ISSN 1007-9327
CN 14-1219/R

World Journal of Gastroenterology®

Indexed and Abstracted in:

Current Contents®/Clinical Medicine, Science Citation Index Expanded (also known as SciSearch®) and Journal Citation Reports/Science Edition, *Index Medicus*, MEDLINE and PubMed, Chemical Abstracts, EMBASE/Excerpta Medica, Abstracts Journals, *Nature Clinical Practice Gastroenterology and Hepatology*, CAB Abstracts and Global Health.
ISI JCR 2003-2000 IF: 3.318, 2.532, 1.445 and 0.993.

Volume 14 Number 23
June 21, 2008
World J Gastroenterol
2008 June 21; 14(23): 3609-3772

Online Submissions
wjg.wjgnet.com
www.wjgnet.com
Printed on Acid-free Paper
世界胃腸病学杂志

A Weekly Journal of Gastroenterology and Hepatology

World Journal of
Gastroenterology ®
Editorial Board
2007-2009

百世登
Baishideng
http://www.wjgnet.com
E-mail: wjg@wjgnet.com

HONORARY EDITORS-IN-CHIEF
Montgomery Bissell, *San Francisco*
James L Boyer, *New Haven*
Ke-Ji Chen, *Beijing*
Li-Fang Chou, *Taipei*
Jacques V Dam, *Stanford*
Martin H Floch, *New Haven*
Guadalupe Garcia-Tsao, *New Haven*
Zhi-Qiang Huang, *Beijing*
Shinn-Jang Hwang, *Taipei*
Ira M Jacobson, *New York*
Derek Jewell, *Oxford*
Emmet B Keeffe, *Palo Alto*
Min-Liang Kuo, *Taipei*
Nicholas F LaRusso, *Rochester*
Jie-Shou Li, *Nanjing*
Geng-Tao Liu, *Beijing*
Lein-Ray Mo, *Tainan*
Bo-Rong Pan, *Xi'an*
Fa-Zu Qiu, *Wuhan*
Eamonn M Quigley, *Cork*
David S Rampton, *London*
Rafiq A Sheikh, *Sacramento*
Rudi Schmid, *Kentfield*[1]
Nicholas J Talley, *Rochester*
Guido NJ Tytgat, *Amsterdam*
Hsiu-Po Wang, *Taipei*
Jaw-Ching Wu, *Taipei*
Meng-Chao Wu, *Shanghai*
Ming-Shiang Wu, *Taipei*
Jia-Yu Xu, *Shanghai*
Ta-Sen Yeh, *Taoyuan*

EDITOR-IN-CHIEF
Lian-Sheng Ma, *Taiyuan*

ASSOCIATE EDITORS-IN-CHIEF
Gianfranco D Alpini, *Temple*
Bruno Annibale, *Roma*
Roger W Chapman, *Oxford*
Chi-Hin Cho, *Hong Kong*
Hugh J Freeman, *Vancouver*
Alexander L Gerbes, *Munich*
Shou-Dong Lee, *Taipei*
Walter E Longo, *New Haven*
You-Yong Lu, *Beijing*
Masao Omata, *Tokyo*
Harry HX Xia, *Hanover*

MEMBERS OF THE EDITORIAL BOARD

Albania
Bashkim Resuli, *Tirana*

Argentina
Julio H Carri, *Córdoba*
Adriana M Torres, *Rosario*

Australia
Minoti V Apte, *Liverpool*
Richard B Banati, *Lidcombe*
Michael R Beard, *Adelaide*
Patrick Bertolino, *Sydney*
Filip Braet, *Sydney*
Andrew D Clouston, *Sydney*
Graham Cooksley, *Queensland*
Darrell HG Crawford, *Brisbane*
Adrian G Cummins, *Woodville South*
Guy D Eslick, *Sydney*
Michael A Fink, *Melbourne*
Robert JL Fraser, *Daw Park*
Mark D Gorrell, *Sydney*
Yik-Hong Ho, *Townsville*
Gerald J Holtmann, *Adelaide*
Michael Horowitz, *Adelaide*
John E Kellow, *Sydney*
Geoffrey W McCaughan, *Sydney*
Finlay A Macrae, *Victoria*
Daniel Markovich, *Brisbane*
Phillip S Oates, *Perth*
Stephen M Riordan, *Sydney*
Ian C Roberts-Thomson, *Adelaide*
Arthur Shulkes, *Melbourne*
Ross C Smith, *Sydney*
Kevin J Spring, *Brisbane*
Nathan Subramaniam, *Brisbane*
Herbert Tilg, *Innsbruck*
Martin J Veysey, *Gosford*
Daniel L Worthley, *Bedford*

Austria
Peter Ferenci, *Vienna*
Valentin Fuhrmann, *Vienna*
Alfred Gangl, *Vienna*
Christoph Gasche, *Vienna*
Kurt Lenz, *Linz*
Markus Peck-Radosavljevic, *Vienna*
Rudolf E Stauber, *Auenbruggerplatz*
Michael Trauner, *Graz*
Harald Vogelsang, *Vienna*
Guenter Weiss, *Innsbruck*

Belarus
Yury K Marakhouski, *Minsk*

Belgium
Rudi Beyaert, *Gent*
Bart Rik De Geest, *Leuven*
Inge I Depoortere, *Leuven*
Olivier Detry, *Liège*
Benedicte Y De Winter, *Antwerp*
Karel Geboes, *Leuven*
Thierry Gustot, *Brussels*
Yves J Horsmans, *Brussels*
Geert G Leroux-Roels, *Ghent*
Louis Libbrecht, *Leuven*
Etienne M Sokal, *Brussels*
Marc Peeters, *De Pintelaan*
Gert A Van Assche, *Leuven*
Yvan Vandenplas, *Brussels*
Eddie Wisse, *Keerbergen*

Brazil
Heitor Rosa, *Goiania*

Bulgaria
Zahariy Krastev, *Sofia*

Canada
Fernando Alvarez, *Québec*
David Armstrong, *Ontario*
Jeffrey P Baker, *Toronto*
Olivier Barbier, *Québec*
Nancy Baxter, *Toronto*
Matthew Bjerknes, *Toronto*
Frank J Burczynski, *Winnipeg*
Michael F Byrne, *Vancouver*
Wang-Xue Chen, *Ottawa*
Chantal Guillemette, *Québec*
Samuel S Lee, *Calgary*
Gary A Levy, *Toronto*
Andrew L Mason, *Alberta*
John K Marshall, *Ontario*
Donna-Marie McCafferty, *Calgary*
Thomas I Michalak, *St. John's*
Gerald Y Minuk, *Manitoba*
Paul Moayyedi, *Hamilton*
William G Paterson, *Kingston*
Eldon Shaffer, *Calgary*
Morris Sherman, *Toronto*
Martin Storr, *Calgary*
Alan BR Thomson, *Edmonton*
Elena F Verdu, *Ontario*
John L Wallace, *Calgary*
Eric M Yoshida, *Vancouver*

Chile
Silvana Zanlungo, *Santiago*

China
Henry LY Chan, *Hongkong*
Xiao-Ping Chen, *Wuhan*
Zong-Jie Cui, *Beijing*
Da-Jun Deng, *Beijing*
Er-Dan Dong, *Beijing*
Sheung-Tat Fan, *Hong Kong*
Jin Gu, *Beijing*
De-Wu Han, *Taiyuan*
Ming-Liang He, *Hong Kong*
Wayne HC Hu, *Hong Kong*
Chee-Kin Hui, *Hong Kong*
Ching-Lung Lai, *Hong Kong*
Kam Chuen Lai, *Hong Kong*
James YW Lau, *Hong Kong*
Yuk-Tong Lee, *Hong Kong*
Suet-Yi Leung, *Hong Kong*
Wai-Keung Leung, *Hong Kong*
Chung-Mau Lo, *Hong Kong*
Jing-Yun Ma, *Beijing*
Lun-Xiu Qin, *Shanghai*
Yu-Gang Song, *Guangzhou*
Qin Su, *Beijing*
Wai-Man Wong, *Hong Kong*
Hong Xiao, *Beijing*
Dong-Liang Yang, *Wuhan*
Winnie Yeo, *Hong Kong*
Yuan Yuan, *Shenyang*
Man-Fung Yuen, *Hong Kong*
Jian-Zhong Zhang, *Beijing*
Xin-Xin Zhang, *Shanghai*
Shu Zheng, *Hangzhou*

Croatia
Tamara Cacev, *Zagreb*
Marko Duvnjak, *Zagreb*

Cuba

Damian C Rodriguez, *Havana*

Czech

Milan Jirsa, *Praha*

Denmark

Peter Bytzer, *Copenhagen*
Asbjørn M Drewes, *Aalborg*
Hans Gregersen, *Aalborg*
Jens H Henriksen, *Hvidovre*
Claus P Hovendal, *Odense*
Fin S Larsen, *Copenhagen*
Søren Møller, *Hvidovre*

Egypt

Abdel-Rahman El-Zayadi, *Giza*
Amr M Helmy, *Cairo*
Sanaa M Kamal, *Cairo*
Ayman Yosry, *Cairo*

Estonia

Riina Salupere, *Tartu*

Finland

Irma E Jarvela, *Helsinki*
Katri M Kaukinen, *Tampere*
Minna Nyström, *Helsinki*
Pentti Sipponen, *Espoo*

France

Bettaieb Ali, *Dijon*
Corlu Anne, *Rennes*
Denis Ardid, *Clermont-Ferrand*
Charles P Balabaud, *Bordeaux*
Soumeya Bekri, *Rouen*
Jacques Belghiti, *Clichy*
Pierre Brissot, *Rennes*
Patrice P Cacoub, *Paris*
Franck Carbonnel, *Besancon*
Laurent Castera, *Pessac*
Bruno Clément, *Rennes*
Benoit Coffin, *Colombes*
Jacques Cosnes, *Paris*
Thomas Decaens, *Cedex*
Francoise L Fabiani, *Angers*
Gérard Feldmann, *Paris*
Jean Fioramonti, *Toulouse*
Jean-Paul Galmiche, *Nantes*
Catherine Guettier, *Villejuif*
Chantal Housset, *Paris*
Juan L Iovanna, *Marseille*
Rene Lambert, *Lyon*
Philippe Mathurin, *Lille*
Patrick Marcellin, *Paris*
Tamara Matysiak–Budnik, *Paris*
Francis Mégraud, *Bordeaux*
Richard Moreau, *Clichy*
Thierry Piche, *Nice*
Raoul Poupon, *Paris*
Jean Rosenbaum, *Bordeaux*
Jose Sahel, *Marseille*
Jean-Philippe Salier, *Rouen*
Jean-Yves Scoazec, *Lyon*
Khalid A Tazi, *Clichy*
Emmanuel Tiret, *Paris*
Baumert F Thomas, *Strasbourg*
Marie-Catherine Vozenin-brotons, *Villejuif*
Jean-Pierre H Zarski, *Grenoble*
Jessica Zucman-Rossi, *Paris*

Germany

Hans-Dieter Allescher, *Garmisch-Partenkirchen*
Martin Anlauf, *Kiel*
Rudolf Arnold, *Marburg*
Max G Bachem, *Ulm*
Thomas F Baumert, *Freiburg*
Daniel C Baumgart, *Berlin*
Hubert Blum, *Freiburg*
Thomas Bock, *Tuebingen*
Katja Breitkopf, *Mannheim*
Dunja Bruder, *Braunschweig*
Markus W Büchler, *Heidelberg*
Christa Buechler, *Regensburg*
Reinhard Buettner, *Bonn*
Elke Cario, *Essen*
Uta Dahmen, *Essen*
Christoph F Dietrich, *Bad Mergentheim*
Rainer J Duchmann, *Berlin*
Volker F Eckardt, *Wiesbaden*
Paul Enck, *Tuebingen*
Fred Fändrich, *Kiel*
Ulrich R Fölsch, *Kiel*
Helmut Friess, *Heidelberg*
Peter R Galle, *Mainz*
Nikolaus Gassler, *Aachen*
Andreas Geier, *Aachen*
Markus Gerhard, *Munich*
Dieter Glebe, *Giessen*
Burkhard Göke, *Munich*
Florian Graepler, *Tuebingen*
Axel M Gressner, *Aachen*
Veit Gülberg, *Munich*
Rainer Haas, *Munich*
Eckhart G Hahn, *Erlangen*
Stephan Hellmig, *Kiel*
Martin Hennenberg, *Bonn*
Johannes Herkel, *Hamburg*
Klaus R Herrlinger, *Stuttgart*
Eberhard Hildt, *Berlin*
Joerg C Hoffmann, *Berlin*
Ferdinand Hofstaedter, *Regensburg*
Werner Hohenberger, *Erlangen*
Jörg C Kalff, *Bonn*
Ralf Jakobs, *Ludwigshafen*
Jutta Keller, *Hamburg*
Andrej Khandoga, *Munich*
Sibylle Koletzko, *München*
Stefan Kubicka, *Hannover*
Joachim Labenz, *Siegen*
Frank Lammert, *Bonn*
Thomas Langmann, *Regensburg*
Christian Liedtke, *Aachen*
Matthias Löhr, *Mannheim*
Christian Maaser, *Muenster*
Ahmed Madisch, *Dresden*
Peter Malfertheiner, *Magdeburg*
Michael P Manns, *Hannover*
Helmut Messmann, *Augsburg*
Stephan Miehlke, *Dresden*
Sabine Mihm, *Göttingen*
Silvio Nadalin, *Essen*
Markus F Neurath, *Mainz*
Johann Ockenga, *Berlin*
Florian Obermeier, *Regensburg*
Gustav Paumgartner, *Munich*
Ulrich KS Peitz, *Magdeburg*
Markus Reiser, *Bochum*
Emil C Reisinger, *Rostock*
Steffen Rickes, *Magdeburg*
Tilman Sauerbruch, *Bonn*
Dieter Saur, *Munich*
Hans Scherubl, *Berlin*
Joerg Schirra, *Munich*
Roland M Schmid, *München*
Volker Schmitz, *Bonn*
Andreas G Schreyer, *Regensburg*
Tobias Schroeder, *Essen*
Hans Seifert, *Oldenburg*
Manfred V Singer, *Mannheim*
Gisela Sparmann, *Rostock*
Jurgen M Stein, *Frankfurt*
Ulrike S Stein, *Berlin*
Manfred Stolte, *Bayreuth*
Christian P Strassburg, *Hannover*
Wolfgang R Stremmel, *Heidelberg*
Harald F Teutsch, *Ulm*
Robert Thimme, *Freiburg*
Hans L Tillmann, *Leipzig*
Tung-Yu Tsui, *Regensburg*
Axel Ulsenheimer, *Munich*
Patrick Veit-Haibach, *Essen*
Claudia Veltkamp, *Heidelberg*
Siegfried Wagner, *Deggendorf*
Henning Walczak, *Heidelberg*
Fritz von Weizsacker, *Berlin*
Jens Werner, *Heidelberg*
Bertram Wiedenmann, *Berlin*
Reiner Wiest, *Regensburg*
Stefan Wirth, *Wuppertal*
Stefan JP Zeuzem, *Homburg*

Greece

Christos Dervenis, *Athens*
Elias A Kouroumalis, *Heraklion*
Ioannis E Koutroubakis, *Heraklion*
Spiros Sgouros, *Athens*

Hungary

Peter L Lakatos, *Budapest*
Zsuzsa Szondy, *Debrecen*

Iceland

Hallgrimur Gudjonsson, *Reykjavik*

India

Philip Abraham, *Mumbai*
Kunissery A Balasubramanian, *Vellore*
Sujit K Bhattacharya, *Kolkata*
Yogesh K Chawla, *Chandigarh*
Radha K Dhiman, *Chandigarh*
Kalpesh Jani, *Vadodara*
Sri Prakash Misra, *Allahabad*
Nageshwar D Reddy, *Hyderabad*

Iran

Seyed-Moayed Alavian, *Tehran*
Reza Malekzadeh, *Tehran*
Seyed A Taghavi, *Shiraz*

Ireland

Billy Bourke, *Dublin*
Ronan A Cahill, *Cork*
Anthony P Moran, *Galway*

Israel

Simon Bar-Meir, *Hashomer*
Abraham R Eliakim, *Haifa*
Yaron Ilan, *Jerusalem*
Avidan U Neumann, *Ramat-Gan*
Yaron Niv, *Pardesia*
Ran Oren, *Tel Aviv*
Ami D Sperber, *Beer-Sheva*

Italy

Giovanni Addolorato, *Roma*
Luigi E Adinolfi, *Naples*
Domenico Alvaro, *Rome*
Vito Annese, *San Giovanni Rotond*
Adolfo F Attili, *Roma*
Giovanni Barbara, *Bologna*
Gabrio Bassotti, *Perugia*
Pier M Battezzati, *Milan*
Stefano Bellentani, *Carpi*
Antomio Benedetti, *Ancona*
Mauro Bernardi, *Bologna*
Livia Biancone, *Rome*
Luigi Bonavina, *Milano*
Flavia Bortolotti, *Padova*
Giuseppe Brisinda, *Rome*
Giovanni Cammarota, *Roma*
Antonino Cavallari, *Bologna*
Giuseppe Chiarioni, *Valeggio*
Michele Cicala, *Rome*
Amedeo Columbano, *Cagliari*
Massimo Conio, *Sanremo*
Dario Conte, *Milano*
Gino R Corazza, *Pavia*
Francesco Costa, *Pisa*
Antonio Craxi, *Palermo*
Silvio Danese, *Milan*
Roberto De Giorgio, *Bologna*
Giovanni D De Palma, *Naples*
Fabio Farinati, *Padua*

Giammarco Fava, *Ancona*
Francesco Feo, *Sassari*
Stefano Fiorucci, *Perugia*
Andrea Galli, *Firenze*
Valeria Ghisett, *Turin*
Gianluigi Giannelli, *Bari*
Edoardo G Giannini, *Genoa*
Paolo Gionchetti, *Bologna*
Mario Guslandi, *Milano*
Pietro Invernizzi, *Milan*
Giacomo Laffi, *Firenze*
Giovanni Maconi, *Milan*
Lucia Malaguarnera, *Catania*
Emanuele D Mangoni, *Napoli*
Paolo Manzoni, *Torino*
Giulio Marchesini, *Bologna*
Fabio Marra, *Florence*
Marco Marzioni, *Ancona*
Giuseppe Montalto, *Palermo*
Giovanni Monteleone, *Rome*
Giovanni Musso, *Torino*
Gerardo Nardone, *Napoli*
Valerio Nobili, *Rome*
Luisi Pagliaro, *Palermo*
Francesco Pallone, *Rome*
Fabrizio R Parente, *Milan*
Francesco Perri, *San Giovanni Rotondo*
Raffaele Pezzilli, *Bologna*
Alberto Pilotto, *San Giovanni Rotondo*
Mario Pirisi, *Novara*
Anna C Piscaglia, *Roma*
Paolo Del Poggio, *Treviglio*
Gabriele B Porro, *Milano*
Piero Portincasa, *Bari*
Bernardino Rampone, *Siena*
Cosimo Prantera, *Roma*
Claudio Romano, *Messina*
Marco Romano, *Napoli*
Gerardo Rosati, *Potenza*
Mario Del Tacca, *Pisa*
Pier A Testoni, *Milan*
Enrico Roda, *Bologna*
Domenico Sansonno, *Bari*
Vincenzo Savarino, *Genova*
Vincenzo Stanghellini, *Bologna*
Giovanni Tarantino, *Naples*
Roberto Testa, *Genoa*
Dino Vaira, *Bologna*

Japan

Kyoichi Adachi, *Izumo*
Yasushi Adachi, *Sapporo*
Taiji Akamatsu, *Matsumoto*
Sk Md Fazle Akbar, *Ehime*
Takafumi Ando, *Nagoya*
Akira Andoh, *Otsu*
Taku Aoki, *Tokyo*
Masahiro Arai, *Tokyo*
Tetsuo Arakawa, *Osaka*
Yasuji Arase, *Tokyo*
Masahiro Asaka, *Sapporo*
Hitoshi Asakura, *Tokyo*
Takeshi Azuma, *Fukui*
Yoichi Chida, *Fukuoka*
Takahiro Fujimori, *Tochigi*
Jiro Fujimoto, *Hyogo*
Kazuma Fujimoto, *Saga*
Mitsuhiro Fujishiro, *Tokyo*
Yoshihide Fujiyama, *Otsu*
Hirokazu Fukui, *Tochigi*
Hiroyuki Hanai, *Hamamatsu*
Kazuhiro Hanazaki, *Kochi*
Naohiko Harada, *Fukuoka*
Makoto Hashizume, *Fukuoka*
Tetsuo Hayakawa, *Nagoya*
Kazuhide Higuchi, *Osaka*
Keisuke Hino, *Ube*
Keiji Hirata, *Kitakyushu*
Yuji Iimuro, *Nishinomiya*
Kenji Ikeda, *Tokyo*
Fumio Imazeki, *Chiba*
Yutaka Inagaki, *Kanagawa*
Yasuhiro Inokuchi, *Yokohama*
Haruhiro Inoue, *Yokohama*
Masayasu Inoue, *Osaka*
Akio Inui, *Kagoshima*
Hiromi Ishibashi, *Nagasaki*
Shunji Ishihara, *Izumo*
Toru Ishikawa, *Niigata*
Kei Ito, *Sendai*
Masayoshi Ito, *Tokyo*
Hiroaki Itoh, *Akita*
Ryuichi Iwakiri, *Saga*
Yoshiaki Iwasaki, *Okayama*
Terumi Kamisawa, *Tokyo*
Hiroshi Kaneko, *Aichi-Gun*
Shuichi Kaneko, *Kanazawa*
Takashi Kanematsu, *Nagasaki*
Mitsuo Katano, *Fukuoka*
Junji Kato, *Sapporo*
Mototsugu Kato, *Sapporo*
Shinzo Kato, *Tokyo*
Norifumi Kawada, *Osaka*
Sunao Kawano, *Osaka*
Mitsuhiro Kida, *Kanagawa*
Yoshikazu Kinoshita, *Izumo*
Tsuneo Kitamura, *Chiba*
Seigo Kitano, *Oita*
Kazuhiko Koike, *Tokyo*
Norihiro Kokudo, *Tokyo*
Satoshi Kondo, *Sapporo*
Shoji Kubo, *Osaka*
Masato Kusunoki, *Tsu Mie*
Shigeki Kuriyama, *Kagawa*[2]
Katsunori Iijima, *Sendai*
Shin Maeda, *Tokyo*
Masatoshi Makuuchi, *Tokyo*
Osamu Matsui, *Kanazawa*
Yasuhiro Matsumura, *Chiba*
Yasushi Matsuzaki, *Tsukuba*
Kiyoshi Migita, *Omura*
Tetsuya Mine, *Kanagawa*
Hiroto Miwa, *Hyogo*
Masashi Mizokami, *Nagoya*
Yoshiaki Mizuguchi, *Tokyo*
Motowo Mizuno, *Hiroshima*
Morito Monden, *Suita*
Hisataka S Moriwaki, *Gifu*
Yasuaki Motomura, *Iizuka*
Yoshiharu Motoo, *Kanazawa*
Kazunari Murakami, *Oita*
Kunihiko Murase, *Tusima*
Masahito Nagaki, *Gifu*
Masaki Nagaya, *Kawasaki*
Yujl Naito, *Kyoto*
Hisato Nakajima, *Tokyo*
Hiroki Nakamura, *Yamaguchi*
Shotaro Nakamura, *Fukuoka*
Mikio Nishioka, *Niihama*
Shuji Nomoto, *Nagoya*
Susumu Ohmada, *Maebashi*
Masayuki Ohta, *Oita*
Tetsuo Ohta, *Kanazawa*
Kazuichi Okazaki, *Osaka*
Katsuhisa Omagari, *Nagasaki*
Saburo Onishi, *Nankoku*
Morikazu Onji, *Ehime*
Satoshi Osawa, *Hamamatsu*
Masanobu Oshima, *Kanazawa*
Hiromitsu Saisho, *Chiba*
Hidetsugu Saito, *Tokyo*
Yutaka Saito, *Tokyo*
Isao Sakaida, *Yamaguchi*
Michiie Sakamoto, *Tokyo*
Yasushi Sano, *Chiba*
Hiroki Sasaki, *Tokyo*
Iwao Sasaki, *Sendai*
Motoko Sasaki, *Kanazawa*
Chifumi Sato, *Tokyo*
Shuichi Seki, *Osaka*
Hiroshi Shimada, *Yokohama*
Mitsuo Shimada, *Tokushima*
Tomohiko Shimatan, *Hiroshima*
Hiroaki Shimizu, *Chiba*
Ichiro Shimizu, *Tokushima*
Yukihiro Shimizu, *Kyoto*
Shinji Shimoda, *Fukuoka*
Tooru Shimosegawa, *Sendai*
Tadashi Shimoyama, *Hirosaki*
Ken Shirabe, *Iizuka*
Yoshio Shirai, *Niigata*
Katsuya Shiraki, *Mie*
Yasushi Shiratori, *Okayama*
Masayuki Sho, *Nara*
Yasuhiko Sugawara, *Tokyo*
Hidekazu Suzuki, *Tokyo*
Minoru Tada, *Tokyo*
Tadatoshi Takayama, *Tokyo*
Tadashi Takeda, *Osaka*
Koji Takeuchi, *Kyoto*
Kiichi Tamada, *Tochigi*
Akira Tanaka, *Kyoto*
Eiji Tanaka, *Matsumoto*
Noriaki Tanaka, *Okayama*
Shinji Tanaka, *Hiroshima*
Wei Tang, *Tokyo*
Hideki Taniguchi, *Yokohama*
Kyuichi Tanikawa, *Kurume*
Akira Terano, *Shimotsugagun*
Hitoshi Togash, *Yamagata*
Kazunari Tominaga, *Osaka*
Takuji Torimura, *Fukuoka*
Minoru Toyota, *Sapporo*
Akihito Tsubota, *Chiba*
Shingo Tsuji, *Osaka*
Takato Ueno, *Kurume*
Naomi Uemura, *Tokyo*
Shinichi Wada, *Tochigi*
Hiroyuki Watanabe, *Kanazawa*
Toshio Watanabe, *Osaka*
Yuji Watanabe, *Ehime*
Toshiaki Watanabe, *Tokyo*
Chun-Yang Wen, *Nagasaki*
Koji Yamaguchi, *Fukuoka*
Takayuki Yamamoto, *Yokkaichi*
Takashi Yao, *Fukuoka*
Masashi Yoneda, *Tochigi*
Hiroshi Yoshida, *Tokyo*
Masashi Yoshida, *Tokyo*
Norimasa Yoshida, *Kyoto*
Kentaro Yoshika, *Toyoake*
Masahide Yoshikawa, *Kashihara*

Lebanon

Bassam N Abboud, *Beirut*
Ala I Sharara, *Beirut*
Joseph D Boujaoude, *Beirut*

Lithuania

Limas Kupcinskas, *Kaunas*

Macedonia

Vladimir C Serafimoski, *Skopje*

Malaysia

Andrew Seng Boon Chua, *Ipoh*
Khean-Lee Goh, *Kuala Lumpur*
Jayaram Menon, *Sabah*

Mexico

Diego Garcia-Compean, *Monterrey*
Eduardo R Marin-Lopez, *Jesús García*
Saúl Villa-Treviño, *México*
Jesus K Yamamoto-Furusho, *México*

Monaco

Patrick Rampal, *Monaco*

Morocco

Abdellah Essaid, Rabat

Netherlands

Ulrich Beuers, *Amsterdam*
Gerd Bouma, *Amsterdam*
Lee Bouwman, *Leiden*
J Bart A Crusius, *Amsterdam*
Janine K Kruit, *Groningen*
Ernst J Kuipers, *Rotterdam*
CBHW Lamers, *Leiden*
Ton Lisman, *Utrecht*

Yi Liu, *Amsterdam*
Servaas Morré, *Amsterdam*
Chris JJ Mulder, *Amsterdam*
Michael Müller, *Wageningen*
Amado S Peña, *Amsterdam*
Robert J Porte, *Groningen*
Ingrid B Renes, *Rotterdam*
Andreas Smout, *Utrecht*
Reinhold W Stockbrugger, *Maastricht*
Luc JW van der Laan, *Rotterdam*
Karel van Erpecum, *Utrecht*
Gerard P VanBerge-Henegouwen,*Utrecht*

New Zealand
Ian D Wallace, *Auckland*

Nigeria
Samuel B Olaleye, *Ibadan*

Norway
Trond Berg, *Oslo*
Tom H Karlsen, *Oslo*
Helge L Waldum, *Trondheim*

Pakistan
Muhammad S Khokhar, *Lahore*
Syed MW Jafri, *Karachi*

Peru
Hector H Garcia, *Lima*

Poland
Tomasz Brzozowski, *Cracow*
Robert Flisiak, *Bialystok*
Hanna Gregorek, *Warsaw*
Dariusz M Lebensztejn, *Bialystok*
Wojciech G Polak, *Wroclaw*
Marek Hartleb, *Katowice*

Portugal
Rodrigues MP Cecília, *Lisbon*
Miguel C De Moura, *Lisbon*

Russia
Vladimir T Ivashkin, *Moscow*
Leonid Lazebnik, *Moscow*
Vasiliy I Reshetnyak, *Moscow*

Saudi Arabia
Ibrahim A Al Mofleh, *Riyadh*

Serbia
Dusan M Jovanovic, *Sremska Kamenica*

Singapore
Bow Ho, *Singapore*
Khek-Yu Ho, *Singapore*
Francis Seow-Choen, *Singapore*

Slovakia
Anton Vavrecka, *Bratislava*

Slovenia
Sasa Markovic, *Ljubljana*

South Africa
Michael C Kew, *Parktown*

South Korea
Byung Ihn Choi, *Seoul*
Ho Soon Choi, *Seoul*
Marie Yeo, *Suwon*
Sun Pyo Hong, *Gyeonggi-do*
Jae J Kim, *Seoul*
Jin-Hong Kim, *Suwon*
Myung-Hwan Kim, *Seoul*
Chang Hong Lee, *Seoul*
Jong Kyun Lee, *Seoul*
Eun-Yi Moon, *Seoul*
Jae-Gahb Park, *Seoul*
Dong Wan Seo, *Seoul*
Dong Jin Suh, *Seoul*

Spain
Juan G Abraldes, *Barcelona*
Agustin Albillos, *Madrid*
Raul J Andrade, *Málaga*
Luis Aparisi, *Valencia*
Fernando Azpiroz, *Barcelona*
Ramon Bataller, *Barcelona*
Josep M Bordas, *Barcelona*
Xavier Calvet, *Sabadell*
Andres Cardenas, *Barcelona*
Vicente Carreño, *Madrid*
Jose Castellote, *Barcelona*
Antoni Castells, *Barcelona*
Vicente Felipo, *Valencia*
Juan C Garcia-Pagán, *Barcelona*
Jaime B Genover, *Barcelona*
Javier P Gisbert, *Madrid*
Jaime Guardia, *Barcelona*
Mercedes Fernandez, *Barcelona*
Angel Lanas, *Zaragoza*
María IT López, *Jaén*
José M Mato, *Derio*
Juan F Medina, *Pamplona*
Miguel A Muñoz-Navas, *Pamplona*
Julian Panes, *Barcelona*
Miguel M Perez, *Valencia*
Miguel Perez-Mateo, *Alicante*
Josep M Pique, *Barcelona*
Jesús M Prieto, Pamplona
Sabino Riestra, *Pola De Siero*
Luis Rodrigo, *Oviedo*
Manuel Romero-Gómez, *Sevilla*

Sweden
Einar S Björnsson, *Gothenburg*
Curt Einarsson, *Huddinge*
Per M Hellström, *Stockholm*
Ulf Hindorf, *Lund*
Hanns-Ulrich Marschall, *Stockholm*
Lars C Olbe, *Molndal*
Lars A Pahlman, *Uppsala*
Matti Sallberg, *Stockholm*
Magnus Simrén, *Göteborg*
Xiao-Feng Sun, *Linköping*
Ervin Tóth, *Malmö*
Weimin Ye, *Stockholm*
Christer S von Holstein, *Lund*

Switzerland
Chrish Beglinger, *Basel*
Pierre A Clavien, *Zurich*
Jean-Francois Dufour, *Bern*
Franco Fortunato, *Zürich*
Jean L Frossard, *Geneva*
Gerd A Kullak-Ublick, *Zurich*
Pierre Michetti, *Lausanne*
Francesco Negro, *Genève*
Bruno Stieger, *Zurich*
Radu Tutuian, *Zurich*
Stephan R Vavricka, *Zurich*
Gerhard Rogler, *Zurich*
Arthur Zimmermann, *Berne*

Turkey
Yusuf Bayraktar, *Ankara*
Figen Gurakan, *Ankara*
Aydin Karabacakoglu, *Konya*
Serdar Karakose, *Konya*
Hizir Kurtel, *Istanbul*
Osman C Ozdogan, *Istanbul*
Özlem Yilmaz, *Izmir*
Cihan Yurdaydin, *Ankara*

United Arab Emirates
Sherif M Karam, *Al-Ain*

United Kingdom
David H Adams, *Birmingham*
Navneet K Ahluwalia, *Stockport*
Ahmed Alzaraa, *Manchester*
Charalambos G Antoniades, *London*
Anthony TR Axon, *Leeds*
Qasim Aziz, *Manchester*
Nicholas M Barnes, *Birmingham*
Jim D Bell, *London*
Mairi Brittan, *London*
Alastair D Burt, *Newcastle*
Simon S Campbell, *Manchester*
Simon R Carding, *Leeds*
Paul J Ciclitira, *London*
Eithne Costello, *Liverpool*
Tatjana Crnogorac-Jurcevic, *London*
Amar P Dhillon, *London*
William Dickey, *Londonderry*
Emad M El-Omar, *Aberdeen*
Annette Fristscher-Ravens, *London*
Elizabeth Furrie, *Dundee*
Daniel R Gaya, *Edinburgh*
Subrata Ghosh, *London*
William Greenhalf, *Liverpool*
Indra N Guha, *Southampton*
Peter C Hayes, *Edinburgh*
Gwo-Tzer Ho, *Edinburgh*
Anthony R Hobson, *Salford*
Stefan G Hübscher, *Birmingham*
Robin Hughes, *London*
Pali Hungin, *Stockton*
David P Hurlstone, *Sheffield*
Rajiv Jalan, *London*
Janusz AZ Jankowski, *Oxford*
Brian T Johnston, *Belfast*
David EJ Jones, *Newcastle*
Roger Jones, *London*
Michael A Kamm, *Harrow*
Peter Karayiannis, *London*
Laurens Kruidenier, *Harlow*
Patricia F Lalor, *Birmingham*
Hong-Xiang Liu, *Cambridge*
Kenneth E L McColl, *Glasgow*
Stuart AC McDonald, *London*
Dermot P Mcgovern, *Oxford*
Giorgina Mieli-Vergani, *London*
Nikolai V Naoumov, *London*
John P Neoptolemos, *Liverpool*
James Neuberger, *Birmingham*
Mark S Pearce, *Newcastle Upon Tyne*
Stephen P Pereira, *London*
D Mark Pritchard, *Liverpool*
Stephen E Roberts, *Swansea*
Marco Senzolo, *Padova*
Soraya Shirazi-Beechey, *Liverpool*
Robert Sutton, *Liverpool*
Simon D Taylor-Robinson, *London*
Paris P Tekkis, *London*
Ulrich Thalheimer, *London*
Nick P Thompson, *Newcastle*
David Tosh, *Bath*
Frank I Tovey, *London*
Chris Tselepis, *Birmingham*
Diego Vergani, *London*
Geoffrey Warhurst, *Salford*
Peter J Whorwell, *Manchester*
Roger Williams, *London*
Karen L Wright, *Bath*
Min Zhao, *Foresterhill*

United States
Gary A Abrams, *Birmingham*
Maria T Abreu, *New York*
Reid B Adams, *Virginia*
Golo Ahlenstiel, *Bethesda*
BS Anand, *Houston*
Frank A Anania, *Atlanta*
Meenakshisundaram Ananthanarayanan, *New York*
Gavin E Arteel, *Louisville*

Jasmohan S Bajaj, *Milwaukee*
Subhas Banerjee, *Palo Alto*
Peter A Banks, *Boston*
Jamie S Barkin, *Miami*
Kim E Barrett, *San Diego*
Marc D Basson, *Detroit*
Wallace F Berman, *Durham*
Timothy R Billiar, *Pittsburgh*
Edmund J Bini, *New York*
Jennifer D Black, *Buffalo*
Herbert L Bonkovsky, *Charlotte*
Andrea D Branch, *New York*
Robert S Bresalier, *Houston*
Alan L Buchman, *Chicago*
Ronald W Busuttil, *Los Angeles*
Alan Cahill, *Philadelphia*
John M Carethers, *San Diego*
David L Carr-Locke, *Boston*
Maurice A Cerulli, *New York*
Ravi S Chari, *Nashville*
Jiande Chen, *Galveston*
Xian-Ming Chen, *Omaha*
Ramsey Chi-man Cheung, *Palo Alto*
William D Chey, *Ann Arbor*
John Y Chiang, *Rootstown*
Parimal Chowdhury, *Arkansas*
Raymond T Chung, *Boston*
James M Church, *Cleveland*
Ram Chuttani, *Boston*
Mark G Clemens, *Charlotte*
Vincent Coghlan, *Beaverton*
David Cronin II, *New Haven*
John Cuppoletti, *Cincinnati*
Mark J Czaja, *New York*
Peter V Danenberg, *Los Angeles*
Kiron M Das, *New Brunswick*
Conor P Delaney, *Cleveland*
Sharon DeMorrow, *Temple*
Deborah L Diamond, *Seattle*
Peter Draganov, *Florida*
Douglas A Drossman, *Chapel Hill*
Katerina Dvorak, *Tucson*
Bijan Eghtesad, *Cleveland*
Hala El-Zimaity, *Houston*
Michelle Embree-Ku, *Providence*
Alessio Fasano, *Baltimore*
Ronnie Fass, *Tucson*
Mark A Feitelson, *Philadelphia*
Ariel E Feldstein, *Cleveland*
Alessandro Fichera, *Chicago*
Robert L Fine, *New York*
Chris E Forsmark, *Gainesville*
Chandrashekhar R Gandhi, *Pittsburgh*
Susan L Gearhart, *Baltimore*
Xupeng Ge, *Boston*
John P Geibel, *New Haven*
Xin Geng, *New Brunswick*
Jean-Francois Geschwind, *Baltimore*
Ignacio Gil-Bazo, *New York*
Shannon S Glaser, *Temple*
Ajay Goel, *Dallas*
Richard M Green, *Chicago*
Julia B Greer, *Pittsburgh*
James H Grendell, *New York*
David R Gretch, *Seattle*
Stefano Guandalini, *Chicago*
Anna S Gukovskaya, *Los Angeles*
Sanjeev Gupta, *Bronx*
David J Hackam, *Pittsburgh*
Stephen B Hanauer, *Chicago*
Gavin Harewood, *Rochester*
Margaret M Heitkemper, *Washington*
Alan W Hemming, *Gainesville*
Samuel B Ho, *San Diego*
Colin W Howden, *Chicago*
Hongjin Huang, *Alameda*
Jamal A Ibdah, *Columbia*
Atif Iqbal, *Omaha*
Hajime Isomoto, *Rochester*
Hartmut Jaeschke, *Tucson*
Dennis M Jensen, *Los Angeles*
Leonard R Johnson, *Memphis*
Michael P Jones, *Chicago*
Peter J Kahrilas, *Chicago*
Anthony N Kalloo, *Baltimore*
Marshall M Kaplan, *Boston*
Neil Kaplowitz, *Los Angeles*
Serhan Karvar, *Los Angeles*
Rashmi Kaul, *Tulsa*
Jonathan D Kaunitz, *Los Angeles*
Ali Keshavarzian, *Chicago*
Miran Kim, *Providence*
Joseph B Kirsner, *Chicago*
Leonidas G Koniaris, *Miami*
Burton I Korelitz, *New York*
Robert J Korst, *New York*
Richard A Kozarek, *Seattle*
Michael Kremer, *Chapel Hill*
Shiu-Ming Kuo, *Buffalo*
Paul Y Kwo, *Indianapolis*
Daryl Tan Yeung Lau, *Galvesto*
Stephen J Lanspa, *Omaha*
Joel E Lavine, *San Diego*
Dirk J van Leeuwen, *Lebanon*
Glen A Lehman, *Indianapolis*
Alex B Lentsch, *Cincinnati*
Andreas Leodolter, *La Jolla*
Gene LeSage, *Houston*
Cynthia Levy, *Gainesville*
Ming Li, *New Orleans*
Zhiping Li, *Baltimore*
Lenard M Lichtenberger, *Houston*
Gary R Lichtenstein, *Philadelphia*
Otto Schiueh-Tzang Lin, *Seattle*
Martin Lipkin, *New York*
Edward V Loftus, *Rocheste*
Robin G Lorenz, *Birmingham*
Michael R Lucey, *Madison*
James D Luketich, *Pittsburgh*
Henry T Lynch, *Omaha*
Patrick M Lynch, *Houston*
John S Macdonald, *New York*
Bruce V MacFadyen, *Augusta*
Willis C Maddrey, *Dallas*
Ashok Malani, *Los Angeles*
Peter J Mannon, *Bethesda*
Charles M Mansbach, *Tennessee*
John F Di Mari, *Texas*
John M Mariadason, *Bronx*
Jorge A Marrero, *Ann Arbor*
Paul Martin, *New York*
Wendy M Mars, *Pittsburgh*
Laura E Matarese, *Pittsburgh*
Lynne V McFarland, *Washington*
Kevin McGrath, *Pittsburgh*
Harihara Mehendale, *Monroe*
Stephan Menne, *New York*
Howard Mertz, *Nashville*
George W Meyer, *Sacramento*
George Michalopoulos, *Pittsburgh*
James M Millis, *Chicago*
Fabrizio Mechelassi, *New York*
Albert D Min, *New York*
Pramod K Mistry, *New Haven*
Smruti R Mohanty, *Chicago*
Satdarshan S Monga, *Pittsburgh*
Timothy H Moran, *Baltimore*
Steven F Moss, *Providence*
Andrew J Muir, *Durham*
Milton G Mutchnick, *Detroit*
Masaki Nagaya, *Boston*
Victor Navarro, *Philadelphia*
Laura E Nagy, *Cleveland*
Hiroshi Nakagawa, *Philadelphia*
Douglas B Nelson, *Minneapolis*
Patrick G Northup, *Charlottesville*
Brant K Oelschlager, *Washington*
Curtis T Okamoto, *Los Angeles*
Stephen JD O'Keefe, *Pittsburgh*
Dimitry Oleynikov, *Omaha*
Natalia A Osna, *Omaha*
Stephen J Pandol, *Los Angeles*
Pankaj J Pasricha, *Galveston*
Zhiheng Pei, *New York*
Michael A Pezzone, *Pittsburgh*
CS Pitchumoni, *New Brunswiuc*
Paul J Pockros, *La Jolla*
Jay Pravda, *Gainesville*
Massimo Raimondo, *Jacksonville*
GS Raju, *Galveston*
Murray B Resnick, *Providence*
Adrian Reuben, *Charleston*
Douglas K Rex, *Indianapolis*
Victor E Reyes, *Galveston*
Basil Rigas, *New York*
Richard A Rippe, *Chapel Hill*
Marcos Rojkind, *Washington*
Philip Rosenthal, *San Francisco*
Hemant K Roy, *Evanston*
Shawn D Safford, *Norfolk*
Bruce E Sands, *Boston*
James M Scheiman, *Ann Arbor*
Eugene R Schiff, *Miami*
Nicholas J Shaheen, *Chapel Hill*
Vanessa M Shami, *Charlottesville*
Prateek Sharma, *Kansas City*
Harvey L Sharp, *Minneapolis*
Stuart Sherman, *Indianapolis*
Shivendra Shukla, *Columbia*
Alphonse E Sirica, *Virginia*
Shanthi V Sitaraman, *Atlanta*
Stuart J Spechler, *Dallas*
Shanthi Srinivasan, *Atlanta*
Michael Steer, *Boston*
Peter D Stevens, *New York*
Gary D Stoner, *Columbus*
Liping Su, *Chicago*
Christina Surawicz, *Seattle*
Ned Snyder, *Galveston*
Robert W Summers, *Iowa City*
Gyongyi Szabo, *Worcester*
Yvette Taché, *Los Angeles*
Seng-Lai Tan, *Seattle*
Andrzej S Tarnawski, *Orange*
K-M Tchou-Wong, *New York*
Neil D Theise, *New York*
Christopher C Thompson, *Boston*
Paul J Thuluvath, *Baltimore*
Swan N Thung, *New York*
Natalie J Torok, *Sacramento*
RA Travagli, *Baton Rouge*
George Triadafilopoulos, *Stanford*
James F Trotter, *Denver*
Chung-Jyi Tsai, *Lexington*
Andrew Ukleja, *Florida*
Michael F Vaezi, *Nashville*
Hugo E Vargas, *Scottsdale*
Arnold Wald, *Wisconsin*
Scott A Waldman, *Philadelphia*
Jian-Ying Wang, *Baltimore*
Timothy C Wang, *New York*
Irving Waxman, *Chicago*
Steven A Weinman, *Galveston*
Steven D Wexner, *Weston*
Keith T Wilson, *Baltimore*
Jacqueline L Wolf, *Boston*
Jackie Wood, *Ohio*
George Y Wu, *Farmington*
Jian Wu, *Sacramento*
Samuel Wyllie, *Houston*
Wen Xie, *Pittsburgh*
Vijay Yajnik, *Boston*
Yoshio Yamaoka, *Houston*
Vincent W Yang, *Atlanta*
Francis Y Yao, *San Francisco*
Hal F Yee, *San Francisco*
Min You, *Tampa*
Zobair M Younossi, *Virginia*
Liqing Yu, *Winston-Salem*
David Yule, *Rochester*
Ruben Zamora, *Pittsburgh*
Michael E Zenilman, *New York*
Zhi Zhong, *Chapel Hill*
Stephen D Zucker, *Cincinnati*

Uruguay

Henry Cohen, *Montevideo*
Javier S Martin, *Punta del Este*

[1]Passed away on October 20, 2007
[2]Passed away on June 11, 2007

Total of 1050 editorial members from 60 countries world wide have been active in peer review and editing

National Journal Award 2005

World Journal of Gastroenterology®

Weekly Established in October 1995

Volume 14 Number 23
June 21, 2008

Contents

EDITORIAL

3609 Minimal hepatic encephalopathy matters in daily life
Bajaj JS

3616 Cystic tumors of the liver: A practical approach
Del Poggio P, Buonocore M

REVIEW

3621 Extended-therapy duration for chronic hepatitis C, genotype 1: The long and the short of it
Pearlman BL

3628 Is there a place for serum laminin determination in patients with liver disease and cancer?
Rosa H, Parise ER

GASTRIC CANCER

3633 Adipokines and ghrelin in gastric cancer cachexia
Kerem M, Ferahkose Z, Yilmaz UT, Pasaoglu H, Ofluoglu E, Bedirli A, Salman B, Sahin TT, Akin M

LIVER CANCER

3642 Secretory Transactivating Transcription-apoptin fusion protein induces apoptosis in hepatocellular carcinoma HepG2 cells
Han SX, Ma JL, Lv Y, Huang C, Liang HH, Duan KM

CLINICAL RESEARCH

3650 Partial overlap of anti-mycobacterial, and anti-*Saccharomyces cerevisiae* mannan antibodies in Crohn's disease
Müller S, Schaffer T, Schoepfer AM, Hilty A, Bodmer T, Seibold F

3662 Methylenetetrahydrofolate reductase C677T genotype affects promoter methylation of tumor-specific genes in sporadic colorectal cancer through an interaction with folate/vitamin B_{12} status
Mokarram P, Naghibalhossaini F, Saberi Firoozi M, Hosseini SV, Izadpanah A, Salahi H, Malek-Hosseini SA, Talei A, Mojallal M

BASIC RESEARCH

3672 Ellagic acid induces apoptosis through inhibition of nuclear factor κB in pancreatic cancer cells
Edderkaoui M, Odinokova I, Ohno I, Gukovsky I, Go VLW, Pandol SJ, Gukovskaya AS

Contents

World Journal of Gastroenterology
Volume 14 **Number** 23 **June** 21, 2008

3681 Experimental treatment of pancreatic cancer with two novel histone deacetylase inhibitors
Haefner M, Bluethner T, Niederhagen M, Moebius C, Wittekind C, Mossner J, Caca K, Wiedmann M

3693 Negundoside, an irridiod glycoside from leaves of *Vitex negundo*, protects human liver cells against calcium-mediated toxicity induced by carbon tetrachloride
Tasduq SA, Kaiser PJ, Gupta BD, Gupta VK, Johri RK

3710 Hepatitis B virus DNA is more powerful than HBeAg in predicting peripheral T-lymphocyte subpopulations in chronic HBV-infected individuals with normal liver function tests
You J, Sriplung H, Geater A, Chongsuvivatwong V, Zhuang L, Chen HY, Huang JH, Tang BZ

RAPID COMMUNICATION

3719 Ineffective oesophageal motility: Manometric subsets exhibit different symptom profiles
Haack HG, Hansen RD, Malcolm A, Kellow JE

3725 Inoperable esophageal cancer and outcome of palliative care
Besharat S, Jabbari A, Semnani S, Keshtkar A, Marjani J

3729 Honey prevents hepatic damage induced by obstruction of the common bile duct
Erguder BI, Kilicoglu SS, Namuslu M, Kilicoglu B, Devrim E, Kismet K, Durak I

3733 Construction and expression of eukaryotic plasmids containing lamivudine-resistant or wild-type strains of Hepatitis B Virus genotype C
Xu WZ, Fang Y, Li D, Wang Y, Shang QL, Li GQ, Teng X, Gu HX

3739 Reduced expression of P120 catenin in cholangiocarcinoma correlated with tumor clinicopathologic parameters
Zhai B, Yan HX, Liu SQ, Chen L, Wu MC, Wang HY

3745 Effects of different *Helicobacter pylori* culture filtrates on growth of gastric epithelial cells
Yan YG, Zhao G, Ma JP, Cai SR, Zhan WH

3750 Clinical value of serum CA19-9 levels in evaluating resectability of pancreatic carcinoma
Zhang S, Wang YM, Sun CD, Lu Y, Wu LQ

3754 Effect of fragile histidine triad gene transduction on proliferation and apoptosis of human hepatocellular carcinoma cells
Xu RH, Zheng LY, He DL, Tong J, Zheng LP, Zheng WP, Meng J, Xia LP, Wang CJ, Yi JL

CASE REPORT

3759 Abdominal neurenteric cyst
Čolović R, Micev M, Jovanović M, Matić S, Grubor N, Atkinson HDE

World Journal of Gastroenterology
Volume 14 **Number** 23 **June** 21, 2008

Contents

	3763	Pathologic complete response confirmed by surgical resection for liver metastases of gastrointestinal stromal tumor after treatment with imatinib mesylate *Suzuki S, Sasajima K, Miyamoto M, Watanabe H, Yokoyama T, Maruyama H, Matsutani T, Liu A, Hosone M, Maeda S, Tajiri T*
ACKNOWLEDGMENTS	**3768**	Acknowledgments to Reviewers of *World Journal of Gastroenterology*
APPENDIX	**3769**	Meetings
	3770	Instructions to authors
FLYLEAF	I-VII	Editorial Board
INSIDE BACK COVER		Online Submissions
INSIDE FRONT COVER		Online Submissions

RESPONSIBLE EDITORS FOR THIS ISSUE

Assistant Editor: *Yan Jiang* **Review Editor:** *Jing Zhu* **Electronic Page Editor:** *De-Hong Yin*
Editor-in-Charge: *Jian-Xia Cheng* **Copy Editor:** *George Y Wu, Professor* **Associate Senior Editor:** *Jian-Xia Cheng*
Layout Editor: *Lian-Sheng Ma*

NAME OF JOURNAL
World Journal of Gastroenterology

RESPONSIBLE INSTITUTION
Department of Science and Technology of Shanxi Province

SPONSOR
Taiyuan Research and Treatment Center for Digestive Diseases, 77 Shuangta Xijie, Taiyuan 030001, Shanxi Province, China

EDITING
Editorial Board of *World Journal of Gastroenterology,* Room 903, Ocean International Center, Building D, No. 62 Dongsihuan Zhonglu, Chaoyang District, Beijing 100025, China
Telephone: +86-10-59080039
Fax: +86-10-85381893
E-mail: wjg@wjgnet.com

PUBLISHING
The WJG Press and Beijing Baishideng BioMed Scientific Co., Ltd., Room 903, Ocean International Center, Building D, No. 62 Dongsihuan Zhonglu, Chaoyang District, Beijing 100025, China
Telephone: +86-10-59080039
Fax: +86-10-85381893
E-mail: wjg@wjgnet.com
http://www.wjgnet.com

PRINTING
Beijing Kexin Printing House

OVERSEAS DISTRIBUTOR
Beijing Bureau for Distribution of Newspapers and Journals
(Code No. 82-261)
China International Book Trading Corporation PO Box 399, Beijing, China (Code No. M4481)

PUBLICATION DATE
June 21, 2008

EDITOR-IN-CHIEF
Lian-Sheng Ma, *Beijing*

SUBSCRIPTION
RMB 50 Yuan for each issue, RMB 2400 Yuan for one year

CSSN
ISSN 1007-9327
CN 14-1219/R

HONORARY EDITORS-IN-CHIEF
Montgomery Bissell, *San Francisco*
James L Boyer, *New Haven*
Chao-Long Chen, *Kaohsiung*
Ke-Ji Chen, *Beijing*
Li-Fang Chou, *Taipei*
Jacques V Dam, *Stanford*
Martin H Floch, *New Haven*
Guadalupe Garcia-Tsao, *New Haven*
Zhi-Qiang Huang, *Beijing*
Shinn-Jang Hwang, *Taipei*
Ira M Jacobson, *New York*
Derek Jewell, *Oxford*
Emmet B Keeffe, *Palo Alto*
Min-Liang Kuo, *Taipei*
Nicholas F LaRusso, *Rochester*
Jie-Shou Li, *Nanjing*
Geng-Tao Liu, *Beijing*
Lein-Ray Mo, *Tainan*
Bo-Rong Pan, *Xi'an*
Fa-Zu Qiu, *Wuhan*
Eamonn M Quigley, *Cork*
David S Rampton, *London*
Rafiq A Sheikh, *Sacramento*
Rudi Schmid, *Kentfield*[1]
Nicholas J Talley, *Rochester*
Sun-Lung Tsai, *Young-Kang City*
Guido NJ Tytgat, *Amsterdam*
Hsiu-Po Wang, *Taipei*
Jaw-Ching Wu, *Taipei*
Meng-Chao Wu, *Shanghai*
Ming-Shiang Wu, *Taipei*
Jia-Yu Xu, *Shanghai*
Ta-Sen Yeh, *Taoyuan*
Ming-Lung Yu, *Kaohsiung*

STRATEGY ASSOCIATE EDITORS-IN-CHIEF
Peter Draganov, *Florida*
Ronnie Fass, *Tucson*
Hugh J Freeman, *Vancouver*
John P Geibel, *New Haven*
Maria C Gutiérrez-Ruiz, *México*
Kazuhiro Hanazaki, *Kochi*
Akio Inui, *Kagoshima*
Kalpesh Jani, *Vadodara*
Sanaa M Kamal, *Cairo*
Ioannis E Koutroubakis, *Heraklion*
Jose JG Marin, *Salamanca*
Javier S Martin, *Punta del Este*
Natalia A Osna, *Omaha*
Jose Sahel, *Marseille*
Ned Snyder, *Galveston*
Nathan Subramaniam, *Brisbane*
Wei Tang, *Tokyo*
Alan BR Thomson, *Edmonton*
Paul Joseph Thuluvath, *Baltimore*
James F Trotter, *Denver*
Shingo Tsuji, *Osaka*
Harry HX Xia, *Hanover*
Yoshio Yamaoka, *Houston*
Jesue K Yamamoto-Furusho, *México*

ASSOCIATE EDITORS-IN-CHIEF
Gianfranco D Alpini, *Temple*
Bruno Annibale, *Roma*
Roger William Chapman, *Oxford*
Chi-Hin Cho, *Hong Kong*
Alexander L Gerbes, *Munich*
Shou-Dong Lee, *Taipei*
Walter Edwin Longo, *New Haven*
You-Yong Lu, *Beijing*
Masao Omata, *Tokyo*

SCIENCE EDITORS
Director: Jian-Xia Cheng, *Beijing*
Deputy Director: Jian-Zhong Zhang, *Beijing*

LANGUAGE EDITORS
Director: Jing-Yun Ma, *Beijing*
Deputy Director: Xian-Lin Wang, *Beijing*

MEMBERS
Gianfranco D Alpini, *Temple*
BS Anand, *Houston*
Manoj Kumar, *Nepal*
Patricia F Lalor, *Birmingham*
Ming Li, *New Orleans*
Margaret Lutze, *Chicago*
Sabine Mihm, *Göttingen*
Francesco Negro, *Genève*
Bernardino Rampone, *Siena*
Richard A Rippe, *Chapel Hill*
Stephen E Roberts, *Swansea*

COPY EDITORS
Gianfranco D Alpini, *Temple*
Sujit Kumar Bhattacharya, *Kolkata*
Filip Braet, *Sydney*
Kirsteen N Browning, *Baton Rouge*
Radha K Dhiman, *Chandigarh*
John Frank Di Mari, *Texas*
Shannon S Glaser, *Temple*
Eberhard Hildt, *Berlin*
Patricia F Lalor, *Birmingham*
Ming Li, *New Orleans*
Margaret Lutze, *Chicago*
MI Torrs, *Jaén*
Sri Prakash Misra, *Allahabad*
Giovanni Monteleone, *Rome*
Giovanni Musso, *Torino*
Valerio Nobili, *Rome*
Osman Cavit Ozdogan, *Istanbul*
Francesco Perri, *San Giovanni Rotondo*
Thierry Piche, *Nice*
Bernardino Rampone, *Siena*
Richard A Rippe, *Chapel Hill*
Ross C Smith, *Sydney*
Daniel Lindsay Worthley, *Bedford*
George Y Wu, *Farmington*
Jian Wu, *Sacramento*

COPYRIGHT
© 2008 Published by The WJG Press. All rights reserved; no part of this publication may be reproduced, stored in a retrieval system, or transmitted in any form or by any means, electronic, mechanical, photocopying, recording, or otherwise without the prior permission of *WJG*. Authors are required to grant *WJG* an exclusive licence to publish.

SPECIAL STATEMENT
All articles published in this journal represent the viewpoints of the authors except where indicated otherwise.

INSTRUCTIONS TO AUTHORS
Full instructions are available online at http://www.wjgnet.com/wjg/help/instructions.jsp. If you do not have web access please contact the editorial office.

ONLINE SUBMISSION
http://wjg.wjgnet.comw

Online Submissions: wjg.wjgnet.com
wjg@wjgnet.com
doi:10.3748/wjg.14.3609

World J Gastroenterol 2008 June 21; 14(23): 3609-3615
World Journal of Gastroenterology ISSN 1007-9327
© 2008 The WJG Press. All rights reserved.

EDITORIAL

Minimal hepatic encephalopathy matters in daily life

Jasmohan S Bajaj

Jasmohan S Bajaj, Division of Gastroenterology and Hepatology, Medical College of Wisconsin, Milwaukee, WI 53226, United States
Author contributions: Bajaj JS contributed all to this paper.
Correspondence to: Jasmohan S Bajaj, MBBS, MD, MS, Division of Gastroenterology and Hepatology, Medical College of Wisconsin, Milwaukee, WI 53226, United States. jasmohan@gmail.com
Telephone: +1-414-4566825 Fax: +1-414-4566214
Received: February 27, 2008 Revised: March 23, 2008
Accepted: March 30, 2008
Published online: June 21, 2008

Abstract

Minimal hepatic encephalopathy is a neuro-cognitive dysfunction which occurs in an epidemic proportion of cirrhotic patients, estimated as high as 80% of the population tested. It is characterized by a specific, complex cognitive dysfunction which is independent of sleep dysfunction or problems with overall intelligence. Although named "minimal", minimal hepatic encephalopathy (MHE) can have a far-reaching impact on quality of life, ability to function in daily life and progression to overt hepatic encephalopathy. Importantly, MHE has a profound negative impact on the ability to drive a car and may be a significant factor behind motor vehicle accidents. A crucial aspect of the clinical care of MHE patients is their driving history, which is often ignored in routine care and can add a vital dimension to the overall disease assessment. Driving history should be an integral part of care in patients with MHE. The lack of specific signs and symptoms, the preserved communication skills and lack of insight make MHE a difficult condition to diagnose. Diagnostic strategies for MHE abound, but are usually limited by financial, normative or time constraints. Recent studies into the inhibitory control and critical flicker frequency tests are encouraging since these tests can increase the rates of MHE diagnosis without requiring a psychologist. Although testing for MHE and subsequent therapy is not standard of care at this time, it is important to consider this in cirrhotics in order to improve their ability to live their life to the fullest.

© 2008 *WJG*. All rights reserved.

Key words: Minimal hepatic encephalopathy; Quality of life; Driving impairment; Diagnosis; Therapy; Prognosis

Peer reviewer: Giovanni Tarantino, MD, Professor, Department of Clinical and Experimental Medicine, Federico II University Medical School, VIA S. PANSINI, 5, Naples 80131, Italy

Bajaj JS. Minimal hepatic encephalopathy matters in daily life. *World J Gastroenterol* 2008; 14(23): 3609-3615 Available from: URL: http://www.wjgnet.com/1007-9327/14/3609.asp DOI: http://dx.doi.org/10.3748/wjg.14.3609

INTRODUCTION

Minimal hepatic encephalopathy is a neuro-cognitive dysfunction which occurs in an epidemic proportion of cirrhotic patients, estimated as high as 80% of the population tested. It is characterized by a specific, complex cognitive dysfunction which is independent of sleep dysfunction or problems with overall intelligence[1]. Although named "minimal", minimal hepatic encephalopathy (MHE) can have a far-reaching impact on quality of life, ability to function in daily life and progression to overt hepatic encephalopathy (OHE)[2]. Importantly, MHE has a profound negative impact on the ability to drive a car and may be a significant factor behind motor vehicle accidents. Research in this field is expanding rapidly, but little consensus has emerged regarding standard diagnostic strategies or therapeutic options[3]. The current editorial will focus on the relevance of MHE as an important clinical entity that is ready for evaluation and regular detection not only in research centers but in routine hepatology practice.

PREVALENCE AND IMPORTANCE

With improving management of cirrhotic patients, including those with end-stage liver disease, the neuropsychological care of these patients is being recognized as an unmet need[4-6]. The importance of MHE has been recognized by hepatologists worldwide and of late an explosion of research in this field has occurred[7,8].

Since its first description in the 1970s, MHE has been diagnosed in several countries around the world at a rate of 30%-80%[9,10]. The European experience has shown a high prevalence of MHE in patients who are predominantly non-alcoholic and without any psychoactive drug use[11,12]. The diagnostic methodologies were a combination of neuro-psychometric and neuro-physiologic testing strategies[11-13]. In the United States, the rate of MHE in several research series has been reported to

be 60%-80%, again using a combination of psychometric and neuro-physiologic techniques[14,15].

Experience in Asian countries, especially India, Japan and China, has reconfirmed the high prevalence using locally modified tools[10,16-22]. The diagnostic tools were adapted to the local language and to include illiterate subjects[17,19]. The patient population in these series has included a higher number of patients with viral hepatitis compared to Western series[21,22].

CHARACTERIZATION OF MINIMAL HEPATIC ENCEPHALOPATHY

The importance of MHE lies in its specific deficits. As outlined by Weissenborn *et al*, patients with MHE have defects in attention, vigilance and orientation[23]. These attention deficits in turn lead to learning impairment and difficulties in working memory[12,24]. Psychometric testing in patients with MHE has consistently demonstrated a preservation of overall IQ compared to age-matched controls, indicating that the defects are restricted to certain aspects only[11]. Patients with cirrhosis can also exhibit motor impairments that include Parkinsonian features and features of hepatic myelopathy[25,26]. However, these motor deficits are not included in the typical impairment seen in MHE.

Importantly, deficits in MHE do not extend to the verbal and communication spheres[11]. Similar to OHE patients, there is evidence that patients with MHE have poor insight into their psychometric impairments[27-29]. The preservation of communication skills, lack of symptoms and the poor insight make MHE patients a difficult group to identify with simple questioning in the office.

CONTRIBUTION OF CONCOMITANT DISEASES TO MHE

Patients with specific etiologies of cirrhosis are more likely to exhibit psychometric impairment, specifically chronic hepatitis C. Investigations in the chronic hepatitis C infected groups (both with and without cirrhosis) show a worse psychometric performance compared to patients without chronic hepatitis C in selected studies[30-33]. However, other studies have not demonstrated a difference in psychometric performance of cirrhotics with chronic hepatitis C compared to those without it[30,34]. In addition, a recent detailed study before and after interferon therapy in chronic hepatitis C cirrhotics failed to find an improvement or deterioration during and after therapy completion[35].

Diabetes mellitus is an important correlate of patients with cirrhosis, with the increasing importance of non-alcoholic steatohepatitis, and is also correlated with chronic hepatitis C in the general population[36]. Diabetes mellitus, possibly due to its adverse effect on gastrointestinal motility, has been associated with hepatic encephalopathy[34,37].

Most studies of MHE exclude patients with alcoholic liver disease; therefore, excluding patients with chronic hepatitis C and diabetes mellitus will seriously hinder the generalization of the study. Therefore, a subgroup analysis of chronic hepatitis C and diabetes mellitus within the cirrhosis group or regression adjustment would be necessary for MHE investigation.

CONCOMITANT SLEEP DISTURBANCES

Hepatic encephalopathy is associated with adverse effects on the sleep-wake cycle, especially causing fragmentation of sleep, sleep deprivation and reports of drowsiness during the day[38]. Sleep deprivation *per se* can result in impaired psychometric test performance and as is evidenced in the case of obstructive sleep apnea, and can independently lead to poor driving outcomes[39]. There is debate whether the MHE-associated psychometric impairment is partly due to the inherent sleep-wake cycle disturbances in this condition. Validated sleep and quality of life questionnaire such as Sickness Impact Profile (SIP) sleep scales, Pittsburgh Sleep Quality index and Epworth Sleepiness scale evaluation demonstrate a worse sleep quality and effect on quality of life in patients with MHE[17,38,40]. Steindl *et al* demonstrated a disrupted melatonin cycle in patients with cirrhosis and MHE which was independent of psychometric performance[41]. However, reports have demonstrated that cirrhotics with MHE and sleep disruption do not have worse psychometric performance compared to those who do not have sleep disruption[38,42,43]. This implies that although there is a significant disruption of the sleep-wake and circadian rhythm in patients with MHE, this phenomenon co-exists with the psychometric impairment and is not the cause of it.

QUALITY OF LIFE AND MHE

Quality of life is an essential assessment component of patients with chronic diseases. Issues pertaining to quality of life are also central to most patient complaints in cirrhosis[44]. Groeneweg *et al* studied the Sickness Impact Profile (SIP) in a cohort of cirrhotics being tested for MHE (Medical Outcomes Trust, Boston, MA)[40]. The SIP consists of 136 items which questions patients about 12 sections; sleep and rest, eating, work, home management, recreation and pastimes, ambulation, mobility, body care and movement (the last three generate a physical sub score), social interaction, alertness behavior, emotional behavior, and communication (comprising the psychosocial sub score). All scales were significantly impaired in MHE patients compared to others. A recent study by Prasad *et al* confirmed these findings in MHE patients in all spheres apart from communication, which was similar between patients with or without MHE[17]. Impaired quality of life has also been demonstrated using the Short Form 36 (SF-36) in MHE populations in several studies across the world[45,46].

Short form-36 (SF-36) is a 36-part questionnaire that has been used in several studies to characterize chronic liver disease and the chronic liver disease questionnaire

has also been used in patients with liver disease[44-47].

The SIP is an extensive survey which requires several minutes to complete, in contrast to the relatively short SF-36. The SF-36, therefore, may be a better tool for clinical practice. However, since quality of life changes in MHE are subtle, the SIP is perhaps the questionnaire better suited for research studies since it can differentiate between small changes in several aspects of QOL.

WORK CAPACITY AND MHE

The specific nature of cognitive dysfunction in MHE results in a disproportionate impairment of workers engaged in "blue-collar" professions compared to "white-collar" professionals. This is essential to remember because cirrhotics engaged in professions that require constant vigilance and coordination, e.g. machinery operators and drivers are affected by MHE more severely compared to those who have predominantly verbal and intellectual functions, such as administrative and company executives[29]. Therefore, MHE not only has the potential to endanger the patients and co-workers during complex occupational tasks, it also can adversely affect their socio-economic status by interfering with work performance[48].

MHE AND PROGRESSION TO OVERT HEPATIC ENCEPHALOPATHY

Overt hepatic encephalopathy portends a poor prognosis and overall survival[49,50]. Patients with MHE have a higher likelihood of development of OHE[14,49,51,52]. Specific subgroups that are more likely to progress to OHE are males, those with a history of OHE, those with alcoholic etiology of cirrhosis and those with varices[19,53,54]. Positive responders to the glutamine tolerance test are also more likely to develop OHE[53]. It is not clear, however, which individual MHE patient will go on to develop OHE. The relative contributions of precipitating factors, such as gastrointestinal bleeding, for OHE development in the context of MHE *versus* no MHE have also not been fully elucidated. Therefore, patients with MHE may be a subgroup requiring close follow-up clinically for OHE development, especially when potential precipitating factors are encountered.

MHE AND DRIVING CAPABILITY

The ability to drive a motor vehicle requires coordination of visual, auditory and vestibular inputs and has the potential to be impaired by metabolic encephalopathies[55].

MHE affects attention, psychomotor function and working memory, all of which are essential for safe driving[56]. Most studies of driving ability using on-road driving tests have demonstrated that MHE patients have significant defects in reaction time, resulting in their pronouncement as unsafe drivers in studies from Germany and Japan[49,57]. Wein *et al* studied the driving ability and rating of driving behavior of 44 patients with cirrhosis using instructors masked to their status. Fourteen of these patients had been diagnosed with MHE[58]. Results showed that patients with MHE required interventions by the driving instructor to prevent an accident at a rate 10 times higher compared to those with MHE and controls. Specific driving behaviors were also rated worse in patients with MHE, especially car handling, adaptation, cautiousness and maneuvering[58].

Another essential skill required for safe driving is navigation, which ensures that the subject is in the right place at the right time[55]. Given the working memory abnormalities in cirrhotic patients, the study of navigation in MHE is important[24]. Our group recently published a study evaluating the performance of cirrhotics to age and education-matched controls on a driving simulator. Navigation skills in MHE are adversely affected[59]. All patients underwent a driving simulation which also included a navigation task. This task consisted of driving through a "virtual city" and illegal turns off the marked path were recorded. There was a significantly higher rate of illegal turns in the MHE group compared to those without MHE and controls. Illegal turns were proportionate to impairment in psychometric performance in cirrhotic group[59]. Therefore, driving difficulties in patients with MHE are likely multi-dimensional and includes impairment in reaction time and navigation skills.

DRIVING OUTCOMES IN PATIENTS WITH CIRRHOSIS AND MHE

Traffic accidents are one the leading causes of death worldwide, especially in young adults, the most productive age group of any society. It is important to determine whether patients with MHE also have poor driving outcomes compared to those without MHE and controls. This would be essential in formulating public health decisions regarding licensing and therapy for MHE. A study published by our group sent an anonymous driving outcome questionnaire to controls, cirrhotics tested for MHE and cirrhotics not tested for MHE due to concurrent psychoactive drug use[60]. As many as 33% of MHE patients reported having a traffic accident or violation within the last year compared to only 4% of MHE negative patients and 12% of the patients using psychoactive drugs. When 5 year data were analyzed a significant majority of MHE patients (53%) reported a traffic accident or violation compared to only 23% of MHE negative patients and 22% of those on psychoactive drugs. This is even more significant since none of the MHE patients were drinking alcohol. On multi-variate analysis, MHE emerged as the sole factor associated with traffic violations [odds ratio 6.0 (CI 1.2-31.3)], motor vehicle accidents [odds ratio 7.3 (CI 2.1-33.2)] and both [odds ratio 7.6 (CI 1.5-37.3)][60]. However, despite these striking numbers, there is still the need to analyze driving data prospectively using identified records before making specific recommendations regarding driving capability[3].

Patients with cirrhosis have a poor prognosis after trauma and surgery, especially with increasing Child-

Pugh score[61]. A combination of coagulation impairment, sepsis and hepatic dysfunction has been noted as contributing factors to this worse prognosis[61]. A study of a large inpatient sample from the United States showed that patients with cirrhosis who were involved in a motor vehicle crash had a higher mortality than those who were admitted for motor vehicle crashes only[62]. Despite a younger average age, patients with cirrhosis and crash had a similar mortality compared to those admitted with cirrhosis only. Hospitalization charges and inpatient stay were also significantly higher in cirrhotics with crash compared to patients admitted for cirrhosis only and those admitted for motor vehicle accidents only. On multi-variate regression within the patients admitted with motor vehicle accidents, age > 65 years and cirrhosis were the variables most significantly associated with mortality[62].

Therefore, not only are patients with MHE more likely to get into an accident, they are also more likely to die from it and utilize greater resources as a result of the accident. All these factors make it essential for a clinician to take a driving history when evaluating patients for cirrhosis and chronic liver disease.

MHE: INSIGHT INTO THE DISEASE PROCESS AND DRIVING SKILLS

Insight into personal deficits is essential in patients in order to seek medical intervention. Anosognosia, defined as the unawareness of a disease, is a key component of the disease process in several metabolic and vascular cerebral disorders[63,64]. This phenomenon is clearly observed in patients with OHE, in which it is the persons in the environment who detect changes in the patients' sensorium rather than the patient[27]. A recent report extended this lack of insight into driving impairment. This study demonstrated that patients with MHE rated themselves as significantly better drivers compared to those without MHE and controls when they were evaluated by independent observers[28]. Therefore, similar to patients with OHE, it may be important to elicit a complete driving history and assessment from relatives familiar with the MHE patients' driving rather than relying on the patients' history alone.

THE HISTORY NOT TAKEN: DRIVING HISTORY

The standard of care of patients with cirrhosis without any ongoing acute issues is focused on strategies aimed to prevent decompensation. These strategies are aimed at reducing mortality and morbidity from a liver disease standpoint. However, as evidenced by recent reports, patients with cirrhosis and MHE also are at risk for developing morbidity and mortality behind the steering wheel[58,60]. An objective driving history, including confirmation from the local supervisory agency, and corroboration of driving skills by relatives is also an essential aspect of patient care. The driving history to the clinical history would arguably be a vital addition to the overall understanding of the disease severity from a clinical and psychosocial view in cirrhosis.

TESTING FOR MHE DURING CLINIC VISITS

Although the majority of surveyed hepatologists in Spain and the United States agreed that MHE was a significant problem requiring testing, the minority were able to actually test for MHE as part of their clinical practice[7,8]. Main barriers to MHE testing were inability to get tests paid for by insurance, adding time to clinic visits and lack of standardized norms for the United States[8].

The psychometric battery recommended by the Working Group on Hepatic Encephalopathy is the PSE-syndrome test published by Weissenborn *et al*[2,11]. This test battery, although quite efficient in diagnosing MHE, requires a psychologist and valid population norms. The difficulty of applying these tests in the United States is the lack of background population norms and the need for a licensed psychologist to order and administer these tests. In addition, these are still not routinely covered by private health care insurance. These logistic barriers have effectively prevented routine clinic diagnosis of MHE.

The AASLD survey also highlighted the need for simpler and rapid testing that can take the place of cumbersome and copyrighted psychometric testing[8]. The inhibitory control and the critical flicker frequency have emerged as tests that can be applied in clinical practice without the need for psychological expertise[3,13,14,20,65]. However, detailed validation studies are still underway for these tests.

POPULATION TO BE TESTED

Patients with cirrhosis who are ambulatory and capable of independent living are the ones most affected by MHE and should definitely be tested. Previous recommendations have been split regarding the specific population to be targeted for testing. Ortiz *et al* and Stewart *et al* have specifically recommended certain patient populations be tested[1,48]. Psychometric performance can be affected by current alcohol use, use of psychoactive drugs and pre-existing neurological disorders[11]. In cirrhotics who do not fulfill these criteria, it is in the best interest of the patient to be offered testing at the initial visit regardless of their subsequent activities. There is no consensus regarding the frequency of testing, but experience has shown relative similarity in psychometric scores at 6 mo intervals in the absence of acute clinical and neurological events such as development of OHE[19].

THERAPY FOR MHE

Treatment of MHE improves psychometric performance and quality of life[16,17].

A recent consensus conference promulgated lactulose as the first choice of therapy for MHE in concor-

dance with the previous study data and the AASLD survey[3,8]. However, whether this would have any effect on development of OHE, driving capability or overall survival remains to be investigated. Since driving and psychometric impairments are highly correlated, it is reasonable to expect that driving performance would also improve after MHE therapy.

However, the adherence rate of lactulose in patients with OHE is low; therefore, to expect an MHE patient, who does not have any specific symptoms and lacks insight into their problems, to be adherent on a medication that could cause diarrhea and flatulence is difficult[3,66]. Therefore, alternatives to lactulose have also been studied for MHE. Liu *et al* showed that fiber and fiber with probiotics improved psychometric function and importantly the Child class of patients[21]. Similar studies have been published using various formulations of probiotics with good improvement in psychometric tests[67-71]. Our group has recently completed a randomized control trial of a probiotic yogurt that resulted in a significant reversal of MHE in the yogurt-randomized group compared to the group randomized to no treatment[72]. The adherence was excellent and none of the yogurt-treated group developed OHE. Although probiotics are attractive options that spare the patients from the poor palatability of lactulose, difficulties in the availability and the standardization of probiotic organisms remain. However, these preliminary data suggests that dietary intervention may be considered in addition to probiotics for amelioration of MHE.

Therefore, although treatment options for MHE are evolving, it is still important to test patients to offer them the available therapeutic options.

CONCLUSION

MHE is an epidemic cognitive dysfunction in patients with cirrhosis which is gaining importance in clinical and research spheres due to improved survival in cirrhotic patients.

MHE patients exhibit a specific cognitive impairment that negatively impacts their driving capability and work performance and importantly is not evident to the patients themselves.

A crucial aspect of the clinical care of MHE patients is their driving history, which is often ignored in routine care and can add a vital dimension to the overall disease assessment. Driving history should be an integral part of care in patients with MHE.

The lack of specific signs and symptoms, the preserved communication skills and lack of insight make MHE a difficult condition to diagnose.

Diagnostic strategies for MHE abound, but are usually limited by financial, normative or time constraints. Recent studies into the inhibitory control and critical flicker frequency tests are encouraging since these tests can increase the rates of MHE diagnosis without requiring a psychologist.

Although testing for MHE and subsequent therapy is not standard of care at this time, it is important to consider this in cirrhotics in order to improve their ability to live their life to the fullest.

REFERENCES

1 **Ortiz M**, Jacas C, Cordoba J. Minimal hepatic encephalopathy: diagnosis, clinical significance and recommendations. *J Hepatol* 2005; **42** Suppl: S45-S53
2 **Ferenci P**, Lockwood A, Mullen K, Tarter R, Weissenborn K, Blei AT. Hepatic encephalopathy--definition, nomenclature, diagnosis, and quantification: final report of the working party at the 11th World Congresses of Gastroenterology, Vienna, 1998. *Hepatology* 2002; **35**: 716-721
3 **Mullen K**, Ferenci P, Bass NM, Leevy CB, E. K. An Algorithm for the Management of Hepatic Encephalopathy. *Seminars in Liver Disease* 2007; **27**: 32-48
4 **Qadri AM**, Ogunwale BO, Mullen KD. Can we ignore minimal hepatic encephalopathy any longer? *Hepatology* 2007; **45**: 547-548
5 **Talwalkar JA**, Kamath PS. Influence of recent advances in medical management on clinical outcomes of cirrhosis. *Mayo Clin Proc* 2005; **80**: 1501-1508
6 **Noble JA,** Caces MF, Steffens RA, Stinson FS. Cirrhosis hospitalization and mortality trends, 1970-87. *Public Health Rep* 1993; **108**: 192-197
7 **Vergara-Gomez M**, Flavia-Olivella M, Gil-Prades M, Dalmau-Obrador B, Cordoba-Cardona J. [Diagnosis and treatment of hepatic encephalopathy in Spain: results of a survey of hepatologists] *Gastroenterol Hepatol* 2006; **29**: 1-6
8 **Bajaj JS**, Etemadian A, Hafeezullah M, Saeian K. Testing for minimal hepatic encephalopathy in the United States: An AASLD survey. *Hepatology* 2007; **45**: 833-834
9 **Rikkers L**, Jenko P, Rudman D, Freides D. Subclinical hepatic encephalopathy: detection, prevalence, and relationship to nitrogen metabolism. *Gastroenterology* 1978; **75**: 462-469
10 **Saxena N**, Bhatia M, Joshi YK, Garg PK, Tandon RK. Auditory P300 event-related potentials and number connection test for evaluation of subclinical hepatic encephalopathy in patients with cirrhosis of the liver: a follow-up study. *J Gastroenterol Hepatol* 2001; **16**: 322-327
11 **Weissenborn K**, Ennen JC, Schomerus H, Ruckert N, Hecker H. Neuropsychological characterization of hepatic encephalopathy. *J Hepatol* 2001; **34**: 768-773
12 **Ortiz M**, Cordoba J, Jacas C, Flavia M, Esteban R, Guardia J. Neuropsychological abnormalities in cirrhosis include learning impairment. *J Hepatol* 2006; **44**: 104-110
13 **Romero-Gomez M**, Cordoba J, Jover R, del Olmo JA, Ramirez M, Rey R, de Madaria E, Montoliu C, Nunez D, Flavia M, Company L, Rodrigo JM, Felipo V. Value of the critical flicker frequency in patients with minimal hepatic encephalopathy. *Hepatology* 2007; **45**: 879-885
14 **Bajaj JS**, Saeian K, Verber MD, Hischke D, Hoffmann RG, Franco J, Varma RR, Rao SM. Inhibitory control test is a simple method to diagnose minimal hepatic encephalopathy and predict development of overt hepatic encephalopathy. *Am J Gastroenterol* 2007; **102**: 754-760
15 **Meyer T**, Eshelman A, Abouljoud M. Neuropsychological changes in a large sample of liver transplant candidates. *Transplant Proc* 2006; **38**: 3559-3560
16 **Watanabe A**, Sakai T, Sato S, Imai F, Ohto M, Arakawa Y, Toda G, Kobayashi K, Muto Y, Tsujii T, Kawasaki H, Okita K, Tanikawa K, Fujiyama S, Shimada S. Clinical efficacy of lactulose in cirrhotic patients with and without subclinical hepatic encephalopathy. *Hepatology* 1997; **26**: 1410-1414
17 **Prasad S**, Dhiman RK, Duseja A, Chawla YK, Sharma A, Agarwal R. Lactulose improves cognitive functions and health-related quality of life in patients with cirrhosis who have minimal hepatic encephalopathy. *Hepatology* 2007; **45**: 549-559
18 **Li YY**, Nie YQ, Sha WH, Zeng Z, Yang FY, Ping L, Jia L. Prevalence of subclinical hepatic encephalopathy in cirrhotic

patients in China. *World J Gastroenterol* 2004; **10**: 2397-2401
19 **Das A**, Dhiman RK, Saraswat VA, Verma M, Naik SR. Prevalence and natural history of subclinical hepatic encephalopathy in cirrhosis. *J Gastroenterol Hepatol* 2001; **16**: 531-535
20 **Sharma P**, Sharma BC, Puri V, Sarin SK. Critical flicker frequency: diagnostic tool for minimal hepatic encephalopathy. *J Hepatol* 2007; **47**: 67-73
21 **Liu Q**, Duan ZP, Ha DK, Bengmark S, Kurtovic J, Riordan SM. Synbiotic modulation of gut flora: effect on minimal hepatic encephalopathy in patients with cirrhosis. *Hepatology* 2004; **39**: 1441-1449
22 **Kato A**, Kato M, Ishii H, Ichimiya Y, Suzuki K, Kawasaki H, Yamamoto SI, Kumashiro R, Yamamoto K, Kawamura N, Hayashi N, Matsuzaki S, Terano A, Okita K, Watanabe A. Development of quantitative neuropsychological tests for diagnosis of subclinical hepatic encephalopathy in liver cirrhosis patients and establishment of diagnostic criteria-multicenter collaborative study in Japanese. *Hepatol Res* 2004; **30**: 71-78
23 **Weissenborn K**, Giewekemeyer K, Heidenreich S, Bokemeyer M, Berding G, Ahl B. Attention, memory, and cognitive function in hepatic encephalopathy. *Metab Brain Dis* 2005; **20**: 359-367
24 **Weissenborn K**, Heidenreich S, Giewekemeyer K, Ruckert N, Hecker H. Memory function in early hepatic encephalopathy. *J Hepatol* 2003; **39**: 320-325
25 **Joebges EM**, Heidemann M, Schimke N, Hecker H, Ennen JC, Weissenborn K. Bradykinesia in minimal hepatic encephalopathy is due to disturbances in movement initiation. *J Hepatol* 2003; **38**: 273-280
26 **Bechar M**, Freud M, Kott E, Kott I, Kravvic H, Stern J, Sandbank U, Bornstein B. Hepatic cirrhosis with post-shunt myelopathy. *J Neurol Sci* 1970; **11**: 101-107
27 **Weissenborn K**. Clinical features of hepatic encephalopathy. In: Zakim D, Boyer TD, editors. Hepatology. 4th ed. Philadelphia: WB Saunders, 2003: 431-444
28 **Bajaj JS**, Saeian K, Hafeezullah M, Hoffmann RG, Hammeke TA. Patients with minimal hepatic encephalopathy have poor insight into their driving skills. *Clinical Gastroenterology and Hepatology* 2008; **6:** 1135-1139
29 **Schomerus H**, Hamster W. Quality of life in cirrhotics with minimal hepatic encephalopathy. *Metab Brain Dis* 2001; **16**: 37-41
30 **Perry W**, Hilsabeck RC, Hassanein TI. Cognitive dysfunction in chronic hepatitis C: a review. *Dig Dis Sci* 2008; **53**: 307-321
31 **Citro V**, Milan G, Tripodi FS, Gennari A, Sorrentino P, Gallotta G, Postiglione A, Tarantino G. Mental status impairment in patients with West Haven grade zero hepatic encephalopathy: the role of HCV infection. *J Gastroenterol* 2007; **42**: 79-82
32 **Weissenborn K**, Krause J, Bokemeyer M, Hecker H, Schuler A, Ennen JC, Ahl B, Manns MP, Boker KW. Hepatitis C virus infection affects the brain-evidence from psychometric studies and magnetic resonance spectroscopy. *J Hepatol* 2004; **41**: 845-851
33 **Hilsabeck RC**, Hassanein TI, Carlson MD, Ziegler EA, Perry W. Cognitive functioning and psychiatric symptomatology in patients with chronic hepatitis C. *J Int Neuropsychol Soc* 2003; **9**: 847-854
34 **Kalaitzakis E**, Olsson R, Henfridsson P, Hugosson I, Bengtsson M, Jalan R, Bjornsson E. Malnutrition and diabetes mellitus are related to hepatic encephalopathy in patients with liver cirrhosis. *Liver Int* 2007; **27**: 1194-1201
35 **Fontana RJ**, Bieliauskas LA, Lindsay KL, Back-Madruga C, Wright EC, Snow KK, Lok AS, Kronfol Z, Padmanabhan L. Cognitive function does not worsen during pegylated interferon and ribavirin retreatment of chronic hepatitis C. *Hepatology* 2007; **45**: 1154-1163
36 **Mehta SH**, Brancati FL, Sulkowski MS, Strathdee SA, Szklo M, Thomas DL. Prevalence of type 2 diabetes mellitus among persons with hepatitis C virus infection in the United States. *Ann Intern Med* 2000; **133**: 592-599
37 **Sigal SH**, Stanca CM, Kontorinis N, Bodian C, Ryan E. Diabetes mellitus is associated with hepatic encephalopathy in patients with HCV cirrhosis. *Am J Gastroenterol* 2006; **101**: 1490-1496
38 **Cordoba J**, Cabrera J, Lataif L, Penev P, Zee P, Blei AT. High prevalence of sleep disturbance in cirrhosis. *Hepatology* 1998; **27**: 339-345
39 **Engleman HM**, Hirst WS, Douglas NJ. Under reporting of sleepiness and driving impairment in patients with sleep apnoea/hypopnoea syndrome. *J Sleep Res* 1997; **6**: 272-275
40 **Groeneweg M**, Quero JC, De Bruijn I, Hartmann IJ, Essink-bot ML, Hop WC, Schalm SW. Subclinical hepatic encephalopathy impairs daily functioning. *Hepatology* 1998; **28**: 45-49
41 **Steindl PE**, Finn B, Bendok B, Rothke S, Zee PC, Blei AT. Disruption of the diurnal rhythm of plasma melatonin in cirrhosis. *Ann Intern Med* 1995; **123**: 274-277
42 **Spahr L**, Coeytaux A, Giostra E, Hadengue A, Annoni JM. Histamine H1 blocker hydroxyzine improves sleep in patients with cirrhosis and minimal hepatic encephalopathy: a randomized controlled pilot trial. *Am J Gastroenterol* 2007; **102**: 744-753
43 **Montagnese S**, Middleton B, Skene DJ, Morgan MY. Sleep-wake abnormalities do not correlate with neuropsychiatric performance in patients with cirrhosis (abstract). *Hepatology* 2008; **46**: 563A
44 **Marchesini G**, Bianchi G, Amodio P, Salerno F, Merli M, Panella C, Loguercio C, Apolone G, Niero M, Abbiati R. Factors associated with poor health-related quality of life of patients with cirrhosis. *Gastroenterology* 2001; **120**: 170-178
45 **Arguedas MR**, DeLawrence TG, McGuire BM. Influence of hepatic encephalopathy on health-related quality of life in patients with cirrhosis. *Dig Dis Sci* 2003; **48**: 1622-1626
46 **Bao ZJ**, Qiu DK, Ma X, Fan ZP, Zhang GS, Huang YQ, Yu XF, Zeng MD. Assessment of health-related quality of life in Chinese patients with minimal hepatic encephalopathy. *World J Gastroenterol* 2007; **13**: 3003-3008
47 **Ferrer M**, Cordoba J, Garin O, Olive G, Flavia M, Vargas V, Esteban R, Alonso J. Validity of the Spanish version of the Chronic Liver Disease Questionnaire (CLDQ) as a standard outcome for quality of life assessment. *Liver Transpl* 2006; **12**: 95-104
48 **Stewart CA**, Smith GE. Minimal hepatic encephalopathy. *Nat Clin Pract Gastroenterol Hepatol* 2007; **4**: 677-685
49 **Poordad FF**. Review article: the burden of hepatic encephalopathy. *Aliment Pharmacol Ther* 2007; **25** Suppl 1: 3-9
50 **Bustamante J**, Rimola A, Ventura PJ, Navasa M, Cirera I, Reggiardo V, Rodes J. Prognostic significance of hepatic encephalopathy in patients with cirrhosis. *J Hepatol* 1999; **30**: 890-895
51 **Romero-Gomez M**, Boza F, Garcia-Valdecasas MS, Garcia E, Aguilar-Reina J. Subclinical hepatic encephalopathy predicts the development of overt hepatic encephalopathy. *Am J Gastroenterol* 2001; **96**: 2718-2723
52 **Saxena N**, Bhatia M, Joshi YK, Garg PK, Dwivedi SN, Tandon RK. Electrophysiological and neuropsychological tests for the diagnosis of subclinical hepatic encephalopathy and prediction of overt encephalopathy. *Liver* 2002; **22**: 190-197
53 **Romero-Gomez M**, Grande L, Camacho I, Benitez S, Irles JA, Castro M. Altered response to oral glutamine challenge as prognostic factor for overt episodes in patients with minimal hepatic encephalopathy. *J Hepatol* 2002; **37**: 781-787
54 **Hartmann IJ**, Groeneweg M, Quero JC, Beijeman SJ, de Man RA, Hop WC, Schalm SW. The prognostic significance of subclinical hepatic encephalopathy. *Am J Gastroenterol* 2000; **95**: 2029-2034
55 **Maguire EA**, Burgess N, Donnett JG, Frackowiak RS, Frith CD, O'Keefe J. Knowing where and getting there: a human navigation network. *Science* 1998; **280**: 921-924

56 **Evans L**. The dominant role of driver behavior in traffic safety. *Am J Public Health* 1996; **86**: 784-786
57 **Watanabe A**, Tuchida T, Yata Y, Kuwabara Y. Evaluation of neuropsychological function in patients with liver cirrhosis with special reference to their driving ability. *Metab Brain Dis* 1995; **10**: 239-248
58 **Wein C**, Koch H, Popp B, Oehler G, Schauder P. Minimal hepatic encephalopathy impairs fitness to drive. *Hepatology* 2004; **39**: 739-745
59 **Bajaj JS**, Hafeezullah M, Hoffmann RG, Varma RR, Franco J, Binion DG, Hammeke TA, Saeian K. Navigation skill impairment: Another dimension of the driving difficulties in minimal hepatic encephalopathy. *Hepatology* 2008; **47**: 596-604
60 **Bajaj JS**, Hafeezullah M, Hoffmann RG, Saeian K. Minimal hepatic encephalopathy: a vehicle for accidents and traffic violations. *Am J Gastroenterol* 2007; **102**: 1903-1909
61 **Teh SH**, Nagorney DM, Stevens SR, Offord KP, Therneau TM, Plevak DJ, Talwalkar JA, Kim WR, Kamath PS. Risk factors for mortality after surgery in patients with cirrhosis. *Gastroenterology* 2007; **132**: 1261-1269
62 **Bajaj JS**, Ananthakrishnan AN, McGinley E, Hoffmann RG, Brasel KJ. Deleterious impact of cirrhosis on outcomes after motor vehicle crashes using the Nationwide Inpatient Sample. *Am J Gastroenterol* 2008; **103:** 1674-1681
63 **Ries ML**, Jabbar BM, Schmitz TW, Trivedi MA, Gleason CE, Carlsson CM, Rowley HA, Asthana S, Johnson SC. Anosognosia in mild cognitive impairment: Relationship to activation of cortical midline structures involved in self-appraisal. *J Int Neuropsychol* Soc 2007; **13**: 450-461
64 **Starkstein SE**, Jorge R, Mizrahi R, Adrian J, Robinson RG. Insight and danger in Alzheimer's disease. *Eur J Neurol* 2007; **14**: 455-460
65 **Kircheis G**, Wettstein M, Timmermann L, Schnitzler A, Haussinger D. Critical flicker frequency for quantification of low-grade hepatic encephalopathy. *Hepatology* 2002; **35**: 357-366
66 **Conn H**. In Hepatic Encephalopathy: Management with lactulose and related carbohydrates. Illinois: Medi-Ed Press, 1988
67 **Malaguarnera M**, Greco F, Barone G, Gargante MP, Malaguarnera M, Toscano MA. Bifidobacterium longum with fructo-oligosaccharide (FOS) treatment in minimal hepatic encephalopathy: a randomized, double-blind, placebo-controlled study. *Dig Dis Sci* 2007; **52**: 3259-3265
68 **Boca M**, Vyskocil M, Mikulecky M, Ebringer L, Kolibas E, Kratochvil'ova H, Buzgova D. [Complex therapy of chronic hepatic encephalopathy supplemented with probiotic: comparison of two studies] *Cas Lek Cesk* 2004; **143**: 324-328
69 **Macbeth WA**, Kass EH, Mcdermott WV Jr. Treatment of hepatic encephalopathy by alteration of intestinal flora with lactobacillus acidophilus. *Lancet* 1965; **1**: 399-403
70 **Uribe M**, Dibildox M, Malpica S, Guillermo E, Villallobos A, Nieto L, Vargas F, Garcia Ramos G. Beneficial effect of vegetable protein diet supplemented with psyllium plantago in patients with hepatic encephalopathy and diabetes mellitus. *Gastroenterology* 1985; **88**: 901-907
71 **Zhao HY**, Wang HJ, Lu Z, Xu SZ. Intestinal microflora in patients with liver cirrhosis. *Chin J Dig Dis* 2004; **5**: 64-67
72 **Bajaj JS**, Saeian K, Christensen KM, Hafeezullah M, Franco J, Varma RR, Pleuss JA, Krakower G, Hoffmann RG, Binion DG. Probiotic yogurt for the treatment of minimal hepatic encephalopathy. *Am J Gastroenterol* 2008; **103:** 1707-1715

S- Editor Li DL **L- Editor** Rippe RA **E- Editor** Liu Y

Online Submissions: wjg.wjgnet.com
wjg@wjgnet.com
doi:10.3748/wjg.14.3621

World J Gastroenterol 2008 June 21; 14(23): 3621-3627
World Journal of Gastroenterology ISSN 1007-9327
© 2008 The WJG Press. All rights reserved.

REVIEW

Extended-therapy duration for chronic hepatitis C, genotype 1: The long and the short of it

Brian L Pearlman

Brian L Pearlman, Atlanta Medical Center, Medical College of Georgia, Emory School of Medicine, 285 Boulevard NE Suite 140 Atlanta, Georgia 30312, United States
Correspondence to: Brian L Pearlman, MD, FACP, Center For Hepatitis C, Atlanta Medical Center, Medical College of Georgia, Emory School of Medicine, 315 Boulevard NE Suite 200, Atlanta, Georgia 30312,
United States. brianpearlman@hotmail.com
Telephone: +1-404-265-4644 Fax: +1-404-265-1047
Received: February 28, 2008 Revised: April 30, 2008
Accepted: May 7, 2008
Published online: June 21, 2008

Abstract

With pegylated interferon and ribavirin, more than half of all chronically-infected hepatitis C patients can achieve a sustained virologic response; however, patients with genotype 1 infections and those with other poor prognostic factors have relatively inferior treatment response rates. Since new therapies are still years away from approval, it is incumbent upon providers to maximize the therapeutic efficacy of today's treatment. The later the virus is undetectable in serum during treatment, the less likely it will be eradicated. Patients with a delayed or slow virologic response to therapy (at least a 2-$\log_{10}$ decrease in baseline hepatitis C RNA yet detectable viremia at 12 wk of therapy and undetectable virus 12 wk subsequently) may, therefore, benefit from an extended therapy course beyond one of standard duration. Although higher rates of treatment discontinuation may plague this approach, 72 wk of treatment for genotype 1-infected slow-responders may improve response rates and diminish relapse rates relative to those of 48 wk. Based on data from both viral kinetic and clinical studies, therapy prolongation in slow responders may be a reasonable strategy to improve response rates in these treatment-refractory patients.

© 2008 The WJG Press. All rights reserved.

Key words: Hepatitis C virus genotype; Peginterferon alpha; Ribavirin; Slow-responder; Extension

Peer reviewers: Dr. George V Papatheodoridis, 2nd Academic Department of Internal Medicine, Hippokration General Hospital, 114 Vas. Sofias ave., Athens 1527, Greece; Akihito Tsubota, Assistant Professor, Institute of Clinical Medicine and Research, Jikei University School of Medicine, 163-1 Kashiwashita, Kashiwa, Chiba 277-8567, Japan

Pearlman BL. Extended-therapy duration for chronic hepatitis C, genotype 1: The long and the short of it. *World J Gastroenterol* 2008; 14(23): 3621-3627 Available from: URL: http://www.wjgnet.com/1007-9327/14/3621.asp DOI: http://dx.doi.org/10.3748/wjg.14.3621

INTRODUCTION

One hundred and seventy million persons worldwide are infected with the hepatitis C virus (HCV)[1], and liver-related deaths from the virus are expected to nearly triple by the year 2020[2]. Three years prior to the virus' identification in 1986, interferon alpha-2b was first utilized for the treatment of non-A, non-B hepatitis[3]. Although sustained virologic response (SVR) rates to interferon monotherapy for 6 mo were only about 8%, treatment extension to 12 mo nearly doubled response rates[4]. With the advent of the nucleoside analog ribavirin, used in combination with interferon, rates of SVR more than doubled again[5,6]. Whereas 48 wk of standard interferon with ribavirin achieved sustained response rates as high as 43%[6], 48 wk of the newer pegylated interferons plus ribavirin improved rates of SVR to 54%-56% as shown in two multinational, randomized controlled trials[7,8].

Nevertheless, SVR rates are inferior for patients with genotype 1 infection[7-9] despite a 48 wk recommended treatment course of peginterferon with weight-based ribavirin[10,11]. Although preliminary evidence indicates that small molecule inhibitors in combination with peginterferon and ribavirin may improve response rates even further for genotype 1-infected patients with merely 24 wk of therapy[12,13], the combination of peginterferon and ribavirin alone is likely to remain the recommended treatment regimen for chronic HCV for the next 3-5 years[14]. Thus, it is incumbent upon clinicians to maximize their patients' chance of treatment success with existing therapy.

Methods utilized to improve the treatment response in genotype 1-infected patients include the bolstering of patient adherence through aggressive side effect management and increasing the dose of therapy through induction dosing of interferon or through higher doses

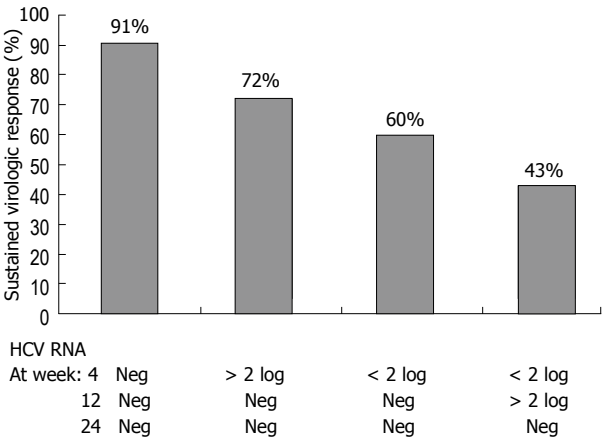

Figure 1 Relationship between hepatitis C viremia and sustained virologic response with pegylated interferon alpha-2a and ribavirin therapy[19]. The later the virus becomes undetectable on therapy, the less likely it will be ultimately cleared. Data are from retrospective analysis[19] of a registration trial for peginterferon alpha-2a plus ribavirin involving over 1000 chronic, treatment-naive hepatitis C-infected patients[8]. Neg: Undetectable RNA; > 2 log: At least a 2 log_{10} decrease in viral RNA compared to pre-treatment value; < 2 log: Less than a 2 log_{10} decrease in viral RNA compared to pre-treatment value.

of either interferon or ribavirin. Another strategy is to lengthen duration of treatment in those that are slow-responders to standard doses of peginterferon and ribavirin. The purpose of this survey is to review the justification for therapy prolongation in appropriate patients using viral kinetic data and to summarize the clinical trials supporting this approach.

VIRAL KINETICS DURING TREATMENT

An initial decrement in HCV RNA level, referred to as phase 1, occurs hours after the administration of interferon; it represents the blocking of viral replication. A subsequent, slower decrease in viremia (phase 2) represents the clearance of HCV-infected hepatocytes and typically occurs days to months after interferon therapy is initiated. The phase 2 decline in virus is the better predictor of ultimate HCV clearance[15,16]. Phase 2 decline is significantly slower in genotype 1-infected patients than in those infected with genotypes 2 and 3[17,18]. Thus, by measuring virus concentrations of various points along a slope of a phase 2 decline in viremia, treatment outcome may be better predicted, and ultimately modified, based on an individual patient's response to therapy.

HCV-infected patients who achieve undetectable viremia as early as 4 wk into standard therapy have excellent sustained response rates; these rapid virologic responders achieve SVR about 90% of the time[19]. In fact, support exists for truncating therapy duration for genotype 1-infected rapid responders with low baseline HCV viral loads[20]. Conversely, patients who show undetectable virus for the first time 24 wk into therapy have less than one-third chance of ultimately achieving SVR[8]. Therefore, the earlier the HCV is undetectable in serum during treatment, the greater the likelihood of a successful treatment response (Figure 1).

Similarly, longer durations of viral suppression on treatment may improve virologic response rates. Investigators have sought to determine if the standard 48 wk treatment duration of patients with genotype 1 infection is adequate. Using data from the peginterferon alpha-2b and ribavirin phase Ⅲ trial[7], Drusano and Preston developed a prediction model based on the duration of viral suppression on therapy[21]. The model was built on the basis of eleven covariables including demographics and virologic characteristics from 771 HCV-infected patients. Among the variables, the durations of viral clearance had the strongest bearing on the likelihood of a SVR. When the model was applied to a validation group of 229 patients, it predicted SVR with a positive predictive value of 97% and a negative predictive value of 91%. To achieve an 80% chance of SVR in genotype 1-infected patients, an undetectable HCV RNA was required for at least 32 wk on therapy, and to achieve a 90% chance of SVR, RNA undetectability was necessary for 36 wk. Since the average time to clear genotype 1 viremia was 30 wk, the authors concluded that the standard 48 wk treatment course for this genotype is inadequate. Problems with this study are its retrospective analysis and the model's requirement for monthly viral loads which may be cost-prohibitive. Furthermore, the model was based on the use of suboptimal ribavirin dosing (800 mg daily) which limits its applicability in genotype 1 infection. However, the study suggests that patients who don't achieve undetectable virus at certain time points may enjoy improved rates of SVR with treatment extension.

A failure to achieve an early virologic response (EVR), defined by an undetectable HCV RNA level or at least a 2-log_{10} decrement in RNA from baseline at 12 wk of therapy, has excellent negative predictive value for treatment success[22,23]. An analysis of the peginterferon with ribavirin registration trials[7,8] suggests that patients who do not achieve a 12 wk EVR have a 3% or lower chance of ultimately achieving SVR[23]. Nonetheless, there is a large disparity in treatment response between patients who, at 12 wk, have at least a 2-log_{10} decrease in baseline HCV RNA yet still have detectable virus (partial EVR) compared to those who achieve undetectable viremia (complete EVR). In the registration trial for peginterferon alpha-2b with ribavirin, patients in the latter group achieved SVR about four times more frequently than those in the former[23]. These former patients are said to be slow or late responders to therapy. Patients have also been characterized as slow responders to therapy if they have detectable virus at 4 wk; either definition necessitates undetectable virus at 24 wk of treatment, since detectable viremia at this time point virtually guarantees treatment failure.

In genotype 1 infection with the standard therapy duration of 48 wk, slow responders have higher relapse rates compared to those that clear virus earlier in treatment[19]. High rates of relapse in slow responding patients may indicate that therapy was of insufficient duration; therefore, it has been hypothesized that extending therapy in these patients may improve rates of SVR (Figure 2).

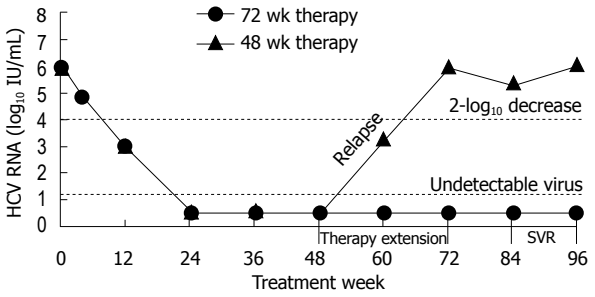

Figure 2 Virologic responses of slow-responders to 48 wk *vs* 72 wk of therapy. Treatment extension may improve chance of SVR by lessening the chance of relapse. Slow-responders to standard duration therapy (48 wk) may see relapse after an end-of-treatment response is achieved; those receiving extended duration therapy (72 wk) are not as apt to relapse after treatment is completed.

EXTENDED DURATION THERAPY WITH STANDARD INTERFERON

Several years before the term slow-responder was popularized, investigators attempted to improve response rates by extending therapy duration utilizing older medications. Using standard interferon monotherapy, authors have demonstrated improved biochemical, histologic and virologic responses with treatment ranging from 60 to 76 wk compared to treatments of shorter durations[24,25]. In one of these studies[24], the investigators noted a reduced tendency for patients to relapse after treatment cessation when therapy was extended to 60 wk relative to previously published studies with shorter durations.

The first randomized, controlled trial to show that prolongation of interferon-based therapy combined with ribavirin for 18 mo reduced rates of relapse was performed in the Netherlands and Belgium[26]. Three hundred treatment-naive chronic HCV patients were randomized to 6 or 18 mo of standard-interferon (3 million units thrice weekly) plus ribavirin (1000-1200 mg daily) or to 18 mo of the same dose of standard interferon monotherapy plus placebo. The majority of patients were genotype 1-infected with high viral loads. Although end-of-treatment responses were similar in the two combination therapy arms (55% and 41% in 6 and 18 mo arms, respectively), relapse rates were significantly lower in the 18 mo combination arm (13%) compared to those in the 6 mo treatment arm (38%, $P = 0.006$). It should be noted that the rate of relapse in the group treated with 18 mo of monotherapy was still high at 38%; these results demonstrate that extending the duration of interferon alone is inadequate to decrease relapse rates and attests to ribavirin's effect on relapse diminution. In an intention-to-treat analysis, SVR rates were 16% for 18 mo monotherapy, 34% for 6 mo combination therapy and 43% for 18 mo of combination therapy ($P < 0.05$). Although 25% of patients withdrew from both 18 mo treatment arms prematurely, this withdrawal rate is similar to those from standard interferon plus ribavirin treatment trials of 48 wk duration (21%-27%)[5,6]. Prolongation of combination therapy had no significant effect on rates of relapse or SVR in genotype 2- or 3- infected patients; nevertheless, extension of treatment from 6 to 18 mo had an independent effect on relapse and SVR rates in patients infected with genotype 1 virus (SVR: OR 4; CI: 2-10, $P = 0.004$). Slow responders, those with detectable viremia at 12 wk, enjoyed a decline in relapse rate from 70% to 30% when treatment was prolonged from 24 to 72 wk. The study's major limitation was the absence of a 12 mo treatment arm.

EXTENDED DURATION THERAPY WITH PEGYLATED INTERFERON

Investigators from Spain and Israel were the first to report successful treatment extension to 72 wk for slow responders to peginterferon and ribavirin[27]. Slow responders were defined as those patients with at least a 2 $\log_{10}$ decline in HCV RNA from baseline, yet detectable viremia at 12 wk after receipt of 1.0 mcg of peginterferon alpha-2b weekly and 800 mg ribavirin daily. Although only 8 patients were treated in this fashion, 7 of the 8 (88%) achieved an SVR, which is a profound improvement relative to a SVR of 21% in slow responders treated for 48 wk in the phase Ⅲ trial of peginterferon alpha-2b and ribavirin[23]. The suboptimal dosing of ribavirin and the paucity of patients studied are the limitations of this analysis.

Furthermore, results from a large, prospective, multicenter trial from Germany support the extension of therapy duration in slow responders to peginterferon and ribavirin[28]. 459 treatment-naïve genotype 1-infected patients were randomized to 48 wk *vs* 72 wk of peginterferon alpha-2a, 180 mcg weekly and ribavirin, 800 mg daily. 22% of patients were slow virologic responders to therapy, defined by virus detectability at 12 wk of treatment, but with viral undetectability at 24 wk. Slow responders in the 72 wk group had lower relapse rates than did slow responders treated for 48 wk (40% *vs* 64%, respectively; $P = 0.021$) and had similar end-of-treatment responses; thus, rates of SVR for this subgroup of patients were significantly higher when treated for 72 wk compared those treated for 48 wk (29% *vs* 17%, respectively; $P = 0.04$). Patients with low levels of viremia (less than 6000 IU/mL) at 12 wk of treatment derived the greatest benefit from extended duration therapy. Thus, the investigators concluded that in slow virologic responders to treatment, relapse rates could be reduced and rates of SVR could be augmented by extending therapy to 72 wk. Nonetheless, the slow responders represented only a subgroup of those randomized, and the conclusions were garnered retrospectively. Moreover, the 800 mg ribavirin used in the trial is an inadequate dose for most genotype 1-infected patients[9]. It should also be emphasized that, for the majority of patients randomized to 72 wk of therapy, there was no statistical benefit relative to 48 wk of treatment. Overall, SVR rates were 54% and 53%, respectively ($P = 0.8$), and relapse rates were likewise statistically similar. Thus, extended duration

therapy is generally not recommended for all treatment-naïve patients with genotype 1 infection and should be considered only for those with the slow responding phenotype. Finally, although patients in both the standard and extended duration treatment arms had similar rates of medication dose reduction and adverse events, the rate of premature therapy discontinuation was higher in the extended treatment arm compared to that in the standard treatment arm (41% and 24%, respectively).

Another randomized, multicenter clinical trial from Spain, the TeraViC-4 study, prospectively evaluated the effects of extended therapy duration with peginterferon alpha-2a (180 mcg weekly) and ribavirin (800 mg daily)[29]. Treatment-naïve patients with detectable HCV RNA levels at week 4 (n = 326) were randomized to a therapy duration of 48 wk (n = 165, 149 of whom were genotype 1-infected) or to 72 wk (n = 161, 142 of whom were genotype 1-infected). Thus, in this case, a slow responder was defined by absence of a rapid virologic response, and only slow responders were randomized to extended therapy. In TeraViC-4, the 12 wk virologic responses were not reported. Although end-of-treatment responses for patients with genotype 1 infections were statistically similar in both extended and standard treatment arms (62% *vs* 58%, respectively; P = 0.53), SVR rates were superior in the extended treatment arm (44% *vs* 28%, respectively; P = 0.003), by virtue of a diminution of relapse rate (17% *vs* 53%, respectively; P = 0.002). The incidence of adverse events and dose reductions were similar in both groups; yet, treatment discontinuation was more frequent in the extended therapy arm compared to the standard duration arm (36% *vs* 18%, respectively; P = 0.0004). In fact, one of the study's limitations was this inordinate number of premature terminations in those randomized to prolonged therapy, largely because of patient preference. Other limitations were the lack of central testing for viral load measurements and the inclusion of patients with other genotypes besides one. Like that of the German study, the primary weakness of this trial may have been the suboptimal dose of ribavirin utilized (800 mg for genotype 1 virus).

In another prospective study from the United States, we randomized genotype 1-infected slow-responders to 48 or 72 wk of peginterferon alpha-2b (1.5 mcg/kg weekly) and weight-based ribavirin (800 to 1400 mg daily)[30]. In our trial, slow response was defined by achieving at least a 2 $\log_{10}$ decrement in HCV RNA from baseline, yet having detectable viremia at 12 wk but undetectable virus at 24 wk (PCR, lower limit of detection 10 IU/mL). One hundred twelve of our treatment-naïve patients were deemed slow-responders who represented about 30% of our patients. This percentage was felt to be high secondary to difficult-to-treat baseline characteristics: 26% had bridging fibrosis or cirrhosis on pre-treatment liver biopsy; 48% were African American; 34% were obese defined by greater than or equal to 30 kg/m^2; 78% had high baseline viral load (more than 800 000 IU/mL) and 18% had impaired fasting glucose, pre-treatment. Similar to the aforementioned European trials, we did not observe a higher number of adverse events or therapy reductions in the extended treatment arm relative to the control arm. However, unlike in the other studies, we did not see a greater treatment cessation rate in the prolonged therapy arm; in fact, none of the therapy terminations occurred between weeks 48 and 72. Growth factors were prohibited, yet peginterferon dose reductions for neutropenia were made only if counts were less than 500/mm^3. Similar to those of the slow-responders in Spain, our randomized patients saw equivalent end-of-treatment response rates in the 72 wk arm *vs* the 48 wk arm (48% *vs* 45%, respectively; P = 0.75), yet enjoyed improved relapse rates with therapy prolongation (20% *vs* 59%, respectively; P = 0.004). Overall, rates of SVR in slow-responders were superior with treatment extension (38%) compared to those of standard duration therapy (18%, P = 0.03). The primary limitation of our analysis is it was conducted in a single medical center.

African Americans, a group with inferior responses to interferon-based therapy[31-33], may likewise benefit from a treatment extension strategy if slowly responsive to treatment. When compared to non-Hispanic whites receiving combination therapy, African Americans showed smaller phase 1 and phase 2 declines in viral load[34]; thus, it was unclear if African Americans' viral kinetics on therapy would be analogous to those of white "late" responders. Nearly half of our slow responders were self-identified as African American (n = 48) and were randomized to 48 and 72 wk treatment arms in our Atlanta study described above[30]. Although overall, African American slow responders had expected inferior SVR rates to those of whites (17% and 39%, respectively), the former group still benefited from treatment extension because of reduced relapse rates. End-of-treatment response rates were 24% *vs* 26% for 48 and 72 wk of treatment, respectively (P > 0.05), and SVR rates were 12% *vs* 21%, respectively (P = 0.02). Results should be interpreted with caution, however, because this ethnic group's response rates were derived from subgroup analysis.

Preliminary results are available from a multicenter trial in Europe that also utilized extended therapy for slow-responders to peginterferon alpha-2a (180 mcg weekly) with weight-based ribavirin (1000-1200 mg daily)[35,36]. Of the 373 patients treated, 11% were slow-responders to therapy, defined by having detectable virus at 12 wk (> 50 IU/mL), yet still at least 2 $\log_{10}$ below baseline, and thus randomized to complete standard duration therapy of 48 wk or extended treatment to 72 wk. None of these slow-responders had achieved undetectable virus at 4 wk. Over 90% of patients had genotype 1 infections, and the remainder was infected with genotype 4 virus. As in the previously described studies, extended therapy compared to that of standard duration improved SVR rates in slow-responders (69% *vs* 52%, respectively; P value not available) by virtue of a decrease in relapse rates (18% *vs* 32%, respectively; P value not available). Although treatment discontinuation data are not available for slow-responders specifically,

Table 1 Studies of extended therapy for treatment-naive, genotype 1-infected slow responders to pegylated interferon with ribavirin

Country(ies) in which studies performed	Number of subjects studied	Treatment duration (wk)	Definition of slow response (assay sensitivity)	Pegylated interferon type and weekly dose	Ribavirin daily dose (mg)	End-of-treatment responses	Relapse rates	Sustained virologic response rates	*P* value (sustained response)	Major study limitation (s)
Spain, Israel[27]	8	72	⩾ 2-$\log_{10}$ 12 wk decrease[1] (100 IU/mL)	Alpha -2b 1.0 mcg/kg	800	100%	13%	88%	Not applicable	Few subjects suboptimal ribavirin dose
Germany[28]	100	48	> 50 IU/mL at wk 12 (50 IU/mL)	Alpha 2-a 180 mcg	800	47%	64%	17%	0.04	Retrospective subgroup analysis suboptimal ribavirin dose
	106	72				49%	40%	29%		
Spain[29]	149	48	> 50 IU/mL at wk 4 (50 IU/mL)	Alpha 2-a 180 mcg	800	58%	53%	28%	0.003	Suboptimal ribavirin dose
	142	72				62%	17%	44%		
United States[30]	49	48	⩾ 2-$\log_{10}$ 12 wk decrease[1] (10 IU/mL)	Alpha 2-b 1.5 mcg/kg	800-1400	45%	59%	18%	0.03	Single center
	52	72				48%	20%	38%		
Europe[35,36]	25[2]	48	⩾ 2-$\log_{10}$ 12 wk decrease[1] (50 IU/mL)	Alpha 2-a 180 mcg	1000–1200	Not available	32%	52%	Not available	Few subjects some genotype four infections
	16[2]	72					18%	69%		
Italy[37]	21	48	⩾ 2-$\log_{10}$ 12 wk decrease[1] (50 IU/mL)	Alpha -2b 1.5 mcg/kg or Alpha -2a 180 mcg	1000-1200	5%[3]	100%[3]	0%[3]	0.3[4]	Subgroup analysis
	52	72				19%	60%	8%		
Europe, Canada, Israel[38]	63	48	⩾ 2-$\log_{10}$ 12 wk decrease[1] (30 IU/mL)	Alpha -2b 1.5 mcg/kg	800-1400	Pending	Pending	Pending	Pending	Pending
	63	72								

[1]Detectable viremia at 12 wk and undetectable viremia at 24 wk required; [2]Less than 10% genotype 4 infections; [3]One of twenty patients had an end-of-treatment response, but relapsed; [4]Not statistically significant.

patients who received extended duration therapy had a greater number of treatment discontinuations (17%) compared to those on standard duration therapy (4%). Limitations of this study are the small numbers of slow-responders analyzed (41 patients) and the mixture of genotype 1- and 4- infected patients.

Finally, a recently published, randomized, multicenter study from Italy assessed the utility of variable therapy duration, including a treatment extension strategy, based on the time to a patient's first undetectable HCV RNA[37]. 696 genotype 1-infected treatment-naive patients were randomized to a standard duration or a variable duration therapy arm in a 2:1 ratio. Patients were treated with either peginterferon alpha-2a (180 mcg weekly) or peginterferon alpha-2b (1.5 mcg/kg weekly), both with weight-based ribavirin (1000-1200 mg daily). Irrespective of first time to viral undetectability in serum (< 50 IU/mL), 237 patients in the standard therapy arm received treatment for 48 wk, unless patients did not achieve EVR at week 12 or had detectable virus at week 24, at which time therapy was discontinued. However, in the variable duration arm, patients were treated for 24, 48 or 72 wk if serum HCV RNA were negative at 4, 8, or 12 wk, respectively. Patients were likewise treated for 72 wk in the variable duration arm if they had at least a 2 $\log_{10}$ decline in serum RNA from baseline yet detectable viremia at 12 wk of therapy (slow-responders).

Overall, based on the rates of SVR, the standard and variable duration treatment arms were statistically equivalent. Nonetheless, the study proved prospectively that the longer the virus is undetectable on therapy, the better the chance of achieving a SVR, regardless if a patient had received treatment of a standard or variable duration. In the standard duration arm, 87%, 70% and 38% of patients first attaining undetectable viremia at 4, 8 or 12 wk, respectively, achieved SVR; in the variable duration group, corresponding SVR rates were 77%, 72% and 64%.

More pertinent to this discussion is the fact that the study's slow-responders in the standard treatment duration arm (n = 21) did not achieve SVR in a single case (0%), and those slow-responders treated for 72 wk (n = 53) saw an SVR of only 7.5%; nonetheless, the results were not statistically significant (P = 0.3). Moreover, 10 of the slow-responders treated for 72 wk voluntarily withdrew from the study compared to only 3 patients treated for 48 wk, suggesting that prolonged therapy was not well-tolerated. Most intriguing, patients who achieved undetectable virus for the first time at 12 wk of therapy (having detectable viremia at week 8), enjoyed improved SVR rates when treated for 72 wk compared to 48 wk in 64% and 38% of cases, respectively (difference -25.4, CI: 22.3-28.4). Extended therapy, even in these "complete" early virologic responders, seemed to have improved SVR rates because of a decline in relapse (43% in standard group, and 15% in variable group). The authors deemed this difference "…substantial, (and) may warrant a prospective trial."

The most important limitations of this last study are the large number of patients in the variable treatment duration arm who discontinued therapy because of poor

compliance (49% of all treatment discontinuations), and the relative paucity of patients on which subgroup analysis was performed. For example, only 21 slow-responders were treated for 48 wk.

The Study to Assess Treatment with Pegylated Interferon Alpha-2b and Ribavirin in Treatment-Naive Patients with Chronic hepatitis C and slow virologic response (SUCCESS) is a multinational study in 133 centers across Europe, Canada and Israel designed to compare response rates of slow-responders to either 48 or 72 wk of therapy[38]. Slow-response is again defined by patients with genotype 1 infection who had at least a 2 $\log_{10}$ reduction, albeit detectable, HCV RNA levels at 12 wk compared to baseline and undetectable virus at week 24. As of late 2006, 126 patients were deemed slow-responders and were randomized into standard and extended therapy duration arms (Table 1). Final results should be available sometime later in 2008 or in early 2009.

CONCLUSION

Treatment extension has been attempted with varying degrees of success using alternative interferons[39,40], in those with relapse[40] or non-response to peginterferon-based therapies[41] and in those who are HCV-HIV coinfected[42,43]. Details of these analyses are beyond the scope of this review.

Certainly, not every treatment-naive patient with genotype-1 infection benefits from therapy prolongation. However, a subgroup with a delayed or slow response to therapy (approximately 15% of patients) may enjoy improved rates of SVR with treatment extension to 72 wk, largely because of a relapse diminution. Data on therapy prolongation in slow-responders are summarized in Table 1. Compared to patients receiving therapy of standard duration, those in extended treatment groups have experienced higher discontinuation rates in most, but not all, studies to date; however, the numbers of adverse events and dose reductions appear to be equivalent. Clearly, if treatment prolongation is utilized, adherence to therapy is paramount. Finally, the use of 72 wk for slow virologic responders to peginterferon and ribavirin may be cost-effective compared to 48 wk, or standard duration therapy[44]. Thus, therapy extension in slow-responders seems to be a reasonable strategy to ameliorate response rates in a group with notoriously poor treatment results.

REFERENCES

1 **Global surveillance and control of hepatitis C**. Report of a WHO Consultation organized in collaboration with the Viral Hepatitis Prevention Board, Antwerp, Belgium. *J Viral Hepat* 1999; **6**: 35-47

2 **Alter MJ**, Kruszon-Moran D, Nainan OV, McQuillan GM, Gao F, Moyer LA, Kaslow RA, Margolis HS. The prevalence of hepatitis C virus infection in the United States, 1988 through 1994. *N Engl J Med* 1999; **341**: 556-562

3 **Hoofnagle JH**, Mullen KD, Jones DB, Rustgi V, Di Bisceglie A, Peters M, Waggoner JG, Park Y, Jones EA. Treatment of chronic non-A,non-B hepatitis with recombinant human alpha interferon. A preliminary report. *N Engl J Med* 1986; **315**: 1575-1578

4 **Carithers RL Jr**, Emerson SS. Therapy of hepatitis C: meta-analysis of interferon alfa-2b trials. *Hepatology* 1997; **26**: 83S-88S

5 **McHutchison JG**, Gordon SC, Schiff ER, Shiffman ML, Lee WM, Rustgi VK, Goodman ZD, Ling MH, Cort S, Albrecht JK. Interferon alfa-2b alone or in combination with ribavirin as initial treatment for chronic hepatitis C. Hepatitis Interventional Therapy Group. *N Engl J Med* 1998; **339**: 1485-1492

6 **Poynard T**, Marcellin P, Lee SS, Niederau C, Minuk GS, Ideo G, Bain V, Heathcote J, Zeuzem S, Trepo C, Albrecht J. Randomised trial of interferon alpha2b plus ribavirin for 48 weeks or for 24 weeks versus interferon alpha2b plus placebo for 48 weeks for treatment of chronic infection with hepatitis C virus. International Hepatitis Interventional Therapy Group (IHIT). *Lancet* 1998; **352**: 1426-1432

7 **Manns MP**, McHutchison JG, Gordon SC, Rustgi VK, Shiffman M, Reindollar R, Goodman ZD, Koury K, Ling M, Albrecht JK. Peginterferon alfa-2b plus ribavirin compared with interferon alfa-2b plus ribavirin for initial treatment of chronic hepatitis C: a randomised trial. *Lancet* 2001; **358**: 958-965

8 **Fried MW**, Shiffman ML, Reddy KR, Smith C, Marinos G, Goncales FL Jr, Haussinger D, Diago M, Carosi G, Dhumeaux D, Craxi A, Lin A, Hoffman J, Yu J. Peginterferon alfa-2a plus ribavirin for chronic hepatitis C virus infection. *N Engl J Med* 2002; **347**: 975-982

9 **Hadziyannis SJ**, Sette H Jr, Morgan TR, Balan V, Diago M, Marcellin P, Ramadori G, Bodenheimer H Jr, Bernstein D, Rizzetto M, Zeuzem S, Pockros PJ, Lin A, Ackrill AM. Peginterferon-alpha2a and ribavirin combination therapy in chronic hepatitis C: a randomized study of treatment duration and ribavirin dose. *Ann Intern Med* 2004; **140**: 346-355

10 **Dienstag JL**, McHutchison JG. American Gastroenterological Association medical position statement on the management of hepatitis C. *Gastroenterology* 2006; **130**: 225-230

11 **Strader DB**, Wright T, Thomas DL, Seeff LB. Diagnosis, management, and treatment of hepatitis C. *Hepatology* 2004; **39**: 1147-1171

12 **Jacobson IM**, Everson GT, Gordon SC, Kauffman R, McNair L, Muir A, McHutchison JG. Interim analysis results from a phase 2 study of telaprevir with peginterferon alfa-2a and ribavirin in treatment-naïve subjects with hepatitis C. *Hepatology* 2007; **46**: 315A-316A

13 **Hezode C**, Ferenci P, Dusheiko GM, Pol S, Goeser T, Bronowicki JP, Gharakhanian S, Devonish D, Kauffman R, Alam J, Pawlotsky JM, Zeuzem S. PROVE 2: phase II study of VX-950 (Telaprevir) in combination with peginterferon alfa-2a with or without ribavirin in subjects with chronic hepatitis C, first interim analysis. *Hepatology* 2007; **46**: 268A-269A

14 **Modi AA**, Hoofnagle JH. New therapies for hepatitis C. *Hepatology* 2007; **46**: 615-617

15 **Lam NP**, Neumann AU, Gretch DR, Wiley TE, Perelson AS, Layden TJ. Dose-dependent acute clearance of hepatitis C genotype 1 virus with interferon alfa. *Hepatology* 1997; **26**: 226-231

16 **Neumann AU**, Lam NP, Dahari H, Gretch DR, Wiley TE, Layden TJ, Perelson AS. Hepatitis C viral dynamics in vivo and the antiviral efficacy of interferon-alpha therapy. *Science* 1998; **282**: 103-107

17 **Neumann AU**, Lam NP, Dahari H, Davidian M, Wiley TE, Mika BP, Perelson AS, Layden TJ. Differences in viral dynamics between genotypes 1 and 2 of hepatitis C virus. *J Infect Dis* 2000; **182**: 28-35

18 **Zeuzem S**, Herrmann E, Lee JH, Fricke J, Neumann AU, Modi M, Colucci G, Roth WK. Viral kinetics in patients with chronic hepatitis C treated with standard or peginterferon alpha2a. *Gastroenterology* 2001; **120**: 1438-1447

19 **Ferenci P**, Fried MW, Shiffman ML, Smith CI, Marinos G, Goncales FL Jr, Haussinger D, Diago M, Carosi G, Dhumeaux D, Craxi A, Chaneac M, Reddy KR. Predicting

sustained virological responses in chronic hepatitis C patients treated with peginterferon alfa-2a (40 KD)/ribavirin. *J Hepatol* 2005; **43**: 425-433

20 **Davis GL**. Tailoring antiviral therapy in hepatitis C. *Hepatology* 2006; **43**: 909-911

21 **Drusano GL**, Preston SL. A 48-week duration of therapy with pegylated interferon alpha 2b plus ribavirin may be too short to maximize long-term response among patients infected with genotype-1 hepatitis C virus. *J Infect Dis* 2004; **189**: 964-970

22 **Zeuzem S**, Lee JH, Franke A, Ruster B, Prummer O, Herrmann G, Roth WK. Quantification of the initial decline of serum hepatitis C virus RNA and response to interferon alfa. *Hepatology* 1998; **27**: 1149-1156

23 **Davis GL**, Wong JB, McHutchison JG, Manns MP, Harvey J, Albrecht J. Early virologic response to treatment with peginterferon alfa-2b plus ribavirin in patients with chronic hepatitis C. *Hepatology* 2003; **38**: 645-652

24 **Reichard O**, Foberg U, Fryden A, Mattsson L, Norkrans G, Sonnerborg A, Wejstal R, Yun ZB, Weiland O. High sustained response rate and clearance of viremia in chronic hepatitis C after treatment with interferon-alpha 2b for 60 weeks. *Hepatology* 1994; **19**: 280-285

25 **Poynard T**, Bedossa P, Chevallier M, Mathurin P, Lemonnier C, Trepo C, Couzigou P, Payen JL, Sajus M, Costa JM. A comparison of three interferon alfa-2b regimens for the long-term treatment of chronic non-A, non-B hepatitis. Multicenter Study Group. *N Engl J Med* 1995; **332**: 1457-1462

26 **Brouwer JT**, Nevens F, Bekkering FC, Bourgeois N, Van Vlierberghe H, Weegink CJ, Lefebvre V, Van Hattum J, Henrion J, Delwaide J, Hansen BE, Schalm SW, For The Benelux Study Group On Treatment Of Chronic Hepatitis C. Reduction of relapse rates by 18-month treatment in chronic hepatitis C. A Benelux randomized trial in 300 patients. *J Hepatol* 2004; **40**: 689-695

27 **Buti M**, Valdes A, Sanchez-Avila F, Esteban R, Lurie Y. Extending combination therapy with peginterferon alfa-2b plus ribavirin for genotype 1 chronic hepatitis C late responders: a report of 9 cases. *Hepatology* 2003; **37**: 1226-1227

28 **Berg T**, von Wagner M, Nasser S, Sarrazin C, Heintges T, Gerlach T, Buggisch P, Goeser T, Rasenack J, Pape GR, Schmidt WE, Kallinowski B, Klinker H, Spengler U, Martus P, Alshuth U, Zeuzem S. Extended treatment duration for hepatitis C virus type 1: comparing 48 versus 72 weeks of peginterferon-alfa-2a plus ribavirin. *Gastroenterology* 2006; **130**: 1086-1097

29 **Sanchez-Tapias JM**, Diago M, Escartin P, Enriquez J, Romero-Gomez M, Barcena R, Crespo J, Andrade R, Martinez-Bauer E, Perez R, Testillano M, Planas R, Sola R, Garcia-Bengoechea M, Garcia-Samaniego J, Munoz-Sanchez M, Moreno-Otero R. Peginterferon-alfa2a plus ribavirin for 48 versus 72 weeks in patients with detectable hepatitis C virus RNA at week 4 of treatment. *Gastroenterology* 2006; **131**: 451-460

30 **Pearlman BL**, Ehleben C, Saifee S. Treatment extension to 72 weeks of peginterferon and ribavirin in hepatitis C genotype 1-infected slow responders. *Hepatology* 2007; **46**: 1688-1694

31 **Muir AJ**, Bornstein JD, Killenberg PG. Peginterferon alfa-2b and ribavirin for the treatment of chronic hepatitis C in blacks and non-Hispanic whites. *N Engl J Med* 2004; **350**: 2265-2271

32 **Jeffers LJ**, Cassidy W, Howell CD, Hu S, Reddy KR. Peginterferon alfa-2a (40 kd) and ribavirin for black American patients with chronic HCV genotype 1. *Hepatology* 2004; **39**: 1702-1708

33 **Conjeevaram HS**, Fried MW, Jeffers LJ, Terrault NA, Wiley-Lucas TE, Afdhal N, Brown RS, Belle SH, Hoofnagle JH, Kleiner DE, Howell CD. Peginterferon and ribavirin treatment in African American and Caucasian American patients with hepatitis C genotype 1. *Gastroenterology* 2006; **131**: 470-477

34 **Layden-Almer JE**, Ribeiro RM, Wiley T, Perelson AS, Layden TJ. Viral dynamics and response differences in HCV-infected African American and white patients treated with IFN and ribavirin. *Hepatology* 2003; **37**: 1343-1350

35 **Ferenci P**, Laferi H, Scherzer T, Maieron A, Gschwantler M, Brunner H, Hubmann R, Bischof M, Staufer K, Datz C, Steindl-Munda P, Kessler H. Customizing treatment with peginterferon alfa-2a plus ribavirin in patients with HCV genotype 1 or 4 infection. Interim analysis of a prospective, randomized trial. *Hepatology* 2006; **44**: 336A

36 **Sanchez-Tapias JM**, Ferenci P, Diago M, Romero-Gomez M, Zeuzem S, Berg T. Which genotype 1 patients may benefit from extended treatment duration with peginterferon alfa-2a plus ribavirin? Proceedings of the 17th Asian Pacific Association Study of Liver Disease conference, Kyoto, Japan. *Hep Intl* 2007; **1**: 242

37 **Mangia A**, Minerva N, Bacca D, Cozzolongo R, Ricci GL, Carretta V, Vinelli F, Scotto G, Montalto G, Romano M, Cristofaro G, Mottola L, Spirito F, Andriulli A. Individualized treatment duration for hepatitis C genotype 1 patients: A randomized controlled trial. *Hepatology* 2008; **47**: 43-50

38 **Buti M**, Lurie Y, Blokhina N, Teuber G, Holota W, Sumskiene J, Vozianova Z, Wong F, Winkler R, Esteban R. Pegylated interferon alfa-2b plus ribavirin in patients with genotype 1 chronic hepatitis C with a slow virologic response: an early enrollers analysis of the SUCCESS study. *Hepatology* 2006; **44**: 342A

39 **Kaiser S**, Holger H, Bissinger L, Bettina L, Sauter B, Gregor M. Extended treatment of 72 versus 48 weeks for chronic hepatitis C patients with genotype 1 and high viral load using daily consensus interferon and ribavirin. *Hepatology* 2006; **44**: 608A

40 **Kaiser S**, Lutze B, Sauter B, Bissinger L, Werner C, Hass H, Gregor M. Retreatment of HCV genotype 1 relapse patients to peginterferon/ribavirin therapy with an extended treatment regimen of 72 weeks of consensus interferon/ribavirin versus peginterferon alpha/ribavirin. *Hepatology* 2007; **46**: 819A

41 **Jensen DM**, Frelich B, Andreone P, DiBisceglie A, Brandao-Mello CE, Reddy KR, Craxi A, Martin AO, Teuber G, Messinger D, Hooper G, Popescu M, Marcellin P. Pegylated interferon alfa-2a plus ribavirin in prior non-responders to pegylated interferon alfa-2b/ribavirin: final efficacy and safety outcomes of the REPEAT study. *Hepatology* 2007; **46**: 291A-292A

42 **Fuster D**, Planas R, Gonzalez J, Force L, Cervantes M, Vilaro J, Roget M, Garcia I, Pedrol E, Tor J, Ballesteros AL, Salas A, Sirera G, Videla S, Clotet B, Tural C. Results of a study of prolonging treatment with pegylated interferon-alpha2a plus ribavirin in HIV/HCV-coinfected patients with no early virological response. *Antivir Ther* 2006; **11**: 473-482

43 **Nunez M**, Miralles C, Berdun MA, Losada E, Aguirre-bengoa K, Ocampo A, Arazo P, Cervantes M, de Los Santos I, San Joaquin I, Echeverria S, Galindo MJ, Asensi V, Barreiro P, Sola J, Hernandez-Burruezo JJ, Guardiola JM, Romero M, Garcia-Samaniego J, Soriano V. Role of weight-based ribavirin dosing and extended duration of therapy in chronic hepatitis C in HIV-infected patients: the PRESCO trial. *AIDS Res Hum Retroviruses* 2007; **23**: 972-982

44 **Nakamura J**, Toyabe SI, Aoyagi Y, Akazawa K. Economic impact of extended treatment with peginterferon alpha-2a and ribavirin for slow hepatitis C virologic responders. *J Viral Hepat* 2008; **15**: 293-299

S- Editor Li DL **L- Editor** Li M **E- Editor** Lin YP

Online Submissions: wjg.wjgnet.com
wjg@wjgnet.com
doi: 10.3748/wjg.14.3616

World J Gastroenterol 2008 June 21; 14(23): 3616-3620
World Journal of Gastroenterology ISSN 1007-9327
© 2008 The WJG Press. All rights reserved.

EDITORIAL

Cystic tumors of the liver: A practical approach

Paolo Del Poggio, Marco Buonocore

Paolo Del Poggio, Marco Buonocore, Hepatology Unit, Treviglio Hospital, Treviglio (Bg) 24047, Italy
Author contributions: Del Poggio P and Buonocore M wrote the paper and contributed equally to the work.
Correspondence to: Paolo Del Poggio, Hepatology Unit, Treviglio Hospital (Bg), Treviglio (Bg) 24047, Italy. pdpoggio@ospedale.treviglio.bg.it
Telephone: +39-036-3424494 Fax: +39-036-3424561
Received: March 13, 2008 Revised: April 22, 2008
Accepted: April 29, 2008
Published online: June 21, 2008

Abstract

Biliary cyst tumors (cystadenoma and cystadenocarcinoma) are an indication for liver resection. They account for only 5% of all solitary cystic lesions of the liver, but differential diagnosis with multiloculated or complicated biliary cysts, atypical hemangiomas, hamartomas and lymphangiomas may be difficult. The most frequent challenge is to differentiate biliary cyst tumors from hemorrhagic cysts. Computerized tomography (CT) and magnetic resonance imaging (MRI) are often not diagnostic and in these cases fine needle aspiration (FNA) is used to confirm the presence of atypical biliary cells. FNA, however, lacks adequate sensitivity and specificity and should always be used in conjunction with imaging. Pre-operative differentiation of cystadenoma from cystadenocarcinoma is impossible and surgery must be performed if a biliary cyst tumor is suspected. When multiple cystic lesions are observed throughout the liver parenchyma, it is important to exclude liver metastasis, of which colonic cancer is the most common primary site. Multiple biliary hamartomas (von Meyenburg complex) can appear as a mixture of solid and cystic lesions and can be confused with cystic metastasis. Strong and uniform T2 hyperintensity on MRI is usually diagnostic, but occasionally a percutaneous biopsy may be required.

© 2008 The WJG Press. All rights reserved.

Key words: Biliary cyst tumor; Liver cystic neoplasia; Cystadenoma; Cystadenocarcinoma; Atypical hepatic cysts

Peer reviewer: Dr. Nahum Méndez-Sánchez, Departments of Gastroenterology and Liver Unit, Medica Sur Clinic and Foundation, Puente de Piedra 150, Col. Toriello Guerra, Mexico City 14050, Mexico

Del Poggio P, Buonocore M. Cystic tumors of the liver: A practical approach. *World J Gastroenterol* 2008; 14(23): 3616-3620 Available from: URL: http://www.wjgnet.com/1007-9327/14/3616.asp DOI: http://dx.doi.org/10.3748/wjg.14.3616

INTRODUCTION

Although rare, cystic neoplasms of the liver may represent a diagnostic challenge in everyday practice. Cystic tumors may be solitary or multiple and vary from the most benign (e.g. simple cysts, hamartomas) to potentially malignant (cystadenoma) or overtly malignant (cystadenocarcinoma). There are also atypical cystic presentations of normally non-cystic tumors, like cystic hemangiomas or cystic hepatocarcinomas and congenital diseases presenting as diffuse cyst-like involvement of the liver (Caroli's disease and von Meyenburg complex) that must be differentiated from cystic metastasis. The most important issue in the case of solitary cystic tumors is to distinguish biliary cystadenoma and cystadenocarcinoma from other benign conditions that require only observation of the patient.

SOLITARY CYSTIC TUMORS

Cystadenoma is a biliary cyst tumor arising from biliary epithelium. With its malignant counterpart (cystadenocarcinoma), it accounts for less than 5% of all cystic lesions of the liver; but it is dangerous for its propensity toward local recurrence and malignant change[1,2]. These tumors usually present in middle aged women with a mean age of 50 years and have a great variability in size, ranging from 1.5 cm to 30 cm. The majority of patients are asymptomatic, but in the case of large tumors they may present with a palpable mass and cause symptoms[3]. Cystadenocarcinoma can arise *de novo* or from a pre-existent cystadenoma, from which it is difficult to differentiate since both have a multiloculated appearance at ultrasound (US), computerized tomography (CT) and magnetic resonance imaging (MRI). Cystadenoma has thinner septa and a less thick and more regular walls than cystadenocarcinoma[4]. However, internal papillary projections and foldings with arterial enhancement of the external wall at dynamic CT scan and MRI may be present in both tumors, so that imaging itself cannot reliably differentiate these

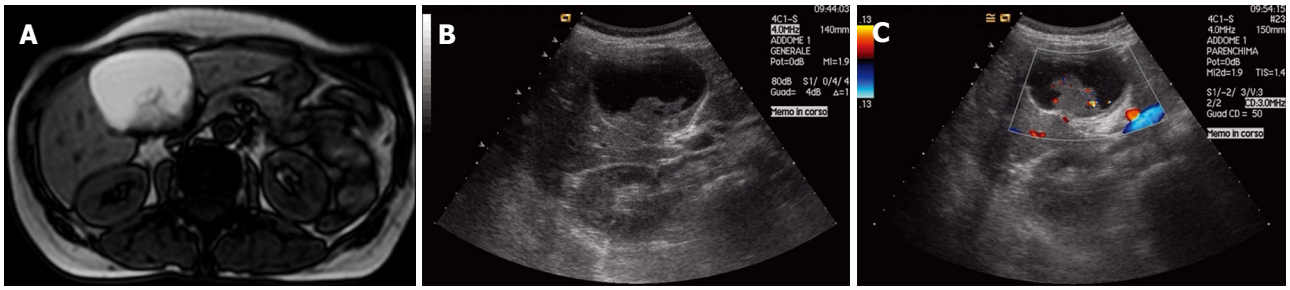

Figure 1 T1 weighted MR image (**A**) and ultrasound examination (**B**) showing a large cystic lesion of the left liver lobe with a thick and irregular septum, raising the suspicion of a biliary cystadenoma, and Doppler ultrasound (**C**) showing vascular signals within the septum disclosing a focus of cystadenocarcinoma confirmed in the surgical specimen.

neoplasms. Internal septa and papillary projections are more often hypovascular in the case of cystadenoma, and the demonstration of vascular signals at color Doppler can be a sign of its malignant transformation (Figure 1). The diagnosis of cystadenocarcinoma is straightforward only when ultrasound, CT scan or MRI shows nodular septa and thick, irregular walls with strong contrast enhancement, but in many cases there are overlapping features. Intracystic hemorrhage and fine punctuate calcifications may present in both conditions and can also be observed in complicated hemorrhagic cysts, their role as diagnostic criterion are, therefore, doubtful[5]. Fine needle aspiration can be used to differentiate a biliary cyst from other benign conditions and from a single metastasis, but is totally unreliable in differentiating cystadenoma from cystadenocarcinoma, since small neoplastic foci are undetectable by fine needle aspiration and may be revealed only in the surgical specimen[6].

In conclusion, there is no definite, reliable criterion for differentiating cystadenoma from cystadenocarcinoma and the correct diagnosis is often made only in the surgical specimen.

The majority of biliary cyst tumors do not usually communicate with the bile ducts, although direct luminal communication is occasionally observed. In these cases, dysplastic mucinous epithelium itself may proliferate within the bile ducts and cause obstruction[7]. This variant is considered an intraductal papillary neoplasm with prominent cystic dilatation rather than a true biliary cyst neoplasm and must be differentiated from biliary papillomatosis and cholangiocarcinoma of intraductal growth type. CT and MRI are insufficient to show the luminal communication, probably because the communication is too narrow, while intraoperative cholangiography can establish the correct diagnosis. Intraductal spreading of neoplastic cells into the bile duct portends a poorer prognosis of this variant of biliary cyst tumor.

If it is practically impossible to distinguish preoperatively cystadenoma from cystadenocarcinoma, every effort should be made to differentiate these neoplasms from biliary cysts and other benign tumors without malignant potential. In case of simple cysts, without internal septa or papillary projections, cystadenoma can be reliably excluded and the patient can only be observed. In case of multiloculated biliary or complicated biliary cyst (hemorrhagic cyst), imaging is often not reliable in ruling out cystadenoma. The most challenging differential diagnosis is hemorrhagic cysts where ultrasound can visualize internal clots as papillary excrescences or nodular and irregular septal images. CT scan is less sensitive than ultrasound in visualizing intracystic blood clots and at times it can only depict homogeneous low density areas inside a huge cyst. In these cases, a discrepancy between US and CT may suggest the correct diagnosis of hemorrhagic cysts. Recently MRI has been shown to be helpful. It was reported that high signals from clot formation could be detected both in T1 and in T2 weighted sequences, and are useful in differentiating it from cystadenocarcinoma, which usually exhibits low signals[8]. It should be noted that if a hemorrhagic cyst is suspected, MRI should not be delayed because hemorrhagic signal intensity becomes rapidly low when clots are liquefied[9]. History, on the contrary, is totally unreliable to suspect a hemorrhagic cyst since intracystic hemorrhage can occur in the absence of any symptom[10]. In the presence of a complicated or multiloculated hepatic cyst, a fine needle aspiration (FNA) of intracystic fluid can be performed to rule out a biliary cyst neoplasm. The presence of atypical cells, mucinous material and elevated levels of CEA and CA19-9 in the cystic fluid has been typically observed both in cystadenoma and in cystadenocarcinoma, but not in hepatic cysts[11,12] although CA19-9 is equally expressed in paraffin-embedded tissues from both hepatic cysts and biliary cyst neoplasms[13]. To complicate things further, high CA19-9 cyst-fluid levels have been occasionally found in complicated hepatic cysts[14] and data on CA19-9 serum levels are scanty and inconclusive[13,15]. The macroscopic appearance of the intracystic fluid is likewise useless since in biliary cyst tumors it can be mucinous, but also bile stained or clear, as it occurs when there is abundance of ovary stroma[16]. On the whole, FNA alone does not have adequate sensitivity and specificity to confirm or exclude biliary cyst tumors and should be always evaluated together with imaging.

Similar to intracystic bleeding, non suppurative, granulomatous infection of a biliary cyst may simulate cystadenoma and cystadenocarcinoma by the presence

of a thickened wall and a solid component infiltrating the peri-cystic surrounding tissue, thus mimicking a neoplastic lesion[17]. On the other hand, suppurated hepatic cysts and echinococcal cysts do not generally pose diagnostic problems. Sonography can easily differentiate the mobile internal debris typical of abscess formation or the multilayered appearance of the echinococcal cystic wall, and only an unexperienced sonographer can confuse the multiloculated appearance of cystadenoma with multiple daughter cysts of echinococcus[18]. When in doubt, the presence of anti-echinococcal antibodies is diagnostic.

Mesenchymal hamartoma is an uncommon benign lesion composed of bile ducts, immature mesenchymal cells and hepatocytes and may appear as a multiseptated cyst, causing confusion with biliary cystadenoma. Isolated septal calcification can be observed in both lesions and does not aid in the correct diagnosis[19]. Most of the cases are diagnosed in childhood when it presents as a large cystic mass[20] and very few cases have been reported in adults[21]. FNA can be diagnostic by showing clusters of both epithelial and mesenchymal spindle-shaped cells with pieces of loose connective tissue[22].

Ciliated hepatic foregut cyst is a very rare benign lesion arising from an abnormal budding of the primitive foregut and lined by stratified ciliated columnar cells, similar to the bronchial epithelium. These cysts are often anechogenic, but at times they may show internal echoes and can reach considerable dimensions posing differential diagnostic problems of cystadenoma. The typical subcapsular location in segment Ⅳ and the presence of a strong T2 hyper-intensity with T1 signal variability on MRI are quite characteristic. Another helpful clue may be the presence of scattered hyperecogenic spots within the cystic wall with no acoustic shadowing, which are related to cartilaginous remnants[23].

Abdominal lymphangioma may be occasionally located in the liver and appear as a single multiseptated lesion[24]. If this diagnosis is suspected, fine needle aspiration is not recommended due to the risk of massive lymphorrhea[25] and complete surgical resection should be accomplished, even without a precise pre-operative diagnosis.

Differential diagnosis with cystic hemangioma may also be a problem, especially in the case of a giant hemangioma, with large hypoechogenic central areas simulating the giant cystadenoma. CT and magnetic resonance imaging point out to the correct diagnosis by showing an enhancing rim with globular vessels and centripetal filling, with sparing of the large central lacunar areas[26].

Hepatocellular carcinoma and cholangiocarcinoma may occasionally present as a large hypodense and multiseptated mass at CT scan, simulating a cystic lesion or a biliary cyst tumor. In these cases, arterial phase enhancement on dynamic CT and washing out of the contrast material in the portal phase, are diagnostic[27].

Isolated mucin producing metastasis from melanoma or colon adenocarcinoma may at times simulate biliary cyst tumors and even benign hepatic cysts. These metastases may be associated to segmental dilatation of the peripheral bile ducts, caused by the presence of mucin casts occluding the bile ducts themselves[28].

Once a diagnosis of cystadenoma is made, surgery should be performed in any case, because differential diagnosis with cystadenocarcinoma is unreliable and cystadenoma itself has a malignant potential. If the pre-operative diagnostic work up, including cytologic aspiration of the lesion, has not produced a definitive diagnosis and surgery is performed because of a suspected bile cyst tumor, an intraoperative biopsy of the lesion is recommended since an extensive lymph node resection would be required if the tumor is proved to be a cholangiocarcinoma[14]. It is important that final decisions regarding indications and type of intervention are jointly discussed by the surgeon and a radiologist expert in liver tumor imaging, particularly in the case of cystic liver tumors, the most frequent mistake is the resection of a complicated biliary cyst incorrectly diagnosed as a cystadenoma.

MULTIPLE CYSTIC TUMORS

When multiple cystic lesions are observed throughout the liver parenchyma, the most important diagnostic problem is to exclude cystic liver metastases. The primary tumor is usually colonic adenocarcinoma, melanoma, carcinoid, breast or renal or ovarian cancer. Colonic cancer is the common, accounting for about 50% of all hepatic metastases[27]. The presence of intra- or peri-tumoral calcifications may suggest a specific diagnosis, being more frequent in the case of gastrointestinal, ovarian, breast and renal metastases compared to other types of tumors[29]. The cystic nature of the metastasis is secondary to the rapid growth and insufficient hepatic arterial supply of the lesion, leading to a large central necrosis simulating a cyst[30].

The differential diagnosis with polycystic liver disease and multiple liver abscesses is usually an easy task on US and CT scan. In case of cystic metastases, the borders of the cystic lesions are heterogeneous and ill-defined, the cystic wall is irregular and the vessels are amputated, but not displaced as in polycystic liver disease. In addition, cystic metastasis has a peripheral enhancing rim on the arterial phase of CT scan and MRI[27], while polycystic liver disease does not show any type of enhancement[31]. Another helpful sign may be the presence of peribiliary cysts, such as small cysts with a diameter of less than 10 mm, located within the hilum and adjacent to the hepatic ducts, more frequently on the left. These small cysts are typically observed only in polycystic liver disease and should not be confused with the segmental biliary dilatations occasionally observed in the case of metastasis or macronodular cirrhosis, which are less regular and never adjacent to the main ducts[32].

Multiple hepatic pyogenic microabscesses are easy to differentiate from metastasis by clinical symptoms and

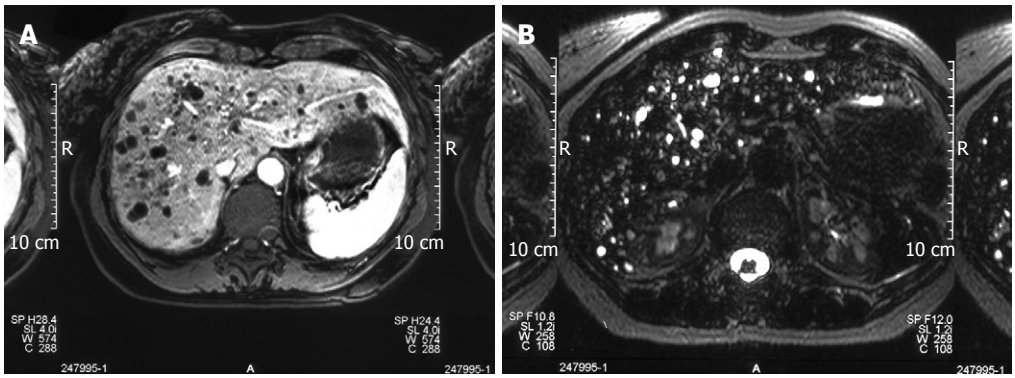

Figure 2 T1 weighted images showing the left multiple hypointense focal lesions of the liver parenchyma simulating metastases (**A**) and T2 weighted images showing a strong hyper-intensity in Von Meyenburg complex disclosing its cystic nature (**B**).

the presence of a late faint enhancing peripheral rim on CT scan and MRI[33]. This rim is quite different from the early arterial enhancing ring observed in the case of metastasis. An additional sign pointing to liver abscesses is the presence of air densities inside the lesions, which is almost never observed in the case of cystic metastasis.

The differential diagnosis with other types of ductal plate malformations, such as Caroli's disease, Caroli's syndrome and von Meyenburg complex, may at times be more difficult. Caroli's disease is a congenital autosomal recessive malformation characterized by diffuse or segmental cystic dilation of the intrahepatic biliary system. In Caroli's syndrome, periportal congenital fibrosis or multicystic renal diseases are observed in addition to biliary dilations. In both cases, these dilations are less regular than in polycystic liver disease and have intraluminal protrusions or may be associated to segmental dilation of the intrahepatic bile ducts, thus simulating cholangiocarcinoma or multiple cystic metastases. The presence of the "dot signs", such as an intracystic portal branch, surrounded by the dilated bile duct and the demonstration of a communication of the cysts with the biliary system on MR cholangiography, is diagnostic and excludes liver metastasis[34].

Von Meyenburg complex and bile duct hamartoma are small focal developmental lesions composed of innumerable dilated bile ducts mixed with a dense collagenous stroma. The dilated bile duct foci, contrary to those observed in Caroli's disease and Caroli's syndrome do not communicate with the biliary system[16]. Depending on the prevalence of fibrous stroma or biliary dilation, these lesions can appear as predominantly solid and cystic or intermediate and may be easily confused with metastases, microabscesses and even biliary cystadenocarcinoma[35]. Occasionally, the differential diagnosis may be a real dilemma. Although biliary hamartomas are more uniform in size and measure less than 1 cm in diameter, CT scan and ultrasound are often not specific. MRI, on the contrary, can be very helpful by identifying strong hyper-intensity in biliary hamartomas on heavily T2 weighted images (Figure 2), often with a signal intensity similar to that of the spleen[36]. These features, however, are not always sufficient to make a precise diagnosis, especially in intermediate or predominantly solid von Meyenburg complex and a percutaneous or even surgical biopsy is occasionally required[37]. The issue is further complicated by very rare reports on malignant transformation of these hamartomas to cholangiocarcinoma, making this type of cystic malformation the most challenging to differentiate from cystic neoplastic lesions.

ACKNOWLEDGMENTS

The authors are indebted to Dr. Luigi Grazioli for kindly providing iconographic material.

REFERENCES

1 **Wheeler DA**, Edmondson HA. Cystadenoma with mesenchymal stroma (CMS) in the liver and bile ducts. A clinicopathologic study of 17 cases, 4 with malignant change. *Cancer* 1985; **56**: 1434-1445
2 **Devaney K**, Goodman ZD, Ishak KG. Hepatobiliary cystadenoma and cystadenocarcinoma. A light microscopic and immunohistochemical study of 70 patients. *Am J Surg Pathol* 1994; **18**: 1078-1091
3 **Kim HG**. [Biliary cystic neoplasm: biliary cystadenoma and biliary cystadenocarcinoma] *Korean J Gastroenterol* 2006; **47**: 5-14
4 **Teoh AY**, Ng SS, Lee KF, Lai PB. Biliary cystadenoma and other complicated cystic lesions of the liver: diagnostic and therapeutic challenges. *World J Surg* 2006; **30**: 1560-1566
5 **Choi BI**, Lim JH, Han MC, Lee DH, Kim SH, Kim YI, Kim CW. Biliary cystadenoma and cystadenocarcinoma: CT and sonographic findings. *Radiology* 1989; **171**: 57-61
6 **Del Poggio P**, Jamoletti C, Forloni B, De Benedictis R, Mattiello M, Corti D, Pezzica E. Malignant transformation of biliary cystadenoma: a difficult diagnosis. *Dig Liver Dis* 2000; **32**: 733-736
7 **Zen Y**, Fujii T, Itatsu K, Nakamura K, Konishi F, Masuda S, Mitsui T, Asada Y, Miura S, Miyayama S, Uehara T, Katsuyama T, Ohta T, Minato H, Nakanuma Y. Biliary cystic tumors with bile duct communication: a cystic variant of intraductal papillary neoplasm of the bile duct. *Mod Pathol* 2006; **19**: 1243-1254
8 **Vilgrain V**, Silbermann O, Benhamou JP, Nahum H. MR imaging in intracystic hemorrhage of simple hepatic cysts. *Abdom Imaging* 1993; **18**: 164-167
9 **Gomori JM**. Head and neck hemorrhage in Kressel HY editor. Magnetic Resonance annual 1987. New York: Raven, 1987: 71-112
10 **Kitajima Y**, Okayama Y, Hirai M, Hayashi K, Imai H, Okamoto T, Aoki S, Akita S, Gotoh K, Ohara H, Nomura T, Joh T, Yokoyama Y, Itoh M. Intracystic hemorrhage of a simple liver cyst mimicking a biliary cystadenocarcinoma. *J Gastroenterol* 2003; **38**: 190-193
11 **Pinto MM**, Kaye AD. Fine needle aspiration of cystic liver lesions. Cytologic examination and carcinoembryonic

antigen assay of cyst contents. *Acta Cytol* 1989; **33**: 852-856
12 **Horsmans Y**, Laka A, Gigot JF, Geubel AP. Serum and cystic fluid CA 19-9 determinations as a diagnostic help in liver cysts of uncertain nature. *Liver* 1996; **16**: 255-257
13 **Park KH**, Kim JS, Lee JH, Kim HJ, Kim JY, Yeon JE, Park JJ, Byun KS, Bak YT, Lee CH. [Significances of serum level and immunohistochemical stain of CA19-9 in simple hepatic cysts and intrahepatic biliary cystic neoplasms] *Korean J Gastroenterol* 2006; **47**: 52-58
14 **Shimada M**, Takenaka K, Gion T, Fujiwara Y, Taguchi K, Kajiyama K, Shirabe K, Sugimachi K. Treatment strategy for patients with cystic lesions mimicking a liver tumor: a recent 10-year surgical experience in Japan. *Arch Surg* 1998; **133**: 643-646
15 **Kim K**, Choi J, Park Y, Lee W, Kim B. Biliary cystadenoma of the liver. *J Hepatobiliary Pancreat Surg* 1998; **5**: 348-352
16 **Precetti S**, Gandon Y, Vilgrain V. [Imaging of cystic liver diseases] *J Radiol* 2007; **88**: 1061-1072
17 **Kawashita Y**, Kamohara Y, Furui J, Fujita F, Miyamoto S, Takatsuki M, Abe K, Hayashi T, Ohno Y, Kanematsu T. Destructive granuloma derived from a liver cyst: a case report. *World J Gastroenterol* 2006; **12**: 1798-1801
18 **Lewall DB**, McCorkell SJ. Hepatic echinococcal cysts: sonographic appearance and classification. *Radiology* 1985; **155**: 773-775
19 **Konez O**, Goyal M, Vyas PK, Boinapally SB. Mesenchymal hamartoma of the liver. *Comput Med Imaging Graph* 2001; **25**: 61-65
20 **Papastratis G**, Margaris H, Zografos GN, Korkolis D, Mannika Z. Mesenchymal hamartoma of the liver in an adult: a review of the literature. *Int J Clin Pract* 2000; **54**: 552-554
21 **Brkic T**, Hrstic I, Vucelic B, Jakic-Razumovic J, Skegro M, Romic B, Cukovic-Cavka S, Pulanic R, Ostojic R. Benign mesenchymal liver hamartoma in an adult male: a case report and review of the literature. *Acta Med Austriaca* 2003; **30**: 134-137
22 **al-Rikabi AC**, Buckai A, al-Sumayer S, al-Damegh S, al-Bassam AR. Fine needle aspiration cytology of mesenchymal hamartoma of the liver. A case report. *Acta Cytol* 2000; **44**: 449-453
23 **Del Poggio P**, Jamoletti C, Mattiello M, Corti D, Pezzica E. Images in Hepatology. Ciliated hepatic foregut cyst. *J Hepatol* 2003; **39**: 1090
24 **Allen JG**, Riall TS, Cameron JL, Askin FB, Hruban RH, Campbell KA. Abdominal lymphangiomas in adults. *J Gastrointest Surg* 2006; **10**: 746-751
25 **Damascelli B**, Spagnoli I, Garbagnati F, Ceglia E, Milella M, Masciadri N. Massive lymphorrhoea after fine needle biopsy of the cystic haemolymphangioma of the liver. *Eur J Radiol* 1984; **4**: 107-109
26 **Coumbaras M**, Wendum D, Monnier-Cholley L, Dahan H, Tubiana JM, Arrive L. CT and MR imaging features of pathologically proven atypical giant hemangiomas of the liver. *AJR Am J Roentgenol* 2002; **179**: 1457-1463
27 **Alobaidi M**, Shirkhoda A. Malignant cystic and necrotic liver lesions: a pattern approach to discrimination. *Curr Probl Diagn Radiol* 2004; **33**: 254-268
28 **Tokai H**, Kawashita Y, Eguchi S, Kamohara Y, Takatsuki M, Okudaira S, Tajima Y, Hayashi T, Kanematsu T. A case of mucin producing liver metastases with intrabiliary extension. *World J Gastroenterol* 2006; **12**: 4918-4921
29 **Sica GT**, Ji H, Ros PR. CT and MR imaging of hepatic metastases. *AJR Am J Roentgenol* 2000; **174**: 691-698
30 **Mortele KJ**, Ros PR. Cystic focal liver lesions in the adult: differential CT and MR imaging features. *Radiographics* 2001; **21**: 895-910
31 **Gupta S**, Seith A, Dhiman RK, Chawla YK, Sud K, Kohli HS, Sakhuja V, Suri S. CT of liver cysts in patients with autosomal dominant polycystic kidney disease. *Acta Radiol* 1999; **40**: 444-448
32 **Terayama N**, Matsui O, Hoshiba K, Kadoya M, Yoshikawa J, Gabata T, Takashima T, Terada T, Nakanuma Y, Shinozaki K. Peribiliary cysts in liver cirrhosis: US, CT, and MR findings. *J Comput Assist Tomogr* 1995; **19**: 419-423
33 **Mortele KJ**, Segatto E, Ros PR. The infected liver: radiologic-pathologic correlation. *Radiographics* 2004; **24**: 937-955
34 **Brancatelli G**, Federle MP, Vilgrain V, Vullierme MP, Marin D, Lagalla R. Fibropolycystic liver disease: CT and MR imaging findings. *Radiographics* 2005; **25**: 659-670
35 **Karahan OI**, Kahriman G, Soyuer I, Ok E. Hepatic von Meyenburg complex simulating biliary cystadenocarcinoma. *Clin Imaging* 2007; **31**: 50-53
36 **Maher MM**, Dervan P, Keogh B, Murray JG. Bile duct hamartomas (von Meyenburg complexes): value of MR imaging in diagnosis. *Abdom Imaging* 1999; **24**: 171-173
37 **Eisenberg D**, Hurwitz L, Yu AC. CT and sonography of multiple bile-duct hamartomas simulating malignant liver disease (case report). *AJR Am J Roentgenol* 1986; **147**: 279-280

S- Editor Zhong XY **L- Editor** Wang XL **E- Editor** Lu W

Online Submissions: wjg.wjgnet.com
wjg@wjgnet.com
doi:10.3748/wjg.14.3628

World J Gastroenterol 2008 June 21; 14(23): 3628-3632
World Journal of Gastroenterology ISSN 1007-9327
© 2008 The WJG Press. All rights reserved.

REVIEW

Is there a place for serum laminin determination in patients with liver disease and cancer?

Heitor Rosa, Edison Roberto Parise

Heitor Rosa, Unit of Gastroenterology and Hepatology, Federal University of Goiás School of Medicine, Goiânia, Goiás 74093-080, Brazil
Edison Roberto Parise, Unity of Hepatology, Federal University of São Paulo (UNIFESP), São Paulo 04024-002, Brazil
Author contributions: Rosa H and Parise ER contributed equally to this work.
Correspondence to: Heitor Rosa, Professor, MD, PhD, Chief, Unit of Gastroenterology and Hepatology, Federal University of Goiás School of Medicine, Rua 126 n. 21, Setor Sul, Goiânia, Goiás 74093-080, Brazil. hrosa@cultura.com.br
Telephone: +55-62-32816128 Fax: +55-62-32096248
Received: January 24, 2008 Revised: April 18, 2008
Accepted: April 25, 2008
Published online: June 21, 2008

Abstract

Laminin is a glycoprotein which has an important role in the mechanism of fibrogenesis and is, thus, related to hepatic fibrosis in addition to presenting increased levels in several types of neoplasias. However, its determination is not routinely considered in the study of hepatic fibrosis. In this review, the authors critically comment on the role of this glycoprotein compared to other markers of fibrosis through non-invasive procedures (Fibroscan). They also consider its clinical investigational potential and believe that the continuation of these investigations might contribute to a better understanding of the fibrogenic mechanism, which could in turn either lead to the identification of patients at risk of developing fibrosis non-alcoholic fatty liver disease (NAFLD) and non-alcoholic steatohepatitis (NASH) or at least be used as an indicator for hepatic biopsy in such patients. Finally, the authors believe that serum laminin determination might contribute to the diagnosis of epithelial tumor metastasis and peritoneal carcinomatosis.

© 2008 The WJG Press. All rights reserved.

Key words: Laminin; Hepatic fibrosis; Cancer; Cirrhosis; Fibrosis markers

Peer reviewers: Dr. Maribel Rodriguez-Torres, Fundacion De Investigacion De Diego, ave. De diego 359 suite 302, Santurce 00909, Puerto Rico; Dr. Devanshi Seth, Drug Health Services & Centenary Institute, Royal Prince Alfred Hospital, Missenden Road, Camperdown NSW 2050, Australia

Rosa H, Parise ER. Is there a place for serum laminin determination in patients with liver disease and cancer? *World J Gastroenterol* 2008; 14(23): 3628-3632 Available from: URL: http://www.wjgnet.com/1007-9327/14/3628.asp DOI: http://dx.doi.org/10.3748/wjg.14.3628

INTRODUCTION

Laminin was initially identified by TIMPL and MARTIN in 1979[1], from a murine fibrosarcoma, the Engelbreth-Holm-Swan (EHS) tumor. Its molecule is a large complex (approximately 850 kilodaltons) made up of three polypeptidic chains called α1 (with approximately 440 kDa), β1 e γ1 (each one with approximately 200 kDa). These chains are intertwined by disulphide bridges, forming a characteristic cross-shaped asymmetrical structure[1-3].

Laminin is one of the main glycoproteins of the basement membrane and participates in a series of such biological phenomena as adhesion, migration, cellular differentiation and growth, inflammatory response and the maintenance of the cytoskeleton upon its binding to several components of the matrix, such as collagen type IV, heparan-sulphate and entacin[3-7].

Laminin receptors are also found on the surface of a wide range of cells, such as platelets, muscle cells, neutrophils, endothelial cells and hepatocytes[3,6]. Recently, the existence of a class of transmembrane receptors for laminin known as integrins has been demonstrated. These integrins are involved in the mechanisms of cell-cell, cell-matrix and, more recently, pathogen-cell adhesion[3,7,8]. Laminin binding proteins have been described in a number of such pathogenic agents as *Staphylococcus aureus*, *Escherichia coli*, *Helicobacter pylori (H pylori)*, and *Candida albicans*.

LAMININ IN THE LIVER

In normal liver, laminin is found around the vessels and biliary ducts, where basement membranes are identified. Little or only a slight reaction for antibodies against laminin can be observed in the hepatic sinusoids[9,10]. In this organ, glycoprotein is also involved in intracellular activities, such as the normal differentiation of the biliary ducts, genetic expressions for albumin messenger RNA in hepatocyte, and regeneration with normal

lobular organization following partial hepatectomy[11-14]. Laminin is thought to be synthesized by hepatocytes and sinusoidal cells[14,15]. Among all cellular types in the sinusoids, special attention should be given to stellate cells or lipocytes, which produce the largest amount of serum laminin.

With the development of hepatic cirrhosis, laminin and collagen deposition occurs both along the fibers of septal fibrosis and subendothelial sinusoids or Disse's space. At the latter site, laminin deposition, together with collagen deposition, determine the formation of a true basement membrane along sinusoids. This phenomenon is called capillarization of Disse's space[16]. Besides the increased production of laminin in the liver an additional effect due to a lack of degradation of this protein by liver endothelial cells should also be taken into consideration. As demonstrated by Smedsrod *et al*[17] in an experimental model, apart from an increase in tissue deposition or turnover, there would be a decrease in the liver's ability to degrade this protein. With the development of anti-laminin antibodies, directed against the laminin P1 portion, increased levels of this circulating protein were observed in the more advanced stages of fibrosis in patients with hepatic disease[18-22] and as expected these serum levels have a positive correlation with portal pressure[21-26]. Kropf *et al* have proposed laminin serum concentration as a sensitive screening test for hepatic fibrotic disease and portal hypertension, if the test is carried out together with hyaluronic acid determination[21,22]. Laminin as an isolated parameter was found to be highly sensitive, but with low specificity to detect portal pressure above 5 mmHg.

We have assessed laminin serum levels in patients with alcoholic liver cirrhosis and with preserved hepatic function in an attempt to evaluate its predictive value for the risk of variceal bleeding, which is assessed through a portal pressure level equal to or higher than 12 mmHg[26]. In these patients, serum laminin levels were significantly correlated with portal pressure levels (r = 0.70). Such correlation enabled us to find a cut-off level for serum laminin that could correspond more closely to a portal pressure of 12 mmHg, accepted as a threshold for esophageal rupture in those patients. As it was found by others, these laminin levels presented very low specificity and negative predictive values to identify those patients with increased portal hypertension. In fact, patients presenting laminin serum concentration of less than 2.20 U/mL have almost 50% chance of having or not a portal pressure of 12 mmHg or higher.

This low specificity of serum laminin determination in portal hypertension could be related to the fact that laminin levels reflect only structural changes and do not take into account changes in the systemic and portal blood flow, which contribute significantly to portal pressure.

On the other hand, due to the great distribution of laminin in the body's basement membranes, and its limited participation in the liver's extracellular matrix, some issues need to be further investigated and clarified as for the origin of this protein. A study of concentrations of serum laminin in different vascular territories showed that its levels in supra-hepatic veins were higher compared to those found in the renal and femoral veins of patients with fibrosis or hepatic cirrhosis[27], which would be indicative of its hepatic synthesis. Similar findings were also demonstrated in control and carbon tetrachloride treated animals; there was also a significant correlation found between laminin serum levels and the degree of hepatic fibrosis[28] and an important increase was observed in the concentration of this glycoprotein in the supra-hepatic vein when compared to its amount in portal blood[29]. However, the hepatic contribution was much smaller in cirrhotic animals than in those with fibrosis as the sole condition. This fact could point towards decreased hepatic extraction of the protein or an increase in laminin synthesis in other organs of the splanchnic circulation, secondary to the venous congestion of this system. The latter possibility seems to be reinforced by studies with patients infected by *Schistosoma mansoni*. In the hepatosplenic form of the disease portal hypertension is due to periportal fibrosis, which determines pre-sinusoidal portal hypertension with large splenomegaly. Because these patients do not present hepatic cirrhosis, collagenization and capillarization of with Disse's space are not usually found. In these patients, initial studies revealed a significant increase in the levels of circulating laminin, when compared to patients presenting hepatointestinal form and the control group[30-32]. This increase correlated with the levels of portal pressure measured *via* the splenic vein[30, 31]. But, when these patients where submitted to splenectomy, a significantly decrease in the levels of type IV collagen and laminin in the serum of these patients was observed[32]. Since an increased synthesis of basement membrane in the spleen of such patients has been reported, the reduced levels of laminin after splenectomy strongly suggest an important participation of an extra-hepatic source for the serum levels of laminin in these patients[33,34].

Thus, not only might circulating levels of laminin reflect the hepatic processes of synthesis and degradation, but also the increase of the synthesis of basement membranes, as a result of the congestion observed in other splanchnic organs.

Hence, the use of serum laminin as a marker of portal hypertension for clinical use suffers from other extra-hepatic factors which might influence its blood concentration. In addition, recent studies with Fibroscan have found sensitivity and specificity for the diagnosis of portal hypertension in cirrhotic patients far higher than those found through the determination of serum laminin[35,36].

Due to this relationship between laminin tissue deposition and advanced fibrosis, serum levels of laminin have been used by several authors as a non-invasive parameter to assess liver fibrosis in alcoholic patients as well as in those presenting with viral hepatitis and hemochromatosis[37]. Such determination, however, was progressively discontinued as it did not demonstrate to be superior to those of other such components of the extracellular matrix as TIMPs and hyaluronic acid. However,

in recent studies laminin determination has been included in a set of test together with PIIINP, hydroxyproline, prothrombin activity, and AST/ALT in the diagnosis of advanced fibrosis in chronic hepatitis C[35,38-41].

In non-alcoholic fatty liver disease (NAFLD), however, laminin serum levels should be further investigated. In this condition, the fibrogenic stimulus in the perisinusoidal region occurs earlier, with the detection of pericellular and perisinusoidal fibrosis in the early stages of fibrosis[39].

We have more recently been able to assess serum laminin values in NAFLD, and to measure collagen type Ⅳ and hyaluronic acid[42]. Ballooning and hepatic fibrosis in these patients is associated with the progression of the disease[43]. In this preliminary study, we analyzed the discriminative ability of serum laminin, type Ⅳ collagen and hyaluronan and hepatic enzymes levels to predict the presence of fibrosis in 30 overweight patients divided into two groups according to the absence or presence of fibrosis upon liver biopsy. All the three biochemical markers of fibrosis were able to differentiate between these two groups, but laminin presented the best correlation (rs = 0.65) with hepatic fibrosis and the best diagnostic performance, with 87% accuracy. When compared with the BAAT criteria proposed by Ratziu *et al*[44], laminin values presented a better diagnostic accuracy for the diagnosis of septal fibrosis (83% × 70%) and for the presence of any fibrosis.

Although laminin was not evaluated, in a study with 112 patients with NAFLD, 70 of whom with at least grade 1 fibrosis, Sakugawa *et al*[38] were able to confirm our findings that hyaluronic acid and type Ⅳ collagen were useful in discriminating the patients with fibrosis from those with steatosis only. The subtle differences in diagnostic accuracy performance for these biochemical markers of liver fibrosis found in our study and that by Sakugawa *et al*[38] might be attributable to the fact that their study included a higher number of patients with any given degree of fibrosis (62% × 37%) or advanced fibrosis (37% × 10%). On the other hand, Lydatakis *et al*[36] showed that HA determination was more useful in the diagnosis of fibrosis than serum laminin and type Ⅳ collagen. No correlation was observed among laminin level and the grade of hepatic fibrosis, possibly due to the method and patients selection. It's important to take into account the small number of studies on fibrosis markers by indirect method.

In studies by Sakugawa *et al*[38] HA serum levels have been well demonstrated to significantly increase in cirrhotic patients when compared to the other degrees of fibrosis. In this manner, the determination of serum laminin values can not only play a useful role in the identification of NAFLD patients with a certain degree of fibrosis, but also in the distinction between patients with simple steatosis and those with non-alcoholic steatohepatitis (NASH) and a certain degree of fibrosis. Finally, the determination of serum laminin values might become a selection parameter of patients for the indication of fibrosis. A study bearing this purpose is currently being conducted in our laboratories.

SERUM LAMININ IN NEOPLASTIC DISEASES

Not only have serum laminin levels been studied in patients with liver diseases, but also in patients with cancer, especially in cases where tumor proliferation and invasion are found. Serum values tend to increase significantly with the emergence of metastases, irrespective of tumor lineage or the organ originating the neoplasm[45-48].

Hence, serum laminin could be regarded as a tumoral marker in cases of alterations in the basement membrane, proliferation and tumoral invasion[48]. In fact serum laminin concentration is increased in metastatic cancer of different origins as melanoma, gastric adenocarcinoma, hepatocellular carcinoma, colorectal cancer, epithelial ovarian tumor[49-52].

Grounded on these observations and the findings by Byers *et al*[53] and Chu *et al*[54], who observed increased concentrations of laminin in the ascites of metastatic breast tumors, we decided to study the discriminative ability for this glycoprotein in serum and in ascites to (differentiate) discriminate between ascites due to peritoneal carcinomatosis and hepatic cirrhotics[55]. By using polyclonal antibodies against laminin isolated from human placenta, a significant increase in serum and ascitic laminin levels was observed in patients with peritoneal carcinomatosis when compared to patients with hepatic cirrhosis with or without hepatocellular carcinoma.

Although immunohistochemical studies have shown important laminin deposition in cases of neoplastic transformation of hepatocytes[56,57] and despite the considerable representation of the group of patients with HCC once they presented advanced disease with large tumor masses with high serum alpha-fetoprotein levels, blood and ascites laminin values did not distinguish these patients from those with liver cirrhosis without tumor complication. In benign and malignant ascites, serum laminin values were higher and showed excellent correlation with its value in the ascitic fluid (r = 0.93, P < 0.0001). Thus, these findings indicated that serum laminin levels can also be a marker of neoplastic ascites. Indeed serum laminin showed high discriminative ability for the diagnosis of malignant ascites, with 75% sensitivity, 100% specificity and 91% accuracy[43].

So, considering the potential of laminin for clinical investigation, it seems to us that more studies are needed in order to clarify if there are still a place for serum laminin determination in the diagnosis of hepatic fibrosis in NAFLD and in the diagnosis of epithelial tumors metastasis and peritoneal carcinomatosis.

ACKNOWLEDGMENTS

The authors thank Mr. Edmilson Chagas for his excellent linguistics assistance.

REFERENCES

1 **Timpl R**, Rohde H, Robey PG, Rennard SI, Foidart JM,

Martin GR. Laminin--a glycoprotein from basement membranes. *J Biol Chem* 1979; **254**: 9933-9937
2 **Burgeson RE**, Chiquet M, Deutzmann R, Ekblom P, Engel J, Kleinman H, Martin GR, Meneguzzi G, Paulsson M, Sanes J. A new nomenclature for the laminins. *Matrix Biol* 1994; **14**: 209-211
3 **Aumailley M**, Smyth N. The role of laminins in basement membrane function. *J Anat* 1998; **193** (Pt 1): 1-21
4 **Kleinman HK**, Cannon FB, Laurie GW, Hassell JR, Aumailley M, Terranova VP, Martin GR, DuBois-Dalcq M. Biological activities of laminin. *J Cell Biochem* 1985; **27**: 317-325
5 **Kershenobich Stalnikowitz D**, Weissbrod AB. Liver fibrosis and inflammation. A review. *Ann Hepatol* 2003; **2**: 159-163
6 **Mecham RP**. Receptors for laminin on mammalian cells. *FASEB J* 1991; **5**: 2538-2546
7 **Haas TA**, Plow EF. Integrin-ligand interactions: a year in review. *Curr Opin Cell Biol* 1994; **6**: 656-662
8 **Valkonen KH**, Ringner M, Ljungh A, Wadstrom T. High-affinity binding of laminin by Helicobacter pylori: evidence for a lectin-like interaction. *FEMS Immunol Med Microbiol* 1993; **7**: 29-37
9 **Martinez-Hernandez A**. The hepatic extracellular matrix. I. Electron immunohistochemical studies in normal rat liver. *Lab Invest* 1984; **51**: 57-74
10 **Parise ER**, Summerfield JA, Hahn E, Wiedmann KH, Doenhoff MJ. Basement membrane proteins and type III procollagen in murine schistosomiasis. *Trans R Soc Trop Med Hyg* 1985; **79**: 663-670
11 **Shah KD**, Gerber MA. Development of intrahepatic bile ducts in humans. Possible role of laminin. *Arch Pathol Lab Med* 1990; **114**: 597-600
12 **Caron JM**. Induction of albumin gene transcription in hepatocytes by extracellular matrix proteins. *Mol Cell Biol* 1990; **10**: 1239-1243
13 **Martinez-Hernandez A**, Delgado FM, Amenta PS. The extracellular matrix in hepatic regeneration. Localization of collagen types I, III, IV, laminin, and fibronectin. *Lab Invest* 1991; **64**: 157-166
14 **Voss B**, Rauterberg J. Investigation on the biosynthesis of connective tissue components by cultured mouse liver macrophages and mouse peritoneal macrophages. In: Sinusoidal liver cells. Amsterdam: Elsevier, 1982; 201-208
15 **Gressner AM**, Bachem MG. Cellular sources of noncollagenous matrix proteins: role of fat-storing cells in fibrogenesis. *Semin Liver Dis* 1990; **10**: 30-46
16 **Schaffner F**, Popper H. Capillarization of hepatic sinusoids in man. *Gastroenterology* 1963; **44**: 239-242
17 **Smedsrod B**, Paulsson M, Johansson S. Uptake and degradation in vivo and in vitro of laminin and nidogen by rat liver cells. *Biochem J* 1989; **261**: 37-42
18 **Hahn E**, Wick G, Pencev D, Timpl R. Distribution of basement membrane proteins in normal and fibrotic human liver: collagen type IV, laminin, and fibronectin. *Gut* 1980; **21**: 63-71
19 **Schneider M**, Voss B, Hogemann B, Eberhardt G, Gerlach U. Evaluation of serum laminin P1, procollagen-III peptides, and N-acetyl-beta-glucosaminidase for monitoring the activity of liver fibrosis. *Hepatogastroenterology* 1989; **36**: 506-510
20 **Niemela O**, Risteli J, Blake JE, Risteli L, Compton KV, Orrego H. Markers of fibrogenesis and basement membrane formation in alcoholic liver disease. Relation to severity, presence of hepatitis, and alcohol intake. *Gastroenterology* 1990; **98**: 1612-1619
21 **Korner T**, Kropf J, Gressner AM. Serum laminin and hyaluronan in liver cirrhosis: markers of progression with high prognostic value. *J Hepatol* 1996; **25**: 684-688
22 **Kropf J**, Gressner AM, Tittor W. Logistic-regression model for assessing portal hypertension by measuring hyaluronic acid (hyaluronan) and laminin in serum. *Clin Chem* 1991; **37**: 30-35
23 **Annoni G**, Colombo M, Cantaluppi MC, Khlat B, Lampertico P, Rojkind M. Serum type III procollagen peptide and laminin (Lam-P1) detect alcoholic hepatitis in chronic alcohol abusers. *Hepatology* 1989; **9**: 693-697
24 **Gressner AM**, Tittor W. Serum laminin--its concentration increases with portal hypertension in cirrhotic liver disease. *Klin Wochenschr* 1986; **64**: 1240-1248
25 **Mal F**, Hartmann DJ, Trinchet JC, Lacombe F, Ville G, Beaugrand M. [Serum laminin and portal pressure in alcoholic cirrhosis. A study of 39 patients] *Gastroenterol Clin Biol* 1988; **12**: 841-844
26 **Kondo M**, Miszputen SJ, Leite-mor MM, Parise ER. The predictive value of serum laminin for the risk of variceal bleeding related to portal pressure levels. *Hepatogastroenterology* 1995; **42**: 542-545
27 **Gressner AM**, Tittor W, Negwer A. Serum concentrations of N-terminal propeptide of type III procollagen and laminin in the outflow of fibrotic livers compared with liver-distal regions. *Hepatogastroenterology* 1986; **33**: 191-195
28 **Neves LB**, Catarino RM, Silva MR, Parise ER. [Increased serum levels of laminin in the experimental cirrhosis induced by carbon tetrachloride] *Arq Gastroenterol* 2003; **40**: 173-176
29 **Neves LB**. Estudo da laminina sérica e de sua deposição no fígado de ratos com fibrose hepática induzida pelo tetracloreto de carbono. Thesis UNIFESP, 2000
30 **Parise ER**, Rosa H. Serum laminin in hepatic schistosomiasis. *Trans R Soc Trop Med Hyg* 1992; **86**: 179-181
31 **Parise ER**, Leite-Mor MM, Rosa H. Serum laminin in hepatosplenic human schistosomiasis. *Mem Inst Oswaldo Cruz* 1992; **87** Suppl 4: 127-128
32 **Grimaud JA**, Borojevic R. Chronic human schistosomiasis mansoni. Pathology of the Disse's space. *Lab Invest* 1977; **36**: 268-273
33 **Wyszomirska RMAF**. Determinação sérica dos marcadores de fibrose hepática em portadores de esquistossomose mansônica: avaliação do colágeno tipo IV e laminina. Thesis. 1999 University of Campinas 1999. Sao Paulo, **118**: 1117-1123
34 **Borojevic R**, Grimaud JA. Collagen fibers in enlarged basement membranes in human schistosomal liver and spleen. *Cell Mol Biol Incl Cyto Enzymol* 1980; **26**: 247-250
35 **Li ZX**, He Y, Wu J, Liang DM, Zhang BL, Yang H, Wang LL, Ma Y, Wei KL. Noninvasive evaluation of hepatic fibrosis in children with infant hepatitis syndrome. *World J Gastroenterol* 2006; **12**: 7155-7160
36 **Lydatakis H**, Hager IP, Kostadelou E, Mpousmpoulas S, Pappas S, Diamantis I. Non-invasive markers to predict the liver fibrosis in non-alcoholic fatty liver disease. *Liver Int* 2006; **26**: 864-871
37 **Lebensztejn DM**, Skiba E, Sobaniec-Lotowska ME, Kaczmarski M. Serum hyaluronan and laminin level in children with chronic hepatitis B during long-term lamivudine treatment. *Hepatogastroenterology* 2007; **54**: 834-838
38 **Sakugawa H**, Nakayoshi T, Kobashigawa K, Yamashiro T, Maeshiro T, Miyagi S, Shiroma J, Toyama A, Nakayoshi T, Kinjo F, Saito A. Clinical usefulness of biochemical markers of liver fibrosis in patients with nonalcoholic fatty liver disease. *World J Gastroenterol* 2005; **11**: 255-259
39 **Attallah AM**, Toson EA, Shiha GE, Omran MM, Abdel-Aziz MM, El-Dosoky I. Evaluation of serum procollagen aminoterminal propeptide III, laminin, and hydroxyproline as predictors of severe fibrosis in patients with chronic hepatitis C. *J Immunoassay Immunochem* 2007; **28**: 199-211
40 **Katayama M**, Funakoshi A, Sumii T, Sanzen N, Sekiguchi K. Laminin gamma2-chain fragment circulating level increases in patients with metastatic pancreatic ductal cell adenocarcinomas. *Cancer Lett* 2005; **225**: 167-176
41 **Gressner OA**, Weiskirchen R, Gressner AM. Biomarkers of liver fibrosis: clinical translation of molecular pathogenesis or based on liver-dependent malfunction tests. *Clin Chim Acta* 2007; **381**: 107-113

42 **Santos VN**, Leite-Mor MM, Kondo M, Martins JR, Nader H, Lanzoni VP, Parise ER. Serum laminin, type IV collagen and hyaluronan as fibrosis markers in non-alcoholic fatty liver disease. *Braz J Med Biol Res* 2005; **38**: 747-753

43 **Matteoni CA**, Younossi ZM, Gramlich T, Boparai N, Liu YC, McCullough AJ. Nonalcoholic fatty liver disease: a spectrum of clinical and pathological severity. *Gastroenterology* 1999; **116**: 1413-1419

44 **Ratziu V**, Giral P, Charlotte F, Bruckert E, Thibault V, Theodorou I, Khalil L, Turpin G, Opolon P, Poynard T. Liver fibrosis in overweight patients. *Gastroenterology* 2000; **118**: 1117-1123

45 **Liotta LA**, Rao CN, Wewer UM. Biochemical interactions of tumor cells with the basement membrane. *Annu Rev Biochem* 1986; **55**: 1037-1057

46 **AbouFarha KM**, Menheere PP, Nieman FH, Arends JW, Janknegt RA. Value of serum laminin P1 as a diagnostic and monitoring parameter in transitional cell carcinoma of the bladder. *Urol Int* 1992; **49**: 130-136

47 **Nakano T**, Iwahashi N, Maeda J, Hada T, Higashino K. Serum laminin P1 in small cell lung cancer: a valuable indicator of distant metastasis? *Br J Cancer* 1992; **65**: 608-612

48 **Rochlitz C**, Hasslacher C, Brocks DG, Herrmann R. Serum concentration of laminin, and course of the disease in patients with various malignancies. *J Clin Oncol* 1987; **5**: 1424-1429

49 **Saito N**, Kameoka S. Serum laminin is an independent prognostic factor in colorectal cancer. *Int J Colorectal Dis* 2005; **20**: 238-244

50 **Gao ZL**, Zhang C, Du GY, Lu ZJ. Clinical significance of changes in tumor markers, extracellular matrix, MMP-9 and VEGF in patients with gastric carcinoma. *Hepatogastroenterology* 2007; **54**: 1591-1595

51 **Qin LX**, Tang ZY. Recent progress in predictive biomarkers for metastatic recurrence of human hepatocellular carcinoma: a review of the literature. *J Cancer Res Clin Oncol* 2004; **130**: 497-513

52 **Burchardt ER**, Hein R, Bosserhoff AK. Laminin, hyaluronan, tenascin-C and type VI collagen levels in sera from patients with malignant melanoma. *Clin Exp Dermatol* 2003; **28**: 515-520

53 **Byers LJ**, Osborne JL, Carson LF, Carter JR, Haney AF, Weinberg JB, Ramakrishnan S. Increased levels of laminin in ascitic fluid of patients with ovarian cancer. *Cancer Lett* 1995; **88**: 67-72

54 **Chu Y**, Yang Y, Lin M, Wang Z. Detection of laminin in serum and ascites from patients with epithelial ovarian tumor. *J Huazhong Univ Sci Technolog Med Sci* 2002; **22**: 58-59, 68

55 **Catarino RM**, Lopes JD, Forones NM, Parise ER. Laminin concentration in ascites of patients with hepatic cirrhosis and peritoneal carcinomatosis. *Braz J Med Biol Res* 2005; **38**: 271-276

56 **Su Q**, Fu Y, Liu YF, Zhang W, Liu J, Wang CM. Laminin induces the expression of cytokeratin 19 in hepatocellular carcinoma cells growing in culture. *World J Gastroenterol* 2003; **9**: 921-929

57 **Yoshida K**, Tadaoka Y, Manabe T. Expression of laminin in hepatocellular carcinoma: an adjunct for its histological diagnosis. *Jpn J Clin Oncol* 1996; **26**: 70-76

S- Editor Li DL **L- Editor** Alpini GD **E- Editor** Yin DH

Online Submissions: wjg.wjgnet.com
wjg@wjgnet.com
doi:10.3748/wjg.14.3633

World J Gastroenterol 2008 June 21; 14(23): 3633-3641
World Journal of Gastroenterology ISSN 1007-9327
© 2008 The WJG Press. All rights reserved.

Adipokines and ghrelin in gastric cancer cachexia

Mustafa Kerem, Zafer Ferahkose, Utku Tonguc Yilmaz, Hatice Pasaoglu, Ebru Ofluoglu, Abdulkadir Bedirli, Bulent Salman, Tevfik Tolga Sahin, Murat Akin

Mustafa Kerem, Zafer Ferahkose, Utku Tonguc Yilmaz, Abdulkadir Bedirli, Bulent Salman, Tevfik Tolga Sahin, Murat Akin, Department of General Surgery, Medical Faculty, Gazi University, Besevler 06510, Ankara, Turkey
Hatice Pasaoglu, Ebru Ofluoglu, Department of Biochemistry, Medical Faculty, Gazi University, Besevler 06510, Ankara, Turkey
Author contributions: Kerem M and Ferahkose Z contributed equally to this work; Kerem M, Ferahkose Z, Yilmaz UT and Bedirli A designed research; Kerem M, Yilmaz UT, Salman B, Akin M, Pasaoglu H, Ofluoglu E and Sahin TT performed research; Kerem M, Salman B and Sahin TT analysed data; Kerem M, Ferahkose Z and Bedirli A wrote the paper.
Supported by Gazi University Scientific Research Projects Centers, No. 01/2006-37
Correspondence to: Mustafa Kerem, MD, Department of General Surgery, Faculty of Medicine, Gazi University, Besevler 06510, Ankara,
Turkey. keremm1@yahoo.com;mkerem@gazi.edu.tr
Telephone: +90-312-2025727 Fax: +90-312-2124647
Received: February 9, 2008 Revised: May 4, 2008
Accepted: May 11, 2008
Published online: June 21, 2008

Abstract

AIM: To investigate the roles of the adipocytokines, ghrelin and leptin in gastric cancer cachexia.

METHODS: Resistin, ghrelin, leptin, adiponectin, insulin and insulin-like growth factor (IGF-Ⅰ), were measured in 30 healthy subjects, and 60 gastric cancer patients of which 30 suffered from cancer-induced cachexia and 30 served as a control group. The relationships between hormones, body mass index (BMI) loss ratio, age, gender, and Glasgow Prognostic Score (GPS) were investigated.

RESULTS: Cachexia patients had higher tumor stage and GPS when compared with non-cachexia patients ($P < 0.05$). Ghrelin, resistin, leptin, adiponectin and IGF-Ⅰ, showed a significant correlation with BMI loss ratio and GPS ($P < 0.05$). A strong correlation was seen between GPS and BMI loss ($R = -0.570$, $P < 0.0001$). Multivariate analysis indicated that BMI loss was significantly independent as a predictor of ghrelin, resistin, leptin and IGF-Ⅰ ($P < 0.05$). Existence of an important significant relationship between resistin and insulin resistance was also noted.

CONCLUSION: These results showed that serum ghrelin, leptin, adiponectin, and IGF-Ⅰ play important roles in cachexia-related gastric cancers. No relationship was found between resistin and cancer cachexia. Also, because of the correlation between these parameters and GPS, these parameters might be used as a predictor factor.

© 2008 The WJG Press. All rights reserved.

Key words: Gastric cancer; Cachexia; Resistin; Ghrelin; Leptin; Adiponectin; Insuline

Peer reviewers: Shingo Tsuji, Professor, Department of Internal Medicine and Therapeutics, Osaka University Graduate School of Medicine(A8), 2-2 Yamadaoka, Suita, Osaka 565-0871, Japan; Reza Malekzadeh, Professor, Director, Digestive Disease Research Center, Tehran University of Medical Sciences, Shariati Hospital, Kargar Shomali Avenue, Tehran 19119, Iran

Kerem M, Ferahkose Z, Yilmaz UT, Pasaoglu H, Ofluoglu E, Bedirli A, Salman B, Sahin TT, Akin M. Adipokines and ghrelin in gastric cancer cachexia. *World J Gastroenterol* 2008; 14(23): 3633-3641 Available from: URL: http://www.wjgnet.com/1007-9327/14/3633.asp DOI: http://dx.doi.org/10.3748/wjg.14.3633

INTRODUCTION

Cachexia, characterized by marked weight loss, anorexia, asthenia and anemia, is often associated with the presence and growth of a tumor and leads to malnutrition secondary to the induction of anorexia or decreased food intake[1]. As major mediators of metabolism; growth hormone (GH) and insulin-like growth factor-Ⅰ (IGF-Ⅰ) have attracted many researchers in the field of cachexia associated gastrointestinal cancer[2,3]. Recent evidence suggests that an intricate interplay between multiple hypothalamic effector pathways and afferent hormonal signals of diverse systemic origin (resistin, leptin and adiponectin from adipocytes, ghrelin and polypeptides from the gastrointestinal tract, and insulin from the pancreas) is important in the regulation of energy intake and expenditure[4].

Ghrelin was discovered as the peptide hormone that stimulates the release of GH from the anterior pituitary and has crucial roles in the regulation of food intake and energy homeostasis in both humans and rodents[5]. It is produced primarily by the mammalian gastric enteroendocrine cells of the oxyntic mucosa, likely the

X/A-like cells[6]. It has been reported that there was an increase in the levels of total ghrelin in cachectic lung[7], breast and colon[8] cancer patients. Ghrelin infusion has recently been shown to increase appetite in subjects with cancer-induced cachexia[9]. Data on the association between ghrelin levels and gastric cancer cachexia are contradictory.

Leptin is a member of a group of adipocyte-secreted proteins, collectively known as the adipocytokines. Leptin acts in the central nervous system, particularly in the hypothalamus, to suppress food intake and stimulate energy expenditure[4]. Leptin levels were reported to be low in gastrointestinal[10] and pancreatic cancers[11], and high in breast and gynecologic cancer patients[12].

Resistin which is an 108-amino acid, 12.5-kDa peptide hormone member of the cysteine-rich secreted protein family, is also referred to as resistin-like molecules or "found in inflammatory zone" molecules. Resistin has mainly been studied in mice, in which there is compelling evidence linking the protein to insulin resistance, obesity, and type 2 diabetes mellitus[13]. There is only 55% amino acid homology between human and murine resistin, and findings have been inconclusive regarding a potential role of resistin in human insulin regulation, obesity and type 2 diabetes mellitus[14]. There is no information about the role of resistin in cancer cachexia.

Adiponectin is a member of the adipocytokine family. It is induced during adipocyte differentiation, and its secretion is stimulated by insulin and IGF- I [4]. A negative correlation between obesity and circulating adiponectin has been well established and adiponectin concentrations increase concomitantly with weight loss[15,16]. Although low adiponectin levels were reported among patients with weight-loss in advanced lung cancer[16], there was no correlation between adiponectin levels and cachexia in breast and colon cancer patients[8]. A more recent study demonstrated that an impaired response of adiponectin, ghrelin, and leptin may play a role in the pathogenesis of cancer cachexia with breast and colon cancer[8]. However, the role of adiponectin in gastric cancer patients is not clearly understood.

There is increasing evidence that the presence of a systemic inflammatory response, as evidenced by elevated concentrations of C-reactive protein (CRP), is a prognostic factor independent of stage, performance status and weight loss in patients with advanced cancer. Recently, Forrest *et al*[17,18] have shown that an elevated CRP and hypoalbuminemia may be combined to form a score, the Glasgow Prognostic score (GPS), which has prognostic value in patients with inoperable non-small-cell lung cancer.

The aim of the present study was to investigate: (1) the nature of the relationship between serum levels of resistin, leptin, adiponectin, ghrelin, and cancer related cachexia; (2) the relationship of these three hormones, insulin, IGF- I and insulin-resistance; and (3) to evaluate the relation between the hormones and GPS.

MATERIALS AND METHODS

The protocol was approved by the Gazi University Medical Faculty Ethics Committee and was conducted between October 2005 and December 2006. All clinical investigations described in this paper were conducted within the guidelines mentioned in The Declaration of Helsinki. Patients with a histopathological diagnosis of gastric adenocarcinoma were included in the study, while patients with gastric lymphoma and malignant stromal tumors were excluded from the study for homogenization. The contributors were informed of the nature of the study and informed consent was obtained.

Exclusion criteria

Patients were excluded if there was evidence of drug or alcohol abuse defined as any use of reactional drugs or more than two drinks per day; presence of congestive heart failure (ejection fraction < 35% on a echocardiogram or signs such as edema, dyspnea, or jugular venous distension); severe liver disease; severe chronic obstructive pulmonary disease; diabetes with hemoglobin A1c levels greater than 7%; fasting plasma glucose greater than 160 mg/dL or random glucose levels greater than 200 mg/dL; presence of thyroid diseases or renal failure; active infection (temperature > 38℃ or other signs or symptoms of infection); history of neuroendocrine tumor; use of glucocorticoids, progesterone, testosterone or other orexigenic agents; history of eating disorders or dysphagia; treatment by chemotherapy, radiotherapy, or a major operation within the last 6 mo prior to hospitalization; malignancy with an obstructing lesion in the cardia or antrum together or if patients refused consent.

Control group patients were chosen from healthy people over 40 years of age, because the majority of the patients were over 50 and most of the parameters studied in the study were affected by age.

Demographic findings and anthropometrical measurements

Clinical parameters obtained in the study included age, gender, BMI, cancer localization and staging, cachexia, performance status, and GPS. All pathology reports were evaluated and data on tumor histology were recorded. The extent of tumor spread was recorded using the American Joint Cancer Committee TNM Classification and Stage System. Patient height and weight were measured and BMI was calculated as body weight divided by height squared (kg/m^2). Patients were defined as cachectic, based on > 10% reduction in BMI within 6 mo prior to admission, as calculated from reported weight differences given by these subjects[1]. Performance status was evaluated by using the World Health Organization (WHO) performance status.

Analytical methods

Blood samples were drawn from each subject between 8 and 9 AM, after an overnight bed rest for measurement of the hormones, CRP, and fasting sugar, as well as a complete blood count and chemistry. All samples were stored at -80℃ until analytical measurements were

performed, except for glucose, which was determined immediately after blood was drawn.

Biochemical parameters

Routine laboratory measurements of hemoglobin, albumin and CRP were conducted. Serum glucose was measured using the glucose oxidase method. Homeostasis model assessment of insulin resistance (HOMA-IR) was calculated from fasting insulin and glucose levels [fasting glucose (millimoles per litre X fasting insulin microunits per millilitre)/22.5] as previously described[19].

Prealbumin

Prealbumin concentrations in the serum were determined using a commercial solid phase sandwich enzyme linked immuno-sorbent assay (ELISA) kit from Immundiagnostic® kit (Bensheim, Germany).

Hormone determination

Resistin, leptin, adiponectin, IGF- I, and insulin concentrations in serum were determined using a commercially available ELISA kit from RayBiotech® (Norcross, GA, USA). The intra- and interassay coefficients of variation were less than 7%-10% for all parameters.

Active ghrelin levels

For human ghrelin assessment, we used a RIA kit (Linco Research®, Missouri, USA) which incorporates an antibody that is specific for active ghrelin. The sensitivity was 100 pg/mL (in a 100 μL sample size) with a range of 100 to 10 000 pg/mL. The intra- and inter assay coefficients of variation were 5.63% and 16%, respectively.

Statistical analysis

All calculations and statistical tests were performed using SPSS (version 13.00 software, SPSS, Inc., Chicago, IL, USA). Descriptive data were expressed as mean ± SD. Categorical parameters were expressed as percentage. The study variables were compared between the study groups using Student *t*-tests or ANOVA for continuous variables and Fisher exact test for categorical variables. For multiple comparisons, the Tukey test was used. Pearson or Kendall's tau-b correlation coefficient was used to determine the relationship between continuous variables. Multiple linear regression analysis was performed to ascertain independent effects of BM, after adjustment for age, gender, and differentiation of tumor on adiponectin, ghrelin, leptin, and IGF- I levels. All significance tests were two-tailed.

RESULTS

Subjects characteristics and demographic finding

Sixty patients (30 cachectic and 30 non-cachectic), who satisfied study criteria, were selected from 76 gastric cancer patients admitted to our unit between the study dates.

The patient demographic characteristics are presented in Table 1. There was no significant difference between the ages of cachectic (63.6 ± 13.8), non-cachectic (55.6 ± 13.3), and control patients (56.4 ± 3.0). There was no difference with respect to gender within the three groups. While 60% of non-cachectic patients had stage 1 and 2 cancers, this rate was only 10% in cachectic patients. The majority of cachectic patients were stage 3 (40%) or 4 (50%) and in non-cachectic patients, this ratio was 25% and 15%, respectively ($P = 0.007$). None of the non-cachectic patients were inoperable. On the other hand, there were 2 inoperable patients (5%) in the cachectic group ($P < 0.05$). There was no difference between the two groups according to tumor location and differentiation ($P = 0.369$). While the WHO score for gastric cancer patients was significantly worse than the control group ($P < 0.001$), there was no significant difference between the WHO scores of cachectic and non-cachectic groups ($P = 0.108$). Baseline biochemical findings and changes in BMI and weights are listed in Table 2. Changes in BMI and weight were significantly higher in cachectic patients than the non-cachectic patients ($P < 0.001$). Hb levels of cachectic patients were significantly lower than the levels of control and non cachectic patients ($P < 0.001$). There were no significant differences in the levels of TSH, AST, creatinine, WBC or lymphocytes in the three groups.

Ghrelin

Mean ghrelin levels were significantly elevated in cachectic patients compared with non-cachectic cancer patients and healthy control subjects (2 305 ± 818 ng/mL *vs* 1980 ± 913 ng/mL, and 1332 ± 620 ng/mL, respectively, $P = 0.013$; Table 3). No significant difference in ghrelin levels between non-cachexia and healthy control groups was observed.

A significant negative correlation was found between the serum ghrelin levels and BMI loss in the previous 6 mo ($R = -0.439$, $P = 0.008$, Figure 1A). There was also a positive significant correlation between the serum ghrelin levels and age ($R = 0.467$, $P = 0.039$, Table 4), and GPS ($R = 0.327$, $P = 0.002$).

Resistin

Mean resistin levels were significantly elevated in cachectic patients compared with non-cachectic cancer patients and healthy control subjects ($P = 0.013$). It was found that resistin levels in non-cachectic gastric cancer patients were significantly higher than the control group ($P = 0.042$, Table 3). A significant negative correlation was found between the serum ghrelin levels and BMI loss in the previous 6 mo ($R = -0.574$, $P < 0.001$, Figure 1B), and GPS ($R = 0.387$, $P < 0.01$, Table 4). There was also a significant correlation between the serum resistin levels and insulin ($R = 0.348$, $P = 0.016$), glucose ($R = 0.418$, $P = 0.0018$), and HOMA-IR ($R = 0.518$, $P = 0.0001$, Table 4).

Adiponectin

The average serum adiponectin levels were 36.5 ± 15.0 μg/mL in patients with cachectic gastric cancer,

Table 1 Clinical characteristics of the subjects (n = 30)

	Healthy controls	Patients with gastric cancer		*P* value
		Non-cachexia	Cachexia	
Age (mean ± SD)	56.4 ± 3.0	55.8 ± 13.3	63.6 ± 13.8	0.001[1]
Gender (%)				0.344[2,3]
Male	20 (67)	25 (84)	23 (77)	
Female	10 (33)	5 (16)	7 (23)	
Tumor stage (%)				0.007[2]
Ⅰ	-	6 (20)	0	
Ⅱ	-	12 (40)	3 (10)	
Ⅲ	-	8 (25)	12 (40)	
Ⅳ	-	4 (15)	15 (50)	
Tumor differentiation				0.347[2]
Differentiated		26 (87)	23 (77)	
Undifferentiated		4 (13)	7 (23)	
Operability				0.351[2]
Operable/No operable	-	30/0	28/2	
Localization (%)				0.369[2]
Cardia	-	3 (10)	2 (6)	
Corpus	-	6 (20)	10 (34)	
Fundus	-	3 (10)	0	
Antrum		18 (60)	18 (60)	
WHO performance status (%)				0.108[2], < 0.001[3]
0	30 (100)	9 (30)	3 (10)	
1	0	14 (45)	11 (36)	
2	0	6 (20)	6 (20)	
3	0	0	7 (24)	
4	0	1 (5)	3 (10)	
GPS				< 0.001[2,3]
0	30 (100)	18 (60)	1 (5)	
1	0	12 (40)	17 (55)	
2	0	0	12 (40)	

[1]Patients with gastric cancer *vs* healthy control (ANOVA); [2]Cachexia *vs* non-cachexia (χ^2); [3]Cachexia and non-cachexia *vs* healthy control (χ^2).

Table 2 Changes in BMI and body weight and baseline biochemical findings (n = 30, mean ± SD)

	Healthy controls (n = 30)	Patients with gastric cancer		*P* value (between groups) (ANOVA)
		Non-cachexia (n = 30)	Cachexia (n = 30)	
Initial BMI (kg/m^2)	25.3 ± 2.3	27 ± 5.1	26.3 ± 2.5	0.985
Final BMI (kg/m^2)	26.7 ± 2.8	24.8 ± 5.0	20.3 ± 2.5[a]	0.002
Change BMI (%)	1.26 ± 2.6	-4.0 ± 2.4[c]	-5.7 ± 5.2[a]	< 0.001
Initial weight (kg)	75.4 ± 11.0	73.8 ± 13.3	70.0 ± 12.3	0.436
Final weight (kg)	76.2 ± 10.2	70.8 ± 16.3[c]	53.6 ± 13.0[a]	0.001
Change weight (kg)	0.15 ± 0.76	-2.9 ± 1.5[c]	-10.4 ± 3.3[a]	< 0.001
Hb (gr/L)	12.8 ± 2.8	12.6 ± 1.9	11.1 ± 1.3[a]	< 0.001
TSH (mIU/mL)	1.96 ± 0.28	1.98 ± 0.85	2.11 ± 0.11	0.492
AST (IU/L)	23.3 ± 8.3	28.7± 8.2	26.5 ± 5.1	0.088
Creatinine (mg/dL)	0.81 ± 0.36	1.03 ± 0.27	0.97 ± 0.28	0.085
WBC (× 10^9)	6.9 ± 1.2	7.1 ± 2.1	7.0 ± 2.2	0.230
Lymphocytes (%)	22.3 ± 4.2	24.3 ± 3.8	23.98 ± 4.8	0.156

[a]P < 0.05 *vs* healthy controls and non cachexia; [c]P < 0.05 *vs* healthy controls.

22.6 ± 12.4 μg/mL in healthy controls, and 27.8 ± 11.9 μg/mL in the non-cachexia group. Thus, there was a significant difference between the cachexia group and healthy and non-cachexia groups (P = 0.006, Table 3). However, there was no significant difference between the serum adiponectin levels of healthy and non-cachectic controls.

The association between adiponectin levels and BMI loss in the last 6 mo is plotted in Figure 1C. A significant negative correlation was found between the serum adiponectin levels and BMI changes in the previous 6 mo (R = -0.283, P = 0.028). Adiponectin showed a strong positive correlation with GPS (R = 0.241, P = 0.008).

Leptin

Cachectic gastric cancer patients had significantly higher serum leptin levels than healthy controls and non-cachectic gastric cancer patients (3 405 ± 640 pg/mL

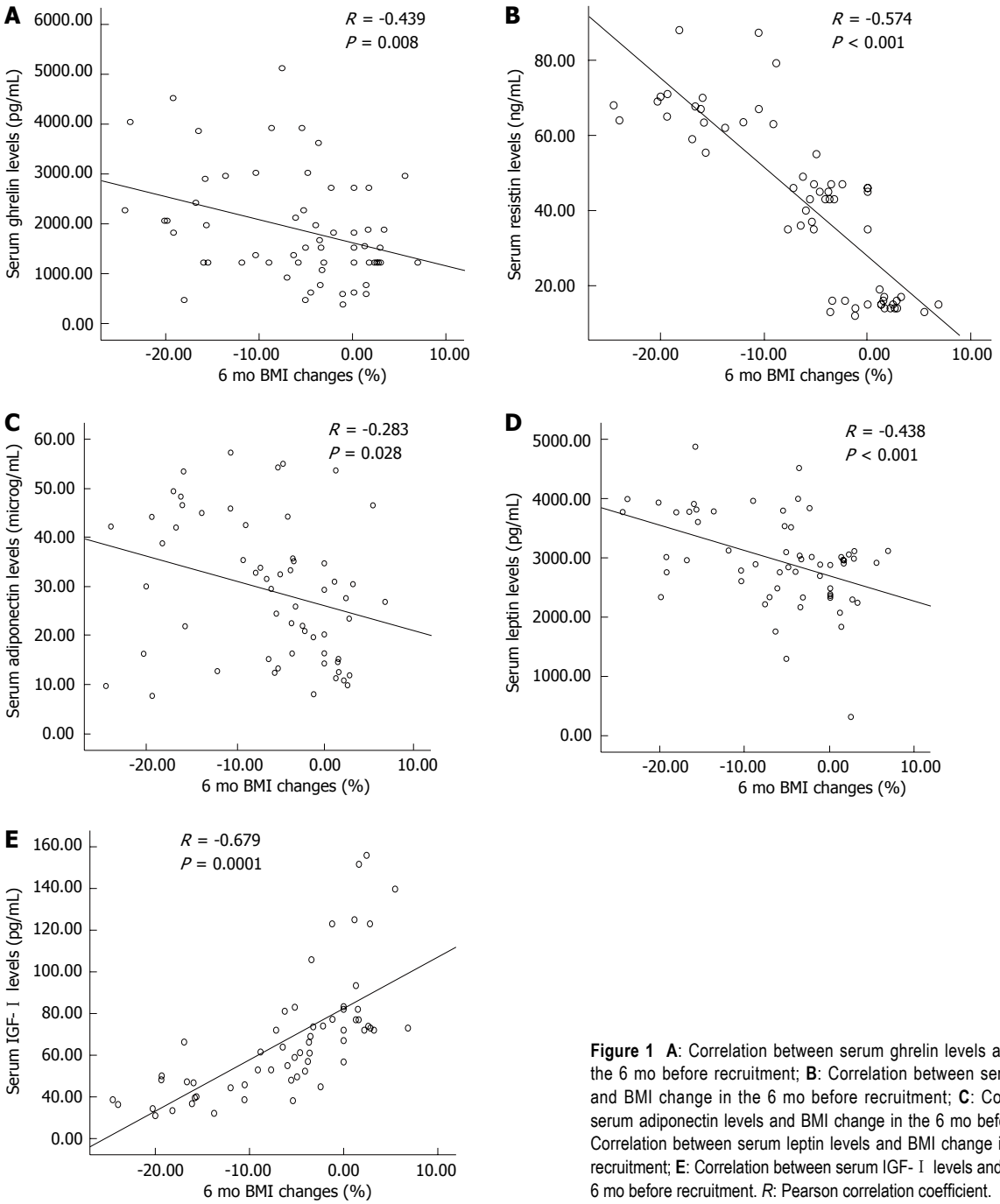

Figure 1 **A**: Correlation between serum ghrelin levels and BMI change in the 6 mo before recruitment; **B**: Correlation between serum resistin levels and BMI change in the 6 mo before recruitment; **C**: Correlation between serum adiponectin levels and BMI change in the 6 mo before recruitment; **D**: Correlation between serum leptin levels and BMI change in the 6 mo before recruitment; **E**: Correlation between serum IGF-I levels and BMI change in the 6 mo before recruitment. *R*: Pearson correlation coefficient.

vs 2623 ± 665 pg/mL and 2 810 ± 818 pg/mL, respectively, $P = 0.003$, Table 3). No significant differences in serum leptin levels between non-cachexia and healthy control groups were observed. A significant negative correlation was found between leptin levels and BMI loss in the previous 6 mo ($R = -0.438$, $P < 0.001$, Figure 1D). Leptin also showed a strong positive correlation with GPS ($R = 0.303$, $P = 0.003$).

Albumin, prealbumin, CRP, and GPS

Albumin and prealbumin, markers of nutritional status, were lower in gastric cancer patients when compared with healthy and non-cachectic subjects ($P = 0.03$, $P = 0.001$, respectively). The mean CRP levels were significantly higher in cachexia patients than the levels of healthy and non-cachexia controls ($P < 0.001$). CRP levels also increased significantly in non-cachectic and healthy subjects ($P < 0.05$, Table 3). The average GPS was significantly higher in cachexia patients than non-cachectic cancer patients and healthy controls ($P < 0.001$). BMI loss in last 6 mo showed a strong negative correlation with GPS ($R = -0.758$, $P < 0.0001$) and CRP ($R = -0.570$, $P < 0.0001$), however, a positive correlation with prealbumin ($R = 0.302$, $P = 0.019$).

Glucose, insulin, and HOMA-IR

Fasting glucose levels increased borderline significantly in cachectic patients compared with the healthy and non-cachectic patients ($P = 0.05$). Insulin levels were increased in non-cachectic gastric cancer patients when

Table 3 All biochemical parameters in blood in whole subjects are shown

	Healthy controls (n = 30)	Patients with gastric cancer		P-value (between groups) (ANOVA)
		Non-cachexia (n = 30)	Cachexia (n = 30)	
Albumin (gr/dL)	4.2 ± 0.2	4.0 ± 0.5	2.9± 0.2[a]	0.03
CRP (mg/L)	5.95 ± 0.8	9.72 ± 4.3[e]	12.9 ± 2.2[a]	< 0.001
Prealbumin (ng/mL)	52.5 ± 8.3	49.2 ± 6.4	41.0 ± 12.3[a]	0.001
Fasting glucose (mg/dL)	102.7 ± 8.3	105.7 ± 13.7	114.3 ± 13.8[a]	0.005
Insulin (μIU/mL)	21.8 ± 9.0	24.4 ± 6.3	18.4 ± 6.0[c]	0.04
HOMA-IR	5.58 ± 2.55	6.58 ± 1.89	5.05 ±1.68	0.07
IGF-1 (pg/mL)	95.0 ± 30.1	63.1 ± 13.1[e]	43.8 ± 9.5[a]	< 0.001
Resistin (ng/mL)	18.1	43.4[e]	66.7[a]	< 0.001
Ghrelin (ng/ml)	1332 ± 620	1980 ± 913	2305 ± 818[a]	< 0.001
Adiponectin (μg/mL)	22.6 ± 12.4	27.8 ± 11.9	36.5 ± 15.0[a]	0.045
Leptin (pg/mL)	2810 ± 818	2623 ± 665	3405 ± 640	0.003

[a]P < 0.05 *vs* healthy controls and non cachexia; [c]P < 0.05 *vs* non-cachexia; [e]P < 0.05 *vs* healthy controls.

Table 4 Bivariate correlation analysis between different hormones and age, GPS and other parameters

		Resistin	Ghrelin	Leptin	Adiponectin	IGF- I
Age	R	0.115	0.267[a]	0.253	-0.092	-0.331[a]
	P	0.687	0.039[a]	0.051	0.486	0.010[a]
GPS	R	0.387[a]	0.327[a]	0.303[a]	0.241[a]	0.363[a]
	P	0.0017[a]	0.002[a]	0.003[a]	0.019[a]	0.004[a]
Insulin	R	0.348[a]	-0.126	-0.225	0.197	0.06
	P	0.016[a]	0.339	0.084	0.132	0.905
Glucose	R	0.418[a]	0.194	-0.324[a]	0.172	-0.358[a]
	P	0.0018[a]	0.138	0.012[a]	0.190	0.005[a]
HOMA-IR	R	0.518[a]	-0.100	-0.181	-0.094	0.073
	P	0.0001[a]	0.449	0.166	0.475	0.581
Prealbumin	R	-0.218	-0.223	-0.097	-0.341[a]	0.287[a]
	P	0.082	0.087	0.461	0.008[a]	0.026[a]

P: Pearson correlation coefficient; R: Kendall's tau-b correlation coefficient. Significantly correlations and [a]P < 0.05.

compared with cachectics (P = 0.04); however, there was no significant difference between non-cachectic cancer patients and healthy subjects (P > 0.05). After adjusting for the presence of diabetes mellitus, HOMA-IR values were not significantly different between groups. Only glucose showed an inverse significant correlation with BMI loss in 6 mo (R = -0.324, P = 0.012).

IGF- I

IGF- I levels significantly decreased in cachectic subjects compared with healthy and non-cachectic subjects (43.8 ± 9.5 pg/mL *vs* 95.0 ± 30.1 pg/mL and 63.1 ± 13.1 pg/mL; P < 0.05). Moreover, there was a significant difference in IGF- I levels between healthy and non-cachectic cancer patients (63.1 ± 13.1 pg/mL *vs* 43.8 ± 9.5 pg/mL; P < 0.05, Figure 1E). IGF- I also showed a positive correlation with BMI loss in the previous 6 mo (R = -0.679, P < 0.0001, Figure 1E) and GPS (R = 0.363, P = 0.004); negative correlations with age (R = -0.331, P =0.01) and fasting glucose (R = -0.358, P = 0.005, Table 4) were observed.

Multivariate analysis results

Multiple regression analysis was used to evaluate the role of BMI loss as a continuous variable, along with age, gender, and BMI change to predict ghrelin, resistin, leptin, adiponectin, and IGF- I levels. The results of the regression model indicated that age was not a significant predictor of hormone levels. Gender was a negative independent significant predictor for leptin, and BMI was found to be a negative independent significant predictor for all parameters, except adiponectin (Table 5).

Table 5 Multiple regression analysis with age, BMI change, gender, and tumor differentiation as predictors of ghrelin, leptin, adiponectin, and IGF- I in gastric cancer patients

		Resistin	Ghrelin	Leptin	Adiponectin	IGF- I
Age	β	0.148	0.168	0.019	-0.323	0.115
	P	0.402	0.305	0.899	0.053	0.377
Gender	β	0.126	0.286	-0.339[a]	0.057	0.073
	P	0.387	0.085	0.032[a]	0.726	0.377
BMI change	β	-0.583[a]	-0.318[a]	-0.418[a]	-0.202	0.699[a]
	P	0.001[a]	0.009[a]	0.008[a]	0.21	< 0.0001[a]

β: Standardized coefficient. Significant regression analysis and [a]P < 0.05 are shown.

DISCUSSION

In this prospective study, BMI loss in gastric cancer patients negatively correlated with serum active ghrelin, resistin, adiponectin and leptin levels, but positively correlated with the level of serum IGF- I . It was also noted that there was a correlation between resistin which was found to be high in cachectic patients, and insulin resistance, insulin and blood glucose.

Ghrelin an anabolic hormone, has several roles in metabolism, appetite, nutrition, weight gain, gastric motility, and gastric emptying. In addition, it has an important role in the regulation of synthesis of GH, IGF- I , insulin, and leptin[4-6]. Total ghrelin levels in cachectic patients with colon, breast and lung cancer were significantly higher than the levels in non-cachectic patients[7,8]. Garcia *et al*[20] showed that the ratio of active to total ghrelin levels increased in cancer-induced cachexia. In the same study, it was stated that the increase in active ghrelin levels could have been explained by ghrelin resistance. As the ratio of active/total ghrelin levels were

in favor of active ghrelin in cancer cachexia, we evaluated active ghrelin levels. Our study showed that active ghrelin levels were higher in healthy subjects and non-cachectic cancer patients, especially females. Although we were not able to confirm the ghrelin resistance mentioned by Garcia *et al*[20], we saw the indirect effects. Under normal conditions, endogenous ghrelin increases GH secretion and indirectly increases IGF- I by stimulation of its own receptors. However in our study, the existence of a negative correlation between decreased IGF- I and ghrelin may show that efficiency decreases while the levels of active ghrelin increase. These findings support the presence of ghrelin resistance. It is also possible that ghrelin levels could increase to compensate for the increased metabolic rate and energy need, which was hypothesized by Nagaya *et al*[21] Several experimental studies have shown that ghrelin has an important role in the regulation of insulin *via* controlling pancreatic endocrine functions[22,23]. No significant relationship between ghrelin and insulin, fasting glucose level and HOMA-IR were found in the present study.

Resistin is a member of the newly discovered family of cysteine-rich secretory proteins, called resistin-like proteins. The role of resistin in pathogenesis of insulin resistance remains questionable, with conflicting data in animal models and negative findings in clinical observation[13,14]. The role of insulin resistance in cancer cachexia occurrence is not fully understood[1,2]. From this point of view, it came to mind whether resistin can have effect in gastric cancer cachexia occurrence. There are no clinical studies of serum resistin levels in cancer cachexia. It has been shown that serum resistin levels are high in lymphoma patients[24], but the resistin-tumor cachexia relationship was not investigated in this study. From this point of view, our study is the first study in the literature. We found that serum resistin levels in cachectic gastric cancer patients were significantly higher than the noncachectic patients and healthy controls. Resistin showed negative correlation with BMI loss. The effect of resistin on cachexia is probably due to insulin resistance and ineffective usage of glucose. The existence of a correlation between serum resistin levels and insulin, insulin resistance and blood glucose levels supports this idea[25]. The role of leptin in modulating the immune response and inflammation has become increasingly evident and has been reviewed recently[26,27]. Complex interactions among the nervous, endocrine and immune systems affect the leptin loop and the potential role of these mediators in cancer-related cachexia-anorexia syndrome[8,11,12]. Wallace *et al*[10] showed that serum levels of leptin did not differ between normal subjects and patients with gastrointestinal cancer. Other studies have shown that there is a relationship between cachexia and leptin levels in pancreatic, lung, breast, and colon cancer patients[8,11,12]. Wolf *et al*[8] showed that changes in leptin levels in cancer cachexia were significantly higher. Our results were similar to this last study. It is known that leptin receptors are found in β islet cells of the pancreas and inhibit insulin secretion[28,29]. However, our study revealed that there was a reverse correlation between leptin and fasting glucose levels, whereas no relation was found between leptin, insulin resistance, and insulin levels.

It also has been showed that insulin resistance and low serum IGF- I levels are important factors for cancer cachexia. These hormones are strongly anabolic and increase muscle protein synthesis[1,2]. IGF- I concentrations increase with growth hormone and testosterone administration, thereby accounting for some of the effects of these hormones on muscle bulk and strength. Low IGF- I concentrations in malnourished humans suggest a role for IGF- I in the pathogenesis of cachexia[30]. These findings showed that IGF- I was one of the most important factors in the gastric cancer cachexia.

GPS was found to be an important parameter for determining the prognosis of advanced cancers[17,18]. In our study, besides the strong correlation between GPS and BMI loss, significant correlations were found between the GPS and the levels of hormones and cytokines which could be very important for clinical evaluation. GPS which is calculated using routine measurements of albumin and CRP can help us in evaluation and management of the cancer cachexia in clinical practice.

Adiponectin, which has an obvious anti-inflammatory effect, is inversely related to weight gain[4]. Serum adiponectin levels were low in cases with increased insulin resistance like obesity, type 2 diabetics, and non-alcoholic fatty liver diseases[30]. However, serum adiponectin levels decreased in patients who lost weight voluntarily. High adiponectin levels are risk factors for endometrial and breast cancer, whereas low levels are risk factors for gastric cancers[31,32]. No relationship was found between adiponectin and cachexia in breast and colon cancer. In our study, a significant positive correlation was found between adiponectin and BMI loss, but multivariate analysis did not show BMI loss as predictive for adiponectin. Adiponectin, which is predominantly secreted from adipose tissues, might have increased due to lipolysis which occurred with muscle loss in the catabolic state. No correlation was found between adiponectin, whose close relationship with insulin resistance was known, and insulin, blood glucose levels, HOMA-IR, or IGF- I [4].

As a result, cachexia in gastric cancer is a complex process in which ghrelin, resistin, leptin, adiponectin, and IGF- I function. It is of note that these hormones have important roles in occurrence of cachexia in gastric cancer patients. This study will be one of the corner stones of the further studies about prevention and treatment of cachexia.

COMMENTS

Background

Adipocytokines are the peptide hormones secreted from adipocytes and have special roles in regulation of metabolism, glucose metabolism, and inflammation. Ghrelin which is secreted from especially from the gastric fundus has roles in regulation of blood glucose level, appetite and secretion of growth hormone. In this study, the role of adiponectin, ghrelin, and insulin like growth factor in gastric cancer patients with cachexia is evaluated.

Research frontiers

Significant correlation between cachexia and ghrelin, leptin adiponectin and IGF-Ⅰ can inform more sophisticated studies about the mechanism of cachexia. Despite sufficient nutritional support, cachexia is always an expected morbidity in cancer patients. This study will help future studies about the pathophysiology of the cachexia.

Innovations and breakthroughs

Although there have been several studies concerning nutritional support and measurement of cachexia in cancer patients, there have not been many studies about the pathophysiology. It is important to understand the behaviour of cancer with cachexia and also to support the patient. Several factors contributing to cancer biology demand attention. However, this study is original for being the first evaluating the correlation between cancer cachexia and resistin. The relationship between adipocytokines and colon, lung and breast cachexia have been studied before. This study has investigated the relationship between gastric cancer cachexia and adipocytokines.

Applications

To date, the treatment of cancer cachexia has gone no further than nutritional and fluid-electrolyte support. Alternative treatment modalities may be identified if the role of hormones and peptides in cachexia is well-understood. For example, administration of recombinant ghrelin induces growth hormone secretion and appetite.

Terminology

Adipocytokines are secreted from adipocytes. They are peptide hormones that have systemic effect. For example: resistin, adiponectin, leptin, *etc.* Cachexia means loss of lipid, carbohydrate and protein in a short time.

Peer review

This paper investigated resistin, ghrelin, leptin, adiponectin, insulin, IGF-Ⅰ in gastric cancer subjects with and without cachexia and healthy controls. Ghrelin, resistin, adiponectin significantly differed between subjects with and without cachexia. The study was well described and appropriately presented. It's an important study.

REFERENCES

1 **Tisdale MJ**. Cachexia in cancer patients. *Nat Rev Cancer* 2002; **2**: 862-871

2 **Yoshikawa T**, Noguchi Y, Doi C, Makino T, Nomura K. Insulin resistance in patients with cancer: relationships with tumor site, tumor stage, body-weight loss, acute-phase response, and energy expenditure. *Nutrition* 2001; **17**: 590-593

3 **Huang Q**, Nai YJ, Jiang ZW, Li JS. Change of the growth hormone-insulin-like growth factor-I axis in patients with gastrointestinal cancer: related to tumour type and nutritional status. *Br J Nutr* 2005; **93**: 853-858

4 **Meier U**, Gressner AM. Endocrine regulation of energy metabolism: review of pathobiochemical and clinical chemical aspects of leptin, ghrelin, adiponectin, and resistin. *Clin Chem* 2004; **50**: 1511-1525

5 **Kojima M**, Hosoda H, Date Y, Nakazato M, Matsuo H, Kangawa K. Ghrelin is a growth-hormone-releasing acylated peptide from stomach. *Nature* 1999; **402**: 656-660

6 **Gualillo O**, Lago F, Gomez-Reino J, Casanueva FF, Dieguez C. Ghrelin, a widespread hormone: insights into molecular and cellular regulation of its expression and mechanism of action. *FEBS Lett* 2003; **552**: 105-109

7 **Shimizu Y**, Nagaya N, Isobe T, Imazu M, Okumura H, Hosoda H, Kojima M, Kangawa K, Kohno N. Increased plasma ghrelin level in lung cancer cachexia. *Clin Cancer Res* 2003; **9**: 774-778

8 **Wolf I**, Sadetzki S, Kanety H, Kundel Y, Pariente C, Epstein N, Oberman B, Catane R, Kaufman B, Shimon I. Adiponectin, ghrelin, and leptin in cancer cachexia in breast and colon cancer patients. *Cancer* 2006; **106**: 966-973

9 **Neary NM**, Small CJ, Wren AM, Lee JL, Druce MR, Palmieri C, Frost GS, Ghatei MA, Coombes RC, Bloom SR. Ghrelin increases energy intake in cancer patients with impaired appetite: acute, randomized, placebo-controlled trial. *J Clin Endocrinol Metab* 2004; **89**: 2832-2836

10 **Wallace AM**, Kelly A, Sattar N, McArdle CS, McMillan DC. Circulating concentrations of "free" leptin in relation to fat mass and appetite in gastrointestinal cancer patients. *Nutr Cancer* 2002; **44**: 157-160

11 **Brown DR**, Berkowitz DE, Breslow MJ. Weight loss is not associated with hyperleptinemia in humans with pancreatic cancer. *J Clin Endocrinol Metab* 2001; **86**: 162-166

12 **Bolukbas FF**, Kilic H, Bolukbas C, Gumus M, Horoz M, Turhal NS, Kavakli B. Serum leptin concentration and advanced gastrointestinal cancers: a case controlled study. *BMC Cancer* 2004; **4:** 29

13 **Steppan CM**, Bailey ST, Bhat S, Brown EJ, Banerjee RR, Wright CM, Patel HR, Ahima RS, Lazar MA. The hormone resistin links obesity to diabetes. *Nature* 2001; **409**: 307-312

14 **Kusminski CM**, McTernan PG, Kumar S. Role of resistin in obesity, insulin resistance and Type II diabetes. *Clin Sci* (Lond) 2005; **109**: 243-256

15 **Faraj M**, Havel PJ, Phelis S, Blank D, Sniderman AD, Cianflone K. Plasma acylation-stimulating protein, adiponectin, leptin, and ghrelin before and after weight loss induced by gastric bypass surgery in morbidly obese subjects. *J Clin Endocrinol Metab* 2003; **88**: 1594-1602

16 **Jamieson NB**, Brown DJ, Michael Wallace A, McMillan DC. Adiponectin and the systemic inflammatory response in weight-losing patients with non-small cell lung cancer. *Cytokine* 2004; **27**: 90-92

17 **Forrest LM**, McMillan DC, McArdle CS, Angerson WJ, Dunlop DJ. Comparison of an inflammation-based prognostic score (GPS) with performance status (ECOG) in patients receiving platinum-based chemotherapy for inoperable non-small-cell lung cancer. *Br J Cancer* 2004; **90**: 1704-1706

18 **Forrest LM**, McMillan DC, McArdle CS, Angerson WJ, Dunlop DJ. Evaluation of cumulative prognostic scores based on the systemic inflammatory response in patients with inoperable non-small-cell lung cancer. *Br J Cancer* 2003; **89**: 1028-1030

19 **Matthews DR**, Hosker JP, Rudenski AS, Naylor BA, Treacher DF, Turner RC. Homeostasis model assessment: insulin resistance and beta-cell function from fasting plasma glucose and insulin concentrations in man. *Diabetologia* 1985; **28**: 412-419

20 **Garcia JM**, Garcia-Touza M, Hijazi RA, Taffet G, Epner D, Mann D, Smith RG, Cunningham GR, Marcelli M. Active ghrelin levels and active to total ghrelin ratio in cancer-induced cachexia. *J Clin Endocrinol Metab* 2005; **90**: 2920-2926

21 **Nagaya N**, Uematsu M, Kojima M, Date Y, Nakazato M, Okumura H, Hosoda H, Shimizu W, Yamagishi M, Oya H, Koh H, Yutani C, Kangawa K. Elevated circulating level of ghrelin in cachexia associated with chronic heart failure: relationships between ghrelin and anabolic/catabolic factors. *Circulation* 2001; **104**: 2034-2038

22 **Prado CL**, Pugh-Bernard AE, Elghazi L, Sosa-Pineda B, Sussel L. Ghrelin cells replace insulin-producing beta cells in two mouse models of pancreas development. *Proc Natl Acad Sci USA* 2004; **101**: 2924-2929

23 **Wierup N**, Yang S, McEvilly RJ, Mulder H, Sundler F. Ghrelin is expressed in a novel endocrine cell type in developing rat islets and inhibits insulin secretion from INS-1 (832/13) cells. *J Histochem Cytochem* 2004; **52**: 301-310

24 **Pamuk GE**, Demir M, Harmandar F, Yesil Y, Turgut B, Vural O. Leptin and resistin levels in serum of patients with hematologic malignancies: correlation with clinical characteristics. *Exp Oncol* 2006; **28**: 241-244

25 **Burcelin R**. Leptin and resistin: master enemy adipokines unified in brain to control glucose homeostasis. *Endocrinology* 2008; **149**: 443-444

26 **La Cava A**, Matarese G. The weight of leptin in immunity. *Nat Rev Immunol* 2004; **4**: 371-379

27 **Kieffer TJ**, Heller RS, Habener JF. Leptin receptors expressed on pancreatic beta-cells. *Biochem Biophys Res Commun* 1996; **224**: 522-527

28 **Ahren B**, Havel PJ. Leptin inhibits insulin secretion induced

by cellular cAMP in a pancreatic B cell line (INS-1 cells). *Am J Physiol* 1999; **277**: R959-R966

29 **Arita Y**, Kihara S, Ouchi N, Takahashi M, Maeda K, Miyagawa J, Hotta K, Shimomura I, Nakamura T, Miyaoka K, Kuriyama H, Nishida M, Yamashita S, Okubo K, Matsubara K, Muraguchi M, Ohmoto Y, Funahashi T, Matsuzawa Y. Paradoxical decrease of an adipose-specific protein, adiponectin, in obesity. *Biochem Biophys Res Commun* 1999; **257**: 79-83

30 **Dal Maso L**, Augustin LS, Karalis A, Talamini R, Franceschi S, Trichopoulos D, Mantzoros CS, La Vecchia C. Circulating adiponectin and endometrial cancer risk. *J Clin Endocrinol Metab* 2004; **89**: 1160-1163

31 **Miyoshi Y**, Funahashi T, Kihara S, Taguchi T, Tamaki Y, Matsuzawa Y, Noguchi S. Association of serum adiponectin levels with breast cancer risk. *Clin Cancer Res* 2003; **9**: 5699-5704

32 **Ishikawa M**, Kitayama J, Kazama S, Hiramatsu T, Hatano K, Nagawa H. Plasma adiponectin and gastric cancer. *Clin Cancer Res* 2005; **11**: 466-472

S- Editor Li DL **L- Editor** Lalor PF **E- Editor** Yin DH

Online Submissions: wjg.wjgnet.com
wjg@wjgnet.com
doi:10.3748/wjg.14.3642

World J Gastroenterol 2008 June 21; 14(23): 3642-3649
World Journal of Gastroenterology ISSN 1007-9327
© 2008 The WJG Press. All rights reserved.

LIVER CANCER

Secretory Transactivating Transcription-apoptin fusion protein induces apoptosis in hepatocellular carcinoma HepG2 cells

Su-Xia Han, Jin-Lu Ma, Yi Lv, Chen Huang, Hai-Hua Liang, Kang-Min Duan

Su-Xia Han, Hai-Hua Liang, Kang-Min Duan, College of Life Sciences, Northwest University, Xi'an 710069, Shaanxi Province, China
Su-Xia Han, Jin-Lu Ma, Yi Lv, the First Affiliated Hospital; College of Medicine, Xi'an Jiaotong University, Xi'an 710061, Shaanxi Province, China
Chen Huang, College of Medicine, Xi'an Jiaotong University, Xi'an 710061, Shaanxi Province, China
Author contributions: Duan KM, Han SX, Ma JL, and Lv Y designed the research; Han SX, Ma JL, Lv Y, and Huang C performed the research; Han SX, Ma JL and Liang HH analyzed the data; and Han SX, Ma JL and Duan KM wrote the paper.
Supported by the National Natural Science Foundation of China, No. 30672069 and No. 30470098
Correspondence to: Kang-Min Duan, College of Life Sciences, Northwest University, 229 Taibai Rd. North, Xi'an 710069, Shaanxi Province, China. kduan@ucalgary.ca
Telephone: +86-29-88302132 Fax: +86-29-88305288
Received: February 22, 2008 Revised: April 16, 2008
Accepted: April 23, 2008
Published online: June 21, 2008

Abstract

AIM: To determine whether SP-TAT-apoptin induces apoptosis and also maintains its tumor cell specificity.
METHODS: In this study, we designed a secretory protein by adding a secretory signal peptide (SP) to the N terminus of Transactivating Transcription (TAT)-apoptin (SP-TAT-apoptin), to test the hypothesis that it gains an additive bystander effect as an anti-cancer therapy. We used an artificial human secretory SP whose amino acid sequence and corresponding cDNA sequence were generated by the SP hidden Markov model.
RESULTS: In human liver carcinoma HepG2 cells, SP-TAT-apoptin expression showed a diffuse pattern in the early phase after transfection. After 48 h, however, it translocated into the nuclear compartment and caused massive apoptotic cell death, as determined by 3-(4,5-dimethylthiazole-2-yl)-2,5-diphenyltetrazolium bromide (MTT) assay and annexin-V binding assay. SP-TAT-apoptin did not, however, cause any cell death in non-malignant human umbilical vein endothelial cells (HUVECs). Most importantly, the conditioned medium from Chinese hamster ovary (CHO) cells transfected with SP-TAT-apoptin also induced significant cell death in HepG2 cells, but not in HUVECs.
CONCLUSION: The data demonstrated that SP-TAT-apoptin induces apoptosis only in malignant cells, and its secretory property might greatly increase its potency once it is delivered *in vivo* for cancer therapy.

© 2008 The WJG Press. All rights reserved.

Key words: Apoptin; Apoptosis; Hepatoma; Human immunodeficiency Virus-Transactivating Transcription protein; Secretory

Peer reviewer: Gianluigi Giannelli, MD, Dipartimento di Clinica Medica, Immunologia e Malattie Infettive, Sezione di Medicina Interna, Policlinico, Piazza G. Cesare 11, 70124 Bari, Italy

Han SX, Ma JL, Lv Y, Huang C, Liang HH, Duan KM. Secretory Transactivating Transcription-apoptin fusion protein induces apoptosis in hepatocellular carcinoma HepG2 cells. *World J Gastroenterol* 2008; 14(23): 3642-3649 Available from: URL: http://www.wjgnet.com/1007-9327/14/3642.asp DOI: http://dx.doi.org/10.3748/wjg.14.3642

INTRODUCTION

Apoptin or viral protein 3 (VP3), a protein of 13.6 kDa derived from the chicken anemia virus (CAV), represents a new anti-cancer tool with great potential[1,2]. It appears to have innate tumor-specific, *p53*-independent[3,4], Bcl-2-enhanced proapoptotic activity[4,5], and hence is of considerable interest for efficient targeting and specific elimination of cancer cells[3,4,6-8]. The antitumor activity of apoptin appears to be linked to its ability to localize in the nuclei of transformed cells, but not in those of primary or non-transformed cells[9]. Therefore, apoptin has been explored to achieve efficient targeting and specific elimination of cancer cells.

To use apoptin in cancer therapy, efficient delivery to or expression of apoptin in cancer cells is required. The Human Immunodeficiency Virus (HIV) Transactivating Transcription (TAT)-derived protein transduction peptide is a small basic peptide that has been successfully shown to deliver a large variety of materials, from small particles to proteins, peptides and nucleic acids, across

the cell membrane[10-12]. The region that conveys the cell-penetrating properties appears to be confined to a small (11 amino acids) stretch of basic amino acids (aa 47-57, YGRKKRRQRRR)[13]. This TAT transduction domain has been successfully used to deliver apoptin to cancer cells[14].

In this study, we designed a secretory TAT-apoptin fusion protein by adding a secretory signal to the N-terminal of the recombinant molecule to gain an additive by-stander effect as an anti-cancer therapy. Secreted TAT-apoptin from transformed cells enters un-transformed cancer cells and causes apoptosis. We employed an artificial human secretory signal peptide (SP) whose amino acid sequence and corresponding cDNA sequences were generated by an SP hidden Markov model (SP-HMM)[15]. We demonstrated expression of the secretory fusion protein (SP-TAT-apoptin) and induction of apoptosis by the secreted protein in HepG2 cells.

MATERIALS AND METHODS

Generation and cloning of SP-TAT-apoptin

The human secretory SP was designed and optimized by an HMM that has been used to predict, identify and generate secretory SP sequences[15]. PCR was used to amplify the apoptin gene and to incorporate the TAT transduction domain and SP sequence upstream. The primers were designed based on the published sequences in GenBank (NC_001427), and synthesized by Shanghai Sangon Biological Engineering Technology & Services (Shanghai, China). The first pair of designed primers were: 5'AAGAATGAACGCTCTGCAGG AAGATACTCC-3' (sense) and 5'-CTGCAGTCTTA TACGCCTTTTTGCGG-3' (antisense), with a product size of 406 bp. The sense primer contains the TAT transduction domain sequence. The second pair of primers, which incorporated the secretory signal sequence into the TAT-apoptin fusion protein, were: 5' GCTGCTGCTGCTGCTGCTGTGGCCCATGGTG TGGGCCTATGGCAGG-3' (sense) and the same antisense primer as the first pair, with a product size of 466 bp. The templates used for generating recombinant TAT-apoptin and TAT-GFP in the first round PCR were the *apoptin* and *gfp* genes carried on pCDNA3.1-apoptin plasmid[16] and pEGFP plasmid, respectively. The conditions for both rounds of PCR were as follows: 30 cycles of 94℃ for 40 s, 56℃ for 40 s, and 72℃ for 1 min. The PCR products obtained were TOPO® cloned into the pLenti6/V5-D-TOPO® vector (Invitrogen, USA) resulting pLenti6/V5-D-TOPO/SP-TAT-apoptin and pLenti6/V5-D-TOPO/SP-TAT-EGFP. The plasmids were transformed into Stbl3™ *Escherichia coli (E.coli)* (Invitrogen) by electroporation. The SP-TAT-apoptin cDNA cloned in pLenti6/V5-D- TOPO® vector was confirmed by restriction enzyme digestion and by DNA sequencing.

Cell lines and cell culture

HepG2 human hepatoma cells, human umbilical vein endothelial cells (HUVECs) and Chinese hamster ovary (CHO) cells were purchased from Keygen Company (Nanjing, China). All cells were maintained and grown at 37℃ in DMEM (Hyclone, USA), supplemented with 1% penicillin–streptomycin, and 10% fetal bovine serum in an incubator with CO_2 controlled at 5%.

Conditioned medium: The conditioned medium from Chinese hamster ovary (CHO) cells transfected with SP-TAT-apoptin. (CHO cells were cultured in a six-well plate. The cells were transfected with the pLenti6/V5-D-TOPO/SP-TAT-apoptin plasmid using the Lipofectamine™ 2000 protocol according to manufacturer's instructions (Invitrogen). After 6 h incubation, the cells were washed with fresh culture medium and cultured for an additional 24 h. The culture supernatants were then collected and added, respectively, to the monolayers of HepG2 cells and HUVECs grown in 24-well plates.)

Stbl3™ *Escherichia coli*: Stbl3™ *E. coli* for transformation as this strain is particularly well-suited for use in cloning unstable DNA such as lentiviral DNA containing direct repeats.

Reverse transcriptase-PCR (RT-PCR)

Cells were rinsed twice with PBS and total RNA was isolated from cells using a Simply P Total RNA Extraction Kit (Bioer, Japan) according to the manufacturer's instructions. One microgram of total RNA was reverse transcribed to first-strand cDNA with Superscript Ⅱ reverse transcriptase (Invitrogen) at 46℃ for 45 min. Synthesized first-strand cDNA was then subjected to PCR analysis using gene-specific primers. The primers used were: CMV forward 5' -CGCAAATGGGCGGTAGGCGTG-3' and V5(C-term) reverse 5'-ACCGAGGAGAGGGTTAGGGAT-3', with a product size of 700 bp. The PCR conditions were as follows: 30 cycles at 94℃ for 40 s, 56℃ for 40 s, and 72℃ for 1 min for SP-TAT-apoptin; 25 cycles at 94℃ for 30 s, 60℃ for 45 s, and 72℃ for 1 min for β-actin control. PCR products were run on 1.5% agarose gels containing ethidium bromide and photographed using a Syngene Gene Genius imaging system (Syngene, USA).

Transient transfection and fluorescence microscopy

Cells were cultivated in 24-well culture plates. In each well, the cells were grown at 50%-80% confluency and transfected with 400 ng plasmid DNA pre-incubated with 1.4 μL Lipofectamine™ 2000 (Invitrogen), according to the manufacturer's instructions. Coverslips were placed at the bottom of the wells to allow the cells grow on the slides. Apoptin expression was detected with anti-V5-FITC antibody (Invitrogen) as green fluorescence, and the cell nuclei were stained by propidium iodide (PI) as red fluorescence. The cells were incubated with anti-V5-FITC antibody in the dark for 1 h and washed twice with PBS before staining with PI. Fluorescence images were recorded on a confocal imaging system equipped with krypton–argon laser (Leica SP2 Confocal System, Germany).

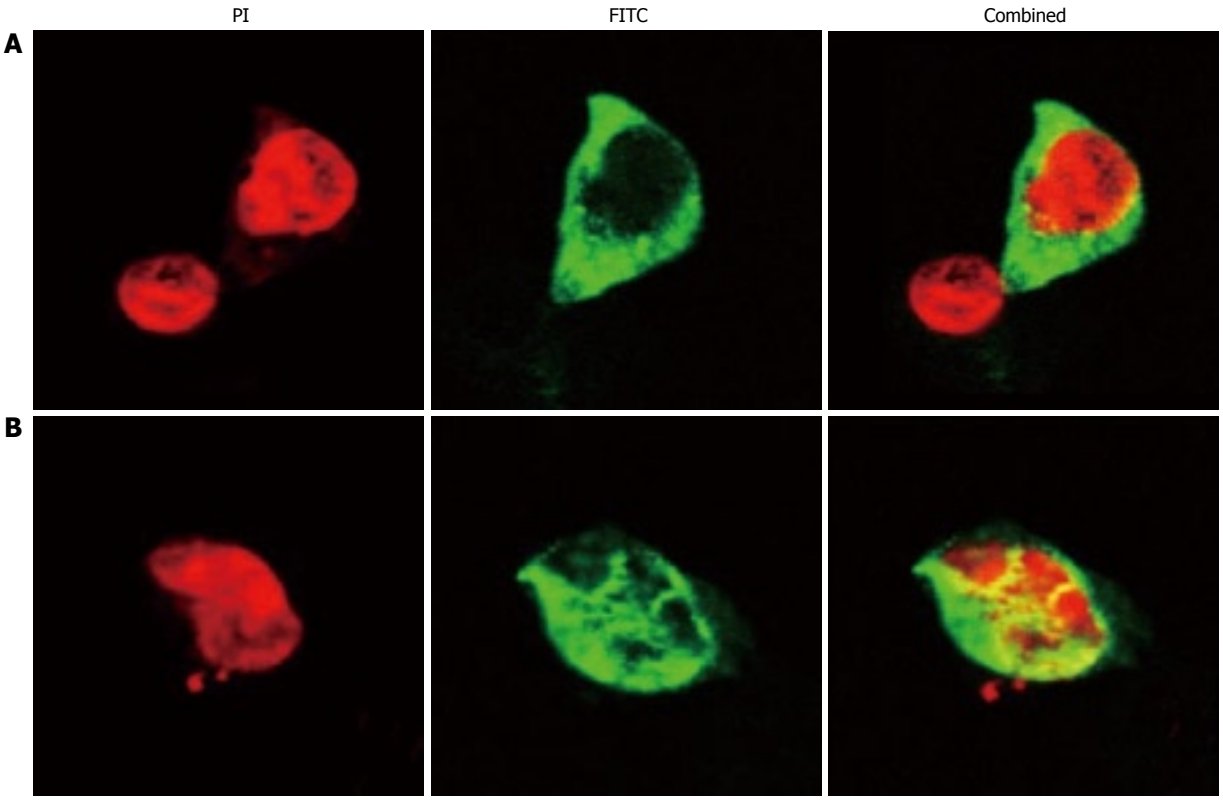

Figure 1 SP-TAT-apoptin expression in HepG2 cells (× 1000). Cells transfected with plenti6/V5-D-TOPO/SP-TAT-apoptin plasmid and fixed at 24 h (**A**) and 48 h (**B**) post-transfection. Recombinant apoptin detected by anti-V5-FITC antibody is shown in green and cell nuclei stained by PI in red. Apoptin protein showed a diffuse pattern in the cytoplasm at 24 h post-transfection, and in the nucleus at 48 h.

Flow cytometry

The loss of cell membrane asymmetry in apoptotic cells was determined by using an Annexin-V FITC Apoptosis Assay Kit (Keygen, China). Apoptin-expressing cells were stained with annexin-V FITC as green fluorescent cells, and the nuclei of the apoptotic cells were stained by PI with red fluorescence. After staining, the cell suspensions were analyzed on a Cytometric FC500 flow cytometer, and 10^5 events were collected for each sample. Viable cells were defined as annexin-V FITC and PI double-negative events.

Cell viability assay

Cell viability was also determined by the 3-(4,5-dimethylthiazol-2-yl)-2,5-diphenyltetrazolium bromide (MTT) dye reduction assay which measures mitochondrial respiratory function[17,18]. Exponentially growing cells were plated in 96-well flat bottom plates (Corning, USA) and allowed to adhere for 24 h. At various times post-transfection with the recombinant plasmid, cells were incubated with MTT dye (1 mg/mL) for 2 h and solubilized with 20 μL 10% SDS. A_{560} was then measured.

DNA laddering assay

DNA fragmentation was detected using an Apoptotic DNA Laddering Kit (Keygen) according to the manufacturer's instructions. DNA was extracted, separated by 1.5% agarose gel electrophoresis, followed by ethidium bromide staining to visualize the laddered DNA.

Immunocytochemical assay and DAPI staining

At various times post-transfection, cells grown in six-well plates were harvested and treated by trypsinization and resuspended in PBS. The cells were then spread on a slide, fixed by 100% methanol for 5 min at room temperature, stained by the Apoptotic/Necrotic Cell Detection Kit (Keygen), and embedded in resin, after permeabilization, for long-term storage.

Cytotoxicity of SP-TAT was also tested by 2,4-diamidino-2-phenylin-dole (DAPI) staining. Transfected cells grown on coverslips that were placed on the bottom of a 24-well plate were washed with PBS and fixed, and apoptotic cells were differentiated by staining with mounting medium containing DAPI, and visualized using an Olympus AX70 fluorescence microscope.

Protein secretion and activity test

CHO cells were cultured in a six-well plate. The cells were transfected with the pLenti6/V5-D-TOPO/SP-TAT-apoptin plasmid using the Lipofectamine™ 2000 protocol according to manufacturer's instructions (Invitrogen). After 6 h incubation, the cells were washed with fresh culture medium and cultured for an additional 24 h. The culture supernatants were then collected and added respectively to the monolayers of HepG2 cells and HUVECs grown in 24-well plates. These cells had also been washed with PBS before adding the supernatants. At various times post co-culture, these cells were fixed and stained, and apoptin localization and apoptosis were analyzed.

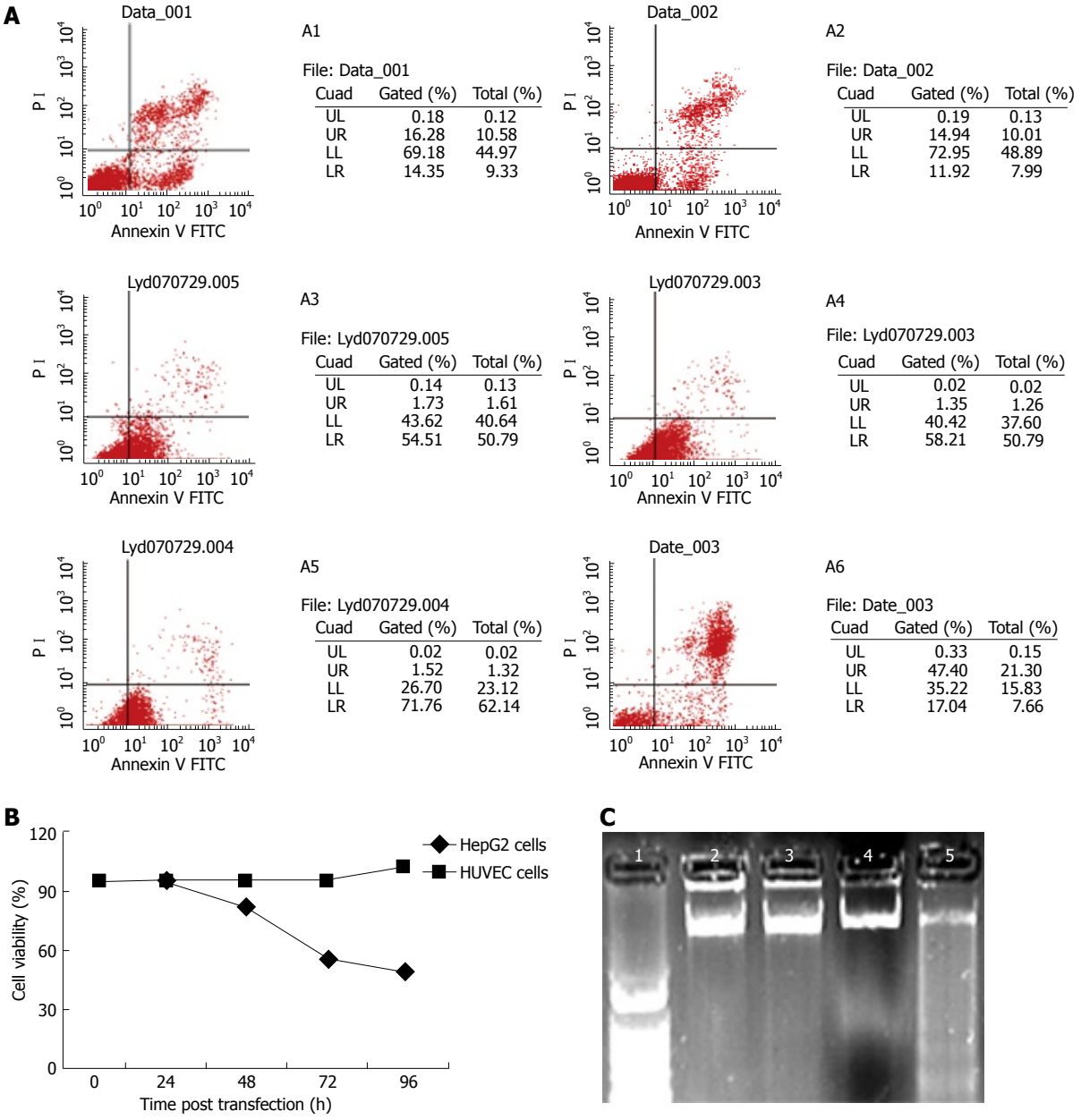

Figure 2 SP-TAT-apoptin-induced cell death. **A:** Cell viability measured by flow cytometry. **A**1 and **A**2: HUVECs at 48 and 72 h post-transfection; **A**3-**A**6: HepG2 cells at 24, 48, 72 and 96 h. HepG2 cells were susceptible to SP-TAT-apoptin-induced apoptosis in a time-dependent manner; **B:** Cell viability determined by MTT dye reduction assay; **C:** DNA fragmentation in HepG2 cells demonstrated by agarose gel electrophoresis. Lane 1: 1 kb DNA marker; Lanes 2-5: DNA from cells at 24, 48, 60 and 72 h post-transfection, respectively.

Statistical analysis

ANOVA was performed for multiple group comparison. In conjunction with ANOVA, post hoc pairwise comparisons were performed by Bonferroni's test, with $P < 0.05$ regarded as statistically significant.

RESULTS

Generation of SP-TAT-apoptin fusion construct and expression of SP-TAT-apoptin

The human secretory SP was constructed and optimized virtually by the HMM, which has been used to describe, predict, identify, and generate secretory SP sequences[13]. It was inserted at the N terminus of recombinant TAT-apoptin to generate SP-TAT-apoptin fusion protein, and it contained a positively charged N region, a hydrophobic central region, and a C region that contained a cleavage site. Two rounds of PCR were carried out to amplify the apoptin gene and to fuse TAT and the synthetic SP into the construct to create recombinant secretory-TAT-apoptin.

To determine whether the SP-TAT-apoptin cDNA construct generated was expressed *in vivo*, the HepG2 cell line was transfected with the plenti6/V5-D-TOPO/SP-TAT-apoptin plasmid. Analysis by RT-PCR revealed that SP-TAT-apoptin was expressed 24 h after transfection (data not shown). The expression of SP-TAT-apoptin in HepG2 cells was confirmed by immunofluorescence microscopy (Figure 1).

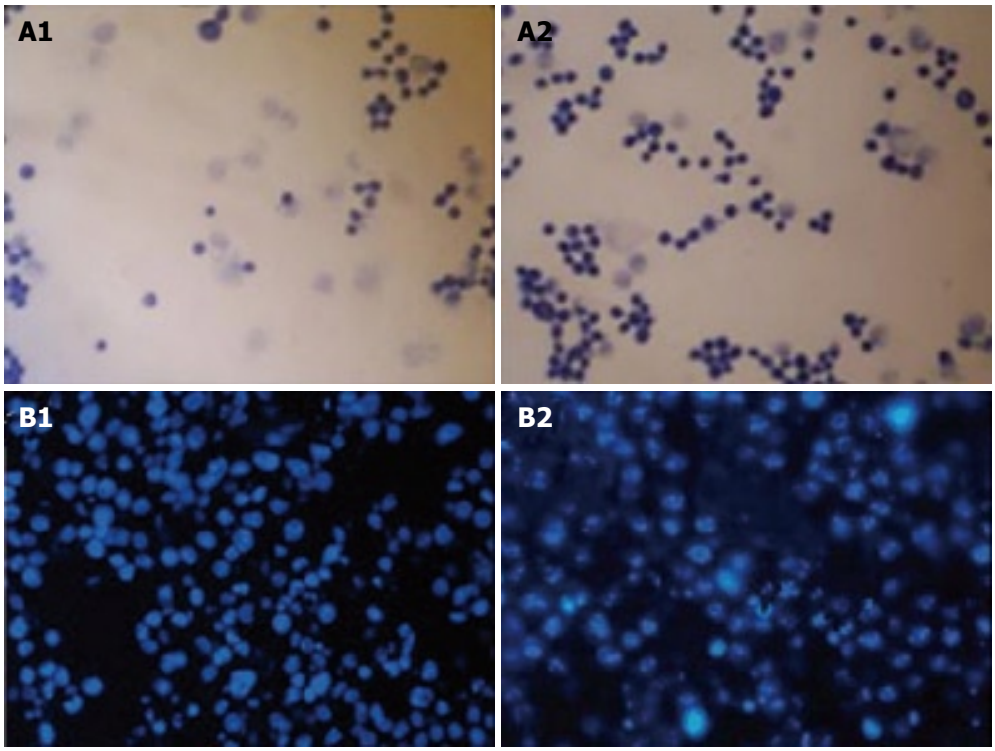

Figure 3 Cytotoxicity of SP-TAT-apoptin compared to SP-TAT. **A:** Micrographs of HepG2 cells transfected with SP-TAT-apoptin construct stained by Apoptotic/Necrotic Cell Detection Kit. An inverted microscope (× 400) was used. The nuclei of apoptotic cells were stained deep blue. **A1** and **A2**: HepG2 cells at 24 and 72 h post-transfection; **B:** HepG2 cells stained with DAPI and observed by fluorescence microscopy (× 400). **B1**: HepG2 cells 72 h after transfection with plenti6/V5-D-TOPO/SP-TAT-GFP plasmid; **B2**: HepG2 cells 72 h after transfection with plenti6/V5-D-TOPO/SP-TAT-apoptin. Arrow indicates apoptotic cells.

Induction of apoptosis by SP-TAT-apoptin

To determine whether SP-TAT-apoptin induces apoptosis and also maintains its tumor cell specificity, HUVECs and HepG2 cells were transfected with the plenti6/V5-D-TOPO/SP-TAT-apoptin plasmid. SP-TAT-apoptin-induced apoptosis was investigated in these two cell lines. Three different assays were used to gauge apoptosis. In the first assay, cell viability was measured by co-staining with annexin-V FITC and PI, followed by flow cytometry. This assay was based on the loss of plasma membrane asymmetry (integrity) as a result of apoptosis. Viable cells were defined as annexin-V FITC and PI double-negative events. As shown in Figure 2A, only HepG2 cells were susceptible to SP-TAT-apoptin-induced apoptosis in a time-dependent manner. These results also confirm previous reports that apoptin has the ability to induce apoptosis specifically in tumor cells[3,4,7,19,20]. In the second assay, cells that were exponentially grown were inoculated in 96-well flat-bottom plates and allowed to adhere for 24 h. After transfection, cell viability was determined at various times by MTT dye reduction assay. Expression of the recombinant protein slightly decreased the viability of HepG2 cells at 24 h post-transfection, and the same was true in HUVECs (Figure 2B). At 48 h post-transfection, the viability of HUVECs was only slightly decreased compared to that at 24 h. However, the viability of HepG2 cells was significantly decreased at 48 h post-transfection. The presence of recombinant apoptin caused a decrease in HepG2 cell viability to < 60% at 72 h and < 50% at 96 h post-transfection (Figure 2B). In the third assay, genomic DNA fragmentation in HepG2 cells and HUVECs was investigated. As shown in Figure 2C, the apoptin fusion protein brought about significant DNA fragmentation in HepG2 cells at 72 h post-transfection. In contrast, detectable apoptotic DNA laddering in HUVECs was not seen during the experiment (data not shown).

Lack of cytotoxicity of SP-TAT

In order to determine the cytotoxicity of SP-TAT, plenti6/V5-D-TOPO/SP-TAT-apoptin plasmid and plenti6/V5-D-TOPO/SP-TAT-GFP plasmids were transfected into HepG2 cells separately. Robust apoptosis of HepG2 cells was observed, as demonstrated by microscopy at different times after transfection, while in contrast, expression of SP-TAT-GFP did not induce noticeable apoptosis in these cells (Figure 3). Therefore, SP-TAT did not seem to exhibit cytotoxicity in HepG2 cells and apoptosis induced by SP-TAT-apoptin was due to apoptin.

Secretion of SP-TAT-apoptin and the effect of secreted TAT-apoptin on HepG2 cells

The presence of synthesized SP enables TAT-apoptin to be secreted outside the transfected cells and re-enter adjacent un-transfected HepG2 cells, potentially increasing the efficacy of apoptin when used as cancer therapy. To test its feasibility, the recombinant construct was used to transfect CHO cells and the culture supernatant was collected. HepG2 cells and HUVECs

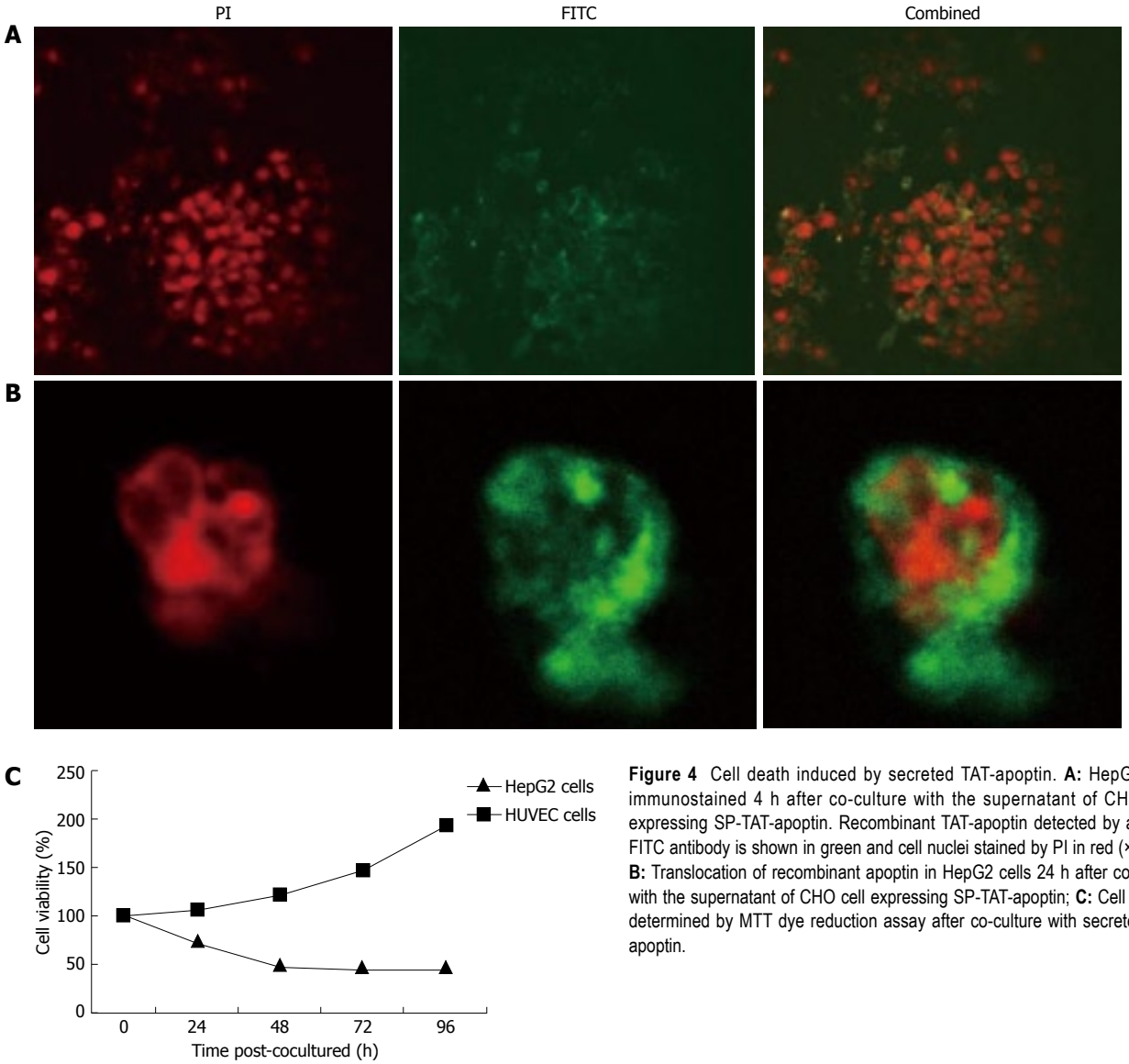

Figure 4 Cell death induced by secreted TAT-apoptin. **A:** HepG2 cells immunostained 4 h after co-culture with the supernatant of CHO cells expressing SP-TAT-apoptin. Recombinant TAT-apoptin detected by anti-V5-FITC antibody is shown in green and cell nuclei stained by PI in red (× 1000); **B:** Translocation of recombinant apoptin in HepG2 cells 24 h after co-culture with the supernatant of CHO cell expressing SP-TAT-apoptin; **C:** Cell viability determined by MTT dye reduction assay after co-culture with secreted TAT-apoptin.

were then co-cultured with this supernatant. At 24 h post co-culture, TAT-apoptin had translocated from the cytoplasm to the nucleus (Figure 4A). At various times post co-culture, cell viability was also determined by MTT dye reduction assay. As shown in Figure 4B, the recombinant protein TAT-apoptin slightly decreased cell viability of HepG2 cells at 24 h post co-culture. In contrast, the viability of HUVECs was actually increased at 24 h, which continued during the course of the experiment. At 48 h post co-culture, viability of HepG2 cells was significantly decreased compared to that of HUVECs. The recombinant apoptin protein decreased HepG2 cell viability to < 50% at 48 h post-transfection.

DISCUSSION

New therapeutic approaches that facilitate selective targeting of cancer cells while sparing normal cells have emerged in recent years. Apoptin represents a new anti-cancer tool in such new approaches with great potential[21-25]. Two routes can be taken using apoptin or its encoding cDNA, i.e. as protein or gene therapy. In any case, efficient systems are required to facilitate the delivery of apoptin to cancer cells or expression of apoptin within these cells[26-30]. The HIV TAT transduction domain has been successfully used to deliver apoptin into cancer cells[14], and no apoptosis of normal cells (HUVECs) was observed with this TAT-apoptin fusion protein. In this study, we generated a cDNA construct of SP-TAT-apoptin. Cancer cells transfected with this construct expressed recombinant apoptin and apoptosis was induced. By incorporating a synthetic SP we also expected apoptin to be secreted from the transfected cells as TAT-apoptin fusion protein and re-enter adjacent untransfected HepG2 cells, which enabled the construct to act as both a protein and gene therapeutic agent, and increased the potency of apoptin in cancer therapy.

SP-TAT-apoptin was expressed in HUVECs and HepG2 cells, and the protein was initially located in the cytoplasm. At 48 h post-transfection, the protein was located in the nucleus of HepG2 cells, which indicated that SP-TAT-apoptin was capable of translocating to the nucleus. SP-TAT-apoptin was also functionally active and efficiently induced HepG2 cell apoptosis, in a time-dependent manner. In HUVECs, SP-TAT-

apoptin remained in the cytoplasm and no induction of apoptosis above the background level was observed. Meanwhile, no apoptosis was observed in cells in which SP-TAT-GFP was expressed, which indicates that SP-TAT alone is not cytotoxic for HepG2 cells. Therefore, SP-TAT-apoptin retained the characteristic expression pattern of apoptin and induced apoptosis in cancer cells.

Having a synthetic SP, recombinant apoptin was able to be secreted from transfected cells and re-enter adjacent untransfected HepG2 cells. The recombinant protein was detected in the cytoplasm in HepG2 cells and HUVECs shortly after co-culture of the cells with the cell-free supernatant of the transfected CHO cells. This indicated that the secreted TAT-apoptin fusion protein contained in the CHO cell culture medium was able to enter these cells. The fusion protein was later found in the nucleus of HepG2 cells and induced HepG2 apoptosis. The new secretory characteristic increased the possibility of apoptin being used in cancer gene therapy. However, there are still a large number of unanswered questions regarding the mechanisms and therapeutic usage of apoptin, and further studies are certainly required.

ACKNOWLEDGMENTS

We thank Dr. Zhi-Xian Sun at the Academy of Military Medical Sciences, China, for providing plasmid pCDNA3.1-apoptin.

COMMENTS

Background

Apoptin is a protein encoded by Constant Angular Velocity (CAV) and it can cause apoptotic cell death. It has been shown to possess a striking specificity for cancer cells. Apoptin, therefore, has great potential for efficient targeting and specific elimination of cancer cells.

Research frontiers

Human Immunodeficiency Virus (HIV)-Transactiviting Transcription (TAT)-fused apoptin has been shown to possess a striking specificity for cancer cells. However, the cancer killing activity is limited in cells transfected with the apoptin expression construct, which spares the untransfected cancer cells. A secretory TAT-apoptin fusion protein with a secretory signal has an additive by-stander effect as an anti-cancer therapy. Secreted TAT-apoptin from transformed cells enters un-transformed cancer cells and causes apoptosis.

Innovations and breakthroughs

The new secretory characteristic increased the possibility of apoptin being used in cancer gene therapy. However, there are still a large number of unanswered questions regarding the mechanisms and therapeutic usage of apoptin, and further studies are certainly required.

Terminology

Apoptin or VP3 is a protein of 13.6 kDa derived from CAV, represents a new anti-cancer tool with great potentials. It appears to have innate tumor-specific, p53-independent, Bcl-2-enhanced pro-apoptotic activity.

Peer review

The authors investigated the role of secretory TAT-apoptin fusion protein in HepG2 cells. They conclude that such a protein induces apoptosis in HCC cell lines, but not in non-cancer cell line HUVEC. This is a very interesting study, which may be applicable for the treatment of human liver cancer in the future.

REFERENCES

1 **Noteborn MH.** Chicken anemia virus induced apoptosis: underlying molecular mechanisms. *Vet Microbiol* 2004; **98**: 89-94
2 **Olijslagers SJ,** Zhang YH, Backendorf C, Noteborn MH. Additive cytotoxic effect of apoptin and chemotherapeutic agents paclitaxel and etoposide on human tumour cells. *Basic Clin Pharmacol Toxicol* 2007; **100**: 127-131
3 **Janssen K,** Hofmann TG, Jans DA, Hay RT, Schulze-Osthoff K, Fischer U. Apoptin is modified by SUMO conjugation and targeted to promyelocytic leukemia protein nuclear bodies. *Oncogene* 2007; **26**: 1557-1566
4 **Burek M,** Maddika S, Burek CJ, Daniel PT, Schulze-Osthoff K, Los M. Apoptin-induced cell death is modulated by Bcl-2 family members and is Apaf-1 dependent. *Oncogene* 2006; **25**: 2213-2222
5 **Russo A,** Terrasi M, Agnese V, Santini D, Bazan V. Apoptosis: a relevant tool for anticancer therapy. *Ann Oncol* 2006; **17** Suppl 7: vii115-vii123
6 **Liu X,** Elojeimy S, El-Zawahry AM, Holman DH, Bielawska A, Bielawski J, Rubinchik S, Guo GW, Dong JY, Keane T, Hannun YA, Tavassoli M, Norris JS. Modulation of ceramide metabolism enhances viral protein apoptin's cytotoxicity in prostate cancer. *Mol Ther* 2006; **14**: 637-646
7 **Maddika S,** Mendoza FJ, Hauff K, Zamzow CR, Paranjothy T, Los M. Cancer-selective therapy of the future: apoptin and its mechanism of action. *Cancer Biol Ther* 2006; **5**: 10-19
8 **Peng DJ,** Sun J, Wang YZ, Tian J, Zhang YH, Noteborn MH, Qu S. Inhibition of hepatocarcinoma by systemic delivery of Apoptin gene via the hepatic asialoglycoprotein receptor. *Cancer Gene Ther* 2007; **14**: 66-73
9 **Wang QM,** Fan GC, Chen JZ, Chen HP, He FC. A putative NES mediates cytoplasmic localization of Apoptin in normal cells. *Acta Biochim Biophys Sin* (Shanghai) 2004; **36**: 817-823
10 **Hashida H,** Miyamoto M, Cho Y, Hida Y, Kato K, Kurokawa T, Okushiba S, Kondo S, Dosaka-Akita H, Katoh H. Fusion of HIV-1 Tat protein transduction domain to poly-lysine as a new DNA delivery tool. *Br J Cancer* 2004; **90**: 1252-1258
11 **Kubo E,** Fatma N, Akagi Y, Beier DR, Singh SP, Singh DP. TAT-mediated PRDX6 protein transduction protects against eye lens epithelial cell death and delays lens opacity. *Am J Physiol Cell Physiol* 2008; **294**: C842-C855
12 **Song HY,** Lee JA, Ju SM, Yoo KY, Won MH, Kwon HJ, Eum WS, Jang SH, Choi SY, Park J. Topical transduction of superoxide dismutase mediated by HIV-1 Tat protein transduction domain ameliorates 12-O-tetradecanoylphorbol-13-acetate (TPA)-induced inflammation in mice. *Biochem Pharmacol* 2008; **75**: 1348-1357
13 **Ziegler A,** Seelig J. Interaction of the protein transduction domain of HIV-1 TAT with heparan sulfate: binding mechanism and thermodynamic parameters. *Biophys J* 2004; **86**: 254-263
14 **Guelen L,** Paterson H, Gaken J, Meyers M, Farzaneh F, Tavassoli M. TAT-apoptin is efficiently delivered and induces apoptosis in cancer cells. *Oncogene* 2004; **23**: 1153-1165
15 **Barash S,** Wang W, Shi Y. Human secretory signal peptide description by hidden Markov model and generation of a strong artificial signal peptide for secreted protein expression. *Biochem Biophys Res Commun* 2002; **294**: 835-842
16 **Sun GJ ,**Tong X, Sun ZX, Gene clone and activity assay of apoptin. *Junshi Yixue Kexueyuan Yuankan* 2001; **2**: 85-87
17 **Hayon T,** Dvilansky A, Shpilberg O, Nathan I. Appraisal of the MTT-based assay as a useful tool for predicting drug chemosensitivity in leukemia. *Leuk Lymphoma* 2003; **44**: 1957-1962
18 **Kubota T.** (Cancer chemosensitivity test-from laboratory to clinic) *Hum Cell* 1995; **8**: 189-194
19 **Lee YH,** Cheng CM, Chang YF, Wang TY, Yuo CY. Apoptin T108 phosphorylation is not required for its tumor-specific nuclear localization but partially affects its apoptotic activity. *Biochem Biophys Res Commun* 2007; **354:** 391-395
20 **Olijslagers SJ,** Zhang YH, Backendorf C, Noteborn MH.

Additive cytotoxic effect of apoptin and chemotherapeutic agents paclitaxel and etoposide on human tumour cells. *Basic Clin Pharmacol Toxicol* 2007; **100:** 127-131

21 **Danen-Van Oorschot AA,** Zhang YH, Leliveld SR, Rohn JL, Seelen MC, Bolk MW, Van Zon A, Erkeland SJ, Abrahams JP, Mumberg D, Noteborn MH. Importance of nuclear localization of apoptin for tumor-specific induction of apoptosis. *J Biol Chem* 2003; **278:** 27729-27736

22 **Alvisi G,** Poon IK, Jans DA. Tumor-specific nuclear targeting: promises for anti-cancer therapy? *Drug Resist Updat* 2006; **9:** 40-50

23 **Poon IK,** Oro C, Dias MM, Zhang J, Jans DA. Apoptin nuclear accumulation is modulated by a CRM1-recognized nuclear export signal that is active in normal but not in tumor cells. *Cancer Res* 2005; **65:** 7059-7064

24 **He X,** Zhang Q, Liu Y, He P. Apoptin Induces Chromatin Condensation in Normal Cells. *Virus Genes* 2005; **31:** 49-55

25 **Gdynia G,** Lehmann-Koch J, Sieber S, Tagscherer KE, Fassl A, Zentgraf H, Matsuzawa S, Reed JC, Roth W. BLOC1S2 interacts with the HIPPI protein and sensitizes NCH89 glioblastoma cells to apoptosis. *Apoptosis* 2008; **13:** 437-447

26 **Maddika S,** Wiechec E, Ande SR, Poon IK, Fischer U, Wesselborg S, Jans DA, Schulze-Osthoff K, Los M. Interaction with PI3-kinase contributes to the cytotoxic activity of apoptin. *Oncogene* 2008; **27:** 3060-3065

27 **Maddika S,** Bay GH, Kroczak TJ, Ande SR, Maddika S, Wiechec E, Gibson SB, Los M. Akt is transferred to the nucleus of cells treated with apoptin, and it participates in apoptin-induced cell death. *Cell Prolif* 2007; **40:** 835-848

28 **Backendorf C,** Visser AE, de Boer AG, Zimmerman R, Visser M, Voskamp P, Zhang YH, Noteborn M. Apoptin: therapeutic potential of an early sensor of carcinogenic transformation. *Annu Rev Pharmacol Toxicol* 2008; **48:** 143-169

29 **Schoop RA,** Kooistra K, Baatenburg De Jong RJ, Noteborn MH. Bcl-xL inhibits p53- but not apoptin-induced apoptosis in head and neck squamous cell carcinoma cell line. *Int J Cancer* 2004; **109:** 38-42

30 **Maddika S,** Mendoza FJ, Hauff K, Zamzow CR, Paranjothy T, Los M. Cancer-selective therapy of the future: apoptin and its mechanism of action. *Cancer Biol Ther* 2006; **5:** 10-19

S- Editor Li DL **L- Editor** Kerr C **E- Editor** Lin YP

Online Submissions: wjg.wjgnet.com
wjg@wjgnet.com
doi:10.3748/wjg.14.3650

World J Gastroenterol 2008 June 21; 14(23): 3650-3661
World Journal of Gastroenterology ISSN 1007-9327
© 2008 The WJG Press. All rights reserved.

CLINICAL RESEARCH

Partial overlap of anti-mycobacterial, and anti-*Saccharomyces cerevisiae* mannan antibodies in Crohn's disease

Stefan Müller, Thomas Schaffer, Alain M Schoepfer, Annamarie Hilty, Thomas Bodmer, Frank Seibold

Stefan Müller, Thomas Schaffer, Alain M Schoepfer, Frank Seibold, Department of Clinical Research, Division of Gastroenterology, University of Bern, Bern CH-3010, Switzerland
Stefan Müller, Thomas Schaffer, Annamarie Hilty, Thomas Bodmer, Institute for Infectious Diseases, University of Bern, Bern CH-3010, Switzerland
Author contributions: Müller S and Schaffer T contributed equally to this work; Müller S contributed to the study design, planned experiments, carried through the animal part of the study and ELISAs with affinity purified sera, and wrote the paper; Schaffer T screened patients' sera by ELISA, performed neutralization experiments and affinity purifications; Schoepfer AM provided clinical data and performed statistic analyses; Hilty A, and Bodmer T prepared and supervised mycobacterial cultures; and Seibold F had the original idea and designed the study.
Supported by The Swiss National Science Foundation grant No. SNSF 3200B0-107527/1 to F. Seibold
Correspondence to: Frank Seibold, Department of Gastroenterology, Inselspital Bern, University Hospital, Freiburgstrasse 10, Bern CH-3010, Switzerland. frank.seibold@insel.ch
Telephone: +41-31-6328025 Fax: +41-31-63297 65
Received: February 11, 2008 Revised: April 14, 2008
Accepted: April 21, 2008
Published online: June 21, 2008

Abstract

AIM: To test whether humoral immune reaction against mycobacteria may play a role in anti-*Saccharomyces cerevisiae* antibodies (ASCA) generation in Crohn's disease (CD) and/or whether it correlates with clinical subtypes.

METHODS: The dominant ASCA epitope was detected by *Galanthus nivalis* lectin (GNL)-binding assay. ASCA and IgG against mycobacterial lysates [*M avium, M smegmatis, M chelonae, M bovis* BCG, *M avium ssp. paratuberculosis* (MAP)] or purified lipoarabinomannans (LAM) were detected by ELISA. ASCA and anti-mycobacterial antibodies were affinity purified to assess cross-reactivities. Anti-mycobacterial IgG were induced by BCG-infection of mice.

RESULTS: GNL bound to different extents to mycobacterial lysates, abundantly to purified mannose-capped (Man) LAM from *M tuberculosis*, but not to uncapped LAM from *M smegmatis*. Fifteen to 45% of CD patients but only 0%-6% of controls were seropositive against different mycobacterial antigens. Anti-mycobacterial IgG correlated with ASCA (r = 0.37-0.64; P = 0.003-P < 0.001). ASCA-positivity and deficiency for mannan-binding lectin synergistically associated with anti-mycobacterial IgG. In some patients, anti-mycobacterial antibodies represent cross-reactive ASCA. Vice-versa, the predominant fraction of ASCA did not cross-react with mycobacteria. Finally, fistulizing disease associated with antibodies against *M avium*, *M smegmatis* and MAP (P = 0.024, 0.004 and 0.045, respectively).

CONCLUSION: Similar to ASCA, seroreactivity against mycobacteria may define CD patients with complicated disease and a predisposition for immune responses against ubiquitous antigens. While in some patients anti-mycobacterial antibodies strongly cross-react with yeast mannan; these cross-reactive antibodies only represent a minor fraction of total ASCA. Thus, mycobacterial infection unlikely plays a role in ASCA induction.

© 2008 The WJG Press. All rights reserved.

Key words: Crohn's disease; Anti-mycobacterial antibodies; Anti-*Saccharomyces cerevisiae* antibodies; Cross-reactivity; Mannan; Lipoarabinomannan

Peer reviewer: Dr. Daniel R Gaya, Gastrointestinal Unit, Molecular Medicine Centre, School of Molecular and Clinical Medicine, University of Edinburgh, Western General Hospital, Crewe Road, Edinburgh EH4 2XU, United Kingdom

Müller S, Schaffer T, Schoepfer AM, Hilty A, Bodmer T, Seibold F. Partial overlap of anti-mycobacterial, and anti-*Saccharomyces cerevisiae* mannan antibodies in Crohn's disease. *World J Gastroenterol* 2008; 14(23): 3650-3661 Available from: URL: http://www.wjgnet.com/1007-9327/14/3650.asp DOI: http://dx.doi.org/10.3748/wjg.14.3650

INTRODUCTION

Crohn's disease (CD) is a multifactorial disease that affects genetically susceptible hosts. The exact pathogenesis is still largely unknown. However, it is generally accepted that the disease, once established,

is driven by antigens of the intestinal flora, reflecting a loss of tolerance against commensal microorganisms[1,2]. The hypothesis that genetic predisposition, together with unfavorable environmental and commensal triggers cause CD with its various phenotypes contradicts the highly controversial idea of a single infectious origin of the disease[3].

A number of serological markers have been detected that have a certain degree of specificity and sensitivity for CD[4,5]. Of the most intriguing antibodies are those directed against outer cell wall mannans of the baker's yeast *Saccharomyces cerevisiae* (anti-*Saccharomyces cerevisiae* antibodies, ASCA)[6-9]. These antibodies are found in more than 50% of CD patients, but rarely in healthy controls or patients with ulcerative colitis (UC)[8]. Yeasts are ubiquitous and ingested on a daily basis. Why an organism that, with a few reported exceptions of virulent mutants[10], is not adapted to live or even grow in the human body elicits a strong IgG response in CD patients has not yet been conclusively answered. A recent report presented experimental data supporting the idea that the facultative opportunistic pathogen *Candida albicans* may be the inducer of ASCA[11]. However, our recent study showed that ASCA and anti-*C albicans* antibodies correlate to a lower degree than ASCA with antibodies to mannans from other ubiquitous yeasts[12]. Thus, whether *C albicans* infection may indeed represent the dominant trigger for ASCA cannot be definitively answered so far and there may be other cross-reactivities that play a role in ASCA induction. Potential candidates are mycobacteria since their cell wall contains lipoarabinomannans with similar mannose side chains as the cell wall mannans of yeast. The exact epitope recognized by ASCA has been demonstrated to be an α-1,3 mannose-(α-1,2 mannose)n with $n = 2$ or 3 by two independent studies[9,13]. Similar or equal oligo-mannose motives are found in other yeasts, as well as in the mannosylated side chains of mycobacterial lipoarabinomannans (LAM)[14,15]. Part of this motif, the terminal α-1,3 linked mannose, can be detected by the *Galanthus nivalis* lectin (GNL)[16,17] and has been shown to be present in the lipo(arabino)mannan of *M chelonae*[18]. Two other publications have demonstrated presence of the GNL-reactive motif in some mycobacterial species, including *M bovis*, *M avium* and *Mycobacterium avium* ssp. paratu-berculosis (MAP)[19,20]. Hence, we were interested whether ASCA-positive CD patients may also more frequently contain antibodies against distinct mycobacterial strains and specifically against LAM, and whether these antibodies would be of cross-reactive nature.

In the case of MAP studies have shown a very high (77%-87%) prevalence of seroreactivity against the MAP antigens p35 and p36 in CD[21,22]. While this is intriguing, the interest in the possible relationship between CD and MAP mainly comes from the fact that Johne's disease in cattle which is caused by MAP infection in some aspects resembles CD.

The acute phase reactant mannose-binding lectin (MBL) specifically binds to mannose residues and is an important first line of defense innate immune effector molecule[23-26]. We have previously shown that deficiency for MBL associates with the ASCA-positive subgroup of CD patients[27,28]. Thus, it was of interest, if in CD, deficiency for MBL might associate with elevated levels of anti-mycobacterial IgG as well. Finally, we correlated our findings regarding anti-mycobacterial antibodies with different clinical CD phenotypes.

MATERIALS AND METHODS

Patients and sera

Sera from 105 patients with CD, 45 patients with UC and 35 healthy controls were obtained with informed consent and with the approval of the local ethical authorities. Diagnosis of CD and UC was established by endoscopic, histological and clinical criteria. CD: 54 women and 51 men, mean age 40 years (19-73); UC: 22 women and 23 men, mean age 38 years (20-65); healthy controls: 21 women and 14 men, mean age 37 years (18-67). Disease activity was graded for CD according to the CD activity index (CDAI), or for UC according to the Mayo-score[29,30]. At the time of blood collection, CD patients were treated as follows: no medical treatment ($n = 29$), 5-ASA ($n = 4$), steroids ($n = 8$), antibiotics ($n = 3$), infliximab ($n = 4$), or immunomodulators such as 6-mercaptopurine or azathioprine (6-MP/aza, $n = 47$), or methotrexate ($n = 20$). Some patients had combined medication: infliximab + methotrexate ($n = 1$), steroids + methotrexate ($n = 4$), steroids + 6-MP/aza ($n = 3$), infliximab + 6-MP/aza ($n = 2$). CDAI ranged between 75 and 380 (mean: 138 points). UC patients were treated as follows: no medical treatment ($n = 9$), 5-ASA ($n = 15$), steroids ($n = 6$), immunomodulators 6-MP/aza ($n = 20$), or tacrolimus ($n = 2$). Some of these patients had combined medication: 5-ASA + 6-MP/aza ($n = 4$), steroids + 6-MP/aza ($n = 3$). CD patients were grouped according to the Montreal classification[31] into a UC-like (purely inflammatory, non-stenosing, non-fistulizing), a stenosing, or a fistulizing phenotype. The latter two are summarized as complicated disease phenotype.

Mycobacteria, yeast and mannan

Mycobacterial strains used in this study were *M avium*, *M smegmatis*, *M chelonae*, MAP (all strains are patients' isolates and property of the Institute of Infectious Diseases, University of Bern), and BCG (commercial vaccination strain). Strains were grown in Middlebrook 7H9 medium (Difco™ BBL™, BD Biosciences, San Jose, CA, USA) with 10% OADC enrichment (Difco™ BBL™, BD Biosciences), 1 mg/mL casein peptone (Merck, Glattbrugg, Switzerland) and 0.5% glycerin, and were collected during logarithmic growth phase. For MAP cultures, growth medium was supplemented with 2 mg/mL Mycobactin J (Synbiotics Europe SAS, Munich, Germany). Bacteria were heat-inactivated for 1 h at 80℃ and then lysed in the presence of trypsin inhibitor and PMSF (Sigma, Buchs, Switzerland) by needle sonication (2 × 1 min. with 100 watts, on ice). The lysate was cleared by centrifugation and protein concentration determined.

Mannose-capped lipoarabinomannan (ManLAM) from M tuberculosis and (non-mannose-capped) phospho-myo-inositol-capped LAM (PILAM, subsequently termed LAM) were kindly provided by J. Belisle, Colorado State University. S cerevisiae Vita Gold was obtained from Deutsche Hefewerke, Nürnberg, Germany. The yeast was grown in 5% yeast peptone D-glucose (YPD, Sigma) and harvested during logarithmic growth. Mannan was extracted according to Kocourek and Balou[32]. Briefly, cells were resuspended in 20 mmol/L Na-citrate buffer (pH 7.0) and autoclaved for 3 h at 125℃. The supernatant was cleared by centrifugation and the pellet resuspended in Na-citrate buffer (1.5 × initial volume). After centrifugation, the supernatants were pooled and cleared from residual debris by centrifugation. The mannans were complexed with equal volumes of Fehling's solutions (Fehling Ⅰ: 6.93 g $CuSO_4 \cdot 5\ H_2O$/100 mL in H_2O; Fehling Ⅱ: 34.6 g $C_4H_4KNaO_6 \cdot 4H_2O$ + 12 g NaOH/100 mL in H_2O) and pelleted by centrifugation. The pellet was resolved in 3 mol/L HCl before precipitating the mannans off the $CuSO_4$ complex with a methanol/acetic acid 8:1 v/v solution while stirring. The precipitate was pelleted and washed repeatedly with methanol/acetic acid 8:1 v/v until the supernatant was colorless and clear and finally washed twice with methanol alone and dried in a desiccator at 4℃.

ELISA

ELISA was performed in Nunc-Immuno™ Maxisorp 96-well plates (Nunc, Wiesbaden, Germany). For mycobacteria-specific ELISA, 50 μL of mycobacterial lysates, purified LAM or ManLAM at 5 μg/mL PBS was added per well and dried over night at 37℃. The next day plates were blocked with 1% skim milk in PBS. For ASCA, tetanus toxoid (TT) or galanthus nivalis lectin (GNL)-binding ELISA, plates were coated with the respective antigen at 0.25 μg/mL carbonate-bicarbonate (25 mmol/L Na_2CO_3, 25 mmol/L $NaHCO_3$) coating buffer pH 9.6, overnight at 4℃. On the next day, plates were blocked with PBS + 0.5% BSA (PBS-BSA). Plates were washed and patients' sera added 1/500 (mycobacteria) or 1/1000 (ASCA, TT) PBS-BSA. Plates were incubated 1.5 h at room temperature (mycobacteria) or overnight at 4℃ (ASCA, TT). For the GNL-binding ELISA, biotinylated GNL (Vector Laboratories, Burlingame, CA, USA) was added at 5 μg/mL to the blocked plates. Plates were washed with PBS-BSA + 0.05% Tween 20 (PBST-BSA). For ASCA and TT ELISA peroxidase-coupled anti-human IgG (Sigma) was added 1/5000 in PBST-BSA and plates incubated for 1 h at room temperature. The plates incubated with biotinylated GNL were further incubated with peroxidase-coupled streptavidin (BD Biosciences). After washing ELISA was developed with TMB substrate (Sigma) for 15-30 min. in the dark. Reaction was stopped with 0.5 mol/L sulphuric acid and plates read at 450 nm. A cut-off value discriminating between negativity and positivity for anti-mycobacterial IgG was defined using the average extinction values for the healthy population (without the clearly positive individuals as defined by $A_{450} \geqslant 0.3$) and addition of 3 standard deviations. To determine the MBL oligomer concentration sera were diluted 1/100 and assessed in an MBL-oligomer ELISA kit according to the manufacturer's instructions (The Antibodyshop, Gentofte, Denmark).

Affinity purification of ASCA

S cerevisiae mannan was separated on an 8% polyacrylamide gel. The separated mannan was transferred to Hybond-ECL nitrocellulose membrane (Amersham GE Healthcare Europe, Otelfingen, Switzerland) and the ASCA-reactive material was localized by Western blot on a small section of the membrane. The ASCA-reactive region of the remaining membrane was cut into 8 equal pieces and the pieces blocked in TBS + 2% BSA.

Eight highly ASCA-positive sera from Crohn's patients were diluted 1/5 in TBS + 2% BSA and incubated with one piece of the membrane overnight at 4℃, on a rocking platform. After incubation the membranes were thoroughly washed with TBS and 1× with H_2O and bound antibodies eluted with 0.2 mol/L glycine, pH 2.8. The eluate was neutralized with Tris-base pH 8.0 and the eluted antibodies stabilized with 0.1% BSA.

Affinity purification of anti-*M smegmatis* antibodies

1 cm × 1 cm pieces of Hybond-ECL nitrocellulose membrane were decorated with *M smegmatis* lysate and sequentially incubated overnight at 4℃ and for 2 h at rt. Membranes were rinsed and blocked in TBS + 2% BSA. Incubation with sera and elution of bound antibodies was performed as described above.

Immunization of mice

C57BL/6 mice were reared in individually ventilated cages (IVC) under specified pathogen-free conditions. Housing and experimental procedures were in accordance with the European regulations on animal experimentation (FELASA). BCG culture was adjusted to a density of A_{600} = 0.5 MacFarland (10^8 cells per mL) with 0.9% sterile NaCl and 100 μL (10^7 viable bacteria) injected into the tail vein per mouse. Mice were 8 wk old and sex-matched. Viability of the mycobacteria was confirmed by reculturing the remaining bacterial suspension. Four weeks after infection serum was prepared from whole blood samples after clipping the tail tips. By week 5, the mice were boosted by iv with the same amount of mycobacteria and sera collected 4 and 13 wk later. Anti-BCG and ASCA IgM and IgG were determined by ELISA. To that end, samples were diluted 1/250 and anti mouse IgM and IgG HRP antibodies (Sigma) used 1/1000 and 1/500, respectively.

Statistical analysis

Raw data were imported into a statistical package program (STATA Versivn 9.0, Texas). Results of numerical data are presented as mean ± SE. Categorical data are summarized as the percentage of the group total. Two-sided Fisher's exact test ($n < 20$) or the Chi square test ($n \geqslant 20$) was used to explore associations of

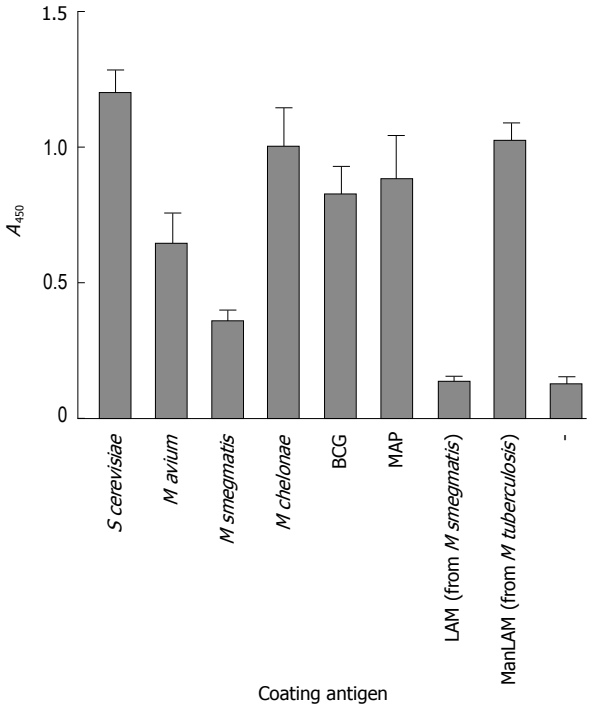

Figure 1 Reactivity of *Galanthus nivalis* lectin (GNL) with mycobacterial lysates and purified LAM or ManLAM. ELISA plates were coated with yeast mannan, mycobacterial lysates, purified LAM or ManLAM or coating buffer alone without antigen (-), and binding of biotinylated GNL to these antigens assessed by further incubation with peroxidase-coupled streptavidin followed by TMB substrate reaction. Shown are mean values ± SE of 3 individual experiments.

categorical data in 2 independent groups. The Wilcoxon rank sum test was used to explore associations of numerical data in 2 independent groups. A $P < 0.05$ was considered statistically significant. Associations between numerical data were evaluated using the Spearman rank correlation coefficient.

RESULTS

The dominant ASCA epitope terminal α-1,3 linked mannose is differentially present in lysates of different mycobacterial species

Phosphopeptidomannan with α-1,3 mannose (α-1,2 mannose α-1,2 mannose)$_n$ (n = 1 or 2) sugar residues represent a prominent epitope recognized by ASCA from CD patients[9,13]. The snowdrop lectin *Galanthus nivalis* agglutinin or lectin (GNL) has been shown to have high specificity for such terminal mannose sugar residues[16,17] and has been used to detect ASCA epitopes from microorganisms directly or in infected tissue[11,20]. After coating ELISA plates with mycobacterial lysates, purified LAM or ManLAM, or, as a positive control, yeast mannan, GNL differentially bound to these antigens. Besides yeast mannan, GNL strongly bound to lysate from *M chelonae* which is in perfect agreement with published observations[18]. Marked binding was further observed with lysates from BCG and MAP followed by *M avium* and *M smegmatis*. While no binding was observed to purified LAM, GNL strongly bound to ManLAM (Figure 1).

Higher frequencies of anti-mycobacterial IgG-positive individuals among patients with IBD compared to healthy controls

A_{450} extinction values of the anti-mycobacterial ELISA obtained with sera from the healthy population were used to define cut-off values for anti-mycobacterial IgG as described in the materials and methods section. According to these cut-off levels, between 13% (anti-LAM) and 45% (anti-*M smegmatis*) of CD patients were designated anti-mycobacterial IgG positive while in the group of healthy controls only 0 (anti-ManLAM) to 6% (anti-*M chelonae*, anti-MAP) were positive (Figure 2). Between 2% (anti-LAM) and 36% (anti-BCG) of UC patients were anti-mycobacterial IgG positive. Despite similar age groups, only one of the 35 healthy volunteers was tested positive for anti-BCG IgG while 42% of CD patients and 36% of UC patients were above the cut-off. Furthermore, while none of the healthy controls reached positivity for anti-ManLAM IgG, 19% of CD and 11% of UC patients did. Using the Chi-square test, differences in frequencies of positive individuals between the groups of CD patients and healthy controls were significant for IgG against all mycobacterial lysates tested and purified ManLAM. Differences between UC patients and controls were significant for *M chelonae*, BCG and ManLAM. Finally, compared to UC patients, CD patients were significantly more frequently positive for anti-*M avium* and anti-*M smegmatis* IgG (Figure 2).

Anti-mycobacterial IgG correlate with ASCA

To test whether seroreactivity against mycobacterial antigens in general and mycobacterial mannans in particular may correlate with that against yeast mannans, we grouped CD patients into ASCA-negative and ASCA-positive categories. ASCA-positive CD patients showed the highest frequencies of seropositivities against all mycobacterial antigens tested. Between 21% (anti-LAM) and 65% (anti-*M smegmatis*) of ASCA-positive CD patients were anti-mycobacterial IgG positive, while only 5% (anti-LAM) to 29% (anti-*M smegmatis*) of ASCA-negative CD patients had anti-mycobacterial IgG titers above the cut-off (Figure 3A). Compared to healthy controls, even the proportion of anti-LAM-positive individuals was significantly elevated in ASCA-positive CD patients (21% *vs* 4%). In addition, ASCA-positive CD patients were also significantly more frequently positive for IgG against *M smegmatis*, *M chelonae*, BCG, MAP and purified ManLAM when compared with ASCA-negative CD patients. On the other hand, ASCA-negative CD patients were significantly more frequently positive than healthy controls only for anti-*M smegmatis* IgG. When ASCA-positive CD patients were further grouped according to the levels of their ASCA titers, we observed a weak trend of increasing titers of IgG against mycobacterial lysates with increasing ASCA titers (data not shown). In contrast, seropositivity against purified LAM or ManLAM was almost exclusively and strongly elevated in the highest ASCA-positive subgroup. While less than 20% of ASCA-negative, or weakly positive CD patients were positive for anti-LAM

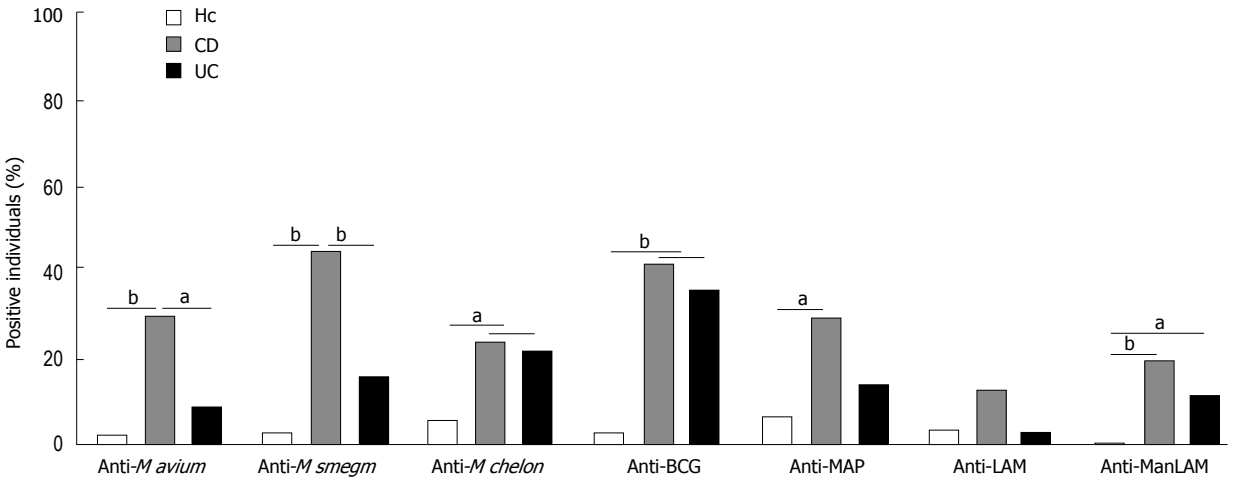

Figure 2 Determination of anti-mycobacterial serum IgG in IBD and healthy controls. ELISA for different mycobacterial lysates and purified LAM or ManLAM were performed with sera from 105 CD patients, 45 UC patients and 35 controls. A negative to positive discrimination level was defined by a cut-off value representing the average of all A_{450} values from the healthy controls (excluding the clearly positive individuals with an $A_{450} \geqslant 0.3$) plus 3 standard deviations. With these cut-off values, individuals positive for antibodies against the various mycobacterial antigens were identified and are shown as a percent of the total population. Asterisks indicate significant differences between the populations. $^{a}P < 0.05$, $^{b}P < 0.01$.

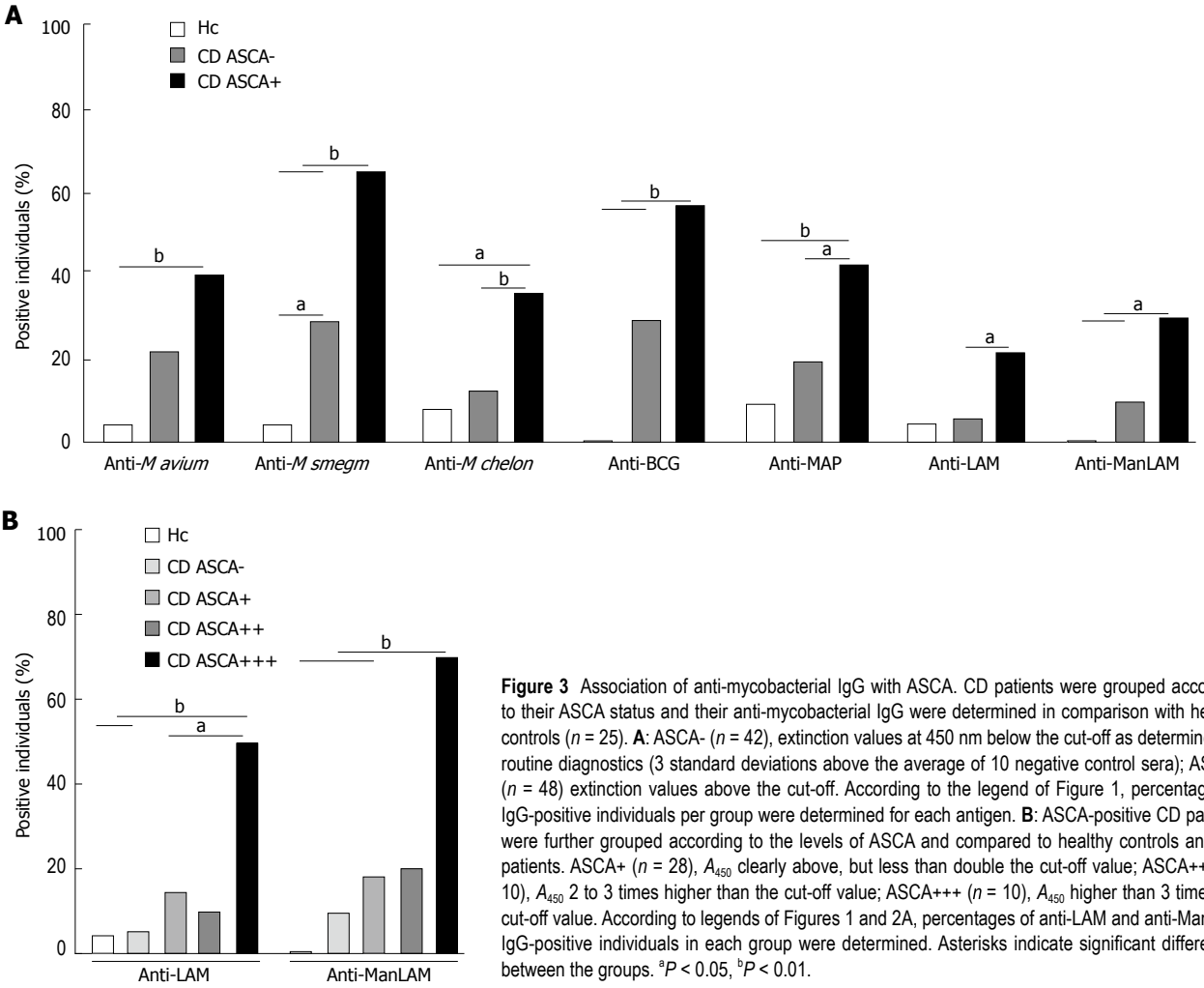

Figure 3 Association of anti-mycobacterial IgG with ASCA. CD patients were grouped according to their ASCA status and their anti-mycobacterial IgG were determined in comparison with healthy controls ($n = 25$). **A**: ASCA- ($n = 42$), extinction values at 450 nm below the cut-off as determined by routine diagnostics (3 standard deviations above the average of 10 negative control sera); ASCA+ ($n = 48$) extinction values above the cut-off. According to the legend of Figure 1, percentages of IgG-positive individuals per group were determined for each antigen. **B**: ASCA-positive CD patients were further grouped according to the levels of ASCA and compared to healthy controls and UC patients. ASCA+ ($n = 28$), A_{450} clearly above, but less than double the cut-off value; ASCA++ ($n = 10$), A_{450} 2 to 3 times higher than the cut-off value; ASCA+++ ($n = 10$), A_{450} higher than 3 times the cut-off value. According to legends of Figures 1 and 2A, percentages of anti-LAM and anti-ManLAM IgG-positive individuals in each group were determined. Asterisks indicate significant differences between the groups. $^{a}P < 0.05$, $^{b}P < 0.01$.

and anti-ManLAM IgG, 50% and 70% of the highest ASCA-positive CD patients were positive for anti-LAM ($P \leqslant 0.0362$, *vs* ASCA-low or ASCA-negative patients) and anti-ManLAM IgG ($P \leqslant 0.0047$, *vs* ASCA-low or ASCA-negative patients; Figure 3B), respectively. To better visualize the extent of correlations between anti-mycobacterial IgG and ASCA, we plotted the extinction values obtained in the mycobacterial ELISA against those of the ASCA ELISA (Figure 4). All correlations were highly significant and ASCA correlated best with

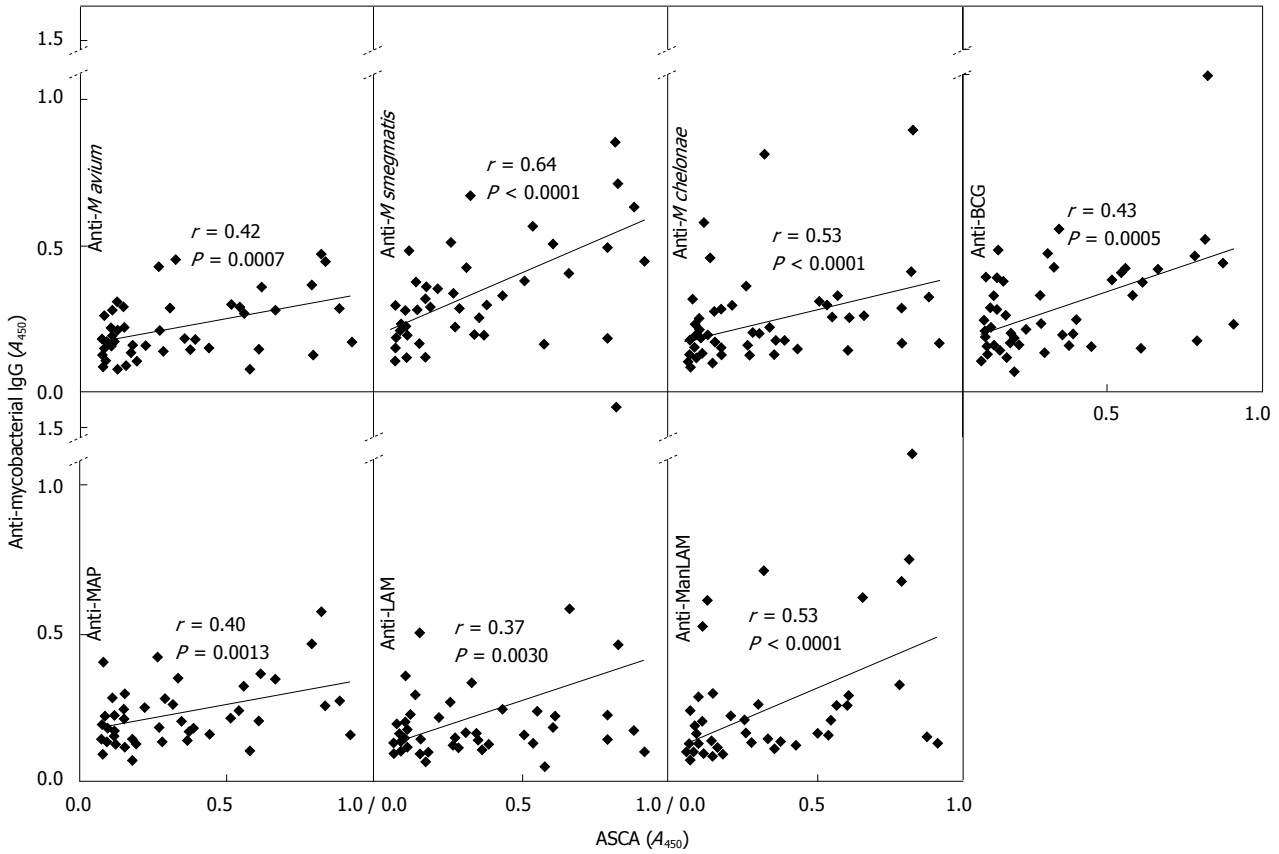

Figure 4 Correlation of ASCA with anti-mycobacterial IgG titers. Sera from 60 CD patients were randomly chosen and used for determination of ASCA titers and anti-mycobacterial IgG levels in the same experiment. Each dot represents one serum sample with the A_{450} obtained in the ASCA-specific ELISA (x-axis) and that obtained with ELISA specific for IgG against different mycobacterial lysates or purified LAM or ManLAM (y-axis).

IgG against *M smegmatis* ($r = 0.64$, $P < 0.0001$), followed by anti- BCG and anti-ManLAM IgG ($r = 0.53$, $P < 0.0001$).

ASCA-positivity and MBL-deficiency synergistically associate with anti-mycobacterial IgG

Since deficiency for MBL associates with the ASCA-positive subgroup of CD patients 27, 28 we asked whether deficiency for MBL might also associate with elevated levels of anti-mycobacterial IgG. We found that similar to ASCA-positivity, MBL-deficiency was associated with higher proportions of anti-mycobacterial IgG-positive individuals for some but not all mycobacterial antigens tested (Figure 5), intriguingly, MBL-negativity synergistically contributed to increased frequencies of anti-mycobacterial IgG-positive individuals in the ASCA-positive/MBL-negative as compared to the ASCA-/MBL-double positive subgroup of CD patients. The synergistic effect that MBL-negativity and ASCA-positivity had regarding increased frequencies of anti-mycobacterial IgG positive individuals was most obvious when the ASCA-positive/MBL-negative group was compared with the ASCA-negative/MBL-positive group of CD patients: between 2.7-fold (from 13.0% to 35.3% for anti-*M chelonae*) and 7.4-fold (from 8.7% to 64.7% for anti-*M avium*) increased proportion of anti-mycobacterial IgG-positive individuals.

Anti-mycobacterial antibodies bind to yeast mannan

To determine potential cross-reactivities between anti-mycobacterial antibodies and ASCA, we affinity-purified eight highly ASCA-positive sera from CD patients on yeast mannan and compared original sera with the corresponding affinity purified antibodies for reactivity with yeast mannan (positive control), mycobacterial lysates and purified LAM and ManLAM. A tetanus toxoid-specific ELISA confirmed that affinity-purified serum antibodies were virtually free of contaminating, non-yeast mannan-specific IgG. Affinity-purified ASCA from individual patients showed individual reactivity patterns. While three of eight patients' ASCA reacted markedly with all mycobacterial preparations (patients No. 1, 4 and 7), 5 patients showed restricted reactivity (Figure 6A). On average, affinity-purified antibodies showed the highest degree of reactivity with LAM (73% ± 34% of original sera) and lowest with MAP lysate (35% ± 16% of original sera). The same 8 highly ASCA-positive sera were also affinity purified on *M smegmatis* lysate and assessed for reactivity with yeast mannan and tetanus toxoid. All sera showed strongly reduced reactivity with yeast mannan after affinity-purification (Figure 6B).

Infection of mice with BCG leads to transient production of immunoglobulins that cross-react with *S cerevisiae* mannan

To test, whether experimentally induced antibodies

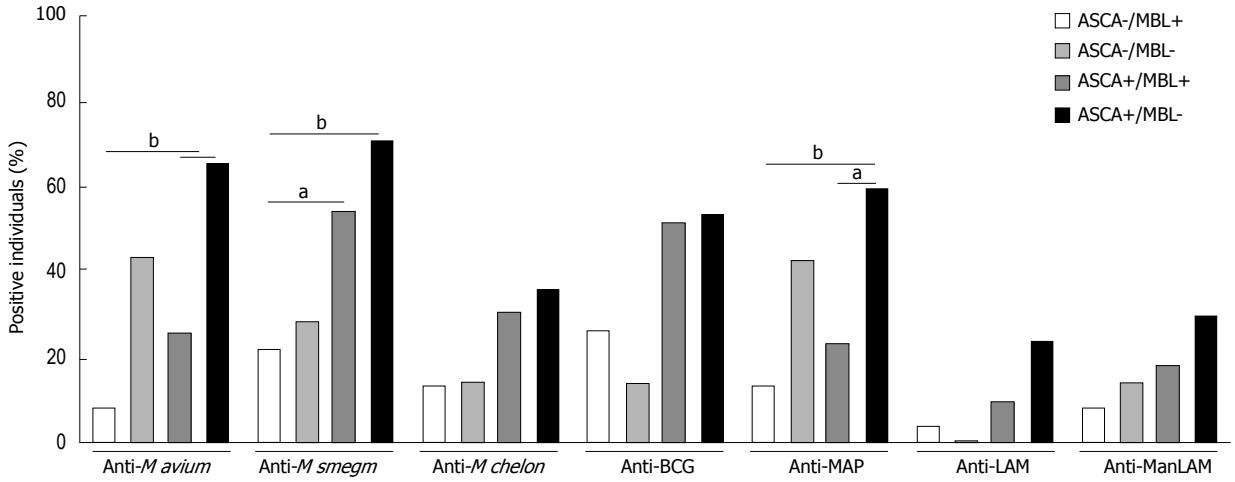

Figure 5 ASCA-positivity and MBL-negativity synergistically associate with anti-mycobacterial seroreactivity. CD patients' sera were grouped according to their ASCA and MBL status. ASCA-negative and ASCA-positive patients were separated into MBL-expressers (> 500 ng/mL, n = 23 and 39, respectively) and MBL-low/deficient ($\leqslant$ 500 ng/mL, n = 7 and 17, respectively) individuals. From each group, average IgG levels against mycobacterial lysates or purified LAM or ManLAM ± SEM were determined. Percentages of individuals per group with anti-mycobacterial IgG titers above the cut-off levels are shown. Significant differences are marked with asterisks. $^{a}P < 0.05$, $^{b}P < 0.01$.

against mycobacteria may cross-react with *S cerevisiae* mannan, we infected mice with 10^7 live BCG, followed by an equal booster injection after 5 wk. Figure 7 shows that infection with BCG induced marked levels of BCG-lysate-specific IgM and moderate levels of specific IgG after 4 wk and up to 13 wk after the booster injection. Intriguingly, BCG infection led to transiently elevated titers of ASCA IgM and IgG which declined to background or near background levels within 2 mo post booster injection.

Higher frequency of anti-mycobacterial IgG-positive individuals in the subgroup of CD patients with fistulizing disease

In order to address the possible significance of anti-mycobacterial IgG in CD, patients were grouped according to the Montreal classification into UC-like (purely inflammatory), or stenosing or fistulizing disease phenotype (the latter two summarized as complicated disease). Sera from these groups of CD patients were compared for anti-mycobacterial IgG and ASCA by ELISA. ASCA were included because earlier reports indicate that ASCA associate with complicated disease[33,34] and increased risk for surgery months[35]. There was a weak tendency for patients with complicated disease to more often express anti-mycobacterial IgG compared to patients with UC-like disease (data not shown). On the other hand, a markedly higher frequency of patients expressed antibodies against mycobacterial lysates, but not purified LAM or ManLAM, when only the subgroup of patients with fistulizing disease was compared with UC-like disease (Figure 8). These differences were statistically significant for anti-*M avium* (P = 0.024), anti-*M smegmatis* (P = 0.004) and anti-MAP IgG (P = 0.045). In contrast, the proportion of patients with stenoses expressing IgG against mycobacterial lysates was not markedly elevated compared to those with UC-like disease. Both subgroups with complicated disease had a markedly higher proportion of individuals being positive for ASCA compared to UC-like disease. Here, the difference was statistically significant for the subgroup with stenoses compared to UC-like disease (P = 0.008, Figure 8). Finally, compared to patients with UC-like disease or stenoses, patients with fistulizing disease on average showed more individual seroreactivities per patient against the mycobacterial antigens tested (2.5 *vs* 1.5/1.6, P = 0.050, Figure 8B).

DISCUSSION

In the present study we have chosen a number of mycobacterial strains with more or less ubiquitous occurrence and - with the exception of BCG-originally isolated from patients suffering from mycobacterial infections to serve as antigens for ELISA with IBD patients' and control sera in order to assess a possible relationship between anti-mycobacterial antibodies and ASCA in CD. In addition, we used purified lipoarabinomannans with or without a richly mannosylated arabinose moiety (LAM from *M smegmatis* and ManLAM from *M tuberculosis*, respectively) because of similar oligomannose side chains as found in mannan from *S cerevisiae*, the specific antigen for ASCA. In agreement with published data[19,20], terminal α-1,3 linked mannose which is part of the dominant ASCA epitope was present at different extents in our mycobacterial preparations. In particular this epitope was strongly present in ManLAM from M tuberculosis while it was completely absent in LAM from *M smegmatis*. In accordance with that, *M smegmatis* lysate showed the weakest binding to GNL among all lysates tested. With the exception of non-mannose-capped LAM, we found significantly higher proportions of anti-mycobacterial IgG-positive individuals in CD compared to the healthy control group. We focused on IgG because initial screenings generally showed much lower levels

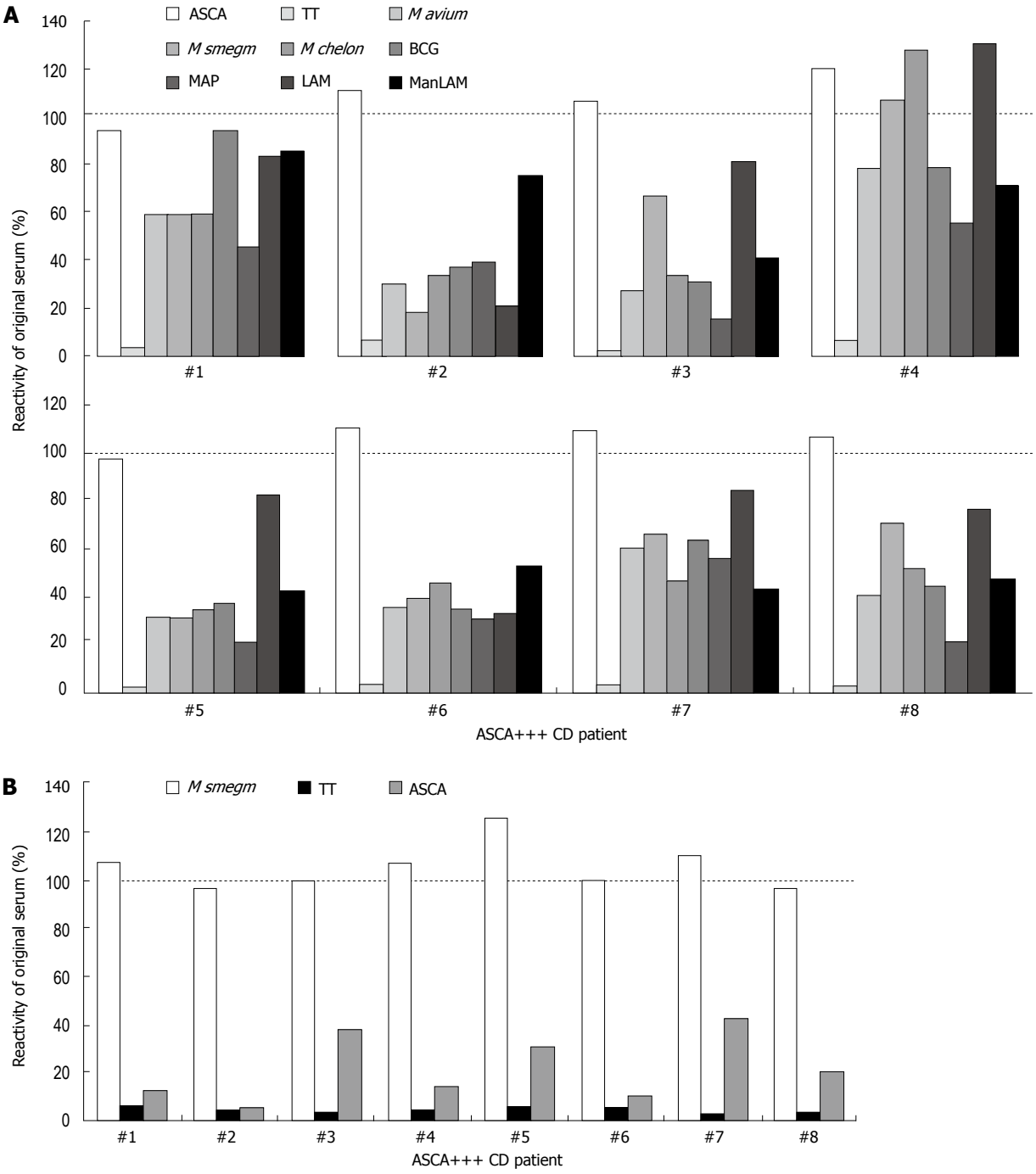

Figure 6 ASCA strongly cross-react with mycobacterial antigens in a subgroup of ASCA-positive CD patients. **A**: Eight sera from highly ASCA-positive CD patients were incubated with membrane sections of yeast mannan Western blots containing the ASCA-reactive material, and bound antibodies were eluted. Eluted antibodies were titrated to yield comparable extinction values in the ASCA ELISA as with the original serum (approx. 100%, empty columns) and used at the corresponding dilution to assess reactivities against mycobacterial antigens. As a specificity control for affinity purification, eluted antibodies were also tested in a tetanus toxoid (TT) ELISA. **B**: The same 8 patients' sera were also affinity purified on nitrocellulose membranes decorated with *M smegmatis* lysate. In analogy to A, eluted antibodies were adjusted for equal reactivity with *M smegmatis* as the original sera (approx. 100%, empty columns) and tested at the corresponding dilution for reactivities against yeast mannan and TT.

or absence of specific IgA (data not shown). Previous studies have mainly focused on seroreactivities against selected antigens from MAP[22,36,37]. Naser *et al* have observed that a large proportion of CD, but neither UC patients nor controls had antibodies reactive with two recombinant antigens (75% and 89%, respectively) from their MAP genomic library[22]. In contrast, less than 30% of our CD patients showed broad MAP-specific seroreactivity. Our results are comparable to those described by Polymeros *et al*, who found that sera of 42% of their small cohort of CD patients reacted with one or more MAP-derived peptides[37]. In our study UC patients showed-although less marked than CD patients - enhanced seroreactivity compared to healthy controls, in particular against some of the crude lysates. This is not surprising as enhanced seroreactivities against unusual,

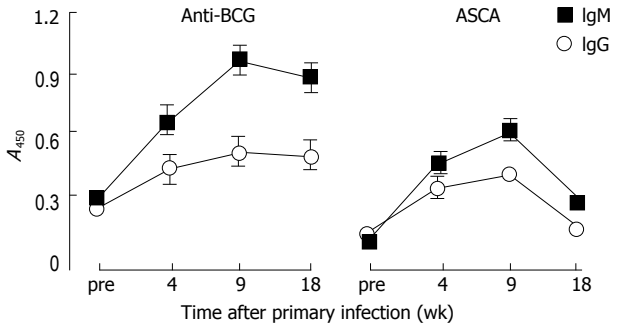

Figure 7 Antibody response of mice infected with *M bovis* BCG. C57BL/6 mice were intravenously infected with 10^7 viable *M bovis* BCG and the infection repeated after 5 wk. Serum was prepared from blood samples collected before infections, 4 wk after primary infection and 4 wk and 13 wk after secondary infection. Serum samples were tested for the presence of IgM (filled squares) and IgG (empty spheres) antibodies specific for *M bovis* BCG (left panel) and for *S cerevisiae* mannan (right panel). Results are shown as average A_{450} values of 4 animals ± SE.

untypical or commensal antigens is not only a hallmark of CD but of IBD in general[38].

While Polymeros *et al*[37] addressed a potential self-cross-reactive nature of anti-MAP antibodies in CD patients, in the present study, we were focusing on potential cross reactivities of CD patients' anti-mycobacterial antibodies with mannan from *S cerevisiae*. We could clearly demonstrate that the frequent seroreactivity against cell wall mannan from *S cerevisiae* (ASCA-positivity) in CD patients significantly correlated with seroreactivity not only against MAP, but also against antigens from all other mycobacteria that we tested. Importantly, correlations were best for *M smegmatis* lysate and purified ManLAM. The *M tuberculosis*-derived ManLAM used in the present study is characterized by highly mannosylated arabinose (similar to the ManLAM from BCG). While Stokes *et al* have also observed binding of GNL to *M tuberculosis*[39], ManLAM from *M tuberculosis* should theoretically not contain the GNL-reactive α-1,3 linked mannose residues according to biochemical analyses[40]. On the other hand, the phospho-myo-inositol-capped LAM of *M smegmatis* has no rich mannose-cap on its arabinose moiety[41,42] and shows no binding to GNL. Collectively, the good correlations between seroreactivities against *S cerevisiae* mannan and mycobacterial antigens shown in the present study do not solely depend on the presence of either the terminal α-1,3 linked mannose residues or a rich mannose-cap. *M chelonae* is one of the rare mycobacterial strains with truly uncapped arabinose moieties on their LAM, also termed AraLAM or CheLAM[18]. On the other hand, this strain's lysate is very well recognized by GNL which may explain the increased reactivity with ASCA-positive CD patients' IgG.

Even in the absence of the dominant ASCA epitope terminal α-1,3 linked mannose there was a good and significant correlation of ASCA-positivity with seroreactivities against purified LAM, most strikingly if only those patients with high ASCA titers were considered.

Because in our cohort of CD patients MBL-deficiency associates with positivity for ASCA[27,28], we wondered whether generation of anti-mycobacterial antibodies may associate with this deficiency as well, and whether such an association may depend on certain strains with differential presence of the terminal α-1,3 linked mannose motive and/or distinctly capped LAM. Indeed, we found an association of MBL deficiency with the prevalence of anti-mycobacterial antibodies. However, this association was not confined to strains with mannose-capped LAM and was not apparent for antibodies to BCG with rich mannose caps or *M chelonae* with the best binding to GNL apart from yeast mannan. It is known that MBL facilitates the entry of mycobacteria into host cells[43,44]. Therefore, in MBL-deficient persons, a stronger systemic immune response may be expected since the mycobacterial (cell wall) antigens are not rapidly eliminated by phagocytes.

The strong association of anti-mycobacterial antibodies with high ASCA titers with the observed synergistic effect of MBL-deficiency may be explained in different ways. First, it may be that these individuals have, due to a genetic predisposition, an increased reactivity to environmental (mannosylated) antigens. Alternatively there could be a true antibody cross-reactivity between the mannan antigens of *S cerevisiae* and mycobacteria. To address this question we affinity-purified ASCA from highly ASCA-positive CD patients and could show that these purified antibodies exert variable degrees of cross-reactivities between yeast mannan and mycobacterial lysates or purified (Man) LAM. On the other hand, affinity-purification of antibodies against *M smegmatis* lysate - the lysate that showed the highest degree of binding with affinity-purified ASCA-led to strongly reduced reactivity with yeast mannan compared to the original serum. Thus, while in some patients anti-mycobacterial IgG are mainly due to cross-reactive ASCA, in others, ASCA and anti-mycobacterial antibodies have separate specificities. In either case, the fact that affinity-purified anti-*M smegmatis* IgG only show weak or no reactivity with yeast mannan suggests that such cross-reactive antibodies only account for a minor fraction of total ASCA. This constellation makes it very unlikely that mycobacterial antigens play a role in the induction of ASCA. Since our purified LAM does not contain the terminal α-1,3 mannose motif but shows a high degree of reactivity with affinity-purified ASCA, it has to be discussed whether the spectrum of antigens recognized by CD patients' ASCA goes beyond terminal α-1,3 linked mannose side chains and may encompass other antigens such as peptide epitopes from the protein part of the mannan. In this context, it is of interest that according to a recent study CD patients contain antibodies that cross-react to an individual extent between β2-glycoprotein I and yeast phosphope ptidomannans[45].

Our experimental mouse model was to test whether mycobacterial infection is theoretically able to trigger induction of ASCA. For infection of mice we have chosen BCG because it is a commercial vaccination strain and is well established for infection and immunization studies in mice. Our finding that ASCA were only transiently expressed and declined by 2 mo post-booster

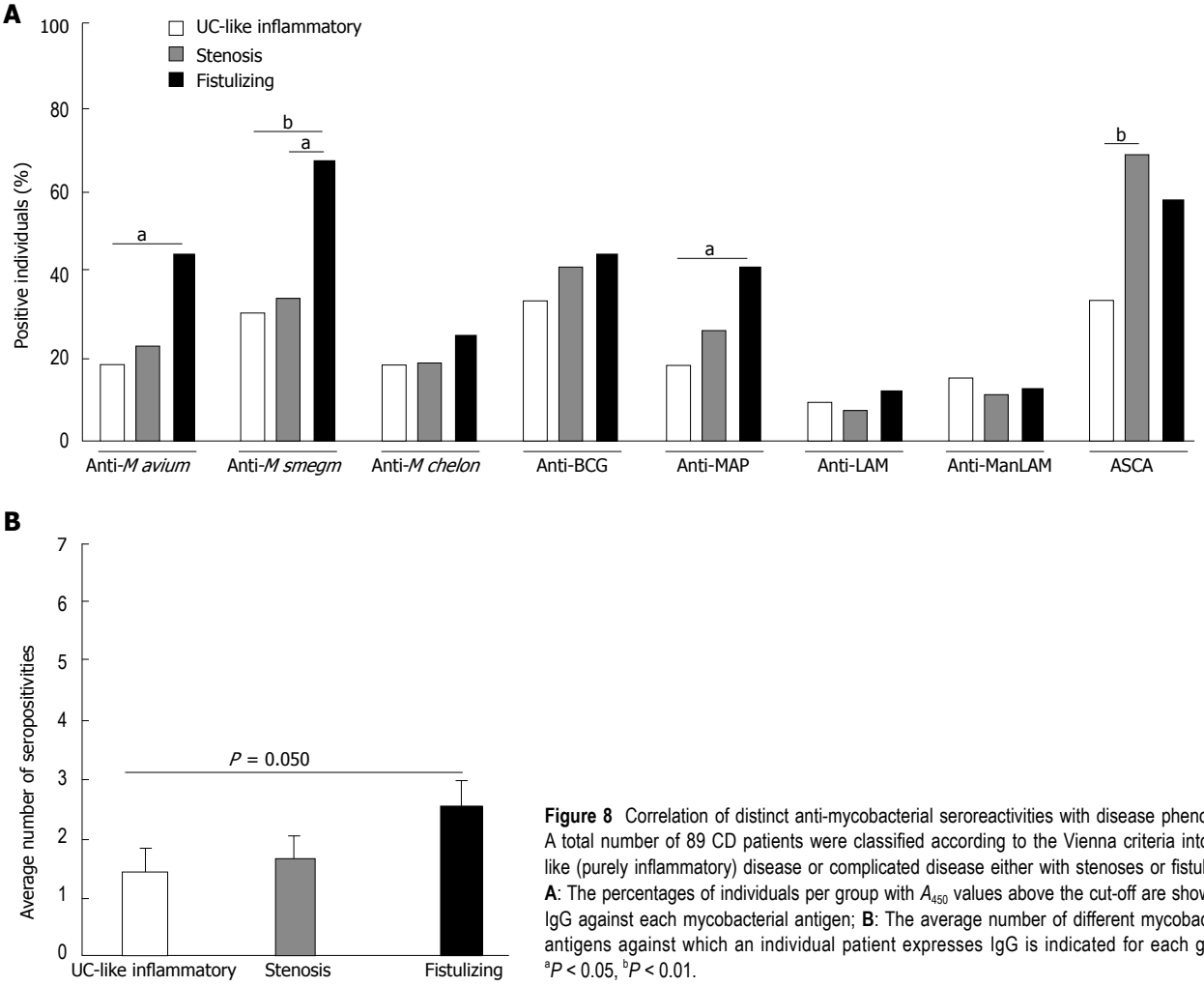

Figure 8 Correlation of distinct anti-mycobacterial seroreactivities with disease phenotype. A total number of 89 CD patients were classified according to the Vienna criteria into UC-like (purely inflammatory) disease or complicated disease either with stenoses or fistulizing. **A**: The percentages of individuals per group with A_{450} values above the cut-off are shown for IgG against each mycobacterial antigen; **B**: The average number of different mycobacterial antigens against which an individual patient expresses IgG is indicated for each group. $^{a}P < 0.05$, $^{b}P < 0.01$.

infection while BCG-specific IgM and IgG remained high, supports our conclusion from the results of the affinity-purification study that an immune reactivity to mycobacterial antigens is unlikely to trigger the induction of a stable phenotype of ASCA-positivity.

We were interested whether seroreactivity to mycobacterial antigens may associate with a certain disease phenotype. We observed that more patients with complicated disease (stenosing or fistulizing) expressed antibodies against mycobacterial lysates compared to patients with purely inflammatory disease. Since we observed strong associations of anti-mycobacterial antibodies with ASCA-positivity and ASCA have been shown to associate with complicated disease[33-35], our findings were not unexpected. However, the fact that this trend was clearly confined to the subgroup with fistulizing disease, while ASCA-positivity even better associated with stenoses, is surprising. Possibly, ingested mycobacteria more easily gain access to systemic immune compartments for priming if the bowel wall is transmurally damaged. Regarding ASCA, the origin of this unusual immune response is still unknown and whatever it is may actually be involved in the progression to more severe CD phenotypes. Finally, patients with fistulizing disease more frequently showed seroreactivities against multiple mycobacterial antigens compared to those with UC-like disease. This observation fits to data published by others showing a more severe phenotype of disease in patients with increasing numbers of seroreactivities to various intestinal (commensal) antigens[46].

In conclusion, we were able to demonstrate that ASCA-positive patients had significantly more immune reactivities to mycobacterial antigens. In a subgroup of ASCA-positive CD patients, anti-mycobacterial immunoglobulins at least partially represent cross-reactive ASCA, while in others there seem to be separate ASCA and anti-mycobacterial antibodies that do not cross-react. Furthermore, purified anti-*M smegmatis* IgG showed low or no binding to yeast mannan. Therefore, we postulate that our results reflect more the predisposition of CD patients to develop increased immune reactivities to various ubiquitous antigens in general and mannosylated antigens in particular, rather than a role of mycobacteria in the induction of ASCA.

ACKNOWLEDGMENTS

The authors would like to thank Martin Sauter for technical assistance with purification and characterization of *S cerevisiae* mannan, Beatrice Flogerzi for lab-technical assistance, Irène Garcia for help with mycobacterial infection, and Linda Bolzern for carefully reading the manuscript.

COMMENTS

Background

A subgroup of patients with Crohn's disease (CD) develops antibodies against *S cerevisiae* cell wall mannan (ASCA). The mechanism of ASCA generation is still unclear. It is possible that some opportunistic or pathogenic infectious microorganism may be the initial inducer of this unusual antibody response because similar (cell wall) mannans also occur in other microorganisms such as mycobacteria with their lipoarabinomannan (LAM).

Research frontiers

It has been shown that the opportunistic pathogen *Candida albicans* is able to experimentally induce ASCA (Standaert-Vitse *et al* 2006) and we have shown that Crohn's patients' ASCA cross-react with cell wall mannans from different yeast strains including *C albicans* (Schaffer *et al* 2007). In contrast to yeast, there exists a highly controversial debate on a possible role for mycobacteria in the etiopathogenesis of Crohn's disease.

Innovations and breakthroughs

Our study clearly shows that (1) mycobacterial infection is very unlikely the origin of ASCA since anti-mycobacterial antibodies and ASCA in an individual patient are either non-overlapping or the former only represents a minor part of all antibodies recognizing yeast mannan; and (2) the correlation of antibodies against mycobacterial antigens with those against yeast mannan reflects - apart from pure cross-reactivity in some patients - increased predisposition for adaptive immune responses against ubiquitous antigens, especially observed in patients with a severe disease phenotype.

Applications

The findings in the present study represent an important basis for further research on the role of antimicrobial immune responses in the pathogenesis of Crohn's disease. Furthermore, antimicrobial antibody patterns may define distinct subgroups of Crohn's patients requiring individual treatment approaches.

Peer review

Similar to ASCA, seroreactivity against mycobacteria may define CD patients with complicated disease and a predisposition for immune responses against ubiquitous antigens. Mycobacterial infection does not likely play a role in ASCA induction.

REFERENCES

1 **Duchmann R**, Kaiser I, Hermann E, Mayet W, Ewe K, Meyer zum Buschenfelde KH. Tolerance exists towards resident intestinal flora but is broken in active inflammatory bowel disease (IBD). *Clin Exp Immunol* 1995; **102**: 448-455

2 **Sartor RB**. Targeting enteric bacteria in treatment of inflammatory bowel diseases: why, how, and when. *Curr Opin Gastroenterol* 2003; **19**: 358-365

3 **Greenstein RJ**. Is Crohn's disease caused by a mycobacterium? Comparisons with leprosy, tuberculosis, and Johne's disease. *Lancet Infect Dis* 2003; **3**: 507-514

4 **Sandborn WJ**. Serologic markers in inflammatory bowel disease: state of the art. *Rev Gastroenterol Disord* 2004; **4**: 167-174

5 **Reumaux D**, Sendid B, Poulain D, Duthilleul P, Dewit O, Colombel JF. Serological markers in inflammatory bowel diseases. *Best Pract Res Clin Gastroenterol* 2003; **17**: 19-35

6 **Main J**, McKenzie H, Yeaman GR, Kerr MA, Robson D, Pennington CR, Parratt D. Antibody to Saccharomyces cerevisiae (bakers' yeast) in Crohn's disease. *BMJ* 1988; **297**: 1105-1106

7 **Seibold F**. ASCA: genetic marker, predictor of disease, or marker of a response to an environmental antigen? *Gut* 2005; **54**: 1212-1213

8 **Seibold F**, Stich O, Hufnagl R, Kamil S, Scheurlen M. Anti-Saccharomyces cerevisiae antibodies in inflammatory bowel disease: a family study. *Scand J Gastroenterol* 2001; **36**: 196-201

9 **Sendid B**, Colombel JF, Jacquinot PM, Faille C, Fruit J, Cortot A, Lucidarme D, Camus D, Poulain D. Specific antibody response to oligomannosidic epitopes in Crohn's disease. *Clin Diagn Lab Immunol* 1996; **3**: 219-226

10 **Wheeler RT**, Kupiec M, Magnelli P, Abeijon C, Fink GR. A Saccharomyces cerevisiae mutant with increased virulence. *Proc Natl Acad Sci USA* 2003; **100**: 2766-2770

11 **Standaert-Vitse A**, Jouault T, Vandewalle P, Mille C, Seddik M, Sendid B, Mallet JM, Colombel JF, Poulain D. Candida albicans is an immunogen for anti-Saccharomyces cerevisiae antibody markers of Crohn's disease. *Gastroenterology* 2006; **130**: 1764-1775

12 **Schaffer T**, Muller S, Flogerzi B, Seibold-Schmid B, Schoepfer AM, Seibold F. Anti-Saccharomyces cerevisiae mannan antibodies (ASCA) of Crohn's patients crossreact with mannan from other yeast strains, and murine ASCA IgM can be experimentally induced with Candida albicans. *Inflamm Bowel Dis* 2007; **13**: 1339-1346

13 **Young M**, Davies MJ, Bailey D, Gradwell MJ, Smestad-Paulsen B, Wold JK, Barnes RM, Hounsell EF. Characterization of oligosaccharides from an antigenic mannan of Saccharomyces cerevisiae. *Glycoconj J* 1998; **15**: 815-822

14 **Chatterjee D**. The mycobacterial cell wall: structure, biosynthesis and sites of drug action. *Curr Opin Chem Biol* 1997; **1**: 579-588

15 **Nigou J**, Gilleron M, Puzo G. Lipoarabinomannans: from structure to biosynthesis. *Biochimie* 2003; **85**: 153-166

16 **Shibuya N**, Goldstein IJ, Van Damme EJ, Peumans WJ. Binding properties of a mannose-specific lectin from the snowdrop (Galanthus nivalis) bulb. *J Biol Chem* 1988; **263**: 728-734

17 **Kaku H**, Goldstein IJ, Oscarson S. Interactions of five D-mannose-specific lectins with a series of synthetic branched trisaccharides. *Carbohydr Res* 1991; **213**: 109-116

18 **Guerardel Y**, Maes E, Elass E, Leroy Y, Timmerman P, Besra GS, Locht C, Strecker G, Kremer L. Structural study of lipomannan and lipoarabinomannan from Mycobacterium chelonae. Presence of unusual components with alpha 1,3-mannopyranose side chains. *J Biol Chem* 2002; **277**: 30635-30648

19 **Michell SL**, Whelan AO, Wheeler PR, Panico M, Easton RL, Etienne AT, Haslam SM, Dell A, Morris HR, Reason AJ, Herrmann JL, Young DB, Hewinson RG. The MPB83 antigen from Mycobacterium bovis contains O-linked mannose and (1-->3)-mannobiose moieties. *J Biol Chem* 2003; **278**: 16423-16432

20 **Mpofu CM**, Campbell BJ, Subramanian S, Marshall-Clarke S, Hart CA, Cross A, Roberts CL, McGoldrick A, Edwards SW, Rhodes JM. Microbial mannan inhibits bacterial killing by macrophages: a possible pathogenic mechanism for Crohn's disease. *Gastroenterology* 2007; **133**: 1487-1498

21 **Shafran I**, Piromalli C, Decker JW, Sandoval J, Naser SA, El-Zaatari FA. Seroreactivities against Saccharomyces cerevisiae and Mycobacterium avium subsp. paratuberculosis p35 and p36 antigens in Crohn's disease patients. *Dig Dis Sci* 2002; **47**: 2079-2081

22 **Naser SA**, Hulten K, Shafran I, Graham DY, El-Zaatari FA. Specific seroreactivity of Crohn's disease patients against p35 and p36 antigens of M. avium subsp. paratuberculosis. *Vet Microbiol* 2000; **77**: 497-504

23 **Turner MW**. Mannose-binding lectin (MBL) in health and disease. *Immunobiology* 1998; **199**: 327-339

24 **Vasta GR**, Quesenberry M, Ahmed H, O'Leary N. C-type lectins and galectins mediate innate and adaptive immune functions: their roles in the complement activation pathway. *Dev Comp Immunol* 1999; **23**: 401-420

25 **Jack DL**, Klein NJ, Turner MW. Mannose-binding lectin: targeting the microbial world for complement attack and opsonophagocytosis. *Immunol Rev* 2001; **180**: 86-99

26 **Dommett RM**, Klein N, Turner MW. Mannose-binding lectin in innate immunity: past, present and future. *Tissue Antigens* 2006; **68**: 193-209

27 **Seibold F**, Konrad A, Flogerzi B, Seibold-Schmid B, Arni S, Juliger S, Kun JF. Genetic variants of the mannan-binding lectin are associated with immune reactivity to mannans in

Crohn's disease. *Gastroenterology* 2004; **127**: 1076-1084
28 **Seibold F**, Boldt AB, Seibold-Schmid B, Schoepfer AM, Flogerzi B, Muller S, Kun JF. Deficiency for mannan-binding lectin is associated with antibodies to Saccharomyces cerevisiae in patients with Crohn's disease and their relatives. *Gut* 2007; **56**: 152
29 **Best WR**, Becktel JM, Singleton JW, Kern F Jr. Development of a Crohn's disease activity index. National Cooperative Crohn's Disease Study. *Gastroenterology* 1976; **70**: 439-444
30 **Schroeder KW**, Tremaine WJ, Ilstrup DM. Coated oral 5-aminosalicylic acid therapy for mildly to moderately active ulcerative colitis. A randomized study. *N Engl J Med* 1987; **317**: 1625-1629
31 **Satsangi J**, Silverberg MS, Vermeire S, Colombel JF. The Montreal classification of inflammatory bowel disease: controversies, consensus, and implications. *Gut* 2006; **55**: 749-753
32 **Kocourek J**, Ballou CE. Method for fingerprinting yeast cell wall mannans. *J Bacteriol* 1969; **100**: 1175-1181
33 **Vasiliauskas EA**, Kam LY, Karp LC, Gaiennie J, Yang H, Targan SR. Marker antibody expression stratifies Crohn's disease into immunologically homogeneous subgroups with distinct clinical characteristics. *Gut* 2000; **47**: 487-496
34 **Dassopoulos T**, Frangakis C, Cruz-Correa M, Talor MV, Burek CL, Datta L, Nouvet F, Bayless TM, Brant SR. Antibodies to saccharomyces cerevisiae in Crohn's disease: higher titers are associated with a greater frequency of mutant NOD2/CARD15 alleles and with a higher probability of complicated disease. *Inflamm Bowel Dis* 2007; **13**: 143-151
35 **Forcione DG**, Rosen MJ, Kisiel JB, Sands BE. Anti-Saccharomyces cerevisiae antibody (ASCA) positivity is associated with increased risk for early surgery in Crohn's disease. *Gut* 2004; **53**: 1117-1122
36 **Olsen I**, Wiker HG, Johnson E, Langeggen H, Reitan LJ. Elevated antibody responses in patients with Crohn's disease against a 14-kDa secreted protein purified from Mycobacterium avium subsp. paratuberculosis. *Scand J Immunol* 2001; **53**: 198-203
37 **Polymeros D**, Bogdanos DP, Day R, Arioli D, Vergani D, Forbes A. Does cross-reactivity between mycobacterium avium paratuberculosis and human intestinal antigens characterize Crohn's disease? *Gastroenterology* 2006; **131**: 85-96
38 **Bossuyt X**. Serologic markers in inflammatory bowel disease. *Clin Chem* 2006; **52**: 171-181
39 **Stokes RW**, Norris-Jones R, Brooks DE, Beveridge TJ, Doxsee D, Thorson LM. The glycan-rich outer layer of the cell wall of Mycobacterium tuberculosis acts as an antiphagocytic capsule limiting the association of the bacterium with macrophages. *Infect Immun* 2004; **72**: 5676-5686
40 **Chatterjee D**, Lowell K, Rivoire B, McNeil MR, Brennan PJ. Lipoarabinomannan of Mycobacterium tuberculosis. Capping with mannosyl residues in some strains. *J Biol Chem* 1992; **267**: 6234-6239
41 **Chatterjee D**, Khoo KH. Mycobacterial lipoarabinomannan: an extraordinary lipoheteroglycan with profound physiological effects. *Glycobiology* 1998; **8**: 113-120
42 **Vercellone A**, Nigou J, Puzo G. Relationships between the structure and the roles of lipoarabinomannans and related glycoconjugates in tuberculosis pathogenesis. *Front Biosci* 1998; **3**: e149-e163
43 **Soborg C**, Madsen HO, Andersen AB, Lillebaek T, Kok-Jensen A, Garred P. Mannose-binding lectin polymorphisms in clinical tuberculosis. *J Infect Dis* 2003; **188**: 777-782
44 **Bonar A**, Chmiela M, Rudnicka W, Rozalska B. Mannose-binding lectin enhances the attachment and phagocytosis of mycobacteria in vitro. *Arch Immunol Ther Exp* (Warsz) 2005; **53**: 437-441
45 **Krause I**, Blank M, Cervera R, Font J, Matthias T, Pfeiffer S, Wies I, Fraser A, Shoenfeld Y. Cross-reactive epitopes on beta2-glycoprotein-I and Saccharomyces cerevisiae in patients with the antiphospholipid syndrome. *Ann N Y Acad Sci* 2007; **1108**: 481-488
46 **Arnott ID**, Landers CJ, Nimmo EJ, Drummond HE, Smith BK, Targan SR, Satsangi J. Sero-reactivity to microbial components in Crohn's disease is associated with disease severity and progression, but not NOD2/CARD15 genotype. *Am J Gastroenterol* 2004; **99**: 2376-2384

S- Editor Zhong XY **L- Editor** Alpini GD **E- Editor** Lin YP

Online Submissions: wjg.wjgnet.com
wjg@wjgnet.com
doi:10.3748/wjg.14.3662

World J Gastroenterol 2008 June 21; 14(23): 3662-3671
World Journal of Gastroenterology ISSN 1007-9327
© 2008 The WJG Press. All rights reserved.

CLINICAL RESEARCH

Methylenetetrahydrofolate reductase C677T genotype affects promoter methylation of tumor-specific genes in sporadic colorectal cancer through an interaction with folate/vitamin B_{12} status

Pooneh Mokarram, Fakhraddin Naghibalhossaini, Mehdi Saberi Firoozi, Seyed Vahid Hosseini, Ahmad Izadpanah, Heshmetalah Salahi, Seyed Ali Malek-Hosseini, Abdoulrasool Talei, Mehra Mojallal

Pooneh Mokarram, Fakhraddin Naghibalhossaini, Department of Biochemistry, Shiraz University of Medical Sciences, School of Medicine, Shiraz 71345, Iran
Mehdi Saberi Firoozi, Department of Internal Medicine and Gastroenterohepatology Research Centre, Shiraz University of Medical Sciences, Shiraz 71345, Iran
Seyed Vahid Hosseini, Ahmad Izadpanah, Department of Surgery (colorectal ward) and Gastroenterohepatology Research Centre, Shiraz University of Medical Sciences, Shiraz 71345, Iran
Heshmetalah Salahi, Seyed Ali Malek-Hosseini, Department of Surgery and Organ Transplantation Research Centre, Namazee Hospital, Shiraz University of Medical Sciences, Shiraz 71345, Iran
Abdoulrasool Talei, Department of Surgery and Institute of Cancer Research, Shiraz University of Medical Sciences, Shiraz 71345, Iran
Mehra Mojallal, Pathology Laboratory, Dena Hospital, Shiraz 71345, Iran
Supported by The office of the Vice Chancellor for Research, Shiraz University of Medical Sciences, No. 83-2212; Grant from the Gastroenterohepatology Research Centre, Shiraz University of Medical Sciences, Shiraz, Iran
Author contributions: Naghibalhossaini F designed research and wrote the paper; Hosseini SV, Saberi Firoozi M, Izadpanah A, Salahi H, Malek-Hosseini SA, Talei A, and Mojallal M provided specimens, reagents and analytical tools; Mokarram P performed research.
Correspondence to: Fakhraddin Naghibalhossaini, Department of Biochemistry, Shiraz University of Medical Sciences, School of Medicine, Zand Street, Shiraz 71345, Iran. fakhraddin.naghibalhossaini@elf.mcgill.ca
Telephone: +98-711-2303029 Fax: +98-711-2303029
Received: February 18, 2008 Revised: April 15, 2008
Accepted: April 22, 2008
Published online: June 21, 2008

Abstract

AIM: To evaluate joint effects of *Methylentetrahydrofolate reductase* (*MTHFR*) *C677T* genotypes, and serum folate/vitamin B_{12} concentrations on promoter methylation of tumor-associated genes among Iranian colorectal cancer patients.

METHODS: We examined the associations between *MTHFR C677T* genotype, and promoter methylation of *P16*, *hMLH1*, and *hMSH2* tumor-related genes among 151 sporadic colorectal cancer patients. The promoter methylation of tumor-related genes was determined by methylation-specific PCR. Eighty six patients from whom fresh tumor samples were obtained and 81 controls were also examined for serum folate and vitamin B_{12} concentrations by a commercial radioimmunoassay kit.

RESULTS: We found 29.1% of cases had tumors with at least one methylated gene promoter. In case-case comparison, we did not find a significant association between methylation in tumors and any single genotype. However, in comparison to controls with the *CC* genotype, an increased risk of tumor methylation was associated with the *CT* genotype (OR = 2.5; 95% CI, 1.1-5.6). In case-case comparisons, folate/vitamin B_{12} levels were positively associated with tumor methylation. Adjusted odds ratios for tumor methylation in cases with high (above median) *versus* low (below median) serum folate/vitamin B_{12} levels were 4.9 (95% CI, 1.4-17.7), and 3.9 (95% CI, 1.1-13.9), respectively. The frequency of methylated tumors was significantly higher in high methyl donor than low methyl donor group, especially in those with *MTHFR CT* (P = 0.01), and *CT/TT* (P = 0.002) genotypes, but not in those with the *CC* genotype (P = 1.0).

CONCLUSION: We conclude that high concentrations of serum folate/vitamin B_{12} levels are associated with the risk of promoter methylation in tumor-specific genes, and this relationship is modified by *MTHFR C677T* genotypes.

© 2008 The WJG Press. All rights reserved.

Key words: *Methylentetrahydrofolate reductase*; Folate; Vitamin B_{12}; Methylation; Colorectal cancer

Peer reviewer: Shu Zheng, Professor, Scientific Director of Cancer Institute, Zhejiang University, Secondary Affiliated Hospital, Zhejiang University, 88# Jiefang Road, Hangzhou 310009, Zhejiang Province, China

Mokarram P, Naghibalhossaini F, Saberi Firoozi M, Hosseini SV, Izadpanah A, Salahi H, Malek-Hosseini SA, Talei A, Mojallal M. Methylenetetrahydrofolate reductase C677T

genotype affects promoter methylation of tumor-specific genes in sporadic colorectal cancer through an interaction with folate/vitamin B_{12} status. *World J Gastroenterol* 2008; 14(23): 3662-3671 Available from: URL: http://www.wjgnet.com/1007-9327/14/3662.asp DOI: http://dx.doi.org/10.3748/wjg.14.3662

INTRODUCTION

Colon cancer (CLC) is one of the most common cancers in the world, with high rates in Western countries[1]. A significant increase in CLC incidence with the predominant localization in the left colon has also been reported in Iran over the last decade[2,3]. However, little is known about the molecular mechanism of CLC in this region.

One of the pathways by which that CLC can progress involves transcriptional silencing by hypermethylation of CpG islands referred as methylator phenotype ($CIMP^+$)[4]. The $CIMP^+$ in CLC is characterized by frequent hypermethyaltion of specific CpG sites, including those present in the promoter regions of tumor suppressor genes such as the cell cycle regulator, *p16* and genes involved in DNA mismatch repair like *hMLH1*[4]. The *hMLH1* promoter region is methylated in about 90% of microsatellite unstable (MSI-positive) colon cancers that leads to the silencing of *hMLH1* expression[5]. The $CIMP^+$ phenotype may be the result of more widespread aberration in methyl-group metabolism in cancer cells.

Interaction of the epigenome with the environment, including nutrition, can alter patterns of gene expression. It has been proposed that polymorphisms in folate-metabolizing enzymes and genes involved in DNA methylation are associated with colon cancer. MTHFR is a key enzyme regulating folate metabolism, which affects DNA methylation and synthesis. MTHFR converts 5, 10-methylentetrahydrofolate to 5-methyl tetrahydrofolate, which is required for homocysteine methylation to methionine. Methionine is then activated to S-adenosylmethionine, a universal methyl donor in numerous transmethylation reactions, including methylation of DNA, RNA, proteins, and other molecules[6]. The *MTHFR* gene is polymorphic with single nucleotide variants within codon 677 in exon 4 (C to T, Ala to Val). This variant encodes a thermolabile enzyme with reduced activity that leads to a reduced plasma folate level[7].

Several case-control studies have shown a reduced risk of CLC for homozygous *MTHFR TT* individuals. The protective effect appears to depend on an adequate level of dietary folate intake, gender, age, and location of the tumor in the proximal or distal colon[8,9]. In some circumstances, the *MTHFR-TT* genotype seems to increase the risk of CLC[10,11]. It has been suggested that deficient activity of MTHFR affects DNA methylation status through an interaction with folate status[12]. Several data provide evidence that individuals with the common *C677T* mutation in the *MTHFR* gene and with low levels of folate had a diminished level of DNA methylation compared with those with the *C/C* wild type. Folate deficiency may be involved in carcinogenesis through impaired synthesis and repair of DNA, or by causing global hypomethylation of DNA, a possible early event in carcinogenesis[13]. Although a protective role against cancer was suggested for the high dietary folate intake, epidemiological evidence has not consistently shown a protective effect of high folate intake against CLC[14,15]. There are few studies addressing joint effects of *MTHFR C677T* genotypes, and methyl donor coenzymes status on promoter methylation of tumor-associated genes in CLC[16,17]. In the current study we investigated the role of *MTHFR C677T* genotype, and serum folate/vitamin B_{12} concentrations on methylation of CpG islands at *p16*, *hMLH1*, and *hMSH2* tumor-associated genes among Iranian sporadic CLC patients.

MATERIALS AND METHODS

Study population, and samples

A total of 151 sporadic primary CLC tumor samples (86 fresh and 65 formalin fixed and paraffin embedded) as well as corresponding normal mucosa were collected from surgical patients at 3 hospitals of the Shiraz University of Medical Sciences in Shiraz, Southern Iran from July, 2003 to September, 2005. Institutional review board approval was granted for this study. The fresh samples were snap frozen in liquid nitrogen immediately after resection and stored at -70℃ until processing. All samples were evaluated and subjected to histological diagnosis by an expert pathologist, who also selected representative tissue sections for DNA extraction, and further molecular analyses. The splenic flexure was used as the anatomical boundary to define proximal and distal CLC. Sociodemographic characteristics such as age and gender were obtained by completion of a detailed questionnaire.

Extraction of DNA and MTHFR genotyping

Genomic DNA was extracted from micro-dissected formalin-fixed, paraffin embedded tumor samples and adjacent normal tissues using the pinpoint slide DNA isolation kit (ZYMORESEARCH, CA, USA). We used the standard phenol/chloroform method for DNA extraction from fresh tumor samples. Genotyping of *MTHFR* at codon 677 of DNA from control and CLC cases was performed using a modification of the mutagenically separated PCR (MS-PCR) method described by Hill and FitzPatrick[18]. Genotyping for *MTHFR* involved analysis of PCR product size by electrophoresis on 3% agarose gels. PCR reactions were carried out in a volume of 50 μL containing 50 ng DNA, 1 × polymerization buffer (MBI Fermentas, Lithuania), 1.5 mmol/L $MgCl_2$, 0.2 mmol/L dNTP, and 1.5 U Taq polymerase. The primers and concentrations used for PCR reactions were as follows: forward mutant (29 bases) 0.35 μmol/L 5´-CACTTGAAGGAGAAGGTGTCTGCGGGACT-3´, forward normal (49 bases) 0.19 μmol/L 5'-GCTTTGAGGCTGACCTGAAGA-CCTTGAAGGAGAAG GTGTCTGCGGCAGC-3'

and the reverse primer (20 bases) 0.23 μmol/L 5'-TCACCTGGATGGGAAAGATC-3'. The two forward primers are complementary to the normal (677C) and mutant (677T) alleles and differed in length by 20 bases at their 5' ends. The cycling parameters were 5 min at 95℃ followed by 35 cycles of 45 s at 95℃, 1 min at 55℃, and 45 s at 72℃ followed by a single 10-min extension at 72℃. Twenty μL of each reaction mixture was separated on agarose gel and stained with ethidium bromide and visualized under UV illumination.

Serum folate and vitamin B_{12} measurement and methylation specific PCR (MSP)

Folate and vitamin B_{12} measurements were limited to sera from 86 patients with freshly studied tumors and 81 age and sex matched normal controls, selected among healthy volunteers from the general population with no history of any cancer. Blood samples were drawn from patients before operation and serum was prepared within two hours of blood collection. Sera were frozen immediately at -70℃ until used. The concentrations of folate and vitamin B_{12} in each specimen were measured in duplicate by a commercial radioimmunoassay kit (SimulTRAC-SNB RIA, DRG International Inc. USA) using a gamma counter (Contron, Switzerland). We determined the *p16*, *hMLH1*, and *hMSH2* promoter methylation status by chemical treatment with sodium bisulfite and subsequent MSP as described[19]. In brief, this technique uses bisulfite modification to convert unmethylated, but not methylated, cytosine to uracil. MSP utilizes this difference to amplify specifically either methylated or unmethylated DNA. The sequences of primers used for amplification of the promoter region of each of the 3 genes were as follows: *p16* methylated, sense 5'-TTATTAGAGGGTGGGGC-GGATCGC-3' and antisense 5'-GACCCCGAACCGCGACCGTAA-3', which produce a 150 bp fragment; *p16* unmethylated: sense 5'-TTATTAGAGGGTGGGGTGGATTGT-3' and antisense 5'- CAACCCCAAACCACAACCATAA-3', which produce a 151 bp fragment; *hMLH1* methylated, sense 5'-ACGTAGACG-TTTTATTAGGGTCGC-3' and antisense 5'-CCTCATCGTAACTACCCGCG-3', which produce a 112 bp fragment; *hMLH1* unmethylated, sense 5'-TTTTGATGTAGATGTTTTATTAGGGTTGT-3' and antisense 5'-ACCACCTCATCATAACTACCCACA-3',which produce a 124 bp fragment; *hMSH2* methylated, sense 5'-TCGTGGTCGGACGTCGTTC-3' and antisense 5'-CAACGTCTCCTTCGACTACACCGG-3', which produce a 133 bp fragment; *hMSH2* unmethylated, sense 5´-GGTTGTTGTGGTTGGATGTTGTTT-3' and antisense 5'-CAACTACAACATCTCCTTCAAC TACACCA-3', which produce a 144 bp fragment. The hot-started PCR reactions were performed in a 50 μL reaction volume containing 25 pmol of each of sense and antisense primer, 0.2 mmol/L dNTPs, and 80 ng bisulfite-modified DNA in 1× PCR buffer provided by Taq enzyme supplier. The reaction mixture was denatured at 95℃ for 5 min, after which 1.5 U Taq polymerase was added; then amplified by 40 cycles, each consisting of 30 s denaturation at 95℃, 45 s annealing at 58℃, and 30 s polymerization at 72℃, followed by a single 10-min extension at 72℃.

Table 1 Frequency distributions of selected characteristics in CLC patients and control subjects

Variables	Cases			Control (n = 81)	P^1
	Proximal	Distal	Total (n = 151)		
Gender					0.8
Male (%)	28 (31.1)	62 (68.9)	90 (59.6)	50 (61.7)	
Female (%)	32 (52.5)	29 (47.5)	61 (40.4)	31 (38.3)	
Smoking status					0.1
Smokers[2] (%)	22 (34.4)	42 (65.6)	64 (42.4)	25 (30.9)	
Non-smokers	38 (43.7)	49 (56.3)	87 (57.6)	56 (69.1)	
Age groups (yr)					0.4
< 60 (%)	24 (36.4)	42 (63.6)	66 (43.7)	40 (49.4)	
≥60 (%)	36 (42.4)	49 (57.6)	85 (56.3)	41 (50.6)	
Median (range)	61 (40-87)	60 (28-90)	60 (28-90)	60 (28-89)	
Mean (SD)	62.22 (10.97)	59.24 (12.7)	60.42 (12)	58.98 (15.66)	

[1]Fisher's exact test; [2]Current and former smokers.

Statistical analysis

Statistical analysis was performed using the SPSS version 11.5 software package (Chicago, IL). Associations between methylation of loci and clinical, biological and genotypic features were evaluated using Chi square and Fisher's exact test as appropriate. Logistic regression was used to calculate odds ratio (OR) and 95% confidence intervals (95% CI). We adjusted for covariates, specifically including age, gender, and smoking status. Comparing serum folate and vitamin B_{12} levels in cases and controls was performed using two-sided *t*-test, Mann-Whitney test, and Kruskal-Wallis test appropriately.

RESULTS

Distribution of selected characteristics of cases and controls

Selected characteristics of the study population are presented in Table 1. One hundred and fifty one patients and 81 controls entered the study. The distribution was similar in cases and controls by virtue of the study design. Sixty percent (91) of patients had distal CLC and 40% (60) had proximal CLC. Cases were more likely to be males and to be non-smokers. No statistically significant differences were found between cases and controls or between proximal and distal cancer cases with respect to distributions of age, and smoking status. The frequency of distal CLC in males and females was 68.9% and 47.5% (Table 1), respectively, indicative of a significantly higher left CLC incidence in males than females (OR = 2.65; 95% CI, 1.3-5.2).

MTHFR genotypes and the methylation status of tumor-associated genes promoter

Illustrative examples of genotyping of *MTHFR* gene are shown in Figure 1. In 42 patients for whom we performed genotyping in both the cancer tissue and adjacent normal tissue, the typing results were identical in the two samples. CpG island promoter

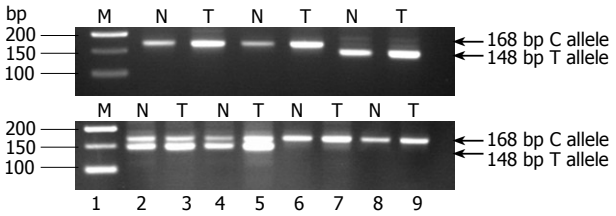

Figure 1 Representative example of MS-PCR assay for genotyping of codon 677 of *MTHFR* gene. For PCR-primers and reaction conditions see methods. In case of the *MTHFR 677 C* allele, a product with 168 base pairs (bp) in length was generated, whereas the *MTHFR 677 T* allele yielded a 148-bp product. The differently sized allele-specific PCR products were separated by agarose gel electrophoresis. In 42 patients genotyping was performed in both cancer tissue (T) and adjacent normal tissue (N). Lanes 2-5 in the lower panel show heterozygote (*CT*) samples. M: DNA size marker.

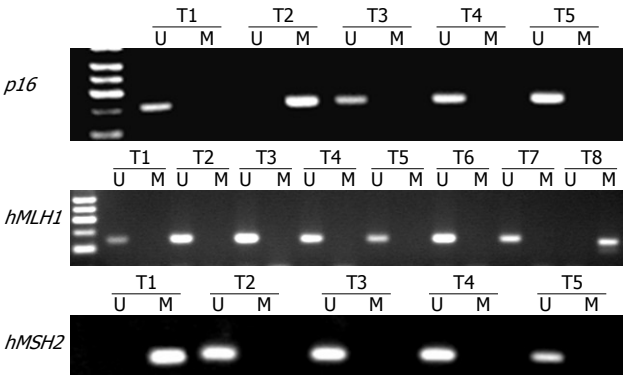

Figure 2 Representative examples of MSP reactions for promoter methylation analysis of *p16*, *hMLH1*, and *hMSH2* genes in primary CLC tumors. The presence of a visible PCR product in those lanes marked U indicates the presence of unmethylated genes; the presence of a product in those lanes marked M indicates the presence of methylated genes. Lane 1 indicates the 50 bp DNA size marker.

hypermethylation was analyzed in the primary tumors by methylation specific PCR as described in "MATERIALS AND METHODS". Illustrative examples are shown in Figure 2. Table 2 summarizes the association of promoter methylation of genes and *MTHFR* genotype, and other clinical-biological characteristics of CLC patients. Several studies have reported age-dependent variation in the frequency of the *MTHFR* genotypes[20,21]. Therefore, we divided both CLC and control groups into $\geqslant$ 60 and < 60-year old groups. The median age of CLC patients (60 years) was chosen for this division. The most frequently methylated locus was *p16* (19.9 %; 30 of 151), followed by *hMLH1* (13.2 %; 20 of 151), and *hMSH2* (2.6 %; 4 of 151). Eight of 151 (5.3 %) of tumors had both P16 and *hMLH1* CpG island hypermethylation while 2 of 151(1.3%) had both *hMLH1* and *hMSH2* promoter hypermethylation. None of the tumors had simultaneous CpG island hypermethylation of all three genes. There were no significant differences in association of methylation of any individual gene investigated by age or sex of patients. The frequency of tumor methylation (tumors with at least one gene methylated) was 44/151 (29.1%). The latter group of tumors is collectively referred to as "methylated tumors". A significantly higher risk of tumor methylation was found in females (OR = 2.3; 95% CI, 1.1-5.04) (Table 2). Gene promoter methylation was also strongly associated with tumor site, the highest frequency (more than 97%) of methylation occurring in the proximal tumors.

We confronted *MTHFR* genotype with the methylation of tumors using the *CC* genotype as the reference group. Results from case-case comparison, showed no statistically significant genotype dependent differences in the frequency of any specific gene promoter methylation (Table 2). In comparison to cases with the *CC* genotype, we did not find any significant association between tumor methylation or "methylated tumors" , defined above and any single genotype in the entire group of patients, but cases with the *CT* genotype were slightly more likely to have methylated tumors (OR = 1.9; 95% CI, 0.9-4.2). Results from the case-control comparison, showed that the *CT* genotype was significantly associated with tumor methylation in the entire group of patients (OR = 2.5; 95% CI, 1.1-5.6; Table 3). More than five-fold increased risk of tumor methylation was also observed for the *CT* genotype, in male CLC cases compared with age-matched male controls. The *CT* genotype also presented significantly increased tumor methylation in the proximal and in the older age group (OR = 2.7, 95% CI, 1.2-6.2; OR = 3.8, 95% CI, 1.2-12, respectively). The same trend was also observed for CT + TT genotypes. These results suggest that the *C677T* genotype of *MTHFR* can predispose some of CLC patients to the methylation of genes promoter.

Serum folate/vitamin B_{12} status and genes promoter methylation

Due to the previously observed interaction between folate and the *MTHFR* genotype in CLC[22], we investigated the influence of serum folate/vitamin B_{12} levels on tumor methylation in 86 fresh tissue samples in which their corresponding blood samples were also available. We observed no significant differences in serum folate/vitamin B_{12} levels between cases and controls (Table 4). There were also no differences in association of serum folate/vitamin B_{12} levels by sex, and tumor location. Comparing two age groups of patients, a trend for higher serum folate/vitamin B_{12} levels was observed in older age group, with the older cases presenting 15% higher serum folate ($P = 0.04$).

In case-control comparisons, we found no significant difference in serum folate/vitamin B_{12} levels by *MTHFR* genotypes (data not shown). However, in case-case comparisons, serum folate levels appear to be associated with *MTHFR* genotypes (Table 5). Patients with the homozygous *TT* genotype had significantly lower concentrations of folate in their blood than those with *CT* or *CC* genotypes (Mann-Whitney test, $P = 0.007$ and $P = 0.03$, respectively). We found no significant difference in serum vitamin B_{12} concentrations between subjects with the CC and *TT* genotypes.

To test the association between serum folate/vitamin B_{12} levels and methylation of genes promoter and tumors methylation, we stratified serum folate/

Table 2 Stratification analysis of tumors and genes promoter methylation frequencies

Variables	Methylation positive (%)						Methylated tumors[2] *n* (%)	OR (95% CI, *P*)[3]
	p16	*P*[1]	*hMLH1*	*P*[1]	*hMSH2*	*P*[1]		
Sex								
Male (90)	13 (14.4)	0.06	10 (11.1)	NS	4 (4.4)	NS	21 (23.3)	1
Female (61)	17 (27.9)		10 (16.4)		0 (0)		23 (37.7)	2.3 (1.1–5.04, 0.03)
Total (151)	30 (19.9)		20 (13.2)		4 (2.6)		44 (29.1)	
Age (yr)								
< 60 (66)	15 (22.7)	NS	7 (10.6)	NS	0 (0)	NS	19 (28.8)	1
⩾ 60 (85)	15 (17.6)		13 (15.3)		4 (4.7)		25 (29.4)	1.1 (0.6–2.4, 0.7)
Tumor site								
Proximal (60)	29 (48.3)	0.00	20 (33.3)	0.00	4 (6.7)	0.02	43 (71.7)	1
Distal (91)	1 (1.1)		0 (0)		0 (0)		1 (1.1)	0.002 (0.00–0.023, 0.00)
Serum folate (86)								
Low (38)	2 (5.3)	0.04	4 (10.5)	NS	0 (0)	NS	4 (10.5)	1
High (48)	10 (20.8)		10 (20.8)		3 (6.3)		16 (33.3)	4.9 (1.4 -17.7, 0.01)
Serum vitamin B_{12} (86)								
Low (42)	2 (4.8)	0.02	5 (11.9)	NS	0 (0)	NS	5 (11.9)	1
High (44)	10 (22.7)		9 (20.5)		3 (6.8)		15 (34.1)	3.9 (1.1-13.9, 0.03)
MTHFR 677 genotype[4]								
CC (64)	13 (20.3)	NS	7 (10.9)	NS	0 (0)	NS	15 (23.4)	1
CT (80)	17 (21.3)	NS	12 (15)	NS	3 (3.8)	NS	28 (35)	1.92 (0.9-4.2, 0.09)
TT (7)	0 (0)	NS	1 (14.3)	NS	1 (14.3)	NS	1 (14.3)	0.7 (0.07-6.1, 0.7)
CT + *TT* (87)	17 (19.5)	NS	13 (14.9)	NS	4 (4.6)	NS	29 (33.3)	1.8 (0.8-3.9, 0.125)

[1]Fisher's exact test; [2]tumors with at least one methylated gene promoter; [3]the first category was taken as reference. Odds ratio adjusted for age, sex, and smoking status; [4]For genotype comparison CC used as the reference category. NS: Not significant.

Table 3 Association between MTHFR genotypes and tumor methylation in relation to clinical-biological features of CLC patients (case-control comparison, *n*)

Genotype (%)	Controls	Cases	Methylated	OR (95% CI, *P*)[1,2]	Unmethylated	OR (95% CI, *P*)[1,2]
Total	81	151	44		107	
CC	40 (49.4)	64 (42.4)	15 (34.1)	1	49 (45.8)	1
CT	31 (38.3)	80 (53)	28 (63.6)	2.5 (1.1-5.6, 0.02)	52 (48.6)	1.4 (0.7-2.6, 0.3)
CT or TT	41 (50.6)	87 (57.6)	29 (65.9)	2.1 (0.9-4.5, 0.07)	58 (54.2)	1.1 (0.7-2.1, 0.6)
Sex						
Male	50	90	21		69	
CC	28 (56)	33 (36.7)	5 (23.8)	1	28 (40.6)	1
CT	17 (34)	51 (56.7)	15 (71.4)	5.3 (1.6-18.2, 0.008)	36 (52.2)	1.9 (0.9-4.3, 0.09)
CT or TT	22 (44)	57 (63.3)	16 (76.2)	4.3 (1.3-14.3, 0.01)	41 (59.4)	1.7 (0.8-3.6, 0.1)
Female	31	61	23		38	
CC	12 (38.7)	31 (50.8)	10 (43.5)	1	21 (55.3)	1
CT	14 (45.2)	29 (47.5)	13 (56.5)	1.1 (0.3-3.6, 0.9)	16 (42.1)	0.7 (0.2-1.9, 0.5)
CT or TT	19 (61.3)	30 (49.2)	13 (56.5)	0.9 (0.3-2.8, 0.8)	17 (44.7)	0.5 (0.2-1.4, 0.2)
Age						
< 60	40	66	19		47	
CC	18 (45)	31 (47)	6 (31.6)	1	25 (53.2)	1
CT	18 (45)	34 (51.5)	13 (68.4)	1.4 (0.4-5.1, 0.6)	21 (44.7)	0.8 (0.3-1.9, 0.6)
CT or TT	22 (55)	35 (53)	13 (68.4)	1.1 (0.3-3.8, 0.9)	22 (46.8)	0.7 (0.3-1.6, 0.3)
⩾ 60	41	85	25		60	
CC	22 (53.7)	33 (38.8)	9 (36)	1	24 (40)	1
CT	13 (31.7)	46 (54.1)	15 (60)	3.8 (1.2-12.0, 0.02)	31 (51.7)	2.6 (0.9-6.6, 0.09)
CT or TT	19 (46.3)	52 (61.2)	16 (64)	2.7 (0.9-8.2, 0.08)	36 (60)	1.9 (0.8-4.2, 0.1)
Site						
Proximal		60	43		17	
CC		22 (36.7)	15 (34.9)		7 (41.2)	
CT		37 (61.7)	27 (62.8)	2.7 (1.2-6.2, 0.02)	10 (58.8)	1.4 (0.5-4.8, 0.4)
CT or TT		38 (63.3)	28 (65.1)	2.1 (1.03-4.99, 0.05)	10 (58.8)	1.2 (0.4-3.7, 0.7)
Distal		91	1		90	
CC		42 (46.2)	0 (0)		42 (46.7)	
CT		43 (47.3)	1 (100)	ND	42 (46.7)	1.3 (0.7-2.5, 0.4)
CT or TT		49 (53.8)	1 (100)	ND	48 (53.3)	0.9 (0.5-1.6, 0.7)

[1,2]For odds ratio and 95% CI calculations, controls with CC genotype was used as reference category, odds ratio adjusted for age, sex and smoking status. ND: Not determined.

vitamin B_{12} levels in two groups of low (below median), and high (above median) levels. The prevalence of

Table 4 Associations between serum folate/vitamin B_{12} concentrations and tumor methylation in relation to the clinical-biological characteristics of patients

Variables	*n* (%)	Folate (ng/mL) mean (range)	*P*[1]	High folate/Low folate[2] *n* (%)	*P*[3]	Vit.B_{12} (pg/mL) mean (range)	*P*[1]	High B_{12}/Low B_{12}[2] *n* (%)	*P*[3]
Controls (81)		6.3 (3.8-12)	0.1[4]	49 (60.5)/32(39.5)	0.6[4]	312.8 (108-995)	0.1[4]	40 (49.4)/41 (50.6)	0.9[4]
Total cases (86)		5.9 (2.1-12)		48 (55.8)/38(44.2)		269 (50-681)		44 (51.2)/42 (48.8)	
Unmethylated	66 (76.7)	5.7 (2.4-12)		32 (48.5)/34 (51.5)		255.2 (79-681)		29 (43.9)/37 (56.1)	
Methyalated	20 (23.3)	6.4 (2.1-10)	0.06	16 (80)/4 (20)	0.02	314.7 (50-571)	0.1	15 (75)/5 (25)	0.02
Sex									
Male (55)		5.9 (2.4-12)		29 (52.7)/26 (47.3)		274.2 (67-681)		28 (50.9)/27(49.1)	
Unmethylated	43 (78.2)	5.8 (2.4-12)		19 (44.2)/24 (55.8)		325.5 (67-571)		18 (41.9)/25 (58.1)	
Methylated	12 (21.8)	6.5 (3.9-9.5)	0.1	10 (83.3)/2 (16.7)	0.02	254.4 (83-681)	0.04	10 (83.3)/2 (16.7)	0.02
Female (31)		5.7 (2.1-10)	0.6[5]	19 (61.3)/12 (38.7)	0.5[5]	259.7 (50-523)	0.7[5]	16(51.6)/15 (48.4)	1.00[5]
Unmethylated	23 (74.2)	5.6 (3-8)		13 (56.5)/10 (43.5)		260. 3 (79-521)		11 (47.8)/12 (52.2)	
Methylated	8 (25.8)	6.2 (2.1-10)	0.4	6 (75)/2 (25)	0.4	257.8 (50-523)	0.9	5 (62.5)/3 (37.5)	0.7
Age									
< 60 yr (36)		5.4 (2.1-8)		18 (50)/18 (50)		238.1(50-571)		14 (38.9)/22(61.1)	
Unmethylated	30 (83.3)	5.4 (3-8)		14 (46.7)/16 (53.3)		229.8 (79-465)		11 (36.7)/19 (63.3)	
Methylated	6 (16.7)	5.5 (2.1-7.9)	0.5	4 (66.6)/2 (33.3)	0.7	279.5 (50-571)	0.8	3 (50)/3 (50)	0.7
⩾ 60 yr (50)		6.3 (2.4-12)	0.04[5]	30 (60)/20 (40)	0.4[5]	291.3 (67-681)	0.1[5]	30 (60)/20(40)	0.1[5]
Unmethylated	36 (72)	6.1 (2.4-12)		18 (50)/18 (50)		276.3 (83-681)		18 (50)/18 (50)	
Methylated	14 (28)	6.8 (3.9-10)	0.1	12 (85.7)/2 (14.3)	0.03	329.7 (67-543)	0.1	12 (85.7)/2 (14.3)	0.03
Site									
Distal (62)		5.8 (2.4-12)		32 (51.6)/30 (48.4)		260.6 (79-681)		28 (45.2)/34 (54.8)	
Unmethylated	61 (98.4)	5.8 (2.4-12)		31 (50.8)/30 (49.2)		255.5 (79-681)		27 (44.3)/34 (55.7)	
Methylated	1 (1.6)	7.9	0.3	1 (100)/0 (0)	ND	271 (271)	0.1	1 (100)/0 (0)	ND
Proximal (24)		6.1 (2.1-10)	0.4[5]	16 (66.7)/8 (33.3)	0.2[5]	290.7 (50-543)	0.5[5]	16 (66.7)/8 (33.3)	0.1[5]
Unmethylated	5 (20.8)	5.3 (4.5-6.4)		1 (20)/4 (80)		251 (109-483)		2 (40)/3 (60)	
Methylated	19 (79.2)	6.3 (2.1-10)	0.06	15 (78.9)/4 (21.1)	0.03	301.2 (50-543)	0.5	14 (73.7)/5 (26.3)	0.3

[1]*P*-value from Mann-Whitney and *t*-test where appropriate; [2]Median was taken as cut off point for low and high categorical value for serum folate/vitamin B_{12} levels (5.5 ng/mL, and 240 pg/mL, respectively); [3]*P* value from Fisher's exact test; [4]Case/control comparison; [5]Subgroups comparison, cases only. ND: Not determined.

Table 5 Combined effects of *MTHFR 677* genotype and serum folate/vitamin B_{12} concentrations on risk of tumor methylation (case-case comparison)

MTHFR 677 genotype	*n* (%)	Folate (ng/mL) mean (range)	*P*[1]	High folate/Low folate[2] *n* (%)	*P*[3]	Vit. B_{12} (pg/mL) mean (range)	*P*[1]	High B_{12}/Low B_{12}[2] *n* (%)	*P*[3]
Cases (86)									
CC (42)		5.8 (2.1-8.8)		25 (59.5)/17 (40.5)		254.6 (50-673)		20 (47.6)/22 (52.4)	
Unmethylated	34 (81)	5.9 (3.4-8.8)		20 (58.8)/14 (41.2)		267.3 (107-673)		16 (47.5)/18 (53.9)	
Methylated	8 (19)	5.4 (2.1-7.8)	0.6	5 (62.5)/3 (37.5)	1.00	200.9 (50-429)	0.2	4 (50)/4 (50)	1.00
CT (38)		6.3 (3-12)	0.5[5]	22 (57.9)/16 (42.1)	1.00	296 (79-681)	0.4[5]	21 (55.3)/17 (44.7)	0.5
Unmethylated	27 (71.1)	5.9 (3-12)		12 (44.4)/15 (55.6)		254.1 (79-681)		11 (40.7)/16 (53.9)	
Methylated	11 (28.9)	7.2 (5.3-10)	0.06	10 (90.9)/1 (9.1)	0.01	398.7 (150-571)	0.007	10 (90.9)/1 (9.1)	0.01
TT (6)[4]		4.2 (2.4-5.9)	0.03[5]	1 (16.7)/5 (83.3)	0.08	198.5 (83-300)	0.4[5]	3 (50)/3(50)	1.00
Unmethylated	5 (83.3)	3.8 (2.4-5.1)		0/5 (100)		178.2 (83-258)		2 (40)/3 (60)	
Methylated	1 (16.7)	5.9		1 (100)/0		300		1 (100)/0	
CT + *TT* (44)		5.9 (2.4-12)	0.9[5]	23 (52.3)/21 (47.7)	0.5	282.7 (79-681)	0.5[5]	24 (54.5)/20 (45.5)	0.7
Unmethylated	32 (72.7)	5.6 (2.4-12)		12 (37.5)/20 (62.5)		242.3 (79-681)		13 (40.6)/19 (59.4)	
Methylated	12 (27.3)	7.1 (5.3-10)	0.002	11(91.7)/1 (8.3)	0.002	390.5 (150-571)	0.002	11 (91.7)/1 (8.3)	0.003

[1]*P*-values for methylated and unmethylated cases, and genotype comparison, Mann-Whitney, *t*-test and Kruskal Wallis where appropriate; [2]Median was taken as cut off point for low and high categorical value for serum folate/vitamin B_{12} levels (5.5 ng/mL, and 240 pg/mL, respectively); [3]*P*-value from Fisher's exact test; [4]Since we did not have enough *TT* cases, the association of serum methyl donors and tumor methylation was not determined in these individuals; [5]Comparison with the *CC* genotype, cases only.

hypermethylation within the promoter of *p16* gene, but not in either *hMLH1* or *hMSH2* genes, was higher in CLCs derived from patients with high serum folate ($P = 0.04$) and vitamin B_{12} ($P = 0.02$) when compared with CLCs from patients with low serum folate/vitamin B_{12} levels status (Table 2).

The association between tumor methylation and serum folate/vitamin B_{12} levels is shown in Table 4. A small trend for higher levels of serum folate was found in the entire group of patients with methylated tumors compared to those with unmethylated tumors ($P = 0.06$). The percentage of methylated tumors in patients with high serum methyl donors was also higher than those with low serum methyl donors (80% in high folate group, and 75% in high B_{12} group; $P = 0.02$), whereas no such difference was found for unmethylated tumor group (Table 4). The OR for tumor methylation was 4.9 (95% CI, 1.4-17.7) for patients with high serum folate

versus low serum folate (Table 2). The risk of tumor methylation was also positively associated with serum vitamin B_{12} status (OR = 3.9, 95% CI, 1.1-13.9). The high serum folate/vitamin B_{12} levels were particularly associated with tumor methylation in males (P = 0.02), but not in females (P = 0.4, Table 4). The association was also age and site dependent, being significant for older cases and those with proximal tumors (Table 4). Since we did not have enough distal methylated tumors, we could not examine the association of tumor methylation with serum folate status in such tumors.

Joint effects of serum methyl donors, and MTHFR C677T genotypes on promoter methylation of tumor-associated genes

To investigate further whether the relationship between serum folate/vitamin B_{12} status and DNA methylation is modified by the *MTHFR* genotype, we evaluated the joint effects of *MTHFR* codon 677 genotypes and serum folate/vitamin B_{12} levels on tumor methylation. The combined effects of serum folate/vitamin B_{12} levels and *MTHFR* polymorphism on tumor methylation are presented in Table 5. While the *CC* genotype showed no association with serum folate/vitamin B_{12} levels with respect to tumors methylation, the *CT* and *CT/TT* genotypes of *MTHFR* exhibited a significant association of tumor methylation with high serum methyl donors. Insufficient *TT* cases eliminated the ability to examine their association with serum methyl donors and tumor methylation in these individuals. The frequency of methylated tumors was significantly different between cases with high and low serum methyl donors only in those with the *CT* and *CT/TT* genotype, but not with the *CC* genotype. More than 90% of methylated tumors in cases with *CT* and *CT/TT* genotypes had high serum methyl donors (Table 5). Among *CC* individuals no significant differences in mean serum folate/vitamin B_{12} levels between cases with methylated and unmethylated tumors or an association between tumor methylation and folate/vitamin B_{12} levels was observed. Therefore, the *677T* allele seems to increase the risk of methylation associated with high serum folate/vitamin B_{12}. We conclude that for the heterozygous or homozygous *C677T* genotypes, increased concentrations of folate and vitamin B_{12} are associated with increased risks of tumor methylation. Our data suggest that the *MTHFR C677T* genotype might be a genetic modifier of the effect of the folate/vitamin B_{12} status on the risk of methylation of genes promoter.

DISCUSSION

It is well established that loss of proper gene expression in human cancer can occur through epigenetic mechanisms. The effect of a common polymorphism in the *MTHFR* gene (*C677T*) on colorectal cancer risk in relation to folate status is controversial. Both global DNA hypomethylation and gene promoter hypermethylation associated with the *MTHFR TT* genotype under low folate intake have been reported[12]. In the present study, we investigated the association between the *MTHFR C677T* genotype and methylation of three putative tumor-associated genes, *p16*, *hMLH1*, and *hMSH2*, in 151 unselected series of sporadic CLC.

In our study (Table 2) the number of CLCs with at least one gene methylated was higher in females than males, and in those with proximal tumor location than those with distal tumors. Proximal tumor location, higher frequency in female subjects, and older age are characteristics that were previously associated with CIMP+ CLC[4,10].

In comparison to controls, *MTHFR C677T* allele was associated with the elevation of tumor methylation in the entire group of cases, as well as in males and older patients (Table 3). Therefore, our finding is consistent with those reports in which increased genes promoter methylation was associated with the *MTHFR C677T* genotype in CLC[10,23]. We found no apparent association between methylation of any of the individual gene examined and the *MTHFR* genotypes. Therefore, DNA methylation at specific loci appears to be random. Consistent with a previous report that there are more frequent CIPM+ proximal tumors in subjects with alleles conferring low MTHFR enzyme activity[23], the majority of methylated tumors with 677T variants in our study were also located in the proximal colon (Table 3).

Vitamin B_{12} and folate are two important cofactors of methyl-group metabolism. We noted a trend for association between serum folate/vitamin B_{12} levels and gene promoter methylation (Table 2). Higher serum folate and vitamin B_{12} levels were strongly associated with promoter methylation of the key tumor suppressor gene *p16* (P = 0.04, and P = 0.02, respectively). There was also a trend, although not statistically significant, in the association between the serum folate/vitamin B_{12} levels with promoter methylation of *hMLH1* and *hMSH2* genes.

Given the interaction between folate and the *MTHFR* genotype for CLC risk, we stratified the analyses of tumor methylation based on *MTHFR* genotypes and serum folate/vitamin B_{12} status (Tables 4 and 5). In case-case comparisons, we found no significant difference in methyl donor status by age, sex, or tumor location. However, the serum folate level was significantly lower in cases homozygous for the *C677T* variant compared to those with the *CT* and *CC* genotypes (P = 0.04, Table 5). We found the *TT* variant of *MTHFR* associated with lower levels of folate in patient's sera. Although the blood folate level is mainly determined by dietary intake, the *MTHFR C677T* polymorphism might modify its metabolism and serum concentration[24].

In our study, we found significant differences in the serum folate and vitamin B_{12} levels in patients with methylated and unmethylated tumors (Table 4). None of the patients in our study used vitamin supplementation. Therefore, the increased tumor methylation observed in our study was associated with the high serum methyl donor status in physiological range. We noted also the same trend in the association between serum vitamin B_{12} levels and tumor methylation (Table 4). Therefore, our data are consistent with those reports where a

positive association of dietary folate intake with DNA methylation and CLC risk was observed[25,26].

Both folate deficiency and the *MTHFR C677T* polymorphism have been previously linked to global DNA hypomethylation in lymphocytes and colon tissue[27,28]. However, few studies have addressed the joint effects of methyl donors in blood and *MTHFR* genotypes on promoter-specific DNA methylation in malignancies[12,29]. Here, we assessed the association between methylation of genes promoter, the circulating levels of folate/vitamin B_{12} and the influence of the *MTHFR* 677 genotypes in CLC patients. While no significant difference in serum folate/vitamin B_{12} status was observed between those with methylated and unmethylated tumors in *CC* individuals, the *CT*, and *CT*/*TT* genotypes of *MTHFR* exhibited a significant positive correlation with elevated folate/vitamin B_{12} levels for promoter methylation silencing (Table 5). Previously, an interaction between dietary folic acid and vitamin B_{12} supplementation with promoter methylation in colorectal adenomas has been suggested, especially for subjects with *MTHFR TT* genotype[16,30]. Because we did not have enough *TT* cases, we could not evaluate correlation of serum folate levels with tumor methylation in these individuals. Among our study group there was only one *TT* individual with a methylated tumor who also had higher serum folate/vitamin B_{12} level than *TT* cases with unmethylated tumors (Table 5). Genomic DNA methylation in leukocytes and in transformed human lymphoblasts was shown to be positively correlated to folate status in those with the *TT* genotype, but not with wild-type *MTHFR CC* genotype[12,27,31]. An inverse trend of serum and erythrocyte folate with DNA hypomethylation was also reported in normal colonic mucosa[28].

In some studies, no interaction was reported between either *MTHFR* genotype and folate intake in association with CIMP + colon tumors[17,32]. Further investigation is needed focusing on ethnic variations in the relationships between the *MTHFR* polymorphism, folate intake, and tumors methylation in CLC. The majority of previous case-control studies have assessed dietary folate or vitamin B intake from questionnaires rather than their blood measurements, a procedure which is prone to some degree of miscalculation. Moreover, other factors like alcohol intake and iron status may be related to folate availability and biological activity[33]. In the present work, the direct measurement of serum folate/vitamin B_{12} was correlated with CLC and tumor methylation. It has been previously reported that the colonic mucosal folate concentration correlates directly with serum folate concentration in the physiological range at each time point[34]. Therefore, the serum folate measurement could be an accurate reflection of the folate status in the colonic mucosa. High intracellular concentrations of folate intermediates are associated with aberrant methylation within promoter regions of cancer – associated genes in colorectal tumors[35].

There is evidence that the epigenetic mechanism of gene silencing by methylation may play a differential role in proximal versus distal colon carcinogenesis. A different role for the *MTHFR 677 TT* genotype in the tumorigenesis of proximal and distal CLC has been also suggested[8]. Our finding of an increased risk of tumor methylation associated with high serum folate/vitamin B_{12} levels in those with proximal tumors, and in older patients (Table 4) might be related to the previous observation of a high concentration of folate in tumors from older patients and proximal CLC[35].

Our results indicate that a high serum folate/vitamin B_{12}, in combination with a heterozygous or homozygous *C677T MTHFR* genotype, predisposes tumor-specific genes to promoter hypermethylation. Conversely, folate could be protective or have no effect in developing CLC in subjects with the wild type *MTHFR 677* CC genotype. The *MTHFR C677T* mutation reduces MTHFR activity, which leads to lower levels of 5-methylTHF in individuals with a marginal folate status. However, in the presence of high folate levels, the negative effect of *MTHFR TT* on the efficiency of the methylation process might be masked possibly by maximizing the catalytic activity of MTHFR[36]. Indeed, under conditions of high folate status no differences in the *K*m or *V*max values were detected between the wild type and mutant enzymes[37]. Therefore, hypermethylation of CpG islands could occur in individuals with the *MTHFR 677T* allele under high folate status.

A major draw-back of the present study is the fact that the serum data collection occurred after the onset of tumor formation. Although, more studies are needed to determine whether *MTHFR C677T* genotypes, together with high serum folate/vitamin B_{12} levels, could serve as risk factors for the CIMP + CLC subgroup, the findings of this study are in agreement with other recent reports which together provide additional evidence for caution in the mandatory fortification of cereals with folic acid.

ACKNOWLEDGMENTS

We would like to thank Dr. Rose M Johnstone of McGill University for her critical review of the manuscript.

COMMENTS

Backgrounds

Transcriptional silencing of tumor suppressor genes by hypermethylation of capillary blood gases (CpG) islands located in the promoter region is very common in human colorectal cancer. *P16, hMLH1, hMSH2* are key tumor suppressor genes frequently silenced by promoter methylation in sporadic colon cancer (CLC). Methylentetrahydrofolate reductase (*MTHFR) C677T* genotype has been associated with reduced enzyme activity and altered cellular folate composition. In this study, we investigated the association between serum folate/vitamin B_{12}, *MTHFR C677T* genotype, and promoter methylation of three tumor-associated genes in solid tumors among sporadic CLC patients.

Research frontiers

Dietary folate/vitamin B_{12} intake and *MTHFR C677T* genotype was suggested to protect against colorectal cancer. However, only a few studies have addressed the joint effects of circulating levels of folate/vitamin B_{12} and the *MTHFR C677T* genotype on the risk of epigenetic inactivation of specific tumor suppressor genes in CLC patients.

Innovations and breakthroughs

Our data indicate that serum folate/vitamin B_{12} levels are directly associated with the DNA hypermethylation of CpG island within promoter of the tumor specific genes and to the *C677T* genotype of *MTHFR*. We identified that

the *T* allele of *MTHFR* has strong influence on the risk of tumor methylation associated with high serum folate/vitamin B_{12} levels.

Applications

The results from the study support other recent reports that high folate and vitamin B_{12} status might serve as risk factors for CLC. This study provides additional evidence for caution in terms of CLC risk because of the mandatory fortification of cereals with folic acid in certain countries.

Peer review

This is a population-based, case-controlled, molecular epidemiological study on the interaction of *MTHFR C677T* genotype and circulating folate/vitamin B_{12} with the CpG island hypermethylation of tumor-associated genes in sporadic colorectal cancer. This result indicated that for the *MTHFR C677T* genotypes, increased concentrations of folate and vitamin B_{12} are associated with increased risks of tumor methylation. This demonstration might give a suggestion to protect against colorectal cancer, at least, in Iranian sporadic CLC population.

REFERENCES

1 **Parkin DM**, Bray F, Ferlay J, Pisani P. Estimating the world cancer burden: Globocan 2000. *Int J Cancer* 2001; **94**: 153-156

2 **Yazdizadeh B**, Jarrahi AM, Mortazavi H, Mohagheghi MA, Tahmasebi S, Nahvijo A. Time trends in the occurrence of major GI cancers in Iran. *Asian Pac J Cancer Prev* 2005; **6**: 130-134

3 **Hosseini SV**, Izadpanah A, Yarmohammadi H. Epidemiological changes in colorectal cancer in Shiraz, Iran: 1980-2000. *ANZ J Surg* 2004; **74**: 547-549

4 **Toyota M**, Ahuja N, Ohe-Toyota M, Herman JG, Baylin SB, Issa JP. CpG island methylator phenotype in colorectal cancer. *Proc Natl Acad Sci USA* 1999; **96**: 8681-8686

5 **Herman JG**. Hypermethylation pathways to colorectal cancer. Implications for prevention and detection. *Gastroenterol Clin North Am* 2002; **31**: 945-958

6 **Cellarier E**, Durando X, Vasson MP, Farges MC, Demiden A, Maurizis JC, Madelmont JC, Chollet P. Methionine dependency and cancer treatment. *Cancer Treat Rev* 2003; **29**: 489-499

7 **Frosst P**, Blom HJ, Milos R, Goyette P, Sheppard CA, Matthews RG, Boers GJ, den Heijer M, Kluijtmans LA, van den Heuvel LP. A candidate genetic risk factor for vascular disease: a common mutation in methylenetetrahydrofolate reductase. *Nat Genet* 1995; **10**: 111-113

8 **Toffoli G**, Gafa R, Russo A, Lanza G, Dolcetti R, Sartor F, Libra M, Viel A, Boiocchi M. Methylenetetrahydrofolate reductase 677 C-->T polymorphism and risk of proximal colon cancer in north Italy. *Clin Cancer Res* 2003; **9**: 743-748

9 **Choi SW**, Mason JB. Folate status: effects on pathways of colorectal carcinogenesis. *J Nutr* 2002; **132**: 2413S-2418S

10 **van Rijnsoever M**, Grieu F, Elsaleh H, Joseph D, Iacopetta B. Characterisation of colorectal cancers showing hypermethylation at multiple CpG islands. *Gut* 2002; **51**: 797-802

11 **Heijmans BT**, Boer JM, Suchiman HE, Cornelisse CJ, Westendorp RG, Kromhout D, Feskens EJ, Slagboom PE. A common variant of the methylenetetrahydrofolate reductase gene (1p36) is associated with an increased risk of cancer. *Cancer Res* 2003; **63**: 1249-1253

12 **Friso S**, Choi SW, Girelli D, Mason JB, Dolnikowski GG, Bagley PJ, Olivieri O, Jacques PF, Rosenberg IH, Corrocher R, Selhub J. A common mutation in the 5,10-methylene tetrahydrofolate reductase gene affects genomic DNA methylation through an interaction with folate status. *Proc Natl Acad Sci USA* 2002; **99**: 5606-5611

13 **Kim YI**. Folate and DNA methylation: a mechanistic link between folate deficiency and colorectal cancer? *Cancer Epidemiol Biomarkers Prev* 2004; **13**: 511-519

14 **Bollheimer LC**, Buettner R, Kullmann A, Kullmann F. Folate and its preventive potential in colorectal carcinogenesis. How strong is the biological and epidemiological evidence? *Crit Rev Oncol Hematol* 2005; **55**: 13-36

15 **Sanjoaquin MA**, Allen N, Couto E, Roddam AW, Key TJ. Folate intake and colorectal cancer risk: a meta-analytical approach. *Int J Cancer* 2005; **113**: 825-828

16 **van den Donk M**, van Engeland M, Pellis L, Witteman BJ, Kok FJ, Keijer J, Kampman E. Dietary folate intake in combination with MTHFR C677T genotype and promoter methylation of tumor suppressor and DNA repair genes in sporadic colorectal adenomas. *Cancer Epidemiol Biomarkers Prev* 2007; **16**: 327-333

17 **Curtin K**, Slattery ML, Ulrich CM, Bigler J, Levin TR, Wolff RK, Albertsen H, Potter JD, Samowitz WS. Genetic polymorphisms in one-carbon metabolism: associations with CpG island methylator phenotype (CIMP) in colon cancer and the modifying effects of diet. *Carcinogenesis* 2007; **28**: 1672-1679

18 **Hill AE**, FitzPatrick DR. MS-PCR assay to detect 677C-->T mutation in the 5,10-methylenetetrahydrofolate reductase gene. *J Inherit Metab Dis* 1998; **21**: 694-695

19 **Herman JG**, Graff JR, Myohanen S, Nelkin BD, Baylin SB. Methylation-specific PCR: a novel PCR assay for methylation status of CpG islands. *Proc Natl Acad Sci USA* 1996; **93**: 9821-9826

20 **Matsushita S**, Muramatsu T, Arai H, Matsui T, Higuchi S. The frequency of the methylenetetrahydrofolate reductase-gene mutation varies with age in the normal population. *Am J Hum Genet* 1997; **61**: 1459-1460

21 **Heijmans BT**, Gussekloo J, Kluft C, Droog S, Lagaay AM, Knook DL, Westendorp RG, Slagboom EP. Mortality risk in men is associated with a common mutation in the methylene-tetrahydrofolate reductase gene (MTHFR). *Eur J Hum Genet* 1999; 7: 197-204

22 **Ueland PM**, Hustad S, Schneede J, Refsum H, Vollset SE. Biological and clinical implications of the MTHFR C677T polymorphism. *Trends Pharmacol Sci* 2001; **22**: 195-201

23 **Oyama K**, Kawakami K, Maeda K, Ishiguro K, Watanabe G. The association between methylenetetrahydrofolate reductase polymorphism and promoter methylation in proximal colon cancer. *Anticancer Res* 2004; **24**: 649-654

24 **Jacques PF**, Bostom AG, Williams RR, Ellison RC, Eckfeldt JH, Rosenberg IH, Selhub J, Rozen R. Relation between folate status, a common mutation in methylenetetrahydrof olate reductase, and plasma homocysteine concentrations. *Circulation* 1996; **93**: 7-9

25 **Van Guelpen B**, Hultdin J, Johansson I, Hallmans G, Stenling R, Riboli E, Winkvist A, Palmqvist R. Low folate levels may protect against colorectal cancer. *Gut* 2006; **55**: 1461-1466

26 **Keyes MK**, Jang H, Mason JB, Liu Z, Crott JW, Smith DE, Friso S, Choi SW. Older age and dietary folate are determinants of genomic and p16-specific DNA methylation in mouse colon. *J Nutr* 2007; **137**: 1713-1717

27 **Stern LL**, Mason JB, Selhub J, Choi SW. Genomic DNA hypomethylation, a characteristic of most cancers, is present in peripheral leukocytes of individuals who are homozygous for the C677T polymorphism in the methylene tetrahydrofolate reductase gene. *Cancer Epidemiol Biomarkers Prev* 2000; **9**: 849-853

28 **Pufulete M**, Al-Ghnaniem R, Rennie JA, Appleby P, Harris N, Gout S, Emery PW, Sanders TA. Influence of folate status on genomic DNA methylation in colonic mucosa of subjects without colorectal adenoma or cancer. *Br J Cancer* 2005; **92**: 838-842

29 **Kraunz KS**, Hsiung D, McClean MD, Liu M, Osanyingbemi J, Nelson HH, Kelsey KT. Dietary folate is associated with p16(INK4A) methylation in head and neck squamous cell carcinoma. *Int J Cancer* 2006; **119**: 1553-1557

30 **van den Donk M**, Pellis L, Crott JW, van Engeland M, Friederich P, Nagengast FM, van Bergeijk JD, de Boer SY, Mason JB, Kok FJ, Keijer J, Kampman E. Folic acid and vitamin B-12 supplementation does not favorably influence uracil incorporation and promoter methylation in rectal mucosa DNA of subjects with previous colorectal adenomas. *J Nutr* 2007; **137**: 2114-2120

31 **Chiang EP**, Wang YC, Tang FY. Folate restriction and

methylenetetrahydrofolate reductase 677T polymorphism decreases adoMet synthesis via folate-dependent remethylation in human-transformed lymphoblasts. *Leukemia* 2007; **21**: 651-658

32 **Clarizia AD**, Bastos-Rodrigues L, Pena HB, Anacleto C, Rossi B, Soares FA, Lopes A, Rocha JC, Caballero O, Camargo A, Simpson AJ, Pena SD. Relationship of the meth ylenetetrahydrofolate reductase C677T polymorphism with microsatellite instability and promoter hypermethylation in sporadic colorectal cancer. *Genet Mol Res* 2006; **5**: 315-322

33 **Konings EJ**, Goldbohm RA, Brants HA, Saris WH, van den Brandt PA. Intake of dietary folate vitamers and risk of colorectal carcinoma: results from The Netherlands Cohort Study. *Cancer* 2002; **95**: 1421-1433

34 **Kim YI**, Fawaz K, Knox T, Lee YM, Norton R, Libby E, Mason JB. Colonic mucosal concentrations of folate are accurately predicted by blood measurements of folate status among individuals ingesting physiologic quantities of folate. *Cancer Epidemiol Biomarkers Prev* 2001; **10**: 715-719

35 **Kawakami K**, Ruszkiewicz A, Bennett G, Moore J, Watanabe G, Iacopetta B. The folate pool in colorectal cancers is associated with DNA hypermethylation and with a polymorphism in methylenetetrahydrofolate reductase. *Clin Cancer Res* 2003; **9**: 5860-5865

36 **Moat SJ**, Ashfield-Watt PA, Powers HJ, Newcombe RG, McDowell IF. Effect of riboflavin status on the homocysteine-lowering effect of folate in relation to the MTHFR (C677T) genotype. *Clin Chem* 2003; **49**: 295-302

37 **Yamada K**, Chen Z, Rozen R, Matthews RG. Effects of common polymorphisms on the properties of recombinant human methylenetetrahydrofolate reductase. *Proc Natl Acad Sci USA* 2001; **98**: 14853-14858

S- Editor Zhong XY **L- Editor** Rippe RA **E- Editor** Lin YP

Online Submissions: wjg.wjgnet.com
wjg@wjgnet.com
doi:10.3748/wjg.14.3672

World J Gastroenterol 2008 June 21; 14(23): 3672-3680
World Journal of Gastroenterology ISSN 1007-9327
© 2008 The WJG Press. All rights reserved.

BASIC RESEARCH

Ellagic acid induces apoptosis through inhibition of nuclear factor κB in pancreatic cancer cells

Mouad Edderkaoui, Irina Odinokova, Izumi Ohno, Ilya Gukovsky, Vay Liang W Go, Stephen J Pandol, Anna S Gukovskaya

Mouad Edderkaoui, Irina Odinokova, Izumi Ohno, Ilya Gukovsky, Vay Liang W Go, Stephen J Pandol, Anna S Gukovskaya, Department of Medicine, Veterans Affairs Greater Los Angeles Healthcare System and University of California, Los Angeles CA 90073, California, United States
Irina Odinokova, Institute of Theoretical and Experimental Biophysics, Russian Academy of Sciences, Pushchino, Moscow Region 142290, Russia
Author contributions: Edderkaoui M and Gukovskaya AS designed research; Edderkaoui M, Odinokova I, Ohno I and Gukovsky I performed research; Edderkaoui M, Go VLW, Pandol SJ and Gukovskaya AS analyzed data; Edderkaoui M and Gukovskaya AS wrote the paper.
Supported by the Department of Veterans Affairs Merit Review (to A.S.G), the Hirshberg foundation and the NIH/NCCAM (1P01AT003960-01)
Correspondence to: Anna S Gukovskaya, PhD, VA Greater Los Angeles Healthcare System, West Los Angeles VA Healthcare Center, 11301 Wilshire Blvd, Blg 258, Rm 340, Los Angeles CA 90073, United States. agukovsk@ucla.edu
Telephone: +1-310-4783711-41525 Fax: +1-310-2684578
Received: December 26, 2007 Revised: April 25, 2008
Accepted: May 2, 2008
Published online: June 21, 2008

Abstract

AIM: To determine the effect of ellagic acid on apoptosis and proliferation in pancreatic cancer cells and to determine the mechanism of the pro-survival effects of ellagic acid.

METHODS: The effect of ellagic acid on apoptosis was assessed by measuring Phosphatidylserine externalization, caspase activity, mitochondrial membrane potential and DNA fragmentation; and proliferation by measuring DNA thymidine incorporation. Mitochondrial membrane potential was measured in permeabilized cells, and in isolated mitochondria. Nuclear factor κB (NF-κB) activity was measured by electromobility shift assay (EMSA).

RESULTS: We show that ellagic acid, a polyphenolic compound in fruits and berries, at concentrations 10 to 50 mmol/L stimulates apoptosis in human pancreatic adenocarcinoma cells. Further, ellagic acid decreases proliferation by up to 20-fold at 50 mmol/L. Ellagic acid stimulates the mitochondrial pathway of apoptosis associated with mitochondrial depolarization, cytochrome C release, and the downstream caspase activation. Ellagic acid does not directly affect mitochondria. Ellagic acid dose-dependently decreased NF-κB binding activity. Furthermore, inhibition of NF-κB activity using IkB wild type plasmid prevented the effect of ellagic acid on apoptosis.

CONCLUSION: Our data indicate that ellagic acid stimulates apoptosis through inhibition of the prosurvival transcription factor NF-κB.

© 2008 The WJG Press. All rights reserved.

Key words: Ellagic acid; Nuclear factor-κB; Apoptosis; Pancreatic cancer

Peer reviewer: Minoti Vivek Apte, Pancreatic Research Group, South Western Sydney Clinical School, the University of New South Wales, Level 2, Thomas and Rachel Moore Education Centre, Liverpool Hospital, New South Wales 2170, Liverpool, Australia

Edderkaoui M, Odinokova I, Ohno I, Gukovsky I, Go VLW, Pandol SJ, Gukovskaya AS. Ellagic acid induces apoptosis through inhibition of nuclear factor κB in pancreatic cancer cells. *World J Gastroenterol* 2008; 14(23): 3672-3680 Available from: URL: http://www.wjgnet.com/1007-9327/14/3672.asp DOI: http://dx.doi.org/10.3748/wjg.14.3672

INTRODUCTION

Pancreatic cancer is a very aggressive disease and is the fourth most common cause of death in Western countries with almost the same rate of incidence and mortality per year[1,2]. Pancreatic cancer is very resistant to radio-and chemo-therapies. One reason for that is the resistance of pancreatic cancer cells to apoptosis[3].

During the past decade, significant progress has been achieved in understanding the molecular mechanisms of apoptosis[4]. The information obtained suggests that the commitment to apoptosis occurs through activation of caspases, a unique family of cysteine proteases[4]. Caspases are synthesized as inactive precursors and are, generally, activated by proteases including caspases themselves. Thus, caspases can function in an activation cascade.

Cancer cells protect themselves from apoptosis by

upregulation of prosurvival mechanisms. Activation of the transcription factor NF-κB is a key pro-survival mechanism in cancer cells[5,6]. NF-κB is constitutively active in pancreatic cancer cells, and its inhibition leads to pancreatic cancer cell death and inhibition of tumor development[7].

Ellagic acid ($C_{14}H_6O_8$) is a polyphenolic compound present in fruits and berries such as pomegranates, strawberries, raspberries and blackberries. It has anticarcinogenic, antioxidant and antifibrosis properties[8-11]. The anticarcinogenic effect of ellagic acid was shown in several types of cancers including skin, esophageal, and colon cancers[11,12]. However, the effects of ellagic acid on pancreatic cancer have not been studied. Furthermore, the mechanisms mediating anticancer effect of ellagic acid, in general, remain unknown.

There is a growing interest in natural compounds for enhancing cancer prevention and treatment. In this study, we show that ellagic acid induces apoptosis and decreases proliferation in pancreatic cancer cells. We demonstrate that ellagic acid stimulates apoptosis in pancreatic cancer cells through inhibiting transcription factor NF-κB activity.

MATERIALS AND METHODS

Reagents

Ac-Asp-Glu-Val-Asp-7-amino-4-methylcoumarin (Ac-DEVD-AMC) was from Peptide Institute, Inc (Osaka, Japan). Antibody against cytochrome C was from BD Biosciences (San Diego, CA). CAPE was from biomol (Plymouth meeting, PA). Ellagic acid and all other reagents were from Sigma Chemical (St. Louis, MO).

Cell culture

Human pancreatic adenocarcinoma cell lines, the poorly differentiated MIA PaCa-2 and the moderately differentiated PANC-1, were obtained from the American Type Culture Collection (Manassas, VA). MIA PaCa-2 and PANC-1 cells were grown in 1/1 D-MEM/F-12 medium (GIBCO Invitrogen Corporation, Grand Island, NY) supplemented with 15% fetal bovine serum (FBS), 4 mmol/L L-glutamine, and 1% antibiotic/antimycotic solution (Omega Scientific, Tarzana, CA). Cells were maintained at 37℃ in a humidified atmosphere containing 5% CO_2 and were used between passages 4 and 12.

MIA PaCa-2 and PANC-1 cells were plated at a density of 2×10^6/mL on 100-mm culture dishes, cultured for up to 48 h in D-MEM/F-12 medium supplemented with FBS, glutamine and the antibiotic/antimycotic solution, collected, and processed for the specified analyses. Inhibitors or vehicle were added to the culture medium just before plating out the cells.

Preparation of cytosolic and membrane fractions

Cells were resuspended in a lysis buffer (250 mmol/L sucrose, 20 mmol/L HEPES, 10 mmol/L KCl, 1 mmol/L Na-EGTA, 1 mmol/L Na-EDTA, 2 mmol/L $MgCl_2$, pH 7.0), allowed to swell for 30 min at 4℃, and then disrupted by 80 strokes in a Dounce homogenizer. Homogenates were centrifuged at 1000 *g* for 5 min to pellet nuclei and cell debris. Supernatants were centrifuged at 16 000 *g* for 30 min, and the cytosolic fractions (supernatants) were collected. Pellets (heavy membranes enriched with mitochondria) were lysed in RIPA buffer (0.15 mol/L NaCl, 50 mmol/L Tris, 1% deoxycholic acid, 1% Triton X-100, 0.1% sodium dodecyl sulfate, pH 7.2) for 1 h. To determine the quality of cytosolic and mitochondrial separation, both fractions were assessed by immunoblotting for the mitochondrial marker cytochrome C oxidase subunit Ⅳ (COX Ⅳ).

Western blot analysis

Cells were incubated in a lysis buffer (0.5 mmol/L EDTA, 150 mmol/L NaCl, 50 mmol/L Tris, 0.5% Nonidet P-40, pH 7.5) for 30 min at 4℃. The lysis buffer was supplemented with 1 mmol/L PMSF, 5 g/mL each of protease inhibitors pepstatin, leupeptin, chymostatin, antipain, and aprotinin. Cell lysates were centrifuged for 10 min at 13 000 *g*. Supernatants were collected and proteins were separated by SDS-PAGE (Invitrogen) and electrophoretically transferred to nitrocellulose membranes. Non-specific binding was blocked with 5% milk in Tris-buffered saline (4 mmol/L Tris base, 100 mmol/L NaCl, pH 7.5). Membranes were washed in Tris-buffered saline containing 0.05% Tween 20 (TTBS) and incubated for 2 h with the indicated primary antibodies and then for 1 h with horseradish peroxidase-conjugated secondary antibody. Blots were developed with the Supersignal Chemiluminescent Substrate (ECL) (Pierce).

Measurements of apoptosis

Apoptosis parameters were measured as previously described[13-16]: Internucleosomal DNA fragmentation was measured by using Cell Death Detection ELISA^{Plus} kit (Roche Molecular Biochemicals, Manheim, Germany) according to the manufacturer's instructions.

Phosphatidylserine (PS) externalization: PS externalization was analyzed with the Annexin-V (AnV)-FLUOS Staining Kit from Roche Biochemicals (Indianapolis, IN) as we described before[13]. Cells were collected and resuspended at a density of 1×10^6 cells in 500 μL of binding buffer containing 2 μL AnV and 1 μL propidium iodide (PI), incubated in the dark for 30 min at room temperature, and analyzed by flow cytometry.

Effector caspase (DEVDase) activity: DEVDase activity was measured by a fluorogenic assay in whole cell lysates using DEVD-AMC as a substrate, as we described before[13]. The lysate (50-100 μg of protein) was incubated with 10 μmol/L substrate

in a reaction buffer (25 mmol/L HEPES (pH 7.5), 10% sucrose, 0.1% CHAPS, 10 mmol/L DTT) at 37℃. Caspase substrate cleavage releases AMC, which emits fluorescent signal with 380 nm excitation and 440 nm emission. Fluorescence was calibrated using a standard curve for AMC.

Measurement of mitochondrial membrane potential ($\Delta\psi m$)

Changes in $\Delta\psi$m were detected with the potential-sensitive probes 3, 3' dihexyloxa-carbocyanine DiOC6 (3) (Molecular Probes, Eugene, OR). Cells were incubated with 100 nmol/L DiOC6 (3) for 30 min at 37℃ in the dark, washed twice with PBS, and analyzed on a FACScan using FL-1. To completely dissipate $\Delta\psi$m, cells were treated with the uncoupling agent CCCP (50 μmol/L) for 1 h before DiOC6 (3) staining.

Registration of mitochondrial respiration and membrane potential in cells permeabilized with digitonin

MIA PaCa-2 cells (5×10^6) were washed twice with PBS and resuspended in 50 μL DMEM/F12 medium without serum. The medium for mitochondrial functional assays contained 250 mmol/L sucrose, 22 mmol/L KCl, 22 mmol/L triethanolamine (pH 7.4), 3 mmol/L $MgCl_2$, 5 mmol/L KH_2PO_4, 0.5% BSA. Glutamate (10 mmol/L) and malate (2 mmol/L) were used as mitochondrial respiratory substrates. Digitonin at concentration 0.001% was added to cell suspension to permeabilize plasma membrane and to allow substrates and chemicals to reach mitochondria immediately after addition into reaction medium. The measurements were performed at 25℃. Membrane potential and oxygen consumption were monitored simultaneously in a 1-mL custom-made chamber. Oxygen consumption was measured using a Clark-type electrode (Instech Lab., Plymouth Meeting, PA) connected to an oxygen meter (Yellow Springs Instruments, Yellow Springs, OH). Mitochondrial membrane potential was registered in the presence of 1 μmol/L tetraphenyl phosphonium (TPP^+) using a TPP^+-sensitive electrode connected to an amplifier (Vernier Software, Beaverton, OR). An increase in $\Delta\psi$m causes TPP^+ uptake by mitochondria and, correspondingly, a decrease in external TPP^+ measured with the electrode.

Another approach applied to measure $\Delta\psi$m is by using $\Delta\psi$m-sensitive fluorescent probe tetramethylrhodamine methyl ester (TMRM; Molecular Probes, Eugene, OR). Changes in the fluorescence intensity were measured in the cell suspension containing 0.5 μmol/L TMRM in the 2-mL cuvette in a RF-1501 spectrofluorophotometer (Simadzu, Japan) with 543 nm excitation, and 578 nm emission. $\Delta\psi$m-driven mitochondrial uptake of TMRM causes TMRM quenching, which results in decreased fluorescence intensity.

Isolation of mitochondria

Mitochondria from Mia PaCa-2 cells were isolated using differential centrifugation. Cells (approximately 2×10^8) were homogenized using motor-driven tissue grinder in the isolation buffer containing 320 mmol/L sucrose, 10 mmol/L Tris-HCl (pH 7.4), 0.5 mmol/L EGTA, 0.5 mmol/L EDTA and 0.2% BSA. Unbroken cells were spun down by centrifugation at 500 *g* for 5 min, followed by nuclei centrifugation at 2000 *g* for 3 min. The resulting supernatant containing mitochondria was spun down at 12500 *g* for 10 min; then mitochondria were washed in a washing buffer containing 320 mmol/L sucrose and 10 mmol/L Tris-HCL (pH 7.4); and finally the mitochondrial pellet was re-suspended in the washing buffer. The obtained mitochondrial suspension contained 8 to 12 mg protein/mL as determined by the Bradford protein assay (BioRad Laboratories). All isolation steps were performed at 4℃, and the mitochondria were kept on ice all the time. Mitochondrial membrane potential and oxygen consumption were measured using TPP^+-sensitive and Clark-type electrodes correspondingly in the same incubation buffer as described above for digitonin-permeabilized cells.

Measurement of cytochrome C release from isolated mitochondria

MIA PaCa-2 cell mitochondria were incubated in the absence or presence of ellagic acid for 10 min. Aliquots of mitochondrial suspension were collected, centrifuged at 13500 *g* for 10 min at 4℃, and cytochrome C levels in the mitochondria (pellet) and the medium (supernatant) were measured by Western blot as previously described[13].

Preparation of nuclear extracts and electromobility shift assay (EMSA)

Preparation of nuclear extracts and EMSA have been described in detail[17-19]. Briefly, pancreatic cancer cells were lysed on ice in a hypotonic buffer A[17] supplemented with 1 mmol/L PMSF, 1 mmol/L DTT, and protease inhibitor cocktail containing 5 μg/mL each of pepstatin, leupeptin, chymostatin, antipain, and aprotinin. Cells were left to swell on ice for a 20 min to 25 min period: 0.3% Igepal CA-630 was then added, and the nuclei were collected by microcentrifugation. The nuclear pellet was resuspended in a high-salt buffer C[17] supplemented with 1 mmol/L PMSF, 1 mmol/L DTT, and the protease inhibitor cocktail described above. After incubating at 4℃, membrane debris was pelleted by microcentrifugation for 10 min, and the clear supernatant (nuclear extract) was aliquoted and stored at -80℃. Protein concentration in the extracts was determined by the Bio-Rad protein assay (Bio-Rad Laboratories, Hercules, CA).

For the EMSA, aliquots of nuclear extracts with equal amounts of protein (5-10 μg) were mixed in 20-μL reactions with a buffer containing 10 mmol/L HEPES (pH 7.8), 50 mmol/L KCl, 0.1 mmol/L EDTA, 1 mmol/L DTT, 10% glycerol, and 3 μg poly (dI-dC). Binding reactions were started by the

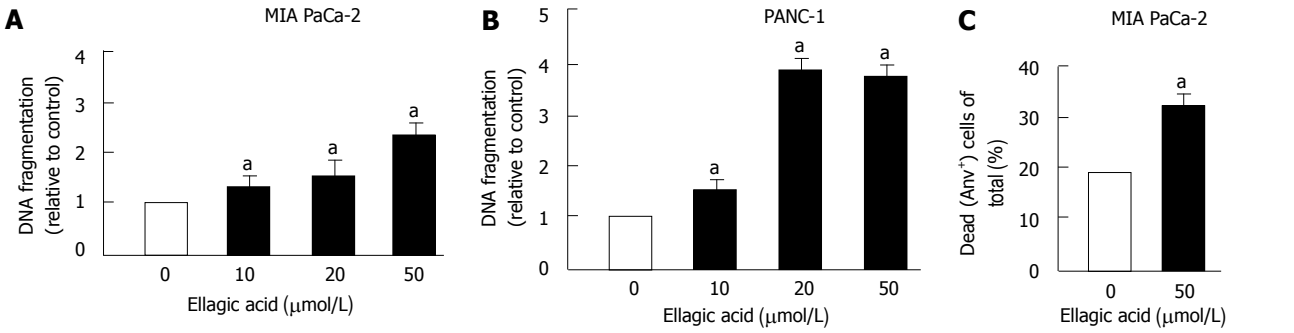

Figure 1 Ellagic acid stimulates apoptosis in pancreatic cancer cells. MIA PaCa-2 (**A**, **C**) and PANC-1 (**B**) cells were cultured for 48 h in the presence or absence of indicated doses of ellagic acid. Internucleosomal DNA fragmentation was measured using the Cell Death Detection ELISA kit (**A**, **B**); Dead cells were assessed by flow cytometry using AnV/PI staining (**C**). AnV^+/PI^- and AnV^+/PI^+ cells were considered dying through apoptosis and/or secondary necrosis. Values are normalized to control (**A**, **B**). Values are mean ± SE (n = 3), $^aP < 0.05$ *vs* control.

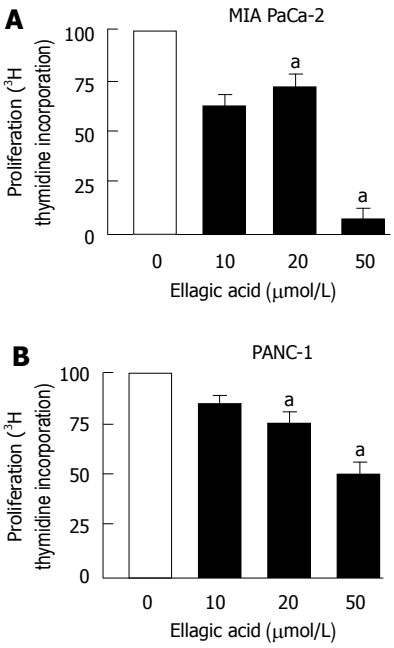

Figure 2 Ellagic acid inhibits proliferation in pancreatic cancer cells. MIA PaCa-2 (**A**, **C**) and PANC-1 (**B**) cells were cultured for 48 h in the presence or absence of indicated doses of ellagic acid. Proliferation was assessed by measuring (^{3}H) thymidine incorporation into DNA. The results are representative of at least 3 independent experiments, $^aP < 0.05$ *vs* control.

addition of 32P-labeled DNA probe and incubated at room temperature for 20 min. The oligo probe 5' -GCAGAGGGGACTTTCCGAGA-3' containing κB binding motif (underlined) was annealed to the complementary oligonucleotide and end-labeled by using T4 polynucleotide kinase. Samples were electrophoresed on a native 4.5% polyacrylamide gel at 200 V in 0.5 TBE buffer (1 × TBE: 89 mmol/L Tris base, 89 mmol/L boric acid, 2 mmol/L EDTA). Gels were dried and densitometrically quantified in the Phosphor-Imager (Molecular Dynamics, Sunnyvale, CA). In pancreatic cancer cells, the NF-κB band has two components: the upper component corresponds to the p50/p65 heterodimer and the lower component to the p50/p50 homodimer. In the present study, we quantified the total (combined) intensity of the NF-κB band.

Cell transfection

For this a luciferase reporter gene system was used. Briefly, MIA PaCa-2 cells were simultaneously transfected with the 4KBwt-pRL-TK luciferase plasmid, which expresses the NF-κB inhibitor I-κB and pRL-TK luciferase (as a reference) using the NucleofectorTM II (Amaxa Inc, Gaithersburg, MD) according to the manufacturer protocol. The transfection efficiency and NF-κB transcriptional activity was assessed by using the Dual-Luciferase Reporter Assay System (Promega Corporation, Madison WI).

Statistical analysis

Results are expressed as mean ± SE from at least 3 independent experiments. Statistical analysis was done using the unpaired Student's *t*-test. $P < 0.05$ was considered statistically significant.

RESULTS

Ellagic acid stimulates apoptosis and inhibits proliferation of pancreatic cancer cells

Ellagic acid dose-dependently increased apoptosis in PaCa cells (Figure 1). To measure apoptosis we used 2 approaches. First, we showed that ellagic acid stimulates apoptotic internucleosomal DNA fragmentation in MIA PaCa-2 (Figure 1A) and PANC-1 cells (Figure 1B). Second, we used flow cytometry and AnV/PI staining to measure the percentage of dead cells as described in Experimental Procedures. We previously showed that the AnV^+/PI^- group includes cells at early stages of apoptosis, whereas the AnV^+/PI^+ group includes both necrotic cells and apoptotic cells associated with secondary necrosis[13]. Ellagic acid increased the percentage of dead MIA PaCa-2 cells (i.e. stained positively for both AnV and PI or for AnV alone) (Figure 1C).

Next, we measured the effect of ellagic acid on proliferation of PaCa cells. The results in Figure 2 show that ellagic acid dose-dependently inhibited proliferation of both MIA PaCa-2 and PANC-1 cell lines as measured by ^{3}H thymidine incorporation (Figure 2A and B). The effect was most pronounced at 50 μmol/L (almost 20 fold inhibition in MIA PaCa-2 cells).

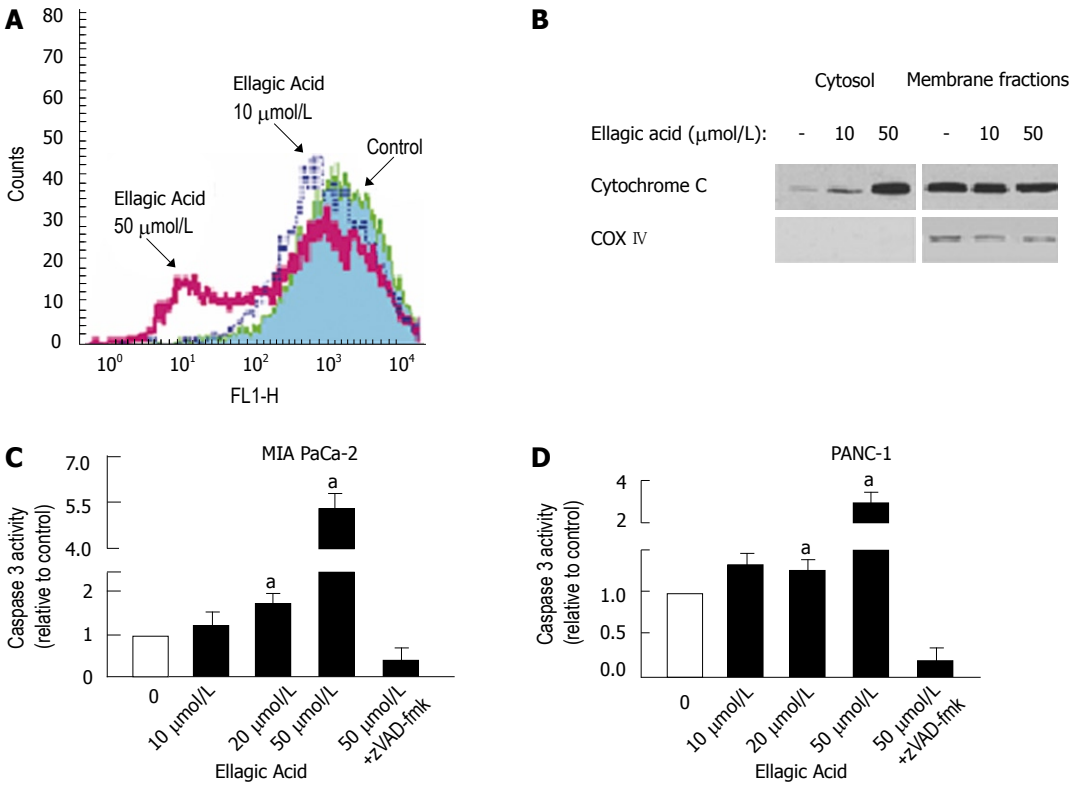

Figure 3 Ellagic acid induces loss of mitochondrial membrane potential, cytochrome C release, and caspase-3 activation in pancreatic cancer cells. MIA PaCa-2 (**A**-**C**) and PANC-1 (**B**) cells were cultured for 48 h in the presence or absence of indicated doses of ellagic acid or broad-spectrum caspase inhibitor zVAD-fmk (100 μmol/L). **A**: Changes in $\Delta\psi$m were measured by flow cytometry using the potential-sensitive probe 3,3'dihexyloxa-carbocyanine DiOC6 (3); **B**: Cytochrome C release was assessed by measuring cytochrome C levels in both cytosolic and mitochondria-enriched membrane fractions using Western blot analysis. Blots were re-probed for cytochrome C oxidase (COX Ⅳ), a specific mitochondrial marker. Western blots of cytosolic fractions re-probed for actin to confirm equal protein loading; **C** and **D**: Caspase-3 activity was assessed by measuring the DEVDase (caspase-3 like) activities in cell lysates using a fluorometric assay with a specific substrate. The results are representative of at least 3 independent experiments. Values are normalized to control (**C** and **D**). Values are mean ± SE (n = 3), $^aP < 0.05$ *vs* control.

Ellagic acid induces mitochondrial depolarization, cytochrome C release, and caspase activation in pancreatic cancer cells

To determine the signaling pathway mediating the proapoptotic effect of ellagic acid, we measured the effects of ellagic acid on mitochondrial membrane potential ($\Delta\psi$m), cytochrome C release, and caspase-3 activity. Ellagic acid decreased $\Delta\psi$m as measured by flow cytometry using the potential-sensitive probe DiOC6 (3). Depolarization was already evident at 10 μmol/L, and was very pronounced at 50 μmol/L ellagic acid (Figure 3A). Ellagic acid also dose-dependently stimulated cytochrome C release, which manifests by its decrease in mitochondria-enriched membrane fractions and its increase in cytosolic fractions (Figure 3B). The increased cytochrome C release was associated with downstream activation of caspase-3 in MIA PaCa-2 (Figure 3C) and PANC-1 (Figure 3D) cells.

These data together indicate that ellagic acid induces the mitochondrial pathway of apoptosis associated with mitochondrial depolarization, cytochrome C release, and downstream caspase activation.

Ellagic acid does not directly affect mitochondria function in pancreatic cancer cells

To test the effect of ellagic acid on mitochondria we isolated functional mitochondria from MIA PaCa-2 cells and measured the effect of ellagic acid on mitochondria respiration, membrane potential, and cytochrome C release (Figure 4). The respiratory control ratio of isolated mitochondria with succinate as a respiratory substrate in all the experiments was greater than 4 in all the experiments. Ellagic acid affected neither oxygen consumption measured with Clark electrode (Figure 4A) nor $\Delta\psi$m measured with TPP^+ electrode (Figure 4B). The protonophore CCCP, which we used as a positive control, depolarized mitochondria (Figure 4B). In agreement with these results, ellagic acid did not increase cytochrome C release from isolated mitochondria into the incubation medium (Figure 4C).

We next assessed the possibility of ellagic acid's effect in permeabilized cells. For this purpose, MIA PaCa-2 cells were permeabilized with digitonin as described by Ohno *et al*[20]. Ellagic acid did not induce any discernable effect on the mitochondrial membrane potential in digitonin-permeabilized cells as measured with TPP^+ electrode (Figure 5B) or by using TMRM fluorescent dye (Figure 5C). CCCP was applied to completely dissipate $\Delta\psi$m (Figure 5B and C). Similarly, ellagic acid did not have any effect on mitochondrial respiration in permeabilized cells (Figure 5A).

The results in Figures 4 and 5 indicate that ellagic acid does not directly affect mitochondria functions in pancreatic cancer cells.

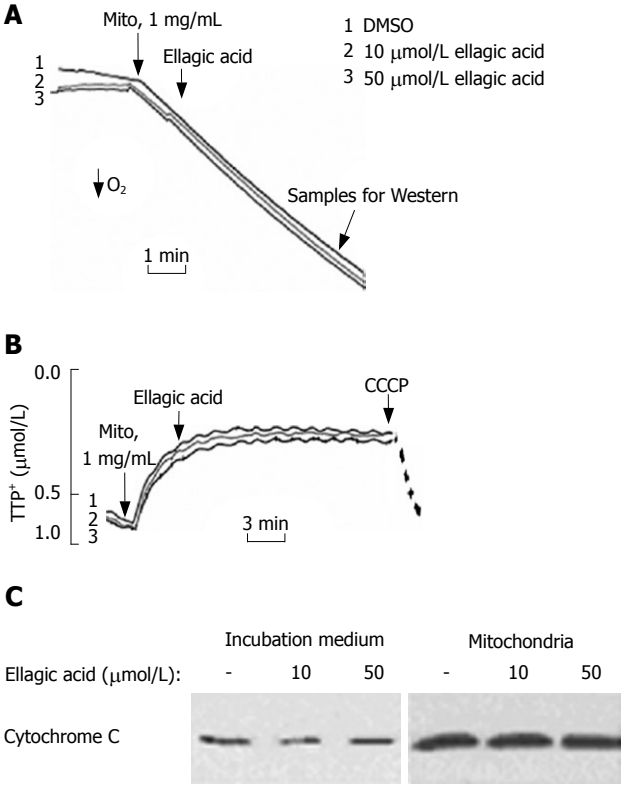

Figure 4 Ellagic acid does not directly affect the function of isolated mitochondria. Mitochondria were isolated from MIA PaCa-2 cells cultured in the absence of ellagic acid. **A**: Oxygen consumption was measured using a Clark-type electrode connected to an oxygen meter; **B**: Mitochondrial membrane potential ($\Delta\psi$m) was monitored in the presence of 2 μmol/L tetraphenyl phosphonium (TPP^+) using a TPP^+-sensitive electrode connected to an amplifier. Protonophore CCCP (10 μmol/L) was added to dissipate $\Delta\psi$m; **C**: Cytochrome C levels were measured in the incubation medium and the mitochondrial pellet by Western blot analysis. The results are representative of 3 independent experiments.

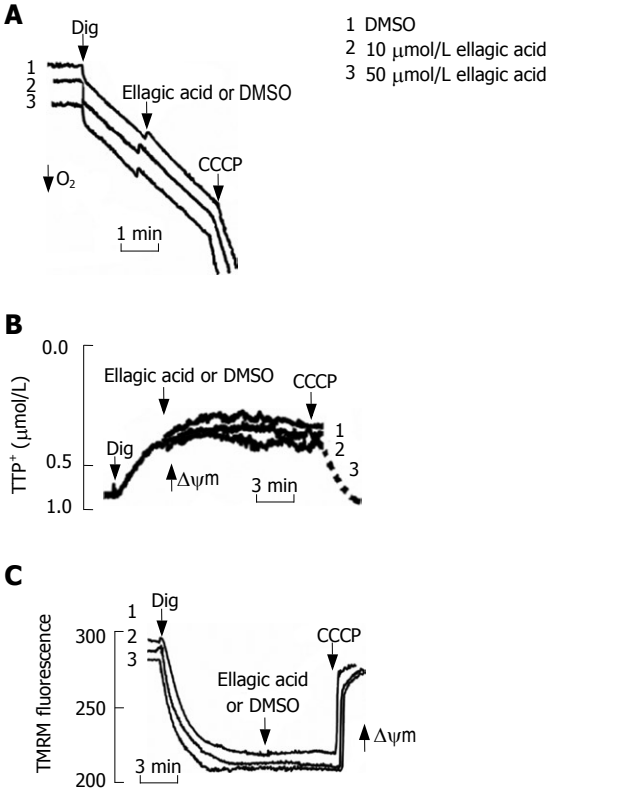

Figure 5 Ellagic acid does not directly affect mitochondria function inpermeabilized MIA PaCa-2 cells. MIA PaCa-2 cells were permeabilized with 0.001% digitonin. **A**: Oxygen consumption was measured using a Clark-type electrode connected to an oxygen meter; **B**: Changes in $\Delta\psi$m were monitored in the presence of 2 μmol/L tetraphenyl phosphonium (TPP^+) using a TPP^+-sensitive electrode connected to an amplifier; **C**: Changes in $\Delta\psi$m were monitored using the $\Delta\psi$m-sensitive fluorescent probe tetramethylrhodamine methyl ester (TMRM); changes in the fluorescence intensities were measured using the excitation at 543 nm and the emission at 578 nm. Protonophore CCCP (10 μmol/L) was added to dissipate $\Delta\psi$m.

Ellagic acid and NF-κB inhibition act through the same mechanism to stimulate apoptosis

We hypothesized that ellagic acid induced the mitochondrial pathway of apoptosis through blocking a key upstream prosurvival mechanisms, namely NF-κB. NF-κB is a key transcription factor, which is usually activated and has anti-apoptotic role in cancer cells including pancreatic cancer[4]. We found that ellagic acid dose-dependently decreased NF-κB binding activity in both MIA PaCa-2 and PANC-1 cell lines (Figure 6A).

We further showed that a pharmacologic inhibitor of NF-κB caffeic acid phenethyl ester (CAPE) stimulated apoptosis in PaCa cells, and that in the presence of CAPE there was no additional stimulation of apoptosis by ellagic acid (50 μmol/L) (Figure 6B). Further, transfection of MIA PaCa-2 cells with 4KBwt-pRL-TK plasmid completely blocked NF-κB transcriptional activity (Figure 6C), and at the same time stimulated apoptosis as measured by DNA fragmentation by > 5-fold (Figure 6D). The addition of ellagic acid to the transfected cells did not further increase DNA fragmentation (Figure 6D), confirming that ellagic acid causes apoptosis through inhibition of NF-κB.

DISCUSSION

Our study aimed to investigate the effect of ellagic acid on cell death and proliferation of pancreatic cancer cells and to determine the mechanism through which ellagic acid affects cell survival. We used the poorly differentiated MIA PaCa-2 and moderately differentiated PANC-1 human pancreatic carcinoma cell lines, which both display K-ras and *p53* mutations characteristic of pancreatic cancer.

We found that ellagic acid: (1) stimulated apoptosis and inhibited proliferation of pancreatic cancer cells; (2) activated the mitochondrial death pathway associated with loss of $\Delta\psi$m, cytochrome C release and caspase-3 activation without directly affecting the mitochondria; and (3) inhibited NF-κB activity in pancreatic cancer cells.

Mechanisms through which ellagic acid inhibits NF-κB remain to be investigated.

One mechanism through which NF-κB inhibits apoptosis is up-regulation of the anti-apoptotic Bcl-xL

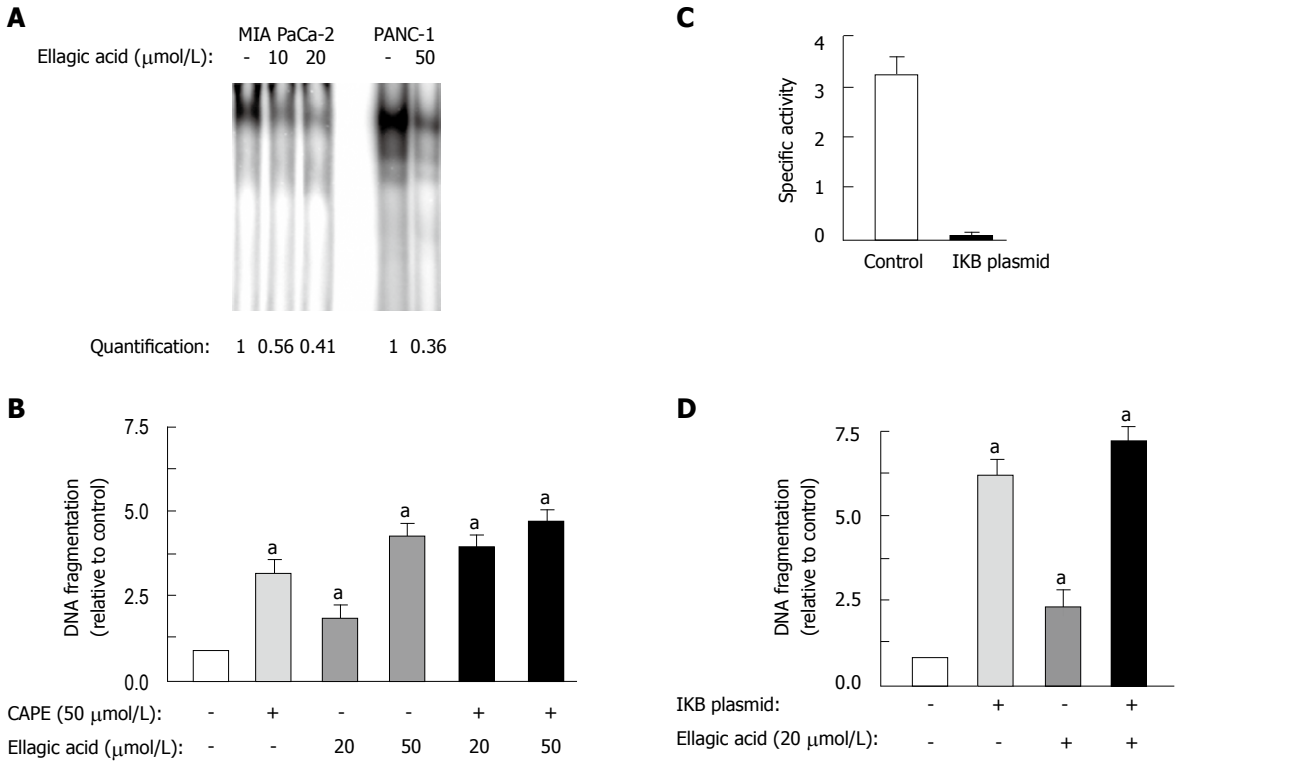

Figure 6 Ellagic acid decreases the activity of the transcription factor NF-κB. The effects of ellagic acid and pharmacological or molecular inhibition of NF-κB on apoptosis are not additive. MIA PaCa-2 (**A** and **B**) cells were cultured for 48 h in the presence or absence of indicated doses of ellagic acid. MIA PaCa-2 cells were transfected with 4KBwt-pRL-TK luciferase plasmid and pRL-TK luciferase as a control using the Nucleofector™ II electroporation system(**C** and **D**). **A**: NF-κB binding activity was measured as described in Experimental procedures; **B** and **D**: Internucleosomal DNA fragmentation was measured using the Cell Death Detection ELISA kit; **C**: NF-κB transcriptional activity was assessed using the dual-Luciferase Reporter Assay System assay. Results are representative of at least 3 independent experiments. Values are normalized to control (**B** and **D**). Values are mean ± SE (n = 3), $^aP < 0.05$ *vs* control.

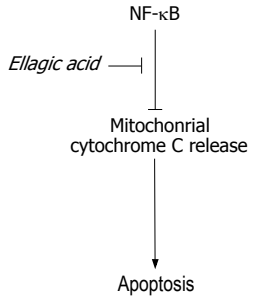

Figure 7 Representative scheme of the proposed mechanism of induction of apoptosis by ellagic acid.

protein. Bcl-xL, in turn, blocks mitochondrial permeabilization resulting in inhibition of cytochrome C release as well as preventing mitochondrial depolarization[21-23]. Our data indicate that ellagic acid decreases NF-κB acivity, leading to activation of the mitochondrial pro-apoptotic pathway and resulting in cytochrome C release and caspase activation. This scheme is depicted in Figure 7.

Our data indicate that ellagic acid inhibits proliferation of pancreatic cancer cells, similar to that in published data of other cells[21,24-28]. Ellagic acid completely abolished proliferation at high concentration, whereas it only increased apoptosis by 2.5-fold. The contribution of necrosis might account for the decreased proliferation.

Our results as well as the published data on the potent inhibitory effect of ellagic acid on the vascular endothelial growth factor receptor and platelet-derived growth factor receptor leading to the inhibition of their signaling[29], indicate that ellagic acid is a powerful phenolic compound with pro-apoptotic and anti-proliferation effects in cancer cells. Understanding the mechanism of action of ellagic acid will allow us to test the effect of the compound alone or in combination with other compounds on cancer growth and survival in an orthotopic model of pancreatic cancer[30].

In summary, the present study shows that ellagic acid induces apoptosis and decreases proliferation in pancreatic cancer cells. This phenolic compound stimulates mitochondrial depolarization, cytochrome C release and caspase activation. Ellagic acid has no direct effect on mitochondria. One mechanism by which it stimulates the mitochondrial death pathway is through inhibiting the transcription factor NF-κB, a major prosurvival factor in pancreatic cancer cells. There is an increasing interest in the use of natural products for cancer treatments. Our results suggest a potential therapeutic role for ellagic acid in the treatment of pancreatic cancer.

COMMENTS

Background

Pancreatic cancer is very resistant to radio- and chemo- therapies. Recently,

there is a growing interest in natural compounds for enhancing cancer prevention and treatment. Ellagic acid is a phenolic compound present in fruits and berries such as pomegranates, strawberries, raspberries and blackberries. It has anticarcinogenic, antioxidant and antifibrosis properties. In the present study the authors investigate the effect of ellagic acid on pancreatic cancer cell proliferation and resistance to death.

Research frontiers

The article focuses on the regulation of pancreatic cancer cell death by a phenolic compound, ellagic acid.

Innovations and breakthroughs

The present study shows that ellagic acid induces apoptosis and decreases proliferation in pancreatic cancer cells. It was shown for the first time that ellagic acid stimulates mitochondrial depolarization, cytochrome C release and caspase activation. Ellagic acid has no direct effect on mitochondria. One mechanism by which it stimulates the mitochondrial death pathway is through inhibiting transcription factor NF-κB, a major prosurvival factor in pancreatic cancer cells.

Applications

The data of this article demonstrate the anti-cancer properties of ellagic acid as well as its mechanism of action. By knowing the mechanism of action of ellagic acid, it can be used in combination with other drugs that target other pro-survival proteins to increase apoptosis in pancreatic cancer cells.

Peer review

This is a carefully performed study with novel findings that have the potential for therapeutic application in pancreatic cancer. It examines the effect of a naturally occurring polyphenolic compound, ellagic acid, on pancreatic cancer cell function, in particular, apoptosis and proliferation. The authors report that ellagic acid stimulates apoptosis of two pancreatic cancer cell lines and the decreased proliferation of ellagic acid-treated cells.

REFERENCES

1 **Giancotti FG,** Ruoslahti E. Integrin signaling. *Science* 1999; **285**: 1028-1032
2 **Parker SL,** Tong T, Bolden S, Wingo PA. Cancer statistics, 1997. *CA Cancer J Clin* 1997; **47**: 5-27
3 **Westphal S,** Kalthoff H. Apoptosis: targets in pancreatic cancer. *Mol Cancer* 2003; **2**: 6
4 **Gukovskaya AS,** Pandol SJ. Cell death pathways in pancreatitis and pancreatic cancer. *Pancreatology* 2004; **4**: 567-586
5 **Ayala GE,** Dai H, Ittmann M, Li R, Powell M, Frolov A, Wheeler TM, Thompson TC, Rowley D. Growth and survival mechanisms associated with perineural invasion in prostate cancer. *Cancer Res* 2004; **64**: 6082-6090
6 **Dutta J,** Fan Y, Gupta N, Fan G, Gelinas C. Current insights into the regulation of programmed cell death by NF-kappaB. *Oncogene* 2006; **25**: 6800-6816
7 **Li L,** Aggarwal BB, Shishodia S, Abbruzzese J, Kurzrock R. Nuclear factor-kappaB and IkappaB kinase are constitutively active in human pancreatic cells, and their down-regulation by curcumin (diferuloylmethane) is associated with the suppression of proliferation and the induction of apoptosis. *Cancer* 2004; **101**: 2351-2362
8 **Mukhtar H,** Das M, Khan WA, Wang ZY, Bik DP, Bickers DR. Exceptional activity of tannic acid among naturally occurring plant phenols in protecting against 7,12-dimethylb enz(a)anthracene-, benzo(a)pyrene-, 3-methylcholanthrene-, and N-methyl-N-nitrosourea-induced skin tumorigenesis in mice. *Cancer Res* 1988; **48**: 2361-2365
9 **Thresiamma KC,** Kuttan R. Inhibition of liver fibrosis by ellagic acid. *Indian J Physiol Pharmacol* 1996; **40**: 363-366
10 **Osawa T,** Ide A, Su JD, Namiki M. Inhibition of lipid peroxidation by ellagic acid. J. Agric. *Food Chem* 1987; **35**: 808-812
11 **Stoner GD,** Gupta A. Etiology and chemoprevention of esophageal squamous cell carcinoma. *Carcinogenesis* 2001; **22**: 1737-1746
12 **Larrosa M,** Tomas-Barberan FA, Espin JC. The dietary hydrolysable tannin punicalagin releases ellagic acid that induces apoptosis in human colon adenocarcinoma Caco-2 cells by using the mitochondrial pathway. *J Nutr Biochem* 2006; **17**: 611-625
13 **Vaquero EC,** Edderkaoui M, Nam KJ, Gukovsky I, Pandol SJ, Gukovskaya AS. Extracellular matrix proteins protect pancreatic cancer cells from death via mitochondrial and nonmitochondrial pathways. *Gastroenterology* 2003; **125**: 1188-1202
14 **Vaquero EC,** Edderkaoui M, Pandol SJ, Gukovsky I, Gukovskaya AS. Reactive oxygen species produced by NAD(P)H oxidase inhibit apoptosis in pancreatic cancer cells. *J Biol Chem* 2004; **279**: 34643-34654
15 **Edderkaoui M,** Hong P, Vaquero EC, Lee JK, Fischer L, Friess H, Buchler MW, Lerch MM, Pandol SJ, Gukovskaya AS. Extracellular matrix stimulates reactive oxygen species production and increases pancreatic cancer cell survival through 5-lipoxygenase and NADPH oxidase. *Am J Physiol Gastrointest Liver Physiol* 2005; **289**: G1137-G1147
16 **Edderkaoui M,** Hong P, Lee JK, Pandol SJ, Gukovskaya AS. Insulin-like growth factor-I receptor mediates the prosurvival effect of fibronectin. *J Biol Chem* 2007; **282**: 26646-26655
17 **Mareninova OA,** Sung KF, Hong P, Lugea A, Pandol SJ, Gukovsky I, Gukovskaya AS. Cell death in pancreatitis: caspases protect from necrotizing pancreatitis. *J Biol Chem* 2006; **281**: 3370-3381
18 **Gukovsky I,** Gukovskaya AS, Blinman TA, Zaninovic V, Pandol SJ. Early NF-kappaB activation is associated with hormone-induced pancreatitis. *Am J Physiol* 1998; **275**: G1402-G1414
19 **Labrecque L,** Lamy S, Chapus A, Mihoubi S, Durocher Y, Cass B, Bojanowski MW, Gingras D, Beliveau R. Combined inhibition of PDGF and VEGF receptors by ellagic acid, a dietary-derived phenolic compound. *Carcinogenesis* 2005; **26**: 821-826
20 **Chauvin C**, De Oliveira F, Ronot X, Mousseau M, Leverve X, Fontaine E. Rotenone inhibits the mitochondrial permeability transition-induced cell death in U937 and KB cells. *J Biol Chem* 2001; **276**: 41394-41398
21 **Shimizu S,** Narita M, Tsujimoto Y. Bcl-2 family proteins regulate the release of apoptogenic cytochrome c by the mitochondrial channel VDAC. *Nature* 1999; **399**: 483-487
22 **Dobbeling U.** Transcription factor profiling shows new ways towards new treatment options of cutaneous T cell lymphomas. *Curr Drug Discov Technol* 2007; **4**: 24-30
23 **Saile B,** Matthes N, El Armouche H, Neubauer K, Ramadori G. The bcl, NFkappaB and p53/p21WAF1 systems are involved in spontaneous apoptosis and in the anti-apoptotic effect of TGF-beta or TNF-alpha on activated hepatic stellate cells. *Eur J Cell Biol* 2001; **80**: 554-561
24 **Mertens-Talcott SU,** Talcott ST, Percival SS. Low concentrations of quercetin and ellagic acid synergistically influence proliferation, cytotoxicity and apoptosis in MOLT-4 human leukemia cells. *J Nutr* 2003; **133**: 2669-2674
25 **Mertens-Talcott SU,** Bomser JA, Romero C, Talcott ST, Percival SS. Ellagic acid potentiates the effect of quercetin on p21waf1/cip1, p53, and MAP-kinases without affecting intracellular generation of reactive oxygen species in vitro. *J Nutr* 2005; **135:** 609-614
26 **Chang WC,** Yu YM, Chiang SY, Tseng CY. Ellagic acid suppresses oxidised low-density lipoprotein-induced aortic smooth muscle cell proliferation: studies on the activation of extracellular signal-regulated kinase 1/2 and proliferating cell nuclear antigen expression. *Br J Nutr* 2008; **99**: 709-714
27 **Ross HA,** McDougall GJ, Stewart D. Antiproliferative

activity is predominantly associated with ellagitannins in raspberry extracts. *Phytochemistry* 2007; **68**: 218-228

28 **Losso JN,** Bansode RR, Trappey A 2nd, Bawadi HA, Truax R. In vitro anti-proliferative activities of ellagic acid. *J Nutr Biochem* 2004; **15**: 672-678

29 **Labrecque L,** Lamy S, Chapus A, Mihoubi S, Durocher Y, Cass B, Bojanowski MW, Gingras D, Beliveau R. Combined inhibition of PDGF and VEGF receptors by ellagic acid, a dietary-derived phenolic compound. *Carcinogenesis* 2005; **26**: 821-826

30 **Eibl G,** Reber HA, Wente MN, Hines OJ. The selective cyclooxygenase-2 inhibitor nimesulide induces apoptosis in pancreatic cancer cells independent of COX-2. *Pancreas* 2003; **26**: 33-41

S- Editor Li DL **L- Editor** Roberts SE **E- Editor** Lin YP

Online Submissions: wjg.wjgnet.com
wjg@wjgnet.com
doi:10.3748/wjg.14.3681

World J Gastroenterol 2008 June 21; 14(23): 3681-3692
World Journal of Gastroenterology ISSN 1007-9327
© 2008 The WJG Press. All rights reserved.

BASIC RESEARCH

Experimental treatment of pancreatic cancer with two novel histone deacetylase inhibitors

Martin Haefner, Thilo Bluethner, Manuel Niederhagen, Christian Moebius, Christian Wittekind, Joachim Mossner, Karel Caca, Marcus Wiedmann

Martin Haefner, Thilo Bluethner, Joachim Mossner, Marcus Wiedmann, Department of Internal Medicine II, University of Leipzig, Philipp-Rosenthal-Str. 27, Leipzig 04103, Germany
Manuel Niederhagen, Christian Wittekind, Institute of Pathology, University of Leipzig, Liebigstr. 26, Leipzig 04103, Germany
Christian Moebius, Department of Surgery II, University of Leipzig, Liebigstrasse 20a, Leipzig 04103, Germany
Karel Caca, Department of Internal Medicine I, Klinikum Ludwigsburg, Posilipostr. 4, Ludwigsburg 71640, Germany
Author contributions: Wiedmann M and Caca K designed research; Haefner M, Bluethner T and Niederhagen M performed research; Wittekind C contributed analytic tools; Moebius C and Mossner J analyzed data and corrected the manuscript; and Wiedmann M wrote the paper.
Supported by Novartis, No. 934000-258
Correspondence to: Dr. Marcus Wiedmann, Department of Internal Medicine II, University of Leipzig, Philipp-Rosenthal-Str. 27, Leipzig 04103,
Germany. wiedm@medizin.uni-leipzig.de
Telephone: +49-341-9712230 Fax: +49-341-9712239
Received: January 25, 2008 Revised: May 4, 2008
Accepted: May 11, 2008
Published online: June 21, 2008

Abstract

AIM: To investigate *in vitro* and *in vivo* treatment with histone deacetylase inhibitors NVP-LAQ824 and NVP-LBH589 in pancreatic cancer.

METHODS: Cell-growth inhibition by NVP-LAQ824 and NVP-LBH589 was studied *in vitro* in 8 human pancreatic cancer cell lines using the 3-(4,5-dimethylthiazole-2-yl)-2,5-diphenyltetrazolium bromide (MTT) assay. In addition, the anti-tumoral effect of NVP-LBH589 was studied in a chimeric mouse model. Anti-tumoral activity of the drugs was assessed by immunoblotting for $p21^{WAF-1}$, acH4, cell cycle analysis, TUNEL assay, and immunohistochemistry for MIB-1.

RESULTS: *In vitro* treatment with both compounds significantly suppressed the growth of all cancer cell lines and was associated with hyperacetylation of nucleosomal histone H4, increased expression of $p21^{WAF-1}$, cell cycle arrest at G2/M-checkpoint, and increased apoptosis. *In vivo*, NVP-LBH589 alone significantly reduced tumor mass and potentiated the efficacy of gemcitabine. Further analysis of the tumor specimens revealed slightly increased apoptosis and no significant reduction of cell proliferation.

CONCLUSION: Our findings suggest that NVP-LBH589 and NVP-LAQ824 are active against human pancreatic cancer, although the precise mechanism of *in vivo* drug action is not yet completely understood. Therefore, further preclinical and clinical studies for the treatment of pancreatic cancer are recommended.

© 2008 The WJG Press. All rights reserved.

Key words: Histone deacetylase inhibitor; Pancreatic cancer; NVP-LAQ824; NVP-LBH589

Peer reviewer: Michael A Fink, MBBS FRACS, Department of Surgery, The University of Melbourne, Austin Hospital, Melbourne, Victoria 3084, Australia

Haefner M, Bluethner T, Niederhagen M, Moebius C, Wittekind C, Mossner J, Caca K, Wiedmann M. Experimental treatment of pancreatic cancer with two novel histone deacetylase inhibitors. *World J Gastroenterol* 2008; 14(23): 3681-3692 Available from: URL: http://www.wjgnet.com/1007-9327/14/3681.asp DOI: http://dx.doi.org/10.3748/wjg.14.3681

INTRODUCTION

Pancreatic cancer is the fifth to sixth leading cause of cancer death in Europe and the fourth leading cause of cancer death in the USA[1]. The lethality of this malignancy is demonstrated by the fact that the annual incidence is approximately equal to the annual deaths. Unfortunately, carcinoma of the pancreas is increasing in incidence, and its risk factors are poorly understood. Although surgical resection remains the only chance for cure, less than 10% of patients diagnosed with pancreatic cancer are eligible for curative (R0) resection, since up to 90% of patients will present with locally advanced or metastatic disease. In addition, there is a high rate of relapse, even in patients who receive adjuvant therapy[2]. A recent evaluation of the Finnish Cancer Registry, which recorded 4922 pancreatic cancer patients between 1990 and 1996, detected only 89 five year survivors (1.8%)[3]. Metastatic cancer tends to be a rapidly progressing disease, often accompanied by significant weight loss, abdominal pain, nausea, and/or depression. For decades, 5-fluorouracil (5-FU) was the most widely used chemotherapeutic agent in

metastatic pancreatic cancer. Today gemcitabine, a nucleoside analogue that is incorporated into replicating DNA resulting in premature chain termination and apoptosis, is the current standard of care[4]. In a phase Ⅲ approval study 126 patients with metastatic disease who had not received prior chemotherapy were randomized to weekly gemcitabine (n = 63) or weekly bolus 5-FU (n = 63)[5]. Overall survival in patients treated with gemcitabine was significantly improved compared with patients treated with 5-FU; However, there was no convincing gain in median survival time (median survival 5.7 mo *vs* 4.4 mo, P = 0.0025). The primary efficacy measure in this study was clinical benefit response, a composite of patient-oriented parameters including pain, Karnofsky performance status, daily analgesic usage, and body weight. Clinical benefit was experienced in 23.8% of patients treated with gemcitabine compared with only 4.5% of the patients treated with 5-FU (P = 0.022). Fixed-dose-rate (FDR) gemcitabine (1500 mg/m^2 at 10 mg/m^2 per minute) has also been investigated by Tempero *et al* in comparison to 2200 mg/m^2 gemcitabine over 30 min[6]. Although median survival time improved from 5.0 mo in the standard arm to 8.0 mo in the FDR arm (P = 0.013), grade 3 and 4 toxicity increased significantly. Many combination regimens with gemcitabine have been tested in open-label phase Ⅱ or Ⅲ studies with higher response and progression-free survival rates, but no definitive benefit in overall survival, with the only exception being a combination with capecitabine[4,7]. As little progress has been made in the past decade, new strategies should focus on targeting cancer cells at the molecular level. Recently, in a randomized phase Ⅲ placebo-controlled trial, Moore *et al* demonstrated that combining gemcitabine with EGFR inhibitor erlotinib was associated with a modest, but statistically significant survival benefit of 15 d[8]. In contrast, a recent phase Ⅲ trial (SWOG S0205 study) failed to demonstrate a clinically significant advantage of the addition of cetuximab, an anti-EGFR monoclonal antibody, to gemcitabine for overall survival, progression free survival and response[9]. Another approach is targeting VEGF as a key player in tumor growth and resistance to therapy. In a phase Ⅱ trial with 52 patients, a combination of VEGF inhibitor bevacizumab and gemcitabine yielded a 21% response rate and a median survival of 8.8 mo[10]. These data led CALGB to conduct a randomized, double-blind, placebo-controlled, phase Ⅲ trial (CALGB 80303). However, the addition of bevacizumab to gemcitabine did not improve survival[11]. Inhibiting histone deacetylases (HDACs), which regulate interactions between histones and DNA together with histone acetylases (HATs) as counter-players, may be another promising molecular target. Clinical studies published so far have shown that HDAC inhibitors (HDACIs) can be administered safely in humans and that treatment of some cancers with such agents seems to be beneficial[12,13]. NVP-LAQ824 and NVP-LBH589 are new chemical entities belonging to a structurally novel class of cinnamic hydroxamic acid compounds[14-17], which are currently in phase Ⅰ clinical evaluation in advanced refractory solid tumors and hematologic malignancies[18-22]. However, little is known about their potential efficacy in pancreatic cancer. Therefore, the objectives of the current study were to investigate the efficacy of *in vitro* and *in vivo* treatment with the novel pan-HDAC inhibitors NVP-LAQ824 and NVP-LBH589 and to evaluate effects of combination with gemcitabine.

MATERIALS AND METHODS

Materials

Eight human pancreatic cancer cell lines (Hs766T, As-PC-1, CFPAC-1, Capan-2, Panc-1, MiaPaca-2, HPAF-2 and L3.6pl) were examined[23-27]. All cell lines were cultured in a 37℃ incubator with 50-100 mL/L CO_2 in appropriate media. The HDACIs NVP-LAQ824 and NVP-LBH589 were provided by Novartis (Basel, Switzerland) and dissolved in dimethyl sulfoxide (DMSO) (10 mmol/L stock). Hoechst dye, sodium butyrate and monoclonal (mc) β-actin antibody were purchased from Sigma (Sigma-Aldrich Chemie GmbH Munich, Germany), mc p21$^{WAF-1/Cip-1}$ from Cell Signaling (Cell Signaling Technology, Beverly, USA), mc acH4 antibody from Upstate (Upstate Biotechnology, Lake Placid, USA), mc MIB-1 antibody from Dako (Glostrub, Denmark), and gemcitabine (diluted in D5W and 50 mL/L DMSO) from our hospital pharmacy. Six to eight-wk-old female athymic NMRI nude mice were supplied by Taconic (Taconic Europe, Ry, Denmark) and held under pathogen-free conditions. Humane care was administered, and study protocols complied with the institutional guidelines.

Inhibition of cell growth

Cytotoxic effects of both drugs were determined by the 3-(4,5-dimethylthiazole-2-yl)-2,5-diphenyltetrazolium bromide (MTT, Sigma-Aldrich Chemie GmbH Munich, Germany) assay. 1-5 × 10^3 cells were seeded in triplicate in 96-well plates (100 μL/well) and allowed to attach overnight. The medium was then replaced with media (100 μL) containing the designated drug or vehicle control (50 mL/L DMSO in D5W) followed by an incubation for 3 or 6 d. For the 6 d experiment, medium was changed after 3 d. Three hours before the end of the incubation period, 10 μL of PBS containing MTT (5 g/L) was added to each well. Following this, the medium was removed. The precipitate was then resuspended in 100 μL of lysis buffer (DMSO, 100 g/L SDS). Absorbance was measured on a plate reader at 590 nm using a reference wavelength of 630 nm. Each experiment was performed in triplicate.

Immunoblotting

Cell culture monolayers were washed twice with ice-cold PBS and lysed with RIPA-buffer containing Tris-HCl (50 mmol/L, pH 7.4), NP-40 (10 g/L), sodium-desoxycholate (2.5 g/L), NaCl (150 mmol/L), EDTA (1 mmol/L), sodium-orthovanadate (1 mmol/L), and

one tablet of complete mini-EDTA-free protease inhibitor cocktail (Boehringer, Mannheim, Germany, in 10 mL buffer). Histones for anti-acH4 immunoblotting were isolated by acid extraction [cells were lysed in ice-cold lysis buffer (HEPES 10 mmol/L; pH 7.9), $MgCl_2$ (1.5 mmol/L), KCl (10 mmol/L), DTT (0.5 mmol/L), PMSF (1.5 mmol/L), and additional protease inhibitor]. One molar HCl was added to a final concentration of 0.2 mol/L, followed by an incubation on ice for 30 min and centrifugation at 13000 r/min for 10 min. The supernatant was retained and dialysed against 200 mL of 0.2 mol/L acetic acid twice for 1 h and against 200 mL H_2O overnight). Proteins were quantified by Bradford protein assay (Bio-Rad, Munich, Germany) and stored at -80℃. 50 μg of cell or tissue lysates were separated on SDS-polyacrylamide gels and electroblotted onto polyvinylidene difluoride membranes (Amersham Pharmacia Biotech, Freiburg, Germany). Membranes were then incubated in blocking solution [50 g/L dry milk in 10 mmol/L Tris-HCl, 140 mmol/L NaCl, 1 g/L Tween-20 (TBS-T)], followed by incubation with the primary antibody at 4℃ overnight (50 g/L BSA in TBS-T). The membranes were then washed in TBS-T and incubated with horseradish peroxidase (HRPO)-conjugated secondary antibodies for 1 h at room temperature. Antibody detection was performed with an enhanced chemoluminescence reaction (SuperSignal West Dura, Pierce, Rockford, USA).

Cell cycle analysis

Cells were seeded in T-25 flasks (2×10^5), treated with various concentrations of NVP-LAQ824 or NVP-LBH589 or vehicle control (50 mL/L DMSO in D5W) for 72 h, washed with PBS, trypsinized, centrifuged, and fixed in 750 mL/L ice-cold ethanol-phosphate-buffered saline containing 10 g/L EDTA. DNA was labeled with 100 mL/L propidium iodide. Cells were sorted by FACScan analysis, and cell cycle profiles were determined using ModFitLT V2.0 software (Becton Dickinson, San Diego, USA). Each experiment was performed in triplicate.

Animal studies

Tumors were induced by injecting 5×10^6 HPAF-2 or L3.6pl cells in 200 μL PBS sc into the flank region of NMRI nude mice. Treatment was started when an average tumor volume of 150 mm^3 was reached (usually after 2 wk). The verum groups received either NVP-LBH589 (25 mg/kg, 5 × weekly) or gemcitabine (5 mg/kg, 1 × weekly) or a combination of both (NVP-LBH589 at 25 mg/kg, 5 × weekly plus gemcitabine at 5 mg/kg, 1 × weekly) ip, whereas the control group received placebo (carrier solution 50 mL/L DMSO in D5W) only. Treatment was continued for 28 consecutive days, tumors were measured daily with a Vernier caliper and tumor volumes were calculated using the formula tumor volume = $0.5 \times L \times W^2$, where L represents the length and W the width of the tumor. When treatment was finished, animals were sacrificed and tumors excised and weighed.

TUNEL POD test

Terminal deoxynucleotidyl transferase-mediated dUTP nick end labeling (*in situ* cell death detection kit, POD) was used to detect apoptosis in paraffin sections from mouse tumor tissue. TUNEL was carried out following the manufacturer's instructions (Roche, Penzberg, Germany) as previously described[28]. Apoptotic cells (red) were counted under a light microscope after fluorescence signal conversion using peroxidase-conjugated antibody and peroxidase substrate (DAB, Roche, Penzberg, Germany). The number of positive cells was counted by an experienced pathologist (M.N.) in a total of 8 high power fields (HPFs) and expressed as mean percentage of total cells in these fields of the tumor. Necrotic tumor cells were excluded from the cell count.

Immunohistochemical staining

For MIB-1 staining, we used paraffin sections following a protocol that has been described elsewhere[29]. The number of positive cells was counted by an experienced pathologist (M.N.) in a total of 4 HPFs and expressed as mean percentage of total cells in these fields of the tumor.

Statistical analysis

Statistical calculations were performed using SPSS, version 10.0 (SPSS Inc., Chicago, USA). Numeric data were presented as mean value with SD or SEM. Inter-group comparisons were performed with the Student *t*-test and ANOVA. $P < 0.05$ was considered significant.

RESULTS

Inhibition of cell growth

After 3 d of incubation, 7 of 8 tested cell lines were sensitive to NVP-LAQ824 (mean IC_{50} (3 d) = 0.18 ± 0.24 μmol/L) and even more to NVP-LBH589 (mean IC_{50} (3 d) = 0.09 ± 0.14 μmol/L). Only cell line Capan-2 demonstrated an IC_{50} (3 d) value > 1 μmol/L for both compounds. Inhibition of cell growth was more pronounced if incubation time was extended to 6 d with a mean IC_{50} value of 0.06 ± 0.07 μmol/L for NVP-LAQ824 and 0.03 ± 0.02 μmol/L for NVP-LBH589. After 6 d of incubation, cell line Capan-2 also became responsive (Figure 1 and Table 1). In addition, DMSO alone (the solvent for NVP-LAQ824 and NVP-LBH589) had no influence on cell growth (data not shown).

Immunoblotting

Treatment of cell lines HPAF-2 and L3.6pl with 0.1 μmol/L NVP-LAQ824 or 0.1 μmol/L NVP-LBH589 for 24 h resulted in acetylation of histone H4 (Figure 2A and B). The same treatment caused an induction of $p21^{WAF-1/CIP-1}$ expression (Figure 2C and D). A dose increase to 0.2 μmol/L NVP-LAQ824 or NVP-LBH589 corresponded with an increase in histone H4 acetylation and $p21^{WAF-1/CIP-1}$ levels. Histone H4 acetylation was higher in treated HPAF-2 than L3.6pl cells, whereas $p21^{WAF-1/CIP-1}$ expression was slightly higher in treated L3.6pl cells.

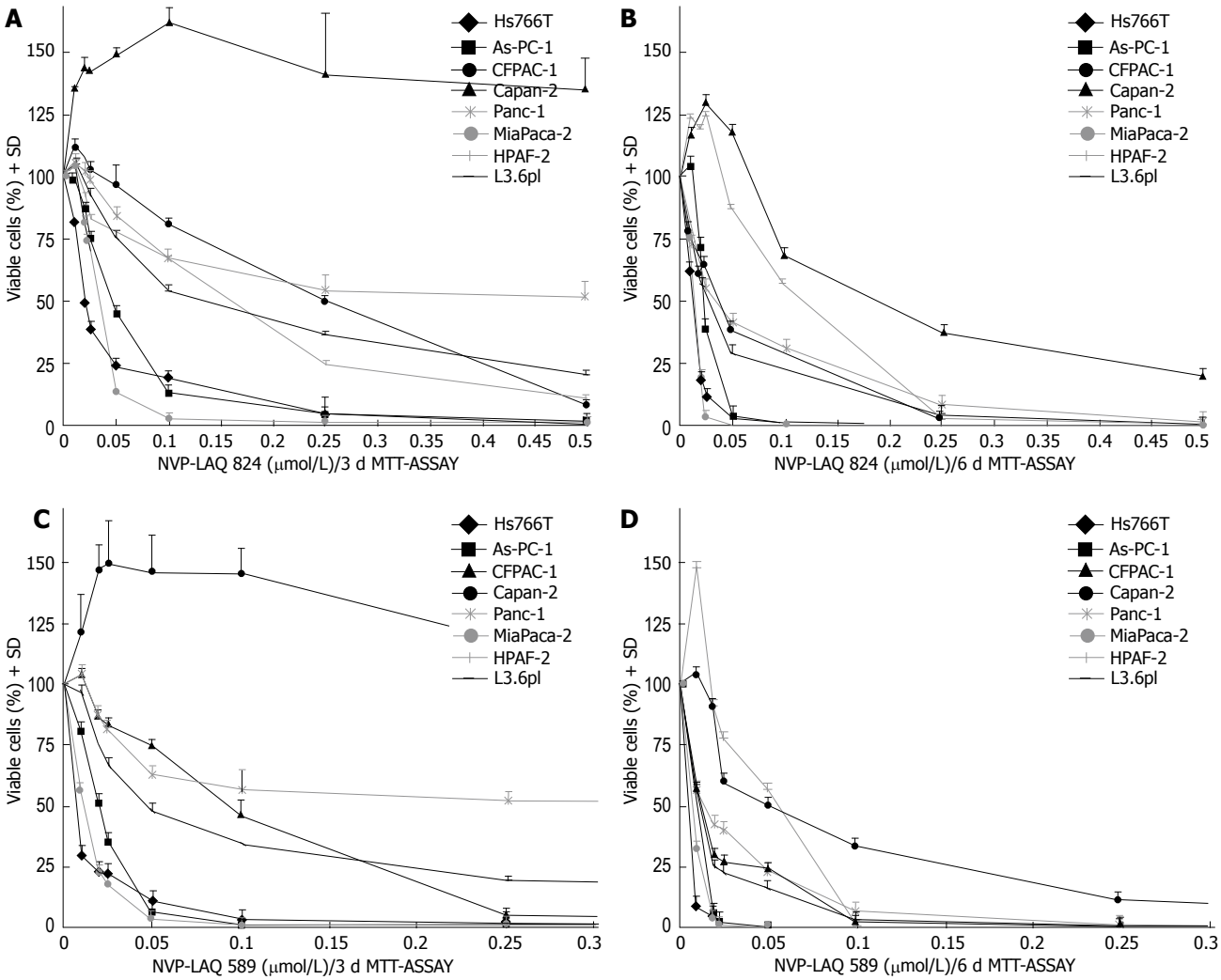

Figure 1 *In vitro* treatment of pancreatic cancer with NVP-LAQ824 and NVP-LBH589 (MTT assay). **A**: 3-d incubation with NVP-LAQ824 (n = 3); **B**: 6-d incubation with NVP-LAQ824 (n = 3); **C**: 3-d incubation with NVP-LBH589 (n = 3); **D**: 6-d incubation with NVP-LBH589 (n = 3).

Table 1 Inhibition of cell growth by NVP-LAQ824 and NVP-LBH589

Cell line	IC_{50} (μmol/L)			
	NVP-LAQ824		NVP-LAQ589	
	3 d	6 d	3 d	6 d
MiaPaca-2	0.03	0.01	0.01	0.01
As-PC-1	0.05	0.02	0.02	0.01
Panc-1	0.70	0.04	0.40	0.02
Hs766T	0.02	0.01	0.01	0.01
CFPAC-1	0.25	0.04	0.09	0.02
HPAF-2	0.16	0.12	0.07	0.06
L3.6pl	0.05	0.02	0.03	0.04
Capan-2	> 1	0.19	> 1	0.05

Cell cycle analysis

Treatment of cell lines HPAF-2 and L3.6pl with 0.1 μmol/L NVP-LAQ824 or NVP-LBH589 for 72 h resulted in G2/M arrest. This arrest was, in general, more pronounced if the dose of NVP-LAQ824 or NVP-LBH589 was increased to 0.2 μmol/L. Percentual G2/M arrest was lower for 0.2 μmol/L than 0.1 μmol/L only for the treatment of HPAF-2 cells with NVP-LBH589. This phenomenon may derive from the fact, that at the same time the sub-G1-peak was much higher for 0.2 μmol/L. For both concentrations, the effect of NVP-LBH589 was stronger than the effect of NVP-LAQ824 with the aforementioned exception of 0.2 μmol/L NVP-LBH589 in HPAF-2 cells (Figure 3). In addition, incubation with NVP-LAQ824 or NVP-LBH589 for 72 h resulted in a dose-dependent significant increase in the sub-G1-peak, which was higher for NVP-LBH589 than NVP-LAQ824 and higher in L3.6pl than in HPAF-2 cells. This result correlated well with the fact that IC_{50} values in the cell growth inhibition experiment (Figure 1) were lower for L3.6pl in comparison to HPAF-2 cells.

Chimeric mouse model

Tumors were induced in nude mice by subcutaneous injection of HPAF-2 and L3.6pl cells. These cell lines were selected because they had the best growth capability in our nude mice in a pilot study. Treatment of mice consisted of ip injections with NVP-LBH589, gemcitabine, NVP-LBH589 plus gemcitabine (COMBO) or placebo (50 mL/L DMSO in D5W). Three days after commencement of NVP-LBH589 or COMBO treatment, HPAF-2 cell tumors showed a signifi-

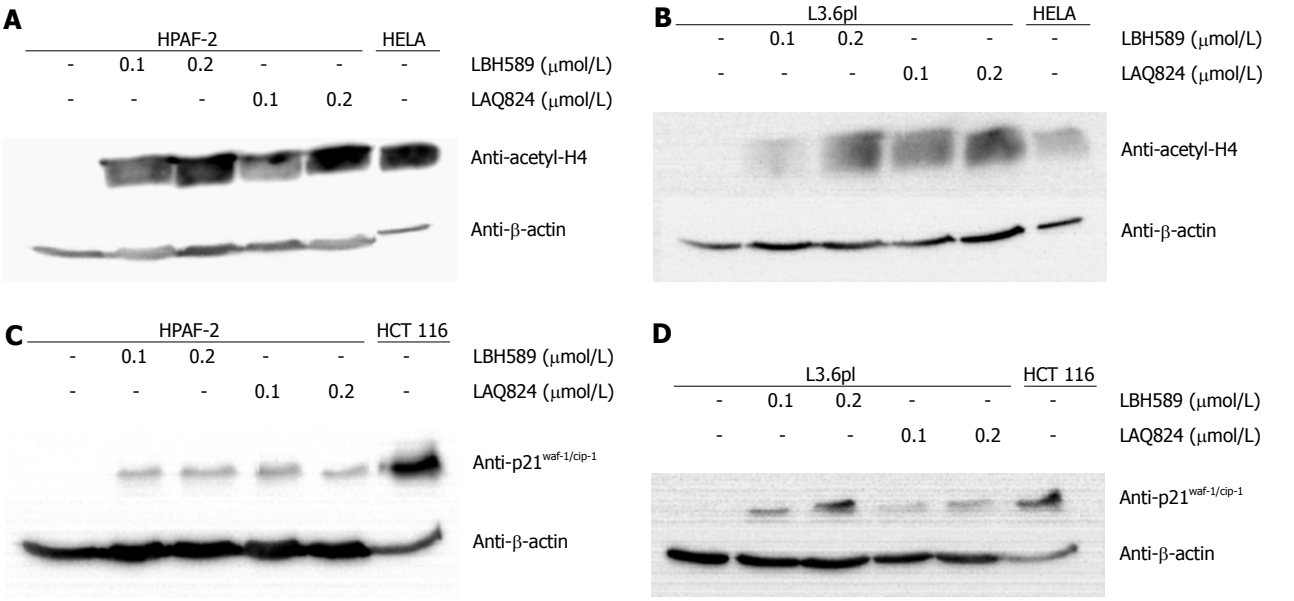

Figure 2 Mechanism of drug action after *in vitro* treatment with NVP-LAQ824 and NVP-LBH589 for 24 h. **A** and **B**: Acetylation of histone H4. Protein extracts from HELA cells that were treated with 5 mmol/L sodium butyrate served as positive controls; **C** and **D**: $p21^{WAF-1/CIP-1}$ expression. Cell lysate from HCT 116 colon cancer cells served as positive control; **A**-**D**: Staining with β-actin antibody confirmed equal protein loading.

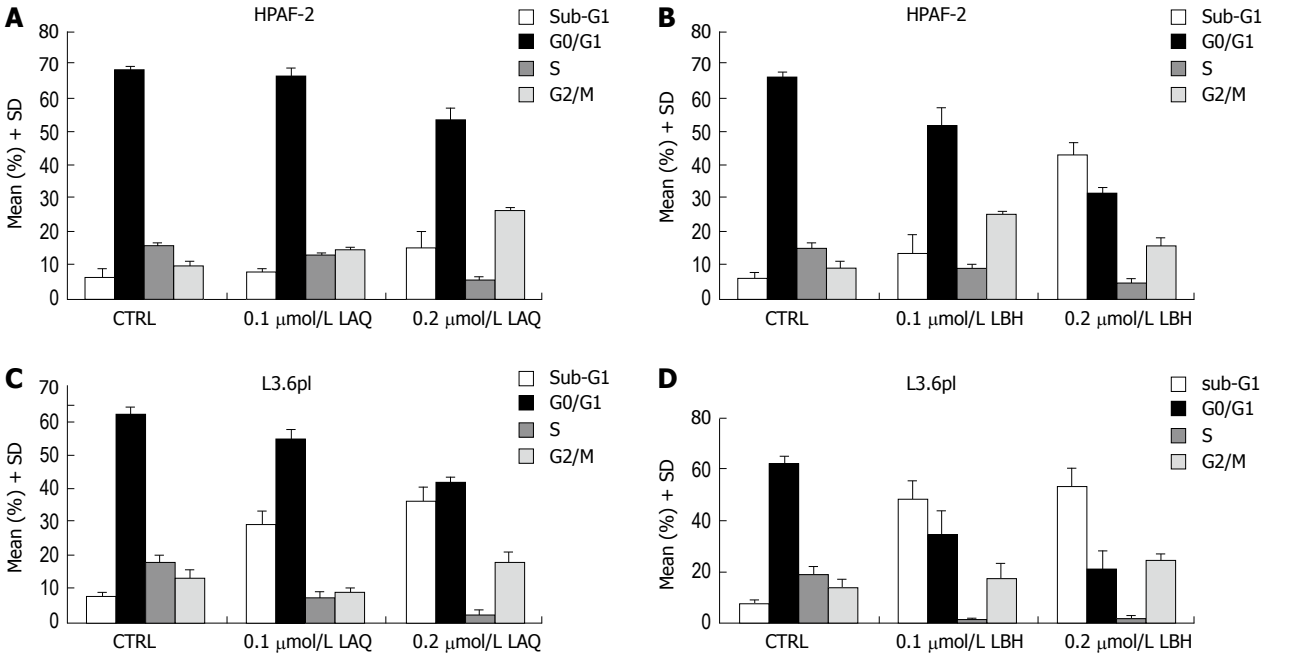

Figure 3 Cell cycle analysis. **A**: Treatment of cell line HPAF-2 with 0.1 or 0.2 μmol/L NVP-LAQ824 for 72 h (n = 3); **B**: Treatment of cell line HPAF-2 with 0.1 or 0.2 μmol/L NVP-LBH589 for 72 h (n = 3); **C**: Treatment of cell line L3.6pl with 0.1 or 0.2 μmol/L NVP-LAQ824 for 72 h (n = 3); **D**: Treatment of cell line L3.6pl with 0.1 or 0.2 μmol/L NVP-LBH589 for 72 h (n = 3).

cantly reduced volume in comparison to control (n = 7 for each group, $P < 0.05$). Treatment of mice with gemcitabine alone resulted in a significant reduction of tumor volume compared to control after 4 d from commencement of treatment. These differences were maintained until the end of the experiment. COMBO therapy was significantly more efficient than gemcitabine treatment alone on treatment day 7, 8, 13, 14, 15, and 16 and was significantly more efficient than NVP-LBH589 therapy alone on treatment day 7 and 14 ($P < 0.05$, Figure 4A). Treatment of L3.6pl tumors with NVP-LBH589 or COMBO resulted in a significantly reduced volume in comparison to control after 4 d ($P < 0.05$) and 3 d ($P < 0.05$) from commencement of therapy, respectively (n = 7 for each group). These differences were also maintained until the end of the experiment. Treatment of mice with gemcitabine alone resulted in a significant reduction of tumor volume compared to control at treatment day 12, 13, 16, 17, and 18 ($P < 0.05$). COMBO therapy was significantly more

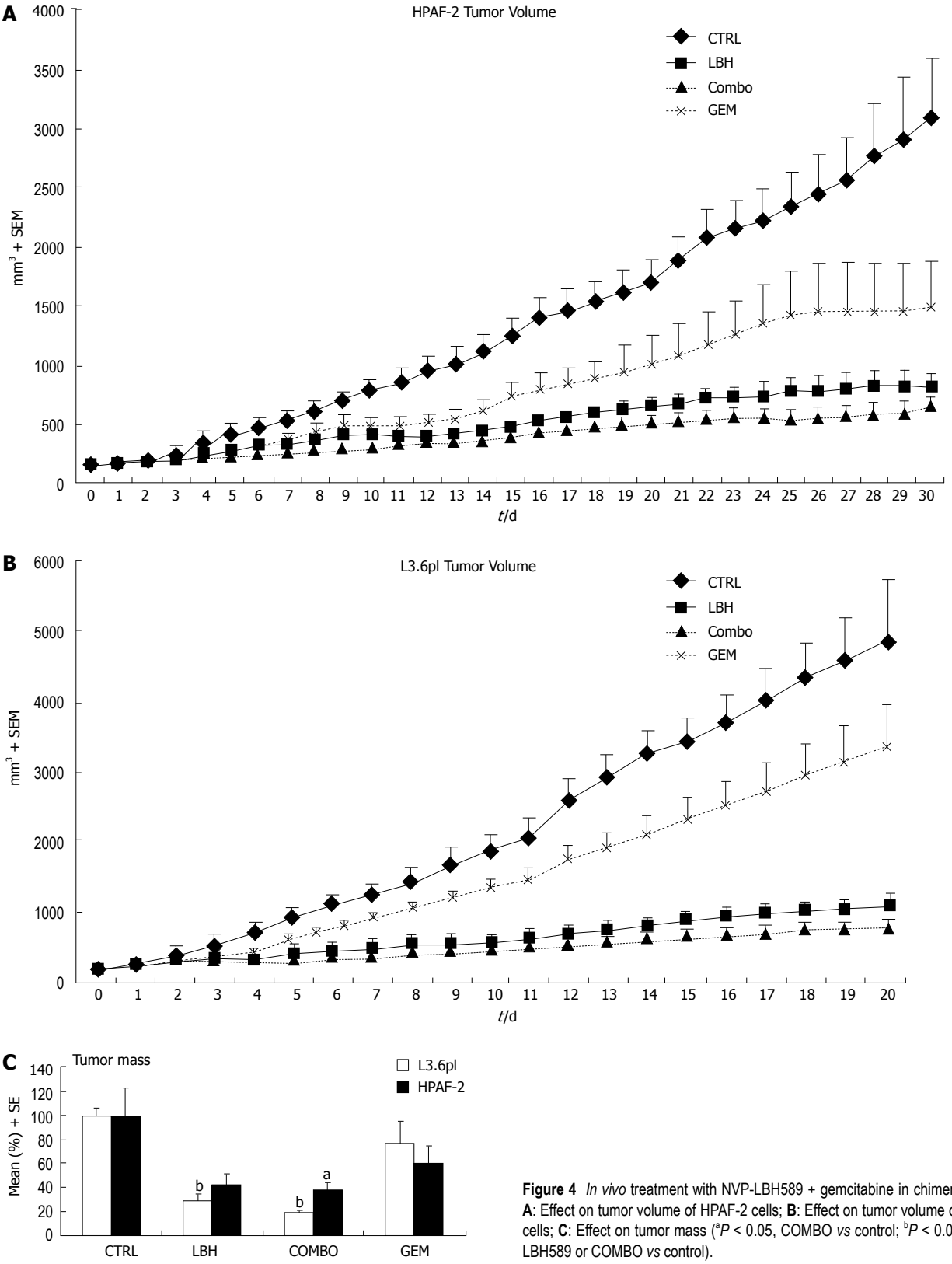

Figure 4 *In vivo* treatment with NVP-LBH589 + gemcitabine in chimeric mice. **A**: Effect on tumor volume of HPAF-2 cells; **B**: Effect on tumor volume of L3.6pl cells; **C**: Effect on tumor mass ($^{a}P < 0.05$, COMBO *vs* control; $^{b}P < 0.01$, NVP-LBH589 or COMBO *vs* control).

efficient than gemcitabine treatment alone on treatment day 3-20 and was significantly more efficient than NVP-LBH589 therapy alone on treatment day 3 ($P < 0.05$). NVP-LBH589 therapy was significantly more efficient than gemcitabine treatment alone on treatment day 5-20 ($P < 0.05$, Figure 4B). At the end of the experiment after 30 d, tumor mass in HPAF-2 cells bearing mice was significantly diminished as compared to placebo after treatment with COMBO (-63%, $P < 0.05$). In contrast, treatment of mice with gemcitabine (-24%, $P = 0.45$) or NVP-LBH589 alone (-58%, $P = 0.056$) did not result in any significant reduction of tumor mass as compared to control (Figure 4C). L3.6pl cell tumor mass in mice was significantly diminished after treatment

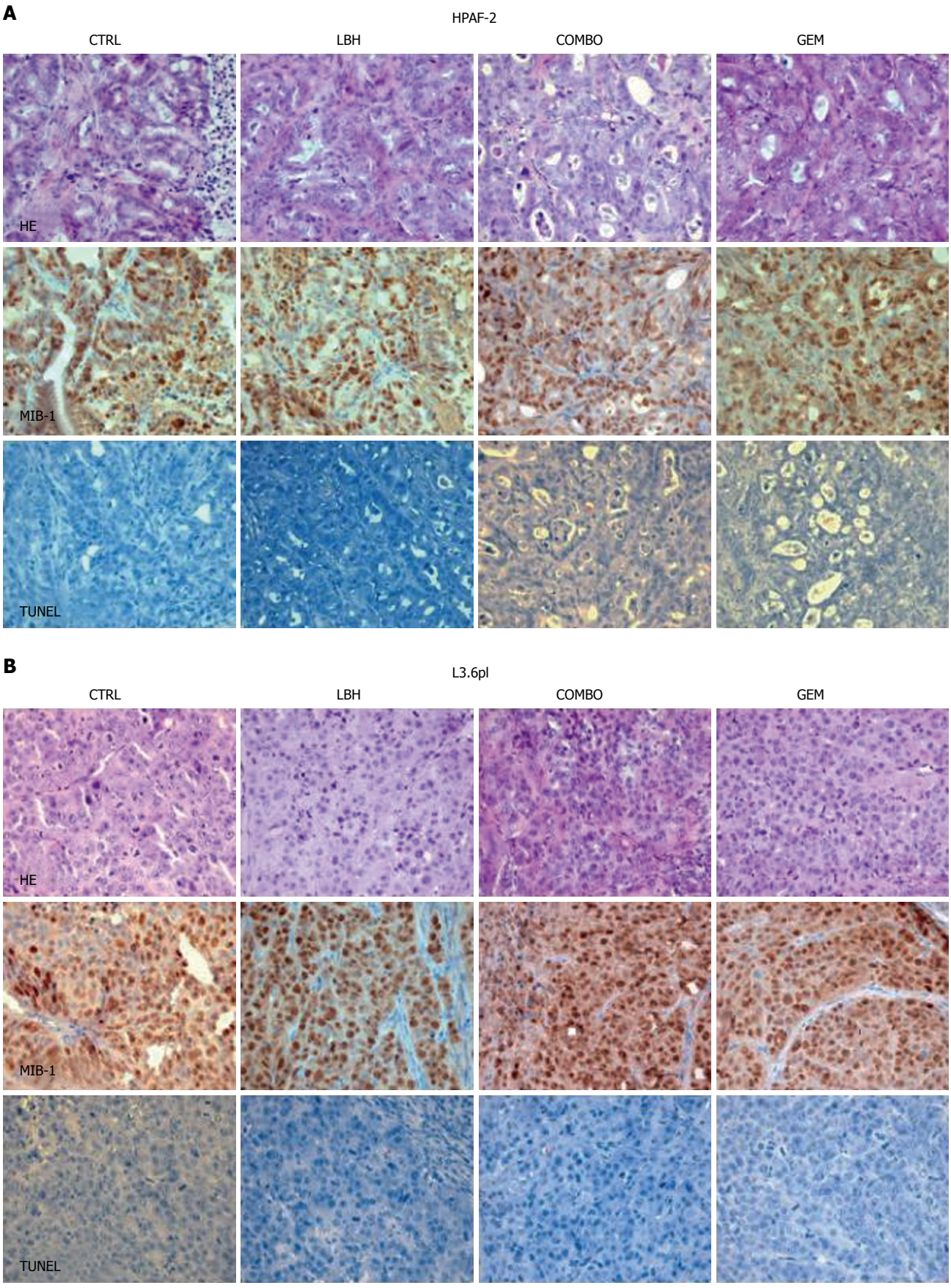

Figure 5 Hematoxylin-eosin (HE), MIB-1 (proliferation marker) and TUNEL (apoptosis marker) staining of mouse tumors (SABC, x 40). **A**: Cell line HPAF-2; **B**: Cell line L3.6pl.

with either NVP-LBH589 (-70%, $P < 0.01$) or COMBO (-81%, $P < 0.01$), but not with gemcitabine (-24%, $P = 0.28$),

Table 2 MIB-1- and TUNEL-staining of mouse tumor specimens

Mean in %	HPAF-2		L3.6pl	
	MIB-1	Apoptosis	MIB-1	Apoptosis
CTRL	67.5	1.3	61.3	0
GEM	66.3	2.5	70	0
LBH	51.3	3.8	76.3	6.3
COMBO	55.0	3.8	78.8	3.8

respectively. In addition, the combination of NVP-LBH589 with gemcitabine was more effective at tumor mass reduction in comparison to gemcitabine alone ($P < 0.05$). The L3.6pl animal experiment was stopped at day 21 for ethical reasons, since animals suffered from tumor burden. Regarding side effects of the different drugs used in HPAF-2 cell tumor bearing mice, weight loss was 2%, 0%, 13%, and 6%, in the control, gemcitabine, NVP-LBH589, and COMBO groups. There was a statistically significant difference between the control and NVP-LBH589 group ($P < 0.05$) and between the gemcitabine and NVP-LBH589 group ($P < 0.01$). Concerning side effects of the different drugs used in L3.6pl cell tumor bearing mice, weight loss was 23%, 17%, 12%, and 25%, in the control, gemcitabine, NVP-LBH589, and COMBO groups. There was a statistically significant difference between the control and NVP-LBH589 group ($P < 0.05$).

In order to assess the anti-tumoral drug mechanism, paraffin sections of mouse tumors were stained with hematoxylin-eosin (H&E), MIB-1 (proliferation marker) and TUNEL (apoptosis marker) (Figure 5). Treatment with NVP-LBH589 and COMBO slightly reduced proliferation (reduced MIB-1 staining) and slightly induced apoptosis (increased TUNEL-staining) in HPAF-2 cell bearing mice, whereas proliferation was not decreased and apoptosis only slightly increased in L3.6pl cell bearing mice (Table 2).

DISCUSSION

Analyzing palliative treatment data, a novel approach for patients with metastatic pancreatic cancer is urgently required. Targeting HDACs may be a new option for this tumor entity. Preliminary studies have demonstrated *in vitro* activity of HDACIs in pancreatic cancer cell lines. Natoni *et al*[30] showed that treatment with sodium butyrate, a carboxyl acid class inhibitor of HDACs, resulted in marked down-regulation of anti-apotoctic Bcl-xL protein expression, mitochondrial membrane depolarization, cytochrome c release from mitochondria, activation of caspase-9 and -3, and apoptosis induction. Garcia-Morales *et al*[31] reported HDACIs induced apoptosis in the pancreatic cancer cell lines IMIM-PC-1, IMIM-PC-2, and RWP-1 that are normally resistant to other antineoplastic drugs. This finding was previously observed by Sato *et al*[32] for five normally chemotherapy-resistant cell lines when treated with FR901228, a cyclic peptide HDACI belonging to the depsipeptides class. Recently, another class of HDACIs, the hydroxamic acids, with representatives such as trichostatin A (TSA), suberoylanilide hydroxamic acid (vorinostat, SAHA), azelaic bis-hydroxamic acid (ABHA), scriptaid, oxamflatin, pyroxamide, m-carboxycinnamic acid bis-hydroxamide (CBHA), and the recently developed NVP-LAQ824, NVP-LBH589, and PXD101 have become the focus for further research, including pancreatic cancer. Gahr *et al*[33] used HDACI trichostatin A for *in vitro* treatment of pancreatic carcinoma cell lines YAP C and DAN G. They described an apoptosis rate of 71% and 66% after 72 h using a drug concentration of 1 μmol/L. Moore *et al*[34] tested trichostatin A in PaCa44 cells using microarrays containing 22283 probe sets. One prominent feature was the increased ratio between the levels of expression of pro-apoptotic (BIM) and anti-apoptotic (Bcl-xL and Bcl-W) genes. In addition, Cecconi *et al*[35] reported for the same cell line PaCa44 that trichostatin A caused cell cycle arrest at the G2 phase and induced apoptotic cell death. Another hydroxamic acid, SAHA, induced growth inhibition in three pancreatic cell lines BxPC3, COLO-357, and PANC-1 by upregulating p21 and sequestering it in the cytoplasm[36]. In our current study, we investigated the two novel cinnamic hydroxamic acid compounds NVP-LAQ824 and NVP-LBH589 for *in vitro* treatment of 8 different human pancreatic cancer cell lines. Cell-growth inhibition by NVP-LAQ824 and NVP-LBH589 was studied by MTT assay. Treatment with both compounds significantly suppressed the growth of 7 cancer cell lines after 3 d of incubation and all cancer cell lines after 6 d of incubation. We hypothezise that the lack of response of Capan-2 cells after 3 d of treatment may be based on the status of the tumor suppressor *p53*. A genetic profile of 10 different human pancreatic cancer cell lines (6 of the 8 cell lines used in our experiment being amongst them) created by a group from John Hopkins University (http://pathology2.jhu.edu/pancreas/geneticsweb/ profiles.htm) discovered *p53* mutations in almost all cell lines, but not in Capan-2 cells. On the other hand, it has been shown that acetylation and deacetylation of *p53* is likely to be part of the mechanism that controls its physiological activity. Whereas HDACs are capable of downregulating p53 function, HDAC inhibition can cause the opposite effect[37]. Interestingly, it has also been shown that HDAC inhibitors, such as FR901228 and trichostatin A, completely deplete mutant p53 in cancer cell lines and restore p53-like functions, which is highly toxic to cell lines with mutant p53[38]. Donadelli *et al* confirmed this finding in *p53* gene mutated pancreatic cancer cell lines which were treated with trichostatin A. The compound induced G2 phase arrest and apoptotic cell death by activation of $p21^{waf1}$, which is normally induced by *p53*[39].

In previous *in vitro* studies, NVP-LAQ824 exhibited potent anti-proliferative activity against colon carcinoma (IC_{50} = 0.01 μmol/L), and biliary tract cancer (IC_{50} = 0.11 μmol/L) as well as against non-small cell lung carcinoma (IC_{50} = 0.15 μmol/L), prostate cancer (IC_{50} = 0.018-0.023 μmol/L), head and neck squamous

carcinoma (IC_{50} = 0.04-0.34 μmol/L), and human breast adenocarcinoma cells (IC_{50} = 0.03-0.039 μmol/L) after 72 h of exposure[16,40-42]. The *in vitro* effects of NVP-LAQ824 on hematologic malignancies have been examined in several human cell lines with a death rate of more than 90% following 48 h of drug incubation, with exposures as low as 0.1 μmol/L[43-45]. Our second compound NVP-LBH589, was even more effective *in vitro* for the treatment of human chronic myeloid leukemia blast crisis K562 and LAMA-84, multiple myeloma, and acute leukemia MV4-11 cells[15,46-48].

The *in vitro* anti-tumoral drug mechanism in our study was assessed by immunoblotting for acH4 (surrogate marker for histone acetylation) $p21^{WAF-1/CIP-1}$, and cell cycle analysis. Treatment with both compounds was associated with hyperacetylation of nucleosomal histone H4, increased expression of $p21^{WAF-1/CIP-1}$, cell cycle arrest at G2/M-checkpoint, and significant induction of apoptosis (increased sub-G1-peak). Therefore, our results are very consistent with the *in vitro* results of the aforementioned studies by Natoni *et al*[30], Garcia-Morales *et al*[31], Sato *et al*[32], Gahr *et al*[33], Donadelli *et al*[39], Cecconi *et al*[35], and Arnold *et al*[36].

Encouraged by our *in vitro* results, we decided to test the most effective drug NVP-LBH589 *in vivo* in comparison to placebo using the chimeric mouse model. The NVP-LBH589 dose of 25 mg/kg (5 d/wk) was selected according to a study testing different iv doses of NVP-LAQ824 between 5 and 100 mg/kg (5 d/wk) in a similar chimeric mouse model using the human colon cancer cell line HCT 116[16]. *In vivo* data for NVP-LBH589 using human prostate carcinoma cell PC-3 xenografts became available only after completion of our study, and showed tumor reduction at a dose of 10 mg/kg per day[49]. In our experiments, NVP-LBH589 significantly reduced tumor mass in comparison to placebo and potentiated the efficacy of gemcitabine. In accordance with our observations, Gahr *et al*[33] and Piacentini *et al*[50] showed that a combination with gemcitabine potentiated the *in vitro* effects of trichostatin A in pancreatic cancer cells, demonstrating a synergistic effect between both agents. This phenomenon has been shown for *in vitro* cotreatment with SAHA, too, where the compound rendered pancreatic cancer cells sensitive to the inhibitory and proapoptotic effects of gemcitabine[36]. In human breast cancer cell lines SKBR-3 and BT-474, NVP-LAQ824 also enhanced gemcitabine-induced apoptosis *in vitro*[41]. For head and neck squamous carcinoma cells, the combination of NVP-LAQ824 with gemcitabine was more effective *in vitro* than a combination with docetaxel, paclitaxel, or cisplatin, especially when the cytotoxic agent was used first for 24 h followed by 48 h of NVP-LAQ824[40]. Unfortunately, in the first recently published randomized, double-blind, placebo-controlled multicenter-phase Ⅱ trial, gemcitabine plus benzamide HDACI CI-994 (N-acetyldinaline) showed no advantage over gemcitabine alone in patients with advanced pancreatic cancer[51]. In this study, a total of 174 patients received combination therapy (CI-994, 6 mg/m^2 per day, day 1-21 plus gemcitabine, 1000 mg/m^2, day 1, 8 and 15 each 28-d cycle) or placebo plus gemcitabine (1000 mg/m^2, day 1, 8 and 15 each 28-d cycle). Median survival was 194 d (combination therapy) *vs* 214 d (gemcitabine) (P = 0.908). The objective response rate was 12% *vs* 14% when investigator-assessed and 1% *vs* 6%, respectively, when assessed centrally. Time to treatment failure did not differ between the two arms (P = 0.304). Quality of life scores at 2 mo were worse with the combination than with gemcitabine alone. Pain response rates were similar between the two groups. There was an increased incidence of neutropenia and thrombocytopenia with combination therapy. However, it is currently unknown whether these clinical observations are also true for the hydroxamic acids class of HDACIs. In addition, recent *in vitro* and *in vivo* data have shown synergistic effects of trichostatin A in combination with DNA methyltransferase inhibitors azacytidine[52,53] and zebularine[54] and proteasome inhibitor PS-341[55], suggesting alternative combination partners for HDACIs. Whereas upregulation of tumor suppressors DUSP6[52] and MUC 2[53] is the proposed mechanism for the additional effect of DNA methyltransferase inhibitors, it is inactivation of NFkappaB signalling, downregulation of anti-apoptotic Bcl-xL and disruption of MAP kinase pathway for combination with the proteasome inhibitor PS-341[55].

Regarding side effects of the different drugs used in our studies, there was no significant additional weight loss in the COMBO group as compared to placebo. Moreover, NVP-LBH589 alone only induced additional weight loss in the HPAF-2 cell experiment. Weight loss in general was apparently more pronounced in the L3.6pl than in the HPAF-2 cell experiment. This may be due to the fact that L3.6pl cells are a selected variant of COLO-357 cells with increased metastatic potential[24,56,57]. Regarding other studies, weight loss of animals was not previously reported for NVP-LAQ824[16], but for NVP-LBH589[42].

In order to assess *in vivo* anti-tumoral drug mechanisms, paraffin sections of mouse tumors were stained with hematoxylin-eosin (H&E), MIB-1 (proliferation marker) and TUNEL (apoptosis marker). Treatment with NVP-LBH589 and COMBO slightly reduced proliferation (reduced MIB-1 staining) and slightly induced apoptosis (increased TUNEL-staining) in HPAF-2 cell bearing mice, whereas proliferation was not decreased and apoptosis only slightly increased in L3.6pl cell bearing mice. Surprisingly, the calculated numbers were much smaller than expected from the *in vitro* experiments. This might be derived from the fact that other pathways, like inhibition of angiogenesis, which we were unable to study in our model due to insufficient tissue quality, may be more important for NVP-LBH589 action in the *in vivo* setting.

Our findings suggest that NVP-LBH589 and NVP-LAQ824 are active against human pancreatic cancer cells *in vitro*, mainly by inhibition of proliferation and induction of apoptosis. NVP-LBH589 is also active in the *in vivo* setting, although the precise mechanism of

drug action is not yet completely understood. Therefore, a clinical study testing NVP-LBH589 for the treatment of pancreaticobiliary cancer has just been initiated at our department.

ACKNOWLEDGMENTS

The authors thank A Kluge for technical assistance, Professor CJ Bruns (Department of Surgery, Klinikum Grosshadern, Ludwig-Maximilian-University, Munich, Germany) for provision of L3.6pl cells and Novartis Pharma for financial support and provision of NVP-LAQ824 and NVP-LBH589.

COMMENTS

Background

Pancreatic adenocarcinoma is essentially an incurable disease, with mortality closely approaching incidence. Single agent gemcitabine is currently considered the standard of care for the treatment of inoperable pancreatic cancer, providing a small but sizable benefit in survival and palliation of symptoms.

Research frontiers

In the past ten years, several molecular-targeting agents have been introduced in the clinical setting. Despite promising results in phase Ⅱ studies, randomized clinical trials exploring the new compounds, such as matrix-metalloprotease-inhibitors (MMPI), farnesyl transferase inhibitors (FTI), signal transduction inhibitors, and angiogenesis inhibitors, either alone or in combination with gemcitabine have been largely disappointing. Polo-like kinase 1 (PLK-1), death receptor 5 (DR5), and histondeacetylase (HDAC) inhibitors are currently under clinical evaluation as new treatment options.

Innovations and breakthroughs

In 2003, fixed-dose-rate (FDR) gemcitabine (1500 mg/m^2 at 10 mg/m^2 per minute) improved median survival time from 5.0 mo in the standard arm to 8.0 mo in a randomized study; However, grade 3 and 4 toxicity increased significantly. In 2005, investigators of a phase Ⅲ study found that the gemcitabine-capecitabine combination significantly improved overall survival over gemcitabine alone (hazard ratio 0.80; 95% CI 0.65-0.98; P = 0.026). Recently, a randomized phase Ⅲ placebo-controlled trial demonstrated that combining gemcitabine with EGFR inhibitor erlotinib was associated with a modest, but statistically significant survival benefit of 15 d.

Applications

The aim of our study was to investigate *in vitro* and *in vivo* treatment with the histone deacetylase inhibitors NVP-LAQ824 and NVP-LBH589 in pancreatic cancer. Our findings suggested that NVP-LBH589 and NVP-LAQ824 are active against human pancreatic cancer *in vitro*. In addition, NVP-LBH589 demonstrated significant *in vivo* activity and potentiated the efficacy of gemcitabine.

Terminology

Histones (positively charged proteins) are the major components of chromatin. Histone acetylation and deacetylation modulate chromosome structure and regulate gene transcription. Two families of enzymes, histone acetyltransferases (HATs) and histone deacetylases (HDACs), activate and repress gene expression, respectively. Aberrant HAT or HDAC activity is associated with various epithelial and hematologic cancers. HDACs may play an important role in human oncogenesis through HDAC-mediated gene silencing and interaction of HDACs with proteins involved in tumorigenesis. HDAC inhibition could potentially restore normal processes in transformed cells without affecting normal cells.

Peer review

This paper addresses the use of histone deacetylase inhibitors in the treatment of pancreatic cancer *in vitro* and *in vivo*. It represents an important experimental assessment of novel agents in the treatment of a cancer for which effective therapy is currently lacking. It's a very interesting paper.

REFERENCES

1 **Jemal A**, Murray T, Ward E, Samuels A, Tiwari RC, Ghafoor A, Feuer EJ, Thun MJ. Cancer statistics, 2005. *CA Cancer J Clin* 2005; **55**: 10-30

2 **Lockhart AC**, Rothenberg ML, Berlin JD. Treatment for pancreatic cancer: current therapy and continued progress. *Gastroenterology* 2005; **128**: 1642-1654

3 **Carpelan-Holmstrom M**, Nordling S, Pukkala E, Sankila R, Luttges J, Kloppel G, Haglund C. Does anyone survive pancreatic ductal adenocarcinoma? A nationwide study re-evaluating the data of the Finnish Cancer Registry. *Gut* 2005; **54**: 385-387

4 **Cardenes HR**, Chiorean EG, Dewitt J, Schmidt M, Loehrer P. Locally advanced pancreatic cancer: current therapeutic approach. *Oncologist* 2006; **11**: 612-623

5 **Burris HA 3rd**, Moore MJ, Andersen J, Green MR, Rothenberg ML, Modiano MR, Cripps MC, Portenoy RK, Storniolo AM, Tarassoff P, Nelson R, Dorr FA, Stephens CD, Von Hoff DD. Improvements in survival and clinical benefit with gemcitabine as first-line therapy for patients with advanced pancreas cancer: a randomized trial. *J Clin Oncol* 1997; **15**: 2403-2413

6 **Tempero M**, Plunkett W, Ruiz Van Haperen V, Hainsworth J, Hochster H, Lenzi R, Abbruzzese J. Randomized phase II comparison of dose-intense gemcitabine: thirty-minute infusion and fixed dose rate infusion in patients with pancreatic adenocarcinoma. *J Clin Oncol* 2003; **21**: 3402-3408

7 **Cunningham D**, Chau I, Stocken D, Davies C, Dunn J, Valle J, Smith D, Steward W, Harper P, Neoptolemos J. Phase III randomised comparison of gemcitabine (GEM) versus gemcitabine plus capecitabine (GEM-CAP) in patients with advanced pancreatic cancer. *EJC Supplements* 2005; **3**: 4

8 **Moore MJ**, Goldstein D, Hamm J, Figer A, Hecht JR, Gallinger S, Au HJ, Murawa P, Walde D, Wolff RA, Campos D, Lim R, Ding K, Clark G, Voskoglou-Nomikos T, Ptasynski M, Parulekar W. Erlotinib plus gemcitabine compared with gemcitabine alone in patients with advanced pancreatic cancer: a phase III trial of the National Cancer Institute of Canada Clinical Trials Group. *J Clin Oncol* 2007; **25**: 1960-1966

9 **Philip PA**, Benedetti J, Fenoglio-Preiser C, Zalupski M, Lenz H, O'Reilly E, Wong R, Atkins J, Abruzzese J, Blanke C. Phase III study of gemcitabine plus cetuximab versus gemcitabine in patients with locally advanced or metastatic pancreatic adenocarcinoma: SWOG S0205 study. *Journal of Clinical Oncology*, 2007 ASCO Annual Meeting Proceedings Part I 2007; **25**: LBA4509

10 **Kindler HL**, Friberg G, Singh DA, Locker G, Nattam S, Kozloff M, Taber DA, Karrison T, Dachman A, Stadler WM, Vokes EE. Phase II trial of bevacizumab plus gemcitabine in patients with advanced pancreatic cancer. *J Clin Oncol* 2005; **23**: 8033-8040

11 **Kindler HL**, Niedzwiecki D, Hollis D, Oraefo E, Schrag D, Hurwitz H, McLeod HL, Mulcahy MF, Schilsky RL, Goldberg RM. A double-blind, placebo-controlled, randomized phase III trial of gemcitabine (G) plus bevacizumab (B) versus gemcitabine plus placebo (P) in patients (pts) with advanced pancreatic cancer (PC): A preliminary analysis of Cancer and Leukemia Group B (CALGB). *Journal of Clinical Oncology*, 2007 ASCO Annual Meeting Proceedings Part I 2007; **25**: 4508

12 **Hess-Stumpp H**. Histone deacetylase inhibitors and cancer: from cell biology to the clinic. *Eur J Cell Biol* 2005; **84**: 109-121

13 **Budillon A**, Bruzzese F, Di Gennaro E, Caraglia M. Multiple-target drugs: inhibitors of heat shock protein 90 and of histone deacetylase. *Curr Drug Targets* 2005; **6**: 337-351

14 **Remiszewski SW**, Sambucetti LC, Bair KW, Bontempo J, Cesarz D, Chandramouli N, Chen R, Cheung M, Cornell-Kennon S, Dean K, Diamantidis G, France D, Green MA, Howell KL, Kashi R, Kwon P, Lassota P, Martin MS, Mou Y, Perez LB, Sharma S, Smith T, Sorensen E, Taplin F, Trogani N, Versace R, Walker H, Weltchek-Engler S, Wood A, Wu A, Atadja P. N-hydroxy-3-phenyl-

2-propenamides as novel inhibitors of human histone deacetylase with *in vivo* antitumor activity: discovery of (2E)-N-hydroxy-3-[4-[[(2-hydroxyethyl)[2-(1H-indol-3-yl)ethyl]amino]methyl]phenyl]-2-propenamide (NVP-LAQ824). *J Med Chem* 2003; **46**: 4609-4624

15 **George P**, Bali P, Annavarapu S, Scuto A, Fiskus W, Guo F, Sigua C, Sondarva G, Moscinski L, Atadja P, Bhalla K. Combination of the histone deacetylase inhibitor LBH589 and the hsp90 inhibitor 17-AAG is highly active against human CML-BC cells and AML cells with activating mutation of FLT-3. *Blood* 2005; **105**: 1768-1776

16 **Atadja P**, Gao L, Kwon P, Trogani N, Walker H, Hsu M, Yeleswarapu L, Chandramouli N, Perez L, Versace R, Wu A, Sambucetti L, Lassota P, Cohen D, Bair K, Wood A, Remiszewski S. Selective growth inhibition of tumor cells by a novel histone deacetylase inhibitor, NVP-LAQ824. *Cancer Res* 2004; **64**: 689-695

17 **Edwards A**, Li J, Atadja P, Bhalla K, Haura EB. Effect of the histone deacetylase inhibitor LBH589 against epidermal growth factor receptor-dependent human lung cancer cells. *Mol Cancer Ther* 2007; **6**: 2515-2524

18 **Giles F**, Fischer T, Cortes J, Garcia-Manero G, Beck J, Ravandi F, Masson E, Rae P, Laird G, Sharma S, Kantarjian H, Dugan M, Albitar M, Bhalla K. A phase I study of intravenous LBH589, a novel cinnamic hydroxamic acid analogue histone deacetylase inhibitor, in patients with refractory hematologic malignancies. *Clin Cancer Res* 2006; **12**: 4628-4635

19 **Rowinsky EK**, Pacey S, Patnaik A, O'Donnell A, Mita MM, Atadja P, Peng B, Dugan M, Scott JW, De Bono JS. A phase I, pharmacokinetic (PK) and pharmacodynamic (PD) study of a novel histone deacetylase (HDAC) inhibitor LAQ824 in patients with advanced solid tumors. *J Clin Oncol* 2004; **22**: abstract 3022 (ASCO 2004)

20 **Ottmann OG**, Deangelo DJ, Stone DJ, Pfeifer H, Lowenberg B, Atadja P, Peng B, Scott JW, Dugan M, Sonneveld P. A Phase I, pharmacokinetic (PK) and pharmacodynamic (PD) study of a novel histone deacetylase inhibitor LAQ824 in patients with hematologic malignancies. *J Clin Oncol* 2004; **22**: 3024

21 **Sharma S**, Vogelzang NJ, Beck J, Patnaik A, Mita M, Dugan M, Hwang A, Masson E, Culver KW, Prince H. Phase I pharmacokinetic (PK) and pharmacodynamic (PD) study of LBH589, a novel deacetylase (DAC) inhibitor given intravenously on a new once weekly schedule. *J Clin Oncol* 2007; **25**: 14019

22 **Prince HM**, George D, Patnaik A, Mita M, Dugan M, Butterfoss D, Masson E, Culver KW, Burris HA, Beck J. Phase I study of oral LBH589, a novel deacetylase (DAC) inhibitor in advanced solid tumors and non-hodgkin's lymphoma. *J Clin Oncol* 2007; **25**: 3500

23 **Ryu B**, Jones J, Blades NJ, Parmigiani G, Hollingsworth MA, Hruban RH, Kern SE. Relationships and differentially expressed genes among pancreatic cancers examined by large-scale serial analysis of gene expression. *Cancer Res* 2002; **62**: 819-826

24 **Bruns CJ**, Harbison MT, Kuniyasu H, Eue I, Fidler IJ. *In vivo* selection and characterization of metastatic variants from human pancreatic adenocarcinoma by using orthotopic implantation in nude mice. *Neoplasia* 1999; **1**: 50-62

25 **Schoumacher RA**, Ram J, Iannuzzi MC, Bradbury NA, Wallace RW, Hon CT, Kelly DR, Schmid SM, Gelder FB, Rado TA. A cystic fibrosis pancreatic adenocarcinoma cell line. *Proc Natl Acad Sci USA* 1990; **87**: 4012-4016

26 **Meck RA**, Clubb KJ, Allen LM, Yunis AA. Inhibition of cell cycle progression of human pancreatic carcinoma cells *in vitro* by L-(alpha S, 5S)-alpha-amino-3-chloro-4,5-dihydro-5-isoxazoleacetic acid, Acivicin (NSC 163501). *Cancer Res* 1981; **41**: 4547-4553

27 **Sipos B**, Moser S, Kalthoff H, Torok V, Lohr M, Kloppel G. A comprehensive characterization of pancreatic ductal carcinoma cell lines: towards the establishment of an *in vitro* research platform. *Virchows Arch* 2003; **442**: 444-452

28 **Tannapfel A**, Geissler F, Kockerling F, Katalinic A, Hauss J, Wittekind C. Apoptosis and proliferation in relation to histopathological variables and prognosis in hepatocellular carcinoma. *J Pathol* 1999; **187**: 439-445

29 **Tannapfel A**, Hahn HA, Katalinic A, Fietkau RJ, Kuhn R, Wittekind CW. Prognostic value of ploidy and proliferation markers in renal cell carcinoma. *Cancer* 1996; **77**: 164-171

30 **Natoni F**, Diolordi L, Santoni C, Gilardini Montani MS. Sodium butyrate sensitises human pancreatic cancer cells to both the intrinsic and the extrinsic apoptotic pathways. *Biochim Biophys Acta* 2005; **1745**: 318-329

31 **Garcia-Morales P**, Gomez-Martinez A, Carrato A, Martinez-Lacaci I, Barbera VM, Soto JL, Carrasco-Garcia E, Menendez-Gutierrez MP, Castro-Galache MD, Ferragut JA, Saceda M. Histone deacetylase inhibitors induced caspase-independent apoptosis in human pancreatic adenocarcinoma cell lines. *Mol Cancer Ther* 2005; **4**: 1222-1230

32 **Sato N**, Ohta T, Kitagawa H, Kayahara M, Ninomiya I, Fushida S, Fujimura T, Nishimura G, Shimizu K, Miwa K. FR901228, a novel histone deacetylase inhibitor, induces cell cycle arrest and subsequent apoptosis in refractory human pancreatic cancer cells. *Int J Oncol* 2004; **24**: 679-685

33 **Gahr S**, Ocker M, Ganslmayer M, Zopf S, Okamoto K, Hartl A, Leitner S, Hahn EG, Herold C. The combination of the histone-deacetylase inhibitor trichostatin A and gemcitabine induces inhibition of proliferation and increased apoptosis in pancreatic carcinoma cells. *Int J Oncol* 2007; **31**: 567-576

34 **Moore PS**, Barbi S, Donadelli M, Costanzo C, Bassi C, Palmieri M, Scarpa A. Gene expression profiling after treatment with the histone deacetylase inhibitor trichostatin A reveals altered expression of both pro- and anti-apoptotic genes in pancreatic adenocarcinoma cells. *Biochim Biophys Acta* 2004; **1693**: 167-176

35 **Cecconi D**, Scarpa A, Donadelli M, Palmieri M, Hamdan M, Astner H, Righetti PG. Proteomic profiling of pancreatic ductal carcinoma cell lines treated with trichostatin-A. *Electrophoresis* 2003; **24**: 1871-1878

36 **Arnold NB**, Arkus N, Gunn J, Korc M. The histone deacetylase inhibitor suberoylanilide hydroxamic acid induces growth inhibition and enhances gemcitabine-induced cell death in pancreatic cancer. *Clin Cancer Res* 2007; **13**: 18-26

37 **Juan LJ**, Shia WJ, Chen MH, Yang WM, Seto E, Lin YS, Wu CW. Histone deacetylases specifically down-regulate p53-dependent gene activation. *J Biol Chem* 2000; **275**: 20436-20443

38 **Blagosklonny MV**, Trostel S, Kayastha G, Demidenko ZN, Vassilev LT, Romanova LY, Bates S, Fojo T. Depletion of mutant p53 and cytotoxicity of histone deacetylase inhibitors. *Cancer Res* 2005; **65**: 7386-7392

39 **Donadelli M**, Costanzo C, Faggioli L, Scupoli MT, Moore PS, Bassi C, Scarpa A, Palmieri M. Trichostatin A, an inhibitor of histone deacetylases, strongly suppresses growth of pancreatic adenocarcinoma cells. *Mol Carcinog* 2003; **38**: 59-69

40 **Tran H**, TShoaf SL. Improved efficacy with sequential use of histone deacetylase inhibitor, LAQ824, with common chemotherapeutic agents in head and neck squamous carcinoma cell lines. *Proc Amer Assoc Cancer Res* 2005; **46**: 5095

41 **Fuino L**, Bali P, Wittmann S, Donapaty S, Guo F, Yamaguchi H, Wang HG, Atadja P, Bhalla K. Histone deacetylase inhibitor LAQ824 down-regulates Her-2 and sensitizes human breast cancer cells to trastuzumab, taxotere, gemcitabine, and epothilone B. *Mol Cancer Ther* 2003; **2**: 971-984

42 **Bluethner T**, Niederhagen M, Caca K, Serr F, Witzigmann H, Moebius C, Mossner J, Wiedmann M. Inhibition of histone deacetylase for the treatment of biliary tract cancer: a new effective pharmacological approach. *World J*

Gastroenterol 2007; **13**: 4761-4770

43 **Catley L**, Weisberg E, Tai YT, Atadja P, Remiszewski S, Hideshima T, Mitsiades N, Shringarpure R, LeBlanc R, Chauhan D, Munshi NC, Schlossman R, Richardson P, Griffin J, Anderson KC. NVP-LAQ824 is a potent novel histone deacetylase inhibitor with significant activity against multiple myeloma. *Blood* 2003; **102**: 2615-2622

44 **Bhalla KN**, Nimmanapalli R, Fuino L, Tao J, Lee H. Histone deacetylase inhibitor LAQ824 down regulates BCR-ABL levels and induces apoptosis of imatinib mesylate -sensitive or -refractory BCR-ABL positive human leukemia cells. *Proc Am Soc Clin Oncol* 2003; **22**: 2322

45 **Rosato RR**, Almenara JA, Maggio SC, Atadja P, Dent P, Grant S. Potentiation of LAQ824-mediated lethality by the cyclin-dependent kinase inhibitor roscovitine in human leukemia cells proceeds through an XIAP- and reactive oxygen species (ROS)-dependent mechanism. *Proc Amer Assoc Cancer Res* 2005; **46**: 5327

46 **Maiso P**, Carvajal-Vergara X, Ocio EM, Lopez-Perez R, Mateo G, Gutierrez N, Atadja P, Pandiella A, San Miguel JF. The histone deacetylase inhibitor LBH589 is a potent antimyeloma agent that overcomes drug resistance. *Cancer Res* 2006; **66**: 5781-5789

47 **Catley L**, Weisberg E, Kiziltepe T, Tai YT, Hideshima T, Neri P, Tassone P, Atadja P, Chauhan D, Munshi NC, Anderson KC. Aggresome induction by proteasome inhibitor bortezomib and alpha-tubulin hyperacetylation by tubulin deacetylase (TDAC) inhibitor LBH589 are synergistic in myeloma cells. *Blood* 2006; **108**: 3441-3449

48 **Fiskus W**, Pranpat M, Bali P, Balasis M, Kumaraswamy S, Boyapalle S, Rocha K, Wu J, Giles F, Manley PW, Atadja P, Bhalla K. Combined effects of novel tyrosine kinase inhibitor AMN107 and histone deacetylase inhibitor LBH589 against Bcr-Abl-expressing human leukemia cells. *Blood* 2006; **108**: 645-652

49 **Qian DZ**, Kato Y, Shabbeer S, Wei Y, Verheul HM, Salumbides B, Sanni T, Atadja P, Pili R. Targeting tumor angiogenesis with histone deacetylase inhibitors: the hydroxamic acid derivative LBH589. *Clin Cancer Res* 2006; **12**: 634-642

50 **Piacentini P**, Donadelli M, Costanzo C, Moore PS, Palmieri M, Scarpa A. Trichostatin A enhances the response of chemotherapeutic agents in inhibiting pancreatic cancer cell proliferation. *Virchows Arch* 2006; **448**: 797-804

51 **Richards DA**, Boehm KA, Waterhouse DM, Wagener DJ, Krishnamurthi SS, Rosemurgy A, Grove W, Macdonald K, Gulyas S, Clark M, Dasse KD. Gemcitabine plus CI-994 offers no advantage over gemcitabine alone in the treatment of patients with advanced pancreatic cancer: results of a phase II randomized, double-blind, placebo-controlled, multicenter study. *Ann Oncol* 2006; **17**: 1096-1102

52 **Xu S**, Furukawa T, Kanai N, Sunamura M, Horii A. Abrogation of DUSP6 by hypermethylation in human pancreatic cancer. *J Hum Genet* 2005; **50**: 159-167

53 **Yamada N**, Hamada T, Goto M, Tsutsumida H, Higashi M, Nomoto M, Yonezawa S. MUC2 expression is regulated by histone H3 modification and DNA methylation in pancreatic cancer. *Int J Cancer* 2006; **119**: 1850-1857

54 **Neureiter D**, Zopf S, Leu T, Dietze O, Hauser-Kronberger C, Hahn EG, Herold C, Ocker M. Apoptosis, proliferation and differentiation patterns are influenced by Zebularine and SAHA in pancreatic cancer models. *Scand J Gastroenterol* 2007; **42**: 103-116

55 **Bai J**, Demirjian A, Sui J, Marasco W, Callery MP. Histone deacetylase inhibitor trichostatin A and proteasome inhibitor PS-341 synergistically induce apoptosis in pancreatic cancer cells. *Biochem Biophys Res Commun* 2006; **348**: 1245-1253

56 **Bruns CJ**, Koehl GE, Guba M, Yezhelyev M, Steinbauer M, Seeliger H, Schwend A, Hoehn A, Jauch KW, Geissler EK. Rapamycin-induced endothelial cell death and tumor vessel thrombosis potentiate cytotoxic therapy against pancreatic cancer. *Clin Cancer Res* 2004; **10**: 2109-2119

57 **Bruell D**, Bruns CJ, Yezhelyev M, Huhn M, Muller J, Ischenko I, Fischer R, Finnern R, Jauch KW, Barth S. Recombinant anti-EGFR immunotoxin 425(scFv)-ETA' demonstrates anti-tumor activity against disseminated human pancreatic cancer in nude mice. *Int J Mol Med* 2005; **15**: 305-313

S- Editor Li DL **L- Editor** Lalor PF **E- Editor** Lin YP

Online Submissions: wjg.wjgnet.com
wjg@wjgnet.com
doi:10.3748/wjg.14.3693

World J Gastroenterol 2008 June 21; 14(23): 3693-3709
World Journal of Gastroenterology ISSN 1007-9327
© 2008 The WJG Press. All rights reserved.

BASIC RESEARCH

Negundoside, an iridiod glycoside from leaves of *Vitex negundo*, protects human liver cells against calcium-mediated toxicity induced by carbon tetrachloride

Sheikh A Tasduq, Peerzada J Kaiser, Bishan D Gupta, Vijay K Gupta, Rakesh K Johri

Sheikh A Tasduq, Peerzada J Kaiser, Bishan D Gupta, Vijay K Gupta, Rakesh K Johri, Indian Institute of Integrative Medicine, CSIR, Jammu-Tawi-180001, Jammu and Kashmir, India

Author contributions: Tasduq SA designed the study, performed the experiments, analyzed the data, drafted the manuscript and contributed in use of new reagents/analytic tools; Kaiser PS was equally responsible as the first author for performing the experiments and helping in data setting, statistics, arrangement of figures and manuscript drafting; Gupta BD performed the chemistry experiments; Gupta VK worked on the data analysis, application of statistics and manuscript correction; Johri RK was the group leader and was responsible for checking the hypothesis of research study and final corrections of the manuscript and acquired funding for the study.

Supported by Indian Institute of Integrative Medicine, Council of Scientific and Industrial Research

Correspondence to: Sheikh A Tasduq, PhD, Scientist, Experimental Toxicology Lab, Division of Pharmacology, Indian Institute of Integrative Medicine, CSIR, Canal Road, Jammu 180001, Jammu and Kashmir, India. tasduq11@gmail.com
Telephone: +91-191-2569000-10 Fax: +91-191-2569333
Received: December 10, 2007 Revised: April 1, 2008
Accepted: April 8, 2008
Published online: June 21, 2008

Abstract

AIM: To evaluate the protective effect of 2'-p-hydroxy benzoylmussaenosidic acid [negundoside (NG), against carbon tetrachloride (CCl_4)-induced toxicity in HuH-7 cells.

METHODS: CCl_4 is a well characterized hepatotoxin, and inducer of cytochrome P450 2E1 (CYP2E1)-mediated oxidative stress. In addition, lipid peroxidation and accumulation of intracellular calcium are important steps in the pathway involved in CCl_4 toxicity. Liver cells (HuH-7) were treated with CCl_4, and the mechanism of the cytoprotective effect of NG was assessed. Silymarin, a known hepatoprotective drug, was used as control.

RESULTS: NG protected HuH-7 cells against CCl_4 toxicity and loss of viability without modulating CYP2E1 activity. Prevention of CCl_4 toxicity was associated with a reduction in oxidative damage as reflected by decreased generation of reactive oxygen species (ROS), a decrease in lipid peroxidation and accumulation of intracellular Ca^{2+} levels and maintenance of intracellular glutathione homeostasis. Decreased mitochondrial membrane potential (MMP), induction of caspases mediated DNA fragmentation and cell cycle arrest, as a result of CCl_4 treatment, were also blocked by NG. The protection afforded by NG seemed to be mediated by activation of cyclic adenosine monophosphate (cAMP) synthesis and inhibition of phospholipases (cPLA2).

CONCLUSION: NG exerts a protective effect on CYP2E1-dependent CCl_4 toxicity *via* inhibition of lipid peroxidation, followed by an improved intracellular calcium homeostasis and inhibition of Ca^{2+}-dependent proteases.

© 2008 The WJG Press. All rights reserved.

Key words: Negundoside; Silymarin; HuH-7; Carbon tetrachloride; CYP 2E1; Oxidative stress; Calcium; Toxicity

Peer reviewers: Kunissery A Balasubramanian, Professor, Christian Medical College, Gastrointestinal Sciences, Ida Scudder Road, Vellore 632004, India; Hitoshi Togashi, Associate Professor, Department of Gastroenterology, Course of Internal Medicine and Therapeutics, Yamagata University School of Medicine, 2-2-2 Iida-Nishi, Yamagata 990-9585, Japan

Tasduq SA, Kaiser PJ, Gupta BD, Gupta VK, Johri RK. Negundoside, an iridiod glycoside from leaves of *Vitex negundo*, protects human liver cells against calcium-mediated toxicity induced by carbon tetrachloride. *World J Gastroenterol* 2008; 14(23): 3693-3709 Available from: URL: http://www.wjgnet.com/1007-9327/14/3693.asp DOI: http://dx.doi.org/10.3748/wjg.14.3693

INTRODUCTION

Natural products from plant sources have extensive past and present use in treatment of diverse diseases and serve as compounds of interest both in their natural form and as templates for synthetic modification. The importance of natural products in modern medicine has been well recognized. More than 20 new drugs, launched world over between 2000 and 2005, originate from natural products. Scrutiny of medical indications by source of compounds has demonstrated that natural products and related drugs are used to treat 87% of all categorized human diseases (infectious and non-

infectious)[1].

Vitex negundo (verbenaceae) is an important source of such natural drugs. It is a reputed medicinal herb and its parts have been employed as a traditional cure in Asian systems of medicine (Indian, Chinese, Malaysian) for a variety of disease conditions. A number of pharmacological activities have been attributed to *V. negundo*, such as: analgesic and anti-inflammatory activity[2], enzymes inhibition[3], nitric oxide scavenging activity[4], snake venom neutralization activity[5], antifeeding activity[6], antiradical and antilipoperoxidative[7], CNS activity[8], hepatoprotective activity[9], anti-bacterial activity[10], anti-fungal[11], larvicidal activity [12], antiandrogenic effects[13], mosquito repellent activity[14].

In the recent past, some of our work and work as reported by others on botanical products from *V. negundo* have shown a promising hepatoprotective activity[9,15]. This activity has been evaluated against various hepatotoxic agents including carbon tetrachloride (CCl_4). CCl_4 is a well established and widely used hepatotoxin and the principle cause of CCl_4-induced liver injury is proposed to be lipid peroxidation by free radical derivatives of CCl_4. CCl_4 is activated by NADH-CYP 450 2E1 system of the liver endoplasmic reticulum and converted into trimethyl CCl_3 radicals (*via* reductive dehalogenation) and, under aerobic conditions, in the more reactive trichloromethyl peroxy radical CCl_3OO^*. Formation of the radicals CCl_3^* and CCl_3OO^* causes oxidative stress. The CYP 2E1-mediated metabolism results in generation of reactive oxygen species, which further contributes to the development of cellular injury[16]. Also, considerable evidence suggests that CCl_4 modifies the expression levels of several pro-apoptotic and anti-apoptotic growth factors and receptors[17] especially during chronic administration. CCl_4 has been shown to be a carcinogen and has been classified as a group 2B carcinogen by inducing gene conversion, homozygosity and intra-chromosomal recombinations[18].

It was, therefore, our interest to investigate, in-depth, the mechanism of modulation of CCl_4-induced toxic manifestations with 2'-p-hydroxybenzoylmussaenosidic acid [negundoside (NG)] (a purified irridoid glycoside from leaves of *Vitex negundo*), particularly inhibition of downstream CYP 2E1 cascade of pro-apoptotic events with reference to the following: (1) role of CYP 450 2E1 activation on calcium-mediated oxidative stress; (2) involvement of calcium in phospholipase A2 (PLA2) and cyclic adenosine monophosphate (cAMP) regulation; (3) effect of activated cPLA2 on mitochondrial depolarization, inducing cytochrome C release resulting in caspase mediated apoptosis.

MATERIALS AND METHODS

Chemicals

DMEM F12 medium, Fetal calf serum, trypsin-EDTA solution, 2', 7'-dichlorofluoresceine diacetate (DCF-DA), rhodamine-123 (Rh-123), propidium iodide (PI), DNase-free RNase, proteinase K, 3-(4,5-dimethylthiazole-2-yl)-2,5-diphenyltetrazolium bromide (MTT), Hoechst 33258, cyclosporine A, penicillin, streptomycin, L-glutamine, pyruvic acid, camptothecin, malondialdehyde (MDA) and other biochemicals were purchased from Sigma Chemicals Co. (St. Louis, Mo). Caspase-3 (ApoAlert caspases assay kits) were from B.D. Clontech, USA. Phospholipase A2 (PLA2) and cyclic adenosine triphosphatase (cAMP) were measured by commercially available kits from Cyman company, USA, and R&D systems, USA respectively. Protein concentration was measured using the BCA Protein Assay Kit from Pierce (Rockford, IL, USA).

Collection and identification of test material

Aerial parts of the plant *Vitex negundo* Linn were collected locally during August to October. Plant material was identified and authenticated by examination of the morphological characteristics by taxonomist of the Institute. A voucher specimen has been deposited in Indian Institute of Integrative Medicine (I.I.I.M.) Jammu Herbarium under collection No. 17814.

Extraction procedure for preparation of NG

The shade dried and powdered leaves (1 kg) of *V. negundo* were soaked in ethanol (5 L) and kept overnight. The percolate was filtered and concentrated under reduced pressure at below 50℃. The extraction procedure was repeated three times more using 3 L of ethanol each time. The combined ethanol extract was stirred with water (300 mL) for 1 h and filtered through Celite. The aqueous extract was concentrated at 50℃ and finally dried in vacuum desiccators.

Isolation of NG

The ethanol extract (50 g) of *V. negungo* was adsorbed over silica gel (100 g) to make slurry which was packed over a column of silica gel (1 kg) packed in chloroform. Elution was done with chloroform followed by mixture of chloroform and methanol. Elution with 10% methanol in chloroform gave agnuside followed by mixture of agnuside and negundoside and then negundoside. The compounds were characterized on the basis of ^{1}HNMR, ^{13}CNMR mass spectral data (data not shown) and standardized by HPLC (Figure 1).

Cell culture

The study was carried out using as a model a human hepatoma HuH-7 cells line (ATCC-USA), a generous gift from Dr. Vijai Kumar, International Centre for Genetic Engineering and Biotechnology (ICGEB), New Delhi, India. Cells were grown in Dulbecco's Modified Eagle's Medium (DMEM) containing 10% fetal calf serum (FCS), supplemented with 100 Units/mL penicillin, 100 mg/L streptomycin in a humidified atmosphere in 5% CO_2 at 37℃, and were sub-cultured at 1:5 ratio once a week.

Cell treatment

FCS was reduced to 3% for the experiments. Cells were plated at a density of 3×10^4 cells/cm^2 and maintained in culture medium for 12 h. Stock solutions of CCl_4, NG and silymarin were prepared fresh to avoid

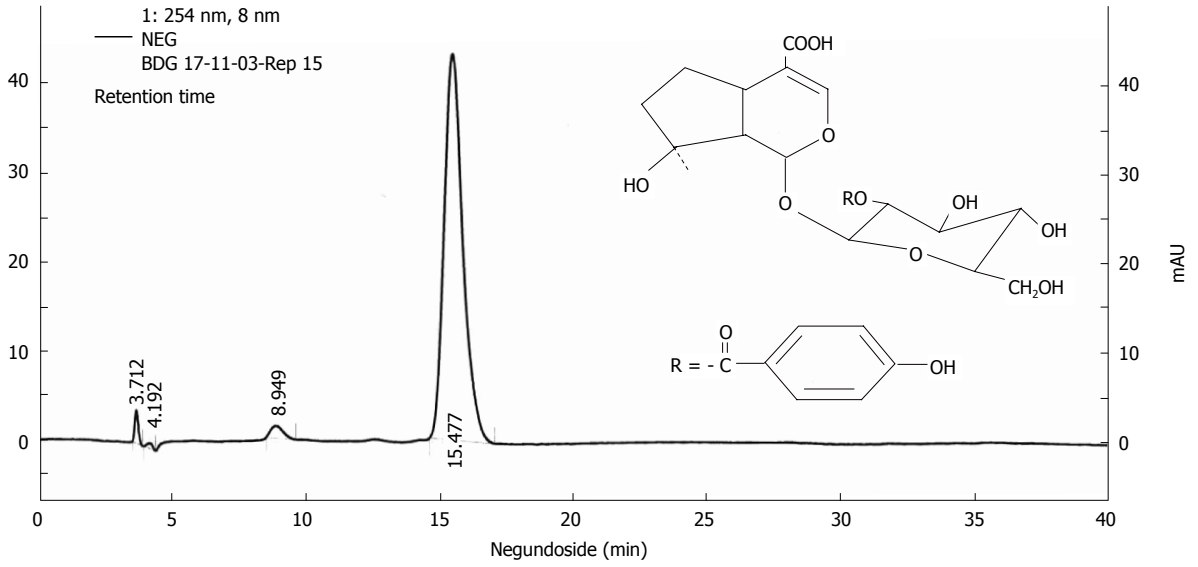

Figure 1 Finger print profile and chemical structure of NG. The HPLC profile of NG was performed by employing Shimadzu HPLC system consisting of a diode array detector and C18 column (5 μm, 250 mm x 4.0 mm I.D.) by UV detection at 254 nm. NG was resolved on a mobile phase consisting of methanol: 2% acetonitrile (30:70) and delivered at a flow rate of 0.6 mL/min. The chromatogram is representative of one of three independent analyses.

oxidation. For CCl_4 toxicity experiments, test substances, were added to the cell cultures an hour prior to CCl_4 treatment. Cells or supernatant were then collected for determination of various parameters.

Cytotoxicity assays

Cells were seeded onto 24-well plates, and after the corresponding treatment, the medium was removed and cell viability was evaluated by assaying for the ability of functional mitochondria to catalyze the reduction of MTT to form formazan salt by mitochondrial dehydrogenases, as described[19] and determined by ELISA reader at 565 nm (Multiskan Spectrum; Thermo Electron Corporation, USA).

Cellular and nuclear morphology

The cellular and nuclear morphology was observed under the light microscope (Nikon Eclipse TE2000U), at 40 × magnification, or under fluorescent microscopy, using Hoechst 33258 staining method as described[20] with certain modifications. Briefly, untreated and treated HuH-7 cells in 6 well plates were harvested by trypsinization, centrifuged at 100 × *g* for 5 min and washed twice with PBS. Cells were gently suspended in 100 μL PBS and fixed in 400 μL cold acetic acid: methanol (v/v = 1:3) overnight at 4℃. Cells were washed again in 1 mL of fixing solution, suspended in the residual volume of about 50 μL, spread on a clean slide and dried overnight at room temperature. One milliliter of staining solution (Hoechst 33258, 10 mg/L in 0.01 mol/L citric acid and 0.45 mol/L disodium phosphate containing 0.05% Tween 20) was poured on each slide and stained for 30 min under subdued light at room temperature. Slides were washed under gentle flow of tap water, rinsed in distilled water followed by in PBS. While wet, 50 μL of mounting fluid (PBS:glycerol, 1:1) was poured over the center of slide and covered with glass cover slip. The slides were sealed with nail polish and observed for any nuclear morphological alterations and apoptotic bodies under inverted fluorescence microscope (Nikon Eclipse TE2000U, magnification 40X) using UV excitation.

Anti-hemolytic activity

Anti-hemolytic activity of NG and silymarin was studied as described[21]. Briefly, blood was collected from healthy volunteers and centrifuged (3000 r/min) with an equal volume of sterilized Alsver solution (2% dextrose, 0.8% sodium citrate, 0.05% citric acid, and 0.42% sodium chloride in water) to obtain the packed cells. The cells were washed with isosaline (0.85%, pH 7.4) and diluted with phosphate buffer (0.15 mol/L, pH 7.4). RBCs (10^8 cells/mL) were incubated with triton × 100 (1 g/L) to induce 100% cell lysis, in absence and presence of test materials at 37℃ for 1 h. The *A* of the supernatant was determined at 540 nm.

CYP2E1 catalytic activity assay

CYP2E1 activity was determined by assaying *P*-nitrophenol hydroxylation in rat liver microsomes prepared by calcium precipitation method as described earlier[22]. In brief, 1 mg microsomes in presence and absence of test material caused hydroxylation of 100 mmol/L aniline hydrochloride in presence of 30 mmol/L cumene hydroperoxide in 0.1 mol/L Tris buffer, pH 7.5. Liberated *p*-aminophenol was treated with 1 mL of 1 mol/L Na_2CO_3 and 1 mL of 2% phenol solution in 0.5 mol/L NaOH. The samples were allowed to stand at room temperature for 30 min and read at 630 nm.

Lipid peroxidation analysis

Cells were plated onto 60 mm Petri dishes, and at the end of the treatment they were washed twice in cold PBS and harvested using rubber policeman in 1 mL PBS. To the resulting cell suspension, we added 2 mL

of TCA-TBA reagent (15% TCA + 0.375% TBA in 5 mol/L HCl) in glass tubes. Tubes were kept in a boiling water bath (100℃) for 1 h, and then cooled to room temp. The contents were centrifuged at 1500 × *g* for 10 min. Absorbance of the supernatants was read at 535 nm against blank. Malonyldialdehyde (MDA) was used to draw the standard curve. The results were expressed as nmoles MDA/mg protein.

In other set of experiments, 1 g/L of rat liver microsomes in 0.15 mol/L NaCl were incubated with 0.1 mmol/L $FeSO_4$ and 35 mmol/L H_2O_2 in the presence and absence of test materials to stimulate lipid peroxidation. Generation of MDA was determined by assaying for thiobarbituric acid-reactive substances (TBARS) as described[22].

Determination of glutathione levels

Cells were seeded onto 60 mm Petri dishes and collected after the corresponding treatments. The total GSH content (reduced form) of samples was assayed as described[23]. Briefly, after treatments, cells were washed with ice cold PBS containing 10 mmol/L EDTA and centrifuged at 1500 × *g*. The cell pellets were resuspended in PBS/EDTA solution with 35% perchloric acid. The cell suspensions were kept on ice for 10 min and vortexed in between 5 times. Cell suspension was centrifuged at 13000 r/min for 10 min at 4℃. The supernatant was transferred to fresh tubes and the pH adjusted to 7 with triethanolamine, 1 mol/L, K_2CO_3 1.65 mol/L and EDTA 30 mmol/L. The contents were centrifuged at 13000 r/min for 10 min. To the 50 μL of the supernatant, we added 1850 μL of PBS/EDTA solution and 100 μL of o-phthaldehyde (1 g/L in methanol). The samples were incubated in the dark for 20 min and read at 350 nm (excitation) and 420 nm (emission) with a fluorescent spectrofluorometer (Perkin Elmer; LS-55).

Determination of cytochrome C by HPLC

Cytochrome C was determined as described[24]. Briefly, the reaction medium (2.5 mL) containing mitochondria (1 mg protein/mL) was 0.2 mol/L sucrose, 1 mmol/L KH_2PO_4, 5 mmol/L succinate, 2 μmol/L rotenone, 10 mmol/L Tris-MOPS, pH 7.3 at 25℃. Mitochondria were preincubated with test materials [NG, silymarin and cyclosporin A (CsA; 0.2 μmol/L)] for 10 min, and then in presence of CCl_4 (2 mmol/L) for 30 min. After incubation, aliquots of mitochondrial suspensions were centrifuged at 11000 × *g* for 8 min to obtain the supernatant. Finally, the supernatant (50 μL) was introduced into an HPLC system equipped with a reverse-phase C4 Cosmosil column (150 mm × 4.6 mm, 5-μm particle size, equipped with a UV-visible detector (393 nm). The column (Spelco; Supercosil LC-304; 24 μm × 4.6 μm × 5 μm) was eluted with a linear gradient of acetonitrile-water (solvents modified with 0.1 mL/L trifluoroacetic acid); the gradient started at 20% acetonitrile and changed to 60% during 12 min and the flow rate was 1.0 mL/min. The column was then washed with the 60% acetonitrile for 5 min followed by reequilibration for 5 min in the 20% acetonitrile.

Preparation of rat liver mitochondria

Mitochondria from livers of rats (Wistar) were prepared as described[25]. In brief, rat livers were washed once with physiological saline, dissected and washed twice in cold isolation solution (200 mmol/L D-mannitol, 70 mmol/L sucrose, 2 mmol/L HEPES, 0.5 g/L BSA). Dissected livers were minced with two volumes of isolation solution and homogenized (IKA homogenizer-WERK, Ultra Turrax, T 25 B). The homogenate was diluted with 7 volumes of isolation buffer and centrifuged for 10 min at 560 × *g*. The supernatant collected was again centrifuged for 15 min at 7000 × *g*. The mitochondrial pellet was collected and resuspended in 2.5 volumes of isolation solution and stored at -80℃ until use.

Measurement of intracellular calcium

Intracellular calcium levels were determined with the fluorescent calcium indicator fura2-AM by ratiometric fluorimetry as described[26]. HuH-7 cells were detached from the plate using HBSS buffer (118 mmol/L NaCl, 4.6 mmol/L KCl, 10 mmol/L glucose, 20 mmol/L Hepes, pH 7.2) containing 0.02% EDTA, resuspended in HBSS with 1 mmol/L $CaCl_2$, and incubated with 1 μmol/L fura2-AM in the dark for 1 h at 37℃. Cells were washed with HBSS/$CaCl_2$, and resuspended in HBSS/$CaCl_2$ at a density of 1×10^6 cells/mL. EGTA (10 mmol/L) was added at the beginning of the experiment, followed by a 60 s-equilibration period[27]. Intracellular free calcium measurements were performed at 37℃ using a ratiometric fluorescence spectrophotometer (Perkin-Elmer LS 50B). Intracellular Ca^{2+} concentration was estimated as described[28] based on the equation: $[Ca^{2+}]_i = K_d[(R-R_{min})/(R_{max}-R)]F_{min(380)}/F_{max(380)}$, where R is F_{340}/F_{380} ratio, R_{min} and R_{max} are the ratios with 50 mmol/L digitonin, and 50 mmol/L digitonin + 11 mmol/L $CaCl_2$, respectively. K_d represents the apparent dissociation constant of Fura-2 (224 nmol/L) and $F_{min(380)}/F_{max(380)}$ are the fluorescence values of digitonized cells without or with 11 mmol/L $CaCl_2$, respectively.

Flow cytometric analysis of mitochondrial membrane potential ($\Delta\psi_m$)

Changes in the mitochondrial membrane potential ($\Delta\psi_m$) were examined by monitoring the cell fluorescence after staining with rhodamine 123 (Rh123) as described[29]. Rh123 is a membrane permeable fluorescent cationic dye that is selectively taken up by mitochondria directly proportional to the MMP[30]. The intensities from Rh123 and PI were determined using a BD-LSR flow cytometer equipped with electronic doublet discriminating capability.

Intracellular measurement of reactive oxygen species (ROS)

The production of ROS was monitored with DCF-DA as the probe[31]. DCF-DA diffuses through the cell membrane and is enzymatically hydrolyzed by

intracellular esterases to nonfluorescent DCF-H, which is then rapidly oxidized to the highly fluorescent DCF in presence of ROS. Treated and non-treated HuH-7 cells were incubated for 1 h with DCF-DA (2 μmol/L) and, after the washing of cells, the production of free radicals were assessed *in situ* as the enhancement of fluorescence at excitation wavelength of 500 nm and emission wavelength of 520 nm and was measured in a fluorescent plate reader (Perkin Elmer LS 55, USA).

Measurement of intracellular H_2O_2

Intracellular H_2O_2 levels were analyzed using 123 dihydrorhodamine (123-DHR) as specific fluorescent dye probe as described by Katiyar *et al* with modifications for HuH-7 cells[32]. Briefly, non-treated and treated HuH-7 were washed twice with PBS and incubated in the culture medium without FCS and loaded with 123-DHR (5 μmol/L). Cells were further incubated for 45 min to irreversibly oxidize and convert DHR to fluorescent compound rhodamine 123 and fluorescence was read with aid of spectrofluorometer (Perkin Elmer LS 55, USA) with excitation wavelength 485 nm and emission wavelength of 530 nm. The cells for fluorescent-based assays were grown onto sterile black fluorescent plates (96 well format; Nunc, Denmark).

Cell cycle analysis (apoptosis)

Cell cycle was analysed as described by Yang *et al*[33]. Briefly, non-treated and treated HuH-7 cells were harvested by trypsinization, centrifuged at 1500 × *g* for 5 min, washed with PBS, and fixed in 70% ethanol at 4℃ overnight. Fixed cells were washed twice with PBS and incubated in PBS containing 1.5 mg/L RNase A for 1 h at 37℃, followed by staining with 5 μL PI (1 mmol/L stock) for 20 min on ice. The cells were analyzed for DNA content using BD-LSR flow cytometer equipped with electronic doublet discrimination capability using blue (488 nm) excitation from argon laser. Data were collected in list mode on 10 000 events for FL2-A *vs* FL2-W.

DNA laddering

DNA fragmentation was analysed as described by Yang *et al*[33]. Briefly, HuH-7 cells treated or untreated were harvested and centrifuged at 1500 × *g* for 5 min. After washing twice with PBS/ethylenediamine-*N, N, N′, N′*-tetraacetic acid (EDTA). Cells were incubated in a lysis buffer [0.5 mL/L Triton X-100, 10 mmol/L EDTA, 0.4 g/L proteinase K, and 10 mmol/L Tris-HCl, pH 7.4] at 56℃ for 1 h. Cell lysate was treated with 0.4 g/L RNase at 37℃ for 30 min. The genomic DNAs were purified by phenol/chloroform extraction and ethanol precipitation, and resuspended in a Tris-EDTA buffer, DNA fragments were stained with ethidium bromide and visualized by 2.5% agarose electrophoresis.

Enzymic assay of caspase 3-activity

Caspase activation was measured using a caspase 3 fluorometric assay kit (BD Apoalert caspase 3 fluorescent assay kit). HuH-7 cells, treated or untreated were harvested, and centrifuged (approximately 1 mg protein) at 400 × *g* for 5 min. The cell pellets were re-suspended in 50 μL of chilled cell lysis buffer and incubated on ice for 10 min, and the lysates were centrifuged at 15 000 × *g* for 10 min at 4℃ to precipitate cellular debris. A total of 50 μL of cell lysates was incubated with 50 μL of reaction buffer/DTT mix. DEVD-CHO was used as an inhibitor of caspase 3 in an induced sample. Five μL of 1 mmol/L caspase-3 substrate (DEVD-AFC at a final concentration of 50 μmol/L) was added to each sample. The samples were incubated at 37℃ for 1 h and read on a spectrofluorometer (Perkin Elmer LS 55) with excitation wavelength 400 nm and emission wavelength of 505 nm.

Cytosolic phospholipase A_2 assay

$cPLA_2$ activity was measured in cell lysates, using $cPLA_2$ assay kit (Cayman Chemical Company $cPLA_2$ assay kit) as per the instructions of the supplier. The kit involves the principle that $cPLA_2$ exhibits specificity towards arachidonic acid. Arachiconyl thio-PC is used as a synthetic substrate to detect the phospholipase activity. Hydrolysis of the arachiconoyl thioester bond at the *sn*-2 position by $cPLA_2$ releases free thiol which are detected by DTNB (5, 5'-dithiobis-2-dinitrobenzoic acid).

Adenosine 3', 5'-cyclic monophosphate (cAMP) assay

cAMP activity was measured in the cell lysates, using cAMP assay kit (R&D Systems, Inc, cAMP assay kit) as per the instructions of the supplier. The kit is based on the competitive binding technique in which cAMP present in a sample competes with a fixed amount of horseradish peroxidase (HRP)-labeled cAMP for sites on a mouse monoclonal antibody. During the incubation, the monoclonal antibody becomes bound to the goat anti-mouse antibody coated onto the microplate. Following a wash to remove excess conjugate and unbound sample, a substrate solution is added to the wells to determine the bound activity. The colour developed was stopped and the absorbance read at 450 nm. The intensity of the colour is inversely proportional to the concentration of cAMP in the sample.

2, 2'-azino-di-[3-ethylbenzthiazoline sulphate] oxidation inhibition assay (ABTS assay)

The assay was performed using antioxidant assay kit from Cayman Chemical Company, as per the instructions by the manufacturer. The assay was used to access the ability of the test materials (NG, Silymarin *etc*) to inhibit the oxidation of ABTS to $ABTS^{\cdot+}$ by metmyoglobin. The amount of $ABTS^{\cdot+}$ produced in absence and presence of test material was monitored by reading absorbance at 750 nm. Suppression of the absorbance at 750 nm in presence of test material is proportional to their antioxidant activity. The capacity of the antioxidant activity (inhibition of $ABTS^{\cdot+}$ formation) in the test sample was compared with that of Trolox, a water-soluble tocopherol analogue.

1,1-diphenyl-2-picrylhydrazyl (DPPH) discolouration assay

This assay was performed as described by Gonzalez

et al[34]. In brief, for the assay, various concentrations of test compound were added to 3 mL of DPPH solution (20 mg/L methanol) and incubated for 5 min at 25℃. The absorbance was measured al 517 nm. A 100% decoloration was established using methanol-water 2:1 and the percentage of DPPH decoloration was calculated.

Superoxide anion scavenging activity

In vitro effect of NG on superoxide anion radical generation was studied as described previously[35]. Two reaction systems used were: (a) enzymic ; (b) non-enzymic. System (a) comprised of 100 μmol/L xanthine, 600 μmol/L nitroblue tetrazolium (NBT) and 0.07 U/mL xanthine oxidase in 50 mmol/L sodium carbonate pH 9.2, incubated for 10 min in presence and absence of test materials and *A* read at 560 nm. System (b) comprised of 10 μmol/L phenazine methosulphate, 78 μmol/L NADH, 25 μmol/L NBT, incubated for 2 min in presence and absence of test materials and *A* read at 560 nm.

Protein estimation

Protein concentration was measured with BCA Protein Assay Kit from Pierce (Rockford, IL, USA) as per the instructions of the manufacturer.

Statistical analysis

Results are expressed as mean ± SD. Comparisons were made between control and treated groups unless otherwise indicated using unpaired Student's *t*-test and *P* values < 0.05 were considered statistically significant.

RESULTS

Standardization of NG

For better scientific and clinical acceptability and proper global positioning of plant based products, it has become implicit to determine their chemical profile data on the basis of purity of compound. In this respect we have developed the HPLC protocol for NG (Figure 1). HPLC profile confirmed that NG was isolated as < 95% pure.

Cytoprotective and membrane stabilizing effect of NG and silymarin against CCl_4-induced cytotoxicity in HuH-7 cells

CCl_4 produced a concentration dependent loss of viability in HuH-7 cells as evaluated by MTT assay. At 24 h of incubation, the IC50 value of CCl_4 was found to be 2 mmol/L approximately (1.958 mmol/L; Figure 2A). This concentration was used to generate oxidative stress to study the cytoprotective effect of NG and silymarin in further experimentations. NG alone was not toxic under the assay conditions up to a concentration of 400 mg/L. However, silymarin at concentrations above 50 mg/L produced loss of cell viability, with an estimated IC50 value of 413.38 mg/L (Figure 2B).

To characterize the protective effect of NG and silymarin on CCl_4 induced cytotoxicity in HuH-7 cells,

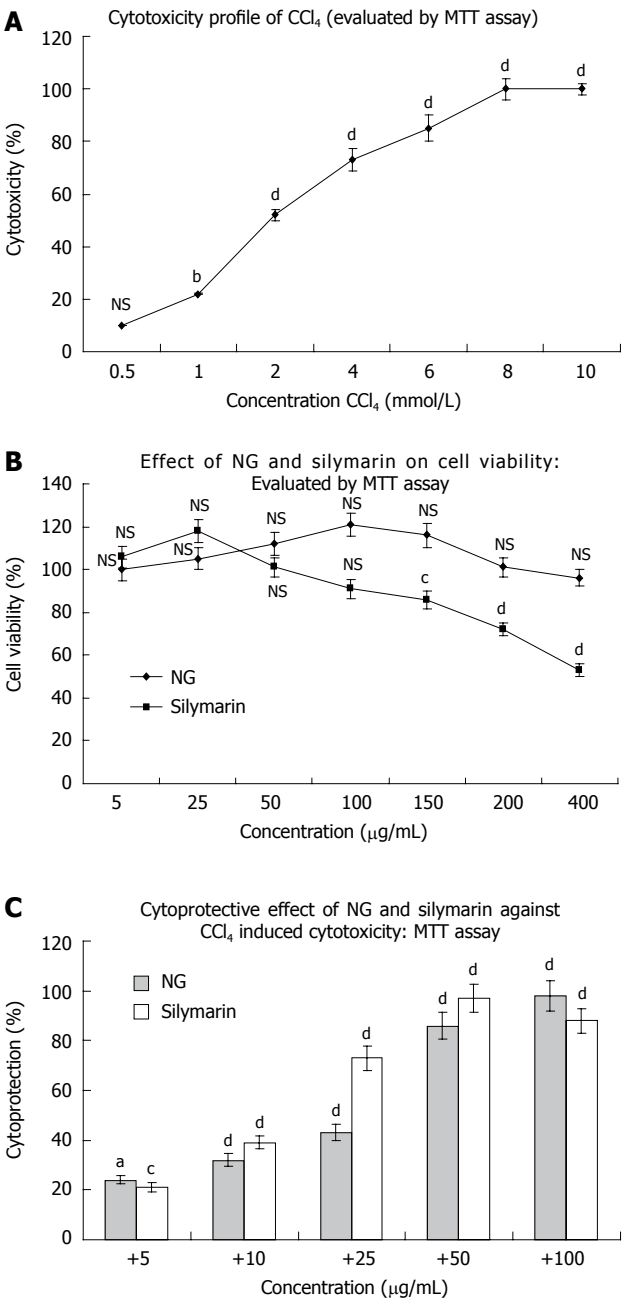

Figure 2 Cytotoxicity profile of CCl_4 and protective effect of NG and silymarin on CCl_4-induced inhibition of cellular proliferation in HuH-7 cells. For cell proliferation assay, HuH-7 cells grown in 24-well culture plate were incubated with indicated concentrations of test materials. Cell proliferation was assessed by MTT reduction assay. **A**, **B**: Represents inhibition of cell proliferation by CCl_4 and test materials (NG and silymarin); **C**: Represents protection of NG and silymarin, against CCl_4 induced inhibition of cell proliferation. HuH-7 cells were treated with various concentrations of NG and silymarin (5 to 100 mg/L) 1 h before treatment with CCl_4 for 24 h and the cell proliferation was determined by MTT reduction assay. Control wells received medium containing DMSO (< 0.2 mL/L). The % cell cytoxicity, % viability and % cytoprotection was calculated as, % Cytotoxicity = (Control - Test)/Control x 100, % Cell viability = % Cytotoxicity - 100, % Cytoprotection = 100 - (Treated - Control)/(CCl_4 - Control) x 100. Data are mean ± SD (n = 8) and representative of one of three similar experiments and statistically significant *P* values: $^bP < 0.01$; $^dP < 0.001$; $^aP < 0.02$; $^cP < 0.05$; NS: Non-significant, CCl_4 treated *vs* control cells; CCl_4 + LIV-1/silymarin *vs* CCl_4 treated cells.

dose-response experiments were conducted using various concentrations of NG and silymarin. NG showed a significant dose dependent protective effect

against CCl_4 induced loss of cell viability. The PC50 (50% protective concentration) for NG was estimated to be 24.46 mg/L and 15.30 mg/L for silymarin (Figure 2C).

Results obtained from MTT assay were in total correlation with the extent of cell death as confirmed by morphological changes observed under light microscope and Hoechst 33258 staining under fluorescence microscopy (Figure 3). Treatment with CCl_4 caused HuH-7 cells to lose their normal structure with signs of cell swelling, most of the cells were detached and monolayer was disturbed (Figure 3 I A compared with Figure 3 I B). These structural changes were prevented to a large extent by 30 and 100 μg/mL of NG and were comparable with the protection offered by silymarin at 50 mg/L (Figure 3 I C-F).

Nuclei of untreated HuH-7 cells appeared prominently round in shape (Figure 3 II A). After exposure with CCl_4, cells showed morphological alterations and condensation of nuclei (Figure 3 II B). The prominent changes were accompanied by an increase in apoptotic bodies and increase in cellular debris. All these alterations were prevented by co-exposure with NG and silymarin in a dose dependent manner (Figure 3 II C-E).

The above mentioned cytoprotective results were further correlated with the membrane stabilizing effect of NG and silymarin against Triton X 100 (1 g/L)-induced membrane disruption in human RBCs. NG showed an effect in the range of 4% to 91% in a concentration dependent manner (5 mg/L to 100 mg/L) against a protective effect of 6% to 88% at the same concentration, shown by silymarin (Figure 4).

Effect of NG and silymarin on CYP2E1 catalytic activity

To study the mechanism by which NG was preventing CCl_4-induced toxicity in HuH-7 cells, the possible interference of NG and silymarin on CYP2E1 activity (aniline hydroxylation) was studied. Hepatic microsomes from Wistar rats were used as a source to assay *in vitro* effect of NG and silymarin on CYP2E1 levels (Figure 5A). In another set of experiments, the CYP2E1 protein levels were analyzed to assay the protective effect of NG and silymarin against oxidation of 2.5 mmol/L ethanol (Figure 5B).

NG alone showed no significant effect on aniline hydroxylation levels at any concentrations used (5 to 100 mg/L), whereas silymarin produced an inhibitory effect in the range of 2.6% to 26.2% at the same concentrations (Figure 5A). Isoniazid (used as a positive control for inhibition of CYP2E1) showed a dose dependent inhibition, with IC50 at 500 μmol/L (data not shown).

Treatment of microsomes with 2.5 mmol/L ethanol caused an increase of 63% in aniline hydroxylation levels. Co-treatment of NG with ethanol showed no inhibitory effect on aniline hydroxylation levels induced by ethanol. However, silymarin caused inhibitions of 8.4%, 41%, 76% and 149% at 10 mg/L, 25 mg/L, 50 mg/L and 100 mg/L, respectively in aniline hydroxylation levels compared to microsomes treated with ethanol alone (Figure 5B).

The results (Figure 5 A and B) show that NG did not inhibit CYP2E21 activity, suggesting that NG is most probably acting as an antioxidant, and not as a CYP2E1 inhibitor and silymarin acts both as an antioxidant, and an inhibitor of CYP2E1.

Effect of NG and silymarin on $FeSO_4$ + H_2O_2 stimulated lipid peroxidation (LPO) in rat liver microsomes and on CCl_4 induced LPO in HuH-7 cells

$FeSO_4$ + H_2O_2 increased LPO in rat liver microsomes by 6.8-fold. Incubation with NG (10 to 100 mg/L) decreased in a range of 3% to 69%, this increase in LPO levels (Figure 6A). Silymarin at the equivalent concentrations showed an enhanced inhibitory effect of 21% to 111%. Treatment of HuH-7 cells with CCl_4, increased LPO levels up to 4.6-fold. NG offered a protective effect against this increase by 10.4%, 21%, 39%, 54% and 131% at 5 mg/L, 10 mg/L, 25 mg/L, 50 mg/L and 100 mg/L, respectively. At similar concentrations, silymarin produced respective inhibitory effects of 17%, 32%, 64%, 146% and 164% (Figure 6B).

Effect of NG and silymarin on the ROS generation induced by CCl_4

Oxidative stress was studied by fluorescence spectrophotometrical analysis of the levels of ROS, using DCF-DA and DHR as the probes. Figure 7 shows the mean values of DCF and DHR fluorescence for cell populations with various treatments. Treatment with CCl_4, increased by 2.1 (DCF) and 2.2-fold (DHR) the production of ROS in HuH-7 cells in comparison with no addition control. NG and silymarin (10 to 100 mg/L) reduced the increase in the ROS levels produced by CCl_4 in a significant and dose dependent manner. NG at 10 mg/L decreased DCF fluorescence intensity by 32% and DHR by 52%. At 50 mg/L, DCF and DHR intensities were decreased by 76% and 105%, respectively. At 100 mg/L, both the fluorescence intensities were down by 104% and 143%. H_2O_2 (500 μmol/L) was used as positive control for ROS generation.

Effect of NG and silymarin on intracellular Ca^{2+} and caspase 3 levels induced by CCl_4

Intracellular Ca^{2+} and caspase 3 levels were increased significantly by CCl_4 treatment, which reflects the requirement of Ca^{2+} and caspase 3 in the overall toxicity pathway of CCl_4 (Figures 8 and 9). CCl_4 caused an increase of 4.8-fold in Ca^{2+} and 2.3-fold in caspase 3 levels in HuH-7 cells. This abnormal rise in Ca^{2+} levels were decreased by NG by 15%, 72% and 106% and caspase 3 levels were decreased by 16%, 92% and 139% at 10 mg/L, 50 mg/L and 100 mg/L, respectively. Silymarin also showed a dose dependent inhibitory effect on Ca^{2+} and caspase 3 levels increased by CCl_4. The effect was 28%, 114% and 207% in Ca^{2+} levels at 10 mg/L, 50 mg/L and 100 mg/L, and 34% and 160% in caspase 3 levels at 10 mg/L and 50 mg/L, respectively. However at 100 mg/L, silymarin showed a less significant effect (28% decrease). Thus, silymarin showed a higher Ca^{2+} inhibitory effect compared to NG, but less caspase 3 inhibition at concentrations

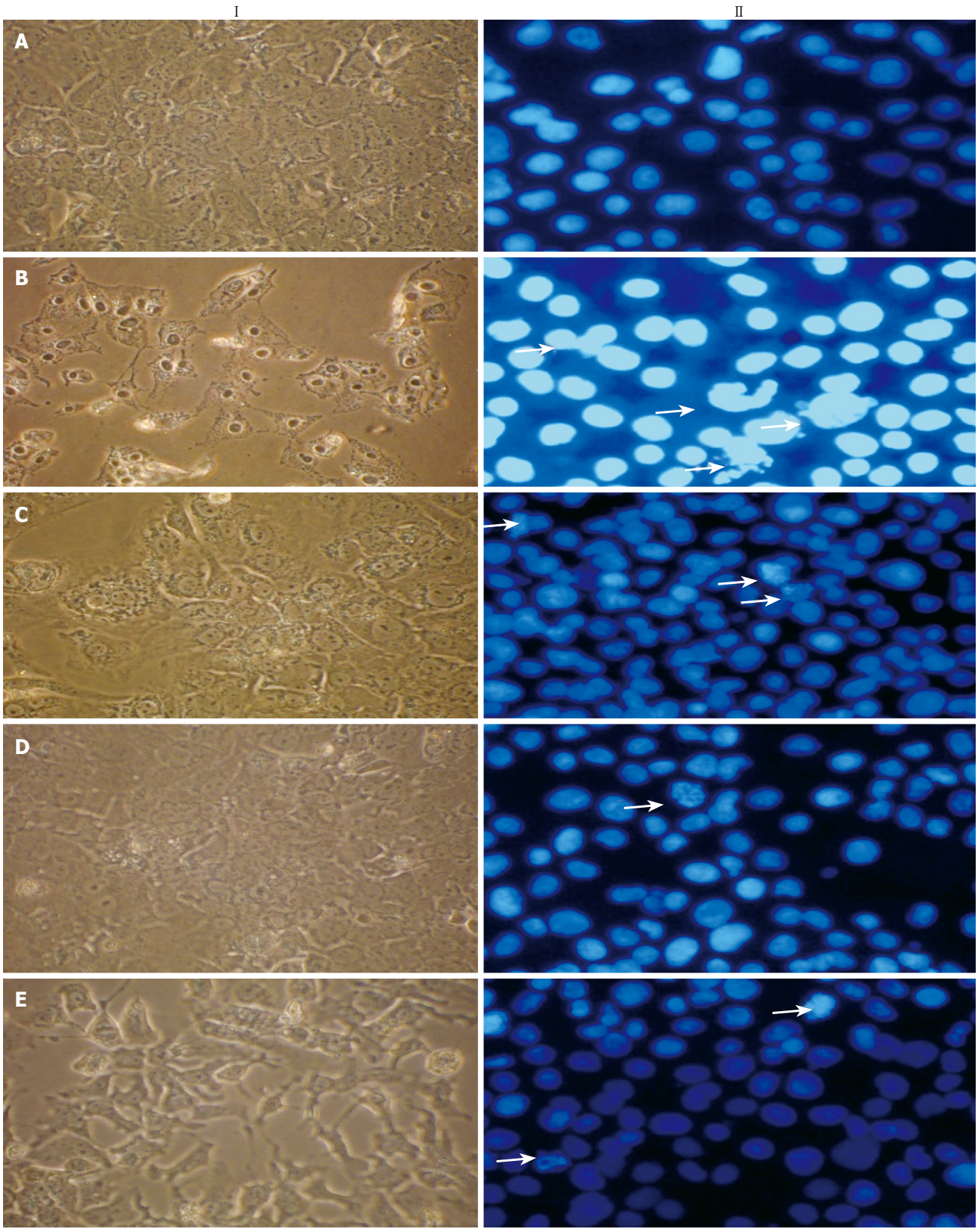

Figure 3 Effect of NG and silymarin against CCl_4-induced altered cellular and nuclear morphology of HuH-7 cells. NG and silymarin rescued CCl_4-induced cellular (Ⅰ) and nuclear morphological (Ⅱ) changes. Cellular morphology was observed by normal phase contrast microscopy, while as nuclear morphology was evaluated by Hoechst 33258 staining of HuH-7 cells and observed under fluorescence microscopy as described in Materials and Methods. These methods detected influences of CCl_4 on cellular and nuclear changes. **A**: Untreated control cells show normal cellular characteristics and rounded nuclei; **B**: Cells treated with CCl_4 (2 mmol/L) for 24 h show altered membrane structure and condensed chromatin/nuclei, apoptotic (arrows) and scattered apoptotic bodies; **C**: Cells incubated with NG (30 mg/L); **D**: Cells incubated with NG (100 mg/L); **E**: Cells incubated with silymarin (50 mg/L), 1 h before the treatment with CCl_4 showed protection against CCl_4-mediated cellular and nuclear alterations.

above 50 mg/L. Cyclosporine (10 μmol/L) was used as positive control for Ca^{2+} inhibition and camptothecin (inducer, 4 μmol/L) and DEVD-CHO (inhibitor, 20 μmol/L) were used as positive controls.

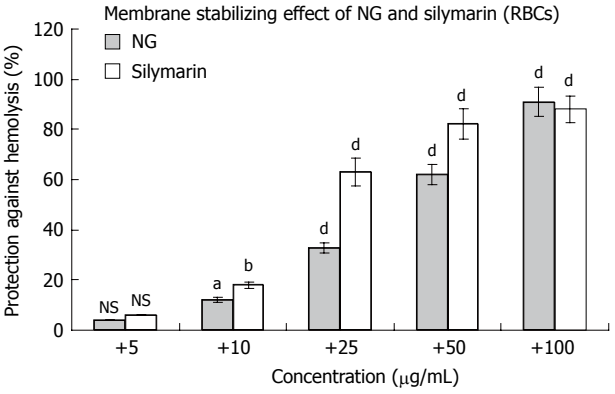

Figure 4 Membrane stabilizing effect of NG and silymarin on human RBCs. RBC suspensions were pre-incubated with or without (control) test materials and triton (1 g/L) in phosphate buffered saline as described in Materials and Methods section. Data are mean ± SD (n = 3) and representative of one of three similar experiments and statistically significant P values: $^{b}P < 0.01$; $^{a}P < 0.05$; $^{d}P < 0.001$; NS = Non-significant. Triton treated *vs* control cells; triton + NG/silymarin *vs* triton treated cells.

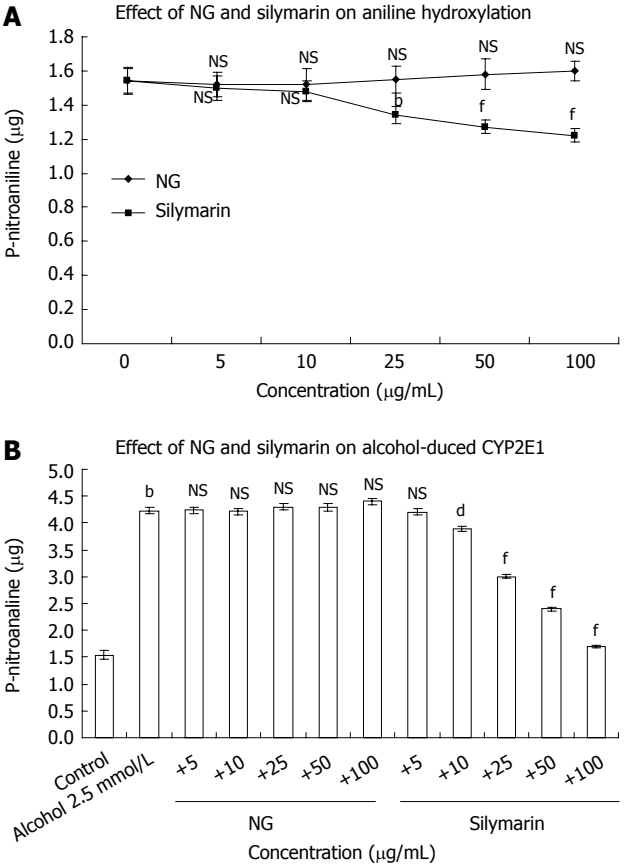

Figure 5 Effect of NG and silymarin *in vitro* on CYP2E1 catalytic activity. **A**: Rat liver microsomes were incubated in the absence or presence of different concentrations (5 to 100 mg/L) of test materials. CYP2E1 activity was assayed by following the hydroxylation of aniline hydrochloride in presence of cumene hydroperoxide as described in Materials and Methods section; **B**: Concentration dependent protection by NG and silymarin against alcohol (2.5 mmol/L)-induced aniline hydroxylase levels in rat liver microsomes. The microsomes were pre-incubated with medium containing various concentrations (5 to 100 mg/L) of test materials for 5 min before addition of alcohol and aniline hydroxylase levels were determined. Data are expressed as mean ± SEM and are from a representative experiments repeated twice and conducted in triplicate. P values: $^{b}P < 0.001$ *vs* the corresponding alcohol-treated microsomes; $^{d}P < 0.001$ and $^{f}P < 0.001$ *vs* alcohol-treated cells in presence of test materials; NS: Non-significant.

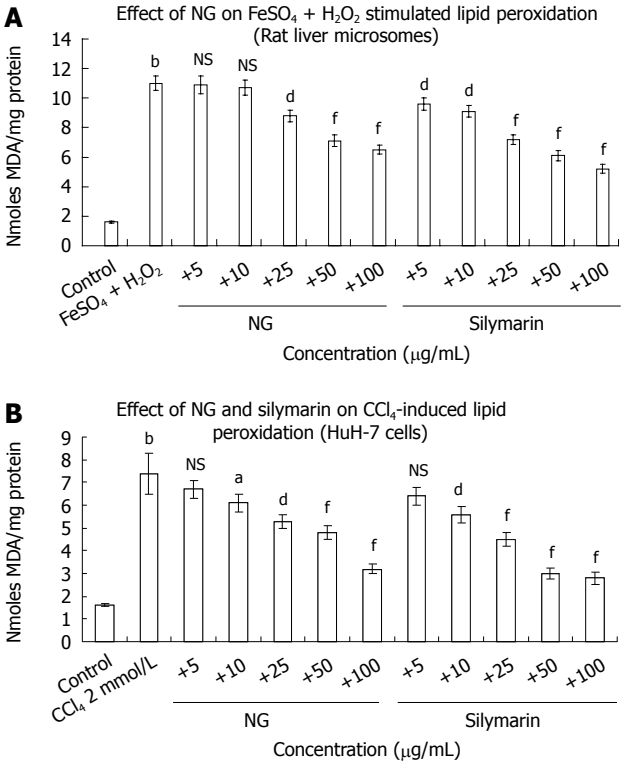

Figure 6 Protective effect of NG and silymarin against stimulated lipid peroxidation. **A**: Anti-lipid peroxidative effect of NG and silymarin *in vitro*. Liver microsomes (1 mg protein/mL, 0.15 mol/L NaCl, pH 7.0) were incubated for 20 min at 37℃ in the absence (control) and presence of 100 mmol/L $FeSO_4$ +/50 mmol/L H_2O_2 (stimulated). In identically set-up Fe^{2+}/H_2O_2-stimulated incubations, NG and silymarin (20 mg/L to 100 mg/L, in 30% DMSO) were added (test C). Control incubations received vehicle only; **B**: HuH-7 cells were pre-incubated for 1 h with medium containing test materials (NG and silymarin) at different concentrations (5 mg/L to 100 mg/L). The cells were further incubated in absence or presence of 2 mmol/L CCl_4 (stimulated) for further 24 h. The cells were harvested by scraping and assayed for the production of MDA using TBARS assay, as described under materials and methods section. Reaction was terminated by the addition of 2.0 mL TCA-TBA reagent (15% TCA, 0.375% TBA in 5mol/L HCl) and LPO content determined as nmol MDA formed/mg protein. Data are expressed as mean ± SD and are from representative experiments repeated twice and conducted in triplicate. Statistical significance, $^{b}P < 0.01$ *vs* the untreated control. $^{d}P < 0.01$; $^{a}P < 0.05$; $^{f}P < 0.001$ and NS: Non-significant *vs* stimulated ($FeSO_4$ + H_2O_2 and CCl_4 treatments).

Effect of NG and silymarin on cytochrome C release from isolated rat liver mitochondria induced by CCl_4

Isolated rat liver mitochondria were used to study the effect of NG and silymarin on cytochrome C release induced by CCl_4 (Figure 10). CCl_4 caused an increase of 2.1-fold in cytochrome C levels, which was inhibited by 75% and 105% at 50 mg/L and 100 mg/L of NG treatment, respectively. Silymarin showed an effect in the range of 27% at 10 mg/L, 135% at 50 mg/L. However at a higher concentration (100 mg/L), silymarin showed a biphasic effect, with a slight increase in cytochrome C levels compared to 50 mg/L (36% increase). Cyclospo-rine 5 μmol/L was used as a positive control for cytochrome C inhibition.

Effect of NG and silymarin on mitochondrial membrane permeability transition onset by CCl_4 in HuH-7 cells

Oxidative damage to mitochondria and the onset of MMP transition seems to play an important role in CCl_4-

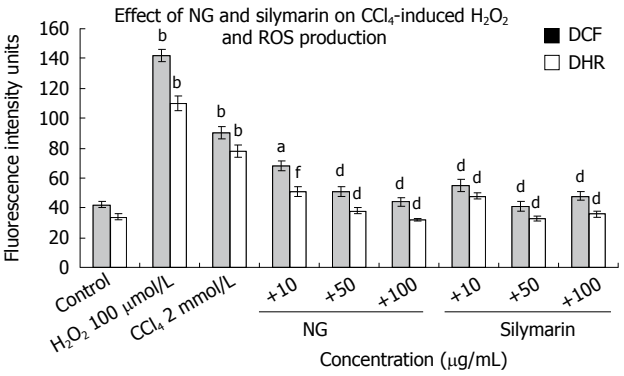

Figure 7 Effect of NG and silymarin on CCl_4-induced ROS production. HuH-7 cells were pre-incubated for 1 h with medium containing test materials (NG and silymarin) at different concentrations (10 to 100 mg/L). The cells were kept for further incubation in absence or presence of 2 mmol/L CCl_4 (stimulated). After 24 h of incubation maintaining the specific treatments, the cells were incubated with serum-free medium containing DCF-DA and 123-DHR and ROS levels were studied as mentioned in material and methods section. H_2O_2 (100 μmol/L) was used as positive control for ROS generation. Data are expressed as mean ± SD and are from representative experiments repeated twice and conducted in triplicate. Statistical significance, $^bP < 0.001$ *vs* the untreated control; $^dP < 0.001$, $^aP < 0.05$; $^fP < 0.01$ *vs* CCl_4-treated cells.

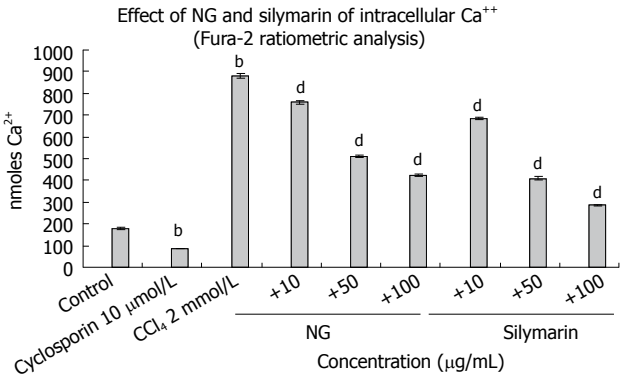

Figure 8 Effect of NG and silymarin against CCl_4-induced cytosolic free Ca^{2+} concentrations. HuH-7 cells pre-incubated for 1 h with medium containing test materials (NG and silymarin) at different concentrations (10 to 100 mg/L) were exposed to CCl_4 (2 mmol/L) for indicated time period, washed and loaded with Fura-2 AM as described in materials and methods section. Cyclosporine (10 μmol/L) was used as positive control. Data are expressed as mean ± SD, and are from a representative experiments repeated twice and conducted in triplicate. Statistical significance: $^bP < 0.001$ *vs* the untreated control, $^dP < 0.001$ *vs* CCl_4 treated cells.

induced toxicity in HuH-7 cells. MMP transitions were analyzed by flow cytometry after staining with Rh123 (Figure 11). Untreated HuH-7 cells were strong in Rh123 fluorescence intensity, suggestive of intact viable cells. A very small percentage of cells (8%) were showing low Rh123 fluorescence, reflective of damaged cells. CCl_4 caused a 6-fold increase in percentage of cells with low Rh123 fluorescence. Incubation in the presence of 50 mg/L and 100 mg/L of NG and silymarin, respectively significantly protected HuH-7 cells from decline in MMP produced by CCl_4.

Effect of NG and silymarin on CCl_4-induced apoptosis in HuH-7 cells

Apoptosis was studied by internucleosomal DNA fragmentation analysis and cell cycle analysis by flow

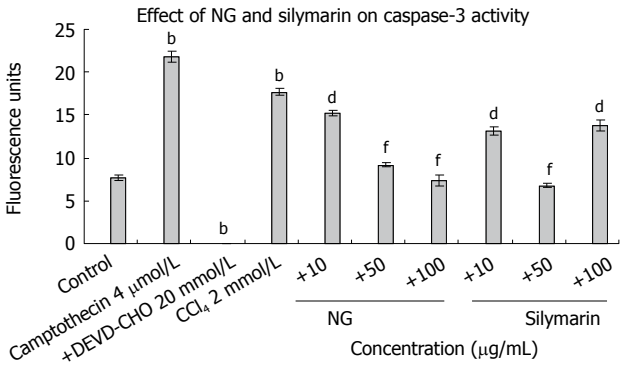

Figure 9 Effect of NG and silymarin against caspase 3-mediated apoptosis. CCl_4 treatment increases caspase 3 activity in HuH-7 cells. HuH-7 cells were treated with CCl_4 in presence or absence of test materials (NG and silymarin) and caspase 3 activity was measured as described in Materials and Methods section. Data are expressed as mean ± SD and are from representative experiments repeated twice and conducted in triplicate. Statistical significance: $^bP < 0.001$ *vs* the untreated control. $^dP < 0.01$; $^fP < 0.001$ *vs* CCl_4-treated cells.

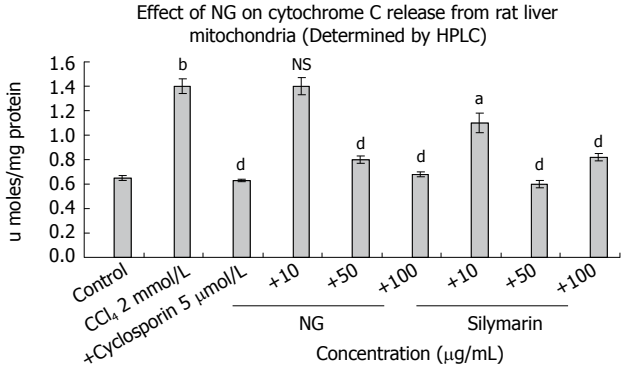

Figure 10 Effect of NG and silymarin against CCl_4-induced cytochrome C release from isolated rat liver mitochondria. CCl_4 treatment causes cytochrome C release form rat liver mitochondria. Mitochondria were treated with CCl_4 in presence or absence of test materials (NG and silymarin) and cytochrome C levels were measured as described in Materials and Methods section. Data are expressed as mean ± SD and are from a representative experiments repeated twice and conducted in triplicate. Statistical significance: $^bP < 0.001$ *vs* the untreated control; $^aP < 0.02$; $^dP < 0.001$ and NS = non-significant *vs* CCl_4 treated mitochondria.

cytometry. A DNA ladder formation was found with cells treated with CCl_4 (Figure 12). Treatment with NG and silymarin protected HuH-7 cells against CCl_4 induced DNA fragmentation.

In cell cycle analysis, treatment with CCl_4 markedly increased proportion of apoptotic cells significantly (49%). NG and silymarin had an obvious anti-apoptosis effect. As shown in Figure 13, the co-treatment with 25 mg/L, 50 mg/L and 100 mg/L of NG markedly reduced the percentage of the apoptotic cells to 27%, 14% and 11%, respectively. Silymarin showed a reduction in apoptotic cells by 21% and 9% at 25 mg/L and 50 mg/L, respectively. At 100 mg/L, however, silymarin had an effect of 18% (Figure 13).

Effect of NG and silymarin on CCl_4-induced alterations in cAMP and $cPLA_2$ levels in HuH-7 cells

To test the effect of CCl_4-induced oxidative stress on cAMP levels in HuH-7 cells, we evaluated cAMP with

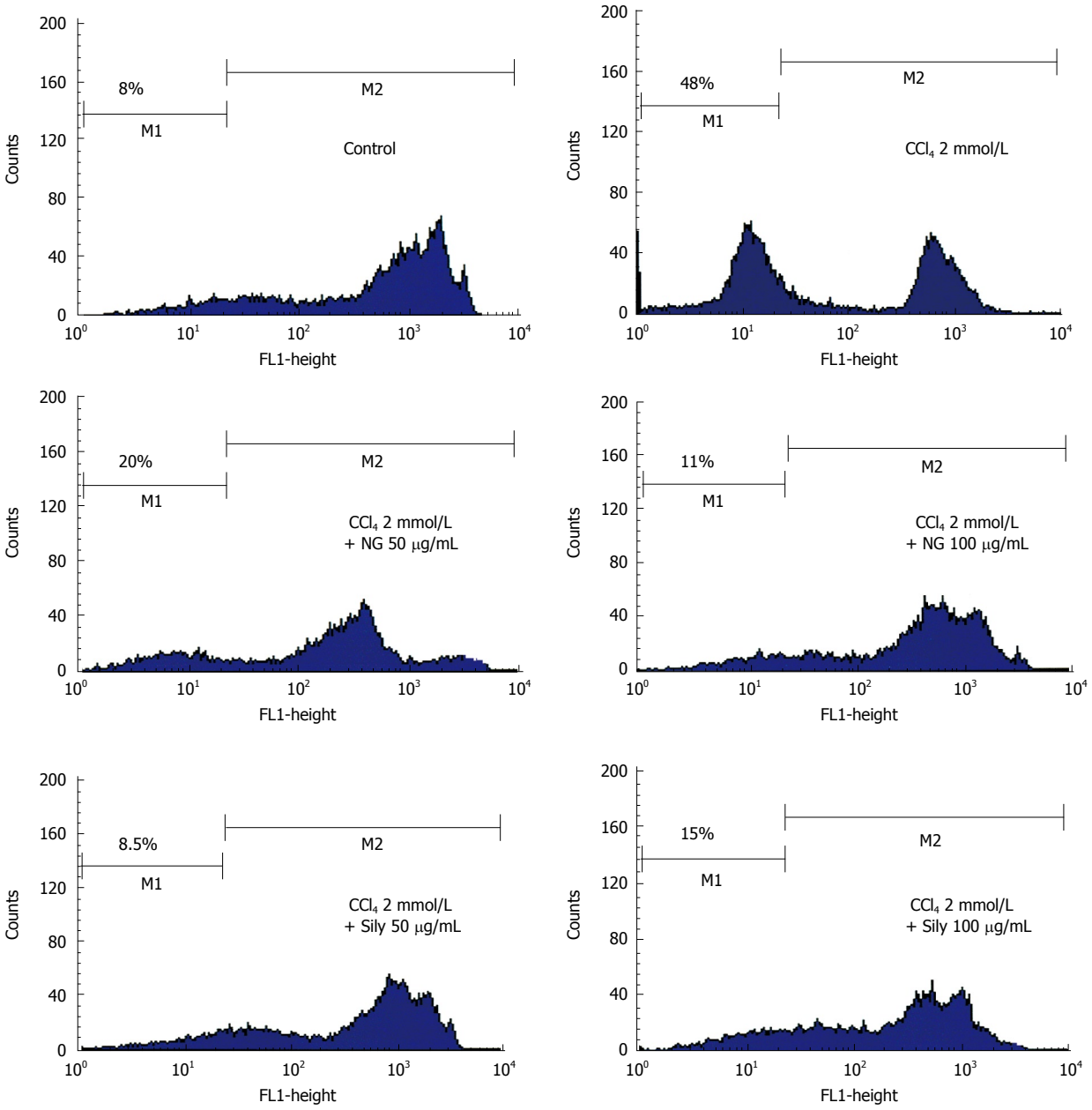

Figure 11 Effect of NG and silymarin against CCl_4-induced loss of mitochondrial membrane potential ($\Delta\psi m$). HuH-7 cells were pre-incubated for 1 h with test materials (NG and silymarin) at mentioned concentrations. The cells were further incubated for 24 h with CCl_4 (2 mmol/L). Thereafter, cells were stained with Rhodamine-123 and analysed by flow cytometry as described in Materials and Methods section. Representative histograms are shown and the percentage of cells in depolarized zone (M1 zone) are shown.

and without CCl_4 and then in the presence of CCl_4 with NG and silymarin. As hypothesized, cAMP levels were significantly reduced by CCl_4. Concomitant treatment of HuH-7 cells with NG significantly increased the levels of cAMP. Similar results were evident with treatment with silymarin. Forskolin (100 μmol/L) was used as a positive inducer of cAMP (Figure 14). On the contrary, phospholipase A2 levels were significantly increased with the CCl_4 treatment (2.3-fold). NG effectively reduced this increase by 44% at 10 mg/L and 304% at 50 mg/L. Silymarin reduced these levels by 97% at 10 mg/L and 136% at 50 mg/L. Bee venom (1 mg/L) was used as positive control to induce cPLA2 levels (Figure 15).

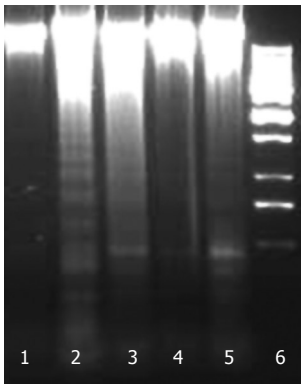

Figure 12 Effect of NG and silymarin against CCl_4-induced DNA fragmentation. HuH-7 cells were pre-incubated for 1 h with test materials (NG and silymarin) at mentioned concentrations. The cells were further incubated for 24 h with CCl_4 (2 mmol/L). Thereafter, genomic DNA was extracted from cells and subjected to gel electrophoresis as mentioned in Materials and Methods section. Lanes: 1: Control; 2: CCl_4 2 mmol/L; 3: CCl_4 2 mmol/L + NG 30 mg/L; 4: CCl_4 2 mmol/L + NG 100 mg/L; 5: CCl_4 2 mmol/L+ Silymarin 50 mg/L; 6: Ladder.

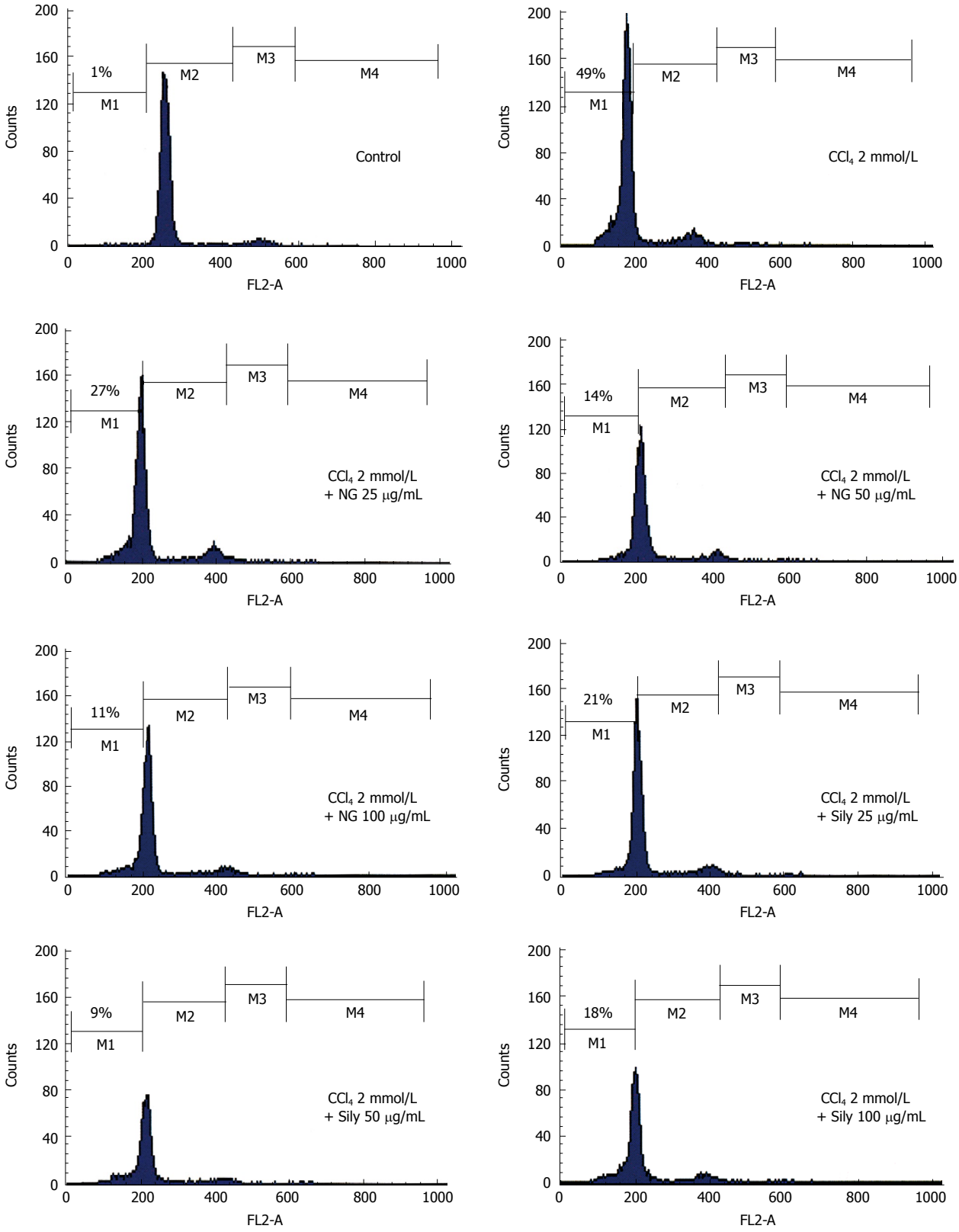

Figure 13 Effect of NG and silymarin against CCl_4-induced cell cycle arrest. HuH-7 cells were pre-incubated for 1 h with test materials (NG and silymarin) at mentioned concentrations. The cells were further incubated for 24 h with CCl_4 (2 mmol/L). Thereafter, cells were harvested by trypsinization, fixed with ethanol, stained with PI , and analyzed using flow cytometry. Representative histograms are shown, and the percentage of cells in the sub G_0/G_1 fraction (M1 zone, hypodiploid area) are shown.

Effect of NG and silymarin on CCl_4-induced depletion of GSH levels in HuH-7 cells

Figure 16 depicts the effect of CCl_4 on GSH levels and restorative effect of NG and silymarin in a dose-response manner. Treatment of HuH-7 cells with CCl_4-depleted the GSH content by 2 folds. Co-exposure with NG and silymarin effectively restored the depleted levels of GSH in a dose response manner. Restorative

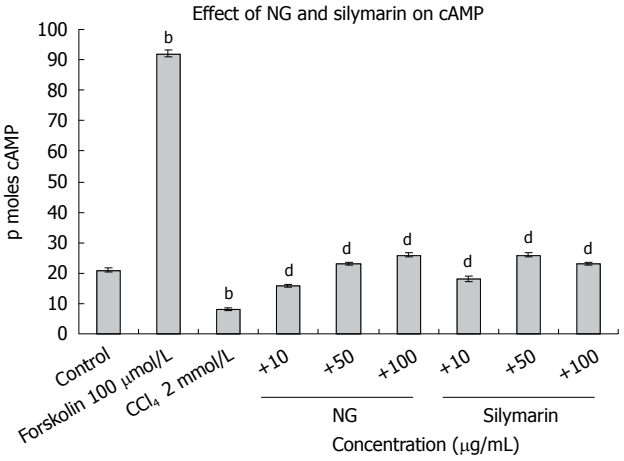

Figure 14 Effect of NG and silymarin against CCl_4-depleted cAMP levels. Pre-incubated, (1 hour at mentioned concentrations of NG and silymarin) HuH-7 cells were exposed to 2 mmol/L CCl_4 for 24 h. cAMP levels were determined in the cell culture supernatants as described in Materials and Methods. Forskolin (100 μmol/L) was used as positive control. Data are expressed as mean ± SD and are from representative experiments repeated twice and conducted in triplicate. Statistical significance: $^bP < 0.001$ *vs* the untreated control. $^dP < 0.001$ *vs* CCl_4-treated cells.

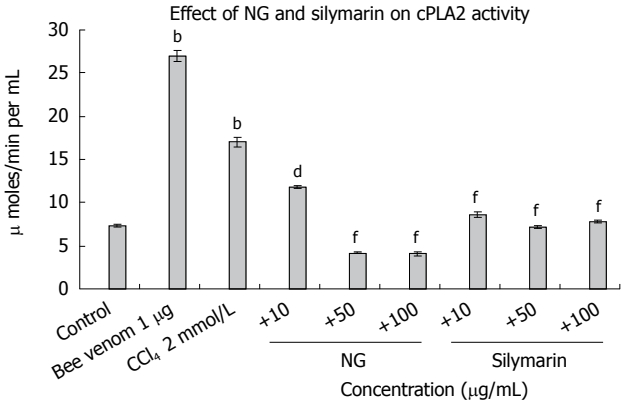

Figure 15 Effect of NG and silymarin against CCl_4-induced cPLA2 levels. Pre-incubated, (1 h with mentioned concentrations of NG and silymarin) HuH-7 cells were exposed to 2 mmol/L CCl_4 for 24 h. cPLA2 levels were determined as described in Materials and Methods. Bee venom (1 μg) was used as positive control. Data are expressed as mean ± SD and are from representative experiments repeated twice and conducted in triplicate. Statistical significance: $^bP < 0.001$ *vs* the untreated control; $^dP < 0.01$; $^fP < 0.001$ *vs* CCl_4-treated cells.

effect of NG was in the range of 17% to 147% at 5 mg/L to 100 mg/L, respectively. Silymarin showed an effect in the range of 23% to 152% at a concentration of 5 to 50 mg/L. However at higher concentration (100 mg/L), there was a slight decrease in this effect. BSO (100 μmol/L) was used as a positive inhibitor of GSH.

In vitro antioxidant activity of NG and silymarin

Figure 17 is representative of anti-oxidant activity of NG and silymarin. NG showed a strong activity, with I.C. 50 values of 17.31 mg/L for DPPH, 22.75 mg/L for enzymatic reaction, 13.49 mg/L for non-enzymatic reaction and 8.71 mg/L for ABTS assay. The IC 50 values of silymarin for the same assays were 34.07, 24.35, 21.10 and 12.36 mg/L respectively.

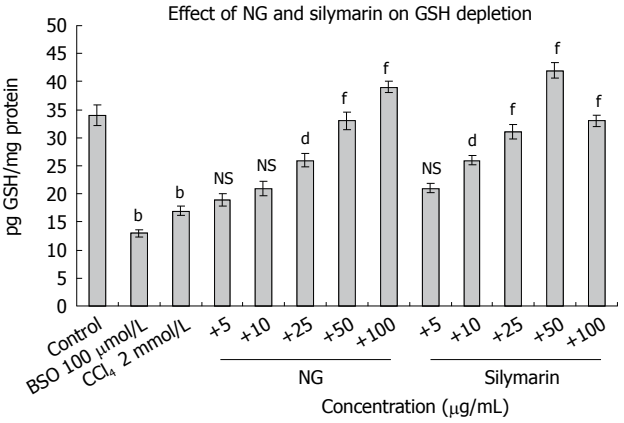

Figure 16 Effect of NG and silymarin on CCl_4-induced decrease in GSH levels. HuH-7 cells were pre-incubated with medium containing test materials (NG and silymarin) for 1 h. The cultures were then further incubated in presence and absence of CCl_4 for 24 h. The cells were harvested by scraping and GSH levels were determined as described under Materials and Methods section. BSO (100 μmol/L) was used as positive control. Data are expressed as mean ± SD and are from representative experiments repeated twice and conducted in triplicate. Statistical significance: $^bP < 0.001$ *vs* the untreated control; $^dP < 0.01$; $^fP < 0.001$; NS = non-significant *vs* CCl_4-treated cells.

DISCUSSION

Liver cells exposed to various chemicals/drugs (pro-oxidants) appear to be a useful *in vitro* model to characterize the biochemical and toxicological properties of such entities, and the possible protection provided by added agents[36]. The main goal of this work was to investigate the influence of an irridoid glycoside compound negundoside (NG) on CYP2E1-mediated toxicity in HuH-7 cells induced by CCl_4. Overall, the results of the present study indicate that NG is effective in protecting against the toxicity and the loss of viability induced by CCl_4.

The main mechanism by which CCl_4 is known to mediate its toxic effects is through oxidative stress and oxidative damage due to an increased production of ROS[37]. Induction of CYP2E1 by CCl_4 is one of the main pathways by which CCl_4 increases ROS production and generates a state of oxidative stress in the liver[38,39]. Since CYP2E1 is a key contributor to injury produced by CCl_4, one possible mechanism involved in the prevention of this toxicity by NG could have been an inhibition of CYP2E1 catalytic activity. Results in this study indicate that NG does not affect *p*-nitrophenol metabolism by CYP2E1 in liver microsomes under the experimental conditions (Figure 5 A and B); therefore, the mechanism by which NG affords its protection is not by inhibition of CYP2E1 activity. This is in confirmation to earlier reports in which many plant derived products like, *Scutellariae radix*[40], *Humulus lupulus*[41], green tea compounds[42] have also been shown to be hepatoprotective in other systems without any effect on CYP2E1 catalytic activity.

Bio-metals, such as iron are powerful catalysts of

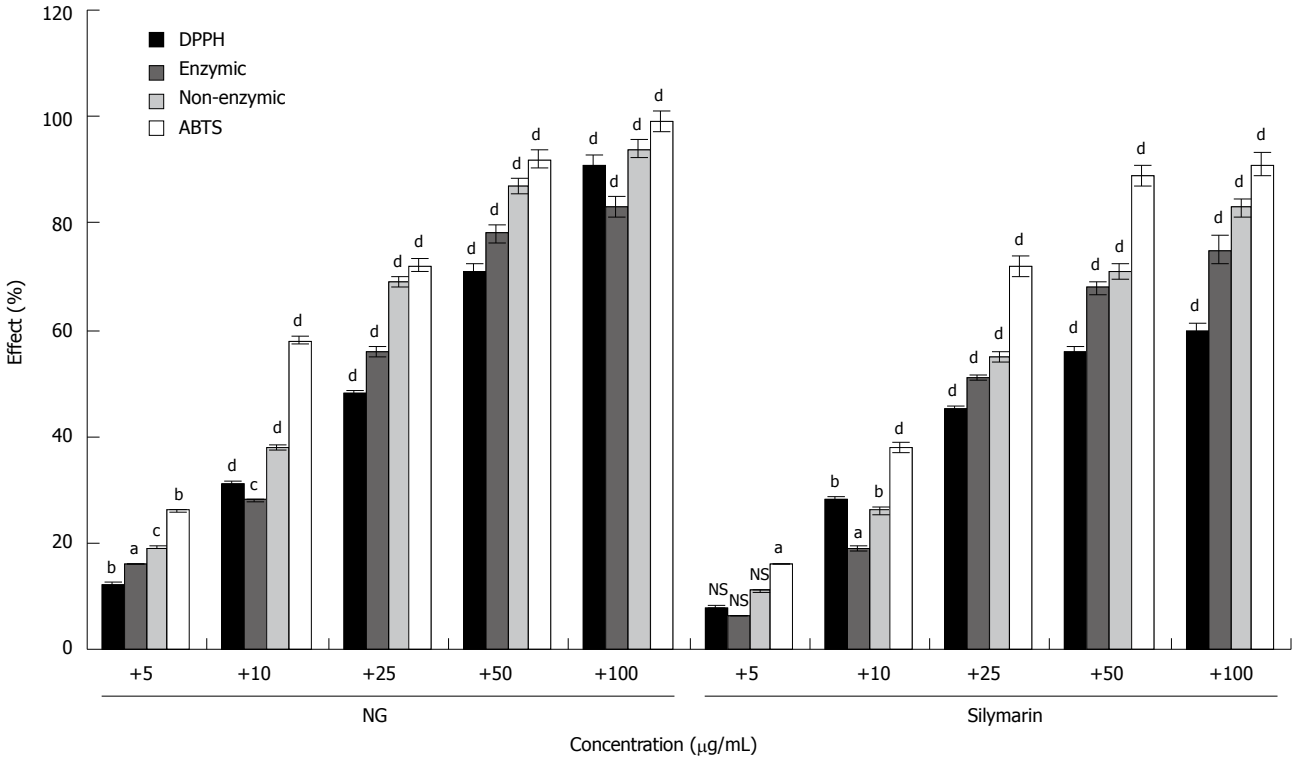

Figure 17 *In vitro* effect of NG and silymarin on free radicals generation. Free radicals scavenging effect of NG and silymarin was studied against DPPH radicals (stable hydroxyl radical), enzymic, non-enzymic (superoxide radicals) and ABTS radical (stable hydroxyl radical). Percentage anti-oxidant activity (% effect) was determined as described in Materials and Methods section. Values are mean from five independent determinations. $^{b}P < 0.001$ versus control. Control O.D. system DPPH, 0.650, system Enzymatic, 0.250 and system Non-enzymatic, 0.300 and system ABTS, 0.750. Data are expressed as mean ± SD and are from a representative experiments repeated twice and conducted in triplicate. Statistical significance: $^{a}P < 0.05$; $^{b}P < 0.01$; $^{c}P < 0.02$; $^{d}P < 0.001$; NS = non-significant *vs* respective controls.

free radical formation and lipid peroxidation processes, and polyunsaturated fatty acids in cellular membranes (microsomes) provide basic substrates for these reactions[43]. Scavenging or preventing formation of lipid radicals may prevent damage when cellular antioxidant defense mechanism is strengthened or iron overload is sequestered by exogenous treatment with cytoprotective drugs as NG. As lipid peroxidation (LPO) has been shown to play an important role in the ensuing toxicities in CYP2E1-induced conditions[44,45], in this respect, NG strongly inhibited lipid peroxidation promoted by H_2O_2+Fe in microsomes and CCl_4 in HuH-7 cells (Figure 6 A and B). It has been reported that glycosides, such as NG, are potent cytoprotective agents against oxidative stress induced cytotoxicity[46]. Therefore, one major mechanism underlying the effectiveness of NG in protecting against the CCl_4-induced LPO in HuH-7 cells may involve its capability to prevent lipid peroxidation chain reactions as a consequence of scavenging free radicals or chelating iron.

Intracellular calcium has been suggested to play a critical role in the oxidative damage of liver cells. Earlier, it has been reported that treatment of liver cells with CCl_4 increases calcium levels and produce cellular toxicity through calcium dependent pathways. Elevated levels of calcium initiates a cascade of signaling events leading to activation of calcium dependent degredative enzymes as phospholipases A2, endonucleases, or proteases[47]. Our results are in corroboration with this and showed that CCl_4-induced cell death in HuH-7 cells was mediated by release of intracellular calcium with subsequent activation of caspase 3 and cPLA2 (Figures 9 and 15) and simultaneous inhibition of cAMP levels (Figure 14). Increased intracellular calcium, activation of PLA2 and inhibition of cAMP were almost parallel to toxicity. Oxidative stress-mediated LPO is suggested to be the initiator of intracellular calcium release[25], which later influences down stream apoptotic signaling processes. cAMP levels are known to be regulated by catalytic activity of adenylate cyclase and phosphodiesterase. Increasing concentration of intracellular cAMP has been directly associated with inhibition of phosphodiesterase, reduced release of ROS and inhibition of chemotaxis, degranulation and cell death[48]. NG restored the calcium and cAMP to normal levels, inhibited lipid peroxidation, activated cPLA2 levels were inhibited and cytotoxicity was reversed without altering CYP2E1 levels. Therefore we hypothesize that NG inhibits CCl_4-induced oxidative stress and, hence LPO, which increases intracellular calcium and PLA2 activation and converge on mitochondria, inducing mitochondrial damage. All these downstream events of CYP2E1 mediated toxicity were effectively inhibited by NG, thus demonstrating its strong anti-oxidant capacity. We also suggest that inhibition of intracellular calcium release mediated cPLA2 activation, increase in cAMP levels, and restoration of MMP are the key factors in cytoprotection afforded by NG. Recently, it has been

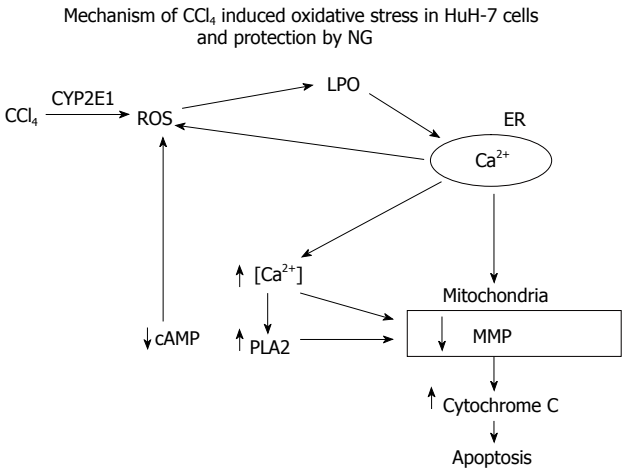

Figure 18 Proposed sequence of events and mechanism involved in the toxicity of CCl_4 and cytoprotection offered by NG. CCl_4 is activated by CYP 450 2E1 system and converted into trimethyl CCl_3 radicals inducing oxidative stress (increased ROS inducing membrane lipid peroxidation) and disturbed cellular Ca^{2+} homeostasis. Increase in intracellular Ca^{2+} concentrations leads to activation of phospholipase A2 and a decline in cAMP levels. All these signaling events converge onto the mitochondrial-initiating mitochondrial pore transition and ultimately to cellular injury. The highly increased levels of ROS is, in part, the consequence of the increase in Ca^{2+}, and also as a result of mitochondrial permeabilization resulting in activation of Ca^{2+} dependent proteases. NG exerts a protective effect *via* inhibition of oxidative stress, maintenance of disrupted intracellular calcium homeostasis and inactivation of Ca^{2+}-dependent proteases.

suggested that calcium levels do not play a direct role in toxicity[26], but that activation of PLA2, promotion of the mitochondrial permeability transition and loss of mitochondrial function, which are secondary manifestations of increased calcium levels, form a general pathway involved in the toxicity: all these events were restored to normal by NG.

As the main antioxidant inside mammalian cells, GSH plays a pivotal role in preventing oxidative stress and mitochondrial damage caused by numerous toxins[49]. Therefore, the effect of CCl_4 in the absence or presence of NG on GSH content was evaluated. CCl_4 treatment drastically depleted intracellular GSH in HuH-7 cells, an effect prevented in the presence of NG (Figure 16). Accordingly, the maintenance of intracellular GSH levels by NG may help in protecting against the oxidative toxicity induced by CCl_4 in HuH-7 cells and avoid cell degeneration and death. Previously as well, depletion of GSH has been shown to enhance CYP2E1 resulting in CYP2E1-derived ROS leading to toxicity[50].

Decreased MMP has been proposed to be a key mechanism by which CYP2E1-dependent LPO causes loss in cell viability. Mitochondria are a main source for generating ROS and, hence, a target for damage by oxidative stress[51]. In this respect, CCl_4 treatment caused a decrease in the MMP in HuH-7 cells, and this effect was prevented by NG as well as by silymarin (Figure 11). These results suggest that NG and silymarin may protect the cells by preventing oxidant-induced MMP transition leading to pathogenesis of necrotic or apoptotic cell death[52]. It has been proposed earlier that mitochondrial injury derived from oxidative damage can lead not only to necrosis by depleting ATP, but also to apoptotic cell death by inducing the release of mitochondrial factors such as cytochrome C, which activates the caspase cascade[53, 54].

Regardless of its precise mechanism of action, numerous studies in various animal models and in humans describe protective effects of NG against oxidative stress-related disease states[2-15]. This enhances its potential usefulness as a preventive agent toward oxidative damage involved in the development of liver injury caused by oxidative stress. Since NG acts as a very potent membrane stabilizer, it is also suggested that NG, may be acting as amphipathic substance, localizing near the membrane surface, trapping any radicals generated in the lipid environment of the membranes as well as in the cytosol. Such localization is suggested from the fact that CYP2E1 is found in the microsomes, and mitochondria appear to be a target for the CYP2E1-mediated damage in the presence of hepatotoxins such as CCl_4, which was effectively inhibited by NG. Moreover, NG is well tolerated without adverse health effects by humans even after oral administration at high doses as evident from its use in Asian traditional medicine practices for various ailments.

In conclusion, this report shows that NG can protect against CCl_4-induced toxicity and oxidative stress. The mechanism of protection involves decreased production of ROS and lipid peroxidation when the CYP2E1 mediated oxidative stress was produced in HuH-7 cells with pro-oxidant as CCl_4. The main mechanism involved in the cytoprotection of NG seems to be its ability to protect the mitochondria against depletion in its membrane potential, an event that is very critical in the loss of cell viability as a consequence of oxidative stress. This mechanism has been postulated in the Figure 18. NG has been shown to prevent CCl_4-induced liver injury, which may be, in part, due to the protection against CYP2E1-dependent oxidative stress as demonstrated in this study. NG supplementation could also prove to be protective against numerous toxicants that involve induction of oxidative stress through increased generation of ROS.

ACKNOWLEDGMENTS

We are grateful to Dr. GN Qazi, Director of this institute for providing constant guidance and support.

COMMENTS

Background

Vitex negundo is a reputed medicinal herb of Indian sub-continent. All plant parts are considered important in Ayurvedic system of medicine for various indications.

Research frontiers

Several pharmacological studies validate the medicinal claims of *Vitex negundo*. Diverse chemical constituents have been reported from various parts of this plant which are considered responsible for its varied pharmacological activities. The negundoside seems to be a potential constituent that exerts a protective effect on CYP2E1-dependent toxicity caused by carbon tetrachloride (CCl_4) *via* inhibition of lipid peroxidation, followed by an improved intracellular calcium homeostasis and inhibition of Ca^{2+}-dependent proteases.

Innovation and breakthrough

The present investigation shows that negundoside is a potent phytopharmaceutical that acts in a novel way in inhibiting liver toxicity by interfering in the key events that are the main causative factors leading to liver

dysfunction.

Applications

Negundoside exerts a protective action on CYP2E1-dependent oxidative stress and toxicity that may contribute to preventing chemically-induced liver injury, and may be useful in preventing toxicity by various other hepatotoxins as well.

Peer review

The authors investigated the anti-apoptotic effect of negundoside (NG), being extracted from leaves of Vitex negundo, on cultured human hepatoma cell line, HuH-7G2. The authors performed a large amount of experiments, and found that NG inhibited ROS formation, lipid peroxidation, intracellular calcium elevation, GSH depletion, elevated anti-oxidant activity, declined MMP, cytochrome C release, and finally carbon tetrachloride-medicated apoptosis. The manuscript addressed the authors' hypothesis with sufficient data.

REFERENCES

1 **Chin YW**, Balunas MJ, Chai HB, Kinghorn AD. Drug discovery from natural sources. *AAPS J* 2006; **8**: E239-E253

2 **Dharmasiri MG**, Jayakody JR, Galhena G, Liyanage SS, Ratnasooriya WD. Anti-inflammatory and analgesic activities of mature fresh leaves of Vitex negundo. *J Ethnopharmacol* 2003; **87**: 199-206

3 **Azhar-Ul-Haq**, Malik A, Khan MT, Anwar-Ul-Haq, Khan SB, Ahmad A, Choudhary MI. Tyrosinase inhibitory lignans from the methanol extract of the roots of Vitex negundo Linn. and their structure-activity relationship. *Phytomedicine* 2006; **13**: 255-260

4 **Jagetia GC**, Baliga MS. The evaluation of nitric oxide scavenging activity of certain Indian medicinal plants in vitro: a preliminary study. *J Med Food* 2004; **7**: 343-348

5 **Alam MI**, Gomes A. Snake venom neutralization by Indian medicinal plants (Vitex negundo and Emblica officinalis) root extracts. *J Ethnopharmacol* 2003; **86**: 75-80

6 **Chandramu C**, Manohar RD, Krupadanam DG, Dashavantha RV. Isolation, characterization and biological activity of betulinic acid and ursolic acid from Vitex negundo L. *Phytother Res* 2003; **17**: 129-134

7 **J Munasinghe TC**, Seneviratne CK, Thabrew MI, Abeysekera AM. Antiradical and antilipoperoxidative effects of some plant extracts used by Sri Lankan traditional medical practitioners for cardioprotection. *Phytother Res* 2001; **15**: 519-523

8 **Gupta M**, Mazumder UK, Bhawal SR. CNS activity of Vitex negundo Linn. in mice. *Indian J Exp Biol* 1999; **37**: 143-146

9 **Avadhoot Y**, Rana AC. Hepatoprotective effect of Vitex negundo against carbon tetrachloride-induced liver damage. *Arch Pharm Res* 1991; **14**: 96-98

10 **Perumal Samy R**, Ignacimuthu S, Sen A. Screening of 34 Indian medicinal plants for antibacterial properties. *J Ethnopharmacol* 1998; **62**: 173-1782

11 **Damayanti M**, Susheela K, Sharma GJ. Effect of plant extracts and systemic fungicide on the pineapple fruit-rotting fungus, Ceratocystis paradoxa. *Cytobios* 1996; **86**: 155-165

12 **Pushpalatha E**, Muthukrishnan J. Larvicidal activity of a few plant extracts against Culex quinquefasciatus and Anopheles stephensi. *Indian J Malariol* 1995; **32**: 14-23

13 **Bhargava SK**. Antiandrogenic effects of a flavonoid-rich fraction of Vitex negundo seeds: a histological and biochemical study in dogs. *J Ethnopharmacol* 1989; **27**: 327-339

14 **Hebbalkar DS**, Hebbalkar GD, Sharma RN, Joshi VS, Bhat VS. Mosquito repellent activity of oils from Vitex negundo Linn. leaves. *Indian J Med Res* 1992; **95**: 200-203

15 **Prabhakar A**, Gupta BD, Suri KA, Satti NK, Malhotra S, Gupta KK, Sharma VK, Johri RK, Jaggi BS, Chandan BK, Shankar L, Bedi KL, Suri OP, Qazi GN. Hepatoprotective activity of 2'-p-hydroxybenzoylmussaenodidic acid. United States patent, US Patent 7, 259, 148, 2007; **259:** 148

16 **Dey A**, Caro AA, Cederbaum AI. S-adenosyl methionine protects ob/ob mice from CYP2E1-mediated liver injury. *Am J Physiol Gastrointest Liver Physiol* 2007; **293**: G91-G103

17 **Kume Y**, Ikeda H, Inoue M, Tejima K, Tomiya T, Nishikawa T, Watanabe N, Ichikawa T, Kaneko M, Okubo S, Yokota H, Omata M, Fujiwara K, Yatomi Y. Hepatic stellate cell damage may lead to decreased plasma ADAMTS13 activity in rats. *FEBS Lett* 2007; **581**: 1631-1634

18 **Beddowes EJ**, Faux SP, Chipman JK. Chloroform, carbon tetrachloride and glutathione depletion induce secondary genotoxicity in liver cells via oxidative stress. *Toxicology* 2003; **187**: 101-115

19 **Jimenez-Lopez JM**, Cederbaum AI. Green tea polyphenol epigallocatechin-3-gallate protects HepG2 cells against CYP2E1-dependent toxicity. *Free Radic Biol Med* 2004; **36**: 359-370

20 **Lee CS**, Kim YJ, Han ES. Glycyrrhizin protection against 3-morpholinosydnonime-induced mitochondrial dysfunction and cell death in lung epithelial cells. *Life Sci* 2007; **80**: 1759-1767

21 **Gandhidasan R**, Thamaraichelvan, Baburaj S. Anti inflammatory action of Lannea coromandelica by HRBC membrane stabilization. *Fitoterapia* 1991; **62**: 81-83

22 **Tasduq SA**, Kaiser P, Sharma SC, Johri RK. Potentiation of isoniazid-induced liver toxicity by rifampicin in a combinational therapy of antitubercular drugs (rifampicin, isoniazid and pyrazinamide) in Wistar rats: A toxicity profile study. *Hepatol Res* 2007; **37**: 845-853

23 **Tietze F**. Enzymic method for quantitative determination of nanogram amounts of total and oxidized glutathione: applications to mammalian blood and other tissues. *Anal Biochem* 1969; **27**: 502-522

24 **Nakagawa Y**, Suzuki T, Kamimura H, Nagai F. Role of mitochondrial membrane permeability transition in N-nitrosofenfluramine-induced cell injury in rat hepatocytes. *Eur J Pharmacol* 2006; **529**: 33-39

25 **Kawamura-Sato K**, Hirama Y, Agata N, Ito H, Torii K, Takeno A, Hasegawa T, Shimomura Y, Ohta M. Quantitative analysis of cereulide, an emetic toxin of Bacillus cereus, by using rat liver mitochondria. *Microbiol Immunol* 2005; **49**: 25-30

26 **Caro AA**, Cederbaum AI. Role of intracellular calcium and phospholipase A2 in arachidonic acid-induced toxicity in liver cells overexpressing CYP2E1. *Arch Biochem Biophys* 2007; **457**: 252-263

27 **Rameh LE**, Rhee SG, Spokes K, Kazlauskas A, Cantley LC, Cantley LG. Phosphoinositide 3-kinase regulates phospholipase Cgamma-mediated calcium signaling. *J Biol Chem* 1998; **273**: 23750-23757

28 **Grynkiewicz G**, Poenie M, Tsien RY. A new generation of Ca2+ indicators with greatly improved fluorescence properties. *J Biol Chem* 1985; **260**: 3440-3450

29 **Caro AA**, Cederbaum AI. Ca2+-dependent and independent mitochondrial damage in HepG2 cells that overexpress CYP2E1. *Arch Biochem Biophys* 2002; **408**: 162-170

30 **Emaus RK**, Grunwald R, Lemasters JJ. Rhodamine 123 as a probe of transmembrane potential in isolated rat-liver mitochondria: spectral and metabolic properties. *Biochim Biophys Acta* 1986; **850**: 436-448

31 **Rothe G**, Valet G. Flow cytometric analysis of respiratory burst activity in phagocytes with hydroethidine and 2',7'-dic hlorofluorescin. *J Leukoc Biol* 1990; **47**: 440-448

32 **Katiyar SK**, Afaq F, Azizuddin K, Mukhtar H. Inhibition of UVB-induced oxidative stress-mediated phosphorylation of mitogen-activated protein kinase signaling pathways in cultured human epidermal keratinocytes by green tea polyphenol (-)-epigallocatechin-3-gallate. *Toxicol Appl Pharmacol* 2001; **176**: 110-117

33 **Yang D**, Yaguchi T, Yamamoto H, Nishizaki T. Intracellularly transported adenosine induces apoptosis in HuH-7 human hepatoma cells by downregulating c-FLIP expression causing caspase-3/-8 activation. *Biochem Pharmacol* 2007; **73**: 1665-1675

34 **Gonzalez-Avila M**, Arriaga-Alba M, de la Garza M, del

Carmen HernandezPretelin M, Dominguez-Ortiz MA, Fattel-Fazenda S, Villa-Trevino S. Antigenotoxic, antimutagenic and ROS scavenging activities of a Rhoeo discolor ethanolic crude extract. *Toxicol In Vitro* 2003; **17**: 77-83

35 **Tasduq SA**, Kaisar P, Gupta DK, Kapahi BK, Maheshwari HS, Jyotsna S, Johri RK. Protective effect of a 50% hydroalcoholic fruit extract of Emblica officinalis against anti-tuberculosis drugs induced liver toxicity. *Phytother Res* 2005; **19**: 193-197

36 **Cao J**, Jiang LP, Liu Y, Yang G, Yao XF, Zhong LF. Curcumin-induced genotoxicity and antigenotoxicity in HepG2 cells. *Toxicon* 2007; **49**: 1219-1222

37 **Arteel GE**. Oxidants and antioxidants in alcohol-induced liver disease. *Gastroenterology* 2003; **124**: 778-790

38 **Morimoto M**, Hagbjork AL, Nanji AA, Ingelman-Sundberg M, Lindros KO, Fu PC, Albano E, French SW. Role of cytochrome P4502E1 in alcoholic liver disease pathogenesis. *Alcohol* 1993; **10**: 459-464

39 **Tsukamoto H**. Cyp2e1 and ALD. *Hepatology* 2000; **32**: 154-156

40 **Kim JY**, Lee S, Kim DH, Kim BR, Park R, Lee BM. Effects of flavonoids isolated from Scutellariae radix on cytochrome P-450 activities in human liver microsomes. *J Toxicol Environ Health A* 2002; **65**: 373-381

41 **Henderson MC**, Miranda CL, Stevens JF, Deinzer ML, Buhler DR. In vitro inhibition of human P450 enzymes by prenylated flavonoids from hops, Humulus lupulus. *Xenobiotica* 2000; **30**: 235-251

42 **Obermeier MT**, White RE, Yang CS. Effects of bioflavonoids on hepatic P450 activities. *Xenobiotica* 1995; **25**: 575-584

43 **Wilhelm J**. Metabolic aspects of membrane lipid peroxidation. *Acta Univ Carol Med Monogr* 1990; **137**: 1-53

44 **Caro AA**, Cederbaum AI. Synergistic toxicity of iron and arachidonic acid in HepG2 cells overexpressing CYP2E1. *Mol Pharmacol* 2001; **60**: 742-752

45 **Chen Q**, Galleano M, Cederbaum AI. Cytotoxicity and apoptosis produced by arachidonic acid in Hep G2 cells overexpressing human cytochrome P4502E1. *J Biol Chem* 1997; **272**: 14532-14541

46 **Moon MK**, Choi BM, Oh GS, Pae HO, Kim JD, Oh H, Oh CS, Kim DH, Rho YD, Shin MK, Lee HS, Chung HT. Catalposide protects Neuro 2A cells from hydrogen peroxide-induced cytotoxicity via the expression of heme oxygenase-1. *Toxicol Lett* 2003; **145**: 46-54

47 **Manibusan MK**, Odin M, Eastmond DA. Postulated carbon tetrachloride mode of action: a review. *J Environ Sci Health C Environ Carcinog Ecotoxicol Rev* 2007; **25**: 185-209

48 **Matsuhashi T**, Otaka M, Odashima M, Jin M, Komatsu K, Konishi N, Wada I, Sato T, Horikawa Y, Ohba R, Oyake J, Hatakeyama N, Watanabe S. Specific type IV phosphodiesterase inhibitor ameliorates thioacetamide-induced liver injury in rats. *J Gastroenterol Hepatol* 2005; **20**: 135-140

49 **Balasubramaniyan V**, Shukla R, Murugaiyan G, Bhonde RR, Nalini N. Mouse recombinant leptin protects human hepatoma HepG2 against apoptosis, TNF-alpha response and oxidative stress induced by the hepatotoxin-ethanol. *Biochim Biophys Acta* 2007; **1770**: 1136-1144

50 **Zhuge J**, Cederbaum AI. Depletion of S-adenosyl-l-methionine with cycloleucine potentiates cytochrome P450 2E1 toxicity in primary rat hepatocytes. *Arch Biochem Biophys* 2007; **466**: 177-185

51 **Wu D**, Cederbaum AI. Cyclosporine A protects against arachidonic acid toxicity in rat hepatocytes: role of CYP2E1 and mitochondria. *Hepatology* 2002; **35**: 1420-1430

52 **Lemasters JJ**, Nieminen AL, Qian T, Trost LC, Elmore SP, Nishimura Y, Crowe RA, Cascio WE, Bradham CA, Brenner DA, Herman B. The mitochondrial permeability transition in cell death: a common mechanism in necrosis, apoptosis and autophagy. *Biochim Biophys Acta* 1998; **1366**: 177-196

53 **Lemasters JJ**, Qian T, Bradham CA, Brenner DA, Cascio WE, Trost LC, Nishimura Y, Nieminen AL, Herman B. Mitochondrial dysfunction in the pathogenesis of necrotic and apoptotic cell death. *J Bioenerg Biomembr* 1999; **31**: 305-319

54 **Hoek JB**, Cahill A, Pastorino JG. Alcohol and mitochondria: a dysfunctional relationship. *Gastroenterology* 2002; **122**: 2049-2063

S- Editor Yang RH **L- Editor** Negro F **E- Editor** Ma WH

Online Submissions: wjg.wjgnet.com
wjg@wjgnet.com
doi:10.3748/wjg.14.3710

World J Gastroenterol 2008 June 21; 14(23): 3710-3718
World Journal of Gastroenterology ISSN 1007-9327
© 2008 The WJG Press. All rights reserved.

BASIC RESEARCH

Hepatitis B virus DNA is more powerful than HBeAg in predicting peripheral T-lymphocyte subpopulations in chronic HBV-infected individuals with normal liver function tests

Jing You, Hutcha Sriplung, Alan Geater, Virasakdi Chongsuvivatwong, Lin Zhuang, Hong-Ying Chen, Jun-Hua Huang, Bao-Zhang Tang

Jing You, Hutcha Sriplung, Alan Geater, Virasakdi Chongsuvivatwong, Epidemiology Unit, Faculty of Medicine, Prince of Songkla University, Hat Yai, Songkhla 90110, Thailand
Lin Zhuang, Department of Hepatology, Third Municipal People's Hospital of Kunming, Kunming 650041, Yunnan Province, China
Hong-Ying Chen, Bao-Zhang Tang, Department of Infectious Diseases, First Affiliated Hospital of Kunming Medical University, Kunming 650032, Yunnan Province, China
Jun-Hua Huang, Department of Infectious Diseases, Yunnan General Hospital of the Chinese People's Armed Police Forces, Kunming 650111, Yunnan Province, China
Author contributions: You J, Sriplung H, Geater A and Chongsuvivatwong V conceptualized the study; You J and staff of the research group assisted with the data collection; You J was responsible for data management and data analysis; You J was responsible for interpretation of data; Sriplung H, Geater A and Chongsuvivatwong V provided advice and review; You J wrote the manuscript; All authors read and approved the final manuscript.
Correspondence to: Jing You, Epidemiology Unit, Faculty of Medicine, Prince of Songkla University, Hat Yai, Songkhla 90110, Thailand. jingyoukm@126.com
Telephone: +66-84-6320906 Fax: +66-74-212900
Received: January 26, 2008 Revised: March 2, 2008
Accepted: March 9, 2008
Published online: June 21, 2008

Abstract

AIM: To investigate the peripheral T-lymphocyte subpopulation profile, and its correlations with hepatitis B virus (HBV) replication level in chronic HBV-infected (CHI) individuals with normal liver function tests (LFTs).
METHODS: Frequencies of T-lymphocyte subpopulations in peripheral blood were measured by flow cytometry in 216 CHI individuals. HBV markers were detected with ELISA. Serum HBV DNA load was assessed with quantitative real-time PCR. Information of age at HBV infection, and maternal HBV infection status was collected. ANOVA linear trend test and linear regression were used in statistical analysis.
RESULTS: CHI individuals had significantly decreased relative frequencies of $CD3^+$, $CD4^+$ subpopulations and $CD4^+/CD8^+$ ratio, and increased $CD8^+$ subset percentage compared with uninfected individuals (all $P < 0.001$). There was a significant linear relationship between the load of HBV DNA and the parameters of T-lymphocyte subpopulations (ANOVA linear trend test $P < 0.01$). The parameters were also significantly worse among individuals whose mothers were known to be HBV carriers, and those having gained infection before the age of 8 years. In multiple regressions, after adjustment for age at HBV infection and status of maternal HBV infection, log copies of HBV DNA maintained its highly significant predictive coefficient on T-lymphocyte subpopulations, whereas the effect of HBeAg was not significant.
CONCLUSION: HBV DNA correlates with modification in the relative T-lymphocyte subpopulation frequencies. High viral load is more powerful than HBeAg in predicting the impaired balance of T-cell subsets.

© 2008 The WJG Press. All rights reserved.

Key words: Hepatitis B virus; Chronic hepatitis B virus infection; Hepatitis B virus DNA; T-lymphocyte subpopulation; Immune function

Peer reviewers: Juan Ramón Larrubia, MD, Gastroenterology Unit and Liver Research Unit, Guadalajara University Hospital, University of Alcalá, Donante de Sangre s/n, Guadalajara 19002, Spain; Jacob George, Professor, University of Sydney, Storr Liver Unit, Westmead Hospital, Westmead 2145, Australia

You J, Sriplung H, Geater A, Chongsuvivatwong V, Zhuang L, Chen HY, Huang JH, Tang BZ. Hepatitis B virus DNA is more powerful than HBeAg in predicting peripheral T-lymphocyte subpopulations in chronic HBV-infected individuals with normal liver function tests. *World J Gastroenterol* 2008; 14(23): 3710-3718 Available from: URL: http://www.wjgnet.com/1007-9327/14/3710.asp DOI: http://dx.doi.org/10.3748/wjg.14.3710

INTRODUCTION

Hepatitis B virus (HBV) infection is a global public

health problem. It is estimated that approximately 2 billion people have serological evidence of past or present HBV infection and more than 350 million individuals worldwide are chronically infected with HBV[1]. In infected adolescents or adults, 5%-10% will develop into a chronic carrier state, whereas in infected neonates up to 90% develop chronicity[1-2]. HBV infection is especially prevalent in African and Asian countries such as Korea, Japan, Taiwan and mainland China because most patients with chronic HBV infection have acquired the infection perinatally from carrier mothers[3]. China has the highest prevalence of HBV, with over one-third of the world's total estimated HBV carriers. Out of the chronic HBV-infected patients, 70%-80% could have persistent normal liver function for many years or a lifetime[1-2]. Further persistent viral infection can, however, lead to subclinical hepatitis and chronic active hepatitis, even liver cirrhosis and the development of hepatocellular carcinoma[1-2].

The pathogenesis of persistent viral infection and hepatitis B is complex. Generally, it is not HBV itself that damages hepatocytes directly, but the result of function disorder of cell-mediated immunity[4-6]. The cellular immune response to HBV is thought to be responsible for viral clearance, and disease pathogenesis during infection. The T-cell response to HBV is vigorous, polyclonal, and multispecific in acutely infected patients who successfully clear the virus, and it is relatively weak and narrowly focused in chronically infected patients[7-8]. The outcome of HBV infection would depend upon the balance between development of immunity (leading to virus elimination) and tolerance (leading to chronic viral persistence). HBeAg may play an important role in the interaction of the virus with the immune system. Secreted HBeAg has been proposed to have an immunoregulatory function in uterus by establishing T-cell tolerance to HBeAg and HBcAg that may predispose neonates born to HBV-infected mothers to develop persistent HBV infection[9]. Recent studies have further demonstrated an immunomodulatory role of HBeAg in antigen presentation and recognition by $CD4^+$ cells[10].

It is essential to study the HBV replication status and its effects on cellular immune function in normal LFTs chronic HBV-infected (CHI) individuals. Firstly, they are the majority of chronic HBV-infected individuals; secondly, the understanding of the immune response upon HBV infection is useful to develop appropriate therapeutic strategies for controlling viral hepatitis and disease progression, as well as to improve current knowledge regarding persistent HBV infection prognosis. However, the correlations between HBV-specific T-cell response, and HBV viral load and HBeAg expression in CHI individuals are complicated. So are the effects of age at first infection and maternal HBV infection status. The aim of the work reported herein was to evaluate the peripheral blood T-lymphocyte subpopulation profile, and its correlations with HBV replication level, and to determine further which active marker of HBV active replication, HBV DNA or HBeAg is more powerful in predicting peripheral T-lymphocyte subpopulation in CHI individuals.

MATERIALS AND METHODS

Enrollment of study subjects

Two hundred and sixteen consecutive CHI individuals with normal LFTs were recruited from the Department of Infectious Diseases and of Hepatology of the First Affiliated Hospital of Kunming Medical University, the Third Municipal People's Hospital of Kunming and the Yunnan General Hospital of The Chinese People's Armed Police Forces, between January 2004 and May 2007.

The following criteria were fulfilled by all individuals: (1) steady positivity for HBsAg in their serum for at least 12 mo and persistently normal liver function tests; and (2) exclusion of other concomitant causes of liver disease (hepatitis C, D and HIV infection and alcohol consumption of more than 60 g/day) and relatively rare liver disease (autoimmune hepatitis and metabolic liver disease) and treated with immunosuppressive therapy or antiviral therapy for HBV-infection within the recent 12 mo before entry. None of the patients was a drug user, or exposed to hepatotoxin. Informed consent was obtained from each study subject. The study protocol conformed to the guidelines of Declaration of Helsinki and was approved by ethics committees of the Faculty of Medicine of Prince of Songkla University and the First Affiliated Hospital of Kunming Medical University.

One hundred individuals who were free of HBsAg were identified from individuals coming to the out-patient service for a health check-up; 61 of the participants were male, 39 were female; mean age, 33.24 (SD, 10.28) years. These served as the control group for comparison of T-lymphocyte subpopulation with those who had HBV infection.

Serological liver function tests and hepatitis B virus markers evaluation

Serum alanine amino-transferase (ALT), aspartate transaminase (AST) and total bilirubin (TBil) were tested with routine automated techniques (upper limit of normal: 40 U/L, 40 U/L and 17.1 μmol/mL, respectively) (AU2700, Japan). HBV markers (HBsAg, HBsAb, HBeAg, HBeAb, HBcAb, and anti-HBcAb IgM) were measured at a virological laboratory with enzyme-linked immunosorbent assay (ELISA) (Anthos 2010, Austria). The experimental methods followed those specified within the reagent kit (Sino-American Biotech Co., Ltd) package insert.

Quantitative measurement HBV DNA (viraemia)

Serum HBV DNA load in individuals was assessed by the real-time fluorescent quantitative polymerase chain reaction method (Real-Time-PCR) using a Lightcycler PCR system (FQD-33A, Bioer) with a lower limit of detection of approximately 1000 viral genome copies/mL. The handling procedures were performed in strict accordance with the reagent kit (Shenzhen PG Biotech Co., Ltd.) package insert. The primer was provided in the kit, the reaction volume was 40 μL, and the reaction condition was 37℃ for 5 min, 94℃ for 1 min then 40 cycles as 95℃ for 5 s and 60℃ for 30 s.

Peripheral blood T lymphocyte subsets measurement

The key components of cellular immunity are T-lymphocyte and its subpopulations. $CD3^+$, $CD4^+$ and $CD8^+$ cells are major functional subgroups of T cells, and play an important role in response to HBV infection, which can reflect the situations of cellular immune function and immunoregulation, and are usually regarded as a valuable index to forecast the changes of patients' immunity[4-5]. These indices were chosen in our study for evaluating cellular immune function status of normal LFTs CHI individuals.

Blood samples were collected in heparinized vacutainer tubes. Whole blood samples were analyzed with a Multi-Q-Prep processor (Coulter, USA) and thereafter Epics-XL flow cytometry (FCM) (Coulter, USA). Lymphocytes were analyzed using a gate set on forward scatter versus side scatter, and a three color flow cytometry to combination reagent of CD3, CD4 and CD8. Anti-human monoclonal antibodies CD3-PE-CY5/CD4-FITC/CD8-PE were purchased from Immunotech, Ltd, USA. The detection was analyzed with the CELLQuest software (Coulter, USA) for each sample. The results were expressed as the percentages of $CD3^+$, $CD3^+/CD4^+$ (short for $CD4^+$ below) and $CD3^+/CD8^+$ (short for $CD8^+$ below) cells found to be positive for the marker antigen in the total T-cell population. The handling procedures were performed in strict accordance with the instructions within the reagent kit package insert.

Maternal HBV infection status (MH)

All mothers of the subjects were reviewed in medical records for previous HBV infection and most of those who were infected could be identified. In addition, all of them were invited to undergo HBV-marker tests. For those with a positive result, a second set of tests was conducted 3 mo after the first test to confirm chronic HBV carrier status. If the mother had died, the cause of death was investigated based on medical records and history taking whether it was from HBV-related liver diseases such as chronic hepatitis B, HBV-related liver cirrhosis or hepatocellular carcinoma. If so, the MH was classified as positive.

Age at HBV infection

In the recent three decades in China, all children have been obligated to be tested for HBV markers when they first enter kindergarten and elementary schools. Subsequent obligatory tests are made when they apply for university or for a job. The results of these tests were obtained from medical records and interview. Based on this setting, we classified the age of first positive test as before 8 years, between 8-20 years and after 20 years.

Statistical analysis

Initial calculation came up with a sample size of 50 subjects with HBV DNA positive and the same number of HBV DNA negative group. This could provide the study with a statistical power of 80% at the 0.025 level of significance to detect a difference in T-cell variation values of 33 *versus* 38. However, to cover the problem of being potentially confounded by other variables and to have enough subjects for stratifying levels of HBV DNA load to examine dose-response relationship, we ultimately recruited 216 CHI individuals and 100 controls.

Descriptive statistics were used to examine the age, gender, serum HBV viral load, HBeAg status, age at HBV-infection and maternal HBV infection status. The levels of T-lymphocyte subpopulation in normal individuals (HBsAg-negative) were summarized as means and standard deviation to serve as a control reference. Effects of various independent demographic, clinical and serological variables on T-cell profile were analyzed only among HBsAg-positive individuals. In univariate analysis, breakdown of these profiles by individual independent variables was carried out. Independent *t* test was done for 2-level independent variables and one-way ANOVA for more than 2-level variables. The relationship of HBV replication level and peripheral T-lymphocyte subpopulation was analyzed by correlation analysis and ANOVA linear trend test. Finally, multiple linear regression models were employed in multivariate analysis to assess the independent effects of variables on peripheral blood T lymphocytes. Variables yielding a P value $\leqslant 0.2$ in the univariate analysis were included in the multivariate analysis, and the models were refined by backward elimination guided by the change in log likelihood of successive models. A final P value of less than 0.05 was considered statistically significant. Computations were carried out with the aid of R softwere version 2.5.1[11].

RESULTS

Demographic characteristics and clinical features of CHI individuals

Demographic, serological, and clinical characteristics of the CHI individuals are summarized in Table 1. They were predominated by male (57.9%). One hundred and twenty four (57.4%) were less than 30 years old.

Of the CHI individuals, 37% got the infection before the age of 8 years. Almost three quarters had detectable serum levels of HBV DNA. Among these, the majority (68.4%, 93/136) had over 10^7 copies per milliliter. Just over half of them were HBeAg positive (56.5%).

Around 60% of the individuals' mothers were HBV positive. Among these individuals, nearly half had young age of infection and five-sixths had detectable serum levels of HBV DNA, of whom the majority (79.2%) had high viral load. Over 75% were HBeAg positive, whereas non-MH individuals were characterized by high age of infection, low viral load and low positivity of HBeAg.

Of those who had young age at infection, 80% (64/80) were HBeAg positive, and the majority (69/80) had detectable serum levels of HBV DNA, of whom nearly 74% (51/69) had high viral load.

Table 1 Characteristics of chronic HBV-infected individuals with normal liver function tests

Characteristics	All individuals	Maternal HBV-infection status (MH)		
	(*n* = 216)	Individuals with MH (*n* = 129)	Individuals without MH (*n* = 87)	*P*
Sex (male/female)	125/91	75/54	50/37	0.922[1]
Mean age (yr)	31.53 ± 11.23	29.11 ± 11.44	35.13 ± 9.94	< 0.001[2]
Age of HBV-infection (yr) (%)				< 0.001[1]
< 8	80 (37.0)	62 (48.1)	18 (20.7)	
8-20	56 (25.9)	36 (27.9)	20 (23.0)	
> 20	58 (26.9)	21 (16.3)	37 (42.5)	
Unknown	22 (10.2)	10 (7.8)	12 (13.8)	
HBV DNA positive (%)	136 (63.0)	106 (82.2)	30 (34.5)	< 0.001[1]
Serum HBV DNA (copies/mL) (%)				< 0.001[1]
$\leqslant 1.0 \times 10^3$	80 (37.0)	23 (17.8)	57 (65.5)	
1.0×10^3-1.0×10^5	14 (6.5)	5 (3.9)	9 (10.3)	
1.0×10^5-1.0×10^7	29 (13.4)	17 (13.2)	12 (13.8)	
$> 1.0 \times 10^7$	93 (43.1)	84 (65.1)	9 (10.3)	
HBV DNA load (log, copies/mL)	5.90 ± 2.61	7.13 ± 2.36	4.07 ± 1.74	< 0.001[2]
HBeAg positive (%)	122 (56.5)	97 (75.2)	25 (28.7)	< 0.001[1]

[1]Chi-square test *P* value; [2]Student *t* test *P* value; HBV: Hepatitis B virus; MH: Maternal HBV-infection status.

Table 2 Peripheral T-cell subsets in normal control and CHI individuals broken down by various factors (mean ± SD)

Groups	*n*	$CD3^+$ (%)	$CD4^+$ (%)	$CD8^+$ (%)	$CD4^+/CD8^+$ ratio
HBV status[1]					
Negative	100	71.07 ± 4.76	38.94 ± 3.39	24.02 ± 4.35	1.67 ± 0.33
Positive	216	57.35 ± 13.81	32.97 ± 7.00	33.08 ± 7.99	1.07 ± 0.41
Maternal HBV-infection status[1]					
Negative	87	64.67 ± 10.74	35.75 ± 6.08	28.71 ± 5.56	1.29 ± 0.35
Positive	129	52.42 ± 13.49	31.10 ± 6.98	36.03 ± 8.04	0.93 ± 0.38
Age at HBV-infection (yr)					
< 8	80	66.35 ± 8.19	30.78 ± 7.03	35.36 ± 7.12	0.91 ± 0.30
8-20	56	66.46 ± 9.33	31.65 ± 5.06	35.80 ± 7.79	0.93 ± 0.28
> 20	58	69.35 ± 9.85	36.37 ± 7.31[df]	28.22 ± 7.11[dh]	1.37 ± 0.46[dh]
Unknown	22	69.35 ± 9.85	35.35 ± 6.62[a]	30.69 ± 7.48[bf]	1.24 ± 0.46[af]
HBV DNA load (copies/mL)[2]					
$\leqslant 1.0 \times 10^3$	80	65.84 ± 9.39	37.11 ± 6.29	28.12 ± 5.65	1.38 ± 0.40
1.0×10^3-1.0×10^5	14	65.36 ± 5.15	34.70 ± 2.79	28.66 ± 6.21	1.28 ± 0.38
1.0×10^5-1.0×10^7	29	66.20 ± 9.99	33.66 ± 6.39	32.40 ± 6.54	1.06 ± 0.24
$> 1.0 \times 10^7$	93	46.09 ± 10.52	28.94 ± 5.95	38.23 ± 7.21	0.79 ± 0.22
HBeAg status[1]					
Negative	94	64.45 ± 10.44	35.81 ± 6.69	29.05 ± 6.43	1.30 ± 0.42
Positive	122	51.89 ± 13.63	30.78 ± 6.46	36.19 ± 7.69	0.89 ± 0.31

[1]$P < 0.001$ for all comparisons of +ve *vs* -ve for each measure and each T-cell parameter; [2]$P < 0.01$ for ANOVA linear trend test; [a]$P < 0.05$, [b]$P < 0.01$, [d]$P < 0.001$ *vs* < 8 yr group; [f]$P < 0.01$,[h]$P < 0.001$ *vs* 8-20 yr group.

Peripheral T lymphocyte subpopulation composition in CHI individuals with normal LFTs

CHI individuals had significantly decreased relative frequencies of $CD3^+$ and $CD4^+$ subpopulations and $CD4^+/CD8^+$ ratio, and increased $CD8^+$ subset percentage compared with the control group. Univariate analyses showed that the impaired balance of T-cell subsets was significantly associated with high viral load, presence of serum HBeAg expression, history of maternal HBV-infection and low age at HBV-infection (Table 2). Linear dose-response relationship between the level of T-lymphocyte subpopulation and log copies of HBV DNA was also highly significant (linear trend test *P* value <0.01). Correlation between T-lymphocyte subpopulations and viral load is also shown in Figure 1 (r = -0.67, -0.54, 0.61, -0.67, respectively, for $CD3^+$, $CD4^+$, $CD8^+$ and $CD4^+/CD8+$ ratio; all $P < 0.0001$) and Figure 2.

Linear regression predicting peripheral blood T-lymphocyte subpopulation from relevant parameters

In Table 3, linear regression models are separately summarized for $CD3^+$, $CD4^+$ and $CD8^+$ cells and $CD4^+/CD8^+$ ratio, which are the dependent variables. After adjustment for all independent variables listed in the table, serum level of HBV viral load was the only significant predictor for each outcome variable, whereas the effects of HBeAg and other variables were not significant.

Figure 3 shows the relationship between T-lym-

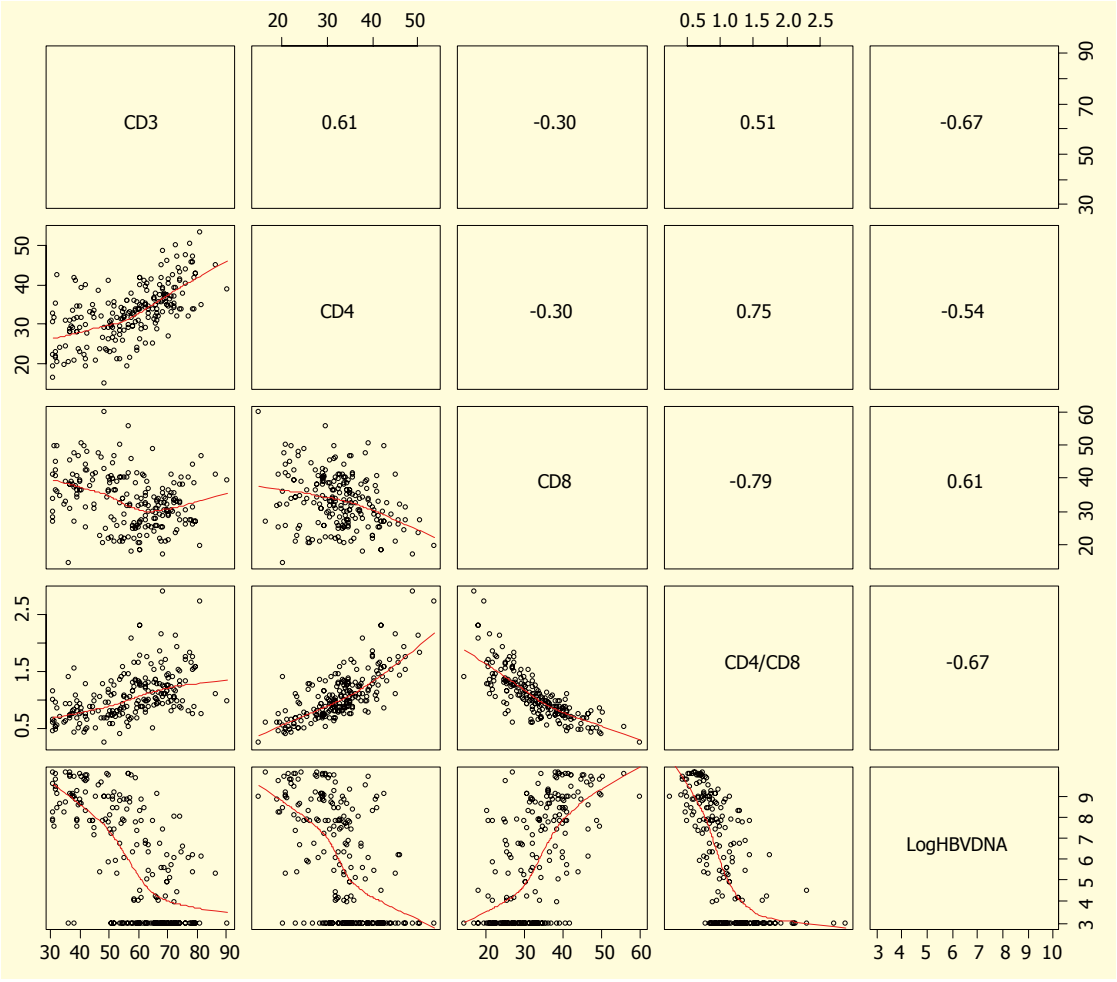

Figure 1 Correlation between peripheral T-cell subsets and serum HBV viral load. The numbers in the boxes refer to correlation coefficients. There is a negative correlation between the $CD3^+$and $CD4^+$ cells and $CD4^+/CD8^+$ ratio and serum viral load in CHI individuals with normal LFTs (r = -0.67, -0.54, -0.67; P < 0.0001), and a positive correlation between the levels of $CD8^+$ cells and viral load (r = 0.61, P < 0.0001).

Table 3 Multiple linear regression predicting peripheral blood T lymphocyte subpopulation (n = 216)

	$CD3^+$ T lymphocyte			$CD4^+$ T lymphocyte			$CD8^+$ T lymphocyte			$CD4^+/CD8^+$ ratio		
	β	SE	P	β	SE	P	β	SE	P	β	SE	P
Intercept	79.54	3.03	-	40.09	1.78	-	25.78	1.88	-	1.5	0.09	-
Serum HBV load (log, copies/mL)[1]	-3.65	0.43	< 0.0001	-1.38	0.25	< 0.0001	1.36	0.26	< 0.0001	-0.08	0.01	< 0.0001
HBeAg negative	0.05	1.98	0.98	0.61	1.16	0.6	0.5	1.22	0.69	-0.02	0.06	0.74
Age at HBV-infection(yr)[2]			0.06			0.63			0.19			0.02
8-20	-1.53	1.8		0.27	1.05		1.52	1.11		-0.03	0.05	
> 20	-4.77	2.08		1.2	1.22		-1.28	1.28		0.15	0.06	
Unknown	1.28	2.55		1.64	1.49		-0.77	1.58		0.13	0.08	
Maternal HBV-infection status	2.17	1.74	0.21	0.31	1.02	0.77	-2.45	1.08	0.02	0.06	0.05	0.27

β: Coefficients from the model; SE: Standard error. [1]Continuous variable; [2]control group, < 8 yr of age at HBV infection.

phocyte subpopulations and viral load stratified by age at HBV infection. There was no significant difference of T-cell subsets among groups of age at HBV infection after adjustment for serum level of HBV viral load. A similar pattern is also seen in the figures that show the relationship between T-lymphocyte subpopulations and viral load stratified by maternal HBV carrier status and by HBeAg status in CHI individuals with normal LFTs respectively.

DISCUSSION

This study demonstrated an impaired balance of the T-cell subsets related to an increased proportion of $CD8^+$ T-lymphocytes and decreased proportion of $CD4^+$ T-lymphocytes and $CD4^+/CD8^+$ ratio in CHI individuals who had normal liver function tests. The level of the T-cell impairment had a linear dose-response relationship with the load of HBV DNA. The study also

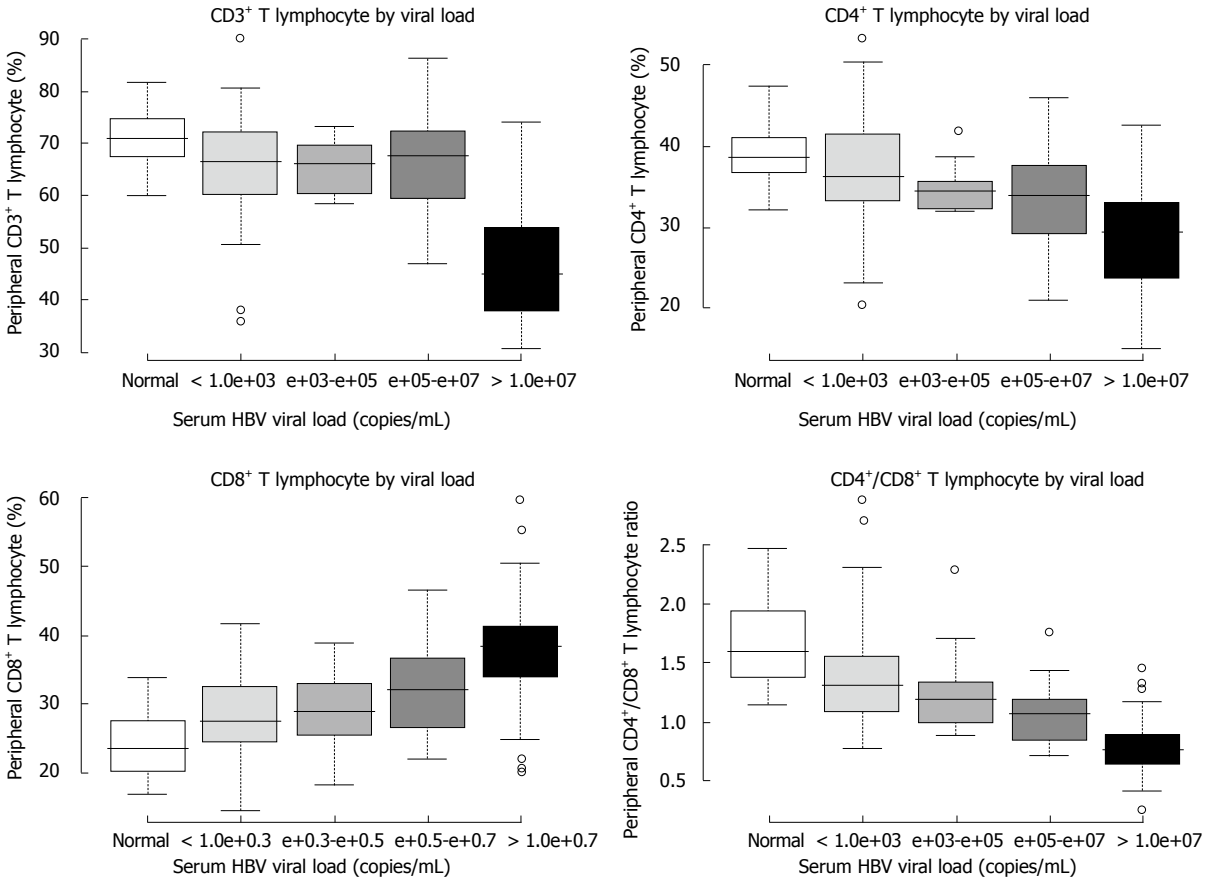

Figure 2 Peripheral T-lymphocyte subpopulations by serum HBV viral load. Composition of T-cell subpopulations from peripheral blood of patients with various serum HBV viral loads. Results are expressed as percentage of cells for each phenotype. Top of the box represents the 75th percentile, the bottom of the box represents the 25th percentile, and the solid line in the middle of the box represents the median. Whiskers above and below the box indicate the 90th and 10th percentiles, while circles represent outliers. Linear dose-response relationship between the level of T-lymphocyte subpopulations and copies of HBV DNA was highly significant (linear trend test, *P* value < 0.001). On the figure, the marks "< 1.0e+03", "e+03-e+05", "e+05-e+07" and "> 1.0e+07" denote "< 10^3", "10^3-10^{5}", "10^5-10^7" and "> 10^7", respectively.

illustrated the strong independent effects of HBV DNA, which eliminate the effects of maternal carrier status, younger age of infection and HBeAg positivity.

Our findings indicate that normal LFTs chronic HBV-infected individuals have an impaired balance of T-cell profile. The same finding also has been proved by previous researches in patients with chronic hepatitis B (CHB) that the chronicity of HBV infection is caused by a deficiency in cellular immune function, and hepatocytic damage is mainly caused by immunological injury[12-21]. However, the mechanism has not been defined[5]. Recently, the results have been reported by Tian *et al*[22] that $CD4^+$ and $CD8^+$ T cells decreased in both 33 CHB patients and 21 asymptomatic HBV carriers. Thus, most evidence has come from research in experimental animals[23-25] and in CHB patients[26-30].

Our results reveal that T-cell impairment was significantly associated with viral replication level. The substantial linear dose-response relationship and strong independent predictive ability of HBV DNA, but not of other variables, on T-cell subpopulations suggests a close proximity between them in the causal pathway. However, cross-sectional study nature of our data does not allow us to identify the temporal direction of the causal relationship between these two variables. Mizukoshi *et al*[31] suggested that antiviral therapy of persistently infected patients appeared to increase the frequency of HBV-specific $CD4^+$ T cell responses during the first year of treatment. Boni *et al*[32-35] reported that antiviral treatment can overcome $CD8^+$ T cell hypo-responsiveness in subjects with chronic HBV infection, suggesting that the T cells are present, but suppressed. It was reported by Pham *et al*[36] in 21 CHB patients that the ratio of $CD4^+$/$CD8^+$ liver-derived lymphocytes, and not of peripheral blood lymphocytes appeared to be related to the level of HBV replication, and it revealed a positive correlation with viral load. The evidence that efficient antiviral T cell response can be restored by mono-antiviral treatment in CHB patients concurrently with reduction of viremia, indicates the importance of viral load in the pathogenesis of T cell hypo-responsiveness in these patients.

The stronger independent effect of viral load on the T-cell impairment and viral factor (viral variants) might explain the disappearance of the effect of other variables in multivariate analysis. Among our research subjects, the majority were characterized by young age of first HBV infection, maternal carrier status and high viral load in serum, and also high HBeAg expression. As a matter of fact, in addition to HBV DNA, HBeAg is also a seromarker for high viral replication which plays

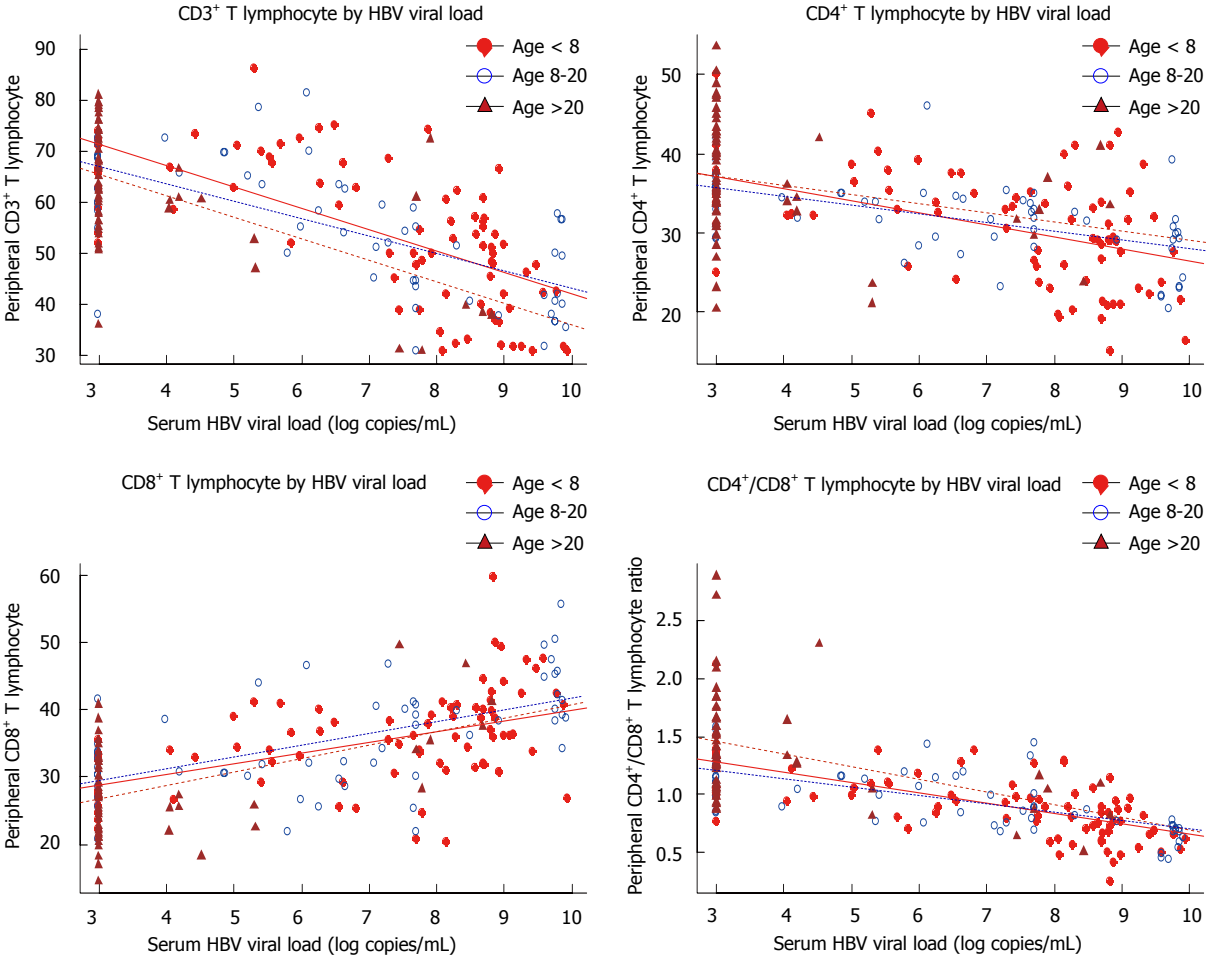

Figure 3 Correlation between T-cell subsets and viral load stratified by age at HBV infection. Three separate regression lines (with different slopes) are drawn for different groups of age at HBV infection. The coefficients of the interaction term "HBV DNA: age-at-HBV-infection" are not statistically significant for each parameter of T lymphocyte subpopulations (all $P > 0.05$). The P value indicates no significant influence of age at HBV infection on peripheral T-cell subpopulations.

a crucial role in chronicity of HBV infection and high viral load by inducing immunological tolerance to HBV in the fetus. The tolerating effect of HBeAg has been well characterized in mice[37-39] and likely contributes to the low level of core-specific T-cell responses present in HBeAg$^+$ chronic patients[4,5]. Clinical evidence supports the tolerogenic effect of HBeAg[4,40]. Also, viral mutations that abrogate or antagonize antigen recognition by virus-specific T cells have been reported in patients with chronic HBV infection[41-42], although the results from univariate analysis in our study showed that dysfunction of T-cell was significantly related with HBeAg, which later disappeared in multivariate analysis. One possible reason is that some of the subjects were infected with pre-C stop codon mutation virus (pre-C/C mutant), which resulted in a loss of HBeAg. In these patients, therefore, viral replication may persist despite elimination of HBeAg and seroconversion to anti-HBe. While the loss of HBeAg appears irrelevant for the biology of the virus, it may play an important role in the interaction of the virus with the immune system. This may weaken the independent association between HBeAg and the T-cell impairment so that the sample size in our study cannot detect this magnitude of association. Those who had maternal carrier history usually got infection at a younger age (Table 1) and a higher HBV viral load was detected in the majority of those who had infection at a younger age. This phenomenon suggests that infection from the mother and/or at younger age predisposes to tolerance to HBV infection and, thus, higher viral load.

The strength of this study lies in the large sample size of CHI individuals with normal LFTs and the measurements of T-lymphocyte subpopulations using modern advanced flow cytometric technology and viral load by the quantitative real-time PCR method. A limitation of this study is the unknown age at HBV-infection of 22 individuals, the specificity of T-lymphocyte subpopulations, and liver-derived T-lymphocyte were not explored concurrently. Although the strong relationship of T-lymphocyte subpopulations with viral load is illustrated, further studies are needed to confirm the causal relationship between them.

Our results, which suggest that high viral load contributes to the impaired balance of the T-cell subsets in normal LFTs CHI individuals, have practical implications for understanding of pathogenesis and controlling of persistent viral infection, disease progression and prognosis because these individuals are also at risk of persistent viral infection leading to sub-clinical hepatitis, and chronic active hepatitis, even

liver cirrhosis and the development of hepatocellular carcinoma[1-3]. Perhaps, we should take this contribution into account in designing interventional strategies such as anti-viral therapeutic and/or immunotherapeutic strategies to prevent the progression and long-term consequences, which have been proved effective in CHB patients. Further clinical studies are needed to explore this possibility not only in CHB patients but also in normal LFTs chronic HBV-infected individuals.

In conclusion, we found that a strong independent predictive effect of HBV DNA load on T-lymphocyte subpopulations suggests a close proximity in the causal pathway between HBV viral load and the T-cell impairment. This information is of great interest because, first, it will be possible to predict the variation of T-lymphocyte subpopulations in peripheral blood in the future by measuring serum viral load level in chronic HBV-infected individuals with normal LFTs and second, this parameter can be monitored in blood easily and cheaply. Therefore, the measurement of viral load in serum of individuals suffering from chronic HBV infection could represent a simple parameter for the evaluation of cellular immune function status.

COMMENTS

Background

Hepatitis B virus (HBV) infection is a serious public health problem worldwide and a major cause of chronic hepatitis, liver cirrhosis, and hepatocellular carcinoma. HBV infection is especially prevalent in African and Asian countries because most patients with chronic HBV infection have acquired the infection perinatally from carrier mothers. The pathogenesis of persistent viral infection is very complex and has not been clarified until now. Generally, it is not HBV itself that damages hepatocytes directly, but the results of disorder of cell-mediated immunity. The outcome of HBV infection would depend on the balance between development of immunity (leading to virus elimination) and tolerance (leading to chronic viral persistence).

Research frontiers

Outcome of HBV infection, and the pathogenesis of liver disease are determined by immune-mediated host-virus interaction, which have been difficult to fully elucidate because the host range of HBV is limited to man and chimpanzees. The pathogenesis of liver disease and interaction between virus and host remain the research hotspots in this field.

Innovations and breakthroughs

The pathogenesis and correlation of cellular immune disorder and HBV viral replication level remain unknown. In the present study, peripheral T-lymphocyte subpopulations of chronic HBV-infected (CHI) individuals who had normal liver function tests in big sample size were measured using advanced flow cytometry technology and HBV viral load with sensitive quantitative real-time-PCR method. The results suggest that the impaired balance of T-cell subpopulations was significantly associated with viral replication level. The substantial linear dose-response relationship and strong independent predictive effect of viral load on T-lymphocyte subpopulations suggests a close proximity of the causal pathway between them, and indicates the importance of viral load in the pathogenesis of T-cell impairment in these patients.

Applications

The results, which suggest that high viral load contributes to the impaired balance of the T-cell subsets in normal liver function tests (LFTs) CHI individuals, have practical implications for understanding of pathogenesis and controlling of persistent viral infection and disease progression and prognosis because these individuals are also at risk of persistent viral infection leading to subclinical hepatitis and chronic active hepatitis, even liver cirrhosis and the development of hepatocellular carcinoma. In addition, it is possible to predict the variation of T-lymphocyte subpopulations in peripheral blood in the future by measuring serum viral load level in chronic HBV-infected patients.

Peer review

The article is clearly written and demonstrates that high viral load is more powerful than HBeAg in predicting the impaired balance of T-cell subsets.

REFERENCES

1 **World Health Organization, Department of Communicable diseases surveillance and response**. Hepatitis B. WHO Fact Sheets. Available from: URL: http://www.who.int. Accessed: August 28, 2007

2 **Pol S**. [Natural history of hepatitis B infection] *Presse Med* 2006; **35**: 308-316

3 **Chen CJ**, Wang LY, Yu MW. Epidemiology of hepatitis B virus infection in the Asia-Pacific region. *J Gastroenterol Hepatol* 2000; **15** Suppl: E3-E6

4 **Baumert TF**, Thimme R, von Weizsacker F. Pathogenesis of hepatitis B virus infection. *World J Gastroenterol* 2007; **13**: 82-90

5 **Bertoletti A**, Gehring AJ. The immune response during hepatitis B virus infection. *J Gen Virol* 2006; **87**: 1439-1449

6 **Liu DX**. A new hypothesis of pathogenetic mechanism of viral hepatitis B and C. *Med Hypotheses* 2001; **56**: 405-408

7 **Michalak TI**, Hodgson PD, Churchill ND. Posttranscriptional inhibition of class I major histocompatibility complex presentation on hepatocytes and lymphoid cells in chronic woodchuck hepatitis virus infection. *J Virol* 2000; **74**: 4483-4494

8 **Khettry U**, Anand N, Gordon FD, Jenkins RL, Tahan SR, Loda M, Lewis WD. Recurrent hepatitis B, hepatitis C, and combined hepatitis B and C in liver allografts: a comparative pathological study. *Hum Pathol* 2000; **31**: 101-108

9 **Milich DR**, Jones JE, Hughes JL, Price J, Raney AK, McLachlan A. Is a function of the secreted hepatitis B e antigen to induce immunologic tolerance in utero? *Proc Natl Acad Sci USA* 1990; **87**: 6599-6603

10 **Milich DR**. Do T cells "see" the hepatitis B core and e antigens differently? *Gastroenterology* 1999; **116**: 765-768

11 **R Development Core Team**. R: A language and environment for statistical computing. R Foundation for Statistical Computing, Vienna, Austria. ISBN 3-900051-07-0. Available from: URL: http://www.R-project.org. Assessed: August, 2007

12 **Wang KX**, Peng JL, Wang XF, Tian Y, Wang J, Li CP. Detection of T lymphocyte subsets and mIL-2R on surface of PBMC in patients with hepatitis B. *World J Gastroenterol* 2003; **9**: 2017-2020

13 **Webster GJ**, Reignat S, Maini MK, Whalley SA, Ogg GS, King A, Brown D, Amlot PL, Williams R, Vergani D, Dusheiko GM, Bertoletti A. Incubation phase of acute hepatitis B in man: dynamic of cellular immune mechanisms. *Hepatology* 2000; **32**: 1117-1124

14 **Webster GJ**, Reignat S, Brown D, Ogg GS, Jones L, Seneviratne SL, Williams R, Dusheiko G, Bertoletti A. Longitudinal analysis of CD8+ T cells specific for structural and nonstructural hepatitis B virus proteins in patients with chronic hepatitis B: implications for immunotherapy. *J Virol* 2004; **78**: 5707-5719

15 **Sarin SK**, Thakur V, Guptan RC, Saigal S, Malhotra V, Thyagarajan SP, Das BC. Profile of hepatocellular carcinoma in India: an insight into the possible etiologic associations. *J Gastroenterol Hepatol* 2001; **16**: 666-673

16 **Shoenfeld Y**, Aron-Maor A. Vaccination and autoimmunity-'vaccinosis': a dangerous liaison? *J Autoimmun* 2000; **14**: 1-10

17 **Trobonjaca Z**, Kroger A, Stober D, Leithauser F, Moller P, Hauser H, Schirmbeck R, Reimann J. Activating immunity in the liver. II. IFN-beta attenuates NK cell-dependent liver injury triggered by liver NKT cell activation. *J Immunol* 2002; **168**: 3763-3770

18 **Rapicetta M**, Ferrari C, Levrero M. Viral determinants and host immune responses in the pathogenesis of HBV

infection. *J Med Virol* 2002; **67**: 454-457
19 **Tanner MS**. Mechanisms of liver injury relevant to pediatric hepatology. *Crit Rev Clin Lab Sci* 2002; **39**: 1-61
20 **Rivero M**, Crespo J, Fabrega E, Casafont F, Mayorga M, Gomez-Fleitas M, Pons-Romero F. Apoptosis mediated by the Fas system in the fulminant hepatitis by hepatitis B virus. *J Viral Hepat* 2002; **9**: 107-113
21 **Okumura A**, Ishikawa T, Yoshioka K, Yuasa R, Fukuzawa Y, Kakumu S. Mutation at codon 130 in hepatitis B virus (HBV) core region increases markedly during acute exacerbation of hepatitis in chronic HBV carriers. *J Gastroenterol* 2001; **36**: 103-110
22 **Tian Y**, Qiu ZF, Li TS. [Difference and significance of peripheral blood T-lymphocyte subsets in patients with chronic hepatitis B and asymptomatic HBV carriers] *Zhonghua Yixue Zazhi* 2005; **85**: 3354-3358
23 **Chen M**, Sallberg M, Thung SN, Hughes J, Jones J, Milich DR. Nondeletional T-cell receptor transgenic mice: model for the CD4(+) T-cell repertoire in chronic hepatitis B virus infection. *J Virol* 2000; **74**: 7587-7599
24 **Lin CM**, Wang FH. Selective modification of antigen-specific CD4(+) T cells by retroviral-mediated gene transfer and in vitro sensitization with dendritic cells. *Clin Immunol* 2002; **104**: 58-66
25 **Chen M**, Sallberg M, Thung SN, Hughes J, Jones J, Milich DR. Modeling the T-helper cell response in acute and chronic hepatitis B virus infection using T-cell receptor transgenic mice. *Antiviral Res* 2001; **52**: 99-111
26 **Thimme R**, Wieland S, Steiger C, Ghrayeb J, Reimann KA, Purcell RH, Chisari FV. CD8(+) T cells mediate viral clearance and disease pathogenesis during acute hepatitis B virus infection. *J Virol* 2003; **77**: 68-76
27 **Lau GK**, Suri D, Liang R, Rigopoulou EI, Thomas MG, Mullerova I, Nanji A, Yuen ST, Williams R, Naoumov NV. Resolution of chronic hepatitis B and anti-HBs seroconversion in humans by adoptive transfer of immunity to hepatitis B core antigen. *Gastroenterology* 2002; **122**: 614-624
28 **Sing GK**, Li D, Chen X, Macnaughton T, Lichanska AM, Butterworth L, Ladhams A, Cooksley G. A molecular comparison of T lymphocyte populations infiltrating the liver and circulating in the blood of patients with chronic hepatitis B: evidence for antigen-driven selection of a public complementarity-determining region 3 (CDR3) motif. *Hepatology* 2001; **33**: 1288-1298
29 **Stoop JN**, van der Molen RG, Baan CC, van der Laan LJ, Kuipers EJ, Kusters JG, Janssen HL. Regulatory T cells contribute to the impaired immune response in patients with chronic hepatitis B virus infection. *Hepatology* 2005; **41**: 771-778
30 **Franzese O**, Kennedy PT, Gehring AJ, Gotto J, Williams R, Maini MK, Bertoletti A. Modulation of the CD8+-T-cell response by CD4+ CD25+ regulatory T cells in patients with hepatitis B virus infection. *J Virol* 2005; **79**: 3322-3328
31 **Mizukoshi E**, Sidney J, Livingston B, Ghany M, Hoofnagle JH, Sette A, Rehermann B. Cellular immune responses to the hepatitis B virus polymerase. *J Immunol* 2004; **173**: 5863-5871
32 **Boni C**, Bertoletti A, Penna A, Cavalli A, Pilli M, Urbani S, Scognamiglio P, Boehme R, Panebianco R, Fiaccadori F, Ferrari C. Lamivudine treatment can restore T cell responsiveness in chronic hepatitis B. *J Clin Invest* 1998; **102**: 968-975
33 **Boni C**, Penna A, Ogg GS, Bertoletti A, Pilli M, Cavallo C, Cavalli A, Urbani S, Boehme R, Panebianco R, Fiaccadori F, Ferrari C. Lamivudine treatment can overcome cytotoxic T-cell hyporesponsiveness in chronic hepatitis B: new perspectives for immune therapy. *Hepatology* 2001; **33**: 963-971
34 **Boni C**, Penna A, Bertoletti A, Lamonaca V, Rapti I, Missale G, Pilli M, Urbani S, Cavalli A, Cerioni S, Panebianco R, Jenkins J, Ferrari C. Transient restoration of anti-viral T cell responses induced by lamivudine therapy in chronic hepatitis B. *J Hepatol* 2003; **39**: 595-605
35 **Boni C**, Fisicaro P, Valdatta C, Amadei B, Di Vincenzo P, Giuberti T, Laccabue D, Zerbini A, Cavalli A, Missale G, Bertoletti A, Ferrari C. Characterization of hepatitis B virus (HBV)-specific T-cell dysfunction in chronic HBV infection. *J Viro*l 2007; **81**: 4215-4225
36 **Pham BN**, Mosnier JF, Walker F, Njapoum C, Bougy F, Degott C, Erlinger S, Cohen JH, Degos F. Flow cytometry CD4+/CD8+ ratio of liver-derived lymphocytes correlates with viral replication in chronic hepatitis B. *Clin Exp Immunol* 1994; **97**: 403-410
37 **Milich D**, Liang TJ. Exploring the biological basis of hepatitis B e antigen in hepatitis B virus infection. *Hepatology* 2003; **38**: 1075-1086
38 **Chen MT**, Billaud JN, Sallberg M, Guidotti LG, Chisari FV, Jones J, Hughes J, Milich DR. A function of the hepatitis B virus precore protein is to regulate the immune response to the core antigen. *Proc Natl Acad Sci USA* 2004; **101**: 14913-14918
39 **Chen M**, Sallberg M, Hughes J, Jones J, Guidotti LG, Chisari FV, Billaud JN, Milich DR. Immune tolerance split between hepatitis B virus precore and core proteins. *J Virol* 2005; **79**: 3016-3027
40 **Liu CJ**, Kao JH, Lai MY, Chen PJ, Chen DS. Precore/core promoter mutations and genotypes of hepatitis B virus in chronic hepatitis B patients with fulminant or subfulminant hepatitis. *J Med Virol* 2004; **72**: 545-550
41 **Bertoletti A**, Costanzo A, Chisari FV, Levrero M, Artini M, Sette A, Penna A, Giuberti T, Fiaccadori F, Ferrari C. Cytotoxic T lymphocyte response to a wild type hepatitis B virus epitope in patients chronically infected by variant viruses carrying substitutions within the epitope. *J Exp Med* 1994; **180**: 933-943
42 **Bertoletti A**, Sette A, Chisari FV, Penna A, Levrero M, De Carli M, Fiaccadori F, Ferrari C. Natural variants of cytotoxic epitopes are T-cell receptor antagonists for antiviral cytotoxic T cells. *Nature* 1994; **369**: 407-410

S-Editor Zhong XY **L- Editor** Ma JY **E-Editor** Yin DH

Online Submissions: wjg.wjgnet.com
wjg@wjgnet.com
doi:10.3748/wjg.14.3719

World J Gastroenterol 2008 June 21; 14(23): 3719-3724
World Journal of Gastroenterology ISSN 1007-9327
© 2008 The WJG Press. All rights reserved.

RAPID COMMUNICATION

Ineffective oesophageal motility: Manometric subsets exhibit different symptom profiles

Horst Gunter Haack, Ross David Hansen, Allison Malcolm, John Edward Kellow

Horst Gunter Haack, Ross David Hansen, Allison Malcolm, John Edward Kellow, Department of Gastroenterology, Gastrointestinal Investigation Unit, Royal North Shore Hospital, University of Sydney, Australia
Author contributions: Haack HG performed research and data analysis; Hansen RD performed conceptual, data and statistical analysis and wrote the paper; Malcolm A discussed the conceptual aspects and the data analysis; Kellow JE designed conceptual aspects, discussed data and statistical analysis and wrote the paper.
Correspondence to: John E Kellow, MD, Department of Gastroenterology, Royal North Shore Hospital, St. Leonards, NSW 2065, Australia. johnk@med.usyd.edu.au
Telephone: +61-2-99267355 Fax: +61-2-94363719
Received: November 7, 2007 Revised: May 19, 2008
Accepted: May 26, 2008
Published online: June 21, 2008

Abstract

AIM: To compare the demographic and clinical features of different manometric subsets of ineffective oesophageal motility (IOM; defined as ⩾ 30% wet swallows with distal contractile amplitude < 30 mmHg), and to determine whether the prevalence of gastro-oesophageal reflux differs between IOM subsets.

METHODS: Clinical characteristics of manometric subsets were determined in 100 IOM patients (73 female, median age 58 years) and compared to those of 100 age-and gender-matched patient controls with oesophageal symptoms, but normal manometry. Supine oesophageal manometry was performed with an eight-channel DentSleeve water-perfused catheter, and an ambulatory pH study assessed gastro-oesophageal reflux.

RESULTS: Patients in the IOM subset featuring a majority of low-amplitude simultaneous contractions (LASC) experienced less heartburn (prevalence 26%), but more dysphagia (57%) than those in the IOM subset featuring low-amplitude propagated contractions (LAP; heartburn 70%, dysphagia 24%; both $P \leqslant 0.01$). LASC patients also experienced less heartburn and more dysphagia than patient controls (heartburn 68%, dysphagia 11%; both $P < 0.001$). The prevalence of heartburn and dysphagia in IOM patients featuring a majority of non-transmitted sequences (NT) was 54% ($P = 0.04$ *vs* LASC) and 36% ($P < 0.01$ *vs* controls), respectively. No differences in age and gender distribution, chest pain prevalence, acid exposure time (AET) and symptom/reflux association existed between IOM subsets, or between subsets and controls.

CONCLUSION: IOM patients with LASC exhibit a different symptom profile to those with LAP, but do not differ in gastro-oesophageal reflux prevalence. These findings raise the possibility of different pathophysiological mechanisms in IOM subsets, which warrants further investigation.

© 2008 The WJG Press. All rights reserved.

Key words: Age; Dysphagia; Heartburn; Ineffective oesophageal motility; Oesophageal manometry; Simultaneous contractions

Peer reviewer: Yvan Vandenplas, Professor, Department of Pediatrics, AZ-VUB, Laarbeeklaan 101, Brussels 1090, Belgium

Haack HG, Hansen RD, Malcolm A, Kellow JE. Ineffective oesophageal motility: Manometric subsets exhibit different symptom profiles. *World J Gastroenterol* 2008; 14(23): 3719-3724 Available from: URL: http://www.wjgnet.com/1007-9327/14/3719.asp DOI: http://dx.doi.org/10.3748/wjg.14.3719

INTRODUCTION

The term ineffective oesophageal motility (IOM), the most common variant of oesophageal dysmotility, was introduced in 1997 to replace the term "non-specific oesophageal motility disorder"[1], as the former term appears to better reflect the functional and clinical relevance of manometric alterations[2,3]. IOM is defined manometrically as ⩾ 30% of swallow sequences with a contractile amplitude < 30 mmHg in the distal oesophagus[4]. Such a definition, however, encompasses three abnormal contractile patterns, namely low-amplitude propagated contractions (LAP), low-amplitude simultaneous contractions (LASC), and non-transmitted contractions. IOM is, therefore, diagnosed if there is a combination of these abnormal contractile patterns.

It is not known if the predominant oesophageal symptom (heartburn, dysphagia, chest pain) experienced by IOM patients is associated with the predominance

of one of these ineffective manometric patterns. In addition, although gastro-oesophageal reflux disease (GORD) has been associated with IOM[5-7], it is not known whether particular manometric subsets of IOM display a higher prevalence of GORD.

This study was thus aimed at (1) comparing the demographic and manometric features of IOM patients with different predominant symptoms (heartburn, dysphagia, chest pain); (2) comparing the demographic and clinical features of different manometric subsets of IOM; (3) comparing the clinical features of IOM subsets with those of patients with oesophageal symptoms, but normal oesophageal manometry; and (4) determining whether the prevalence of gastro-oesophageal reflux differs between the IOM manometric subsets.

MATERIALS AND METHODS

Patients

A total of 100 consecutive patients (73 females, mean ± SD age 56 ± 18 years) were studied. Patients with oesophageal symptoms were referred to the Gastrointestinal Investigation Unit of the Royal North Shore Hospital. All patients fulfilled the current manometric criteria for IOM: ⩾ 30% of wet swallows with low-amplitude propagated sequences (distal contractile amplitude < 30 mmHg), LASC, or non-transmitted contractions[4]. Swallow sequences were considered to be simultaneous when propagation velocity was > 8 cm/s between two or more manometric channels, and were considered to be non-transmitted when contractile amplitude was ⩽ 10 mmHg at any site. A group of 100 age- and gender-matched patients (73 females, age 56 ± 20 years) referred with oesophageal symptoms, but exhibiting normal oesophageal manometry[8] served as a patient control group. Patients in the two groups had undergone upper gastrointestinal endoscopy and/or barium studies to exclude structural disease of the oesophagus, apart from the presence of reflux oesophagitis and sliding hiatus hernia. Patients with systemic diseases that could alter oesophageal motility, such as diabetes mellitus or scleroderma, were excluded. The study was approved by the Human Research Ethics Committee of the Northern Sydney Area Health Service.

Symptom assessment

A standardized symptom assessment was completed by all patients. This assessment comprised the Rome Ⅱ Integrative Questionnaire[9] with an additional evaluation of oesophageal symptoms. This additional evaluation determined the predominant (i.e. most troublesome) oesophageal symptom (heartburn, dysphagia, chest pain, or others)[10] and the time period since its first appearance. The usual intensity, frequency, and duration of all reported symptoms were assessed, and symptom severity scores for heartburn, dysphagia, and chest pain were calculated as the product of these intensity, frequency, and duration data.

Oesophageal manometry

All patients were studied after an overnight fast. Oesophageal manometry was performed using an eight-channel DentSleeve water-perfused manometric catheter with an external diameter of 4.5 mm (DentSleeve Pty. Ltd., Belair, SA, Australia) and a computer-based data acquisition and charting system (Acquidata, Neomedix Systems, Warriewood, NSW, Australia). The catheter was introduced transnasally and swallowing was recorded via a port positioned in the pharynx, 25 cm above the proximal end of the hydraulic sleeve segment of the catheter. Oesophageal contractions were measured by ports located 5, 10, 15, and 20 cm above the proximal end of the sleeve and gastric pressure by a side hole 1 cm below the distal end of the 6 cm long sleeve. Each patient made approximately 10 swallows, each of 5 mL water of room temperature, in the seated position to acclimatize to the procedure. The patient was then placed in the supine position, and a minimum of 10 supine water swallows, each of 5 mL water, with at least 30 s in between swallows, were performed. A station pull-through technique was then used to accurately locate the position of the lower oesophageal sphincter (LOS). The LOS function was assessed by measuring mid-respiratory LOS resting pressure and swallow-induced LOS relaxation[8].

24-h pH monitoring

A subset of patients (54 IOM, 72 patient controls with normal manometry) underwent an ambulatory oesophageal pH study. A probe with an antimony pH sensor (Flexilog, Oakfield Instruments Ltd., Eynsham, England) was introduced transnasally and the sensor was positioned 5 cm above the upper edge of the LOS, which was determined manometrically as described above. The probe was connected to a data logger (Digitrapper Mark Ⅱ, Synectics, Sweden), which sampled pH at 5-s intervals for approximately 24 h. Mealtimes, symptom events, and supine periods were recorded in a patient diary. The computerized analysis (Esophagram, Synectics, Sweden) included the percentage of time pH was below 4 (Acid Exposure Time, AET)[11], and the symptom association probability (SAP)[12] was calculated when possible.

Data analysis

Analysis based on predominant symptom: Proportions of total abnormal swallows, and proportions of LAP, LASC, and non-transmitted sequences (NT) were calculated for each of the three main predominant symptoms (heartburn, dysphagia, chest pain). Differences in proportions were then determined between symptom subgroups.

Analysis based on predominant contractile abnormality: All IOM manometric studies were further categorized into the following three subsets according to the predominant contractile abnormality contributing to the 30% or more abnormal swallows: those exhibiting a majority of LAP, those exhibiting a majority of LASC,

Table 1 Gender, age, time since onset of symptom, and proportion of total abnormal swallows in IOM patients according to the predominant oesophageal symptom[1]

	Gender (F:M)	Median age [yr (range)]	Median time since symptom onset (yr)	Total abnormal swallows (mean ± SD) (%)
Heartburn	37:16	57 (26-82)	6.7	69 ± 22
Dysphagia	28:8	63 (19-86)	2.5	68 ± 22
Chest pain	8:1	59 (31-76)	6.1	61 ± 25

[1]Two male patients reported "other" predominant symptoms (hiccoughs, halitosis).

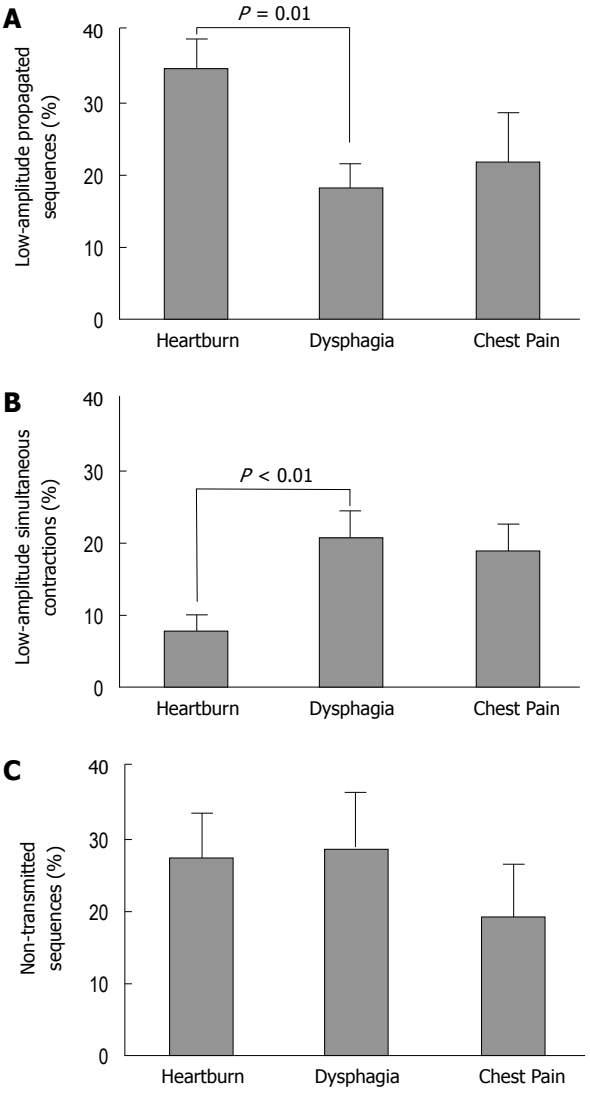

Figure 1 Proportions of low-amplitude propagated sequences (**A**), LASC (**B**), and NT (**C**) in the three predominant symptom subgroups. Proportions are expressed as (mean ± SE) % of total swallows.

and those exhibiting a majority of NT. Differences in clinical features between these three subsets were then determined.

Statistical analysis: Results are presented as mean ± SE, unless otherwise stated. χ^2 and Fisher's exact tests were used to determine differences in gender distribution between symptom subgroups, and differences in symptom prevalence between manometric subsets. Age differences between subsets, and between IOM patients and patient controls, were determined via Kruskal-Wallis tests with post-hoc Mann-Whitney U comparisons. Similarly, differences between symptom subgroups in proportions of contractile abnormalities and in LOS pressure and AET were determined via one-way analysis of variance (ANOVA) with post-hoc Scheffe tests. Correlation and regression analysis was used to describe relationships between variables. All analyses were performed using the SPSS statistical program (Release 14, SPSS Inc., Chicago, IL), with $P < 0.05$ considered significant.

RESULTS

Analysis based on the predominant symptom

Symptom, gender, and age distribution: The prevalence of predominant heartburn, predominant dysphagia, and predominant chest pain in IOM patients was 53%, 36%, and 9%, respectively. The prevalence of heartburn was significantly lower in IOM patients than in patient controls (68%, $P = 0.03$), and the prevalence of dysphagia was significantly higher in IOM patients than in patient controls (11%, $P < 0.001$).

There were no significant differences in gender and age distribution, and in time period since symptom onset, between the three symptom subgroups in IOM (Table 1).

Proportions of abnormal swallows: The mean proportion of LAP was significantly higher in patients with heartburn than in those with dysphagia, and the mean proportion of LASC was significantly higher in patients with dysphagia than in those with heartburn. The mean proportion of NT was similar across the three symptom subgroups (Figure 1; ANOVA and post-hoc tests). The proportion of total abnormal swallows did not differ between the three symptom subgroups (Table 1).

When all reported symptoms were considered (i.e. predominant symptom plus additional symptoms), the relationships between symptom severity scores and proportions of abnormal sequences were examined. There were positive correlations between dysphagia severity score and proportion of LASC ($r = 0.2$, $P = 0.05$), and between chest pain severity score and proportion of LAP ($r = 0.22$, $P < 0.05$).

LOS mid-respiratory resting pressure: Mean LOS pressure was significantly higher in patients with predominant dysphagia (12.5 ± 1.2 mmHg) than in those with heartburn (9.2 ± 0.6 mmHg; $P = 0.03$). The mean value for chest pain patients was 11.1 ± 1.0 mmHg.

Ambulatory pH data: The gender and age distribution of the patients who underwent a pH study closely reflected that of the total subject pool, and mean LOS pressures of subgroups were almost identical to those of the total subject pool. There were no significant

Table 2 Gender and age distribution, and ambulatory oesophageal pH data[1], for IOM manometric subsets and for patient controls who exhibited normal manometry

	Gender (F:M)	Median age [yr (range)]	AET[2] (%)	Abnormal AET[3] (%)	SAP+[4] (%)
IOM-LAP	25:12	58 (26-77)	8.8 ± 1.8	58	52
IOM-LASC	17:7	60 (29-86)	14.7 ± 5.1	90	60
IOM-NT	31:8	61 (19-76)	11.6 ± 2.5	81	33
Patient controls	73:27	58 (19-91)	8.6 ± 0.8	69	51

[1]pH data was available in 54 IOM patients and 72 patient controls; [2]AET (% of time pH < 4), reported as mean ± SE; [3]% of patients with an AET > 4%; [4]Expressed as % of patients with a significant SAP value.

differences between the three subgroups in terms of AET or proportion of patients with an abnormal AET, or proportion with significant SAP values.

Analysis based on predominant contractile abnormality

Gender and age distribution: The gender and age distribution for the three IOM manometric subsets and the patient controls is shown in Table 2. There were no statistical differences in gender and age distribution between patient controls and any of the IOM manometric subsets, or between IOM subsets.

Predominant symptoms: Figure 2 shows the distribution of predominant symptoms for the three manometric subsets and for patient controls. Heartburn was highly prevalent (70%) in the LAP subset, but was significantly less common (26%) in the LASC subset. Conversely, dysphagia was more prevalent in LASC (57%) than in LAP (24%) (χ^2 tests). There were no significant differences between IOM subsets, however, in severity scores for heartburn, dysphagia or chest pain, or in time since the onset of the primary symptom.

LOS mid-respiratory resting pressure: There were no statistically significant differences between the mean LOS pressures of the IOM subsets: values for LAP, LASC, and NT were 10.1 ± 0.9, 11.3 ± 1.4, and 10.9 ± 0.8 mmHg, respectively. There was a trend ($P = 0.05$) for the LAP subset to have a lower value than that of patient controls (12.0 ± 0.5 mmHg).

Ambulatory pH data: There were no significant differences in the prevalence of abnormal AET between IOM subsets. Analysis of mean AET values between the IOM subsets, and compared to patient controls, also revealed no significant differences (Table 2). Similarly, there were no differences in upright and supine AET values between subsets and groups. There were no significant SAP differences between the IOM subsets or in comparison to the control group (Table 2).

DISCUSSION

Despite almost 10 years of usage of the category IOM, and recent studies evaluating IOM with combined intraluminal impedance and manometry[3], the extent

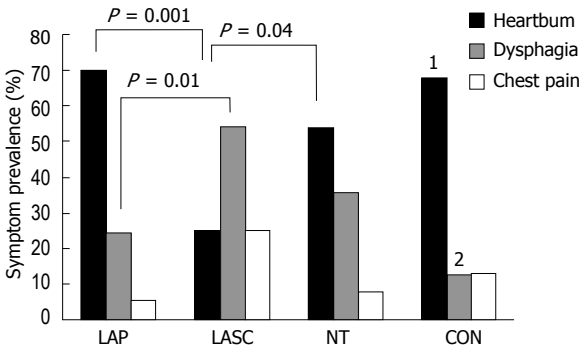

Figure 2 Prevalence of predominant symptoms in the three manometrically-determined IOM subsets, and in patient controls (CON) who exhibited normal manometry. [1]CON significantly higher than LASC ($P < 0.001$); [2]CON significantly lower than LASC ($P < 0.001$) and NT ($P < 0.01$) (χ^2 tests).

to which the various contractile patterns of IOM differ according to the predominant symptom has remained largely unexplored. Our study in a large patient cohort shows that IOM is indeed a heterogeneous clinical entity with regard to the predominant symptom reported. We focused on the type of contractile abnormality, rather than solely considering the contractile amplitude. The novel finding was that two specific contractile patterns, namely LASC and LAP, were closely related to predominant dysphagia and predominant heartburn, respectively. Additional analyses provided further support for these findings in that as the proportion of LASC increased, the dysphagia severity score also increased. Consistent with these findings, there were notable differences in symptom distribution between IOM manometric subsets, categorized according to the most frequent type of contractile pattern in an individual patient. Differences were particularly prominent between patients with low-amplitude propagated sequences and those with LASC; the latter experienced more dysphagia and less heartburn than the former patients.

We did not find a difference in age distribution between manometric subsets. Others have noted that simultaneous contractions are more likely to occur in older than in younger patients[13,14], especially in the presence of severe GORD[15]. The effect of age in relation to the occurrence of simultaneous contractions in healthy volunteers, however, remains unclear, as one study revealed no relationship between simultaneous contractions and age[16], whereas a more recent study did find a direct correlation between the proportion of simultaneous contractions and age[17]. The most recent study revealed differences in muscle thickness between similarly-categorized IOM subsets, and a significant correlation between muscle thickness, and the occurrence of simultaneous contractions[14]. Whether muscle thickness actually plays a causative role in the pathophysiology of simultaneous contractions remains unclear, and this needs to be further evaluated. It is possible that the clinical profile of IOM patients with a majority of LASC is similar to that of patients with diffuse oesophageal spasm (DOS), a disorder that also features intermittent simultaneous (but moderate- to

high-amplitude) contractions[4]. Hence, treatments currently considered for DOS patients[18-20] may prove beneficial for selected IOM patients, and this should also be further evaluated.

In the subset of IOM patients with mainly non-transmitted swallow patterns, it is feasible that this pattern could represent an evolving achalasia-like dysmotility, although these patients exhibited only a modest prevalence of dysphagia. As long-term follow-up of IOM patients has scarcely been reported[21], findings regarding disease progression remain inconclusive, and further studies are needed.

Neither the prevalence nor the severity of gastro-oesophageal acid reflux differed between IOM subsets. In addition, we found no significant differences in symptom/reflux association or heartburn severity score between IOM subsets, despite some differences in LOS resting pressure. A low LOS tone and transient LOS relaxation[22] are regarded as the main mechanisms of gastro-oesophageal reflux. As the LOS tone was lower in IOM patients with low-amplitude propagated sequences compared with patient controls, and heartburn prevalence was highest in this IOM subset, these patients could be expected to have the highest acid exposure. This was not the case, and our findings are consistent with those of Lemme *et al*, who found that the proportion of low-amplitude swallows did not differ between IOM patients with erosive *versus* non-erosive GORD[23]. It is feasible that the presence of propagating (albeit low-amplitude) sequences equates to more efficient clearance[24] of refluxate in these patients, and novel approaches to stimulating clearance[25] may prove beneficial in this IOM subset. Another explanation for the high heartburn prevalence is that these patients exhibit oesophageal hypersensitivity[26]. Despite the lack of difference in acid exposure between IOM subsets, pooled analyses of all IOM patients showed that a low LOS tone was associated with both high heartburn severity scores and high AETs. These findings indicate the complex interactions between LOS characteristics, oesophageal body dysfunction and symptomatology in IOM patients with gastro-oesophageal reflux, which require further investigation.

The current study focused primarily on oesophageal body dysmotility in IOM. LOS swallow-induced relaxation is assessed via manometry, but does not feature in the diagnosis of IOM. Conchillo *et al* have recently shown that, in addition to inadequate LOS relaxation, a shorter duration of LOS relaxation could contribute to abnormal bolus transit in IOM patients[27]. This might represent an additional manometric discriminator of dysmotility, and warrants further investigation.

In summary, we have examined subsets of IOM patients based on symptoms and manometrically-determined oesophageal body dysmotility. These subsets differ in regard to symptom profile, but do not differ in acid exposure or symptom/reflux association. Patients with LASC experience more dysphagia, but less heartburn, than IOM patients with low-amplitude, but propagated sequences. These findings raise the possibility of different pathophysiological mechanisms in IOM subsets, and this warrants further investigation.

ACKNOWLEDGMENTS

Financial support from the Bowel Cancer & Digestive Research Institute Australia is gratefully acknowledged.

COMMENTS

Background

The term ineffective oesophageal motility (IOM) encompasses a variety of symptoms and three types of abnormal oesophageal body peristalsis.

Research frontiers

The pathogenesis of IOM remains unknown, particularly whether it is related to GORD or represents a primary oesophageal motor disorder.

Innovations and breakthroughs

This study raises the possibility of different pathophysiologic mechanisms in the different subsets of IOM.

Applications

Further study of the IOM subsets using novel technologies such as impedance and topographic manometry is required.

Terminology

IOM refers to low-amplitude, simultaneous, or non-transmitted oesophageal body contractions.

Peer review

The authors compared the demographic and clinical features of different manometric subsets of ineffective oesophageal motility and determined whether the prevalence of gastro-oesophageal reflux differs between IOM subsets. This is an interesting and well-written study.

REFERENCES

1 **Leite LP**, Johnston BT, Barrett J, Castell JA, Castell DO. Ineffective esophageal motility (IEM): the primary finding in patients with nonspecific esophageal motility disorder. *Dig Dis Sci* 1997; **42**: 1859-1865
2 **Kahrilas PJ**, Dodds WJ, Hogan WJ. Effect of peristaltic dysfunction on esophageal volume clearance. *Gastroenterology* 1988; **94**: 73-80
3 **Tutuian R**, Castell DO. Clarification of the esophageal function defect in patients with manometric ineffective esophageal motility: studies using combined impedance-manometry. *Clin Gastroenterol Hepatol* 2004; **2**: 230-236
4 **Spechler SJ**, Castell DO. Classification of oesophageal motility abnormalities. *Gut* 2001; **49**: 145-151
5 **Ho SC**, Chang CS, Wu CY, Chen GH. Ineffective esophageal motility is a primary motility disorder in gastroesophageal reflux disease. *Dig Dis Sci* 2002; **47**: 652-656
6 **Fouad YM**, Katz PO, Hatlebakk JG, Castell DO. Ineffective esophageal motility: the most common motility abnormality in patients with GERD-associated respiratory symptoms. *Am J Gastroenterol* 1999; **94**: 1464-1467
7 **Diener U**, Patti MG, Molena D, Fisichella PM, Way LW. Esophageal dysmotility and gastroesophageal reflux disease. *J Gastrointest Surg* 2001; **5**: 260-265
8 **Kahrilas PJ**, Clouse RE, Hogan WJ. American Gastroenterological Association technical review on the clinical use of esophageal manometry. *Gastroenterology* 1994; **107**: 1865-1884
9 **Drossman DA**, Corraziari EC, Talley NJ, Thompson WG, Whitehead WE. Rome II integrative questionnaire. In: Drossman DA, Corraziari EC, Talley NJ, Thompson WG, Whitehead WE. Rome II: the functional gastrointestinal disorders. McLean VA: Degnon Associates, 2000: 691-710
10 **Bak YT**, Lorang M, Evans PR, Kellow JE, Jones MP, Smith RC. Predictive value of symptom profiles in patients with suspected oesophageal dysmotility. *Scand J Gastroenterol*

1994; **29**: 392-397
11 **Kahrilas PJ**, Quigley EM. Clinical esophageal pH recording: a technical review for practice guideline development. *Gastroenterology* 1996; **110**: 1982-1996
12 **Weusten BL**, Roelofs JM, Akkermans LM, Van Berge-Henegouwen GP, Smout AJ. The symptom-association probability: an improved method for symptom analysis of 24-hour esophageal pH data. *Gastroenterology* 1994; **107**: 1741-1745
13 **Ribeiro AC**, Klingler PJ, Hinder RA, DeVault K. Esophageal manometry: a comparison of findings in younger and older patients. *Am J Gastroenterol* 1998; **93**: 706-710
14 **Kim JH**, Rhee PL, Park EH. Evaluation of esophageal muscle thickness in patients with ineffective esophageal motility using a high-frequency intraluminal ultrasound. *Gastroenterology* 2005; **128**: W1551
15 **Achem AC**, Achem SR, Stark ME, DeVault KR. Failure of esophageal peristalsis in older patients: association with esophageal acid exposure. *Am J Gastroenterol* 2003; **98**: 35-39
16 **Richter JE**, Wu WC, Johns DN, Blackwell JN, Nelson JL 3rd, Castell JA, Castell DO. Esophageal manometry in 95 healthy adult volunteers. Variability of pressures with age and frequency of "abnormal" contractions. *Dig Dis Sci* 1987; **32**: 583-592
17 **Grande L**, Lacima G, Ros E, Pera M, Ascaso C, Visa J, Pera C. Deterioration of esophageal motility with age: a manometric study of 79 healthy subjects. *Am J Gastroenterol* 1999; **94**: 1795-1801
18 **Storr M**, Allescher HD, Classen M. Current concepts on pathophysiology, diagnosis and treatment of diffuse oesophageal spasm. *Drugs* 2001; **61**: 579-591
19 **Storr M**, Allescher HD, Rosch T, Born P, Weigert N, Classen M. Treatment of symptomatic diffuse esophageal spasm by endoscopic injections of botulinum toxin: a prospective study with long-term follow-up. *Gastrointest Endosc* 2001; **54**: 754-759
20 **Miller LS**, Pullela SV, Parkman HP, Schiano TD, Cassidy MJ, Cohen S, Fisher RS. Treatment of chest pain in patients with noncardiac, nonreflux, nonachalasia spastic esophageal motor disorders using botulinum toxin injection into the gastroesophageal junction. *Am J Gastroenterol* 2002; **97**: 1640-1646
21 **Achem SR**, Crittenden J, Kolts B, Burton L. Long-term clinical and manometric follow-up of patients with nonspecific esophageal motor disorders. *Am J Gastroenterol* 1992; **87**: 825-830
22 **Sifrim D**, Tack J, Lerut T, Janssens J. Transient lower esophageal sphincter relaxations and esophageal body muscular contractile response in reflux esophagitis. *Dig Dis Sci* 2000; **45**: 1293-1300
23 **Lemme EM**, Abrahao-Junior LJ, Manhaes Y, Shechter R, Carvalho BB, Alvariz A. Ineffective esophageal motility in gastroesophageal erosive reflux disease and in nonerosive reflux disease: are they different? *J Clin Gastroenterol* 2005; **39**: 224-227
24 **Simren M**, Silny J, Holloway R, Tack J, Janssens J, Sifrim D. Relevance of ineffective oesophageal motility during oesophageal acid clearance. *Gut* 2003; **52**: 784-790
25 **Grossi L**, Cappello G, Marzio L. Effect of an acute intraluminal administration of capsaicin on oesophageal motor pattern in GORD patients with ineffective oesophageal motility. *Neurogastroenterol Motil* 2006; **18**: 632-636
26 **Fass R**, Tougas G. Functional heartburn: the stimulus, the pain, and the brain. *Gut* 2002; **51**: 885-892
27 **Conchillo JM**, Nguyen NQ, Samsom M, Holloway RH, Smout AJ. Multichannel intraluminal impedance monitoring in the evaluation of patients with non-obstructive Dysphagia. *Am J Gastroenterol* 2005; **100**: 2624-2632

S- Editor Li DL **L- Editor** Mihm S **E- Editor** Lin YP

Online Submissions: wjg.wjgnet.com
wjg@wjgnet.com
doi:10.3748/wjg.14.3725

World J Gastroenterol 2008 June 21; 14(23): 3725-3728
World Journal of Gastroenterology ISSN 1007-9327
© 2008 The WJG Press. All rights reserved.

RAPID COMMUNICATION

Inoperable esophageal cancer and outcome of palliative care

Sima Besharat, Ali Jabbari, Shahryar Semnani, Abbasali Keshtkar, Jeran Marjani

Sima Besharat, Ali Jabbari, Shahryar Semnani, Abbasali Keshtkar, Jeran Marjani, Golestan University of Medical Sciences, Golestan Research Center of Gastroenterology and Hepatology, Gorgan 49177-65181, Iran
Author contributions: Besharat S designed the research and wrote the paper; Jabbari A contributed new references and edited the paper; Semnani S gave the idea of the research and handled it scientifically; Keshtkar A analyzed data and Marjani J gathered data.
Correspondence to: Shahryar Semnani, MD, Gastroenterologist, Golestan University of Medical Sciences, Golestan Research center of Gastroenterology and Hepatology, 2nd Floor, Nabavi Polyclinic, 4th Azar, 5 Azar Boulevard, Gorgan 49177-65181, Golestan Province, Iran. sh_semnani@yahoo.com
Telephone: +98-171-2240835 Fax: +98-171-2269210
Received: January 20, 2008 Revised: April 9, 2008
Accepted: April 16, 2008
Published online: June 21, 2008

Abstract

AIM: To determine the outcome of esophageal cancer patients referred for palliative care, in Gorgan and Gonbad gastrointestinal clinics, northeast of Iran.

METHODS: This cross-sectional study was done on inoperable esophageal cancer cases referred to gastrointestinal clinics in Gorgan and Gonbad city (2005-2006). Demographic data were collected during the procedure and cases were followed up every one month. Improvement proportion was calculated with 95% confidence interval, to determine the rate of improvement. Survival analysis and Kaplan-Meier methods were used to estimate the duration of palliative care effectiveness.

RESULTS: We recruited 39 cases into the study. Squamous cell carcinoma was the most prevalent (92.3%). The middle third of the esophagus was involved predominantly (51.3%). Dilation was the most preferred method (89.7%) and stenting was done in 4 cases. Decreasing dysphagia score was not related to palliation method or pathology type of carcinoma. Age of the patients was significantly related to the improvement of dysphagia score. Mean survival time was 137.6 d and median was 103 d.

CONCLUSION: Results of this study showed a low survival rate after palliative care in esophageal cancer cases despite dysphagia scores' improvement after dilating or stenting.

© 2008 The WJG Press. All rights reserved.

Key words: Esophageal cancer; Palliative care; Survival; Dysphagia; Iran

Peer reviewer: Robert J Korst, MD, Department of Cardiothoracic Surgery, Weill Medical College of Cornell University, Room M404, 525 East 68th Street, New York 10032, United States

Besharat S, Jabbari A, Semnani S, Keshtkar A, Marjani J. Inoperable esophageal cancer and outcome of palliative care. *World J Gastroenterol* 2008; 14(23): 3725-3728 Available from: URL: http://www.wjgnet.com/1007-9327/14/3725.asp DOI: http://dx.doi.org/10.3748/wjg.14.3725

INTRODUCTION

Esophageal cancer patients have poor prognosis. Due to the lack of widespread screening methods, diagnosis is usually made at advanced stages; therefore, they have a short survival when diagnosed. The 5-year survival rate of patients with esophageal cancer is < 20%[1].

This is more obvious especially in some regions like the northeast of Iran, where the prevalence rate of esophageal cancer is high.

Esophageal cancer five-year survival has slightly increased during past 20 years (5%-9%), but still remains low. Most patients present with locally advanced, unresectable or metastatic disease. At the time of diagnosis, 60% of the patients are only suitable for palliative therapy. Recent advances in therapeutic endoscopy have allowed improving dysphagia, and quality of life. Endoscopic techniques are chosen according to tumor characteristics, since the diagnosis is often made at an advanced stage, when radical treatment is unfeasible[1-3].

Dysphagia, or the inability to swallow, is one of the most distressing and debilitating symptoms in patients with cancer-related oesophageal obstruction. Dysphagia leads to nutritional compromise, pain, and deterioration of quality of life[1,4-5].

As the quality of life, and to some extent the quantity of life remaining to these patients depends to a large degree on their ability to swallow, the relief of dysphagia plays a vital role in the palliation of this disease[5].

Endoscopic palliation aims to restore swallowing,

avoid re-intervention and reduce hospitalization[1,4-5].

Palliation is an important goal of esophageal cancer therapy. Current management options for the palliation of dysphagia include: esophageal dilation, intraluminal stents, Nd:YAG laser therapy, photodynamic therapy, argon laser, systemic chemotherapy, external beam radiation therapy, brachytherapy, and combined chemoradiation therapy. The clinical situation, local expertise, and cost effectiveness play an important role in choosing the appropriate treatment modality[1].

Treatment should ensure that the majority of these patients could avoid the consternation of total dysphagia, regardless of which stent is offered[5].

Palliative treatment methods for esophageal and cardiac cancer include dilation, laser vaporization and other thermal methods, alcohol injection, and stent insertion. None of these procedures, however, has proved to be a simple, well-tolerated, and lasting method[5]. The aim of this study was to determining the rate of recovery after two methods of palliation in patients with inoperable esophageal carcinoma, in Golestan province, northeast of Iran.

MATERIALS AND METHODS

This descriptive cross-sectional study was designed in two main and unique clinics of gastroenterology in the province (located in the central and eastern part of Golestan Province) and all inoperable esophageal cancer cases which referred from January 2005 to March 2007 were recruited. A basic checklist was completed for each case before the procedure and their demographic data were registered.

Dysphagia was graded as follows: 0 = able to eat normal diet/no dysphagia; 1 = able to swallow some solid foods; 2 = able to swallow only semi solid foods; 3 = able to swallow liquids only; 4 = unable to swallow anything/total dysphagia[5].

Subjects were followed up every month, and the endpoint was considered as death or finishing the 6-mo period, due to the short survival of them. Improvement in dysphagia was evaluated 1 wk after stent placement and during monthly interviews.

Complications of palliative therapy were defined as major (aspiration, bleeding, stent misplacement or dislocation, perforation) or minor (reflux esophagitis, chest pain, pharyngeal discomfort). Tumor ingrowth or overgrowth was considered a treatment failure[6].

The decrease in dysphagia severity for at least one degree was registered as dysphagia recovery.

After coding data and entering into the computer, improvement proportion was calculated with 95% confidence interval, to determine the rate of improvement. Survival analysis and Kaplan-Meier methods were used to estimate the duration of palliative care effectiveness.

RESULTS

Thirty and nine cases fulfilled the inclusion criteria. Male to female ratio was 1.6 to 1. Mean age was 67.5 ± 13.7 years. Among these cases, 89.7% were palliated with dilation method, and others (n = 3) with stenting. Most of them (92.3%) were diagnosed as having SCC. The middle third of the esophagus was the most (51.3%) involved site.

Table 1 Report of dysphagia after palliative care in patients suffering from inoperable esophageal cancer in Golestan province, northeast of Iran

Dysphagia	Frequency	Percent
Recovery		
The first degree	18	46.2
The second degree	7	17.9
No recovery	4	10.3
Dysphagia aggravation	3	7.7
Not available	7	17.9
Total	39	100

Table 2 Dysphagia relief after palliative care regarding the different variables in patients suffering from inoperable esophageal cancer in Golestan province, northeast of Iran

Dysphagia relief	Variables	No recovery		Recovery	
		n	%	*n*	%
Type of palliative care	Stent	1	25	3	75
	Dilation	13	37.1	22	62.9
	Total	14	35.9	25	64.1
Age (yr)	< 65	3	21.4	11	78.6
	⩾ 65	10	40	15	60
Pathology	SCC	13	36.1	23	63.9
	Adenocarcinoma	1	33.3	2	66.7

At the beginning of the study, 22 cases (56.4%) had grade three dysphagia (dysphagia to water) and other 17 had complete or grade four dysphagia.

At the first follow up (one month after procedure), seven cases were not available (died). They passed away between 6-31 d (Table 1).

We considered these deaths as non-recovery of dysphagia, and then categorized the cases into two groups: 1, recovered and 2, not recovered (death, dysphagia aggravation or no change in dysphagia) and evaluated the relation between various variables with this condition (Table 2).

No significant relation was seen between relieving dysphagia, and method of palliative care or pathology type of the esophageal cancer (P = 0.96). Age of the patients and the dysphagia recovery was not significantly related, too (P = 0.238). Mean dysphagia score was significantly improved in the first follow up (3.37 *vs* 2.43; 95% CI, 0.62-1.25; P < 0.0001).

Among other 32 cases which were available at the first follow up, 25 were free of dysphagia. Survival analysis method was used to estimate the length of dysphagia relieving persistency after palliation. Aggravation of dysphagia at any time was considered as recurrence.

The mean time of persistent recovery was 172.1 d, and the median was 120 d. Among these 25 patients, only in ten cases no recurrence of dysphagia was reported up to the end of follow-up. At the end of 6-mo follow-up, only 6 (15.4%) patients were alive. The overall mean and median survival time was 137.6 d and 103 d after palliation, respectively.

In the recovered group, mean and median survival

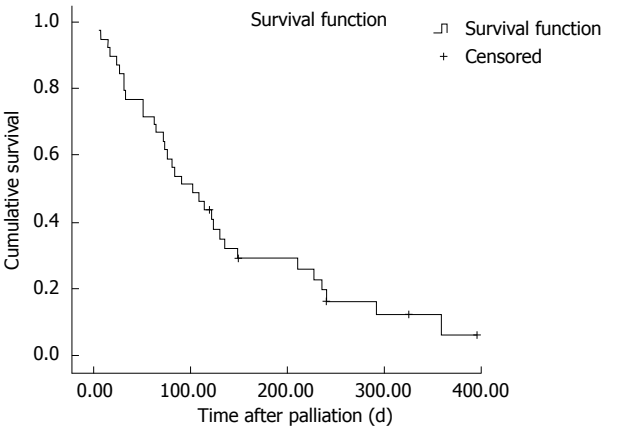

Figure 1 Survival function dysphagia recovery after palliative care by Kaplan-Meyer method.

time were 177.1 d and 135 d after palliation, respectively; while it was 60.7 d and 31 d in the other group; respectively. Kaplan-Meyer survival analysis and Log-rank used to evaluate the relation between dysphagia relief and the survival rate of the cases and significant differences were reported ($\chi^2 = 13.21$, $P < 0.0001$; Figure 1).

DISCUSSION

Diagnostic and therapeutic management of esophageal cancer is a multidisciplinary challenge. Male to female ratio in our patients was 1.6 to 1. This proportion is reported in other similar studies[5].

The most involved part of the esophagus was the middle third, and SCC was the most prominent type. While, in Western countries, the distal third is involved most[2,3], maybe the higher incidence of adenocarcinoma, and its potentiality to appear in the distal part can explain this discrepancy. Among 39 recruited cases, 25 (64%) reported a relief in dysphagia. One grade decrease in dysphagia was seen in 46.2% and 2 grade in 17.9%.

In a study in France, a total of 120 patients treated in a single center by insertion of SEMS (Self-expanding Metal Stent), dysphagia scores decreased in 89.1% of patients, with median scores decreasing from 3.0 to 1.0 ($P < 0.05$)[7]. In the present study, mean dysphagia score in the first follow-up decreased significantly compared to pre-operation (from 3.37 to 2.43). Mean survival time after procedure was 177 d (5.9 mo) in recovered group, and 60.7 d (2 mo) in the other group, which was much lower than reported in other studies[8-10].

In a study in the Netherlands (2006), data from 78 patients, rendered incurable at exploration, and who subsequently underwent palliative interventions, were analyzed retrospectively. Overall, intraluminal stenting was the palliative measure of dysphagia in 25 patients (32.3%). The median survival in the whole group was 8.9 (1-105) mo. Patients treated with chemotherapy had a higher median survival of 11.6 mo compared to that of the other palliatively-treated patients: 8.4 mo ($P = 0.003$). They concluded that patients with incurable oesophageal carcinoma have a poor overall survival of less than 9 mo[8].

In India (2006), thirty patients with inoperable esophageal carcinoma were treated with SEMS. Quality of life score improved significantly from 62-94 before stenting to 80-133 after the procedure. There was improvement in dysphagia grades. Pain was the most common complaint noted on follow up. There was no major morbidity or mortality related to the procedure[11].

In the present study, no complaints were reported immediately after procedure and in the next follow-up, except for the seven cases that reported aggravation or no recovery of dysphagia. One important and disappointing result of this investigation was the high mortality rate of esophageal cancer in our area. Seven deaths occurred between procedures until the first follow-up (one-month later) and at the end of the study, only 6 cases were alive. Ross *et al* (USA, 2007) studied ninety-seven patients with malignant dysphagia who had SEMS placed from 2000 to 2003. Dysphagia scores improved in 86%. Early unexpected deaths occurred in 2 patients. Adenocarcinoma and female sex were factors associated with increased odds of a major complication. Median survival was 77 d[10].

In the present study, dysphagia aggravation and re-dilation was implicated in 7.7%. This is a usual problem seen in all other investigations[9,11]. In a study in Norway (2006), 37 patients with unresectable esophageal and cardial carcinoma treated with SEMS (January 1997-May 2004) were retrospectively analyzed. One patient died the day the stent was introduced. The median time to repeated hospital contact was 25 d, most often due to recurrence of dysphagia. Ten patients underwent repeated stent insertion. The median survival time after the first stent insertion was 88 d[9].

In an Italian report (2007), in 60 cases with malignant dysphagia due to the various etiologies stent insertion was done. The mean dysphagia score of 2.8 improved to a mean score of 1.0 after stenting ($P < 0.001$). Overall median survival time was 4.6 mo[4]. In Germany (2007), stent insertion was done in eighteen patients with esophageal carcinoma. Seventeen of 18 stents were placed technically successful in a single endoscopic procedure. Mean dysphagia score improved from 2.2 to 0.6. In 10 patients, a re-intervention was necessary mainly due to dislocation of the stent[12].

Although placement of a stent is technically feasible, its application is hampered by frequent stent migration and insufficient prevention of gastroesophageal reflux. Further technical improvements of stents or alternative methods like brachytherapy are required for satisfactory palliation of malignant gastroesophageal stenosis[12,13].

Comparing dilation and stenting in the present survey showed that dysphagia recovered in 63.6% after dilation and in 75% after stent insertion.

Although, dysphagia relief and median survival rate were lower in our study, maybe due to the delay in referring and the developed stages at the presentation; however, it seems that palliative care is effective in relieving dysphagia of inoperable esophageal carcinoma, and is suggested for increasing quality of life in the

remaining life-span of the patients.

Implantation of stents proved to be an effective and safe method in palliating severe dysphagia in patients with obstructing esophageal cancer[14-16]; but dilation seems more popular especially in our area; while stents are more expensive, and dilation is more preferred by patients and physicians.

Larger studies with higher sample size and facilities for screening in the lower dysphagia stages and evaluating other factors that impact on the survival rate of the patients are necessary.

Accurate and expanded results could not be achieved in the present report, due to the unavailability of some data and deaths occurred between the procedure and the first follow-up. Also, all included patients had grade 3 and 4 dysphagia, which can itself have an important impact on survival rate, because of prolonged inability of swallowing and the resulting malnutrition.

ACKNOWLEDGMENTS

Authors tend to appreciate all who assist us in gathering data from Atrak clinic (Gonbad city) and 5th Azar endoscopy center (Goragn city).

COMMENTS

Background

Esophageal cancer 5-year survival has slightly increased during past 20 years (5%-9%), but still remains low. Most patients present with locally advanced, unresectable or metastatic disease. At the time of diagnosis, 60% of the patients are only relevant for palliative therapy. As the quality of life, and to some extent the quantity of life remaining to these patients depends to a large degree on their ability to swallow, the relief of dysphagia plays a vital role in the palliation of this disease.

Research frontiers

The clinical situation, local expertise, and cost effectiveness play an important role in choosing the appropriate treatment modality in these patients. Treatment should ensure that the majority of these patients could avoid the consternation of total dysphagia, regardless to which stent is offered.

Innovations and breakthroughs

Although, dysphagia relief and median survival rate were lower in our study, maybe due to the delay in referring and developed stages at the presentation time; however, it seems that palliative care is effective in relieving dysphagia of inoperable esophageal carcinoma, and is suggested for increasing quality of life in the remaining life-span of the patients.

Applications

Implantation of stents proved to be an effective and safe method in palliating severe dysphagia in patients with obstructing esophageal cancer; but dilation seems more popular especially in our area; while stents are more expensive and dilation is more preferred by patients and physicians.

Peer review

Inoperable esophageal cancer cases face many challenges due to the difficulty in eating. When the tumor is considered not resectable, palliative care would be performed to provide a temporary canal for patients. Our area is placed on the esophageal cancer belt of the world, thus, investigators try to determine different aspects of this cancer in the region and help patients have a better life expectancy. Here, we assessed the outcome of esophageal cancer patients which underwent ballooning and stenting as a palliation for their dysphagia.

REFERENCES

1 **Javle M**, Ailawadhi S, Yang GY, Nwogu CE, Schiff MD, Nava HR. Palliation of malignant dysphagia in esophageal cancer: a literature-based review. *J Support Oncol* 2006; **4**: 365-373, 379
2 **Ferrante M**, Feliziani M, Imperatori A, Ferraris L, Bernasconi G. Endoscopic palliation of esophageal cancer. *Rays* 2006; **31**: 3-7
3 **Dahan L**, Ries P, Laugier R, Seitz JF. [Palliative endoscopic treatments for esophageal cancers] *Gastroenterol Clin Biol* 2006; **30**: 253-261
4 **Conigliaro R**, Battaglia G, Repici A, De Pretis G, Ghezzo L, Bittinger M, Messmann H, Demarquay JF, Togni M, Blanchi S, Filiberti R, Conio M. Polyflex stents for malignant oesophageal and oesophagogastric stricture: a prospective, multicentric study. *Eur J Gastroenterol Hepatol* 2007; **19**: 195-203
5 **Tate H**. The Palliation of Dysphagia in Oesophageal Malignant Obstructions Using Endoprostheses: A Review of the Literature. Newcastle upon Tyne: Priory Lodge Education Ltd, 2007
6 **Winkelbauer FW**, Schofl R, Niederle B, Wildling R, Thurnher S, Lammer J. Palliative treatment of obstructing esophageal cancer with nitinol stents: value, safety, and long-term results. *AJR Am J Roentgenol* 1996; **166**: 79-84
7 **Lecleire S**, Di Fiore F, Antonietti M, Ben Soussan E, Hellot MF, Grigioni S, Dechelotte P, Lerebours E, Michel P, Ducrotte P. Undernutrition is predictive of early mortality after palliative self-expanding metal stent insertion in patients with inoperable or recurrent esophageal cancer. *Gastrointest Endosc* 2006; **64**: 479-84
8 **Pultrum BB**, van Westreenen HL, Mulder NH, van Dullemen HM, Plukker JT. Outcome of palliative care regimens in patients with advanced oesophageal cancer detected during explorative surgery. *Anticancer Res* 2006; **26**: 2289-2293
9 **Tangen M**, Andresen SJ, Moum B, Hauge T. [Stent insertion as palliation of cancer in the esophagus and cardia] *Tidsskr Nor Laegeforen* 2006; **126**: 1607-1609
10 **Ross WA**, Alkassab F, Lynch PM, Ayers GD, Ajani J, Lee JH, Bismar M. Evolving role of self-expanding metal stents in the treatment of malignant dysphagia and fistulas. *Gastrointest Endosc* 2007; **65**: 70-76
11 **Maroju NK**, Anbalagan P, Kate V, Ananthakrishnan N. Improvement in dysphagia and quality of life with self-expanding metallic stents in malignant esophageal strictures. *Indian J Gastroenterol* 2006; **25**: 62-65
12 **Schoppmeyer K**, Golsong J, Schiefke I, Mossner J, Caca K. Antireflux stents for palliation of malignant esophagocardial stenosis. *Dis Esophagus* 2007; **20**: 89-93
13 **Keller R**, Flieger D, Fischbach W, Christl SU. Self-expanding metal stents for malignant esophagogastric obstruction: experience with a new design covered nitinol stent. *J Gastrointestin Liver Dis* 2007; **16**: 239-243
14 **Cwikiel W**, Tranberg KG, Cwikiel M, Lillo-Gil R. Malignant dysphagia: palliation with esophageal stents--long-term results in 100 patients. *Radiology* 1998; **207**: 513-518
15 **Carreira Villamor JM**, Reyes Perez R, Gorriz Gomez E, Pulido-Duque JM, Argiles Vives JM, Pardo Moreno MD, Maynar Moliner M. [Wallstent endoprostheses implanted by fluoroscopic guidance in the palliative treatment of malignant esophageal obstructions and esophago-tracheal fistulas] *Nutr Hosp* 1997; **12**: 141-146
16 **Carreira JM**, Gorriz E, Reyes R, Argiles JM, Pulido JM, Pardo MD, Maynar M. [Treatment of dysphagia of malignant origin with the endoprosthesis of Strecker] *Med Clin* (Barc) 1998; **110**: 727-730

S-Editor Zhong XY **L-Editor** Kremer M **E-Editor** Ma WH

Online Submissions: wjg.wjgnet.com
wjg@wjgnet.com
doi:10.3748/wjg.14.3729

World J Gastroenterol 2008 June 21; 14(23): 3729-3732
World Journal of Gastroenterology ISSN 1007-9327
© 2008 The WJG Press. All rights reserved.

RAPID COMMUNICATION

Honey prevents hepatic damage induced by obstruction of the common bile duct

B Imge Erguder, Sibel S Kilicoglu, Mehmet Namuslu, Bulent Kilicoglu, Erdinc Devrim, Kemal Kismet, Ilker Durak

B Imge Erguder, Mehmet Namuslu, Erdinc Devrim, Ilker Durak, Department of Biochemistry, Ankara University Faculty of Medicine, Ankara 06100, Turkey
Sibel S Kilicoglu, Department of Histology and Embriology, Ufuk University Faculty of Medicine, Ankara 06800, Turkey
Bulent Kilicoglu, Kemal Kismet, Ankara Research and Training Hospital, Clinics of General Surgery, Ankara 06100, Turkey
Author contributions: Erguder BI, Devrim E and Namuslu M performed biochemical analysis in this work, Kilicoglu SS performed histological examination, Kilicoglu B removed the tissues surgically, Kismet K analyzed data; and Erguder BI, Durak I, and Kilicoglu B wrote the paper.
Correspondence to: B Imge Erguder, Ankara Universitesy Tıp Fakultesi, Biyokimya Anabilim Dali Dekanlık Binasi, Sihhiye 06100, Ankara 06100, Turkey. imgeerguder@yahoo.com
Telephone: +90-312-3103010 Fax: +90-312-3106370
Received: January 11, 2008 Revised: March 19, 2008
Accepted: March 26, 2008
Published online: June 21, 2008

Abstract

AIM: To examine the possible effects of honey supplementation on hepatic damage due to obstruction of the common bile duct in an experimental rat model.

METHODS: The study was performed with 30 male rats divided into three groups: a sham group, an obstructive jaundice group, and an obstructive jaundice plus honey group. At the end of the study period, the animals were sacrificed, and levels of nitric oxide (NO), and NO synthase (NOS) activities were measured in liver tissues, and levels of adenosine deaminase (ADA) and alanine transaminase (ALT) activities were measured in serum.

RESULTS: Blood ALT and ADA activities were significantly elevated in the jaundice group as compared to those of the sham group. In the obstructive jaundice plus honey group, blood ALT and ADA activities were significantly decreased as compared to those of the jaundice group. In erythrocytes and liver tissues, NO levels were found to be significantly higher in the obstructive jaundice plus honey group compared to those of the sham group. Additionally, NO levels were found to be significantly higher in liver tissues from the animals in the obstructive jaundice plus honey group than those of the jaundice group.

CONCLUSION: Honey was found to be beneficial in the prevention of hepatic damage due to obstruction of the common bile duct.

© 2008 The WJG Press. All rights reserved.

Key words: Honey; Obstructive jaundice; Adenosine deaminase; Nitric oxide

Peer reviewer: Syed MW Jafri, Professor, Medicine/Gastroenterology, Aga Khan University, POB 3500, Karachi 74800, Pakistan

Erguder BI, Kilicoglu SS, Namuslu M, Kilicoglu B, Devrim E, Kismet K, Durak I. Honey prevents hepatic damage induced by obstruction of the common bile duct. *World J Gastroenterol* 2008; 14(23): 3729-3732 Available from: URL: http://www.wjgnet.com/1007-9327/14/3729.asp DOI: http://dx.doi.org/10.3748/wjg.14.3729

INTRODUCTION

Honey is produced by honeybees. They obtain nectar from various flowers, and digest it in their bodies, enrich it with their salivary and enzymatic secretions, and put it in honeycombs, so that ripe honey is formed[1]. Since ancient times, honey has been known as both flavorful food and a traditional therapeutic material. It has rich flavonoid components, such as luteolin, quercetin, apigenin, fisetin, kaempferol, isorhamnetin, acacetin, tamarixetin, chrysin, and galangin, and therefore, exhibits antioxidant activity. Additionally, honey provides antibacterial, anti-inflammatory, immune-stimulant, anti-ulcer and wound/burn healing (regenerative) effects[2].

Free radicals lead to oxidative damage in many molecules, such as lipids, proteins and nucleic acids. Many complications have been attributed to oxidative damage, including atherosclerosis, aging, and cancerous diseases. Antioxidant foods that are rich in flavonoids are protective agents against these ailments[3].

Obstructive jaundice leads to oxidative injury and inflammation in hepatocytes[4,5]. Over production of hydroxyl radicals in blood and liver from rats with obstructive jaundice has been reported[6].

Nitric oxide synthase (NOS) converts arginine to

citrulline and nitric oxide (NO). Nitric oxide leads to activation of guanylyl cyclase, formation of cyclic guanosine 3',5'-monophosphate (cGMP), stimulation of cGMP-protein kinases, and subsequent relaxation in smooth muscle. It has been reported that NOS gene knockout in mice causes an elevation in blood pressure and increased synthesis of cGMP prevents platelet aggregation[7].

Adenosine deaminase (ADA; E.C. 3.5.4.4) is an enzyme that catalyses conversion of adenosine to inosine and ammonia[8]. ADA activity has been found to increase in cirrhotic patients, and increased ADA activity has been suggested as a nonspecific hepatic marker for disease with liver damage[9].

Alanine transaminase (ALT; E.C. 2.6.1.1) is a transaminase enzyme that catalyzes the inter-conversion of the amino acid L-alanine to L-glutamate and vice versa. In liver diseases associated with hepatic necrosis, ALT levels characteristically are elevated[10].

In this study, we investigated the effects of honey on the NO pathway and ADA enzyme activity in rats that had induced obstructive jaundice.

MATERIALS AND METHODS

Thirty male Wistar albino type rats of 12 wk old (250 ± 25 g in weight) were housed individually in wire cages under constant temperature (21℃ ± 2℃) with a 12 h light-dark cycle. Twelve hours before anesthesia animals were deprived of food, but had free access to water until 2 h before anesthesia. No enteral or parenteral antibiotics were administered at any time. The animals were divided randomly into 3 groups of 10 rats each: the sham group (group Ⅰ), the obstructive jaundice group (group Ⅱ) and the obstructive jaundice plus honey group (group Ⅲ). The animals were anesthetized by intramuscular injection of 30 mg/kg ketamine hydrochloride (Ketalar; Parke-Davis, Istanbul, Turkey) and 5 mg/kg xylasine (Rompun, Bayer, Istanbul, Turkey). Midline laparotomy was performed under sterile conditions. In group Ⅰ, the common bile duct (CBD) was freed from the surrounding soft tissue, and was manipulated without ligation and transection. In groups Ⅱ and Ⅲ, the CBDs of the rats were identified, double ligated with 5-0 silk, and divided between the ligatures. Group Ⅲ was nourished with honey 10 mg/kg per day by using a nasogastric tube that was inserted daily and removed after honey supplementation (Balparmak LTD, Istanbul, Turkey). The animals were sacrificed on postoperative day 7 with high-dose diethyl ether inhalation. Subsequently, their liver tissues were removed and blood samples were obtained. The blood samples were put in tubes, and then centrifuged at 2000 *g* for 5 min. Upper clear supernatant (serum) was taken and used in the enzymatic analyses. The liver tissues were first homogenized in physiologic saline (1 g in 5 mL) and then were centrifuged at 4000 *g* for 20 min. Upper clear supernatants were removed to use in the analyses. Protein levels of the supernatants were determined using Lowry's method[11] were adjusted to equal concentrations before analyses.

NO levels and NOS enzyme activities were measured in liver tissues, and ADA and ALT enzymes activities were measured in serum.

The level of NO was estimated by the method based on the diazotization of sulfanilic acid by NO at acid pH, and subsequent coupling to N-(1-naphthyl-ethylene diamine) (Griess reaction) as described previously[12]. Since nitrate anion does not give a diazotization reaction with sulfanilic acid, the samples were treated by cadmium (a reducing agent) to reduce nitrate anions into nitrite anions before the NO estimation[13]. The results were expressed as μmoL/mg protein. The total NOS activity (IU/mL) method is based on the Griess reaction[12]. The results were expressed as IU/mg protein.

Adenosine deaminase activity was studied by the method of Guisti based on spectrophotometric detection of ammonia formation[8]. The results were expressed as IU/L.

Serum ALT levels were determined by using a spectrophotometric method[14]. The results were expressed as U/L.

The histopathological analyses were carried out in the Histology and Embryology Department of Ankara University School of Medicine. Histopathological examination was performed by using light microscopic analyses. The samples were obtained from the liver and fixed in 10% neutral buffered formalin solution for 2 d. Tissues were washed in flowing water, and were dehydrated with rising concentrations of ethanol (50%, 75%, 96% and 100%). After dehydration, specimens were put into xylene to obtain transparency and were then infiltrated with, and embedded in paraffin. Embedded tissues were cut into sections of 5 μm thicknesses by Leica RM 2125 RT and were then stained with hematoxylin and eosin. Histopathologic examinations were performed and photographed by Nikon Eclipse E 600.

In the statistical evaluation of the results, one-way ANOVA, and post hoc LSD tests were used. *P* values of less than 0.05 were considered as significant.

RESULTS

The results are given in Table 1. Serum ALT and ADA enzymes activities were significantly elevated in group Ⅱ compared to those of the sham group. In group Ⅲ, serum ALT and ADA enzymes activities were found to be significantly decreased compared to those of group Ⅱ. In liver tissues, NO levels were found to be higher in group Ⅲ than those of the sham group. Additionally, NO levels were found to be significantly higher in liver tissues of group Ⅲ compared to those of group Ⅱ. There were no significant differences between groups for NOS activities.

In group Ⅰ, there were no morphological alterations in the portal tract and whole liver tissue (Figure 1A). Group Ⅱ tissues displayed some histopathological changes in the portal tract, such as proliferation of the duct epithelial cells, and looping and reduplication of

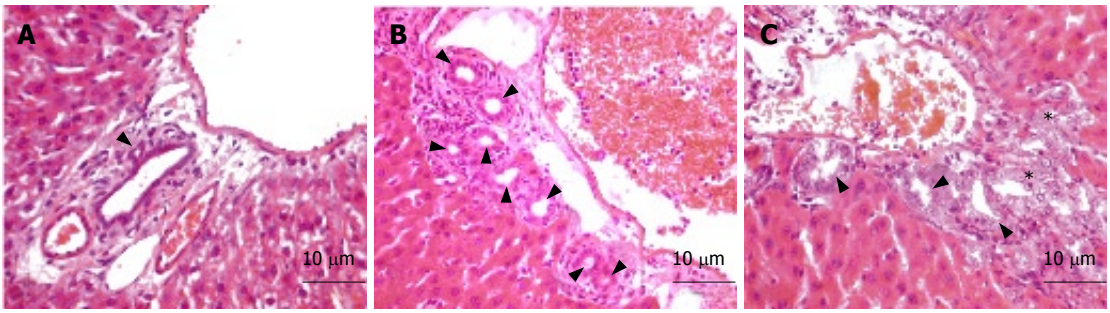

Figure 1 Portal areas of liver biopsies shown for group Ⅰ (**A**), group Ⅱ (**B**) and group Ⅲ (**C**). Bile ducts (arrow heads) and the degenerating and regressing of bile ducts (*) viewed with HE staining by light microscope.

Table 1 The biochemical parameters for each group (mean ± SD, *n* = 10)

Parameters	Group Ⅰ	Group Ⅱ	Group Ⅲ
Serum			
ALT (U/L)	28.98 ± 7.24[a]	59.49 ± 13.42[c]	17.40 ± 5.71
ADA (IU/L)	6.13 ± 4.40[a]	11.02 ± 3.14[c]	6.05 ± 3.69
Liver			
NO (μmoL/mg)	0.281 ± 0.080[a]	0.265 ± 0.065[c]	0.396 ± 0.085
NOS (IU/mg)	0.175 ± 0.031	0.183 ± 0.048	0.180 ± 0.032

ADA: Adenosine deaminase; ALT: Alanine transaminase; NO: Nitric oxide; NOS: NO synthase. Group Ⅰ: Sham operated; Group Ⅱ: Obstructive jaundice; Group Ⅲ: Obstructive jaundice + honey. [a]$P < 0.05$ *vs* Ⅱ; [c]$P < 0.05$ *vs* Ⅲ.

the ducts and ductules. The surrounding hepatocytes were enlarged (Figure 1B). Histopathological evidence showing bile ductule proliferation was markedly reduced in group Ⅲ. Regression of the bile duct epithelial cells, and phagocytosis of the debris from dying bile duct epithelial cells were observed. We also examined the conspicuous reduction in the size of enlarged hepatocytes (Figure 1C).

DISCUSSION

Since ancient times, honey has been known to have antibacterial and antioxidant properties due to its phenolic compounds[3]. It has been emphasized that honey has a rapid wound healing property[15]. Gethin *et al* demonstrated that honey has repairing potential in leg ulceration when wounds are dressed with honey[16]. The antimicrobial property of honey on some microbial isolates has also been reported[17]. Moreover, the antibacterial effect of honey on ocular flora has been displayed[18]. Furthermore, the scolicidal efficacy of propolis, which is a resinous material obtained by honey bees from plants or flowers, has been shown in cystic hydatid disease[19]. Recently, it has been found that honey leads to increased levels of NO in biological fluids and to reduced liver enzymes, such as AST and ALT, in blood[20].

In the obstructive jaundice group in our study, elevated serum ALT and ADA activities indicated liver damage. Additionally, reduced serum ALT and ADA activities in the obstructive jaundice plus honey group showed significant improvement in liver tissues. Histopathological examination also showed damage in the obstructive jaundice group with improvement in the obstructive jaundice plus honey group.

Our results showed the protective potential of honey with liver damage. It is possible that NO levels increased in the liver tissue due to the rich NO content of the honey itself, which is supported by our finding of unchanged NOS activity in liver tissue. Increased NO levels in the obstructive jaundice plus honey group may contribute to the protective result possibly through the elimination of toxic free radicals by NO.

In conclusion, we suggest that honey supplementation may give beneficial results in the prevention of hepatic damage induced by obstruction of the common bile duct.

COMMENTS

Background

In liver diseases associated with hepatic necrosis, the enzyme level characteristically is elevated. In this study, it was aimed to investigate the effects of honey on NO pathway, and adenosine deaminase (ADA) enzyme activity in rats which have induced obstructive jaundice.

Research frontiers

The authors suggest that honey supplementation may give beneficial results to prevent the hepatic damage induced by obstruction of common bile duct.

Innovations and breakthroughs

This study tries to elucidate possible mechanism for honey supplementation in the hepatic damage induced by obstruction of common bile duct.

Applications

Histopathological examination was performed by using light microscopic analyses.

Peer review

This is a valuable study indicating hepatocellular damage in obstructive jaundice group and protective potential of honey in this process. It's a well-designed and important paper.

REFERENCES

1 **Naef R,** Jaquier A, Velluz A, Bachofen B. From the linden flower to linden honey-volatile constituents of linden nectar, the extract of bee-stomach and ripe honey. *Chem Biodivers* 2004; **1**: 1870-1879

2 **Fiorani M,** Accorsi A, Blasa M, Diamantini G, Piatti E. Flavonoids from italian multifloral honeys reduce the extracellular ferricyanide in human red blood cells. *J Agric Food Chem* 2006; **54**: 8328-8334

3 **Perez E,** Rodriguez-Malaver AJ, Vit P. Antioxidant capacity of Venezuelan honey in wistar rat homogenates. *J Med Food*

2006; **9**: 510-516
4 **Celebi F,** Yilmaz I, Aksoy H, Gumus M, Taysi S, Oren D. Dehydroepiandrosterone prevents oxidative injury in obstructive jaundice in rats. *J Int Med Res* 2004; **32**: 400-405
5 **Takaoka M,** Kubota Y, Tsuji K, Yamamoto S, Ogura M, Yanagitani K, Shimatani M, Shibatani N, Inoue K. Human neutrophil functions in obstructive jaundice. *Hepatogastroenterology* 2001; **48**: 71-75
6 **Liu TZ,** Lee KT, Chern CL, Cheng JT, Stern A, Tsai LY. Free radical-triggered hepatic injury of experimental obstructive jaundice of rats involves overproduction of proinflammatory cytokines and enhanced activation of nuclear factor kappaB. *Ann Clin Lab Sci* 2001; **31**: 383-390
7 **Murray RK.** Muscle and the cytoskeleton. In: Murray RK, Granner DK, Mayes PA, Rodwell VW. Eds. Harper's Biochemistry. Stamford: Appleton & Lange, 2000: 729-730
8 **Guisti G.** Enzyme activities. In: Bergmayer UH, ed. Methods of enzymatic analysis. Weinheim Bergest: Verlag Chemia, 1974; 1087-1091
9 **Fernandez E,** Rodrigo L, Riestra S, Carcia S, Gutierrez F, Ocio G. Adenosine deaminase isoenzymes and neopterin in liver cirrhosis. *J Clin Gastroenterol* 2000; **30**: 181-186
10 **Moss DW,** Henderson AR. Clinical Enzymology. In: Burtis CA, Ashwood ER, eds. Tietz textbook of Clinical Chemistry. Philadelphia, Pennsylvania: W.B. Saunders Company, 1999: 652-654
11 **Lowry O,** Rosebrough N, Farr L, Randall R.Protein measurement with the Folin phenol reagent. *J Biol Chem* 1951; **193**: 265-275
12 **Durak I,** Kavutcu M, Kacmaz M, Avci A, Horasanli E, Dikmen B, Cimen MY, Ozturk HS. Effects of isoflurane on nitric oxide metabolism and oxidant status of guinea pig myocardium. *Acta Anaesthesiol Scand* 2001; **45**: 119-122
13 **Ridnour LA,** Sim JE, Hayward MA, Wink DA, Martin SM, Buettner GR, Spitz DR. A spectrophotometric method for the direct detection and quantitation of nitric oxide, nitrite, and nitrate in cell culture media. *Anal Biochem* 2000; **281**: 223-229
14 **Reitman S,** Frankel S. A colorim method for the determination of serum glutamic oxalacetic and glutamic pyruvic transaminases. *Am J Clin Pathol* 1957; **28**: 56-63
15 **Henriques A,** Jackson S, Cooper R, Burton N. Free radical production and quenching in honeys with wound healing potential. *J Antimicrob Chemother* 2006; **58**: 773-777
16 **Gethin G,** Cowman S. Case series of use of Manuka honey in leg ulceration. *Int Wound J* 2005; **2**: 10-15
17 **Al-Waili NS,** Akmal M, Al-Waili FS, Saloom KY, Ali A. The antimicrobial potential of honey from United Arab Emirates on some microbial isolates. *Med Sci Monit* 2005; **11**: BR433-BR438
18 **Albietz JM,** Lenton LM. Effect of antibacterial honey on the ocular flora in tear deficiency and meibomian gland disease. *Cornea* 2006; **25**: 1012-1019
19 **Kismet K,** Kilicoglu B, Koru O, Tanyuksel M, Oruc MT, Sorkun K, Salih B, Akkus MA. Evaluation on scolicidal efficacy of propolis. *Eur Surg Res* 2006; **38**: 476-481
20 **Al-Waili NS,** Saloom KY, Akmal M, Al-Waili F, Al-Waili TN, Al-Waili AN, Ali A. Honey ameliorates influence of hemorrhage and food restriction on renal and hepatic functions, and hematological and biochemical variables. *Int J Food Sci Nutr* 2006; **57**: 353-362

S- Editor Zhong XY L- Editor Lutze M E- Editor Lin YP

Online Submissions: wjg.wjgnet.com
wjg@wjgnet.com
doi:10.3748/wjg.14.3733

World J Gastroenterol 2008 June 21; 14(23): 3733-3738
World Journal of Gastroenterology ISSN 1007-9327
© 2008 The WJG Press. All rights reserved.

RAPID COMMUNICATION

Construction and expression of eukaryotic plasmids containing lamivudine-resistant or wild-type strains of Hepatitis B Virus genotype C

Wei-Zhen Xu, Yong Fang, Di Li, Yan Wang, Qing-Long Shang, Gui-Qiu Li, Xu Teng, Hong-Xi Gu

Wei-Zhen Xu, Yong Fang, Di Li, Yan Wang, Qing-Long Shang, Gui-Qiu Li, Xu Teng, Hong-Xi Gu, Department of Microbiology, Harbin Medical University, Harbin 150081, Heilongjiang Province, China

Author contributions: Xu WZ and Li D contributed equally to this study; Xu WZ and Li D designed the research, preformed the study and wrote the paper; Fang Y, Wang Y and Shang QL performed the study; Li GQ and Teng X analyzed the data; Gu HX was an instructor.

Supported by The PhD Foundation of Education Ministry, China, No. 20050226002; the Doctor Foundation of Harbin Medical University; The Youth Foundation of Heilongjiang Province, No. QC06C061; The Foundation of Education Department, Heilongjiang Province, No. 11521089

Correspondence to: Hong-Xi Gu, Department of Microbiology, Harbin Medical University, No. 157, Baojian Road, Nangang District, Harbin 150081, Heilongjiang Province, China. hxgu2432@163.com
Telephone: +86-451-86685122 Fax: +86-451-86685122
Received: March 3, 2008 Revised: April 23, 2008
Accepted: April 30, 2008
Published online: June 21, 2008

Abstract

AIM: To construct eukaryotic expression plasmids of full-length Hepatitis B Virus (HBV) genotype C genome, which contain lamivudine-resistant mutants (YIDD, YVDD) or wild-type strain (YMDD), and to observe the expression of HBV DNA and antigens [hepatitis B surface antigen (HBsAg) and hepatitis B e antigen (HBeAg)] of the recombinant plasmids in HepG2 cells.

METHODS: Three HBV full-length genomes were amplified from the plasmids pMD18T-HBV/YIDD, pMD18T-HBV/YVDD and pMD18T-HBV/YMDD, using PCR. Three recombinant plasmids were generated by inserting each of the PCR products into the eukaryotic expression vector pcDNA3.1 (+), between the *Eco*RI and *Hind*Ⅲ sites. After being characterized by restriction endonuclease digestion, and DNA sequence analysis, the recombinant plasmids were transfected into HepG2 cells. At 48 and 72 h post-transfection, the levels of intracellular viral DNA replication were detected by real-time PCR, and the expression of HBsAg and HBeAg in the cell culture supernatant was determined by ELISA.

RESULTS: Restriction endonuclease digestion and DNA sequence analysis confirmed that the three recombinant plasmids were correctly constructed. After transfecting the plasmids into HepG2 cells, high levels of intracellular viral DNA replication were observed, and HBsAg and HBeAg were secreted into the cell culture supernatant.

CONCLUSION: Eukaryotic expression plasmids pcDNA3.1 (+)-HBV/YIDD, pcDNA3.1 (+)-HBV/YVDD or pcDNA3.1 (+)-HBV/YMDD, which contained HBV genotype C full-length genome, were successfully constructed. After transfection into HepG2 cells, the recombinant plasmids efficiently expressed HBV DNA, HBsAg and HBeAg. Our results provide an experimental basis for the further study of HBV lamivudine-resistant mutants.

© 2008 The WJG Press. All rights reserved.

Key words: Hepatitis B virus; Lamivudine-resistant mutant; Wild-type strain

Peer reviewer: Eva Herrmann, Professor, Saarland University, Kirrberger Str., Homburg/Saar 66421, Germany

Xu WZ, Fang Y, Li D, Wang Y, Shang QL, Li GQ, Teng X, Gu HX. Construction and expression of eukaryotic plasmids containing lamivudine-resistant or wild-type strains of Hepatitis B Virus genotype C. *World J Gastroenterol* 2008; 14 (23): 3733-3738 Available from: URL: http://www.wjgnet.com/1007-9327/14/3733.asp DOI: http://dx.doi.org/10.3748/wjg.14.3733

INTRODUCTION

Hepatitis B Virus (HBV) infection has become one of the most serious health problems worldwide. In China, HBV prevalence is especially high. Presently, eight genotypes of HBV (A-H) have been identified, based on divergence over the entire genomic sequence of ⩾ 8%[1-4]. Different HBV genotypes have specific geographical distributions[2,5]. According to previous studies, genotypes B and C are predominant in China[6,7]. In Heilongjiang Province in northern China, HBV genotype C is dominant[8,9].

Lamivudine, a potent, non-toxic inhibitor of HBV replication in chronically infected patients, is currently one of the most effective anti-HBV drugs in the clinic.

Unfortunately, it has been found that long-term use of lamivudine leads to emergence of HBV YMDD mutants, which has been demonstrated to be associated with lamivudine resistance[10,11]. In YMDD variants, the methionine of the YMDD motif in HBV polymerase is substituted with either isoleucine, designated as YIDD, or valine, designated as YVDD. Much clinical data has indicated that patients who have developed HBV YMDD mutations show deterioration of their physical condition, and rebound of virus load in their serum[12-14]. In this study, we constructed the eukaryotic expression plasmids of HBV genotype C full-length genome, which contained wild-type, YVDD mutation or YIDD mutation, respectively. All these recombinant plasmids were shown to be able to express HBV DNA and antigens *in vitro*.

MATERIALS AND METHODS

Materials

Platinum Pfx DNA polymerase, T4 DNA ligase, and Lipofection 2000 reagent were purchased from Invitrogen (Carlsbad, CA, USA). Restriction endonucleases *Eco*RI and *Hin*dⅢ were purchased from New England Biolabs (Beijing, China). Dulbecco's modified Eagle's medium (DMEM) was purchased from GIBCO BRL (Gaithersburg, MD, USA). PCR primers were synthesized by Shanghai Sangon Biological Engineering, Technology and Services (Shanghai, China). DNA sequencing was performed by Invitrogen (Beijing, China). Enzyme immunoassay kit was purchased from Shanghai Kehua Biochemical Laboratory (Shanghai, China). Quantitative HBV PCR Fluorogence Diagnostic Kit was purchased from PG Biotechnology (Nanjing, China). Axygen DNA Mini kit was purchased from Axygen Biosciences (Union City, CA, USA). The recombinant plasmids pMD18T-HBV were constructed in our laboratory. The HBV genotype C full-length genome of wild-type strain or YIDD, YVDD mutants were obtained from serum of chronic HBV patients, and inserted into the vector pMD18T. The expression vector pcDNA3.1 (+), HepG2 cells and Escherichia coli DH5α were maintained in our laboratory.

Construction of the recombinant plasmids

The HBV full-length genome of wild-type HBV DNA, YVDD or YIDD mutants was amplified from the plasmids pMD18T-HBV, by PCR using a primer set that consisted of a sense primer: 5'TACCATGGCCCTTTT TCACCTCTGCCTAATC-3', and an antisense primer: 5'CGAGCTCTTCAAAAAGTTGCATGGTGCTGG -3'. Amplification was performed for 30 cycles using the Platinum Pfx DNA Polymerase. The PCR hot-start procedure was as follows: 95℃ for 6 min, 94℃ for 40 s, 68℃ for 3 min, plus 1 min after each 10 cycles, and 68℃ for 10 min. The *Hin*dIII/*Eco*RI-digested PCR products were ligated into *Hin*dIII/*Eco*RI-digested pcDNA3.1 (+) vector using T4 DNA ligase. The recombinant plasmids were then transformed into Escherichia coli (*E. coli*) DH5α and confirmed by restriction endonuclease digestion and DNA sequence analysis. The sequences were aligned using the Gene Runner version 3.05 (Hastings Softerware Inc., Hastings, NY, USA).

Cell culture and transfection

HepG2 cells were cultured in DMEM, supplemented with 10% fetal calf serum, penicillin (100 U/mL) and streptomycin (100 g/mL) at 37℃ in a humidified incubator with 5% CO_2. HepG2 cells in the exponential phase of growth were strictly counted and seeded onto 24-well culture plates with 1.0×10^5 cells/well. After 24 h, cells at 80%-90% confluence were transfected with the recombinant plasmids using Lipofection 2000 reagent, following the manufacturer's guidelines. The transfected cells and supernatants were then harvested after 48 or 72 h. Vector pcDNA3.1 (+) was used as a mock transfection control.

Assays of hepatitis B surface antigen (HBsAg) and hepatitis B e antigen (HBeAg)

At 48 or 72 h post-transfection, the culture supernatant was collected, centrifuged at 3000 r/min for 5 min to remove cellular debris, and transferred to a clean tube for further analysis. The expression levels of HBsAg and HBeAg were separately assayed using an enzyme immunoassay kit. According to the instructions, a ratio of sample/negative (S/N) $\geqslant$ 2.1 was considered as a positive response to HBsAg or HBeAg antigen.

Real-time fluorimetry PCR analysis of HBV DNA

Real-time fluorimetry PCR using TaqMan probe was performed to quantify HBV DNA at 48 or 72 h post-transfection. HBV DNA was extracted from the intracellular core particles using Axygen DNA Mini kit, and then examined by Quantitative HBV PCR Fluorogence Diagnostic kit. According to the instructions, an HBV DNA level $\geqslant 5.0 \times 10^2$ copies/mL was considered as a positive response.

Statistical analysis

All experiments were performed at least three times. All data were indicated as mean ± SD. Data analysis was performed by SPSS 10.0 software (Spss Inc., Chicago, IL, USA).

RESULTS

Construction and characterization of recombinant plasmids pcDNA3.1 (+)-HBV/C-YMDD, YIDD or YVDD

As shown in Figure 1A, the PCR products had the expectant molecular weight (3.2 kb). The target genes were cloned to the expression vector pcDNA3.1 (+), and transformed into *E. coli* DH5α, which generated the reconstructed plasmids pcDNA3.1 (+)/HBV/C-YMDD, YIDD or YVDD. After amplification by *E. coli*, the recombinant plasmids were extracted from the positive clones, and then characterized by digestion with restriction enzymes *Hin*dⅢ/*Eco*R Ⅰ (Figure 1B, lanes 2-4) and *Eco*R Ⅰ (Figure 1C, lanes 2-4). Vector pcDNA3.1 (+),

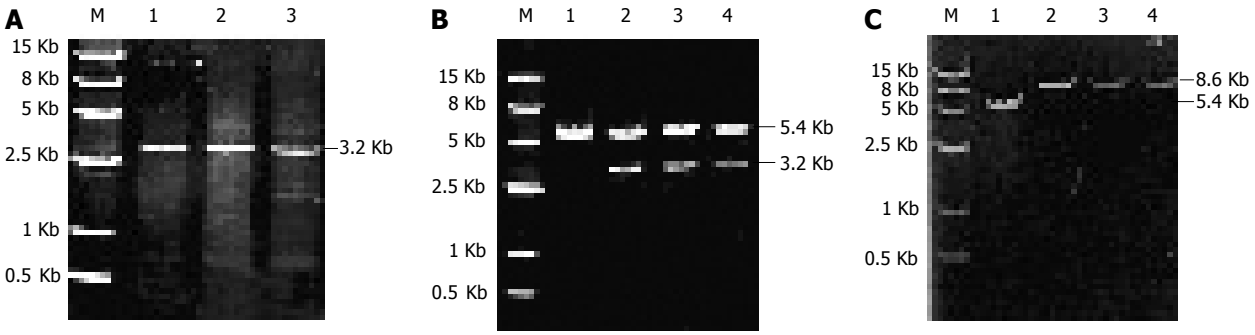

Figure 1 **A**: Electrophoresis of PCR results of HBV genotype C full-length genomes. M: Marker; lanes 1-3: PCR products of YMDD, YIDD and YVDD, respectively; **B**: Electrophoresis of digestion with *Eco*R Ⅰ/*Hind*Ⅲ. M: marker; lane 1: pcDNA3.1 (+)/*Eco*R Ⅰ; lane 2: pcDNA3.1 (+)/HBV-YMDD/*Eco*R Ⅰ/*Hind*Ⅲ; lane 3: pcDNA3.1 (+)/HBV-YIDD/*Eco*R Ⅰ/*Hind*Ⅲ; lane 4: pcDNA3.1(+)/HBV-YVDD/*Eco*R Ⅰ/*Hind*Ⅲ; **C**: Electrophoresis of digestion with *Eco*R Ⅰ. M: marker; lane 1:pcDNA3.1 (+)/*Eco*R Ⅰ; lane 2: pcDNA3.1 (+)/HBV-YMDD/*Eco*R Ⅰ; lane 3: pcDNA3.1 (+)/HBV-YIDD/*Eco*R Ⅰ; lane 4: pcDNA3.1 (+)/HBV-YVDD/*Eco*R Ⅰ.

used as a negative control, was also digested with *Eco*R Ⅰ,which yielded a product of approximate 5.4 kb in size (Figure 1B and C, lane 1). The digested products of the recombinant plasmids were visualized on 7 g/L agarose gel (Figure 1B), which demonstrated that recombinant plasmids were digested to 5.4 and 3.2 kb DNA fragments, which corresponded to the lined vector pcDNA3.1 (+) (5.4 kb) and the target gene HBV full-length genome (3.2 kb), respectively. As shown in Figure 1C, the fragment digested from the recombinant plasmids by *Eco*R Ⅰ was approximate 8.6 kb in size, as expected.

DNA sequence analysis of recombinant plasmids

DNA sequence analysis of positive clones confirmed the result. The inserted HBV full-length genome had the correct reading frame and length. Compared with the sequence of the recombinant plasmids that contained wild-type strain (Figure 2A), it was clearly shown that, in the HBV YIDD mutant (Figure 2B), the 741th base G mutated to T, and in the HBV YVDD mutant (Figure 2C), the 739th base A mutated to G. These mutations resulted in replacement of the methionine residue (amino acid 204) by isoleucine (rtM204Ⅰ), or valine (rtM204V), respectively.

Extracellular expression of HBsAg and HBeAg

At 48 or 72 h post-transfection, culture supernatants were collected. The expression levels of HBV HBsAg and HBeAg were then detected by ELISA. According to the instructions, an S/N ratio ≥ 2.1 was considered as positive HBeAg response. As shown in Table 1, our results indicated that each of the recombinant plasmids could express the antigens, HBsAg and HBeAg in HepG2 cells. The blank control group had a negative HBsAg and HBeAg response.

Intracellular expression of HBV DNA

At 48 or 72 h post-transfection, HepG2 cells were harvested and real-time fluorimetry PCR was then performed. As shown in Table 2, the three transfection groups could be considered as positive (all ≥ 5.0×10^2 copies/mL), which indicated that HBV DNA was expressed efficiently. The blank control group was negative.

DISCUSSION

Lamivudine, a potent inhibitor of HBV replication has been the main therapeutic option for treatment of chronic hepatitis B. It functions by interfering with HBV reverse transcriptase activity, and leads to a marked decrease in serum HBV DNA levels, a significant increase in the rate of HBeAg seroconversion, as well as improvement in serum alanine aminotransferase (ALT) levels[15] and liver histopathological parameters[16]. Several data have revealed that lamivudine can efficiently promote the treatment of hepatitis B in the short term. However, the long-term effectiveness of lamivudine is hampered by the development of viral resistance[15,17]. Lamivudine resistance is associated with mutations in the highly conserved YMDD motif of the reverse transcriptase, in which, methionine 204 is replaced by either isoleucine (rtM204Ⅰ, YIDD variant) or valine (rtM204V, YVDD variant).

It has been reported that the rate of HBV YMDD mutation increases with the duration of lamivudine therapy, with an increase from 15% in one year to 38% and 53% after two and three years of treatment, respectively[18]. Our previous research has also indicated that in northern China, the YMDD mutation rate is approximate 56.3% after four years of lamivudine treatment[8]. YMDD mutations not only result in a reduction in the susceptibility to lamivudine, but also cause virological and biochemical breakthrough, which are represented as rebound of HBV DNA and ALT levels[19,20]. Moreover, acute exacerbation of hepatitis and hepatic failure may occur after the emergence of YMDD mutants. Therefore, the antiviral treatment of YMDD mutants has become a crucial issue in the clinic.

HBV genotypes have distinct geographical distributions and are potential factors that affect virus replication, virus variation, clinical course, and therapy of HBV infection. In northern China, genotype C is predominant, and accounts for 77%-88% of cases of chronic hepatitis B[6,8]. Sugiyama reported that the

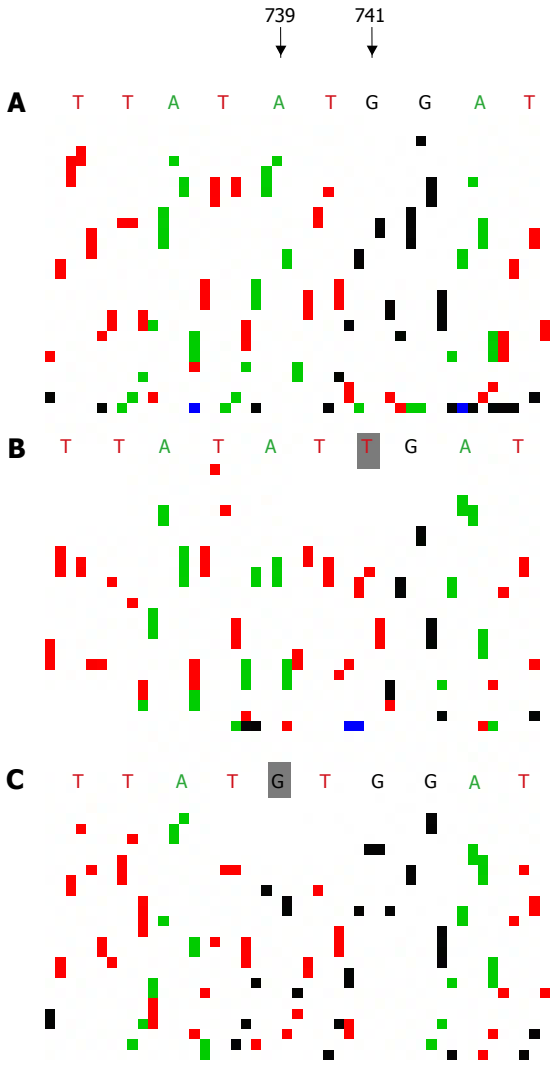

Figure 2 Sequence analysis of wild-type strain and YMDD mutants (YIDD, YVDD). **A:** Wild-type strain: 739th base is A; 741th base is G. **B**: YIDD mutant: 741th base G mutated to T. **C:** YVDD mutant: 739th base A mutated to G.

replication capacity of HBV in transfected Huh7 cells varied among genotype A and B, as well as C and D, with genotype C having the highest replication capacity[21]. HBV genotype C is associated with more severe histological liver damage and low-grade responses to interferon therapy[22]. Moreover, patients with genotype C show poor responses to embolization therapy and may die from hepatic failure because of rapid hepatocellular carcinoma (HCC) progression[23]. Another study has reported that HBV genotype C has more rapid selection of lamivudine resistance than genotype B[17].Therefore, further studies of HBV YMDD mutants with genotype C are of great significance.

To date, many *in vitro* studies on lamivudine resistance have been reported[24-27]. In most of these, recombinant plasmids containing HBV full-length or fragment genome were constructed first, and then expressed in liver-derived cell lines. For example, Gunther *et al* have reported an original and efficient method of amplifying full-length HBV genomes by PCR[24]. Chen *et al* have described a

Table 1 HBsAg and HBeAg in transfected HepG2 cells determined by ELISA

Clone	HBsAg (Sample/Negative)		HBeAg (Sample/Negative)	
	48 h	72 h	48 h	72 h
pcDNA3.1 (+)	0.33 ± 0.028	0.37 ± 0.094	0.39 ± 0.046	0.38 ± 0.050
pcDNA3.1 (+)-HBV/C YMDD	3.14 ± 0.069	3.47 ± 0.413	8.72 ± 0.059	8.77 ± 0.256
pcDNA3.1 (+)-HBV/C YIDD	6.77 ± 0.099	8.26 ± 0.334	2.06 ± 0.318	2.18 ± 0.028
pcDNA3.1 (+)-HBV/C YVDD	10.30 ± 0.065	10.37 ± 0.205	5.03 ± 0.132	5.30 ± 0.117

The ratio of sample/negative (S/N) ⩾ 2.1 was considered as positive HBsAg and HBeAg response.

Table 2 Real-time PCR detection of HBV DNA in transfected HepG2 cells (× 10^8 copies/mL)

Clone	48 h	72 h
pcDNA3.1 (+)[1]	-	-
pcDNA3.1 (+)-HBV/C YMDD	3.57 ± 0.084	3.80 ± 0.078
pcDNA3.1 (+)-HBV/C YIDD	6.85 ± 0.143	6.90 ± 0.038
pcDNA3.1 (+)-HBV/C YVDD	17.64 ± 0.240	18.55 ± 0.127

The HBV DNA levels ⩾ 5 × 10^2 copies/mL was considered as positive HBV DNA response. [1]The results were negative.

method of constructing baculovirus recombinants that contain multiple HBV lamivudine-resistant mutations, introduced by successive rounds of site-directed mutagenesis in laboratory strains[25]. However, in all these studies, either one type of HBV YMDD mutant or wild-type strains was included in the plasmids without specification of HBV genotype. Therefore, to date, serial plasmids that contain a specific HBV genotype, such as genotype C, and lamivudine-resistant sequences, which allow systematic studies on the combined effects of HBV genotype together with lamivudine-resistant mutations, have not been reported.

In this study, we successfully constructed a series of eukaryotic expression plasmids that contained genotype C HBV strain with either wild-type, YVDD or YIDD mutation, namely the plasmids pcDNA3.1 (+)-HBV/C-YMDD, pcDNA3.1 (+)-HBV/C-YVDD and pcDNA3.1 s(+)-HBV/C-YIDD, respectively. In order to achieve high-level expression *in vitro*, the Kozak sequence, ACCATGGCC-which has been found to contribute to the fidelity and efficiency of initiation and expression[28]-was coupled to the 5' end of the sense primer. Moreover, to further assure high fidelity, the PCR analyses were performed following a hot-start protocol and using high-fidelity enzymes. After transfecting the constructed plasmids into HepG2 cells, we analyzed the expression levels of HBsAg and HBeAg by ELISA, and the replication level of HBV DNA by real-time PCR. It was found that both HBV DNA and the antigens were expressed in the transfected cells, but not in the negative control cells transfected with pcDNA3.1 (+). As shown in Table 1, all the recombinant plasmids could express HBsAg in HepG2 cells. At 48 and 72 h, the expression levels of HBeAg were 8.723 ± 0.0585 and 8.77 ± 0.256,

respectively, in YMDD strains and 5.03 ± 0.132 and 5.3 ± 0.117 in YVDD mutants. However, HBeAg expression levels in YIDD mutants were only 2.06 ± 0.318 and 2.18 ± 0.028 at 48 and 72 h, respectively. This difference was probably caused by the emergence of BCP mutations (A1762T/G1764A) in YIDD mutants, while this mutation was not present in YVDD mutants. Our observation is consistent with previous reports that BCP mutation can result in a decrease in HBeAg levels[29]. In addition, HBV DNA expression levels of each of the recombination plasmids were $\geqslant 10^8$ copies/mL in HepG2 cells (Table 2), which indicates that the three recombinant plasmids can be expressed efficiently. Successful construction of the three eukaryotic plasmids pcDNA3.1 (+)-HBV/C-YMDD, pcDNA3.1 (+)-HBV/C-YVDD and pcDNA3.1 (+)-HBV/C-YIDD, provides an experimental basis for the establishment of stable expression system of HBV genotype C lamivudine-resistant mutants. The results may contribute to future in vitro antiviral studies of HBV genotype C lamivudine-resistant mutants.

ACKNOWLEDGMENT

We thank Dr. Wei Ming Xu from Columbia University Medical Center (New York, NY, USA) for her helpful suggestions when it came to written English.

COMMENTS

Background

HBV infection remains a major public health problem worldwide. Lamivudine is currently one of the most effective anti-hepatitis B virus (HBV) drugs in use clinically. However, the long-term use of lamivudine leads to the emergence of lamivudine-resistant mutants (YMDD mutants). It was reported that the rate of YMDD mutations was up to 70% after three years of treatment. The development of YMDD mutants has hampered anti-HBV therapy.

Research frontiers

In vivo and *in vitro* studies on the HBV drug-resistance mechanism have been of great interest. *In vivo* studies have mainly focused on the rate, types and detection method of YMDD mutation. However, there is still little known about the effects of YMDD mutations *in vitro*.

Innovations and breakthroughs

Appropriate and effective eukaryotic expression plasmids that are able to efficiently express HBV DNA and antigens are necessary for further *in vitro* investigations. However, to date, serial plasmids that contain a specific HBV genotype, such as genotype C, and a certain lamivudine-resistance mutation, which allow systematic studies of the combined effects of HBV genotype, together with lamivudine-resistance mutations, have not been reported. In this study, authors successfully constructed eukaryotic expression plasmids pcDNA3.1 (+)-HBV/C-YMDD, pcDNA3.1 (+)-HBV/C-YVDD and pcDNA3.1 (+)-HBV/C-YIDD, which contained genotype C HBV strain with either wild-type, YVDD or YIDD mutations, respectively, and had the ability to express HBV DNA and antigens *in vitro* with a high capacity.

Applications

The successful construction of three eukaryotic plasmids, pcDNA3.1 (+)-HBV/C-YMDD, pcDNA3.1 (+)-HBV/C-YVDD and pcDNA3.1 (+)-HBV/C-YIDD, provides an experimental basis for the establishment of a stable expression system of HBV genotype C lamivudine-resistant mutants. The results may contribute to further *in vitro* antiviral studies of HBV genotype C lamivudine-resistant mutants. This could include establishing a stable expression system for HBV genotype C lamivudine-resistant mutants for studying the mechanism of HBV lamivudine resistance.

Terminology

HBV genotype C is predominant in China, and is associated with more severe histological liver damage, lower response to anti-HBV treatment, and more rapid development of lamivudine resistance.

Peer review

The paper describes a technique for constructing eukaryotic expression plasmids of HBV genotype C with lamivudine-resistant mutants. This is an interesting topic and the manuscript is well written.

REFERENCES

1 **Miyakawa Y**, Mizokami M. Classifying hepatitis B virus genotypes. *Intervirology* 2003; **46**: 329-338
2 **Stuyver L,** De Gendt S, Van Geyt C, Zoulim F, Fried M, Schinazi RF, Rossau R. A new genotype of hepatitis B virus: complete genome and phylogenetic relatedness. *J Gen Virol* 2000; **81:** 67-74
3 **Kao JH,** Chen PJ, Lai MY, Chen DS. Genotypes and clinical phenotypes of hepatitis B virus in patients with chronic hepatitis B virus infection. *J Clin Microbiol* 2002; **40:** 1207-1209
4 **Arauz-Ruiz P,** Norder H, Robertson BH, Magnius LO. Genotype H: a new Amerindian genotype of hepatitis B virus revealed in Central America. *J Gen Virol* 2002; **83:** 2059-2073
5 **Jazayeri M,** Basuni AA, Sran N, Gish R, Cooksley G, Locarnini S, Carman WF. HBV core sequence: definition of genotype-specific variability and correlation with geographical origin. *J Viral Hepat* 2004; **11:** 488-501
6 **Gu HX,** Xu ZL, Liu JY, Zhong ZH, Wang HQ, Zhang SY, Li D, Zhang HH, Abe K. Epidemiology of HBV genotypes by nested PCR with multi-paired primers. *Shijie Huaren Xiaohua Zazhi* 2004; **12:** 1073–1076
7 **Ding X,** Mizokami M, Yao G, Xu B, Orito E, Ueda R, Nakanishi M. Hepatitis B virus genotype distribution among chronic hepatitis B virus carriers in Shanghai, China. *Intervirology* 2001; **44:** 43-47
8 **Li D,** Gu HX, Zhang SY, Zhong ZH, Zhuang M, Hattori T. YMDD mutations and genotypes of hepatitis B virus in northern China. *Jpn J Infect Dis* 2006; **59:** 42-45
9 **Ding X,** Gu H, Zhong ZH, Zilong X, Tran HT, Iwaki Y, Li TC, Sata T, Abe K. Molecular epidemiology of hepatitis viruses and genotypic distribution of hepatitis B and C viruses in Harbin, China. *Jpn J Infect Dis* 2003; **56:**19-22
10 **Allen MI,** Deslauriers M, Andrews CW, Tipples GA, Walters KA, Tyrrell DL, Brown N, Condreay LD. Identification and characterization of mutations in hepatitis B virus resistant to lamivudine. Lamivudine Clinical Investigation Group. *Hepatology* 1998; **27:** 1670-1677
11 **Stuyver L,** Van Geyt C, De Gendt S, Van Reybroeck G, Zoulim F, Leroux-Roels G, Rossau R. Line probe assay for monitoring drug resistance in hepatitis B virus-infected patients during antiviral therapy. *J Clin Microbiol* 2000; **38:** 702-707
12 **Sun J,** Wang Z, Ma S, Zeng G, Zhou Z, Luo K, Hou J. Clinical and virological characteristics of lamivudine resistance in chronic hepatitis B patients: a single center experience. *J Med Virol* 2005; **75:** 391-398
13 **Pallier C,** Castera L, Soulier A, Hezode C, Nordmann P, Dhumeaux D, Pawlotsky JM. Dynamics of hepatitis B virus resistance to lamivudine. *J Virol* 2006; **80:** 643-653
14 **Suzuki Y,** Yotsuyanagi H, Okuse C, Nagase Y, Takahashi H, Moriya K, Suzuki M, Koike K, Iino S, Itoh F. Fatal liver failure caused by reactivation of lamivudine-resistant hepatitis B virus: a case report. *World J Gastroenterol* 2007; **13:** 964-969
15 **Lai CL,** Chien RN, Leung NW, Chang TT, Guan R, Tai DI, Ng KY, Wu PC, Dent JC, Barber J, Stephenson SL, Gray DF. A one-year trial of lamivudine for chronic hepatitis B. Asia Hepatitis Lamivudine Study Group. *N Engl J Med* 1998; **339:** 61-68
16 **Dienstag JL,** Goldin RD, Heathcote EJ, Hann HW, Woessner M, Stephenson SL, Gardner S, Gray DF, Schiff ER. Histological outcome during long-term lamivudine therapy.

Gastroenterology 2003; **124:** 105-117
17 **Pan XP,** Li LJ, Du WB, Li MW, Cao HC, Sheng JF. Differences of YMDD mutational patterns, precore/core promoter mutations, serum HBV DNA levels in lamivudine-resistant hepatitis B genotypes B and C. *J Viral Hepat* 2007; **14:** 767-774
18 **Leung NW,** Lai CL, Chang TT, Guan R, Lee CM, Ng KY, Lim SG, Wu PC, Dent JC, Edmundson S, Condreay LD, Chien RN. Extended lamivudine treatment in patients with chronic hepatitis B enhances hepatitis B e antigen seroconversion rates: results after 3 years of therapy. *Hepatology* 2001; **33:** 1527-1532
19 **Yuen MF,** Sablon E, Hui CK, Yuan HJ, Decraemer H, Lai CL. Factors associated with hepatitis B virus DNA breakthrough in patients receiving prolonged lamivudine therapy. *Hepatology* 2001; **34:** 785-791
20 **Wang JH,** Lu SN, Lee CM, Lee JF, Chou YP. Fatal hepatic failure after emergence of the hepatitis B virus mutant during lamivudine therapy in a patient with liver cirrhosis. *Scand J Gastroenterol* 2002; **37:** 366-369
21 **Sugiyama M,** Tanaka Y, Kato T, Orito E, Ito K, Acharya SK, Gish RG, Kramvis A, Shimada T, Izumi N, Kaito M, Miyakawa Y, Mizokami M. Influence of hepatitis B virus genotypes on the intra-and extracellular expression of viral DNA and antigens. *Hepatology* 2006; **44:** 915-924
22 **Wai CT,** Chu CJ, Hussain M, Lok AS. HBV genotype B is associated with better response to interferon therapy in HBeAg (+) chronic hepatitis than genotype C. *Hepatology* 2002; **36:** 1425-1430
23 **Tsubota A,** Arase Y, Ren F, Tanaka H, Ikeda K, Kumada H. Genotype may correlate with liver carcinogenesis and tumor characteristics in cirrhotic patients infected with hepatitis B virus subtype adw. *J Med Virol* 2001; **65:** 257-265
24 **Gunther S,** Li BC, Miska S, Kruger DH, Meisel H, Will H. A novel method for efficient amplification of whole hepatitis B virus genomes permits rapid functional analysis and reveals deletion mutants in immunosuppressed patients. *J Virol* 1995; **69:** 5437-5444
25 **Chen RY,** Edwards R, Shaw T, Colledge D, Delaney WE 4th, Isom H, Bowden S, Desmond P, Locarnini SA. Effect of the G1896A precore mutation on drug sensitivity and replication yield of lamivudine-resistant HBV *in vitro*. *Hepatology* 2003; **37:** 27-35
26 **Sun D,** Nassal M. Stable HepG2- and Huh7-based human hepatoma cell lines for efficient regulated expression of infectious hepatitis B virus. *J Hepatol* 2006; **45:** 636-645
27 **Brunelle MN,** Jacquard AC, Pichoud C, Durantel D, Carrouee-Durantel S, Villeneuve JP, Trepo C, Zoulim F. Susceptibility to antivirals of a human HBV strain with mutations conferring resistance to both lamivudine and adefovir. *Hepatology* 2005; **41:** 1391-1398
28 **Kozak M.** An analysis of vertebrate mRNA sequences: intimations of translational control. *J Cell Biol* 1991; **115:** 887-903
29 **Parekh S,** Zoulim F, Ahn SH, Tsai A, Li J, Kawai S, Khan N, Trepo C, Wands J, Tong S. Genome replication, virion secretion, and e antigen expression of naturally occurring hepatitis B virus core promoter mutants. *J Virol* 2003; **77:** 6601-6612

S- Editor Li DL **L- Editor** Kerr C **E- Editor** Lin YP

Online Submissions: wjg.wjgnet.com
wjg@wjgnet.com
doi:10.3748/wjg.14.3739

World J Gastroenterol 2008 June 21; 14(23): 3739-3744
World Journal of Gastroenterology ISSN 1007-9327
© 2008 The WJG Press. All rights reserved.

RAPID COMMUNICATION

Reduced expression of P120 catenin in cholangiocarcinoma correlated with tumor clinicopathologic parameters

Bo Zhai, He-Xin Yan, Shu-Qin Liu, Lei Chen, Meng-Chao Wu, Hong-Yang Wang

Bo Zhai, Department of Ultrasonic Intervention, Eastern Hepatobiliary Surgery Hospital, Second Military Medical University, Shanghai 200438, China
He-Xin Yan, Shu-Qin Liu, Lei Chen, Meng-Chao Wu, Hong-Yang Wang, International Cooperation Laboratory on Signal Transduction, Eastern Hepatobilliary Surgery Institute, Second Military Medical University, Shanghai 200438, China
Author contributions: Zhai B wrote the paper and organized the figures and patient data, Yan HX and Liu SQ did the immunohistochemical staining assays; Chen L carried out the statistical analysis; Wu MC and Wang HY helped write, organize, and correct the paper; Wang HY supervised the writing and organization process.
Correspondence to: Hong-Yang Wang, International Cooperation Laboratory on Signal Transduction, Eastern Hepatobilliary Surgery Institute, Second Military Medical University, Shanghai 200438, China. hywangk@online.sh.cn
Telephone: +86-21-25070846 Fax: +86-21-65566851
Received: March 22, 2007 Revised: May 9, 2008
Accepted: May 16, 2008
Published online: June 21, 2008

Abstract

AIM: To investigate the relationship between the expression of P120 and the clinicopathologic parameters in intrahepatic cholangiocarcinoma (ICC).

METHODS: An immunohistochemical study of E-cadherin and P120 catenin was performed on 42 specimens of ICC with a Dako Envision kit.

RESULTS: The expression of E-cadherin and P120 was reduced in 27 cases (64.3%) and 31 cases (73.8%), respectively. Both E-cadherin and P120 expressions were significantly correlated with the tumor histological grade (χ^2 = 9.333, P = 009 and χ^2 = 11.71, P = 0.003), TNM stage (χ^2= 8.627, P = 0.035 and χ^2 = 13.123, P = 0.004), intrahepatic metastasis (χ^2= 7.292, P = 0.007 and χ^2 = 4.657, P = 0.041, respectively) and patients' survival (χ^2= 6.351, P = 0.002 and χ^2 = 4.023, P = 0.000, respectively). In addition, the expression of P120 was in concordance with that of E-cadherin (χ^2 = 13.797, P = 0.000), indicating that the expression of P120 may be dependent on that of E-cadherin. Finally, only P120 expression was found to be an independent prognostic factor in Cox regression model (r = 0.088, P = 0.049).

CONCLUSION: Down-regulated expression of E-cadherin and P120 occurs frequently in ICC and contributes to the progression and development of tumor. Both of them may be valuable biologic markers for predicting tumor invasion, metastasis and patients' survival, but only P120 is an independent prognostic factor for ICC.

© 2008 The WJG Press. All rights reserved.

Key words: P120; Intrahepatic cholangiocarcinoma; Clinicopathologic feature; Invasion and metastasis; Survival

Peer reviewer: Toru Ishikawa, MD, Department of Gastroenterology, Saiseikai Niigata Second Hospital, Teraji 280-7, Niigata, Niigata 950-1104, Japan

Zhai B, Yan HX, Liu SQ, Chen L, Wu MC, Wang HY. Reduced expression of P120 catenin in cholangiocarcinoma correlated with tumor clinicopathologic parameters. *World J Gastroenterol* 2008; 14(23): 3739-3744 Available from: URL: http://www.wjgnet.com/1007-9327/14/3739.asp DOI: http://dx.doi.org/10.3748/wjg.14.3739

INTRODUCTION

P120-catenin is a member of the Armadillo (ARM)/β-catenin gene family and is essential for mesenchymal cadherin-mediated regulation of cell motility and invasiveness[1,2]. Cadherin, one of the transmembrane cell-cell adhesion receptors involved in development, and morphogenesis of ICC[3], is necessary and sufficient for P120 targeting cell-cell junctions.

A main function of P120 is to stabilize cadherins at the cell membrane by regulating cadherin turnover and degradation. In this way, P120 level acts as a set point mechanism underlying cell-cell adhesive interactions. P120 may function as a "cap" to bind to the cadherin cytoplasmic tail and prevent cadherin interactions with endocytic membrane trafficking machinery. Alternatively, P120 may stabilize cell junctions or regulate membrane trafficking machinery through interactions with small GTPases, such as Rho A, Rac and Cdc42. Through these mechanisms, P120 exerts its influence over a wide range of biological processes that are dependent upon tight regulation of cell surface cadherin levels[4].

Intrahepatic cholangiocarcinoma (ICC) is the second most common tumor of primary liver cancers in adults worldwide, accounting for about 15% of liver cancers, and its incidence has increased in recent years[5]. Despite

improved diagnostic and operative techniques, the prognosis of ICC remains poor. In addition, molecular events involving the development of ICC are not well understood. Some studies examined the expression of E-cadherin/catenin complex in ICC, but the conclusion is still controversial. Moreover, to our knowledge, no study has demonstrated the expression characteristics of P120 and the relationship between the expression of P120, and the clinicopathologic parameters in ICC. Therefore, in the present study, we used immunohistochemical staining for the E-cadherin/P120 complex in primary ICC to correlate its expression with its clinicopathologic features.

MATERIALS AND METHODS

Selection of patients and definition of clinicopathologic parameters

In this study, we selected 42 specimens of intrahepatic cholangiocarcinoma collected and diagnosed at the Eastern Hepatobilliary Surgery Hospital, the Second Military Medical University from October 1997 to March 2004. The patients were consisted of 32 men and 10 women. Their age ranged from 27 to 73 years, with an average age of 51 years. Cancer tissue and non-tumorous liver tissue were obtained from each patient for pathological examination. The detailed pathologic data were obtained from the Department of Pathology of Eastern Hepatobilliary Surgery Hospital. Background liver showed cirrhosis in 19 (45.2%) patients, and chronic hepatitis in 15 (35.7%) patients.

Clinicopathologic parameters included histological grade, pTNM stage, tumor size, capsular and vascular invasion, satellite nodules, intrahepatic metastasis, lymph node status and patients' survival. Histological grade of ICC was sub-classified into well, moderately and poorly differentiated ICC based on the criteria for a liver cancer study in Japan[6]. Tumor staging was performed according to the pTNM staging system of the International Union against Cancer UICC[7].

Immunohistochemistry

Formalin-fixed and paraffin-embedded tissues were cut to 5-μm thick sections. Immunohistochemical staining for E-cadherin and P120 was performed with a Dako EnVisionTM kit (Dakocytomation Company, Denmark). The sections were dewaxed, incubated with methanol containing 30% H_2O_2 for 20 min to block endogenous peroxidase activity, immersed in 0.01 mol/L citrate buffer(pH 6.0), heated at 100℃ in a microwave oven for 20 min, washed three times with distilled water and blocked with 1% BSA for 30 min. The sections were then incubated overnight at 4℃ with rabbit polyclonal IgG of E-cadherin (H-297, SC-7870, Santa Clauze Corporation, USA) and rabbit polyclonal IgG of P120 (H-90, SC-13957, Santa Clauze Corporation, USA) at a 1:200 dilution. A subsequent reaction was carried out using second antibodies (Dakocytomation Company, Denmark) at 37℃ for 30 min. Then, the sections were washed three times with phosphate-buffered saline (PBS) and subsequently the color was displayed with DAB (Dakocytomation Company, Denmark) for about 5 min. Nuclei were lightly counterstained with hematoxylin. No staining was obtained when immune serum or PBS was used instead of primary antibodies, thus confirming the specificity of each primary antibody.

Evaluation of immunostaining

A scoring system was used to semiquantitatively evaluate the immunoexpression of E-cadherin and P120 in ICC as described previously[8]. The expression of E-cadherin and P120 in nontumorous tissue was used as an internal control. Briefly, immune activities of E-cadherin and P120 were assessed by the extent (broadness) and intensity (color strength). Depending on the percentage of positive cells, the extent was scored as follows: 0 = no positive cells or less than 5%, +1 = 5%-25% positive cells, +2 = 26%-50% positive cells, +3 = 51%-75% positive cells, and +4 = 76%-100% positive cells. The intensity was also scored as follows: 0 = no immunoreaction, +1 = mild immunoreaction, +2 = moderate immunoreaction, +3 =marked immunoreaction. E-cadherin or P120 expression was defined as positive when the composite score was 6 or 7, and as "absent or loss" when the total score was 0.

Statistical analysis

Results from immunohistochemistry were analyzed by χ^2 or Fisher's exact test. $P < 0.05$ was considered statistically significant. Survival analysis was performed using the log-rank test ($P < 0.05$). Survival curves were plotted according to the method of Kaplant and Meier. The prognosis value of E-cadherin and P120 for ICC was evaluated with univariate (log-rank test) and multivariate analysis (Cox regression model). SPSS 10.1 software package for Windows (SPSS, Inc., Chicago, IL) was used.

RESULTS

Observation under microscope

In nontumorous liver tissue, both E-cadherin and P120 were expressed strongly on cell membranes, but the staining intensity was gradually decreased. In addition, these molecules were normally expressed on cell membranes of bile ducts, proliferating ductules and intra-hepatic vessels. No expression was found in other types of cells in the liver.

In ICC, the expression of E-cadherin and P120 catenin was reduced in 27 (64.3%) and 31 cases (73.8%), being absent in 8 and 10 cases, respectively. In addition, P120 was expressed in 17 cases (40.5%) (Figure 1).

Relationship between expression of E-cadherin/P120 and histological features of ICC

As shown in Table 1, the membranous expression of E-cadherin and P120 was significantly correlated with the tumor grade ($P = 0.009$ and $P = 0.003$, respectively).

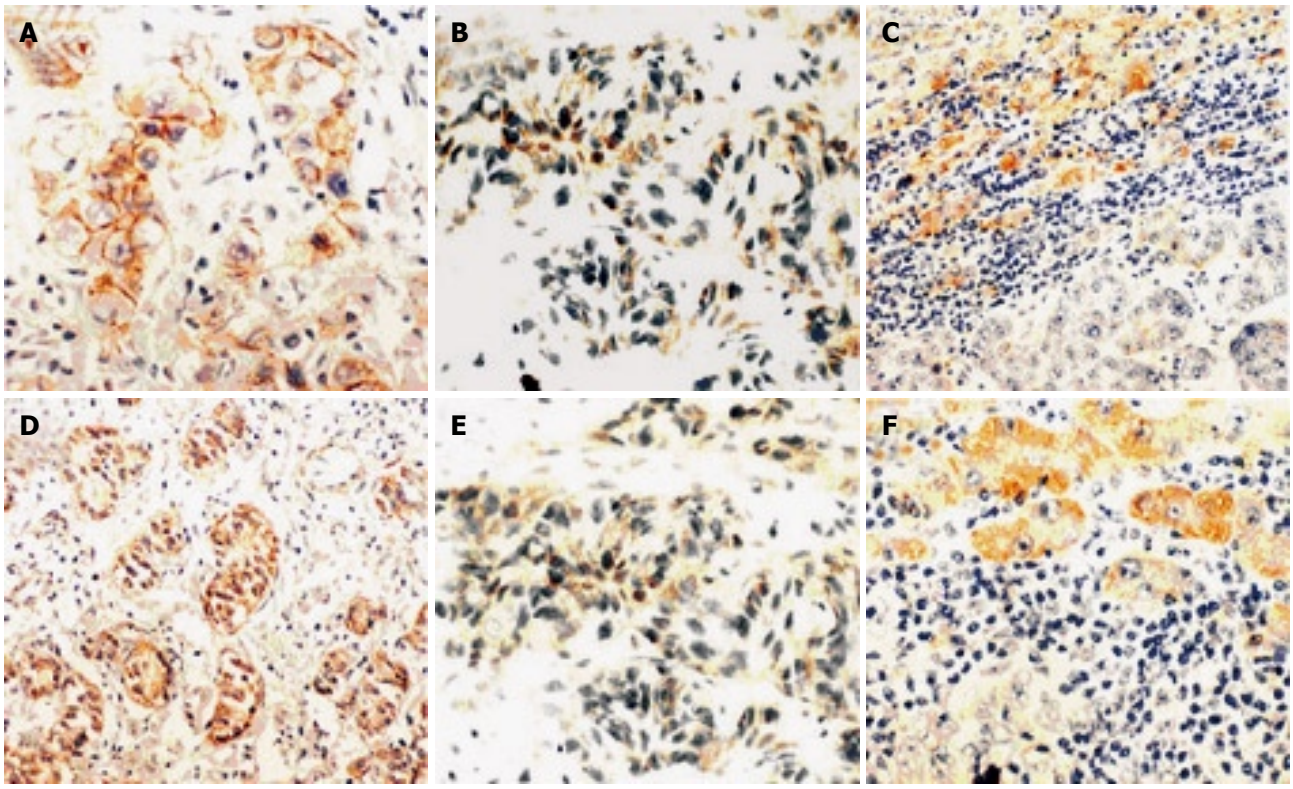

Figure 1 Immunoreactivity of E-cadherin and P120 in intrahepatic cholangiocarcinomas. "Preserved type"(+) (**A**, **D**), "reduced type"(-) (**B**, **E**), and "complete absent" (**C**, **F**) of E-cadherin and P120 induced type"(-) and staining, respectively (× 200).

Table 1 Relationship between expressions of E-cadherin/P120 catenin and histological features of ICC *n* (%)

		E-cadherin			P120 catenin		
	n	+	-	*P* value	+	-	*P* value
Differentiation grade							
Well	3	3 (100)	0 (0)	0.009	3 (100)	0 (0)	0.003
Mediate	14	7 (50.0)	7 (50.0)		5 (35.7)	9 (64.3)	
Poor	25	5 (20.0)	20 (80.0)		3 (12.0)	22 (88.0)	
pTNM							
Ⅰ	2	2 (100)	0 (0)	0.035	2 (100)	0 (0)	0.004
Ⅱ	9	5 (55.6)	4 (44.4)		5 (55.6)	4 (44.4)	
Ⅲ	25	8 (32.0)	17 (68.0)		4 (16.0)	21 (84.0)	
Ⅳ	6	0 (0)	6 (100)		0 (0)	6 (100)	

The expression of E-cadherin and P120 tended to be reduced in poorly-differentiated tumors compared with well- and moderately-differentiated tumors. In addition, the expression of E-cadherin and P120 was inversely associated with the pTNM stage of tumors ($P = 0.035$ and $P = 0.004$, respectively).

Relationship between expression of E-cadherin and P120 and clinical parameters of ICCs

As shown in Table 2, the expression of E-cadherin or P120 was significantly associated with intrahepatic matestasis of ICC ($P = 0.007$ and $P = 0.041$, respectively). No statistically significant difference was observed between the expression level of E-cadherin or P120 and tumor size, capsular and vascular invasion, lymph node permission and satellite nodules.

Relationship between expressions of E-cadherin and P120 in ICC

As shown in Table 3, positive and negative expression of E-cadherin and P120 was found in 9 and 25 cases, respectively. However, negative expression of P120 was observed in 7 cases. There was a significant concordance between the expressions of E-cadherin and P120 ($P = 0.000$).

Relationship between expression of E-cadherin/P120 and survival of ICC patients

The patients were followed up for 4-67 months. The overall survival rate of patients according to the expression of E-cadherin and P120 in tumor is shown in Figure 2. Analysis of the survival of all patients showed that abnormal expression of E-cadherin and P120 was

Table 2 Relationship between expressions of E-cadherin/P120 catenin and clinical parameters of ICC *n* (%)

		E-cadherin			P120 catenin		
	n	+	-	*P* value	+	-	*P* value
Size							
< 5 cm	17	7 (41.2)	10 (58.8)	0.826	6 (35.3)	11 (64.7)	0.584
5-10 cm	16	5 (31.3)	11 (68.7)		3 (18.8)	12 (81.2)	
> 10 cm	9	3 (33.3)	6 (66.7)		2 (22.2)	7 (77.8)	
Capsular invasion							
+	6	4 (66.7)	2 (33.3)	0.164	3 (50)	3 (50)	0.391
-	36	11 (30.6)	25 (69.4)		8 (22.2)	28 (77.8)	
Satellite nodules							
+	11	4 (36.4)	7 (65.6)	1	3 (27.3)	8 (72.7)	0.314
-	31	11 (35.5)	20 (64.5)		8 (25.8)	23 (74.2)	
Vascular invasion							
+	13	2 (15.4)	11 (84.6)	0.089	1 (7.7)	12 (92.3)	0.127
-	29	13 (44.8)	16 (55.2)		10 (34.5)	19 (65.5)	
L.N.P							
+	7	1 (14.3)	6 (85.7)	0.39	0 (0)	7 (100)	0.161
-	35	14 (40)	21 (60)		11 (31.4)	24 (68.6)	
I.M.							
+	10	0 (0)	10 (100)	0.007	0 (0)	10 (100)	0.041
-	32	15 (46.9)	17 (53.1)		11 (34.4)	21 (65.6)	

Table 3 Relationship between expression of E-cadherin and P120 catenin in ICC

E-cadherin	P120 +	P120 -	*P* value
+	9	6	0.000
-	2	25	

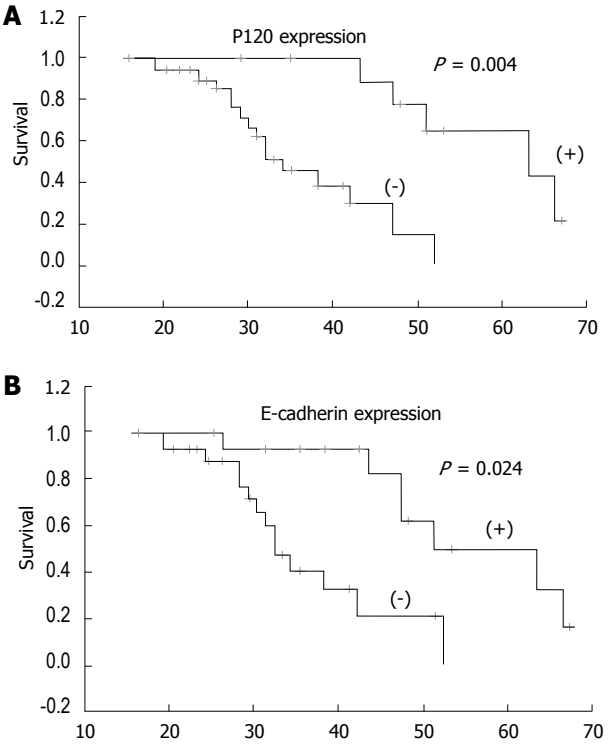

Figure 2 Kaplan-Meier survival curves. **A**: Expression of P120 induced type"(-) and **B**: Expression of E-cadherin.

significantly correlated with the poor survival of patients ($P = 0.024$ and $P = 0.004$, respectively). However,

Table 4 Cox multivariate analysis for survival of 37 patients

	Sig	RR	95% CI	
			Lower	Upper
E-cadherin expression	0.724	1.525	0.147	15.827
P120 expression	0.049	0.088	0.008	0.991
Differentiation	0.194	0.407	0.105	1.583
pTNM stage	0.073	2.898	0.904	9.288
Tumor size	0.037	0.387	0.159	0.944
Capsular invasion	0.052	17.046	0.981	6.166
Satellite nodules	0.709	1.597	0.137	18.578
Vascular invasion	0.948	0.961	0.284	3.247
Limph node invasion	0.087	4.72	0.8	27.855
Intrahepatic metastasis	0.786	1.352	0.154	11.899

Sig: Significance; RR: Relative risk; CI: Confidence interval.

when the expression of E-cadherin or P120 and the clinicopathological parameters were analyzed by the Cox regression model, abnormal expression of P120 was found to be an independent prognostic factor for ICC patients ($P = 0.049$) (Table 4).

DISCUSSION

Usually, ICC is an adenocarcinoma and may arise from the large intra-hepatic bile ducts near the hepatic hilus or from the bile ducts at the border of hepatic parenchyma. It was reported that altered expression of E-cadherin/catenins complex in ICC occurs frequently and is significantly correlated with tumor histological features and/or vascular invasion and metastasis[9-14].

It was recently reported that P120 plays a role in the occurrence of various cancers, and that P120 may behave either as a tumor suppressor or as a metastasis promoter, depending on the loss of E-cadherin and P120. If E-cadherin is lost first, P120 may directly and actively promote metastasis. If P120 is lost first, E-cadherin levels would fall significantly, which is likely to be parallel to

the reduced levels of α-and β-catenins[15]. P120 down-regulation results in a striking dose-dependant loss of endogenous cadherins, indicating that P120 is essential for cadherin stability. Moreover, P120 down-regulation occurs frequently in almost all carcinomas[16]. P120 loss is often associated with the stage and poor prognosis of tumors, suggesting that its loss may be associated with biological aggressiveness and progression of tumors. Nevertheless, to our knowledge, no report is available on the expression of P120 in human intrahepatic chola-giocarcinoma.

The present study showed that reduced or absent expression of E-cadherin and P120 was associated with the histological grade of tumors, which is consistent with reported data[17-21]. In well-differentiated tumors, there were obvious and strong staining along the cell-cell boundaries, whereas in poorly- differentiated tumors, the immunohistostaining was focally and heterogeneously distributed, with patchy or spotty features along the cell-cell boundaries, indicating that the staining of E-cadheri and P120 is related with the differentiation of ICC, namely both E-cadherin and P120 may be regarded as differentiation markers of tumor. In addition, the staining intensity of the E-cadheri and P120 complex was gradually decreased, suggesting that P120 may play a critical role in ICC progression.

Microscopy revealed that E-cadherin was located on the membrane either in non-tumor tissues or in tumor cells, whereas P120 was expressed on the membrane or in cytoplasm of tumor cells. However, it was reported that P120 is also in nuclei[22], suggesting that P120 plays an important role in cell signal transduction. P120 has an intrinsic nucleocytoplasmic shuttling activity that is modulated, in part, by extrinsic factors such as cadherin binding and interactions with the microtubule network[22]. Julia and his colleagues reported[23] that P120 displays up-regulation and nuclear expression in pancreatic cancer. No expression of P120 in nuclei of cancer cells, however, was observed in our study, suggesting that it is necessary to further investigate the mechanism underlying P120 expression in nuclei of cancer cells.

In this study, we observed the relationship between reduced expression of E-cadherin and P120 and several clinicopathologic parameters of ICC. The expression of P120 and E-cadherin was significantly associated with tumor pTNM stage and intrahepatic metastasis (IM), but not with tumor stage and size, capsular and vascular invasion, and lymph node invasion. Osada and his colleagues[24] revealed that E-cadherin is involved in intra-hepatic metastasis of hepatocellular carcinoma. Asayama *et al*[13] detected the expression of E-cadherin in hepatocellular carcinoma and cholangiocarcinoma, and found that reduced expression of E-cadherin is significantly correlated with the grade and IM of ICC. Therefore, E-cadherin and P120 may be important mediators in tumor progression, and can be considered as invasion and metastasis markers of ICC.

Several studies on other cancers have evaluated the relationship between the expression of E-cadherin/P120 and the survival of patients, but the results remain debatable[25-29]. In the present study, reduced expression of both E-cadherin and P120 was significantly related with the survival of patients. However, when the expression of E-cadherin/P120 and the clinicopathological parameters of ICC were analyzed by the Cox regression model, only the abnormal expression of P120 was found to be an independent prognostic factor for ICC, suggesting that P120 can be considered a valuable biological marker for predicting the prognosis of ICC patients.

In summary, abnormal expression of E-cadherin and P120 catenin occurs frequently in intrahepatic cholangiocarcinoma. Reduced expression of P120 catenin and E-cadherin is correlated with tumor differentiation, pTNM stage, intrahepatic metastasis and survival of patients. Both P120 catenin and E-cadherin may play an important role in the development and progression of human intrahepatic cholangiocarcinoma.

ACKNOWLEDGMENTS

The authors thank Miss Guo LN, International Cooperation Laboratory on Signal Transduction, Eastern Hepatobilliary Surgery Institute, Second Military Medical University, for her valuable advice on cell staining.

COMMENTS

Background

P120-catenin is a member of the E-cadherin/catenin complex family and may be associated with biological aggressiveness and progression of tumors. However, no report is available on the expression of P120 catenin in human intra-hepatic cholangiocarcinoma.

Research frontiers

P120 down-regulation occurs frequently in almost all carcinomas. P120 loss is often associated with the stage and poor prognosis of tumors.

Innovations and breakthroughs

Our results suggest that down-regulated expression of E-cadherin and P120 catenin occurred frequently in intrahepatic cholangiocarcinoma (ICC) and contributed to the progression and development of tumors. Both E-cadherin and P120 catenin may be valuable biologic markers for predicting tumor invasion, metastasis and survival of patients, but only P120 catenin is an independent prognostic factor for ICC.

Applications

Because down-regulated expression of P120 contributes to the progression and development of ICC, P120 can be used as a valuable biologic marker for predicting the invasion and metastasis of ICC, and the survival of patients.

Peer review

This is an interesting report on E-cadherin and P120 catenin in human intrahepatic cholangiocarcinoma. The study was performed on 42 specimens of ICC with a Dako Envision kit, indicating that. Both E-cadherin and P120 catenin may be valuable biological markers for predicting tumor invasion, metastasis and survival of patients. However, its clinical application should be further studied.

REFERENCES

1 **Reynolds AB**, Herbert L, Cleveland JL, Berg ST, Gaut JR. p120, a novel substrate of protein tyrosine kinase receptors and of p60v-src, is related to cadherin-binding factors beta-catenin, plakoglobin and armadillo. *Oncogene* 1992; **7**: 2439-2445

2 **Yanagisawa M**, Anastasiadis PZ. p120 catenin is essential for mesenchymal cadherin-mediated regulation of cell motility and invasiveness. *J Cell Biol* 2006; **174**: 1087-1096

3 **Nollet F**, Berx G, van Roy F. The role of the E-cadherin/catenin adhesion complex in the development and

progression of cancer. *Mol Cell Biol Res Commun* 1999; **2**: 77-85
4 **Xiao K**, Oas RG, Chiasson CM, Kowalczyk AP. Role of p120-catenin in cadherin trafficking. *Biochim Biophys Acta* 2007; **1773**: 8-16
5 **Patel T**. Increasing incidence and mortality of primary intrahepatic cholangiocarcinoma in the United States. *Hepatology* 2001; **33**: 1353-1357
6 **The general rules for the clinical and pathological study of primary liver cancer.** Liver Cancer Study Group of Japan. *Jpn J Surg* 1989; **19**: 98-129
7 **Hermanek P**, Hutter RVP, Sobin LH. TNM Atlas, UICC. 4 th ed. Berlin: *Springer* 1997: 115-123
8 **Gamallo C**, Palacios J, Suarez A, Pizarro A, Navarro P, Quintanilla M, Cano A. Correlation of E-cadherin expression with differentiation grade and histological type in breast carcinoma. *Am J Pathol* 1993; **142**: 987-993
9 **Ashida K**, Terada T, Kitamura Y, Kaibara N. Expression of E-cadherin, alpha-catenin, beta-catenin, and CD44 (standard and variant isoforms) in human cholangiocarcinoma: an immunohistochemical study. *Hepatology* 1998; **27**: 974-982
10 **Sato K**, Murai H, Ueda Y, Katsuda S. Intrahepatic sarcomatoid cholangiocarcinoma of round cell variant: a case report and immunohistochemical studies. *Virchows Arch* 2006; **449**: 585-590
11 **Settakorn J**, Kaewpila N, Burns GF, Leong AS. FAT, E-cadherin, beta catenin, HER 2/neu, Ki67 immuno-expression, and histological grade in intrahepatic cholangiocarcinoma. *J Clin Pathol* 2005; **58**: 1249-1254
12 **Tokumoto N**, Ikeda S, Ishizaki Y, Kurihara T, Ozaki S, Iseki M, Shimizu Y, Itamoto T, Arihiro K, Okajima M, Asahara T. Immunohistochemical and mutational analyses of Wnt signaling components and target genes in intrahepatic cholangiocarcinomas. *Int J Oncol* 2005; **27**: 973-980
13 **Asayama Y**, Taguchi Ki K, Aishima Si S, Nishi H, Masuda K, Tsuneyoshi M. The mode of tumour progression in combined hepatocellular carcinoma and cholangiocarcinoma: an immunohistochemical analysis of E-cadherin, alpha-catenin and beta-catenin. *Liver* 2002; **22**: 43-50
14 **Sugimachi K**, Taguchi K, Aishima S, Tanaka S, Shimada M, Kajiyama K, Sugimachi K, Tsuneyoshi M. Altered expression of beta-catenin without genetic mutation in intrahepatic cholangiocarcinoma. *Mod Pathol* 2001; **14**: 900-905
15 **Thoreson MA**, Reynolds AB. Altered expression of the catenin p120 in human cancer: implications for tumor progression. *Differentiation* 2002; **70**: 583-589
16 **Reynolds AB**, Carnahan RH. Regulation of cadherin stability and turnover by p120ctn: implications in disease and cancer. *Semin Cell Dev Biol* 2004; **15**: 657-663
17 **Bremnes RM**, Veve R, Gabrielson E, Hirsch FR, Baron A, Bemis L, Gemmill RM, Drabkin HA, Franklin WA. High-throughput tissue microarray analysis used to evaluate biology and prognostic significance of the E-cadherin pathway in non-small-cell lung cancer. *J Clin Oncol* 2002; **20**: 2417-2428
18 **Sarrio D**, Perez-Mies B, Hardisson D, Moreno-Bueno G, Suarez A, Cano A, Martin-Perez J, Gamallo C, Palacios J. Cytoplasmic localization of p120ctn and E-cadherin loss characterize lobular breast carcinoma from preinvasive to metastatic lesions. *Oncogene* 2004; **23**: 3272-3283
19 **Ishizaki Y**, Omori Y, Momiyama M, Nishikawa Y, Tokairin T, Manabe M, Enomoto K. Reduced expression and aberrant localization of p120catenin in human squamous cell carcinoma of the skin. *J Dermatol Sci* 2004; **34**: 99-108
20 **Qian ZR**, Sano T, Yoshimoto K, Asa SL, Yamada S, Mizusawa N, Kudo E. Tumor-specific downregulation and methylation of the CDH13 (H-cadherin) and CDH1 (E-cadherin) genes correlate with aggressiveness of human pituitary adenomas. *Mod Pathol* 2007; **20**: 1269-1277
21 **Bremnes RM**, Veve R, Gabrielson E, Hirsch FR, Baron A, Bemis L, Gemmill RM, Drabkin HA, Franklin WA. High-throughput tissue microarray analysis used to evaluate biology and prognostic significance of the E-cadherin pathway in non-small-cell lung cancer. *J Clin Oncol* 2002; **20**: 2417-2428
22 **Roczniak-Ferguson A**, Reynolds AB. Regulation of p120-catenin nucleocytoplasmic shuttling activity. *J Cell Sci* 2003; **116**: 4201-4212
23 **Mayerle J**, Friess H, Buchler MW, Schnekenburger J, Weiss FU, Zimmer KP, Domschke W, Lerch MM. Up-regulation, nuclear import, and tumor growth stimulation of the adhesion protein p120 in pancreatic cancer. *Gastroenterology* 2003; **124**: 949-960
24 **Osada T**, Sakamoto M, Ino Y, Iwamatsu A, Matsuno Y, Muto T, Hirohashi S. E-cadherin is involved in the intrahepatic metastasis of hepatocellular carcinoma. *Hepatology* 1996; **24**: 1460-1467
25 **Bellovin DI**, Bates RC, Muzikansky A, Rimm DL, Mercurio AM. Altered localization of p120 catenin during epithelial to mesenchymal transition of colon carcinoma is prognostic for aggressive disease. *Cancer Res* 2005; **65**: 10938-10945
26 **Wang EH**, Liu Y, Xu HT, Dai SD, Liu N, Xie CY, Yuan XM. Abnormal expression and clinicopathologic significance of p120-catenin in lung cancer. *Histol Histopathol* 2006; **21**: 841-847
27 **Wijnhoven BP**, Pignatelli M, Dinjens WN, Tilanus HW. Reduced p120ctn expression correlates with poor survival in patients with adenocarcinoma of the gastroesophageal junction. *J Surg Oncol* 2005; **92**: 116-123
28 **Bantis A**, Giannopoulos A, Gonidi M, Liossi A, Aggelonidou E, Petrakakou E, Athanassiades P, Athanassiadou P. Expression of p120, Ki-67 and PCNA as proliferation biomarkers in imprint smears of prostate carcinoma and their prognostic value. *Cytopathology* 2004; **15**: 25-31
29 **Nakopoulou L**, Gakiopoulou-Givalou H, Karayiannakis AJ, Giannopoulou I, Keramopoulos A, Davaris P, Pignatelli M. Abnormal alpha-catenin expression in invasive breast cancer correlates with poor patient survival. *Histopathology* 2002; **40**: 536-546

S- Editor Sun YL **L- Editor** Wang XL **E- Editor** Lin YP

Online Submissions: wjg.wjgnet.com
wjg@wjgnet.com
doi:10.3748/wjg.14.3745

World J Gastroenterol 2008 June 21; 14(23): 3745-3749
World Journal of Gastroenterology ISSN 1007-9327
© 2008 The WJG Press. All rights reserved.

RAPID COMMUNICATION

Effects of different *Helicobacter pylori* culture filtrates on growth of gastric epithelial cells

Yan-Guo Yan, Gang Zhao, Jin-Ping Ma, Shi-Rong Cai, Wen-Hua Zhan

Yan-Guo Yan, Department of General Surgery, The Affiliated Hospital of Wuhan University of Science & Technology, Wuhan 430064, Hubei Province, China
Gang Zhao, The Second Department of General Surgery, Guangdong Province Hospital, Guangzhou 510080, Guangdong Province, China
Jin-Ping Ma, Shi-Rong Cai, Wen-Hua Zhan, Department of Gastrointestinal and Pancreatic Surgery, The First Affiliated Hospital, Research Center for Gastric Cancer, Sun Yat-sen University, Guangzhou 510080, Guangdong Province, China
Supported by The National Natural Science Foundation of China, No. 30271276
Author contributions: Yan YG, Zhao G, performed the research and wrote the paper and contributed equally to this work; Zhan WH and Ma JP designed the research; Cai SR recorded the data.
Correspondence to: Yan-Guo Yan, Department of General Surgery, The Affiliated Hospital of Wuhan University of Science & Technology, Wuhan 430064, Hubei Province, China. yan969400@yahoo.com.cn
Telephone: +86-27-51164927 Fax: +86-27-51163527
Received: January 6, 2008 Revised: April 21, 2008
Accepted: April 28, 2008
Published online: June 21, 2008

Abstract

AIM: To study the effects of different *Helicobacter pylori* (*H pylori*) culture filtrates on growth of gastric epithelial cells.

METHODS: Broth culture filtrates of *H pylori* were prepared. Gastric epithelial cells were treated with the filtrates, and cell growth was determined by growth curve and flow cytometry. DNA damage of gastric epithelial cells was measured by single-cell microgel electrophoresis.

RESULTS: Gastric epithelial cells proliferated actively when treated by *CagA*-gene-positive broth culture filtrates, and colony formation reached 40%. The number of cells in S phase increased compared to controls. Comet assay showed 41.2% comet cells in GES-1 cells treated with CagA-positive filtrates ($P < 0.05$).

CONCLUSION: CagA-positive filtrates enhance the changes in morphology and growth characteristics of human gastric epithelial tumor cells. DNA damage maybe one of the mechanisms involved in the growth changes.

© 2008 The WJG Press. All rights reserved.

Key words: *CagA* gene; Gastric epithelial cell; *Helicobacter pylori*; Single cell microgel electrophoresis

Peer reviewer: Yvan Vandenplas, Professor, Department of Pediatrics, AZ-VUB, Laarbeeklaan 101, Brussels 1090, Belgium

Yan YG, Zhao G, Ma JP, Cai SR, Zhan WH. Effects of different *Helicobacter pylori* culture filtrates on growth of gastric epithelial cells. *World J Gastroenterol* 2008; 14(23): 3745-3749 Available from: URL: http://www.wjgnet.com/1007-9327/14/3745.asp DOI: http://dx.doi.org/10.3748/wjg.14.3745

INTRODUCTION

Infection with the gastric bacterium *Helicobacter pylori* (*H pylori*) the causative agent of chronic gastritis is associated with an increased risk of developing gastric cancer[1-6]. The international agency for research on cancer has classified *H pylori* as a type I carcinogen[7-10]. A number of studies have pointed to a link between carriage of CagA+ strains and an increased risk of gastric cancer[11-13]. The mechanism by which *H pylori* promotes the development of gastric cancer is presently unclear. Studies have shown that CagA can bind to other signaling molecules, such as SHP2, GRB2, c-MET and phospholipase C to promote gastric carcinogenesis[14-19], which depends on a type Ⅳ secretion system to translocate CagA into host cells.

The aim of this study was to investigate the effects of *H pylori* culture filtrates that contained CagA protein on the growth of gastric epithelial cells. *CagA*-gene-positive and negative *H pylori* culture filtrates were prepared to treat gastric epithelial cells, to observe DNA damage and growth changes.

MATERIALS AND METHODS

Bacterial strains

H pylori strains NCTC11639 (CagA-positive, VacA-negative) and G50 (CagA-negative, VacA-negative) were provided by the Chinese Center for Disease Control and Prevention.

Production of culture filtrates

H pylori was grown in Brucella broth, supplemented with 5% fetal calf serum (Gibco, Grand Island, NY,

USA), for 24-36 h at 37℃ in a thermostatic shaker under microaerophilic conditions. As described by Sommi *et al*[20], when bacterial suspensions reached A_{450} 1.2 (corresponding to a bacterial concentration of 5×10^8 CFU/mL), to obtain the *H pylori* culture filtrate, we then removed bacteria by centrifugation (12000 *g* for 10 min) and sterilized the supernatants by passage through a 0.22 μm cellulose acetate filters (Nalge, Rochester, NY, USA). Uninoculated broth filtrate served as a blank control. To remove ammonia, we dialyzed control and culture filtrates against Hanks' balanced salt solution for 36 h in dialysis tubing, with a 12 kDa molecular mass cutoff (Sigma, St. Louis, MO, USA). The presence of CagA in the culture filtrates was tested by means of SDS-PAGE, followed by Western blotting[21,22]. Total protein content was determined by measuring A_{280}. The conditioned broth was stored at -70℃ until use. There were three groups: CagA+, CagA- and blank control.

Western blotting

Culture filtrates were subjected to 12% SDS-PAGE and transferred to polyvinylidene membranes using standard procedures, and incubated with primary monoclonal anti-CagA antibodies (1:5000) (Santa Cruz Biotechnology, Santa Cruz, CA, USA). Horseradish peroxidase-conjugated secondary antibodies (Boster, China) were used and the immunoreactive proteins were visualized by an ECL detection system (Amersham Biosciences, Uppsala, Sweden).

Human gastric epithelial cells

GES-1 cells (Beijing Institute for Cancer Research Collection) were maintained in DMEM high-glucose medium (Gibco) containing 10% FCS (Sigma, Poole, UK) and different *H pylori* culture filtrates (10% v/v), in 24-well plates. Cell cultures were maintained at 37℃ in a humidified atmosphere of 95% air and 5% CO_2, continuously for 1 mo. The culture medium was changed every 3 d.

MTT assay for cell proliferation

The effect of culture filtrate on endothelial cell proliferation was determined by MTT assay (Sigma). Briefly, GES-1 cells were plated in 24-well plates and cultured overnight in growth medium for 1 mo. 2.5×10^4 cells were inoculated in three groups: CagA+, CagA- and blank control. The viable cells were quantified by, MTT assay at 1-7 d, following the manufacturer's instructions.

Flat clone formation test

The gastric epithelial cells in logarithmic phase were digested to produce single-cell suspension by 0.25% tryptase. Five hundred cells were dispersed in a culture dish (diameter 60 mm); culture medium was added, and the cells were cultured for 2 wk. When clones were visible, the supernatant was removed, and fixed in methanol for 15 min. The samples were stained with 0.4% crystal violet for 20 min, rinsed in water, air dried, and the number of clones that contained above 50 cells was calculated, according to the formula: cloning rate = average clone number/500 × 100%.

Cell cycle and apoptosis rate analysis by flow cytometry

For analysis of DNA content, cells treated with different *H pylori* culture broths were harvested after 72 h and fixed with 70% cold ethanol for 4 h. The apoptosis rate was detected by flow cytometry (FACSalibur, BD Biosciences). Briefly, 1×10^6 cells/mL were suspended in 0.2% triton X-100/PBS solution containing 1 g/L ribonuclease A. After incubation for 20 min, DNA was stained with 50 mg/L propidium iodide. Flow cytometry was performed to determine the apoptosis rate.

Single-cell microgel electrophoresis (comet assay)

The alkaline comet assay in single-cell suspensions was performed according to the method of Singh *et al*[23], with some modifications[24]. Briefly, 15 μL of the single cell suspension (2×10^4 cells) was embedded in 0.5% low-melting-point agarose (Sigma) and spread on agarose-precoated microscope slides. Slides were immersed overnight at 4℃ in freshly prepared cold lysis solution [2.5 mol/L NaCl, 100 mmol/L EDTA, 10 mmol/L Tris, 1% sodium salt N-lauryl sarcosine (pH 10), with 1% triton X-100, and 10% DMSO added fresh; all supplied by Sigma]. Subsequently, the cells were exposed to alkaline buffer (1 mmol/L EDTA and 300 mmol/L NaOH, pH 13.4) at 4℃ for 40 min, to allow DNA unwinding, and expression of alkali-labile sites. In the same solution, electrophoresis was conducted at 4℃ for 20 min, at 25 V and 300 mA. After electrophoresis, the slides were neutralized (0.4 mol/L Tris, pH 7.5), stained with 40 μL ethidium bromide (EtBr) (20 μg/mL), and analyzed with a fluorescence microscope (Axioplan Ⅱ; Zeiss, Oberkochen, Germany), under green light at 400 nm, using an image analysis system (Comet Assay Ⅱ; Perceptive Instruments, Suffolk, UK). Two hundred randomly selected cells (100 from each of two replicate slides) were evaluated from each sample, and the mean of the tail moment was determined. Tail moment according to Comet Assay Ⅱ is defined as "the product of DNA in the tail, and the mean distance of migration in the tail. It is calculated by multiplying tail intensity/sum of comet intensity by tail center of gravity minus peak position." Using this method, the extent of DNA migration is related to the level of DNA damage in each cell, which creates the comet tail images.

Gastric epithelial cell morphology

Gastric epithelial cells treated continuously for 1 mo were collected and digested by 0.25% tryptase to yield a cell suspension, centrifuged at 1000 *g* for 10 min. The supernatant was removed, and the precipitate was fixed with 5% glutaraldehyde. Ultrathin sections were cut and observed under an electron microscope (H-600, Hitachi, Japan).

Statistical analysis

All data were expressed as mean ± SE. SPSS 10.0

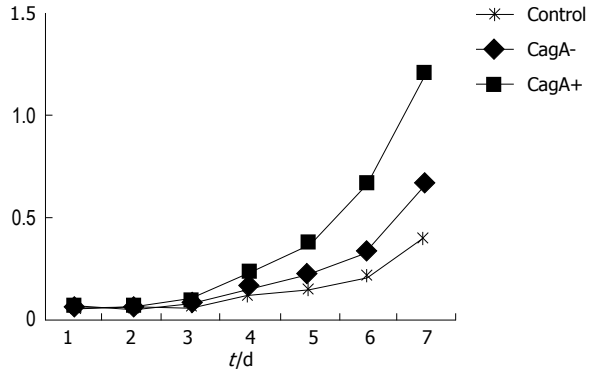

Figure 1 Cell proliferation determined by MTT assay. $P < 0.05$, CagA+ *vs* control and CagA+ *vs* CagA-.

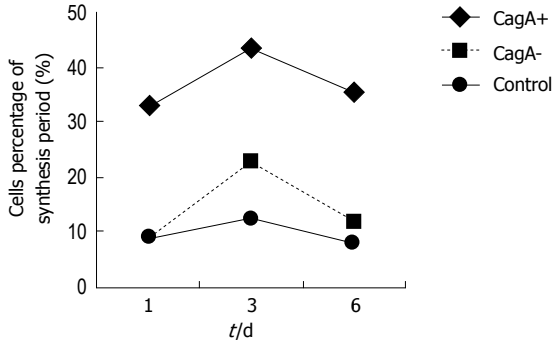

Figure 2 S-phase cells. $P < 0.05$, CagA+ *vs* CagA-.

software was used for one-way analysis of variance and *q* test. $P < 0.05$ was considered statistically significant.

RESULTS

Western blotting of CagA and cell proliferation determined by MTT assay

CagA expression was detected in the CagA+, CagA- and control groups. GES-1 cells proliferated actively when treated by CagA and *H pylori* culture filtrates. There were significant differences between the two groups (Figure 1).

Flat clone formation test

After treatment with *H pylori* culture filtrates, the flat clone formation test in the CagA+ group showed that the GES-1 clone number was larger than that of the CagA-, and control groups (200 *vs* 88.12, $P = 0.005$). The clone formation rates were 40%, 17.6% and 2.4%, respectively. Statistical analysis revealed a significant difference between the CagA+ and CagA- groups.

Effects of culture filtrates on GES-1 cell cycle and apoptosis rate

Flow cytometry showed that the number of S-phase cells increased more in the CagA+ group than in the control group at 1, 3 and 6 d (33.03% *vs* 9.16%, 53.46% *vs* 6.83%, and 35.55% *vs* 8.10%, respectively), which was higher than in the CagA-group ($P = 0.034$). After GES-1 cells had been treated with different *H pylori* culture filtrates for 1 mo, the detection of apoptotic cells was carried out by flow cytometry, and repeated eight times. The mean percentage of hypodiploid cells in the CagA+, CagA- and control cells was 5.6%, 4.4% and 3.7%, respectively. Statistical analysis revealed no significant difference among the three groups (Figure 2).

Table 1 Determination of DNA damage by single-cell microgel electrophoresis

	CagA+	CagA-	Control
Comet cell rate (%)	41.2[a]	12.5	5
Comet tail length	78.6 ± 5.0[a]	14.2 ± 6.3	6.8 ± 2.1

[a]$P < 0.05$ *vs* control and CagA-.

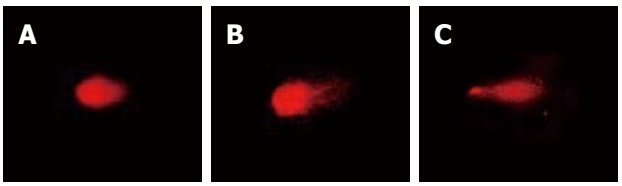

Figure 3 DNA damage measured by single-cell microgel electrophoresis. **A**: Comet tails in control group; **B**: Comet tails in CagA- group; **C**: Comet tails in CagA+ group.

Determination of DNA damage by single-cell microgel electrophoresis

Single-cell microgel electrophoresis showed in the control group that the ratio of comet cells was 5%, less than that in the CagA+ and CagA- groups. There were more comet cells after treatment with CagA+ broth than in the CagA- group, (41.2% *vs* 12.5%, $P = 0.024$, Table 1). The average comet tail length in the CagA+ group was 78.6 ± 5.0, which was larger than that in the CagA- group (14.2 ± 6.3, $P = 0.036$, Figure 3).

Cell morphology

Electron microscopy revealed dyskaryosis, nucleolar hypertrophy and karyokinesis in CagA-treated cells (Figure 4C), compared to the control and CagA- groups.

DISCUSSION

Infection with strains of *H pylori* that carry the *CagA*-gene is associated with gastric carcinoma. The mechanism is still not clear. Recent studies have shown that the *CagA*-gene product is delivered to gastric epithelial cells by the bacterial type Ⅳ secretion system to deregulate the SHP2 oncoprotein, which can promote gastric carcinogenesis[14-19].

In the present study, we prepared different *H pylori* culture filtrates containing the CagA protein to treat gastric epithelial cells. We found that GES-1 cells, after being treated with *CagA*-gene-positive culture filtrates, showed dyskaryosis, nucleolar hypertrophy and karyokinesis. The growth curve showed that GES-1 cells proliferated actively, and colony formation reached 40%. The number of S-phase cells obviously increased compared to the

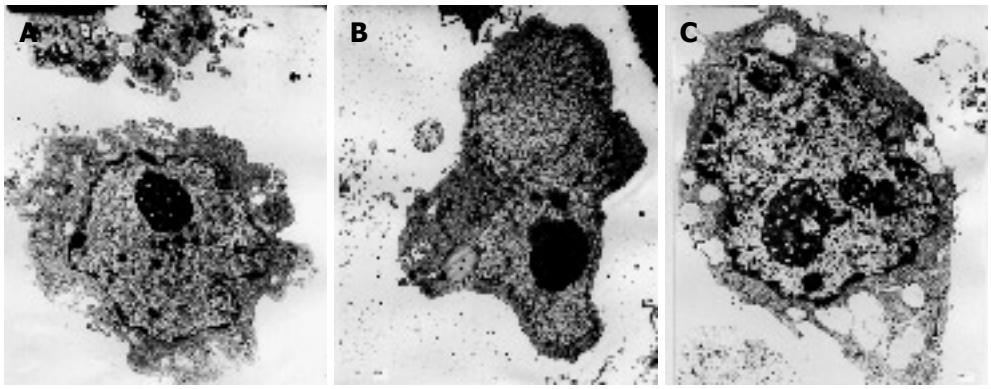

Figure 4 GES-1 treated with different *H pylori* filtrates. **A**: Control group; **B**: CagA-group; **C**: CagA+ group.

controls. These results demonstrate that CagA+ filtrates of *H pylori* can induce carcinogenesis in gastric epithelial cells. Research has shown that reconstruction of CagA fragment induces paraplastic changes in epithelial cells *in vitro*, which supports the suggestion that CagA is involved in gastric carcinogenesis[20-21]. All these results support our findings.

Ladeira *et al*[25] have used the comet assay or single-cell gel electrophoresis to investigate the status of DNA damage in gastric epithelial cells from the antrum and corpus in patients with *H pylori* infection, and gastritis of varying degrees. They have demonstrated that the level of DNA damage in *H pylori*-infected individuals is significantly higher than that in non-infected individuals, with the levels of DNA damage significantly higher in those aged $\geqslant$ 50 years.

The DNA repair enzyme human oxoguanine glycosylase 1 (hOGG1) is known to be responsible for the repair of the 8-hydroxy-deoxyguanosine (8-OHdG) region. Of the hOGG1 polymorphisms identified, a Ser→Cys polymorphism at position 326 has been found to interact with atrophic gastritis, but not with antioxidant dietary or nutrient intakes. It is likely that this makes patients with atrophic gastritis, who also have the hOGG1 Cys allele, more susceptible to gastric cancer[26]. The concentrations of 8-OHdG, inducible nitric oxide synthase (iNOS), nuclear factor κB, myeloid cell leukemia-1, and inhibitor of apoptosis protein are significantly higher in patients with *H pylori* infection, and in those with stage 3 and 4 gastric cancer. This points to the pivotal role that oxygen-free-radical-mediated DNA damage caused by *H pylori* infection plays in the development of gastric carcinoma from chronic gastritis[27]. Single-cell gel electrophoresis is a simple and sensitive method for detecting DNA damage in cells. In this study, we found 41.2% of CagA+ cells formed comet tails. This shows that CagA+ culture broth filtrate has the ability to cause DNA breakage or damage, which may lead to the transformation of gastric epithelial cells.

H pylori-associated inflammation related to DNA damage is indicated by increased levels of oxidative DNA damage, increased occurrence of apoptosis and proliferation, as well as increased expression of iNOS, which seems to provide the mechanistic link between *H pylori* infection and gastric carcinogenesis[28,29]. Upregulation of iNOS expression might contribute to the oxidative DNA damage observed during *H pylori* infection[30]. Yabuki *et al*[31] have investigated cell proliferation and DNA damage in ablation samples from 35 cases of gastric carcinoma, and have indicated that cell damage in *H pylori*-infected human gastric mucosa increases cell proliferation.

We found that CagA+ culture broth filtrate induced DNA damage in human gastric epithelial cells *in vitro*, which suggests that CagA is involved in DNA damage in gastric epithelial cells. All results showed that CagA+ broth culture filtrates of *H pylori* could accelerate human gastric epithelial cell growth and alter their morphology. It is not clear that there are other factors apart from CagA involved in the transformation of gastric epithelial cells induced by CagA+ culture broth filtrate.

ACKNOWLEDGMENTS

We thank Dr. Wei Cheng and Dr. Ji-Zong Zhao and Zheng Lin, Director of General Surgery Laboratory, for their assistance with the culture of *H pylori*. We are also grateful to Dr. Bo Hu who provided assistance with molecular biology.

COMMENTS

Background

It is widely accepted that there is a strong association between *Helicobacter pylori* (*H pylori* infection) and gastric cancer, but the exact molecular mechanism of the pathogen in gastric carcinogenesis has not yet been clarified. DNA damage is involved in the carcinogenesis process. Single-cell gel electrophoresis is a simple and sensitive method for detecting DNA damage in cells.

Research frontiers

There has been considerable interest in recent years in virulence factors, such as CagA protein, which predispose individuals to develop gastric carcinoma. Understanding DNA damage in gastric epithelial cells will provide us with a new strategy for effective prevention of gastric cancer induced by *H pylori* infection. It is also helpful to clarify CagA protein carcinogenesis.

Innovations and breakthroughs

In this study, the mechanism of *H pylori* infection in gastric carcinogenesis was explored by studying its effects on DNA damage in gastric epithelial cells *in vitro*. The results suggest that *H pylori* can induce DNA damage in cultured gastric epithelial cells, and the effect of CagA+ strains was more significant than CagA- strains.

Applications

This study emphasizes the close relationship between *H pylori*, especially CagA+ strains, and gastric carcinoma. It provides a new approach to elucidating the mechanism of *H pylori* gastric carcinogenesis. It also implies that compounds able to repair DNA damage in *H pylori*-infected cells may be used to create new strategies for the prevention and/or treatment of human gastric malignancy.

Peer review

This study seems innovative and interesting. Products of DNA damage have been observed in various pathological processes of the digestive tract, including gastric cancer. To the best of our knowledge, there are still many aspects of the mechanism of *H pylori* infection in gastric carcinogenesis to explore, by studying its effects on DNA damage in gastric epithelial cells *in vitro*.

REFERRENCES

1 **Nomura A**, Stemmermann GN, Chyou PH, Kato I, Perez-Perez GI, Blaser MJ. Helicobacter pylori infection and gastric carcinoma among Japanese Americans in Hawaii. *N Engl J Med* 1991; **325**: 1132-1136

2 **Ekstrom AM**, Held M, Hansson LE, Engstrand L, Nyren O. Helicobacter pylori in gastric cancer established by CagA immunoblot as a marker of past infection. *Gastroenterology* 2001; **121**: 784-791

3 **An international association between Helicobacter pylori infection and gastric cancer.** The EUROGAST Study Group. *Lancet* 1993; **341**: 1359-1362

4 **Camargo MC**, Piazuelo MB, Mera RM, Fontham ET, Delgado AG, Yepez MC, Ceron C, Bravo LE, Bravo JC, Correa P. Effect of smoking on failure of *H. pylori* therapy and gastric histology in a high gastric cancer risk area of Colombia. *Acta Gastroenterol Latinoam* 2007; **37**: 238-245

5 **Sun LP**, Gong YH, Wang L, Gong W, Yuan Y. Follow-up study on a high risk population of gastric cancer in north China by serum pepsinogen assay. *J Dig Dis* 2008; **9**: 20-26

6 **Ogura K**, Hirata Y, Yanai A, Shibata W, Ohmae T, Mitsuno Y, Maeda S, Watabe H, Yamaji Y, Okamoto M, Yoshida H, Kawabe T, Omata M. The effect of Helicobacter pylori eradication on reducing the incidence of gastric cancer. *J Clin Gastroenterol* 2008; **42**: 279-283

7 **Schistosomes, liver flukes and Helicobacter pylori.** IARC Working Group on the Evaluation of Carcinogenic Risks to Humans. Lyon, 7-14 June 1994. *IARC Monogr Eval Carcinog Risks Hum* 1994; **61**: 177-241

8 **Amieva MR**, El-Omar EM. Host-bacterial interactions in Helicobacter pylori infection. *Gastroenterology* 2008; **134**: 306-323

9 **Lambert R**, Hainaut P. The multidisciplinary management of gastrointestinal cancer. Epidemiology of oesophagogastric cancer. *Best Pract Res Clin Gastroenterol* 2007; **21**: 921-945

10 **Vauhkonen H**, Heino S, Myllykangas S, Lindholm PM, Savola S, Knuutila S. Etiology of specific molecular alterations in human malignancies. *Cytogenet Genome Res* 2007; **118**: 277-283

11 **Huang JQ**, Zheng GF, Sumanac K, Irvine EJ, Hunt RH. Meta-analysis of the relationship between cagA seropositivity and gastric cancer. *Gastroenterology* 2003; **125**: 1636-1644

12 **Jackson CB**, Judd LM, Menheniott TR, Kronborg I, Dow C, Yeomans ND, Boussioutas A, Robb L, Giraud AS. Augmented gp130-mediated cytokine signalling accompanies human gastric cancer progression. *J Pathol* 2007; **213**: 140-151

13 **Loh JT**, Torres VJ, Cover TL. Regulation of Helicobacter pylori cagA expression in response to salt. *Cancer Res* 2007; **67**: 4709-4715

14 **Tsutsumi R**, Higashi H, Higuchi M, Okada M, Hatakeyama M. Attenuation of Helicobacter pylori CagA x SHP-2 signaling by interaction between CagA and C-terminal Src kinase. *J Biol Chem* 2003; **278**: 3664-3670

15 **Mimuro H**, Suzuki T, Tanaka J, Asahi M, Haas R, Sasakawa C. Grb2 is a key mediator of helicobacter pylori CagA protein activities. *Mol Cell* 2002; **10**: 745-755

16 **Churin Y**, Al-Ghoul L, Kepp O, Meyer TF, Birchmeier W, Naumann M. Helicobacter pylori CagA protein targets the c-Met receptor and enhances the motogenic response. *J Cell Biol* 2003; **161**: 249-255

17 **Penta R**, De Falco M, Iaquinto G, De Luca A. Helicobacter pylori and gastric epithelial cells: from gastritis to cancer. *J Exp Clin Cancer Res* 2005; **24**: 337-345

18 **Lee YC**. [Pathogenesis of Helicobacter pylori infection] *Korean J Gastroenterol* 2005; **46**: 159-165

19 **Chen Y**, Wang Y, Xu W, Zhang Z. Analysis on the mechanism of Helicobacter pylori-induced apoptosis in gastric cancer cell line BGC-823. *Int J Mol Med* 2005; **16**: 741-745

20 **Sommi P**, Ricci V, Fiocca R, Romano M, Ivey KJ, Cova E, Solcia E, Ventura U. Significance of ammonia in the genesis of gastric epithelial lesions induced by Helicobacter pylori: an *in vitro* study with different bacterial strains and urea concentrations. *Digestion* 1996; **57**: 299-304

21 **Stein M**, Bagnoli F, Halenbeck R, Rappuoli R, Fantl WJ, Covacci A. c-Src/Lyn kinases activate Helicobacter pylori CagA through tyrosine phosphorylation of the EPIYA motifs. *Mol Microbiol* 2002; **43**: 971-980

22 **Azuma T**, Yamakawa A, Yamazaki S, Ohtani M, Ito Y, Muramatsu A, Suto H, Yamazaki Y, Keida Y, Higashi H, Hatakeyama M. Distinct diversity of the cag pathogenicity island among Helicobacter pylori strains in Japan. *J Clin Microbiol* 2004; **42**: 2508-2517

23 **Singh NP**, McCoy MT, Tice RR, Schneider EL. A simple technique for quantitation of low levels of DNA damage in individual cells. *Exp Cell Res* 1988; **175**: 184-191

24 **Klaude M**, Eriksson S, Nygren J, Ahnstrom G. The comet assay: mechanisms and technical considerations. *Mutat Res* 1996; **363**: 89-96

25 **Ladeira MS**, Rodrigues MA, Salvadori DM, Queiroz DM, Freire-Maia DV. DNA damage in patients infected by Helicobacter pylori. *Cancer Epidemiol Biomarkers Prev* 2004; **13**: 631-637

26 **Tsukino H**, Hanaoka T, Otani T, Iwasaki M, Kobayashi M, Hara M, Natsukawa S, Shaura K, Koizumi Y, Kasuga Y, Tsugane S. hOGG1 Ser326Cys polymorphism, interaction with environmental exposures, and gastric cancer risk in Japanese populations. *Cancer Sci* 2004; **95**: 977-983

27 **Chang CS**, Chen WN, Lin HH, Wu CC, Wang CJ. Increased oxidative DNA damage, inducible nitric oxide synthase, nuclear factor kappaB expression and enhanced antiapoptosis-related proteins in Helicobacter pylori-infected non-cardiac gastric adenocarcinoma. *World J Gastroenterol* 2004; **10**: 2232-2240

28 **Selbach M**, Moese S, Hauck CR, Meyer TF, Backert S. Src is the kinase of the Helicobacter pylori CagA protein *in vitro* and in vivo. *J Biol Chem* 2002; **277**: 6775-6778

29 **Azuma T**. Helicobacter pylori CagA protein variation associated with gastric cancer in Asia. *J Gastroenterol* 2004; **39**: 97-103

30 **Argent RH**, Kidd M, Owen RJ, Thomas RJ, Limb MC, Atherton JC. Determinants and consequences of different levels of CagA phosphorylation for clinical isolates of Helicobacter pylori. *Gastroenterology* 2004; **127**: 514-523

31 **Yabuki N**, Sasano H, Tobita M, Imatani A, Hoshi T, Kato K, Ohara S, Asaki S, Toyota T, Nagura H. Analysis of cell damage and proliferation in Helicobacter pylori-infected human gastric mucosa from patients with gastric adenocarcinoma. *Am J Pathol* 1997; **151**: 821-829

S- Editor Zhong XY **L- Editor** Kerr C **E- Editor** Lin YP

Online Submissions: wjg.wjgnet.com
wjg@wjgnet.com
doi: 10.3748/wjg.14.3750

World J Gastroenterol 2008 June 21; 14(23): 3750-3753
World Journal of Gastroenterology ISSN 1007-9327
© 2008 The WJG Press. All rights reserved.

RAPID COMMUNICATION

Clinical value of serum CA19-9 levels in evaluating resectability of pancreatic carcinoma

Shun Zhang, Yi-Ming Wang, Chuan-Dong Sun, Yun Lu, Li-Qun Wu

Shun Zhang, Yi-Ming Wang, Chuan-Dong Sun, Yun Lu, Li-Qun Wu, Department of Hepatobiliary Surgery, Affiliated Hospital of Medical College, Qingdao University, Qingdao 266003, Shandong Province, China
Author contributions: Zhang S designed the study; Wang YM collected and analyzed the data; Wang YM wrote the paper; Sun CD, Lu Y and Wu LQ revised the paper.
Correspondence to: Shun Zhang, Department of Hepatobiliary Surgery, Affiliated Hospital of Medical College, Qingdao University, No. 16 Jiangsu Road, Qingdao 266003, Shandong Province, China. wym0066@sina.com
Telephone: +86-532-82911369 Fax: +86-532-82911999
Received: February 29, 2008 Revised: April 30, 2008
Accepted: May 7, 2008
Published online: June 21, 2008

Peer reviewers: Dr. Bernd Sido, Department of General and Abdominal Surgery, Teaching Hospital of the University of Regensburg, Hospital Barmherzige Brüder, Prüfeninger Strasse 86, Regensburg D-93049, Germany; Giuseppe Tisone, Professor, Department of Surgery, University of Rome Tor Vergata, Ospedale S.Eugenio, Piazzale dell'Umanesimo 10, Rome 00144, Italy

Zhang S, Wang YM, Sun CD, Lu Y, Wu LQ. Clinical value of serum CA19-9 levels in evaluating resectability of pancreatic carcinoma. *World J Gastroenterol* 2008; 14(23): 3750-3753
Available from: URL: http://www.wjgnet.com/1007-9327/14/3750.asp DOI: http://dx.doi.org/10.3748/wjg.14.3750

Abstract

AIM: To evaluate the clinical value of serum CA19-9 levels in predicting the respectability of pancreatic carcinoma according to receiver operating characteristic (ROC) curve analysis.

METHODS: Serum CA19-9 levels were measured in 104 patients with pancreatic cancer which were possible to be resected according to the imaging. ROC curve was plotted for the CA19-9 levels. The point closest to the upper left-hand corner of the graph were chosen as the cut-off point. The sensitivity, specificity, positive and negative predictive values of CA19-9 at this cut-off point were calculated.

RESULTS: Resectable pancreatic cancer was detected in 58 (55.77%) patients and unresectable pancreatic cancer was detected in 46 (44.23%) patients. The area under the ROC curve was 0.918 and 95% CI was 0.843-0.992. The CA19-9 level was 353.15 U/mL, and the sensitivity and specificity of CA19-9 at this cut-off point were 93.1% and 78.3%, respectively. The positive and negative predictive value was 84.38% and 90%, respectively.

CONCLUSION: Preoperative serum CA19-9 level is a useful marker for further evaluating the resectability of pancreatic cancer. Obviously increased serum levels of CA19-9 (> 353.15 U/mL) can be regarded as an ancillary parameter for unresectable pancreatic cancer.

© 2008 The WJG Press. All rights reserved.

Key words: Pancreatic carcinoma; Resection; Tumor markers; CA19-9; Receiver operating characteristic curve

INTRODUCTION

The prognosis of pancreatic cancer is extremely poor and its early diagnosis is difficult[1,2]. Surgical resection offers the best chance of cure. However, local vascular involvement, nodal and distant metastases are frequently found at the time of diagnosis, thus losing the opportunity of operation[3]. At present, the best way for preoperative staging of pancreatic cancer is bolus-contrast, and triple-phase helical computed tomography, which has been shown to be almost 100% accurate in predicting unresectable disease[4-6]. However, approximately 25%-50% of patients with resectable disease on computed tomography are found to have unresectable lesions at laparotomy[7].

CA19-9 is the most widely used pancreatic cancer serum marker. Serum CA19-9 level has been shown to correlate with the thyroid node metastasis (TNM) staging, and tumor size in patients with pancreatic cancer[8]. However, little is known about the value of serum CA19-9 level in evaluating the resectability of pancreatic carcinoma.

Receiver operating characteristic (ROC) curve has been widely accepted as the standard method for dscribing and comparing the accuracy of medical diagnostic tests[9,10]. ROC curve is an efficient way to display and assess the predictive value of cut-off points.

In this study, we evaluated the clinical value of serum CA19-9 level in predicting the resectability of pancreatic carcinoma according to ROC curve analysis.

MATERIALS AND METHODS

We retrospectively reviewed the clinical and imaging data

Table 1 Characteristics of patients (n = 104)

Characteristics	Data, n (%)
Age (yr)	59 ± 9 (mean ± SD)
Sex	
Male	72 (69.2)
Female	32 (30.8)
Location of tumors	
Head	86 (82.7)
Body	8 (7.7)
Body and tail	10 (9.6)
Type of operation	
Pancreaticoduodenectomy	48 (46.2)
Distal pancreatectomy	10 (9.6)
Exploratory laparotomy and biopsy	46 (44.2)

Table 2 CA19-9 levels in patients with resectable and unresectable pancreatic cancer

Group	n	CA19-9 (U/mL)			Wilcoxon	
		Q_1	Q_2	Q_3	Z	P
Resectable	58	15.57	130.10	270.25	-5.132	0.000
Unresectable	46	361.30	656.20	1780.00		

including preoperative CA19-9 level in 104 patients with pancreatic cancer who underwent surgical resection at the Affiliated Hospital of Qingdao University Medical College from January 2001 to July 2007. Pancreatic adenocarcinoma was histologically confirmed. Resectability of pancreatic cancer was evaluated at least by preoperative bolus-contrast, triple-phase helical computer tomography (CT) scan.

Resectability was defined as a tumour limited to the pancreas with no invasion of the superior mesenteric artery and vein, portal vein and metastases (celiac lymph, peritoneum or liver).

Serum levels of CA19-9 and total serum bilirubin levels were measured before surgery (normal 0-39.0 U/mL for CA19-9, 3.4-17.1 μmol/L for total serum bilirubin).

The data were described using Q_{1-3}. Differences between groups were detected using the Wilcoxon 2-sample test. Serum CA19-9 levels were used to plot the ROC curve, and calculate the area under the curve (AUC). We chose the point closest to the upper left-hand corner of the graph as the cut-off point. The sensitivity, specificity, positive and negative predictive values of CA19-9 at this cut-off point were calculated. $P < 0.05$ was considered statistically significant.

RESULTS

Of the 104 patients, 72 were males and 32 were females with a mean age of 59 years (range 41-75 years). The pancreatic tumor was confined to the head, body and tail of the pancreas in 86, 8, and 10 patients, respectively. Forty-eight patients underwent pancreatic- coduodenectomy, 10 patients distal pancreatectomy, and 46 only exploratory laparotomy and biopsy. The general characteristics of the patients are listed in Table 1.

The distribution of preoperative serum CA19-9 levels

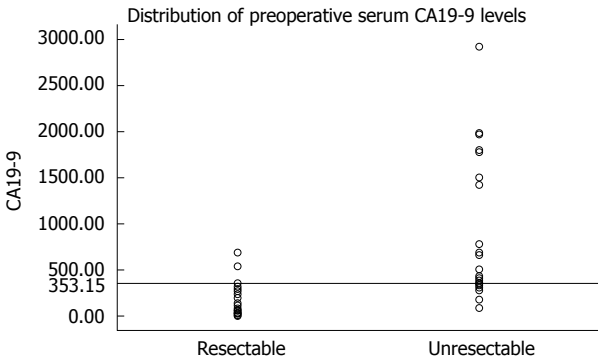

Figure 1 Distribution of preoperative serum CA19-9 levels. The horizon marker is set according to the cut-off point of CA19-9 (353.15 U/mL).

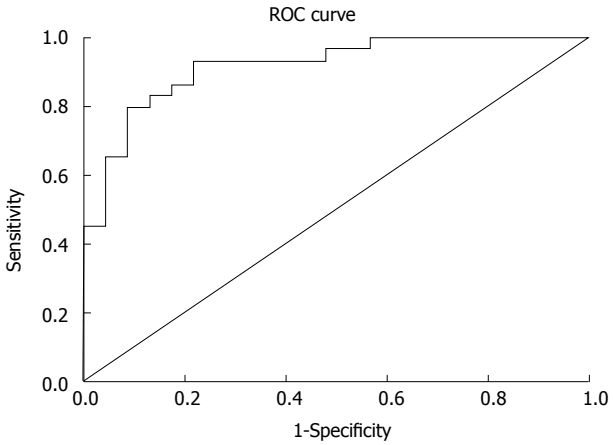

Figure 2 ROC analysis of CA19-9. Perfect discrimination has a ROC plot passing through the upper left corner (100% sensitivity, 100% specificity). The closer the ROC plot to the upper left corner, the higher the overall accuracy of the test (AUC: 0.9-1 indicating excellent; 0.8-0.9 indicating very good; 0.7-0.8 indicating good; 0.6-0.7 indicating average; 0.5-0.6 indicating poor). The AUC of CA19-9 was 0.918.

is shown in Figure 1. The Q_2 (median) preoperative serum CA19-9 level in patients with unresectable tumor was 5-fold higher than that in patients with resectable tumor (Table 2). The difference between two groups was significant ($P < 0.01$). The mean total serum bilirubin level in patients with resectable and unresectable tumor was 28.6 μmol/L and 34.4 μmol/L, respectively ($P > 0.05$). Therefore, the CA19-9 levels were not adjusted.

Figure 2 shows the ROC curve. The AUC was 0.918 and 95% CI was 0.843-0.992, suggesting that changes in serum CA19-9 levels may have a direct relation to resectability[11,12]. When the cut-off value of CA19-9 was 353.15 U/mL according to the point closest to the upper left-hand corner of the graph, the sensitivity and specificity were 93.1% and 78.3%, respectively. The preoperative resectability according to the cut-off point was compared with the actual operation, and the positive and negative predictive value of CA19-9 was 84.38% and 90.00%, respectively (Table 3).

DISCUSSION

Pancreatic cancer is one of the most common causes for

Table 3 Positive and negative predictive values of CA19-9 at the cut-off point

		Resection		Total	Predictive value
		Yes	No		
CA19-9 (U/mL)	≤ 353.15	54	10	64	84.38% (+)
	> 353.15	4	36	40	90.00% (-)
Total		58	46	104	

cancer-related death. The overall five-year survival rate ranges from 0.4% to 4%, the lowest for any cancer[1,13]. Early diagnosis of pancreatic cancer is difficult because its early symptoms are usually non-specific. Local vascular involvement, nodal and distant metastases are frequently found at the time of diagnosis[14].

Recently, considerable improvements in radiological imaging make it possible to limit surgery for patients who will benefit[15,16]. The current methods of choice for diagnosing and staging pancreatic cancer are thin section, contrast-enhanced, and triple-phase helical computed tomography[17,18]. However, approximately 25%-50% of patients with resectable disease on computed tomography are found to have unresectable lesions at laparotomy[7,19]. Although magnetic resonance imaging is increasingly used in the evaluation of pancreatic tumor, it was reported that it offers no significant diagnostic advantage over computed tomography[20]. Endoscopic retrograde cholangio pancreatography (ERCP) is more controversial for patients with a mass on CT[21]. B-mode ultrasonography is operator-dependent and may be inaccurate due to factors such as large body habitus, presence of ascites, or overlying bowel gas. Therefore we should find other ways to further evaluate the resectability of pancreatic cancer.

CA19-9 is a tumor-associated antigen, initially described by Koprowski *et al*[22]. The sensitivity and specificity of CA19-9 for the diagnosis of pancreatic cancer are higher than than those of CEA, CA50 and CA242[23-25]. CA19-9 has become a predominant tumor marker for the diagnosis of pancreatic adenocarcinoma. It was reported that CA19-9 level is useful in diagnosis and prognosis of pancreatic cancer[26,27]. However, little is known about the value of serum CA19-9 levels in evaluating the resectability of pancreatic carcinoma[28]. This study was to find whether preoperative serum CA19-9 is a useful marker for evaluating the resectability of pancreatic cancer.

In the present study, the differences between patients with resectable and unresectable pancreatic cancer were significant ($P < 0.01$). The AUC was 0.918 and 95% CI was 0.843-0.992, suggesting that the preoperative serum CA19-9 level is an efficient marker for evaluating the resectability of pancreatic carcinoma. When the cut-off value of CA19-9 was 353.15 U/mL according to the point closest to the upper left-hand corner of the graph, the sensitivity, specificity, positive and negative predictive value was 93.1%, 78.3%, 84.38% and 90%, respectively, indicating that increased serum levels of CA19-9 (> 353.15 U/mL) can be regarded as an ancillary parameter for the unresectable pancreatic cancer[29]. Pancreatic cancer was resectable only in 4 patients whose preoperative serum CA19-9 level was over 353.15 U/mL (Table 3 and Figure 1).

Kilic *et al*[30] reported that the sensitivity, specificity, positive and negative predictive value are 82.4%, 92.3%, 91.4% and 83.9%, respectively, in 51 patients, and the cut-off value of CA19-9 is 256.4 U/mL. Their results are similar to our data, but the cut-off value was lower than that in our study (256.4 U/mL *vs* 353.15 U/mL). The discrepancy may be due the sample size, and the unadjusted CA19-9 level according to the bilirubin level.

In conclusion, a preoperative serum CA19-9 level is a useful marker for evaluating the resectability of pancreatic cancer. Increased serum levels of CA19-9 (> 353.15 U/mL) can be regarded as an ancillary parameter for unresectable pancreatic cancer.

COMMENTS

Background

At present, the best way of preoperative staging of pancreatic cancer is bolus-contrast and triple-phase helical computed tomography. However, approximately 25%-50% of patients with resectable disease on computed tomography are found to have unresectable lesions at laparotomy.

Research frontiers

CA19-9 is the most widely used serum marker of pancreatic cancer. CA19-9 has been shown to correlate with the thyroid node metastasis (TNM) staging and tumor size in patients with pancreatic cancer. However, little is known about the value of serum CA19-9 levels in evaluating the resectability of pancreatic carcinoma.

Innovations and breakthroughs

Receiver operating characteristic (ROC) curve analysis was used to evaluate the clinical value of serum CA19-9 levels in predicting the resectability of pancreatic carcinoma.

Applications

Preoperative serum CA19-9 level may be a useful marker for evaluating the resectability of pancreatic cancer. Increased serum level of CA19-9 (> 353.15 U/mL) may be regarded as an ancillary parameter for unresectable pancreatic cancer.

Terminology

CA19-9 is a tumor-associated antigen initially described by Koprowski *et al* and has been widely used as a serum marker of pancreatic cancer. ROC curve has been widely accepted as the standard method for describing and comparing the accuracy of medical diagnostic tests. ROC curve is an efficient way to display and assess the predictive value of cut-off points.

Peer review

This is a very interesting study. The authors used ROC analysis as an appropriate statistical method for defining the cut-off value of serum CA19-9 to discriminate between resectable and unresectable pancreatic cancer.

REFERENCES

1 **Jemal A**, Siegel R, Ward E, Hao Y, Xu J, Murray T, Thun MJ. Cancer statistics, 2008. *CA Cancer J Clin* 2008; **58**: 71-96
2 **Wang L**, Yang GH, Lu XH, Huang ZJ, Li H. Pancreatic cancer mortality in China (1991-2000). *World J Gastroenterol* 2003; **9**: 1819-1823
3 **Warshaw AL**, Fernandez-del Castillo C. Pancreatic carcinoma. *N Engl J Med* 1992; **326**: 455-465
4 **Tamm EP**, Silverman PM, Charnsangavej C, Evans DB. Diagnosis, staging, and surveillance of pancreatic cancer. *AJR Am J Roentgenol* 2003; **180**: 1311-1323
5 **Vargas R**, Nino-Murcia M, Trueblood W, Jeffrey RB Jr. MDCT in Pancreatic adenocarcinoma: prediction of vascular invasion and resectability using a multiphasic technique with curved planar reformations. *AJR Am J Roentgenol* 2004; **182**: 419-425

6 **Wakabayashi H**, Nishiyama Y, Otani T, Sano T, Yachida S, Okano K, Izuishi K, Suzuki Y. Role of 18F-fluorodeoxyglucose positron emission tomography imaging in surgery for pancreatic cancer. *World J Gastroenterol* 2008; **14**: 64-69
7 **Pisters PW**, Lee JE, Vauthey JN, Charnsangavej C, Evans DB. Laparoscopy in the staging of pancreatic cancer. *Br J Surg* 2001; **88**: 325-337
8 **Koopmann J**, Rosenzweig CN, Zhang Z, Canto MI, Brown DA, Hunter M, Yeo C, Chan DW, Breit SN, Goggins M. Serum markers in patients with resectable pancreatic adenocarcinoma: macrophage inhibitory cytokine 1 versus CA19-9. *Clin Cancer Res* 2006; **12**: 442-446
9 **Zou KH**, O'Malley AJ, Mauri L. Receiver-operating characteristic analysis for evaluating diagnostic tests and predictive models. *Circulation* 2007; **115**: 654-657
10 **Walter SD**, Sinuff T. Studies reporting ROC curves of diagnostic and prediction data can be incorporated into meta-analyses using corresponding odds ratios. *J Clin Epidemiol* 2007; **60**: 530-534
11 **Altman DG**, Bland JM. Diagnostic tests 2: Predictive values. *BMJ* 1994; **309**: 102
12 **Altman DG**, Bland JM. Diagnostic tests 3: receiver operating characteristic plots. *BMJ* 1994; **309**: 188
13 **Jemal A**, Murray T, Samuels A, Ghafoor A, Ward E, Thun MJ. Cancer statistics, 2003. *CA Cancer J Clin* 2003; **53**: 5-26
14 **Pappas S**, Federle MP, Lokshin AE, Zeh HJ 3rd. Early detection and staging of adenocarcinoma of the pancreas. *Gastroenterol Clin North Am* 2007; **36**: 413-429, x
15 **Takhar AS**, Palaniappan P, Dhingsa R, Lobo DN. Recent developments in diagnosis of pancreatic cancer. *BMJ* 2004; **329**: 668-673
16 **Misek DE**, Patwa TH, Lubman DM, Simeone DM. Early detection and biomarkers in pancreatic cancer. *J Natl Compr Canc Netw* 2007; **5**: 1034-1041
17 **Delbeke D**, Pinson CW. Pancreatic tumors: role of imaging in the diagnosis, staging, and treatment. *J Hepatobiliary Pancreat Surg* 2004; **11**: 4-10
18 **Sahani DV**, Shah ZK, Catalano OA, Boland GW, Brugge WR. Radiology of pancreatic adenocarcinoma: current status of imaging. *J Gastroenterol Hepatol* 2008; **23**: 23-33
19 **Karmazanovsky G**, Fedorov V, Kubyshkin V, Kotchatkov A. Pancreatic head cancer: accuracy of CT in determination of resectability. *Abdom Imaging* 2005; **30**: 488-500
20 **Hanbidge AE**. Cancer of the pancreas: the best image for early detection--CT, MRI, PET or US? *Can J Gastroenterol* 2002; **16**: 101-105
21 **Andersson R**, Vagianos C, Williamson R. Preoperative staging and evaluation of resectability in pancreatic ductal adenocarcinoma. *HPB* (Oxford) 2004; **6**: 5-12
22 **Koprowski H**, Steplewski Z, Mitchell K, Herlyn M, Herlyn D, Fuhrer P. Colorectal carcinoma antigens detected by hybridoma antibodies. *Somatic Cell Genet* 1979; **5**: 957-971
23 **Wu X**, Lu XH, Xu T, Qian JM, Zhao P, Guo XZ, Yang XO, Jiang WJ. [The diagnostic value of serum carcinoma markers, fecal K-ras and p53 gene mutation in pancreatic cancers] *Zhonghua Neike Zazhi* 2005; **44**: 741-744
24 **Okusaka T**, Okada S, Sato T, Wakasugi H, Saisho H, Furuse J, Ishikawa O, Matsuno S, Yokoyama S. Tumor markers in evaluating the response to radiotherapy in unresectable pancreatic cancer. *Hepatogastroenterology* 1998; **45**: 867-872
25 **Liao Q**, Zhao YP, Yang YC, Li LJ, Long X, Han SM. Combined detection of serum tumor markers for differential diagnosis of solid lesions located at the pancreatic head. *Hepatobiliary Pancreat Dis Int* 2007; **6**: 641-645
26 **Kang CM**, Kim JY, Choi GH, Kim KS, Choi JS, Lee WJ, Kim BR. The use of adjusted preoperative CA 19-9 to predict the recurrence of resectable pancreatic cancer. *J Surg Res* 2007; **140**: 31-35
27 **Zhao JZ**, Wu BH. Clinical significance of CA19-9 in diagnosis of digestive tract tumors. *China Nati J New Gastroenterol* 1997; **3**: 253-254
28 **Schlieman MG**, Ho HS, Bold RJ. Utility of tumor markers in determining resectability of pancreatic cancer. *Arch Surg* 2003; **138**: 951-955; discussion 955-956
29 **Zakowski L**, Seibert C, VanEyck S. Evidence-based medicine: answering questions of diagnosis. *Clin Med Res* 2004; **2**: 63-69
30 **Kilic M**, Gocmen E, Tez M, Ertan T, Keskek M, Koc M. Value of preoperative serum CA 19-9 levels in predicting resectability for pancreatic cancer. *Can J Surg* 2006; **49**: 241-244

S- Editor Li DL **L- Editor** Wang XL **E- Editor** Liu Y

Online Submissions: wjg.wjgnet.com
wjg@wjgnet.com
doi:10.3748/wjg.14.3754

World J Gastroenterol 2008 June 21; 14(23): 3754-3758
World Journal of Gastroenterology ISSN 1007-9327
© 2008 The WJG Press. All rights reserved.

RAPID COMMUNICATION

Effect of fragile histidine triad gene transduction on proliferation and apoptosis of human hepatocellular carcinoma cells

Rong-Hua Xu, Liang-Yan Zheng, Dong-Lei He, Jian Tong, Li-Ping Zheng, Wu-Ping Zheng, Jin Meng, Li-Ping Xia, Cong-Jun Wang, Ji-Lin Yi

Rong-Hua Xu, Liang-Yan Zheng, Dong-Lei He, Jian Tong, Li-Ping Zheng, Wu-Ping Zheng, Jin Meng, Li-Ping Xia, The Affiliated Hospital of Hainan Medical College, Haikou 570102, Hainan Province, China
Cong-Jun Wang, Department of General Surgery, First People's Hospital Affiliated to Shanghai Jiaotong University, Shanghai 200080, China
Ji-Lin Yi, Department of General surgery, Tongji Hospital, Tongji Medical College of Huazhong University of Science and Technology, Wuhan 430030, Hubei Province, China
Author contributions: Xu RH and Zheng LY wrote the paper and organized the figures; Xu RH, He DL, Tong J, Zheng LP, Zheng WP, Meng J, Xia LP did cell culture, transduction, RT-PCR, Western blot and animal experiments; Wang CJ carried out the statistical analysis; Yi JL supervised the writing and organization process.
Correspondence to: Dr. Rong-Hua Xu, Department of Oncology Surgery, The Affiliated Hospital of Hainan Medical College, Haikou 570102, Hainan Province, China. xu_ronghua2231@hotmail.com
Telephone: +86-898-66528115
Received: October 29, 2007 Revised: April 19, 2008
Accepted: April 26, 2008
Published online: June 21, 2008

Abstract

AIM: To evaluate the inhibitory effects of human fragile histidine triad (FHIT) gene on cell proliferation and apoptosis in human hepatocellular carcinoma line Hep3B *in vitro*.

METHODS: A recombinant pcDNA3.1 (+)/FHIT including the functional region of FHIT gene was constructed and transferred into human hepatocellular carcinoma cells *in vitro*. mRNA and protein expression of the *FHIT* gene in the transfected cells was detected by RT-PCR and Western blot, respectively. The effect of FHIT on proliferation was detected by MTT assay. Changes in cell cycle and apoptosis were assayed by flow cytometry. Five mice received subcutaneous transplantation of Hep3B-FHIT; 5 mice received subcutaneous transplantation of normal Hep3B and Hep3B-C as controls. The body weight of nude mice and tumor growth were measured.

RESULTS: RT-PCR and Western blot analysis showed that the expression level of FHIT-mRNA and FHIT protein was higher in Hep3B cells after infection with pcDNA3.1 (+)/FHIT. The growth of Hep3B cells treated with pcDNA3.1 (+)/FHIT was significantly inhibited. The pcDNA3.1 (+)/FHIT-transfected Hep3B cells showed a significantly higher cell rate at G_0-G_1 phase and increased apoptosis in comparison with controls ($P < 0.05$). The growth of transplanted tumor was inhibited markedly by FHIT. Tumors arising from the Hep3B-FHIT cells occurred much later than those arising from the Hep3B and Hep3B-C cells. The growth of Hep3B-FHIT cells was slow and the tumor volume was low.

CONCLUSION: Transduction of *FHIT* gene inhibits the growth of human hepatocellular carcinoma cells and induces cell apoptosis *in vivo* and *in vitro*.

© 2008 The WJG Press. All rights reserved.

Key words: Hepatocellular carcinoma; Gene therapy; Fragile histidine triad gene

Peer reviewer: Luis Rodrigo, Professor, Gastroenterology Service, Hospital Central de Asturias, c/ Celestino Villamil, s.n., Oviedo 33.006, Spain

Xu RH, Zheng LY, He DL, Tong J, Zheng LP, Zheng WP, Meng J, Xia LP, Wang CJ, Yi JL. Effect of fragile histidine triad gene transduction on proliferation and apoptosis of human hepatocellular carcinoma cells. *World J Gastroenterol* 2008; 14(23): 3754-3758 Available from: URL: http://www.wjgnet.com/1007-9327/14/3754.asp DOI: http://dx.doi.org/10.3748/wjg.14.3754

INTRODUCTION

Fragile histidine triad (FHIT) gene has been successfully cloned on chromosome 3p14.2 using an exon trapping method for gene capture[1-4]. It was reported that abnormal *FHIT* gene exists in majority of tumors, and is an important candidate tumor-suppressing gene[5-10]. In the hepatoma cell line Hep3B, the *FHIT* gene, mRNA, and protein are abnormal[11]. We constructed a recombinant pcDNA3.1 (+) /FHIT vector containing human (FHIT) gene, which was used to transfect human hepatoma Hep3B cells *in vitro* and *in vivo* to explore the

effect of *FHIT* gene on proliferation or apoptosis of hepatocellular carcinoma cells.

MATERIALS AND METHODS

Bacteria, plasmids and cells

E.coli DH5α and eukaryotic expression vector pcDNA3.1 (+) were routinely kept in our laboratory. PBluescript SK FHIT plasmid with a full-length FHIT cDNA was kindly given by Professor Xiao-Fan Wang, Duke University, USA. Hep3B cells were purchased from the Chinese Academy of Sciences in Shanghai.

Main reagents

A reverse transcription-polymerase chain reaction (RT-PCR) kit was purchased from Takara, Japan. FHIT antibody was purchased from Zymed, USA. A cell cycle assay kit was purchased from Becton Dickinson, USA.

Enzyme cutting and identification of DNA sequence

To establish an enzyme-cutting reaction, pcDNA3.1 (or PBluescript SK FHIT), *Bam*H I and *Xba* I were mixed in a water bath at 37℃ for 2 h. The mixture was electrophoresed, and 1.0 kb *FHIT* gene fragments, and a 5.4 kb linear pcDNA3.1 were retrieved separately with electrophoresis coagulation plastic boxes. For constructing the pcDNA3.1 (+) /FHIT vector, *FHIT* gene fragments, linear pcDNA3.1 and T4 ligase were mixed in an Eppendorf tube at 16℃ for 12 h to establish a recombinant plasmid reaction. The pcDNA3.1 FHIT vector was transferred into competent bacteria DH5, and the clones were cultured and identified.

Cell culture and transfection

Hep3B cells were cultured at 37℃ in Dulbecco's modified Eagle's medium containing 10% fetal calf serum (Gibco), 1.0 mmol/L sodium pyruvate, 0.1 mmol/L non-indispensable amino acid and 5% CO_2, at a saturated humidity. Hep3B cells with strong growth were seeded in 6-well plates. pcDNA3.1 (+) /FHIT was transfected into the Hep3B cells at the density of 70% with Lipofectamine 2000 (liposome transfection kit) following its manufacturer's instructions. After transfection, the cells were screened using G418 (500 mg/L) and the screening was maintained with G418 (250 mg/L). Hep3B cells transfected with *FHIT* gene and empty vector were named Hep3B-FHIT and Hep3B-C, respectively. Parent Hep3B cells were used as an untransfected control.

RT-PCR

FHIT gene was amplified with primers (P1: 5' -ATGTCGTTCAGA-3', P2: 5'-CTGAAAGTACAC-3') using the Hep3B-FHIT cells screened by G418[12]. Total RNA was extracted with TRIZOL method and underwent reverse-transcription PCR. The PCR products were electrophoresed on a 1% agarose gel. One μL of the resulting cDNA was added into the PCR reaction mixture (containing 1.0 μL of forward primer (10 pmol/μL), 1.0 μL of reverse primer(10 pmol/μL), 1.0 μL of dNTPs(10 mmol/L), 0.5 μL Taq DNA polymerase). PCR was performed for 30 cycles, each amplification cycle consisting of denaturation at 94℃ for 1 min, primer annealing at 44℃ for 1 min, and extension at 72℃ for 45 s. The PCR products were analyzed on 10 g/L agarose gel containing ethidium bromide.

Western blot

The screened Hep3B-FHIT cells were lysed with a cell-lysing solution. The protein concentration in the supernatant after centrifugation was measured by Bradford assay. The supernatant was electrophoresed on a 12% SDS-polyacrylamide gel. The electrophoresed proteins were transferred to nitrocellulose membrane, blocked with calf serum, combined with FHIT antibody and horseradish peroxidase secondary antibody, developed by enhanced chemiluminescence (ECL) and photographed.

Measurements of growth capacity of transfected cells by thiazolyl tetrazolium (MTT) assay

Ten thousand cells/well were seeded in 96-well plates (200 μL/well), with 6 wells for each cell group and 3 wells for control. MTT (5 g/L) was used as an incubation solution. DMSO was added to the cell culture for 4 h. The luminous absorbance was measured by ELISA (wavelength of 570 nm). The measurement was repeated once a day for 6 days.

Flow cytometry analysis of cell cycle and apoptosis

After trypsinization, the cells were washed twice with phosphate-buffered saline (PBS), fixed with cold ethanol (70%) overnight, suspended in PBS after ethanol was purged from PBS, and stained with propidium iodide (50 μg/mL). The samples were examined by flow cytometry.

Animal experiments

After forty-eight hours, 2 μg of pcDNA3.1 (+) and pcDNA3.1 (+)/FHIT plasmid was transfected with Lipofectamine 2000 into Hep3B cell lines, and clones were obtained by screening with G418 for 14 d. The clones were cultured. The study was approved by the Experimental Animal Committee of Tongji Medical College, Huazhong University of Science and Technology, and all animal experiments adhered to the Animal Welfare Committee Guidelines. Male athymic BALB/c nu/ nu mice (4-6 wk old) were obtained from the Institute of Materia Medica (Tongji Medical College, Wuhan, China) and housed in laminar-flow cabinets under specific pathogen-free (SPF) conditions. Fifteen male mice were randomized into Hep3B-FHIT/nude, Hep3B-C/nude and Hep3B/nude groups, 5 in each group. A suspension of Hep3B-FHIT or Hep3B-C or Hep3B cells (10^7 cells in 0.15 mL Hanks' solution) was injected into the back of mice in each group. After implantation, tumor growth was detected weekly by measuring its diameter with a Vernier caliper. Tumor volume (TV) was calculated using the following formula: TV (mm^3) = $d^2 \times D/2$, where d is the shortest diameter and D

is the longest diameter. Animals were sacrificed 7 wk after implantation, and samples were harvested. The body weight of mice, and tumor growth were measured.

Statistical analysis

The data were expressed as mean ± SD. Student's two-sided *t*-test was used to compare the values of the test and control samples by software SPSS11.5. $P < 0.05$ was considered statistically significant.

RESULTS

Identification of plasmid

The sequence of PBluescript SK FHIT detected in Shanghai Biological Engineering Company was identical to that of FHIT mRNA in GenBank (Lot. Number: NM-002012). After enzyme-cut, agarose gel electrophoresis showed two DNA bands of plasmid PBluescript FHIT (1.0 kb and 2.7 kb), two DNA bands of plasmid pcDNA3.1 (+)/FHIT (1.0 kb and 5.4 kb) (Figure 1); thus, pcDNA3.1 (+)/FHIT was successfully constructed.

FHIT-mRNA expression in transfected cells

After transfected with pcDNA3.1 (+)/FHIT, RT-PCR showed a 400 bp band of Hep3B-FHIT cells. However, the empty vector-transfected, or native cells did not show any band (Figure 2A).

FHIT protein expression in transfected cells

Western blotting demonstrated FHIT protein (17 kDa) in the cells transfected with pcDNA3.1 (+)/FHIT, but no FHIT protein in empty vector-transfected or native cells (Figure 2B).

Growth rates before and after transfection

Thiazolyl tetrazolium (MTT) assay showed that the growth rate of transfected cells was significantly lower than that of native or empty vector-transfected cells, especially after the logarithm growth phase ($P < 0.05$, Figure 3A).

Changes in cell cycle and apoptosis rate

Flow cytometry analysis revealed that the number of Hep3B cells decreased in the G_2/M and S phases, but increased in the G_0/G_1 phase. The apoptosis rate was higher for transfected cells than for empty vector-transfected or native cells ($P < 0.05$, Table 1).

Tumor growth

The growth of transplanted tumor was inhibited markedly by FHIT, showing that tumors arising from the Hep3B-FHIT cells occur much later than those arising from the Hep3B and Hep3B-C cells. Hep3B-FHIT cells grew slowly and their volume was small (Table 2, Figure 3B).

DISCUSSION

It has been reported that FHIT is the first cancer-suppressive gene which links fragile sites to tumors.

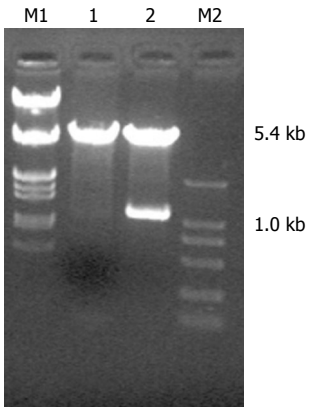

Figure 1 Identification of pcDNA3.1 (+)/FHIT by enzyme-cutting assay. M1: Marker λ/DNA/*Eco*R Ⅰ+*Hin*d Ⅲ; M2: Marker DL2000, lane 1: pcDNA3.1 (+)/FHIT, lane 2: pcDNA3.1 (+)/FHIT post enzyme cutting.

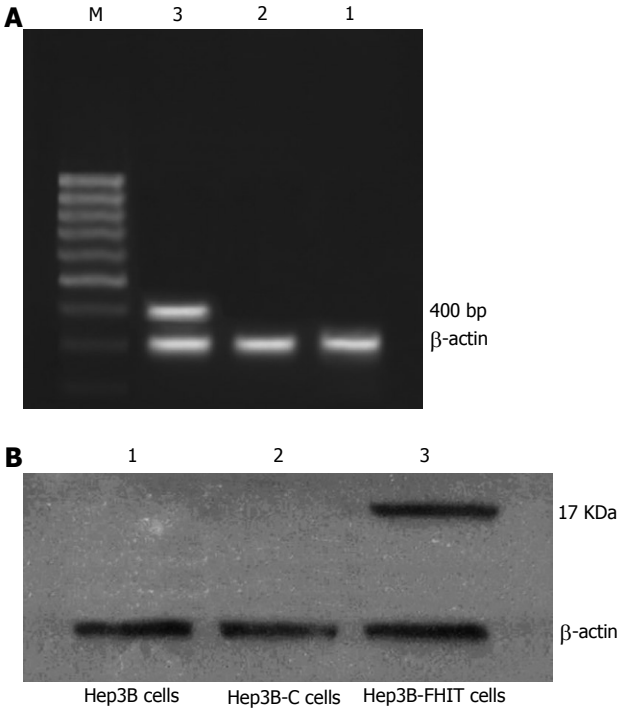

Figure 2 Expression of FHIT mRNA and protein in Hep3B-FHIT, Hep3B-C and Hep3B cells. **A**: FHIT mRNA; **B**: FHIT protein. M: 1000 bp marker; Lane 1: Hep3B cells; lane 2: Hep3B-C cells; lane 3: Hep3B-FHIT cells.

Abnormality of the *FHIT* gene is an early event during tumor development[13-17]. Fracture at the fragile site results in mutation and inactivation of the *FHIT* gene; thus leading to abnormal cell growth[18-22]. Like many other tumors, hepatoma is characterized by highly mutated *FHIT* gene or gene loss. Yuan *et al*[11] found that down-regulation of the *FHIT* gene is detected in 64.3% cell lines (four cell lines showing mRNA down-regulation did not express FHIT protein); allelic loss of intron 5 of the *FHIT* gene was detected in 29.4% hepatomas by *in situ* hybridization; structural alterations of chromosome 3p were identified in 61.5% of hepatocellular carcinomas; expression of FHIT protein was not detectable in 50% primary tumors with immunostaining[11].

FHIT may modulate APnA by hydrolysis of ApnA to yield adenosine 5'-monophosphate (AMP). Due to mutation of FHIT, loss of ApnA hydrolase activity results in elevated Ap3A levels, intracellular accumulation of APnA strengthens the growth signal transduction,

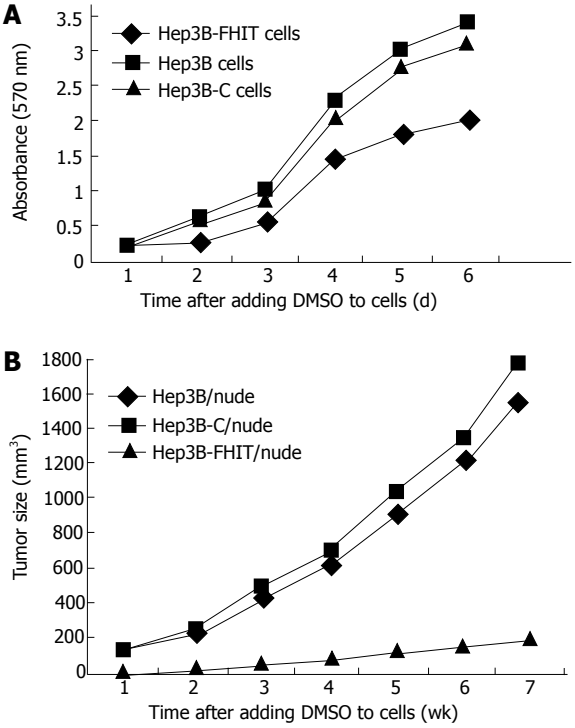

Figure 3 Growth curves. **A**: Growth curves of human hepatocellular carcinoma cells. Luminous absorbance of Hep3B-FHIT, Hep3B-C and Hep3B cells was measured by ELISA (wavelength of 570 nm) after DMSO was added. The measurement was done once a day for 6 d; **B**: Growth curves of tumors after implantation of Hep3B, Hep3B-C or Hep3B-FHIT cells in nude mice. The mice were injected *sc* with 1×10^7 (0.15 mL/mouse) Hep3B, Hep3B-C or Hep3B-FHIT cells. After implantation, tumor growth was detected weekly.

and blocks growth inhibition and apoptosis, thus contributing to carcinogenesis. Additionally, the activity of FHIT on mRNA cap analogs raises the possibility that failure of a decapping function might be tumorigenic[12,23,24].

Gramantieri *et al*[13] examined the mRNA FHIT expression in both cancerous and matched non-cancerous tissues in 28 cases of hepatocellular carcinoma (HCC) and 10 normal livers, and abnormal FHIT transcripts were detected in 13 cases (in cancerous tissue from 11 cases and in non-cancerous tissue from 2 cases). No abnormal FHIT transcripts were found in normal livers. It was recently reported that many other factors can also induce liver carcinogenesis in rats[25-29].

Siprashvili *et al*[30] found that transduction of wild-type FHIT or mutative FHIT with no hydrolase activity into tumor cells lacking *FHIT* gene did not show any advantage to cell growth, and no difference was found in suppression of tumorigenicity, suggesting that FHIT suppresses the tumorigenicity through FHIT protein in combination with its substrate rather than through hydrolysis of APnA. Its more precise mechanism needs to be further explored.

In this study, the full-length of the FHIT cDNA eukaryotic expression vector was transfected into human hepatocellular carcinoma cell line, Hep3B, to manipulate FHIT expression, which alters the biological features of Hep3B cell line. The results indicate that successfully

Table 1 Effect of FHIT gene on cell growth and apoptosis in human hepatocellular carcinoma (mean ± SD)

Cell type	G_0/G_1	S	G_2/M	Apoptosis rate (%)
Hep3B	54.36 ± 0.78	17.40 ± 1.32	28.01 ± 1.12	3.78 ± 0.36
Hep3B-C	53.17 ± 0.52	18.23 ± 2.51	28.55 ± 0.55	3.52 ± 0.33
Hep3B-FHIT[a]	72.23 ± 0.84	12.57 ± 0.42	15.12 ± 1.31	9.74 ± 0.43

[a]$P < 0.05$ *vs* Hep3B or Hep3B-C.

Table 2 Mean tumor formation time and mean tumor weight in nude mice implanted with Hep3B, Hep3B-C or Hep3B-FHIT cells (n = 5, mean ± SD)

Group	Mean tumor formation time (d)	Mean tumor weight (g)
Hep3B/nude	3.22 ± 0.31	3.66 ± 0.40
Hep3B-C/nude	3.08 ± 0.34	3.94 ± 0.39
Hep3B-FHIT/nude	12.17 ± 1.19	0.60 ± 0.04
Total F value	72.38	168.36
Total P value	0.00	0.00

transfected Hep3B cells could express FHIT mRNA and FHIT protein, whereas the empty-vector transfected Hep3B or native cells did not express them. Moreover, cell proliferation and differentiation were significantly decreased at the G_2/M and S phases, and cell apoptosis increased at the G_0/G_1 phases of Hep3B cells transfected with *FHIT* gene as compared with the control group, suggesting that *FHIT* gene plays an important role in blocking cell growth at the G_1 phase, and in inducing cell apoptosis synergized by other apoptosis-inducing factors. Furthermore, transfer of *FHIT* gene could inhibit the growth of human hepatocellular carcinoma cells, and induce cell apoptosis *in vivo*.

In conclusion, FHIT mRNA, and protein are expressed in FHIT-infected Hep3B cells, thus leading to low proliferation, and high apoptosis of HCC cells. Transfection of *FHIT* gene into human hepatocellular carcinoma cells is a promising therapeutic approach to HCC.

COMMENTS

Background

Abnormal fragile histidine triad (FHIT) gene, an important candidate tumor-suppressing gene, exists in a majority of tumors. In the hepatoma cell line Hep3B, the *FHIT* gene, mRNA, and protein is abnormal. Therefore, we constructed a recombinant pcDNA3.1 (+)/FHIT vector containing human fragile histidine triad (FHIT) gene, which was used to transfect human hepatoma Hep3B cells *in vitro* and *in vivo* to explore the effect of *FHIT* gene on proliferation or apoptosis of hepatocellular carcinoma cells.

Research frontiers

Application of gene transfer technologies in treatment of cancer has led to the development of new experimental strategies like inhibition of oncogenes, restoration of tumor-suppressor genes and enzyme/prodrug therapy (GDEPT). These strategies are being evaluated for the treatment of primary and metastatic liver cancer.

Innovations and breakthroughs

In this study, we constructed a recombinant pcDNA3.1 (+)/FHIT vector containing human *FHIT* gene, which can be used to transfect human hepatoma Hep3B cells (FHIT null) *in vitro* and *in vivo*. Transfection of *FHIT* gene could

inhibit the growth of human hepatocellular carcinoma cells, and induce cell apoptosis.

Applications

Transfection of *FHIT* gene into human hepatocellular carcinoma cells is a promising therapeutic approach to HCC.

Peer review

In this paper, the authors evaluated the effect of human *FHIT* gene on cell proliferation and apoptosis in hepatocellular carcinoma *in vitro* and *in vivo*. It is a very interesting paper, and the study is well designed. It provides a potential therapeutic target for hepatocellular carcinoma.

REFERENCES

1 **Ohta M,** Inoue H, Cotticelli MG, Kastury K, Baffa R, Palazzo J, Siprashvili Z, Mori M, McCue P, Druck T, Croce CM, Huebner K. The FHIT gene, spanning the chromosome 3p14.2 fragile site and renal carcinoma-associated t(3;8) breakpoint, is abnormal in digestive tract cancers. *Cell* 1996; **84**: 587-597

2 **Sozzi G,** Veronese ML, Negrini M, Baffa R, Cotticelli MG, Inoue H, Tornielli S, Pilotti S, De Gregorio L, Pastorino U, Pierotti MA, Ohta M, Huebner K, Croce CM. The FHIT gene 3p14.2 is abnormal in lung cancer. *Cell* 1996; **85**: 17-26

3 **Negrini M,** Monaco C, Vorechovsky I, Ohta M, Druck T, Baffa R, Huebner K, Croce CM. The FHIT gene at 3p14.2 is abnormal in breast carcinomas. *Cancer Res* 1996; **56**: 3173-3179

4 **Virgilio L,** Shuster M, Gollin SM, Veronese ML, Ohta M, Huebner K, Croce CM. FHIT gene alterations in head and neck squamous cell carcinomas. *Proc Natl Acad Sci USA* 1996; **93**: 9770-9775

5 **Sozzi G,** Pastorino U, Moiraghi L, Tagliabue E, Pezzella F, Ghirelli C, Tornielli S, Sard L, Huebner K, Pierotti MA, Croce CM, Pilotti S. Loss of FHIT function in lung cancer and preinvasive bronchial lesions. *Cancer Res* 1998; **58**: 5032-5037

6 **Campiglio M,** Pekarsky Y, Menard S, Tagliabue E, Pilotti S, Croce CM. FHIT loss of function in human primary breast cancer correlates with advanced stage of the disease. *Cancer Res* 1999; **59**: 3866-3869

7 **Sorio C,** Baron A, Orlandini S, Zamboni G, Pederzoli P, Huebner K, Scarpa A. The FHIT gene is expressed in pancreatic ductular cells and is altered in pancreatic cancers. *Cancer Res* 1999; **59**: 1308-1314

8 **Birrer MJ,** Hendricks D, Farley J, Sundborg MJ, Bonome T, Walts MJ, Geradts J. Abnormal Fhit expression in malignant and premalignant lesions of the cervix. *Cancer Res* 1999; **59**: 5270-5274

9 **Thiagalingam S,** Lisitsyn NA, Hamaguchi M, Wigler MH, Willson JK, Markowitz SD, Leach FS, Kinzler KW, Vogelstein B. Evaluation of the FHIT gene in colorectal cancers. *Cancer Res* 1996; **56**: 2936-2939

10 **Huebner K,** Croce CM. Cancer and the FRA3B/FHIT fragile locus: it's a HIT. *Br J Cancer* 2003; **88**: 1501-1506

11 **Yuan BZ,** Keck-Waggoner C, Zimonjic DB, Thorgeirsson SS, Popescu NC. Alterations of the FHIT gene in human hepatocellular carcinoma. *Cancer Res* 2000; **60**: 1049-1053

12 **Barnes LD,** Garrison PN, Siprashvili Z, Guranowski A, Robinson AK, Ingram SW, Croce CM, Ohta M, Huebner K. Fhit, a putative tumor suppressor in humans, is a dinucleoside 5',5"'-P1,P3-triphosphate hydrolase. *Biochemistry* 1996; **35**: 11529-11535

13 **Gramantieri L,** Chieco P, Di Tomaso M, Masi L, Piscaglia F, Brillanti S, Gaiani S, Valgimigli M, Mazziotti A, Bolondi L. Aberrant fragile histidine triad gene transcripts in primary hepatocellular carcinoma and liver cirrhosis. *Clin Cancer Res* 1999; **5**: 3468-3475

14 **Zochbauer-Muller S,** Wistuba II, Minna JD, Gazdar AF. Fragile histidine triad (FHIT) gene abnormalities in lung cancer. *Clin Lung Cancer* 2000; **2**: 141-145

15 **Ishii H,** Ozawa K, Furukawa Y. Alteration of the fragile histidine triad gene early in carcinogenesis: an update. *J Exp Ther Oncol* 2003; **3**: 291-296

16 **Guler G,** Uner A, Guler N, Han SY, Iliopoulos D, McCue P, Huebner K. Concordant loss of fragile gene expression early in breast cancer development. *Pathol Int* 2005; **55**: 471-478

17 **Weiske J,** Albring KF, Huber O. The tumor suppressor Fhit acts as a repressor of beta-catenin transcriptional activity. *Proc Natl Acad Sci USA* 2007; **104**: 20344-20349

18 **Ishii H,** Furukawa Y. Alterations of common chromosome fragile sites in hematopoietic malignancies. *Int J Hematol* 2004; **79**: 238-242

19 **Lee SH,** Kim HY, Kim TJ, Park HK, Kim WH, Woo KM, Cho MH. Aberrant splicing of FHIT transcripts in human gastric cancer cell lines. *Res Commun Mol Pathol Pharmacol* 2002; **112**: 39-49

20 **McAvoy S,** Ganapathiraju SC, Ducharme-Smith AL, Pritchett JR, Kosari F, Perez DS, Zhu Y, James CD, Smith DI. Non-random inactivation of large common fragile site genes in different cancers. *Cytogenet Genome Res* 2007; **118**: 260-269

21 **Smith DI,** McAvoy S, Zhu Y, Perez DS. Large common fragile site genes and cancer. *Semin Cancer Biol* 2007; **17**: 31-41

22 **Iliopoulos D,** Guler G, Han SY, Druck T, Ottey M, McCorkell KA, Huebner K. Roles of FHIT and WWOX fragile genes in cancer. *Cancer Lett* 2006; **232**: 27-36

23 **Zawacka-Pankau J,** Podhajska AJ. Expression and simple, one-step purification of fragile histidine triad (Fhit) tumor suppressor mutant forms in Escherichia coli and their interaction with protoporphyrin IX. *Biotechnol Lett* 2007; **29**: 877-883

24 **Huang K,** Frey PA. Engineering human Fhit, a diadenosine triphosphate hydrolase, into an efficient dinucleoside polyphosphate synthase. *J Am Chem Soc* 2004; **126**: 9548-9549

25 **Tsujiuchi T,** Sasaki Y, Oka Y, Konishi Y, Tsutsumi M. Fhit gene alterations in hepatocarcinogenesis induced by a choline-deficient L-amino acid-defined diet in rats. *Mol Carcinog* 2003; **36**: 147-152

26 **Golebiowski F,** Kowara R, Pawelczyk T. Distribution of Fhit protein in rat tissues and its intracellular localization. *Mol Cell Biochem* 2001; **226**: 49-55

27 **Tsujiuchi T,** Sasaki Y, Kubozoe T, Tsutsumi M, Konishi Y, Nakae D. Alterations of the Fhit gene in hepatocellular carcinomas induced by N-nitrosodiethylamine in rats. *Mol Carcinog* 2002; **34**: 19-24

28 **Asensio AC,** Rodriguez-Ferrer CR, Oaknin S, Rotllan P. Biochemical and immunochemical characterisation of human diadenosine triphosphatase provides evidence for its identification with the tumour suppressor Fhit protein. *Biochimie* 2006; **88**: 461-471

29 **Han SY,** Iliopoulos D, Druck T, Guler G, Grubbs CJ, Pereira M, Zhang Z, You M, Lubet RA, Fong LY, Huebner K. CpG methylation in the Fhit regulatory region: relation to Fhit expression in murine tumors. *Oncogene* 2004; **23**: 3990-3998

30 **Siprashvili Z,** Sozzi G, Barnes LD, McCue P, Robinson AK, Eryomin V, Sard L, Tagliabue E, Greco A, Fusetti L, Schwartz G, Pierotti MA, Croce CM, Huebner K. Replacement of Fhit in cancer cells suppresses tumorigenicity. *Proc Natl Acad Sci USA* 1997; **94**: 13771-13776

S- Editor Sun YL **L- Editor** Wang XL **E- Editor** Lin YP

Online Submissions: wjg.wjgnet.com
wjg@wjgnet.com
doi: 10.3748/wjg.14.3759

World J Gastroenterol 2008 June 21; 14(23): 3759-3762
World Journal of Gastroenterology ISSN 1007-9327
© 2008 The WJG Press. All rights reserved.

CASE REPORT

Abdominal neurenteric cyst

Radoje Čolović, Marjan Micev, Miodrag Jovanović, Slavko Matić, Nikica Grubor, Henry Dushan E Atkinson

Radoje Čolović, Marjan Micev, Miodrag Jovanović, Slavko Matić, Nikica Grubor, Clinical Center of Serbia, Institute for Digestive Diseases, Belgrade 11000, Serbia
Henry Dushan E Atkinson, Surgical Directorate, Imperial College School of Medicine, St Mary's Hospital, Praed St, London W2 1NY, United Kingdom
Author contributions: Čolović R took part at the operation and wrote the article; Micev M did the histology and immunohistochemistry investigation; Jovanović M operated the patient; Matić S did the literature analysis, made an original translation to English, did all the corrections of the manuscript and the correspondence; Grubor N did the literature analysis; Atkinson HDE obtained some of the cited references and corrected the final English article.
Correspondence to: Slavko Matić, MD, PhD, Surgeon, Assistant professor of Surgery, Clinical Center of Serbia, Institute for Digestive Diseases, K. Todorovića 6 Street, Belgrade 11000, Serbia. slavko.matic@med.bg.ac.yu
Telephone: +381-64-2181949 Fax: +381-11-3031830
Received: December 24, 2007 Revised: April 30, 2008
Accepted: May 7, 2008
Published online: June 21, 2008

Abstract

Neurenteric cysts are extremely rare congenital anomalies, often presenting in the first 5 years of life, and are caused by an incomplete separation of the notochord from the foregut during the third week of embryogenesis. They are frequently accompanied with spinal or gastrointestinal abnormalities, but the latter may be absent in adults. Although usually located in the thorax, neurenteric cysts may be found along the entire spine. We present a 24-year-old woman admitted for epigastric pain, nausea, vomiting, low grade fever and leucocytosis. She underwent cystogastrostomy for a loculated cyst of the distal pancreas at the age of 4 years, which recurred when she was at the age of 11 years. Ultrasound and computer tomography (CT) scan revealed a 16 cm × 15 cm cystic mass in the body and tail of pancreas, with a 6-7 mm thickened wall. Laboratory data and chest X-ray were normal and spinal radiographs did not show any structural abnormalities. The patient underwent a complete cyst excision, and after an uneventful recovery, remained symptom-free without recurrence during the 5-year follow-up. The cyst was found to contain 1200 mL of pale viscous fluid. It was covered by a primitive single-layered cuboidal epithelium, along with specialized antral glandular parenchyma and hypoplastic primitive gastric mucosa. Focal glandular groups resembling those of the body of the stomach were also seen. In addition, ciliary respiratory epithelium, foci of squamous metaplasia and mucinous glands were present. The wall of the cyst contained a muscular layer, neuroglial tissue with plexogenic nerve fascicles, Paccini corpuscle-like structures, hyperplastic neuro ganglionar elements and occasional psammomatous bodies, as well as fibroblast-like areas of surrounding stroma. Cartilagenous tissue was not found in any part of the cyst. Immunohistochemistry confirmed the presence of neurogenic elements marked by S-100, GFAP, NF and NSE. The gastric epithelium showed mostly CK7 and EMA immunoexpression, and the respiratory epithelium revealed a CK8 and CK18 immunoprofile without CK 10/13 positive elements, though neither CEA or AFP positive cells were found. To our knowledge, this is the first reported case of an abdominally located neurenteric cyst with no associated spinal anomalies.

© 2008 The WJG Press. All rights reserved.

Key words: Neurenteric cyst; Congenital; Abdomen; Pancreas; Surgical excision

Peer reviewers: David Adams, Professor, Liver Research Laboratories, Institute for Biomedical Research, Queen Elizabeth Hospital, University of Birmingham, Birmingham B15 2TT, United Kingdom; Werner Hohenberger, Professor, Chirurgische Klinik und Poliklinik, Krankenhausstrasse 12, Erlangen D-91054, Germany

Čolović R, Micev M, Jovanović M, Matić S, Grubor N, Atkinson HDE. Abdominal neurenteric cyst. *World J Gastroenterol* 2008; 14(23): 3759-3762 Available from: URL: http://www.wjgnet.com/1007-9327/14/3759.asp DOI: http://dx.doi.org/10.3748/wjg.14.3759

INTRODUCTION

Foregut duplications can be classified into three groups: enteric cysts (lined with intestinal epithelium), bronchogenic cysts (lined with respiratory epithelium), and neurenteric cysts (where enteric cysts are associated with vertebral anomalies or communications with the nervous system)[1,2].

Neurenteric cysts are extremely rare congenital anomalies, usually diagnosed in infancy[3,4] and tend to be located in the right upper posterior mediastinum, but can be found anywhere along the spine or even intracra-

nially[1,5,6]. They may be associated with spinal anomalies such as hemivertebrae and anterior spina bifida[5], and esophageal atresia[7,8], though these associated abnormalities may be absent in adults[5].

We describe the first reported case of an abdominal neurenteric cyst, with no associated spinal anomalies.

CASE REPORT

A 24-year-old woman presented to our unit in 2001 with epigastric pain, nausea, vomiting, low grade fever and leucocytosis.

Her medical history and case notes showed that she underwent surgery for an 8 cm multi-loculated cyst in the region of the distal pancreas at the age of 4 years, and this was anastomosed to the posterior wall of the stomach. At the age of 11 years, a 2.5 cm recurrent cyst was found, though no significant enlargement was noted over the following decade, and she was largely symptom-free in almost 20 years.

On examination she was found to have a tender palpable mass in the upper left epigastrium. Ultrasonography (US) and computer tomography (CT) scan revealed a cystic mass in the region of the body and tail of the pancreas, measuring 16 cm × 15 cm, with a 6-7 mm thickened wall, and filled with dense fluid (Figure 1). Laboratory data and chest X-ray were normal and spinal radiographs did not show any structural abnormalities. Barium swallow revealed that the stomach displaced to the right and anteriorly, and a gastroscopy did not show any sign of the previous cystogastrostomy on the posterior wall of the stomach.

With a working diagnosis of a mucinous cystadenoma of the pancreas, the patient underwent laparotomy. The cystic tumor was located in the body and tail of the pancreas, and was adherent to the stomach, splenic vessels, prevertebral fascia, and spine. The pancreatic parenchyma in the region of the cyst was completely atrophied, and the previously performed anastomosis was obliterated. The cyst was completely excised, and was found to contain 1200 mL of pale viscous fluid. Laboratory analyses did not show any elevation of amylase or polymorphonuclears cells, and no growth occurred on microbiological culture.

The postoperative recovery was uneventful, the preoperative symptoms completely resolved, and the patient remained symptom-free, without recurrence during the 5-year follow-up.

Macroscopically, the cyst wall, dark brown in color, was up to 14 mm in thickness and partly hyalinized. The inner surface of the cyst was smooth with some coarse sections, and some areas of the cyst wall also contained smaller cysts. Microscopic examination showed organoid organization resembling tissues, and organs similar to the embryonic foregut, including intestinal wall epithelial formation, partly covered by a primitive single-layered cuboidal epithelium, along with specialized antral glandular parenchyma, and hypoplastic primitive gastric mucosa. Focal glandular groups resembling those of the body of the stomach were also seen. In addition, ciliary

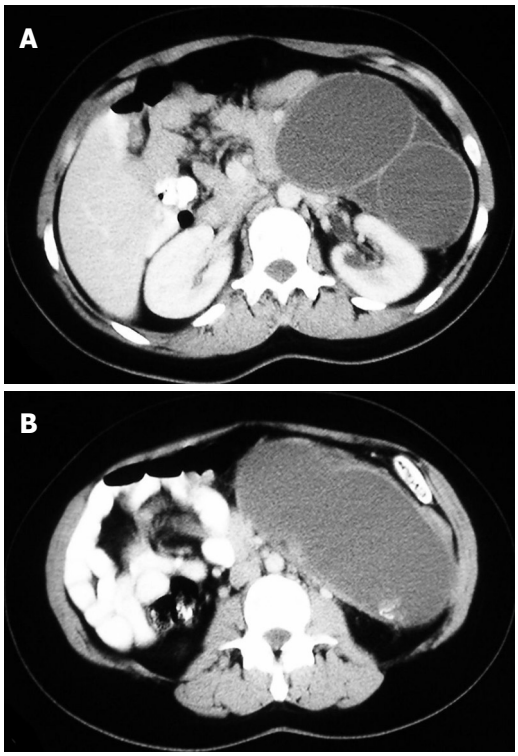

Figure 1 Axial CT scan showing a large bilocular cyst in the region of the body and tail of the pancreas (**A**) and a second more caudal axial CT slice (**B**).

respiratory epithelium, foci of squamous metaplasia, and mucinous glands were present. The wall of the cyst contained a muscular layer, neuroglial tissue with plexogenic nerve fascicles, Paccini corpuscle-like structures, hyperplastic neuro ganglionar elements, and occasional psammomatous bodies, as well as fibroblast-like areas of surrounding stroma (Figures 2 and 3).

Immunohistochemistry confirmed the presence of neurogenic elements marked by S-100, GFAP, NF and NSE. The gastric epithelium showed mostly CK7 and EMA immunoexpression, and the respiratory epithelium revealed a CK8 and CK18 immunoprofile without CK 10/13 positive elements, though neither CEA or AFP positive cells were found (Figure 4A-D).

DISCUSSION

Neurenteric cysts may appear at any age, but are usually discovered during the first five years of life[4,9]. They are thought to develop early in the course of embryogenesis either due to incomplete separation of the notochord from the embryonic foregut (which are apposed), or due to herniation of the endoderm of the embryonic foregut into the dorsal ectoderm[10,11]. This attachment of the cyst to the notochord may prevent fusion of the vertebral bodies and lead to spinal anomalies[1,5], indeed one third of patients have associated anomalies of the central nervous system or gastrointestinal tract[5].

Neurenteric cysts may be multiloculated or septate, lined with ciliated, non-ciliated, columnar or cuboidal epithelium, and may resemble intestinal, duodenal or gastric mucosa. These cells are usually PAS-positive and

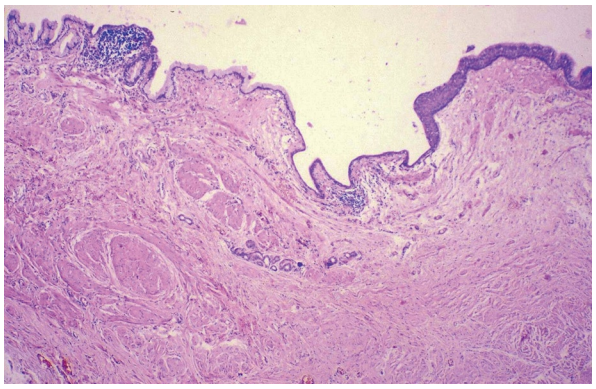

Figure 2 Histological slides showing the full spectrum of epithelia within the cyst lining.

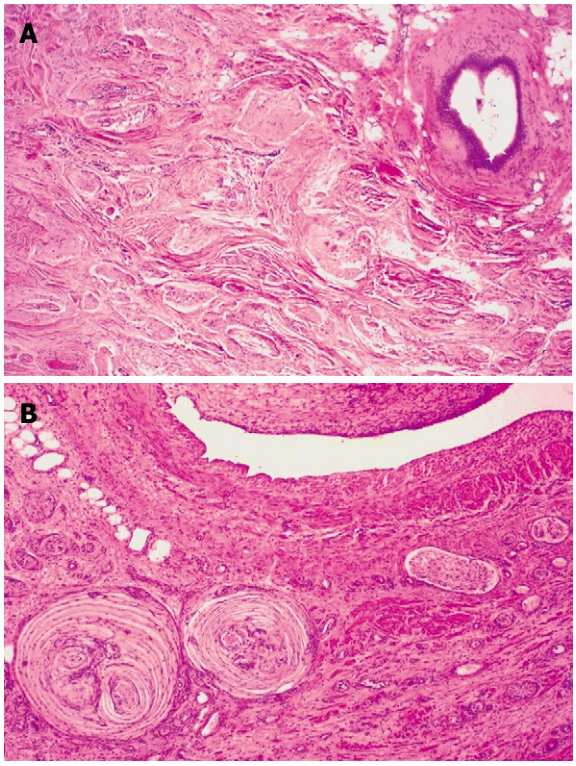

Figure 3 Histological slide showing elements of an abortive muscular layer and focal irregular neuronal hyperplasia in the cyst wall (**A**) and a more irregular configuration of the cyst with various ganglio-neuronal elements including Paccinian corpuscles (**B**).

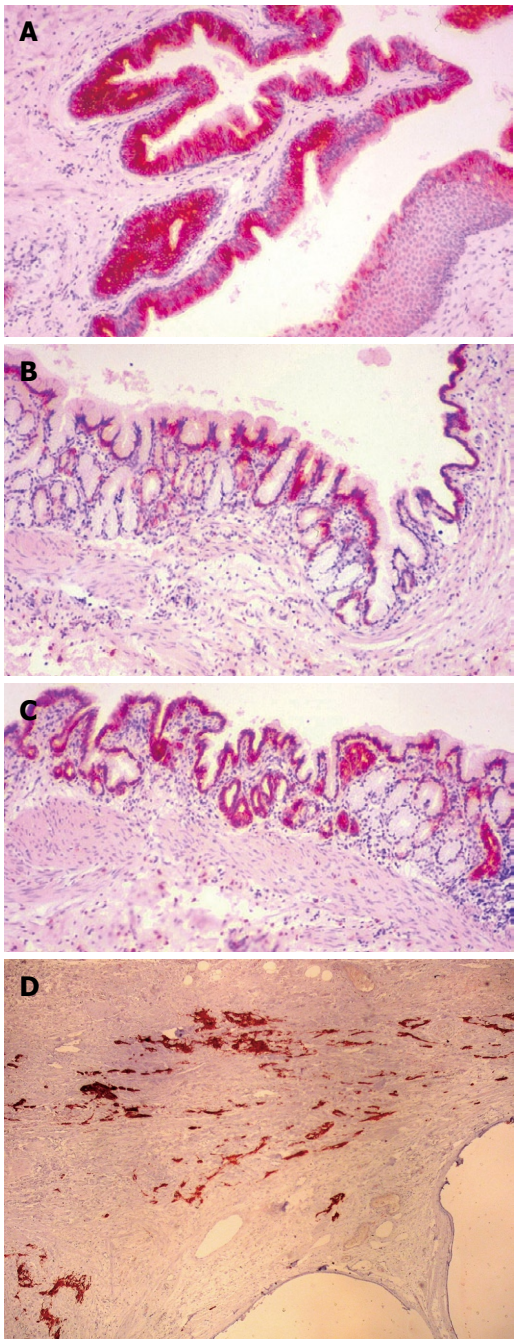

Figure 4 Histological slides showing more specialized epithelia with consistent immunoreactivity to anti-cytokeratin 7 (**A**), anti-cytokeratin 18 (**B**), CA19-9 (**C**), and mixed abundant neuro-ganglionic/neuro-glial elements that were immunohistochemically verified (immunostaining is with the monoclonal antibody to glial fibrillar acidic protein) (**D**).

can contain mucus and globules, with occasional squamous cell metaplasia. A basal membrane is always present and the capsule consisting of fibrovascular tissue is fragile. The wall of the cyst may contain ganglionar cells, lymphatic tissue, pancreatic tissue, salivary glands or muscular tissue without serosa[1]. Cartilaginous tissue is never present[6]. The cysts usually contain clear, pale, yellowish or green viscous or mucinous fluid, depending on the presence or absence of previous hemorrhage[5].

They are classified into Types A-C according to the histology. Type A cysts, the most described in the literature[5], consist of simple lined cuboidal or columnar epithelium with or without cilia. Type B cysts include more complex gastrointestinal or tracheobronchial elements, including mucous glands and smooth muscle cells in the cyst walls. In addition to these elements, type C cysts also contain ependymal and/or glial tissue[5]. Our patient had a septated type C cyst containing respiratory epithelium, gastric epithelium, and ependymal and glial tissue.

The clinical presentation usually depends on the size and location of the cyst. The patient, typically a small infant, often presents with respiratory distress, dyspnoea, stridor or a persistent cough, caused by pressure of the cyst on the lung. Respiratory distress is usually found with a mediastinal mass, and a vertebral anomaly coexisting

in more than 70% of pediatric patients with neurenteric cysts[3,9]. When located intraspinally, the cysts may cause motor and sensory neurological disturbance[9]. Chest pain, cardiac arrhythmias and dysphagia can also present, and in the rare cases of ulcer formation in ectopic gastric mucosa in the cyst wall, the patient can present with melaena or perforation of the cyst[1,12].

The diagnosis is usually made by US, which characterizes the cyst and can evaluate for chest masses, and with the advent of high resolution US, these cysts can be detected as early as 18 wk gestation[1,5,13]. CT and nuclear magnetic resonance imaging (MRI) also have their place[14], though the final diagnosis is based on histopathological examination.

Complete cyst excision is the recommended treatment[6,15], with some patients requiring a simultaneous laminectomy[16]. If the cyst consists of two components, the symptomatic cyst should be excised first. If there is a combination of asymptomatic intraspinal and extraspinal cysts, the spinal cyst should be excised first in order to avoid any neurological deterioration which might occur during mediastinal cyst excision[6].

Our patient underwent a cystogastrostomy at the age of 4 years, presumably with an underlying misdiagnosis of a pancreatic pseudocyst. However, the cyst was covered with an epithelial layer, and recurred. This case nicely demonstrates that the cyst should have previously been completely excised, and when this was finally done, the patient's symptoms resolved, with no cyst recurrence.

REFERENCES

1 **Singh D**, Singh S, Kiraw R, Bhagwat SS. Neurenteric Cyst 2003. Available from URL: http://www.bhj.org/journal/2003_4502_april/neurentericcyst_373.htm

2 **Ravitch MM**. Mediastinal cysts and tumours. In: Welsch KJ, Randolph JG, Ravitch MN, O Neill JAJ, Rowe MJ, editors. Pediatric Surgery Chicago: Year Book Medical Publishers, 1986: 606-614

3 **Fernandes ET**, Custer MD, Burton EM, Boulden TF, Wrenn EL Jr, Whittle AP, Edwards OP. Neurenteric cyst: surgery and diagnostic imaging. *J Pediatr Surg* 1991; **26**: 108-110

4 **Viladevall H**. Primitive gut morphogenesis 2004; 2006. Available from URL: http://sprojects.mmi.mcgill.ca/embryology/gi/pgm.htm

5 **Olavarria SA**, Diaz Guerrero DL, Yanis A. Neurenteric cyst 2000; 2006. Available from URL: http://www.thefetus.net/page.php?id=230

6 **Birmole BJ**, Kulkarni BK, Vaidya AS, Borwankar SS. Intrathoracic enteric foregut duplication cyst. *J Postgrad Med* 1994; **40**: 228-230

7 **Kapouleas GP**, Keramidas DC, Soutis M. Bochdalek's hernia combined with agenesis of the pericardium and intrathoracic solitary cyst of the liver. *Z Kinderchir* 1989; **44**: 377-378

8 **Hemalatha V**, Batcup G, Brereton RJ, Spitz L. Intrathoracic foregut cyst (foregut duplication) associated with esophageal atresia. *J Pediatr Surg* 1980; **15**: 178-180

9 **Mancini M**, Eggerstedt IM. Mediastinal Cysts 2006; 2006. Available from URL: http://www.emedicine.com/med/topic2985.htm

10 **Bourne A**. Congenital and developmental abnormalities. In: Whitehead R, editor. Gastrointestinal and esophageal pathology New York: Churchill Livingstone, 1995: 275-301

11 **Sen S**, Bourne AJ, Morris LL, Furness ME, Ford WD. Dorsal enteric cysts--a study of eight cases. *Aust N Z J Surg* 1988; **58**: 51-55

12 **Cohen SR**, Geller KA, Birns JW, Thompson JW, Meyer BW, Lindesmith GG. Foregut cysts in infants and children. Diagnosis and management. *Ann Otol Rhinol Laryngol* 1982; **91**: 622-627

13 **Perera GB**, Milne M. Neurenteric cyst: antenatal diagnosis by ultrasound. *Australas Radiol* 1997; 41: 300-302

14 **Rattan KN**, Magu S, Rohilla S. Mediastinal foregut duplication cysts. *Indian J Pediatr* 2004; **71**: 103-105

15 **Cahill JF**. An unusual cause of neonatal respiratory distress. RDS in a neonate with a neuro-enteric cyst. *Anaesthesia* 1981; **36**: 790-794

16 **Bilik R**, Ginzberg H, Superina RA. Unconventional treatment of neuroenteric cyst in a newborn. *J Pediatr Surg* 1995; **30**: 115-117

S- Editor Li DL **L- Editor** Wang XL **E- Editor** Liu Y

Online Submissions: wjg.wjgnet.com
wjg@wjgnet.com
doi:10.3748/wjg.14.3763

World J Gastroenterol 2008 June 21; 14(23): 3763-3767
World Journal of Gastroenterology ISSN 1007-9327
© 2008 The WJG Press. All rights reserved.

CASE REPORT

Pathologic complete response confirmed by surgical resection for liver metastases of gastrointestinal stromal tumor after treatment with imatinib mesylate

Seiji Suzuki, Koji Sasajima, Masayuki Miyamoto, Hidehiro Watanabe, Tadashi Yokoyama, Hiroshi Maruyama, Takeshi Matsutani, Aimin Liu, Masaru Hosone, Shotaro Maeda, Takashi Tajiri

Seiji Suzuki, Koji Sasajima, Masayuki Miyamoto, Hidehiro Watanabe, Tadashi Yokoyama, Hiroshi Maruyama, Takeshi Matsutani, Department of Surgery, Tama-Nagayama Hospital, Nippon Medical School, 1-7-1 Nagayama, Tama, Tokyo 206-8512, Japan
Aimin Liu, Masaru Hosone, Shotaro Maeda, Department of Pathology, Tama-Nagayama Hospital, Nippon Medical School, 1-7-1 Nagayama, Tama, Tokyo 206-8512, Japan
Takashi Tajiri, Department of Surgery, Nippon Medical School, 1-1-5 Sndagi, Bunkyo-Ku, Tokyo 113-8603, Japan
Author contributions: Suzuki S, Miyamoto M and Yokoyama T performed hepatectomy; Watanabe H evaluated the effect of the treatment with imatinib; Suzuki S, Maruyama H and Matsutani T treated the patient with imatinib; Liu A, Hosone M and Maeda S evaluated the histopathological findings; Suzuki S wrote the paper; Sasajima K and Tajiri T reviewed the paper.
Correspondence to: Seiji Suzuki, Department of Surgery, Tama-Nagayama Hospital, Nippon Medical School, 1-7-1 Nagayama, Tama, Tokyo 206-8512, Japan. seiji@nms.ac.jp
Telephone: +81-42-3712111 Fax: +81-42-3727384
Received: March 22, 2008 Revised: May 6, 2008
Accepted: May 13, 2008
Published online: June 21, 2008

Abstract

A 39-year-old male underwent distal gastrectomy for a high grade gastrointestinal stromal tumor (GIST). Computed tomography (CT) and magnetic resonance imaging (MRI) 107 mo after the operation, revealed a cystic mass (14 cm in diameter) and a solid mass (9 cm in diameter) in the right and left lobes of the liver, respectively. A biopsy specimen of the solid mass showed a liver metastasis of GIST. The patient received imatinib mesylate (IM) treatment, 400 mg/day orally. Following the IM treatment for a period of 35 mo, the patient underwent partial hepatectomy (S4 + S5). The effect of IM on the metastatic lesions was interpreted as pathologic complete response (CR). Pathologically verified cases showing therapeutic efficacy of IM have been rarely reported.

© 2008 The WJG Press. All rights reserved.

Key words: Gastrointestinal stromal tumor; Liver metastasis; Imatinib mesylate; Pathologic complete response

Peer reviewer: Dr. Xin-Yuan Guan, Department of Clinical Oncology, University of Hong Kong, Room 109, Estate Building, 10 Sassoon Road, Hong Kong 852, China

Suzuki S, Sasajima K, Miyamoto M, Watanabe H, Yokoyama T, Maruyama H, Matsutani T, Liu A, Hosone M, Maeda S, Tajiri T. Pathologic complete response confirmed by surgical resection for liver metastases of gastrointestinal stromal tumor after treatment with imatinib mesylate. *World J Gastroenterol* 2008; 14(23): 3763-3767 Available from: URL: http://www.wjgnet.com/1007-9327/14/3763.asp DOI: http://dx.doi.org/10.3748/wjg.14.3763

INTRODUCTION

Gastrointestinal stromal tumor (GIST) is the most common soft tissue tumor of the gastrointestinal tract. It was reported that GIST derived from interstitial cells of Cajal is characterized by the expression of CD34 and c-kit (CD117). Immunohistochemical positivity for c-kit gene product-CD117, a tyrosine kinase receptor, reflects the presence of gained function of c-kit gene mutation[1]. Imatinib mesylate (IM) (Glivec; Novartis Pharmaceuticals, Basel, Switzerland) is a small-molecule tyrosine kinase inhibitor that suppresses the mutated c-kit product[2]. Clinical trials[3,4] for recurrent or metastatic GIST have demonstrated that the partial response (PR) rate is 47% to 54% based on radiographic evaluation. However, a complete response (CR) is rarely reported. Pathologically verified cases showing therapeutic efficacy have been rarely reported. Up to present, only seven cases of locally advanced or metastatic GIST with a pathologic CR to IM treatment have been reported in the literature[5-10].

The initial treatment for a metastatic GIST is to use IM, and then surgical treatment directing toward complete resection is to be considered when the tumor has responded and reduced in size[11-13]. However, neither the adequate intervals between the start of treatment with IM and operation, nor the significance of surgical resection for the patients with metastatic GIST who have been treated with IM, has been completely elucidated.

In this paper, we present a case of GIST with meta-

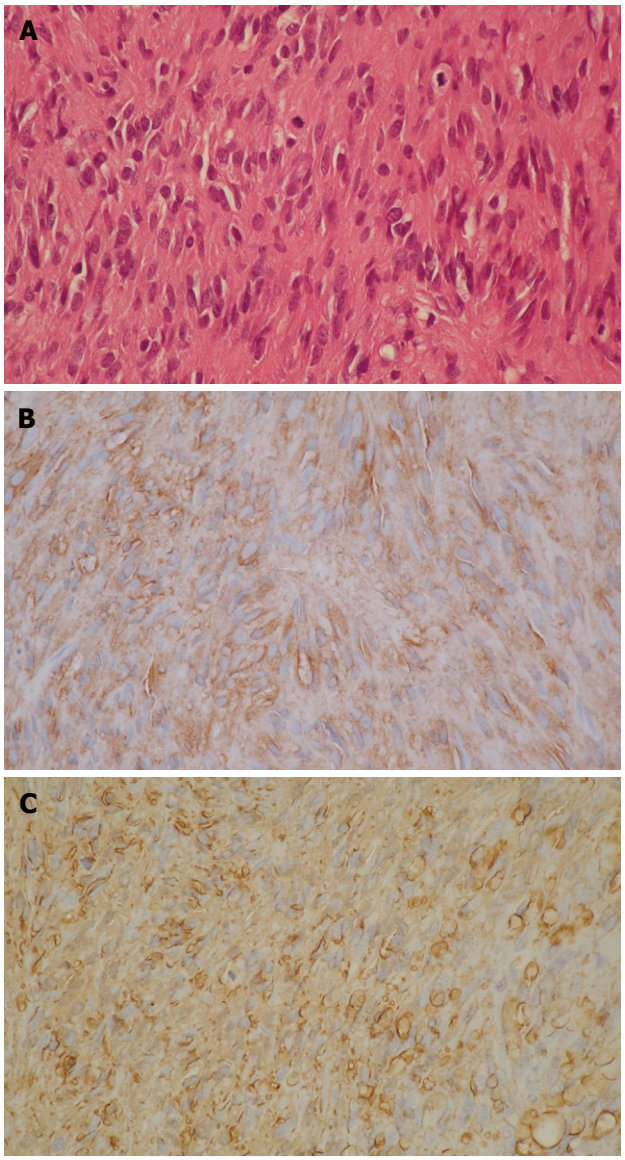

Figure 1 Histological study showing spindle cells with mitoses (HE, × 200) (**A**) and immunohistochemistry findings revealing positive staining for CD117 (**B**) and CD34 (× 200) (**C**) in primary GIST of the stomach.

chronous liver metastasis treated with IM, and describe confirmed the therapeutic efficacy of such a molecular targeting drug as IM, which was confirmed by virtue of pathologic CR following complete surgical resection.

CASE REPORT

A 39-year-old male complaining of epigastralgia was found to have a 3 cm × 2 cm submucosal tumor on the anterior surface of the body along the lesser curvature of the stomach, and underwent partial gastrectomy. Pathological examination of the surgical specimen revealed a high grade leiomyosarcoma showing spindle cells with 20 mitoses/10HPF and 17% in the MIB-1 index. The patient was subsequently diagnosed as having an uncommitted type of high grade GIST, since he was immunohistochemically positive for CD34 and CD117 (Figure 1). One hundred and seven months after the initial operation, the patient developed right upper

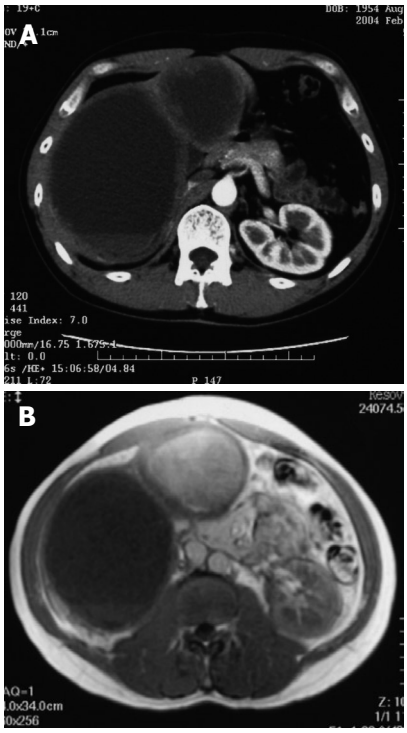

Figure 2 Contrast-enhanced CT scan (**A**) and MRI (**B**) on T1-weighted image 107 mo after the initial operation.

quadrant pain during exercise. Physical examination revealed marked hepatomegaly and the lower margin of the liver could be palpated at five-finger widths below the costal margin. Computed tomography (CT) and magnetic resonance imaging (MRI) showed a cystic mass (14 cm in diameter) and a solid mass (9 cm in diameter) in the right and left lobes of the liver, respectively (Figure 2). Open biopsy was attempted and specimens were obtained from the solid tumor mass in the left lobe of the liver. Pathologically, spindle cells were positive for CD34 and CD117 with 15 mitoses/10 HPF and 15% in the MIB-1 index, which was indicative of a metastatic GIST of the liver (Figure 3). Only fluid was obtained from the cystic mass in the right lobe. A drainage tube was inserted into the cystic mass through the abdominal wall. Cytological examination of the fluid showed that the cystic mass was Class Ⅱ. Since the cystic and solid tumors in the liver were considered too huge to be resected entirely and curatively, molecular targeting therapy using a daily dose of 400 mg of IM was started 3 mo after the liver biopsy. The drainage tube inserted into the cystic mass was removed after a three-week treatment with IM. A follow-up abdominal CT, one month after the start of IM treatment, showed apparent reduction in size of both the cystic and solid masses. The reduction of the solid mass in the left lobe was a partial response (PR). MRI, 30 mo after the treatment with IM, showed that the contrast-enhanced wall of the solid mass became thinner and central necrosis increased in size (Figure 4A). Although CT, 34 mo after the treatment, showed a 5 cm ring-enhanced mass in the left lobe (S4) and a 6 cm enhanced mass in the right lobe (S5) of the liver, the total volume of the

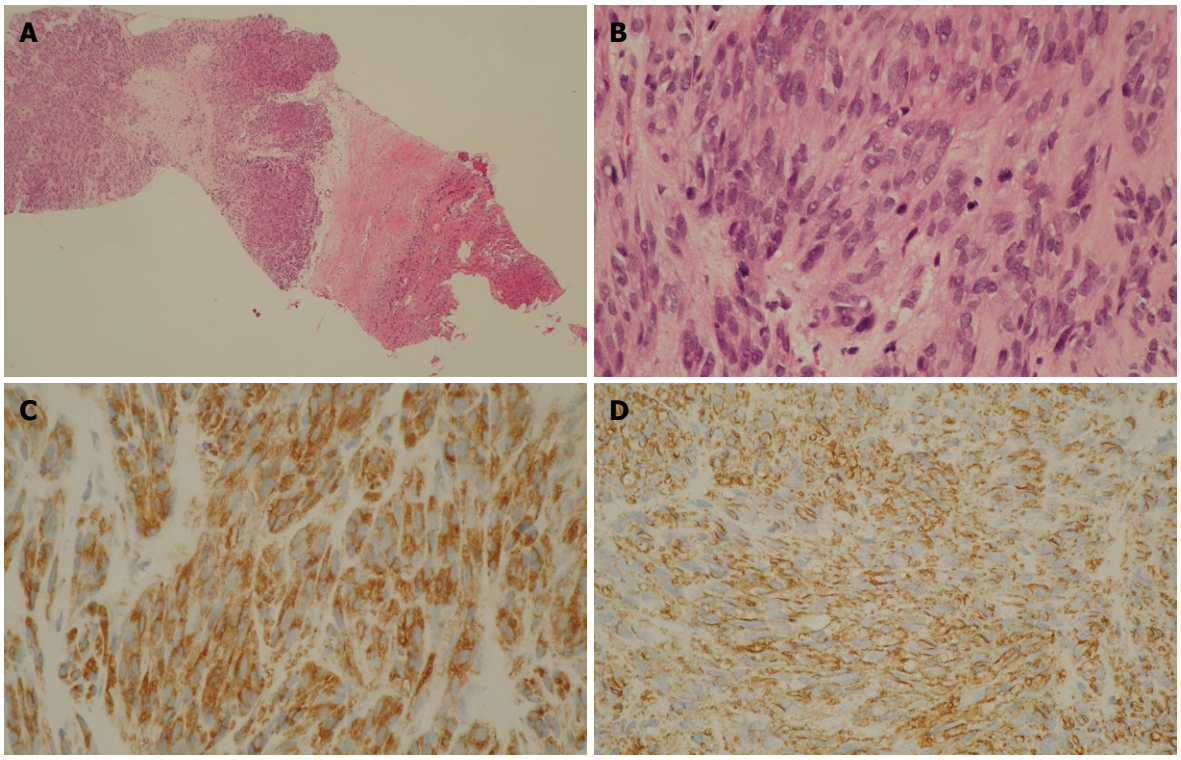

Figure 3 Scanning view of metastatic GIST (× 15) (**A**), histological study revealed spindle cells with mitoses (HE, × 200) (**B**), immunohistochemistry findings revealed positive staining for CD117 (**C**) and CD34 (× 200) (**D**) in metastatic GIST of the liver obtained from liver biopsy.

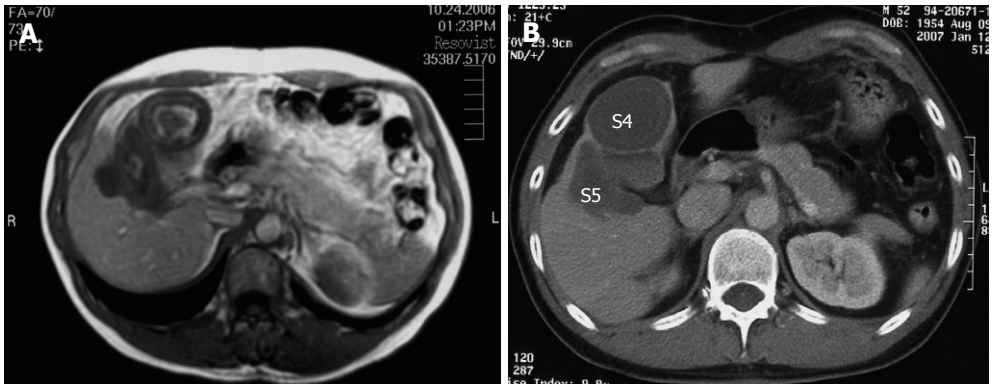

Figure 4 MRI on T1-WI 30 mo after treatment with Imatinib (**A**) and contrast-enhanced CT 34 mo after the treatment with Imatinib (**B**). The metastatic lesions (S4 + S5) are indicated.

neoplastic masses in the liver was sufficiently reduced after the curative resection of the masses (Figure 4B). The IM treatment was interrupted after 35 mo, and then the patient underwent partial hepatectomy (S4 + S5). The cut-surface of the resected specimens from S5 and S4 showed a homogenous yellow-white hard mass and a necrotic soft mass, respectively, forming a scrollwork structure, containing hemorrhagic foci, and surrounded by a yellow-white hard layer (Figure 5). Pathologically, most of the specimens were replaced with hyaline-degenerated tissue, adjacent to which, cystic-degenerated tissue and necrotic tissue with hemorrhage and macrophages containing hemosider-in granules stained with Berlin blue were observed. Since no viable tumor cells stained with CD34 or CD117 were observed in any of the whole sections at the maximum cut surface of the resected specimen, the effect of the IM treatment on the metastatic GIST was interpreted as the pathologic CR (Figure 6).

One week after the operation, oral administration of 400 mg IM daily for 12 mo was performed. Fourteen months after the partial hepatectomy at the time of writing this paper, no recurrent lesion was observed on CT and MRI examinations.

DISCUSSION

The efficacy of aggressive surgical resection for locally advanced or metastatic GIST has been reported before the development of IM treatment[14,15]. Furthermore, clinical studies on the surgical resection after Imatinib treatment have also been reported[5,6,9-12,16,17]. Indeed, surgical resection of GIST makes it possible to elucidate the histopathologic effect of IM treatment on advanced or metastatic GIST. However, biopsy specimens from the lesion alone are usually not enough to assess the histopathologic effect of IM treatment on GIST.

As far as we know, only six clinical reports on the

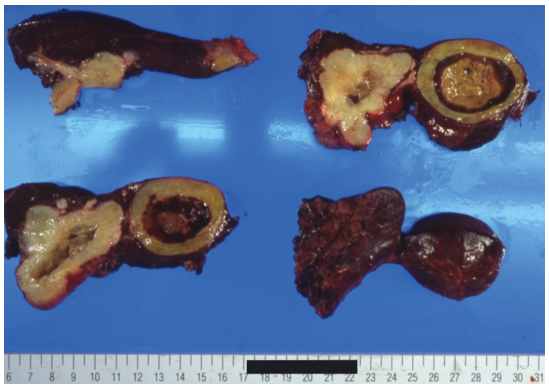

Figure 5 Serous and cut-surface views of resected specimen obtained from partial hepatectomy (S4 + S5) after treatment with Imatinib.

pathological effect of IM treatment on locally advanced or metastatic GIST have been published[5,6,9,10,16,18]. According to Gronchi *et al*[18], no case with a pathological CR was obtained in a series of 38 patients, although the degree of pathologic changes varied widely. Furthermore, Andtbacka *et al*[10] pointed out that radiographic and metabolic CR based upon ^{18}F-fluorodeoxyglucose positron emission tomography (FDG-PET) are not always concordant with a pathologic CR; therefore, it should be born in mind that the pathological evaluation on the surgically resected materials obtained from patients treated with IM might be indispensable for the elucidation of the therapeutic effect of IM on GIST. They also emphasized that the changes in the degree as well as the extent of contrast-enhancement, and the internal structure within the solid tumor should be carefully evaluated on CT and MRI[10]. According to their categorization, our case presented in this paper is compatible with 'initial regression then stabilization' on CT and MRI. MRI, five months prior to the operation in our case, disclosed thickening of the enhanced wall and a change of the signal intensity of the internal structure of the mass in the left lobe of the liver. In fact, the changes in internal density reflected the central necrosis on the cut-surface of the resected mass. Histopathologic changes induced by IM in GIST have been reported to be hyaline degeneration, myxoid degeneration, and appearance of scattered inflammatory cells, hemosider in granules and foamy cells, but seldom necrosis[3,5-8]. Bauer *et al*[6] who found no necrosis in a series of twelve patients treated with IM, speculated that IM would mainly induce apoptosis, but not so much necrosis. As for the timing of surgical resection in patients with recurrent or metastatic GIST, Andtbacka *et al*[10] have reported a complete resection rate of 31.4% after IM therapy for a period of 6.9-37.5 mo (mean, 10 mo). They also emphasized that surgical resection for the IM-responsive recurrent or metastatic GIST should be considered as early as possible before the development of progression and secondary resistance to IM[10]. Surgical resection, 6-12 mo after the start of IM treatment, is recommended among responders[9]. Although the time of operation in our case was markedly

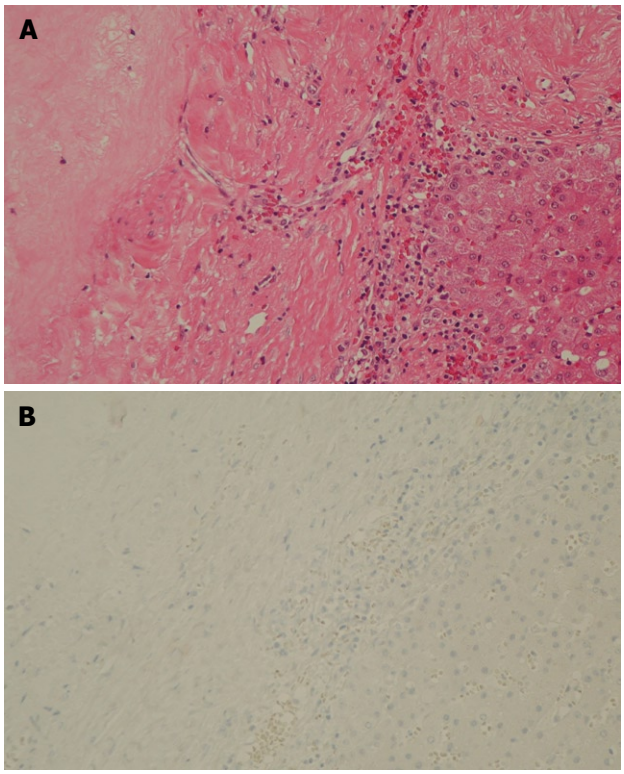

Figure 6 Histological study showing no viable tumor cells and hyaline degenerative tissues (HE, × 200) (**A**) and immunohistochemistry findings revealing negative staining for CD117 (× 200) (**B**) in the resected specimen after treatment with Imatinib.

delayed (35 mo) in comparison with the time suggested by other investigators, it is thought to be adequate for avoidance of the secondary resistance to IM treatment.

In summary, we report a case of GIST with metachronous liver metastases who underwent complete surgical resection following IM treatment. The resected specimen was pathologically proven as a CR. Preoperative radiographic CT, MRI, findings and microscopic findings of the resected specimen were described from the view point of the effect of the molecular targeting therapy.

REFERENCES

1 **Hirota S**, Isozaki K, Moriyama Y, Hashimoto K, Nishida T, Ishiguro S, Kawano K, Hanada M, Kurata A, Takeda M, Muhammad Tunio G, Matsuzawa Y, Kanakura Y, Shinomura Y, Kitamura Y. Gain-of-function mutations of c-kit in human gastrointestinal stromal tumors. *Science* 1998; **279**: 577-580

2 **Joensuu H**, Roberts PJ, Sarlomo-Rikala M, Andersson LC, Tervahartiala P, Tuveson D, Silberman S, Capdeville R, Dimitrijevic S, Druker B, Demetri GD. Effect of the tyrosine kinase inhibitor STI571 in a patient with a metastatic gastrointestinal stromal tumor. *N Engl J Med* 2001; **344**: 1052-1056

3 **Demetri GD**, von Mehren M, Blanke CD, Van den Abbeele AD, Eisenberg B, Roberts PJ, Heinrich MC, Tuveson DA, Singer S, Janicek M, Fletcher JA, Silverman SG, Silberman SL, Capdeville R, Kiese B, Peng B, Dimitrijevic S, Druker BJ, Corless C, Fletcher CD, Joensuu H. Efficacy and safety of imatinib mesylate in advanced gastrointestinal stromal tumors. *N Engl J Med* 2002; **347**: 472-480

4 **Verweij J**, Casali PG, Zalcberg J, LeCesne A, Reichardt P, Blay JY, Issels R, van Oosterom A, Hogendoorn PC, Van Glabbeke M, Bertulli R, Judson I. Progression-free survival in gastrointestinal stromal tumours with high-dose imatinib: randomised trial. *Lancet* 2004; **364**: 1127-1134

5 **Scaife CL**, Hunt KK, Patel SR, Benjamin RS, Burgess MA, Chen LL, Trent J, Raymond AK, Cormier JN, Pisters PW, Pollock RE, Feig BW. Is there a role for surgery in patients with "unresectable" cKIT+ gastrointestinal stromal tumors treated with imatinib mesylate? *Am J Surg* 2003; **186**: 665-669

6 **Bauer S**, Hartmann JT, de Wit M, Lang H, Grabellus F, Antoch G, Niebel W, Erhard J, Ebeling P, Zeth M, Taeger G, Seeber S, Flasshove M, Schutte J. Resection of residual disease in patients with metastatic gastrointestinal stromal tumors responding to treatment with imatinib. *Int J Cancer* 2005; **117**: 316-325

7 **Chacon M**, Roca E, Huertas E, Loria FS, Domenechini E. CASE 3. Pathologic complete remission of metastatic gastrointestinal stromal tumor after imatinib mesylate. *J Clin Onco*l 2005; **23**: 1580-1582

8 **Salazar M**, Barata A, Andre S, Venancio J, Francisco I, Cravo M, Nobre-Leitao C. First report of a complete pathological response of a pelvic GIST treated with imatinib as neoadjuvant therapy. *Gut* 2006; **55**: 585-586

9 **Bonvalot S**, Eldweny H, Pechoux CL, Vanel D, Terrier P, Cavalcanti A, Robert C, Lassau N, Cesne AL. Impact of surgery on advanced gastrointestinal stromal tumors (GIST) in the imatinib era. *Ann Surg Oncol* 2006; **13**: 1596-1603

10 **Andtbacka RH**, Ng CS, Scaife CL, Cormier JN, Hunt KK, Pisters PW, Pollock RE, Benjamin RS, Burgess MA, Chen LL, Trent J, Patel SR, Raymond K, Feig BW. Surgical resection of gastrointestinal stromal tumors after treatment with imatinib. *Ann Surg Oncol* 2007; **14**: 14-24

11 **Gold JS**, Dematteo RP. Combined surgical and molecular therapy: the gastrointestinal stromal tumor model. *Ann Surg* 2006; **244**: 176-184

12 **DeMatteo RP**, Maki RG, Singer S, Gonen M, Brennan MF, Antonescu CR. Results of tyrosine kinase inhibitor therapy followed by surgical resection for metastatic gastrointestinal stromal tumor. *Ann Surg* 2007; **245**: 347-352

13 **Soft Tissue Sarcoma**. National Comprehensive Cancer Network (NCCN) Clinical Practice Guidelines in Oncology 2006. Available from: URL: http://www.nccn.org/professionals/physician_gls/PDF/sarcoma.pdf

14 **DeMatteo RP**, Shah A, Fong Y, Jarnagin WR, Blumgart LH, Brennan MF. Results of hepatic resection for sarcoma metastatic to liver. *Ann Surg* 2001; **234**: 540-547; discussion 547-548

15 **Nunobe S**, Sano T, Shimada K, Sakamoto Y, Kosuge T. Surgery including liver resection for metastatic gastrointestinal stromal tumors or gastrointestinal leiomyosarcomas. *Jpn J Clin Oncol* 2005; **35**: 338-341

16 **Bumming P**, Andersson J, Meis-Kindblom JM, Klingenstierna H, Engstrom K, Stierner U, Wangberg B, Jansson S, Ahlman H, Kindblom LG, Nilsson B. Neoadjuvant, adjuvant and palliative treatment of gastrointestinal stromal tumours (GIST) with imatinib: a centre-based study of 17 patients. *Br J Cancer* 2003; **89**: 460-464

17 **Wu PC**, Langerman A, Ryan CW, Hart J, Swiger S, Posner MC. Surgical treatment of gastrointestinal stromal tumors in the imatinib (STI-571) era. *Surgery* 2003; **134**: 656-665; discussion 665-666

18 **Gronchi A**, Fiore M, Miselli F, Lagonigro MS, Coco P, Messina A, Pilotti S, Casali PG. Surgery of residual disease following molecular-targeted therapy with imatinib mesylate in advanced/metastatic GIST. *Ann Surg* 2007; **245**: 341-346

S- Editor Zhong XY **L- Editor** Wang XL **E- Editor** Yin DH

Online Submissions: wjg.wjgnet.com
wjg@wjgnet.com
www.wjgnet.com

World J Gastroenterol 2008 June 21; 14(23): 3768
World Journal of Gastroenterology ISSN 1007-9327
© 2008 The WJG Press. All rights reserved.

ACKNOWLEDGMENTS

Acknowledgments to Reviewers of *World Journal of Gastroenterology*

Many reviewers have contributed their expertise and time to the peer review, a critical process to ensure the quality of *World Journal of Gastroenterology*. The editors and authors of the articles submitted to the journal are grateful to the following reviewers for evaluating the articles (including those published in this issue and those rejected for this issue) during the last editing time period.

Minoti V Apte, Associate Professor
Pancreatic Research Group, South Western Sydney Clinical School, The University of New South Wales. Liverpool, NSW 2170, Australia

Masahiro Arai, MD, PhD
Department of Gastroenterology, Toshiba General Hospital, 6-3-22 Higashi-ooi, Shinagawa-ku,Tokyo 140-8522, Japan

Tomasz Brzozowski, Professor
Department of Physiology, Jagiellonian University Medical College, 16 Grzegorzecka Str, Cracow 31-531, Poland

Dr. Ronan A Cahill
Department of General Surgery, Waterford Regional Hospital, Waterford, Cork, Ireland

Chi-Hin Cho, Chair and Professor
Departmentof Pharmacology, The University of Hong Kong, 21 Sassoon Road, Hong Kong, China

Deng Da-Jun, Professor
Department of Cancer Etiology, Peking University School of Oncology, 1 Da-Hong-Luo-Chang Street, Western District, Beijing 100034, China

Volker F Eckardt, MD, Professor, Chief
Department of Gastroenterology, Deutsche Klinik für Diagnostik, Aukammallee 33, 65191 Wiesbaden, Germany

Abdellah Essaid, Professor
Hospital Ibn Sina, Rabat 10100, Morocco

Roberto de Franchis, Professor of Medicine (Gastroenterology)
Department of Medical Siences, University of Milan, Head, Gastroenterology 3 Unit, IRCCS Ospedale Maggiore Policlinico, Mangiagalli and Regina Elena Foundation, Via Pace 9, 20122 Milano, Italy

Maria Concepción Gutiérrez-Ruiz, PhD
Departamento de Ciencias de la Salud, Universidad Autónoma Metropolitana-Iztapalapa, DCBS, Av San Rafael Atlixco 186, Colonia Vicentina, México, DF 09340, México

Kazuhiro Hanazaki, MD, Professor and Chairman
Department of Surgery, Kochi Medical School, Kochi University, Kohasu, Okohcho, Nankoku, Kochi 783-8505, Japan

Toru Hiyama, MD, PhD
Health Service Center, Hiroshima University, 1-7-1 Kagamiyama, Higashihiroshima 739-8521, Japan

Ikejima Kenichi, MD, PhD
Department of Gastroenterology, Juntendo University School of Medicine, 2-1-1, Hongo, Bunkyo-ku, 113-8421, Japan

Peter L Lakatos, MD, PhD, Assistant Professor
1st Department of Medicine, Semmelweis University, Koranyi S 2A, Budapest H1083, Hungary

Anders E Lehmann, PhD, Associate Professor
Senior Principal Scientist, Bioscience, AstraZeneca R&D Mölndal, Mölndal, Sweden

Zhe-Xiong Lian, MD, PhD, Associate Adjunct Professor
Division of Rheumatology, Allergy and Clinical Immunology, Genome and Biomedical Sciences Facility, University of California at Davis, 451 Health Sciences Drive, Suite 6605A, Davis, CA 95616, United States

Reza Malekzadeh, Professor, Director
Digestive Disease Research Center, Tehran University of Medical Sciences, Shariati Hospital, Kargar Shomali Avenue, 19119 Tehran, Iran

Kevin McGrath, MD
Division of Gastroenterology, Hepatology and Nutrition, University of Pittsburgh Medical Center, M2, C wing, PUH, 200 Lothrop St, Pittsburgh, PA 15213, United States

Fock Kwong Ming, Professor Senior Consultant
Department of Medicine, Changi General Hospital, 2 Simei Street 3, Singapore 529889, Singapore

Chris JJ Mulder, Professor
Department of Gastroenterology, VU University Medical Center, PO Box 7057, 1007 MB Amsterdam, The Netherlands

Amado S Peña, Professor
Department of Pathology, Immunogenetics, VU University Medical Centre, De Boelelaan 1117, PO Box 7057, Amsterdam 1007 MB, The Netherlands

Dr. Philip Abraham, Professor
Consultant Gastroenterologist & Hepatologist, P. D. Hinduja National Hospital & Medical Research Centre, Veer Savarkar Marg, Mahim, Mumbai 400016, India

Carlos J Pirola, PhD, FAHA
Instituto de Investigaciones Medicas A Lanari, Combatientes de Malvinas 3150, Buenos Aires-1427, Argentina

Sakhawat Rahman, Mr, Consultant in HPB & Minimally Invasive Surgery
Royal Free Hampstead NHS Trust, 133 King Henrys Road, Primrose Hill, London, NW3 3RD, United Kingdom

Vasiliy I Reshetnyak, MD, PhD, Professor
Scientist Secretary of the Scientific Research Institute of General Reanimatology, 25-2, Petrovka str., 107031, Moscow, Russia

Ian C Roberts-Thomson, Professor
Department of Gastroenterology and Hepatology, The Queen Elizabeth Hospital, 28 Woodville Road, Woodville South 5011, Australia

Sammy Saab, MD, MPH, AGAF
Departmentsof Medicine and Surgery, Pfleger Liver Institute, 200 UCLA Medical Plaza, Suite 214, Box 957302, Los Angeles, CA 90095-7302, United States

James M Scheiman, Professor
Division of Gastroenterology, University of Michigan Medical Center, 3912 Taubman Center, Box 0362, Ann Arbor, Michigan 48109-0362, United States

Mitsuo Shimada, Professor
Department of Digestive and Pediatric Surgery, Tokushima University, Kuramoto 3-18-15, Tokushima 770-8503, Japan

Wing-Kin Syn, MD
Division of Gastroenterology, GSRB-1, Suite 1073, DUMC 3256, 595 LaSalle Street, Durham, NC27710, United States

Akihito Tsubota, Assistant Professor
Institute of Clinical Medicine and Research, Jikei University School of Medicine, 163-1 Kashiwa-shita, Kashiwa, Chiba 277-8567, Japan

Satoshi Yamagiwa, MD, PhD
Division of Gastroenterology and Hepatology, Niigata University Graduate School of Medical and Dental Sciences, 757 Asahimachi-dori, Chuo-ku, Niigata, 951-8510, Japan

Online Submissions: wjg.wjgnet.com
wjg@wjgnet.com
www.wjgnet.com

World J Gastroenterol 2008 June 21; 14(23): 3769
World Journal of Gastroenterology ISSN 1007-9327
© 2008 The WJG Press. All rights reserved.

Meetings

Events Calendar 2008-2009

FALK SYMPOSIA 2008
January 24-25, Frankfurt, Germany
Falk Workshop: Perspectives in Liver
Transplantation

International Gastroenterological Congresses 2008
February 14-16, Paris, France
EASL-AASLD-APASL-ALEH-IASL Conference Hepatitis B and C virus resistance to antiviral therapies
www.easl.ch/hepatitis-conference

February 14-17, Berlin, Germany
8th International Conference on New Trends in Immunosuppression and Immunotherapy
www.kenes.com/immuno

February 28, Lyon, France
3rd Congress of ECCO - the European Crohn's and Colitis Organisation
Inflammatory Bowel Diseases 2008
www.ecco-ibd.eu

February 29, Québec, Canada
Canadian Association of Gastroenterology
E-mail: general@cag-acg.org

March 10-13, Birmingham, UK
British Society of Gastroenterology Annual Meeting
E-mail: BSG@mailbox.ulcc.ac.uk

March 14-15, HangZhou, China
Falk Symposium 163: Chronic Inflammation of Liver and Gut

March 23-26, Seoul, Korea
Asian Pacific Association for the Study of the Liver
18th Conference of APASL: New Horizons in Hepatology
www.apaslseoul2008.org

March 29-April 1, Shanghai, China
Shanghai-Hong Kong International Liver Congress
www.livercongress.org

April 05-09, Monte-Carlo (Grimaldi Forum), Monaco
OESO 9th World Congress, The Gastro-esophageal Reflux Disease: from Reflux to Mucosal Inflammation-Management of Adeno-carcinomas
E-mail: robert.giuli@oeso.org

April 9-12, Los Angeles, USA
SAGES 2008 Annual Meeting - part of Surgical Spring Week
www.sages.org/08program/html/

April 18-22, Buenos Aires, Argentina
9th World Congress of the International Hepato-Pancreato Biliary Association
Association for the Study of the Liver
www.ca-ihpba.com.ar

April 23-27, Milan, Italy
43rd Annual Meeting of the European Association for the Study of the Liver
www.easl.ch

May 2-3, Budapest, Hungary
Falk Symposium 164: Intestinal Disorders

May 18-21, San Diego, California, USA
Digestive Disease Week 2008

May 21-22, California, USA
ASGE Annual Postgraduate Course
Endoscopic Practice 2008: At the Interface of Evidence and Expert Opinion
E-mail: education@asge.org

June 4-7, Helsinki, Finland
The 39th Nordic Meeting of Gastroenterology
www.congrex.com/ngc2008

June 5-8, Sitges (Barcelona), Spain
Semana de las Enfermedades Digestivas
E-mail: sepd@sepd.es

June 6-8, Prague, Czech Republic
3rd Annual European Meeting: Perspectives in Inflammatory Bowel Diseases
E-mail: meetings@imedex.com

June 10-13, Istanbul, Turkey
ESGAR 2008 19th Annual Meeting and Postgraduate Course
E-mail: fca@netvisao.pt

June 11-13, Stockholm, Sweden
16th International Congress of the European Association for Endoscopic Surgery
E-mail: info@eaes-eur.org

June 13-14, Amsterdam, Netherlands
Falk Symposium 165: XX International Bile Acid Meeting. B ile Acid Biology and Therapeutic Actions

June 13-14, Prague, Czech Republic
Central and Eastern European Conference on Colorectal "Cancer" Screening, Prevention and Management
E-mail: idca2008@guarant.cz

June 25-28, Barcelona, Spain
10th World Congress on Gastrointestinal Cancer
Imedex and ESMO
E-mail: meetings@imedex.com

June 25-28, Lodz, Poland
Joint Meeting of the European Pancreatic Club (EPC)
and the International Association of Pancreatology (IAP)
E-mail: office@epc-iap2008.org
www.e-p-c.org
www.pancreatology.org

June 26-28, Bratislava, Slovakia
5th Central European Gastroenterology Meeting
www.ceurgem2008.cz

July 9-12, Paris, France
ILTS 14th Annual International Congress
www.ilts.org

September 10-13, Budapest, Hungary
11th World Congress of the International Society for Diseases of the Esophagus
E-mail: isde@isde.net

September 13-16, New Delhi, India
Asia Pacific Digestive Week
E-mail: apdw@apdw2008.net

III FALK GASTRO-CONFERENCE
September 17, Mainz, Germany
Falk Workshop: Strategies of Cancer Prevention in Gastroenterology

September 18-19, Mainz, Germany
Falk Symposium 166:
GI Endoscopy - Standards & Innovations

September 18-20, Prague, Czech Republic
Prague Hepatology Meeting 2008
www.czech-hepatology.cz/phm2008

September 20-21, Mainz, Germany
Falk Symposium 167:
Liver Under Constant Attack - From Fat to Viruses

September 24-27, Nantes, France
Third Annual Meeting
European Society of Coloproctology
www.escp.eu.com

October 8-11, Istanbul, Turkey
18th World Congress of the International Association of Surgeons,
Gastroenterologists and Oncologists
E-mail: orkun.sahin@serenas.com.tr

October 18-22, Vienna, Austria
16th United European Gastroenterology Week
www.negf.org
www.acv.at

October 22-25, Minnesota, USA
Anstralian Gastroenterology Week 2008
E-mail: gesa@gesa.org.au

October 22-25, Brisbane, Australia
71st Annual Colon and Rectal Surgery Conference
E-mail: info@colonrectalcourse.org

October 31-November 4, Moscone West Convention Center, San Francisco, CA
59th AASLD Annual Meeting and Postgraduate Course
The Liver Meeting
Information: www.aasld.org

November 6-9, Lucerne, Switzerland
Neurogastroenterology & Motility Joint International Meeting 2008
E-mail: ngm2008@mci-group.com
www.ngm2008.com

November 12, Santiago de Chile, Chile
Falk Workshop: Digestive Diseases: State of the Art and Daily Practice

November 28-29, Cairo, Egypt
1st Hepatology and Gastroenterology Post Graduate Course
www.egyptgastrohep.com

December 7-9, Seoul, Korea
6th International Meeting
Hepatocellular Carcinoma: Eastern and Western Experiences
E-mail: sglee@amc.seoul.kr

INFORMATION FOR ALL
FALK FOUNDATION e.V.
E-mail: symposia@falkfoundation.de
www.falkfoundation.de

Advanced Courses - European Institute of Telesurgery EITS - 2008
Strasbourg, France
January 18-19, March 28-29, June 6-7, October 3-4

N.O.T.E.S
April 3-5, November 27-29
Laparoscopic Digestive Surgery

June 27-28, November 7-8
Laparoscopic Colorectal Surgery

July 3-5
Interventional GI Endoscopy Techniques
Contact address for all courses:
E-mail: info@eits.fr

International Gastroenterological Congresses 2009
March 23-26, Glasgow, Scotland
Meeting of the British Society of Gastroenterology (BSG)
E-mail: bsg@mailbox.ulcc.ac.uk

May 17-20, Denver, Colorado, USA
Digestive Disease Week 2009

November 21-25, London, UK
Gastro 2009 UEGW/World Congress of Gastroenterology
www.gastro2009.org

Global Collaboration for Gastroenterology

For the first time in the history of gastroenterology, an international conference will take place which joins together the forces of four pre-eminent organisations: Gastro 2009, UEGW/WCOG London. The United European Gastroenterology Federation (UEGF) and the World Gastroenterology Organisation (WGO), together with the World Organisation of Digestive Endoscopy (OMED) and the British Society of Gastroenterology (BSG), are jointly organising a landmark meeting in London from November 21-25, 2009. This collaboration will ensure the perfect balance of basic science and clinical practice, will cover all disciplines in gastroenterology (endoscopy, digestive oncology, nutrition, digestive surgery, hepatology, gastroenterology) and ensure a truly global context; all presented in the exciting setting of the city of London. Attendance is expected to reach record heights as participants are provided with a compact "all-in-one" programme merging the best of several GI meetings. Faculty and participants from all corners of the earth will merge to provide a truly global environment conducive to the exchange of ideas and the forming of friendships and collaborations.

Online Submissions: wjg.wjgnet.com
wjg@wjgnet.com
www.wjgnet.com

World J Gastroenterol 2008 June 21; 14(23): 3770-3772
World Journal of Gastroenterology ISSN 1007-9327
© 2008 The WJG Press. All rights reserved.

Instructions to authors

GENERAL INFORMATION

World Journal of Gastroenterology (*World J Gastroenterol* ISSN 1007-9327 CN 14-1219/R) is a weekly open access peer-reviewed journal supported by an editorial board consisting of 1208 experts in gastroenterology and hepatology from 60 countries. The aim of the journal is to deliver the most clinically relevant original and commentary articles to readers, and to make the full text publicly available to all clinicians, scientists, patients and biomedical students on an unrestricted platform, so that they can access and learn about the most recent key advances in the field.

In addition to the open access nature, another key characteristic of *WJG* is its reading guidance for each article which includes background, research frontier, related reports, breakthroughs, applications, terminology, and comments of peer reviewers for the general readers.

WJG publishes articles on esophageal, gastrointestinal, hepatobiliary and pancreatic tumors, and other esophageal, gastrointestinal, hepatic-biliary and pancreatic diseases in relation to epidermiology, immunology, microbiology, motility & nerve-gut interaction, endocrinology, nutrition & obesity, endoscopy, imaging and advanced hi-technology.

The main goal of *WJG* is to publish high quality commentary articles contributed by leading experts in gastroenterology and hepatology and original articles that combine the clinical practice and advanced basic research, to provide an interactive platform for clinicians and researchers in internal medicine, surgery, infectious diseases, traditional Chinese medicine, oncology, integrated Chinese and Western medicine, imaging, endoscopy, interventional therapy, pathology and other basic medical specialities, and thus eventually improving the clinical practice and healthcare for patients.

Indexed and abstracted in

Current Contents®/Clinical Medicine, Science Citation Index Expanded (also known as SciSearch®) and Journal Citation Reports/Science Edition, Index Medicus, MEDLINE and PubMed, Chemical Abstracts, EMBASE/Excerpta Medica, Abstracts Journals, *Nature Clinical Practice Gastroenterology* and *Hepatology*, CAB Abstracts and Global Health. ISI JCR 2003-2000 IF: 3.318, 2.532, 1.445 and 0.993.

Published by

The WJG Press

SUBMISSION OF MANUSCRIPTS

Manuscripts should be typed in 1.5 line spacing and 12 pt. Book Antiqua with ample margins. Number all pages consecutively, and start each of the following sections on a new page: Title Page, Abstract, Introduction, Materials and Methods, Results, Discussion, Acknowledgements, References, Tables, Figures, and Figure Legends. Neither the editors nor the publisher are responsible for the opinions expressed by contributors. Manuscripts formally accepted for publication become the permanent property of The WJG Press, and may not be reproduced by any means, in whole or in part, without the written permission of both the authors and the publisher. We reserve the right to copy-edit and put onto our website accepted manuscripts. Authors should follow the relevant guidelines for the care and use of laboratory animals of their institution or national animal welfare committee. For the sake of transparency in regard to the performance and reporting of clinical trials, we endorse the policy of the International Committee of Medical Journal Editors to refuse to publish papers on clinical trial results if the trial was not recorded in a publicly-accessible registry at its outset. The only register now available, to our knowledge, is http://www. clinicaltrials.gov sponsored by the United States National Library of Medicine and we encourage all potential contributors to register with it. However, in the case that other registers become available you will be duly notified. A letter of recommendation from each author's organization should be provided with the contributed article to ensure the privacy and secrecy of research is protected.

Authors should retain one copy of the text, tables, photographs and illustrations because rejected manuscripts will not be returned to the author(s) and the editors will not be responsible for loss or damage to photographs and illustrations sustained during mailing.

Online submissions

Manuscripts should be submitted through the Online Submission System at: http://wjg.wjgnet.com. Authors are highly recommended to consult the ONLINE INSTRUCTIONS TO AUTHORS (http://www.wjgnet.com/wjg/help/instructions.jsp) before attempting to submit online. For assistance, authors encountering problems with the Online Submission System may send an email describing the problem to submission@wjgnet.com, or by telephone: +86-10-85381892. If you submit your manuscript online, do not make a postal contribution. Repeated online submission for the same manuscript is strictly prohibited.

MANUSCRIPT PREPARATION

All contributions should be written in English. All articles must be submitted using word-processing software. All submissions must be typed in 1.5 line spacing and 12 pt. Book Antiqua with ample margins. Style should conform to our house format. Required information for each of the manuscript sections is as follows:

Title page

Full manuscript title, running title, all author(s) name(s), affiliations, institution(s) and/or department(s) where the work was carried out; author contributions; disclosure of any financial support for the research; and the name, full address, telephone and fax numbers and email address of the corresponding author should be included. Titles should be concise and informative (remove all unnecessary words), emphasize what is new, and avoid abbreviations. A short running title of less than 40 letters should be provided. List the author(s)' name(s) as follows: initial and/or first name, middle name or initial(s), and full family name.

Author controbutions: The format of this section should be like this: Author contributions: Wang CL and Liang L contributed equally to this work; Wang CL, Liang L, Fu JF, Zou CC, Hong F and Wu XM designed research; Wang CL, Zou CC, Hong F and Wu XM performed research; Xue JZ and Lu JR contributed new reagents/analytic tools; Wang CL, Liang L and Fu JF analyzed data; and Wang CL, Liang L and Fu JF wrote the paper.

Peer reviewers: All articles received are subject to peer review. Normally, three experts are invited for each article. Decision for acceptance is made only when at least two experts recommend an article for publication. Reviewers for accepted manuscripts are acknowledged in each manuscript, and reviewers of articles which were not accepted will be acknowledged at the end of each issue. To ensure the quality of the articles published in *WJG*, reviewers of accepted manuscripts will be announced by publishing the name, title/position and institution of the reviewer in the footnote accompanying the printed article. For example, reviewers: Professor Jing-Yuan Fang, Shanghai Institute of Digestive Disease, Shanghai, Affiliated Renji Hospital, Medical Faculty, Shanghai Jiaotong University, Shanghai, China; Professor Xin-Wei Han, Department of Radiology, The First Affiliated Hospital, Zhengzhou University, Zhengzhou, Henan Province, China; and Professor Anren Kuang, Department of Nuclear Medicine, Huaxi Hospital, Sichuan University, Chengdu, Sichuan Province, China.

Abstract

An informative, structured abstract of no more than 350 words should accompany each manuscript. Abstracts for original contributions should be structured into the following sections: AIM: Only the purpose should be included. METHODS: The materials, techniques, instruments and equipment, and the experimental procedures should be included. RESULTS: The observed and experimental results, including data, effects, outcome, *etc.* should be included. Authors should present *P* value where necessary, and also include any significant data. CONCLUSION: Accurate view and the value of the results should be included.

The format for structured abstracts can be found at: http://www.wjgnet.com/wjg/help/11.doc.

Key words

Please list 5-10 key words, selected mainly from *Index Medicus*, which reflect the content of the study.

Text

For articles of these sections, original articles, rapid communication

and case reports, the main text should be structured into the following sections: INTRODUCTION, MATERIALS AND METHODS, RESULTS and DISCUSSION, and should include appropriate Figures and Tables. Data should be presented in the body text or in Figures and Tables, but not in both. The main text format of these sections, editorial, topic highlight, case report, letters to the editors, should be found at: http://www.wjgnet.com/wjg/help/instructions.jsp.

Illustrations

Figures should be numbered as 1, 2, 3, *etc.*, and mentioned clearly in the main text. Provide a brief title for each figure on a separate page. Detailed legends should not be provided under the figures. This part should be added into the text where the figures are applicable. Figures should be either Photoshop or Illustrator files (in tiff, eps, jpeg formats) at high-resolution. Examples can be found at: http://www.wjgnet.com/1007-9327/13/4520.pdf; http://www.wjgnet.com/1007-9327/13/4554.pdf; http://www.wjgnet.com/1007-9327/13/4891.pdf; http://www.wjgnet.com/1007-9327/13/4986.pdf; http://www.wjgnet.com/1007-9327/13/4498.pdf. Keeping all elements compiled is necessary in line-art image. Scale bars should be used rather than magnification factors, with the length of the bar defined in the legend rather than on the bar itself. File names should identify the figure and panel. Avoid layering type directly over shaded or textured areas. Please use uniform legends for the same subjects. For example: Figure 1 Pathological changes in atrophic gastritis after treatment. A: ...; B: ...; C: ...; D: ...; E: ...; F: ...; G: …*etc.* It is our principle to publish high resolution-figures for the printed and E-versions.

Tables

Three-line tables should be numbered 1, 2, 3, *etc.*, and mentioned clearly in the main text. Provide a brief title for each table. Detailed legends should not be included under tables, but rather added into the text where applicable. The information should complement but not duplicate the text. Use one horizontal line under the title, a second under column heads, and a third below the Table, above any footnotes. Vertical and italic lines should be omitted.

Notes in tables and illustrations

Data that are not statistically significant should not be noted. $^{a}P < 0.05$, $^{b}P < 0.01$ should be noted ($P > 0.05$ should not be noted). If there are other series of P values, $^{c}P < 0.05$ and $^{d}P < 0.01$ are used. A third series of P values can be expressed as $^{e}P < 0.05$ and $^{f}P < 0.01$. Other notes in tables or under illustrations should be expressed as ^{1}F, ^{2}F, ^{3}F; or sometimes as other symbols with a superscript (Arabic numerals) in the upper left corner. In a multi-curve illustration, each curve should be labeled with ●, ○, ■, □, ▲, △, *etc.*, in a certain sequence.

Acknowledgments

Brief acknowledgments of persons who have made genuine contributions to the manuscripts and who endorse the data and conclusions should be included. Authors are responsible for obtaining written permission to use any copyrighted text and/or illustrations.

REFERENCES

Coding system

The author should number the references in Arabic numerals according to the citation order in the text. Put reference numbers in square brackets in superscript at the end of citation content or after the cited author's name. For citation content which is part of the narration, the coding number and square brackets should be typeset normally. For example, "Crohn's disease (CD) is associated with increased intestinal permeability[1,2]". If references are cited directly in the text, they should be put together within the text, for example, "From references[19,22-24], we know that..."

When the authors write the references, please ensure that the order in text is the same as in the references section, and also ensure the spelling accuracy of the first author's name. Do not list the same citation twice.

PMID requirement

PMID roots in the abstract serial number indexed by PubMed (http://www.ncbi.nlm.nih.gov/entrez/query.fcgi?db=PubMed). The author should supply the PMID for journal citation. For those references that have not been indexed by PubMed, a printed copy of the first page of the full reference should be submitted.

The accuracy of the information for journal citations is very important. Using the reference testing system, the authors and editor should check the authors name, title, journal title, publication date, volume number, start page, and end page. We will interlink all references with PubMed in an ASP file so that the readers can immediately access the abstract of the citations online.

DOI requirement

A CrossRef DOI® (Digital Object Identifier) name is a unique string created to identify a piece of scholarly content in the online environment. The author should supply the DOIs for journal citation(doi:10.3748/wjg.13.6458). This link (http://www.crossref.org/SimpleTextQuery/) allows you to retrieve Digital Object Identifiers (DOIs) for journal articles, books, and chapters by simply cutting and pasting the reference list into the box. You may use the form with any reference style, although the tool works most reliably if references are formatted in a standard style such as shown in this example: Assimakopoulos SF, Scopa CD, Vagianos CE. Pathophysiology of increased intestinal permeability in obstructive jaundice. *World J Gastroenterol* 2007; 13(48): 6458-6464

The accuracy of the information of journal citations is very important. We will interlink all references with DOI in ASP file so that readers can access the abstracts of cited articles online immediately.

Style for journal references

Authors: the name of the first author should be typed in bold-faced letters. The family name of all authors should be typed with the initial letter capitalized, followed by their abbreviated first and middle initials. (For example, Lian-Sheng Ma is abbreviated as Ma LS, Bo-Rong Pan as Pan BR). The title of the cited article and italicized journal title (journal title should be in its abbreviated form as shown in PubMed), publication date, volume number (in black), start page, and end page [PMID: 11819634 DOI: 10.3748/wjg.13.5396].

Style for book references

Authors: the name of the first author should be typed in bold-faced letters. The surname of all authors should be typed with the initial letter capitalized, followed by their abbreviated middle and first initials. (For example, Lian-Sheng Ma is abbreviated as Ma LS, Bo-Rong Pan as Pan BR) Book title. Publication number. Publication place: Publication press, Year: start page and end page.

Format

Journals

English journal article (list all authors and include the PMID where applicable)

1 **Jung EM**, Clevert DA, Schreyer AG, Schmitt S, Rennert J, Kubale R, Feuerbach S, Jung F. Evaluation of quantitative contrast harmonic imaging to assess malignancy of liver tumors: A prospective controlled two-center study. *World J Gastroenterol* 2007; **13**: 6356-6364 [PMID: 18081224 DOI: 10.3748/wjg.13.6356]

Chinese journal article (list all authors and include the PMID where applicable)

2 **Lin GZ**, Wang XZ, Wang P, Lin J, Yang FD. Immunologic effect of Jianpi Yishen decoction in treatment of Pixu-diarrhoea. *Shijie Huaren Xiaohua Zazhi* 1999; **7**: 285-287

In press

3 **Tian D**, Araki H, Stahl E, Bergelson J, Kreitman M. Signature of balancing selection in Arabidopsis. *Proc Natl Acad Sci USA* 2006; In press

Organization as author

4 **Diabetes Prevention Program Research Group**. Hypertension, insulin, and proinsulin in participants with impaired glucose tolerance. *Hypertension* 2002; **40**: 679-686 [PMID: 12411462]

Both personal authors and an organization as author

5 **Vallancien G**, Emberton M, Harving N, van Moorselaar RJ; Alf-One Study Group. Sexual dysfunction in 1, 274 European men suffering from lower urinary tract symptoms. *J Urol* 2003; **169**: 2257-2261 [PMID: 12771764]

No author given

6 21st century heart solution may have a sting in the tail. *BMJ* 2002; **325**: 184 [PMID: 12142303]

Volume with supplement

7 **Geraud G**, Spierings EL, Keywood C. Tolerability and safety of frovatriptan with short- and long-term use for treatment

of migraine and in comparison with sumatriptan. *Headache* 2002; **42** Suppl 2: S93-99 [PMID: 12028325]

Issue with no volume

8 **Banit DM**, Kaufer H, Hartford JM. Intraoperative frozen section analysis in revision total joint arthroplasty. *Clin Orthop Relat Res* 2002; (**401**): 230-238 [PMID: 12151900]

No volume or issue

9 Outreach: Bringing HIV-positive individuals into care. *HRSA Careaction* 2002; 1-6 [PMID: 12154804]

Books

Personal author(s)

10 **Sherlock S**, Dooley J. Diseases of the liver and billiary system. 9th ed. Oxford: Blackwell Sci Pub, 1993: 258-296

Chapter in a book (list all authors)

11 **Lam SK**. Academic investigator's perspectives of medical treatment for peptic ulcer. In: Swabb EA, Azabo S. Ulcer disease: investigation and basis for therapy. New York: Marcel Dekker, 1991: 431-450

Author(s) and editor(s)

12 **Breedlove GK**, Schorfheide AM. Adolescent pregnancy. 2nd ed. Wieczorek RR, editor. White Plains (NY): March of Dimes Education Services, 2001: 20-34

Conference proceedings

13 **Harnden P**, Joffe JK, Jones WG, editors. Germ cell tumours V. Proceedings of the 5th Germ cell tumours Conference; 2001 Sep 13-15; Leeds, UK. New York: Springer, 2002: 30-56

Conference paper

14 **Christensen S**, Oppacher F. An analysis of Koza's computational effort statistic for genetic programming. In: Foster JA, Lutton E, Miller J, Ryan C, Tettamanzi AG, editors. Genetic programming. EuroGP 2002: Proceedings of the 5th European Conference on Genetic Programming; 2002 Apr 3-5; Kinsdale, Ireland. Berlin: Springer, 2002: 182-191

Electronic journal (list all authors)

15 Morse SS. Factors in the emergence of infectious diseases. Emerg Infect Dis serial online, 1995-01-03, cited 1996-06-05; 1(1): 24 screens. Available from: URL: http//www.cdc.gov/ncidod/EID/eid.htm

Patent (list all authors)

16 **Pagedas AC**, inventor; Ancel Surgical R&D Inc., assignee. Flexible endoscopic grasping and cutting device and positioning tool assembly. United States patent US 20020103498. 2002 Aug 1

Inappropriate references

Authors should always cite references that are relevant to their article, and avoid any inappropriate references. Inappropriate references include those linked with a hyphen when the difference between the two numbers is greater than five. For example, [1-6], [2-14] and [1, 3, 4-10, 22] are all considered inappropriate references. Authors should not cite their own unrelated published articles.

Statistical data

Write as mean ± SD or mean ± SE.

Statistical expression

Express *t* test as *t* (in italics), *F* test as *F* (in italics), chi square test as χ^2 (in Greek), related coefficient as *r* (in italics), degree of freedom as υ (in Greek), sample number as *n* (in italics), and probability as *P* (in italics).

Units

Use SI units. For example: body mass, m (B) = 78 kg; blood pressure, p (B) = 16.2/12.3 kPa; incubation time, t (incubation) = 96 h, blood glucose concentration, c (glucose) 6.4 ± 2.1 mmol/L; blood CEA mass concentration, p (CEA) = 8.6 24.5 μg/L; CO_2 volume fraction, 50 mL/L CO_2, not 5% CO_2; likewise for 40 g/L formaldehyde, not 10% formalin; and mass fraction, 8 ng/g, *etc.* Arabic numerals such as 23, 243, 641 should be read 23 243 641.

The format for how to accurately write common units and quantums can be found at: http://www.wjgnet.com/wjg/help/15.doc.

Abbreviations

Standard abbreviations should be defined in the abstract and on first mention in the text. In general, terms should not be abbreviated unless they are used repeatedly and the abbreviation is helpful to the reader. Permissible abbreviations are listed in Units, Symbols and Abbreviations: A Guide for Biological and Medical Editors and Authors (Ed. Baron DN, 1988) published by The Royal Society of Medicine, London. Certain commonly used abbreviations, such as DNA, RNA, HIV, LD50, PCR, HBV, ECG, WBC, RBC, CT, ESR, CSF, IgG, ELISA, PBS, ATP, EDTA, mAb, can be used directly without further explanation.

Italics

Quantities: *t* time or temperature, *c* concentration, *A* area, *l* length, *m* mass, *V* volume.
Genotypes: *gyrA*, *arg* 1, *c myc*, *c fos*, *etc.*
Restriction enzymes: *Eco*RI, *Hin*dI, *Bam*HI, *Kbo* I, *Kpn* I, *etc.*
Biology: *H pylori*, *E coli*, *etc.*

SUBMISSION OF THE REVISED MANUSCRIPTS AFTER ACCEPTED

Please revise your article according to the revision policies of *WJG*. The revised version including manuscript and high-resolution image figures (if any) should be copied on a floppy or compact disk. The author should send the revised manuscript, along with printed high-resolution color or black and white photos, copyright transfer letter, and responses to the reviewers by courier (such as EMS/DHL).

Editorial Office

World Journal of Gastroenterology
Editorial Department: Room 903
Ocean International Center, Building D
No. 62 Dongsihuan Zhonglu
Chaoyang District, Beijing 100025, China
E-mail: wjg@wjgnet.com
http://www.wjgnet.com
Telephone: +86-10-59080039
Fax: +86-10-85381893

Language evaluation

The language of a manuscript will be graded before it is sent for revision. (1) Grade A: priority publishing; (2) Grade B: minor language polishing; (3) Grade C: a great deal of language polishing needed; (4) Grade D: rejected. Revised articles should reach Grade A or B.

Copyright assignment form

Please download a Copyright assignment form from http://www.wjgnet.com/wjg/help/9.doc.

Responses to reviewers

Please revise your article according to the comments/suggestions provided by the reviewers. The format for responses to the reviewers' comments can be found at: http://www.wjgnet.com/wjg/help/10.doc.

Proof of financial support

For paper supported by a foundation, authors should provide a copy of the document and serial number of the foundation.

Links to documents related to the manuscript

WJG will be initiating a platform to promote dynamic interactions between the editors, peer reviewers, readers and authors. After a manuscript is published online, links to the PDF version of the submitted manuscript, the peer-reviewers' report and the revised manuscript will be put on-line. Readers can make comments on the peer reviewer's report, authors' responses to peer reviewers, and the revised manuscript. We hope that authors will benefit from this feedback and be able to revise the manuscript accordingly in a timely manner.

Science news releases

Authors of accepted manuscripts are suggested to write a science news item to promote their articles. The news will be released rapidly at EurekAlert/AAAS (http://www.eurekalert.org). The title for news items should be less than 90 characters; the summary should be less than 75 words; and main body less than 500 words. Science news items should be lawful, ethical, and strictly based on your original content with an attractive title and interesting pictures.

Publication fee

Authors of accepted articles must pay a publication fee.
EDITORIAL, TOPIC HIGHLIGHTS, BOOK REVIEWS and LETTERS TO THE EDITOR are published free of charge.